Harnessing Natural Product Biosynthesis to Access Macrocycles

by

Graham William Heberlig

Thesis submitted to the
Faculty of Graduate & Postdoctoral Studies
in partial fulfillment of the requirements for the
Ph.D. degree in Chemistry

Ottawa-Carleton Chemistry Institute

Department of Chemistry and Biomolecular Sciences, Faculty of Science
University of Ottawa

Table of Contents

Table of Figures

Abstract

Macrocyclic natural products are conformationally restricted molecules that often have improved ability to bind with high affinity and selectivity on a target. Within macrocycle chemistry, macrolactone formation is a particularly challenging transformation and has spurred the development of highly diverse synthetic strategies. A key strategy that is missing is a chemoenzymatic approach to this challenge, and the logical place to look for such a catalyst is the thioesterases (TEs) from the biosynthetic pathways that generate these molecules in Nature. These TEs are α/β-hydrolases containing an active site serine or cysteine and a conserved histidine/aspartate catalytic diad. The research presented here describes the development of two related TE domains from resorcylic acid lactone polyketide synthases found in various fungi. Unlike their bacterial counterparts these macrocyclization catalysts have proven to be stereotolerant with regard to the secondary alcohols involved in macrocyclization. Further work has demonstrated that they are also amenable to generating 12- to 18-member macrolactones. These TE domains can also catalyze macrolactam and cyclic depsipeptide formation, setting the stage for these enzymes to serve as a platform for catalyst development. The development of 2,3-diaminopropionate (DAP) incorporation in place of the active site Ser to trap acyl-enzyme intermediates was used to structurally characterize the formation of a macrocyclic trimer. This technique will be broadly applicable to characterizing other TEs. Overall the research presented here lays the foundation for the long term development of TEs as macrocyclization biocatalysts.

Acknowledgements

First, I would like to thank my parents for their love and support throughout my degree. Secondly, Grandma for her love, support, and cards on every holiday and birthday.

A huge thank you to Chris Boddy for taking me on as grad student and for being an incredibly supportive and enthusiastic supervisor.

Thank you to Profs. Jeff Keillor and John Pezacki for their support and advice over my degree.

Finally, a thank you to all the Boddy lab members past and present I have had the pleasure of working with. Sharing the lab with you made the long hours much more bearable. And a thank you to Richenda for sharing the Chipits.

Dedicated to William "Grumps" Walker

A quick calculation on the stoichiometry of caffeine involved in a Ph.D

An average of 15 - 6oz. cups per week at 68 mg/cup

Roughly 297 g or 1.54 mol of caffeine can get you a Ph.D.

1. Synthetic and biosynthetic approaches to macrocycles

1.1 Introduction

1.1.1 Macrocycles - An Enduring Synthetic Challenge

Natural products are structurally diverse and often possess exceptional biological activity. These molecules have captured the interest of synthetic chemists for centuries from Fischer's synthesis of glucose in 1897 to the hundreds of total synthesis papers published each year.[1–3] Natural products are also used as drugs or serve as the inspiration in drug design. Approximately 30-40% of all approved drugs from 1981 to 2014 were derived or based on natural products.[4] A special class of natural products are the macrocycles, while they only comprise about 3% of all natural products[5] they have led to intense study both as synthetic targets and as drug leads owing to their exquisite structures and unusual and varied biological activities.

Since the bulk of my thesis work focuses on enzymatic formation for macrolactones this chapter will review their chemical synthesis and biogenesis this synthetic portion of the review will focus on macrocyclic lactones. Carbocyclic natural products are outside the scope of this review as the chemistries used to generate them are highly diverse, and (depsi)peptidic natural products are almost universally macrocyclized by the formation of an amide bond. Synthetic chemistry efforts toward macrocyclic natural products have been spurred on by the challenge of generating often functionally and stereochemically dense molecules with the additional problem of cyclization. Advances in ester bond formation[6] and macrolactonization strategies in natural product synthesis have been previously reviewed.[7] Macrocyclization is an inherently difficult

synthetic transformation as it introduces complexity, is entropically disfavored, and typically occurs late in the synthetic route, which may limit the amount of material available for testing. This has resulted the development of many different methods for ester/macrolactone formation, though the selection of the best conditions for a particular synthetic target is difficult to predict.

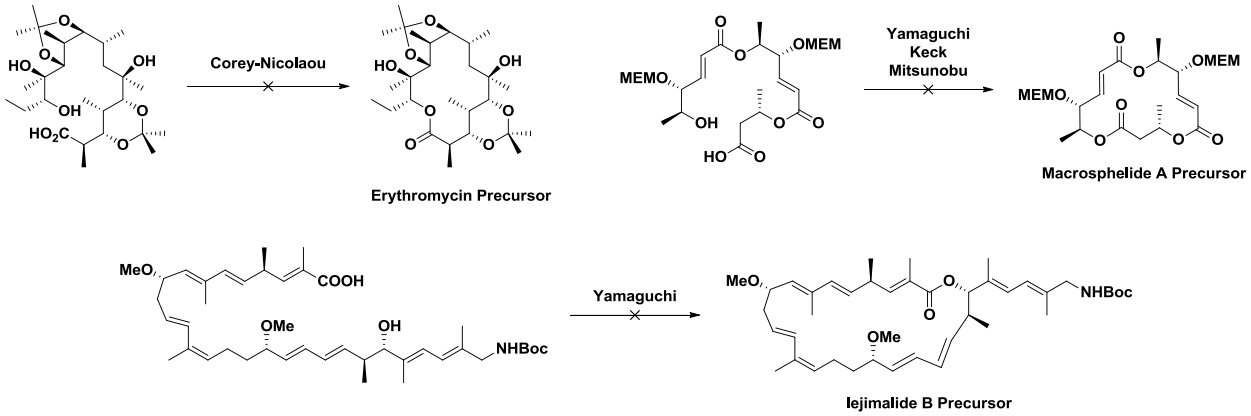

Figure 1.1 Several total synthesis examples where macrolactonization chemistry has failed to yield the desired macrocycle.

A prominent early example of this problem is Woodward's synthesis of erythromycin in 1981.[8] The initial seco-acid intermediate subjected to the Corey-Nicolaou macrolactionization[9] conditions (**Fig 1.1**) failed to yield any macrocycle. Achieving efficient cyclization required the screening of several dozen additional compounds with variable C9 configuration and alcohol protection strategies. The screening library could fortunately be generated by degradation of natural material. If this option was not available, finding macrocyclization conditions would have required carrying large quantities of material through a 27 step sequence.[10]

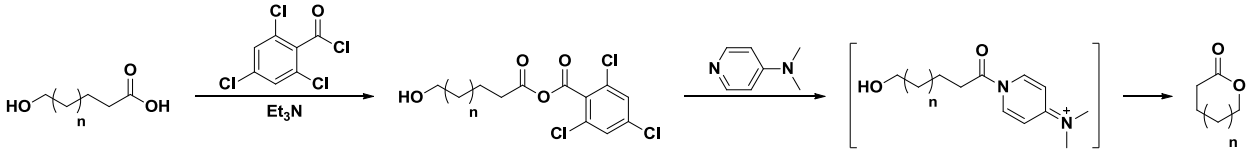

Figure 1.2 Generalized Yamaguchi macrolactionization reaction scheme

One of the most consistent macrolactone forming reactions has been the Yamaguchi mixed anhydride macrolactonization[11] (**Fig 1.2**) and the later Yonemitsu modifications.[12] This reaction has been used in over 340 syntheses for a wide variety of ring sizes.[7] However it can still fail to deliver the desired macrocycle as in the total synthesis of macrosphelide A[13] and iejimalide B (**Fig 1.1**).[14] Fürstner's synthesis of iejimalide B is an interesting case where the macrolactonization route was abandoned entirely and the macrocycle was formed using a surprisingly selective ring-closing metathesis (RCM).[15] This change in strategy for iejimalide B highlights the C-C bond forming alternative to C-O bond forming strategies, in particular the rise of RCM in natural product total synthesis.[16] While RCM based macrocyclization strategies have been successful[17] there are also many examples where RCM has failed outright or fallen short of the yield from macrolactonization (Fig 1.3). Additionally there is a dizzying variety of commercial RCM catalysts available and it is almost impossible to predict which, if any, will provide the best performance.[18] Taken as a whole macrolactone formation and RCM should be used as complementary strategies rather than replacements for one another.

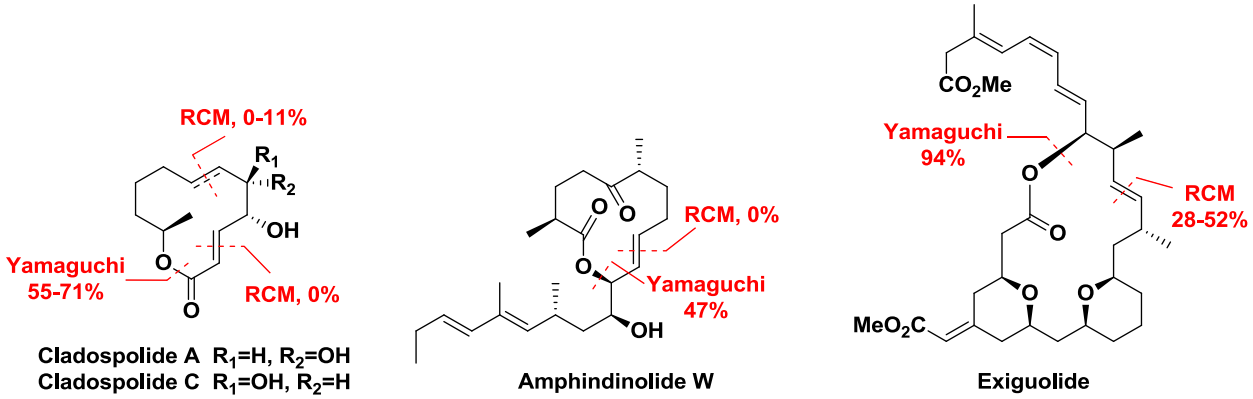

Figure 1.3 Yamaguchi macrocyclization verses RCM as a method for forming macrolactones.[19–22]

As the chemistry to access them has matured, medicinal chemists have become increasingly interested in macrocycles as drugs in the past 20 years as evidenced by a growing number of papers and reviews on this class of compounds.[5,23–28] Many of these compounds, particularly those based on natural products, are in "beyond Rule of 5" space[29,30] and can bind to large, flat, and featureless areas of proteins allowing them to stick on protein surfaces. This can disrupt protein-protein interactions and allow macrocycles to hit what are typically thought of as "undruggable" targets while maintaining oral bioavailablity.[29,31] Another important feature of macrocyclization in drug discovery is the ability to screen more chemical space in a library without adding molecular weight. Given the privileged activity and increasing synthetic availability of macrocycles, it is not surprising that there are now over 20 companies engaged in or associated with the development of macrocyclic drugs including Bicycle Therapeutics, Ra Pharmaceuticals, Polyphor, Aileron Therapeutics, and others.

The majority of these companies build and screen macrocyclic peptide libraries due in large part to the synthetic challenges of constructing macrocyclic lactones. Additionally, robust amide bond forming chemistry, solid phase synthesis, and commercial availability of orthogonally protected amino acids offers easy access to these molecules.[32] New methods to access macrocyclic compounds, particularly macrocyclic lactones, will be important additions to the chemist's toolbox.

1.1.2 PKS/NRPS Machinery - A Natural Source of Macrocycles

Synthetic and medicinal chemistry efforts towards macrocycles have been inspired by molecules from Nature.[5,7] Understanding how this diversity of structure and function come

about can provide insight in designing analogs and developing new chemistry. One of the largest sources of macrocyclic products in nature are the polyketide synthases (PKS) and non-ribosomal peptide synthetases (NRPS).[33] PKS systems are an exceptional source of macrocyclic lactones of various ring sizes and activity (**Fig 1.4**) and have been the targets of many total synthesis efforts (**Fig 1.1, 1.3**).

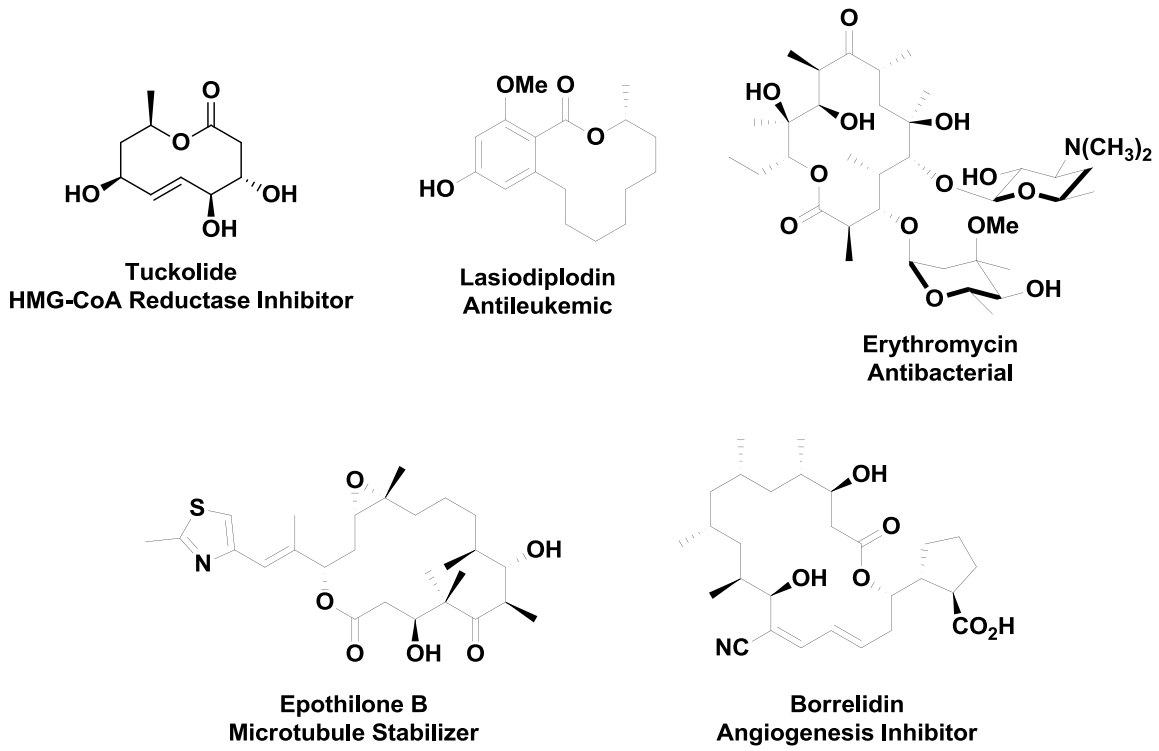

Figure 1.4 Selected macrocyclic polyketide natural products ranging from 10- to 18-member rings and their biological activities.

These products are assembled using large multi-domain PKS megasynthases that extend the growing chain by two carbons during each extension similar to fatty acid biosynthesis. These pathways differ from fatty acid biosynthesis as they can vary the amount of reduction that takes place after each extension to yield products containing alcohols, olefins, and fully reduced carbon chains (**Fig 1.5**). The most well studied of these pathways is the 6-deoxyerythronolide B

(DEBS) synthase (**Fig 1.5**) pathway which is a type-I modular pathway.[34] These are most common in bacterial producers of polyketides. There are several other types of polyketide pathways (type-I iterative, type-II, and type-III)[34] but this review will only cover the modular variety since they generate the majority of macrolatone polyketide products.

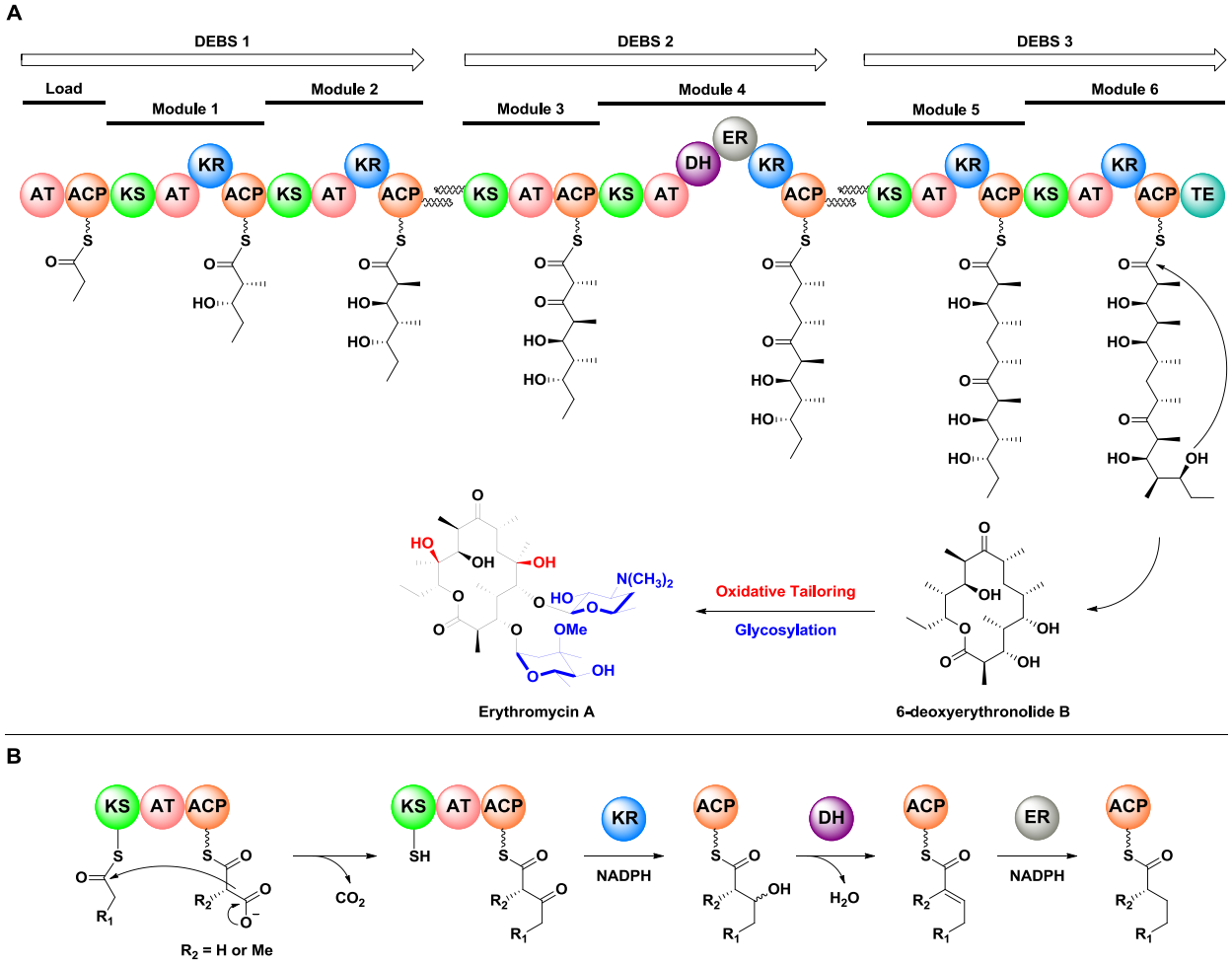

Figure 1.5 A) The DEBS PKS pathway with each ACP-bound intermediate showing the product that is generated after all in-module reductive steps are performed. **B)** The KS-catalyzed decarboxylative Claisen condensation of an acyl-carrier protein (ACP) bound malonyl extender unit with the ketosynthase (KS) bound growing polyketide chain. Subsequent optional reductive chemistry on the ACP-bound extended chain is also shown.

The biosynthesis of these compounds begins with the loading of an acyl-CoA to the acyl carrier protein (ACP) in the loading domain and passage of the acyl chain to the active site Cys on the downstream ketosynthase (KS) domain. The acyltranferase (AT) domain selects the appropriate malonyl-CoA extender unit, most often malonyl-CoA or (2*S*)-methylmalonyl-CoA, and loads this onto the phosphopantethine (Ppant) arm of the in-module ACP. A KS catalyzed decarboxylative Claisen condensation simultaneously extends the chain by two carbons and generates a β-keto thioester attached to the ACP. This product can then be immediately passed to the downstream module for further extension (Module 3) or undergo some amount of sequential β-reductive processing depending on what reductive domains are located within the module. These can include the ketoreductase (KR), which generates a β-hydroxyl, the dehydrotase (DH), which eliminates the alcohol to generate an olefin, and an enoylreductase (ER), which reduces the olefin to a saturated system. This process is summarized in **Figure 1.5B**. Once the final extension and reductive reactions have been carried out the product must be released from the megasynthase to allow the system to turn over. In most pathways this function is performed by a thioesterase (TE) domain which will be discussed in detail below (§ 1.1.3)

Cyclic peptide natural products can be generated both on and off the ribosome. This review will cover non-ribosomal peptides as these predominantly use a TE domain to form macrolactams and macrolactones. Much like the PKS pathways above NRPS pathways are built in a modular fashion with each module extending the growing peptide by one amino acid during each extension (**Fig 1.6**).[33] The extending amino acid is selected and activated as an AMP-ester by the adenylation (A) domain and this is loaded on to the thiolation (T) domain. The T domain is analogous to the ACP domain in polyketide biosynthesis and also has a Ser linked PPant arm. Extension of the amino acid chain is catalyzed by condensation (C) domain, which, as the name

suggests, condenses the upstream amino acid with the loaded in-module T domain. This continues until the chain reaches its full length at the terminus of the pathway where it is released typically by the action of a TE domain.

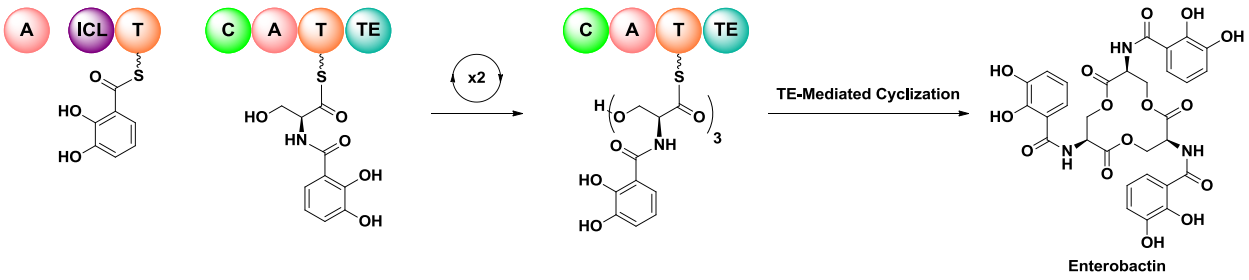

Figure 1.6 The biosynthesis of enterobactin illustrating the basic biosynthesis of non-ribosomal peptides. This pathway acts iteratively to generate a trimeric product that is then cyclized and released from the pathway by a thioesterase (TE) domain.

PKS and NRPS biosynthesis are two strategies that Nature uses to generate complex bioactive molecules. The complex intermediates at the end of biosynthesis must be released from the megasynthases to allow for enzymatic turnover. This is often affected by a TE domain, which can take these highly complex and functionally rich intermediates and selectively macrocyclize them to generate the active metabolite. These TE domains are Nature's macrocyclization catalyst and are the subject of the macrocyclization research presented in this thesis.

1.1.3 Structure and Mechanism of TEs

The previous section covered the basics of PKS and NRPS biosynthesis and noted that many pathways terminate in thioesterase (TE) domains. These domains are α/β-hydrolase like enzymes with an active site Ser or Cys and a conserved His-Asp catalytic dyad. The topology diagram of the TE involved with aflatoxin biosynthesis (**Fig 1.7**) is shown below and illustrates the beta-sheet core of the protein and two extended helices (L1 and L2) with a loop between

them. This region sits over the active site pocket and is referred to as the lid region. This lid forms one part of the channel that the Ppant bound substrate needs to move through to acces the active site of the TE. The lid is also the most mobile portion of the TE domain particularly when acting on larger substrates for macrocyclization.[35,36]

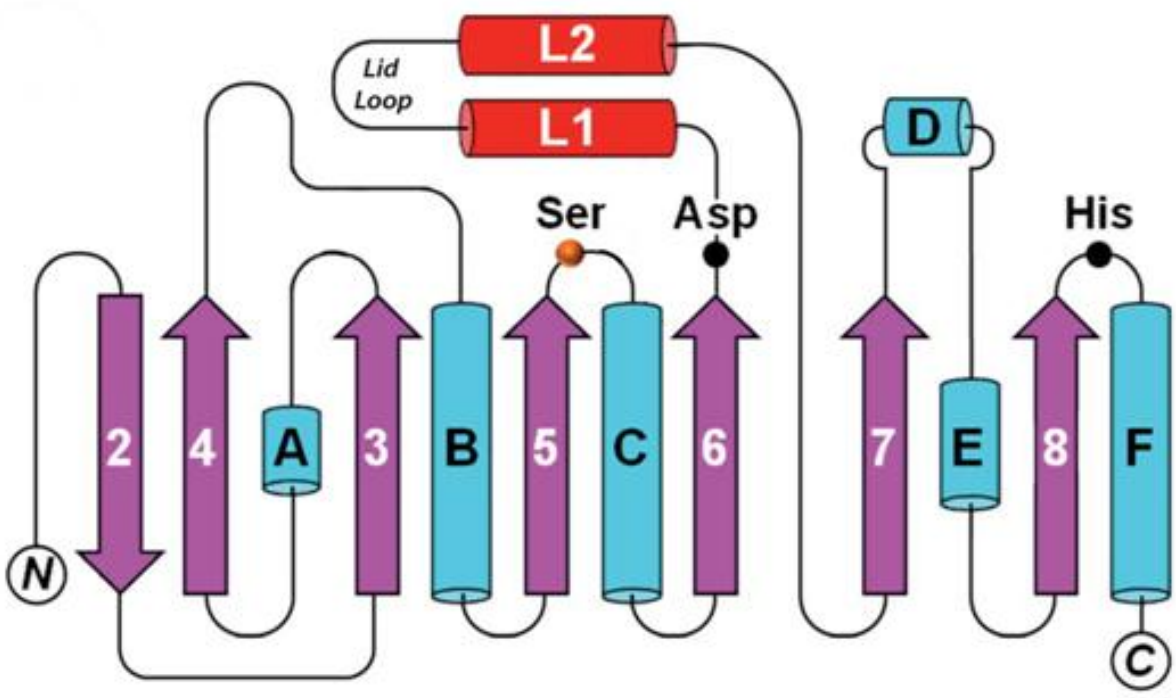

Figure 1.7 General topological map of a thioesterase (PksA from aflatoxin) involved in secondary metabolism. Adapted from Horsman, et al.[37] and Korman et al.[38]

TEs function using a two step mechanism to offload the terminal T/ACP bound intermediate by attack of the Ser side chain on the Ppant thioester with the tetrahedral-intermediate stabilized by the *i*+1 backbone amide group. Collapse of this intermediate leaves the acyl-chain bound to the Ser side chain and the Ppant thiol regenerated and free to participate in elongation. Once the acyl-TE intermediate is generated the offloading step to release the mature product can begin. The nucleophile, whether inter- or intramolecular, approaches and the active

site His is known to serve as an activating base.[36,39,40] This mechanism requires the His side chain to be deprotonated. Townsend, *et al.* have suggested that the departing Ppant thiolate anion may serve this purpose.[38,41] Once activated the nucleophile attacks the acyl-TE intermediate forming another tetrahedral intermediate, which collapses releasing the substrate from the megasynthase and priming the TE to accept another substrate (**Fig 1.8**).

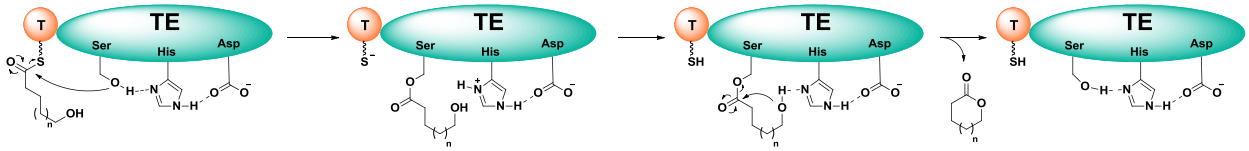

Figure 1.8 General mechanism illustrating the loading of a TE from the T domain and offloading to generate a general macrocyclic product.

1.1.4 PKS/NRPS Release Chemistry

Up to this point all examples of TE catalyzed offloading reactions have resulted in a macrocyclic product however other intermolecular nucleophiles can also particapate in offloading the acyl-TE intermediate. In addition to macrocyclization a common method for chain release is the use of water as a nucleophile, which results in the generation of a free acid such as in the biosynthesis of gephyronic acid (**Fig 1.9a**).[42] External nucleophiles other than water can also function to affect intermolecular release. The most common outcome of this type of release is the generation of di- or trimeric product, which then offloads from the TE through macrocyclization or hydrolysis. The enterobactin pathway discussed in § 1.1.2 (**Fig 1.6**) is a typical example of this trimerization/macrocyclization dual function and this is discussed in detail in chapter 4. One of the two TEs in salinamide biosynthesis has been characterized to transfer a small polyketide/non-ribosomal peptide (PK/NRP) hybrid product to a serine side

chain priming the molecule for oxidative cyclization to form the active product (Fig 1.9b).[43] Combined with the macrocycle forming release discussed above there are three release reactions possible for the offloading step in the TE catalytic cycle.

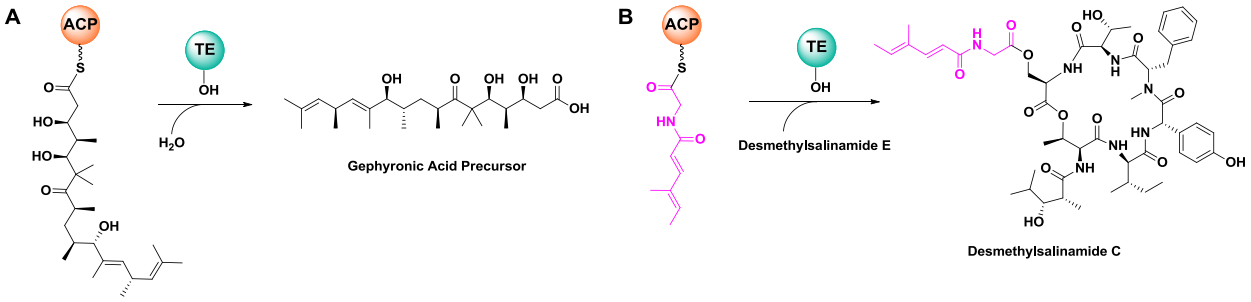

Figure 1.9 Biosynthetically characterized examples of intermolecular nucleophiles in the thioesterase (TE) catalyzed offloading.

Currently there is no way to predict the release selectivity of a TE based on its sequence or even with the context of its associated pathway.[44] Phylogenetic analysis of 295 TE sequences with assigned release reactions did not find any associated between sequence and product type.[37] The sequences clustered primarily based on pathway type (NRPS, PKS, *trans*-AT PKS) or by host organism (bacteria or fungi). Truncated alignment of these sequences also revealed that there is little sequence consensus across TEs and the L1-L2 lid region is particularly variable both in sequence and length.

Recently computational methods have been applied to several characterized TEs with the intent to determine the interacting amino acids responsible for either hydrolysis or macorcyclization.[36,39,40] Application of these methods to the 6-DEBS system found that macrocyclization-competent substrates loading on the TE results in an induced-fit mutual recognition mediated by hydrophobic packing with Leu-183,186, and 190 in the lid.[40] This packing also sequesters the active site away from the bulk solvent and prevents hydrolytic

cleavage to the free acid. This is in agreement with the earlier work by Wang and Boddy, which found that substrate specificity was dominated by hydrophobic interactions rather than hydrogen bonding.[45]

Application of recent non-canonical 2,3-diaminoproionate (DAP) incorporation in the valinomycin TE allowed Chin, Schmeing, and Boddy to biochemically characterize for the first time several native-like intermediates in valinomycin oligomerization and cyclization.[35] This technology will likely be applied to other TEs in the future as attempts to crystallize the DEBS TE with native like substrates tethered via phosphonate esters inhibited the enzyme but could not be visualized in complex.[46] Broad application of this technique to bacterial TEs may reveal the specific determinants for offloading chemistry and would be a welcome addition to the literature and would be a large step forward in our ability to predict the products of orphan pathways.

1.2 Bio-Catalysis: A Brief Overview

The importance of biocatalytic technology was recently highlighted by the 2018 Nobel Prize in chemistry given to Francis H. Arnold for the directed evolution of enzymes. Methods to develop biocatalysts have moved from blind mutagenesis to modern computational prediction and designed directed evolution. Developments in this field have been reviewed.[47–49] Application of enzymes to industrial processes has been a driver in the field for several decades and this mini-review will focus on examples toward pharmaceuticals by Codexis.

Codexis, Inc. developed a biocatalytic process to perform a stereoselective ketone reduction in the synthesis of montelukast (Singulair).[50] This drug is used in the control of asthma symptoms and was prescribed over 25 million times in 2018. The original chemical route to montelukast involved the stereoselective reduction of a ketone using super stioichiometric

amounts of (-)-DIP-Cl under cryogenic conditions.[51] A key challenge in the development of a biocatalyst to affect the same transformation is the high (>7) clogP of the starting material. Through 5 rounds of directed evolution a ketoreductase (KRED) was evolved to function in a blend of toluene, isopropanol and buffer and at 100 g/L substrate loadings. Additionally optical purity exceeded 99.9% *ee* and eliminated necessary crystallization upgrade step in the chemical process. This KRED reaction reduces the process mass intensity (PMI) from 52 to 34 at the same scale and was eventually scaled to 200 kg for manufacturing purposes.

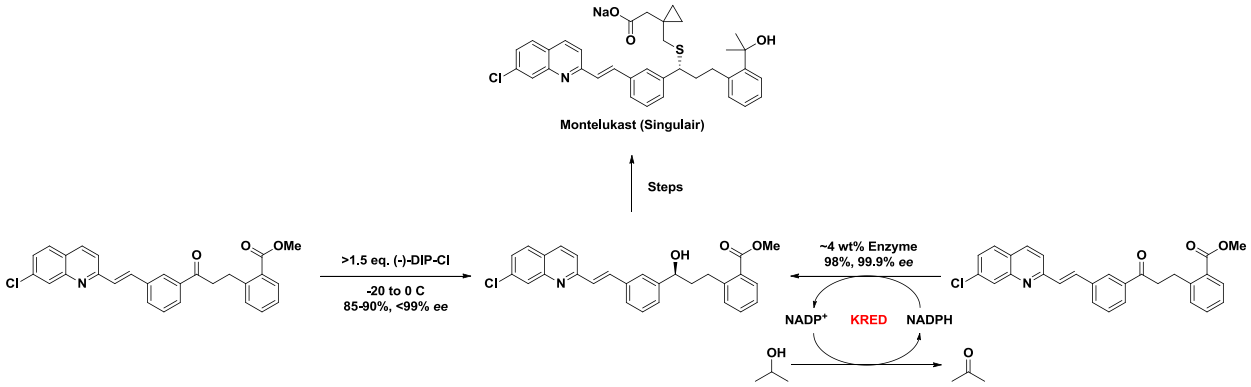

Figure 1.10 Overview of the chemical and biocatalytic reactions to access the enantiopure alcohol intermediate in montelukast production.[50]

Last year Codexis developed a system to perform stereoselective sulfoxidation as the final step to generate the proton pump inhibitor esomeprazole.[52] This method used a cocktail of three enzymes to replace the titanium catalyzed Kagan-Sharpless-Pitchen oxidation used in commercial production.[53,54] The sulfur oxidizing enzyme was a Baeyer-Villiger monooxygenase (BVMO) that was evolved over 19 generations to produce the chiral sulfoxide with >99% *ee* and less than 0.1% of sulfone (under USP limits) using O_2 as the oxidant and catalytic $NADP^+$. Combination with a KRED to regenerate the cofactor and catalase to remove hydrogen peroxide completed the process, which was scalable to 50 g/L.

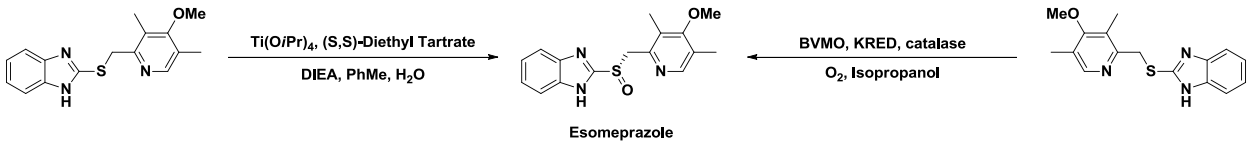

Figure 1.11 Overview of the chemical and biocatalytic reactions oxidize the thioether pyrmetazole to the chiral sulfoxide esomeprazole.[52]

From the preceding examples it is apparent that enzymes as catalysts have lived up to the expectation of highly selective activity and operation under mild reaction conditions. With advances in directed evolution the initial concerns regarding low activity on non-native substrates, function at high substrate loading or product inhibition have largely been overcome for a variety of enzyme classes. halogenases[55,56], dehalogenases[57], imine reductase[58,59], ene-reductases[60], and others have been developed for industrial processes.

1.3 Thioesterases as Biocatalysts

Application of enzymes to complex late stage reactions such as macrocyclization would be a welcome addition to the biocatalyst toolbox. As presented previously (§ 1.1.1) generating macrocycles is a formidable synthetic challenge[61] and designing a biocatalyst from scratch would impractical. Early work on enzyme catalyzed macrolactonization reactions were lipase mediated transesterification reactions using simple ω-hydroxyesters.[62–65] Work by Nanda in 2005[66] used a lipase to macrocyclize a precursor to herbarumin III. That work also claimed to be the first reported use of an enzymatic route to a macrocyclic lactone natural product; however Boddy and coworkers generated epothilone C two years earlier using the native thioesterase.[67] Building off the TE-catalyzed macrocyclization of epothilone many other TEs have been probed

both *in vivo* and *in vitro* for macrocylization activity.[37] The cases presented below are several examples of TEs that can access non-native macrocycles and form the basis of efforts toward a more general macrocyclization biocatalyst.

1.3.1 NRPS TE

Many non-ribosomal peptides longer than 4 residues are macrocyclic and this is proposed to decrease the ability of proteases to cleave and inactivate them, increase membrane permeability, and limit flexibility to promote binding to their target(s). NRPS pathways can incorporate non-proteogenic amino acids and thus have access to extraordinarily diverse peptide intermediates. It is expected that the TEs from these pathways should be able to access highly diverse macrocycles. An early example of substrate flexibility in a macrocyclizing TE from an NPRS pathway is the tyrocidine pathway.[68] This initial report on the TycC TE demonstrated that it could perform macrocylization release as a standalone domain, a first in the field of NRPS biosynthesis, and it possessed the ability to cyclize the related non-ribosomal peptide gramicidin S. Later work by Walsh and coworkers would establish the immense substrate flexibility this of this TE. Using solid-phase peptide synthesis every position of the linear decapeptide was replaced with alanine and the only requirements for cyclization were an aromatic amino acid at position 1, proline at 2, and ornithine as the penultimate amino acid.[68] This preorganization of the substrate for macrocyclization (**Fig 1.12**) provides chemical flexibility for the rest of linear precursor. Additional work allowed the incorporation of ester linkages[69], polyketide-like insertions[70], and the ability to directly macrocyclize substrates from PEGA resin so long as the three essential amino acids were in the correct position.[70] With the addition of Brij 58, a nonionic detergent, the lifetime of the catalyst could be extended and the strict requirement of

ornithine as the penultimate residue was overcome; however, it could only be replaced by amino acids with some ability to hydrogen bond.[71]

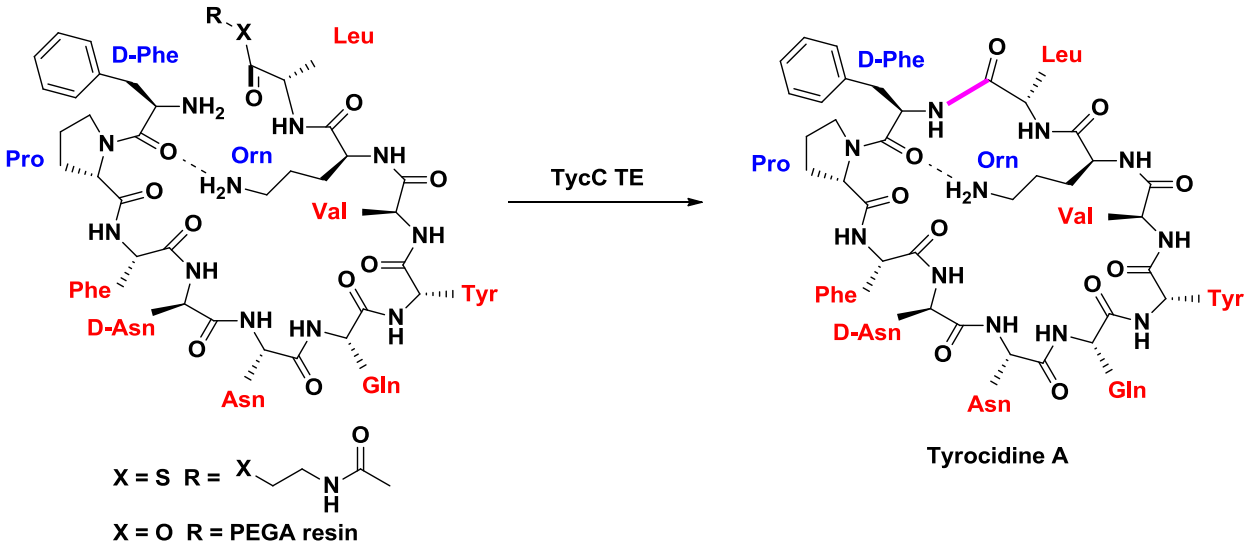

Figure 1.12 Model of tyrocidine substrate preorganization and essential residues for pre-organization shown in blue. The critical hydrogen bond between Orn-9 and Phe-1 is shown as a dashed line. The amide bond formed from this reaction is shown in purple. Adapted from Horsman et al.[37]

1.3.2 Bacterial PKS TEs

Modular type-1 PKS TEs from bacteria tend to be selective for the release mode they catalyze and there are no characterized pathways to date where both a macrocyclic and linear product are both produced in substantial amounts. Additionally these TEs are known to be highly regioselective, the DEBS TE natively only generates a 14-member ring though the possibility to generate a 6- or 12-member macrocycle is also available.[72,73] The DEBS pathway is the most well characterized PKS system and its TE is no exception and it will be discussed here as a macrocyclizing biocatalyst. As this review is focused on TEs as standalone macrocyclization

catalysts the extensive analogs generated by this TE *in vivo* by module and domain shuffling will not be covered and has been reviewed previously.[37] The *in vitro* characterization of the DEBS TE has challenged the enzyme with highly non-native substrates. Work by Pinto et al. challenged the TE with simplified substrates containing an amide linkage and all four possible diastereomers of the C11 and C13 alcohols.[74] Much like previous *in vivo* work only the 14-member ring was generated and only with the native D-configured nucleophile. Intriguingly the TE was also diastereoselective with regard to the configuration at C11, hydrolyzing the substrate bearing the native L-configuation. This result likely rules out substrate driven preorganization in the macrocyclization process. Attempts to explain this unexpected outcome by crystallizing DEBS TE in complex with these substrates unfortunately failed though recent 2,3-diaminopropionate incorporation into TE active sites could remedy this.[35,46]

Hari *et al.* simplified the substrate further by eliminating the C11 alcohol entirely and replacing it with an olefin.[75] Incubation of these substrates with DEBS TE yielded the expected hydrolysis for the L-configured nucleophile but the D-configured substrate underwent hydrolysis, macrocyclization, and transesterification to yield linear and cyclic dimers (**Fig 1.13**). This result indicates the possibility that some modular type-I TEs may be able to access diverse chemistries *in vivo* however there are no characterized pathways to date with this ability.

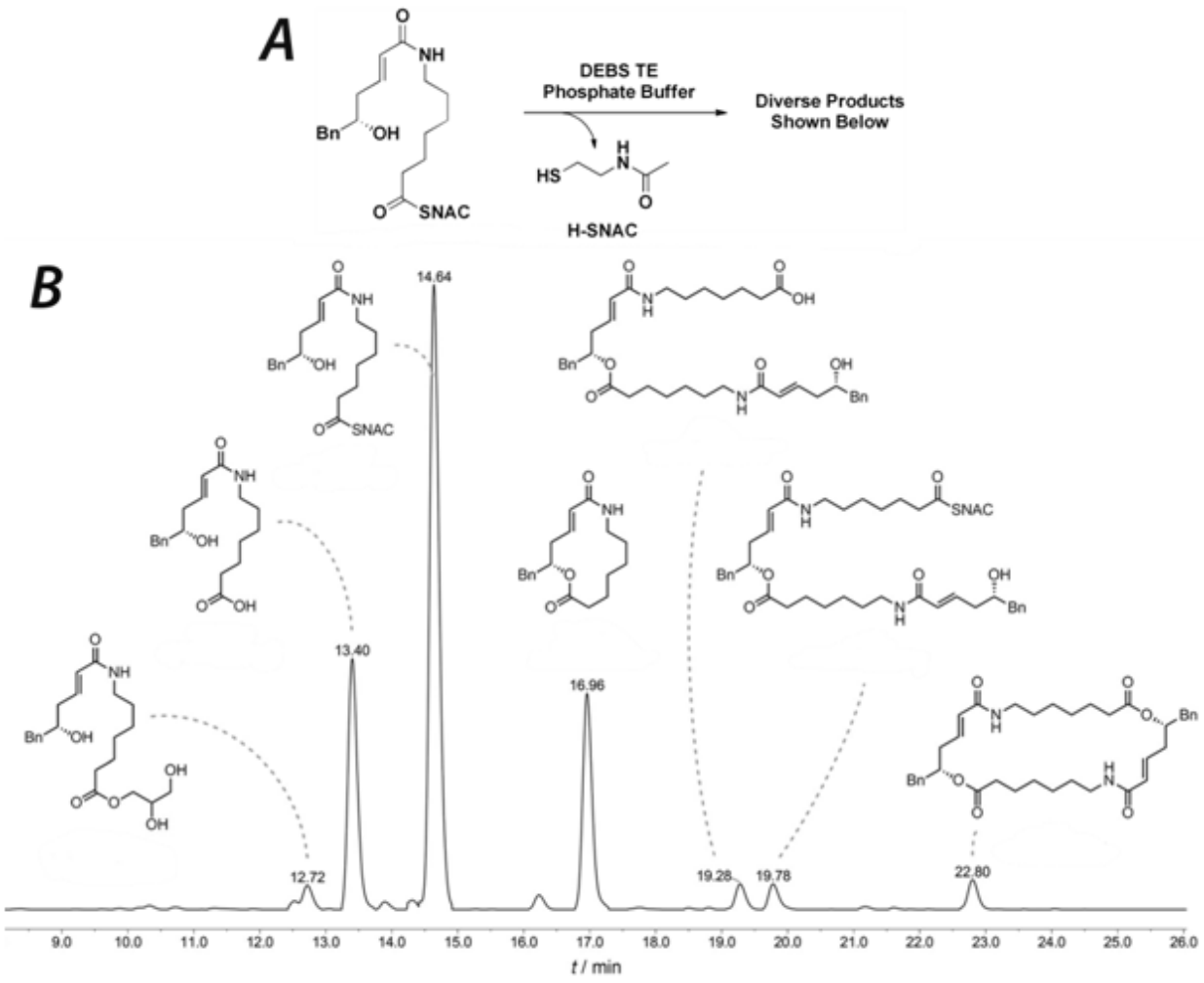

Figure 1.13 A) Overall reaction for DEBS TE acting on a non-native substrate and the products of this reaction are shown in **B)** LC analysis showing the diverse release chemistry accessible to the DEBS TE when challenged with a non-native substrate. Adapted from Hari *et al.*[75]

1.3.3 Fungal PKS TEs

While the bacterial PKS TEs are known to be quite selective, the characterized fungal PKS TEs to date have been more flexible. *In vitro* characterization of the TEs from radicicol (Rdc) and zearalenone (Zea) biosynthetic pathways has shown them to be stereotolerant with regard to the nucleophile secondary alcohol.[76] This work is described in detail in chapter 2. In addition

both the Rdc and Zea TEs are able to generate 12- to 18-member macrocycles and cyclize a depsipeptide substrate.[77] They are however unable to macrocyclize either fully saturated and α,β-unsaturated thioesters. This work is described in detail in Chapter 3.

1.4 Summary and Conclusions

The challenge of efficient macrolactonization has plagued chemists for many decades and spurred on the development and application of diverse reactions to overcome it. One avenue that has not been extensively explored is the search for a biocatalyst to affect macrolactonization. Though robust methods have been developed for evolving enzymes for a specific reaction on a particular substrate, these have not been applied to the challenge of macrocyclization. Generation of a macrocyclization biocatalyst would be a welcome addition to the chemists toolbox and the identification of a tolerant TE as a parent sequence would be required. While the tyrocidine TE is one of the most flexible to date the strict positional requirements for preorganization of the substrate in the active site limits its substrate scope. The TEs from modular PKS pathways typified by the DEBS TE are generally regio- and (dia)stereo-selective and may make good starting points if a structurally related macrocycle is the desired product. The final class of TE discussed, from fungal PKS pathways, are the most general to date and may provide springboard sequences to facilitate engineering efforts toward general catalysts. Chapters 2 and 3 focus on the *in vitro* characterization of two such fungal TEs. Chapter 4 describes the incorporation of 2,3-diaminopropionate (DAP) non-canonical amino acid as a serine mimic which will prove extremely useful in the structural characterization of enzyme bound intermediates which will lead to a better understanding of the sequence determinants of release chemistry.

1.5 References

[1] K. C. Nicolaou, E. J. Sorensen, *Classics in Total Synthesis: Targets, Strategies, Methods*, VCH, Weinheim ; New York, **1996**.
[2] K. C. Nicolaou, S. A. Snyder, E. J. Corey, *Classics in Total Synthesis. 2: More Targets, Strategies, Methods*, Wiley-VCH, Weinheim, **2003**.
[3] K. C. Nicolaou, J. S. Chen, *Classics in Total Synthesis III: Further Targets, Strategies, Methods*, Wiley-VCH, Weinheim, **2011**.
[4] D. J. Newman, G. M. Cragg, *J. Nat. Prod.* **2016**, *79*, 629–661.
[5] L. A. Wessjohann, E. Ruijter, D. Garcia-Rivera, W. Brandt, *Mol. Divers.* **2005**, *9*, 171–186.
[6] M. Tsakos, E. S. Schaffert, L. L. Clement, N. L. Villadsen, T. B. Poulsen, *Nat. Prod. Rep.* **2015**, *32*, 605–632.
[7] A. Parenty, X. Moreau, G. Niel, J.-M. Campagne, *Chem. Rev.* **2013**, *113*, PR1–PR40.
[8] R. B. Woodward, B. W. Au-Yeung, P. Balaram, L. J. Browne, D. E. Ward, B. W. Au-Yeung, P. Balaram, L. J. Browne, P. J. Card, C. H. Chen, *J. Am. Chem. Soc.* **1981**, *103*, 3213–3215.
[9] E. J. Corey, K. C. Nicolaou, *J. Am. Chem. Soc.* **1974**, *96*, 5614–5616.
[10] R. B. Woodward, E. Logusch, K. P. Nambiar, K. Sakan, D. E. Ward, B. W. Au-Yeung, P. Balaram, L. J. Browne, P. J. Card, C. H. Chen, *J. Am. Chem. Soc.* **1981**, *103*, 3210–3213.
[11] J. Inanaga, K. Hirata, H. Saeki, T. Katsuki, M. Yamaguchi, *BCSJ* **1979**, *52*, 1989–1993.
[12] M. Hikota, H. Tone, K. Horita, O. Yonemitsu, *J. Org. Chem.* **1990**, *55*, 7–9.
[13] S. Kusaka, S. Dohi, T. Doi, T. Takahashi, *Tetrahedron Letters* **2003**, *44*, 8857–8859.
[14] A. Fürstner, C. Aïssa, C. Chevrier, F. Teplý, C. Nevado, M. Tremblay, *Angew. Chem. Int. Edit.* **2006**, *45*, 5832–5837.
[15] A. Fürstner, C. Nevado, M. Tremblay, C. Chevrier, F. Teplý, C. Aïssa, M. Waser, *Angew. Chem. Int. Edit.* **2006**, *45*, 5837–5842.
[16] A. Fürstner, *Angew. Chem. Int. Edit.* **2000**, *39*, 3012–3043.
[17] C. Lecourt, S. Dhambri, L. Allievi, Y. Sanogo, N. Zeghbib, R. B. Othman, M.-I. Lannou, G. Sorin, J. Ardisson, *Nat. Prod. Rep.* **2018**, *35*, 105–124.
[18] M. Bieniek, A. Michrowska, D. L. Usanov, K. Grela, *Chem.: Eur. J.* **2008**, *14*, 806–818.
[19] C.-Y. Chou, D.-R. Hou, *J. Org. Chem.* **2006**, *71*, 9887–9890.
[20] D. Si, N. M. Sekar, K. P. Kaliappan, *Org. Biomol. Chem.* **2011**, *9*, 6988–6997.
[21] A. K. Ghosh, G. Gong, *J. Org. Chem.* **2006**, *71*, 1085–1093.
[22] H. Fuwa, T. Suzuki, H. Kubo, T. Yamori, M. Sasaki, *Chem.: Eur. J.* **2011**, *17*, 2678–2688.
[23] F. Giordanetto, J. Kihlberg, *J. Med. Chem.* **2014**, *57*, 278–295.
[24] E. M. Driggers, S. P. Hale, J. Lee, N. K. Terrett, *Nat. Rev. Drug Discov.* **2008**, *7*, 608–624.
[25] J. Levin, *Macrocycles in Drug Discovery*, Royal Society of Chemistry ; Cambridge, UK, **2014**.
[26] X. Yu, D. Sun, *Molecules* **2013**, *18*, 6230–6268.
[27] J. Mallinson, I. Collins, *Future Med. Chem.* **2012**, *4*, 1409–1438.
[28] E. Marsault, M. L. Peterson, *J. Med. Chem.* **2011**, *54*, 1961–2004.
[29] B. C. Doak, J. Zheng, D. Dobritzsch, J. Kihlberg, *J. Med. Chem.* **2016**, *59*, 2312–2327.
[30] C. A. Lipinski, *Drug Discovery Today: Technologies* **2004**, *1*, 337–341.
[31] E. A. Villar, D. Beglov, S. Chennamadhavuni, J. A. P. Jr, D. Kozakov, S. Vajda, A. Whitty, *Nat. Chem. Biol.* **2014**, *10*, 723–731.

[32] A. K. Yudin, *Chem. Sci.* **2014**, *6*, 30–49.
[33] R. Finking, M. A. Marahiel, *Annu. Rev.Microbiol.* **2004**, *58*, 453–488.
[34] J. Staunton, K. J. Weissman, *Nat. Prod. Rep.* **2001**, *18*, 380–416.
[35] N. Huguenin-Dezot, D. A. Alonzo, G. W. Heberlig, M. Mahesh, D. P. Nguyen, M. H. Dornan, C. N. Boddy, T. M. Schmeing, J. W. Chin, *Nature* **2019**, *565*, 112.
[36] S. Fan, R. Wang, C. Li, L. Bai, Y.-L. Zhao, T. Shi, *Int. J. Mol. Sci.* **2019**, *20*, 877.
[37] M. E. Horsman, T. P. A. Hari, C. N. Boddy, *Nat. Prod. Rep.* **2016**, *33*, 183–202.
[38] T. P. Korman, J. M. Crawford, J. W. Labonte, A. G. Newman, J. Wong, C. A. Townsend, S.-C. Tsai, *PNAS* **2010**, *107*, 6246–6251.
[39] T. Shi, L. Liu, W. Tao, S. Luo, S. Fan, X.-L. Wang, L. Bai, Y.-L. Zhao, *ACS Catal.* **2018**, *8*, 4323–4332.
[40] X.-P. Chen, T. Shi, X.-L. Wang, J. Wang, Q. Chen, L. Bai, Y.-L. Zhao, *ACS Catal.* **2016**, *6*, 4369–4378.
[41] N. M. Gaudelli, C. A. Townsend, *Nat. Chem. Biol.* **2014**, *10*, 251–258.
[42] J. Young, D. C. Stevens, R. Carmichael, J. Tan, S. Rachid, C. N. Boddy, R. Müller, R. E. Taylor, *J. Nat. Prod.* **2013**, *76*, 2269–2276.
[43] L. Ray, K. Yamanaka, B. S. Moore, *Angew. Chem. Int. Edit.* **2016**, *55*, 364–367.
[44] K. R. Conway, C. N. Boddy, *Nucleic Acids Res.* **2013**, *41*, D402-407.
[45] M. Wang, C. N. Boddy, *Biochemistry* **2008**, *47*, 11793–11803.
[46] P. Argyropoulos, F. Bergeret, C. Pardin, J. M. Reimer, A. Pinto, C. N. Boddy, T. M. Schmeing, *Biochim. Biophy. Acta* **2016**, *1860*, 486–497.
[47] R. J. Fox, G. W. Huisman, *Trends Biotechnol.* **2008**, *26*, 132–138.
[48] U. T. Bornscheuer, G. W. Huisman, R. J. Kazlauskas, S. Lutz, J. C. Moore, K. Robins, *Nature* **2012**, *485*, 185–194.
[49] J. Lalonde, *Curr. Opin.Biotechnol.* **2016**, *42*, 152–158.
[50] J. Liang, J. Lalonde, B. Borup, V. Mitchell, E. Mundorff, N. Trinh, D. A. Kochrekar, R. Nair Cherat, G. G. Pai, *Org. Process Res. Dev.* **2010**, *14*, 193–198.
[51] M. Zhao, A. O. King, R. D. Larsen, T. R. Verhoeven, P. J. Reider, *Tetrahedron Lett.* **1997**, *38*, 2641–2644.
[52] Y. K. Bong, S. Song, J. Nazor, M. Vogel, M. Widegren, D. Smith, S. J. Collier, R. Wilson, S. M. Palanivel, K. Narayanaswamy, et al., *J. Org. Chem.* **2018**, *83*, 7453–7458.
[53] E. P. Talsi, K. P. Bryliakov, *Catal. Today* **2017**, *279*, 84–89.
[54] P. Pitchen, H. B. Kagan, *Tetrahedron Lett.* **1984**, *25*, 1049–1052.
[55] J. Latham, E. Brandenburger, S. A. Shepherd, B. R. K. Menon, J. Micklefield, *Chem. Rev.* **2018**, *118*, 232–269.
[56] A. E. Fraley, D. H. Sherman, *Bioorg. Med. Chem. Lett.* **2018**, *28*, 1992–1999.
[57] S. K. Ma, J. Gruber, C. Davis, L. Newman, D. Gray, A. Wang, J. Grate, G. W. Huisman, R. A. Sheldon, *Green Chem.* **2010**, *12*, 81–86.
[58] G. A. Aleku, S. P. France, H. Man, J. Mangas-Sanchez, S. L. Montgomery, M. Sharma, F. Leipold, S. Hussain, G. Grogan, N. J. Turner, *Nat. Chem.* **2017**, *9*, 961–969.
[59] C. K. Savile, J. M. Janey, E. C. Mundorff, J. C. Moore, S. Tam, W. R. Jarvis, J. C. Colbeck, A. Krebber, F. J. Fleitz, J. Brands, et al., *Science* **2010**, *329*, 305–309.
[60] H. S. Toogood, N. S. Scrutton, *ACS Catal.* **2018**, *8*, 3532–3549.
[61] J. R. Donald, W. P. Unsworth, *Chem.: Eur. J.* **2017**, *23*, 8780–8799.
[62] M. Lobell, M. P. Schneider, *Tetrahedron: Asymmetry* **1993**, *4*, 1027–1030.
[63] A. Makita, T. Nihira, Y. Yamada, *Tetrahedron Lett.* **1987**, *28*, 805–808.

[64] H. Yamada, S. Ohsawa, T. Sugai, H. Ohta, S. Yoshikawa, *Chem. Lett.* **1989**, *18*, 1775–1776.
[65] Z. W. Guo, C. J. Sih, *J. Am. Chem. Soc.* **1988**, *110*, 1999–2001.
[66] S. Nanda, *Tetrahedron Lett.* **2005**, *46*, 3661–3663.
[67] C. N. Boddy, T. L. Schneider, K. Hotta, C. T. Walsh, C. Khosla, *J. Am. Chem. Soc.* **2003**, *125*, 3428–3429.
[68] J. W. Trauger, R. M. Kohli, H. D. Mootz, M. A. Marahiel, C. T. Walsh, *Nature* **2000**, *407*, 215–218.
[69] J. W. Trauger, R. M. Kohli, C. T. Walsh, *Biochemistry* **2001**, *40*, 7092–7098.
[70] R. M. Kohli, M. D. Burke, J. Tao, C. T. Walsh, *J. Am. Chem. Soc.* **2003**, *125*, 7160–7161.
[71] E. Yeh, H. Lin, S. L. Clugston, R. M. Kohli, C. T. Walsh, *Chem.Biol.* **2004**, *11*, 1573–1582.
[72] C. M. Kao, L. Katz, C. Khosla, *Science* **1994**, *265*, 509–512.
[73] B. A. Pfeifer, S. J. Admiraal, H. Gramajo, D. E. Cane, C. Khosla, *Science* **2001**, *291*, 1790–1792.
[74] A. Pinto, M. Wang, M. Horsman, C. N. Boddy, *Org. Lett.* **2012**, *14*, 2278–2281.
[75] T. P. A. Hari, P. Labana, M. Boileau, C. N. Boddy, *ChemBioChem* **2014**, *15*, 2656–2661.
[76] G. W. Heberlig, M. Wirz, M. Wang, C. N. Boddy, *Org. Lett.* **2014**, *16*, 5858–5861.
[77] G. W. Heberlig, J. T. C. Brown, R. D. Simard, M. Wirz, W. Zhang, M. Wang, L. I. Susser, M. E. Horsman, C. N. Boddy, *Org. Biomol. Chem.* **2018**, *16*, 5771–5779.

Chapter 2. Resorcyclic acid lactone biosynthesis relies on a stereotolerant macrocyclizing thioesterase

2.1 Introduction

The research presented in this chapter was born out of our desire to identify and develop a thioesterase to function as a macrocyclic lactone forming biocatalyst. Initial work was focused on the 6-deoxyerythronolide B thioesterase (DEBS TE) as it had previously shown some flexibility *in vivo* generating 6-, 8-, 12-, and 16-member macrocyclic lactones. As these substrates were generated by modifying the native pathway, all of these products possessed the natural D-configured secondary alcohol in lactone formation, limiting their chemical diversity.[1–5]

Work in the Boddy lab on thioesterases (TEs) has focused on characterizing them as stand-alone domains *in vitro*. Prior efforts in the lab on characterizing the DEBS TE using simplified substrates found that a D-configured nucleophile was also needed *in vitro* for macrocyclization activity. Surprisingly the TE was also found to be diastereoselective with regard to the alcohol at C11. The only substrate to undergo macrocyclization from this panel was the C11 D-, C13 D-configured diastereomer. The natural C11 L-,C13 D-configured substrate only hydrolyzed further muddling any simple predictive rules governing the type of release chemistry a non-native substrate would undergo.[6]

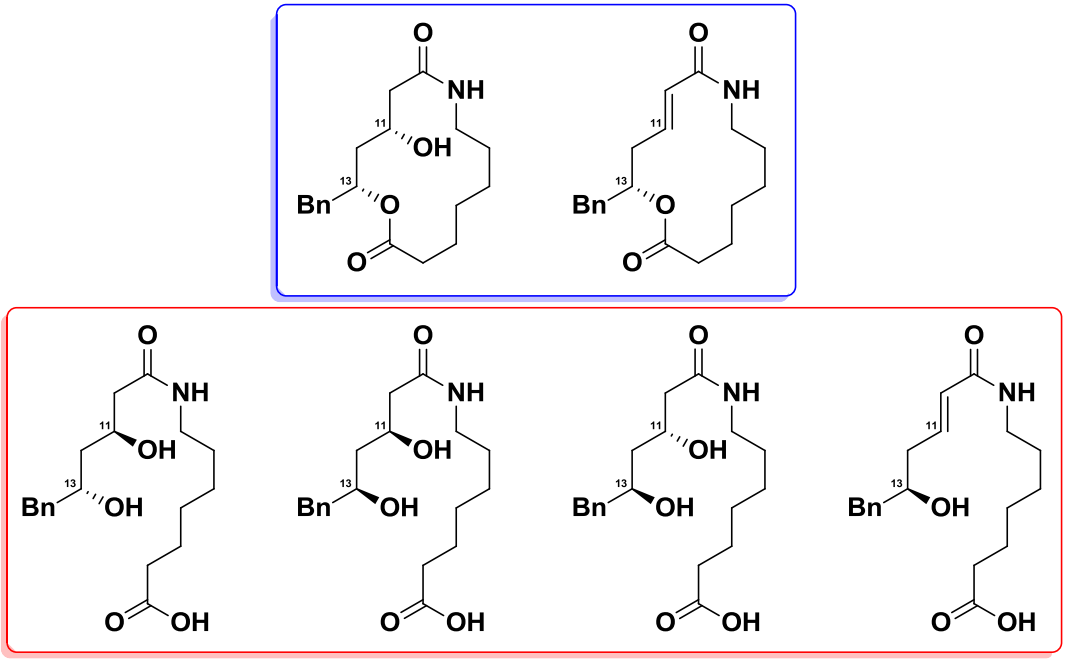

Figure 2.1 Summary of testing DEBS TE *in vitro* by Pinto et al. and Hari et al.[6,7] The compounds circled in blue were the only macrocycles generated in these studies. The compounds circled in red are the hydrolysis products of substrates that failed to cyclize.

Follow up work with two new substrates, generated by elimination (literally!) of the C11 stereocenter, further probed the offloading selectivity of the DEBS TE.[7] Similar to previous observations, only the D-configured nucleophile macrocyclized. In addition, the TE generated linear and macrocyclic dimers, hydrolysis, and glycerolysis products from this same substrate (**Fig 1.13**). Due to the highly capricious nature of *in vitro* macrocycle formation by the DEBS TE its viability as a platform for developing a more general macrolactone forming catalyst dwindled. Efforts toward this goal moved to the TEs from the fungal polyketides radicicol and zearalenone as they seemed likely to be naturally stereotolerant.[8]

2.2 References

[1] J. R. Jacobsen, C. R. Hutchinson, D. E. Cane, C. Khosla, *Science* **1997**, *277*, 367–369.

[2] C. M. Kao, G. Luo, L. Katz, D. E. Cane, C. Khosla, *J. Am. Chem. Soc.* **1995**, *117*, 9105–9106.
[3] R. McDaniel, A. Thamchaipenet, C. Gustafsson, H. Fu, M. Betlach, M. Betlach, G. Ashley, *Proc. Natl. Acad. Sci. U.S.A.* **1999**, *96*, 1846–1851.
[4] C. M. Kao, G. Luo, L. Katz, D. E. Cane, C. Khosla, *J. Am. Chem. Soc.* **1996**, *118*, 9184–9185.
[5] C. M. Kao, M. McPherson, R. N. McDaniel, H. Fu, D. E. Cane, C. Khosla, *J. Am. Chem. Soc.* **1997**, *119*, 11339–11340.
[6] A. Pinto, M. Wang, M. Horsman, C. N. Boddy, *Org. Lett.* **2012**, *14*, 2278–2281.
[7] T. P. A. Hari, P. Labana, M. Boileau, C. N. Boddy, *ChemBioChem* **2014**, *15*, 2656–2661.
[8] G. W. Heberlig, M. Wirz, M. Wang, C. N. Boddy, *Org. Lett.* **2014**, *16*, 5858–5861.

2.3 Author contributions

GWH resynthesized **8** and ***ent-8*** and synthesized all other compounds, characterized all compounds, expressed and purified the proteins, collected HPLC data, analyzed the data, and performed kinetic analysis. **M Wirz** initially synthesized compounds **8** and ***ent-8***. **M Wang** cloned the expression vectors for Rdc and Zea TEs. **GWH** and **CNB** wrote the paper with input from all authors.

Copyright

Organic LETTERS

Letter

pubs.acs.org/OrgLett

Resorcylic Acid Lactone Biosynthesis Relies on a Stereotolerant Macrocyclizing Thioesterase

Graham W. Heberlig, Monica Wirz, Meng Wang, and Christopher N. Boddy*

Department of Chemistry, Centre for Catalysis Research and Innovation, University of Ottawa, Ottawa, ON K1N 6N5, Canada

Supporting Information

ABSTRACT: Zearalenone and radicicol are highly related resorcylic acid lactones with the rare property of having opposite stereochemical configurations of the secondary alcohol involved in lactone formation. The ability of the thioesterases from the zearalenone and radicicol biosynthetic pathways to macrocyclize both D and L configured synthetic substrate analogs was biochemically characterized and showed that both enzymes were highly stereotolerant, macrocyclizing both substrates with similar kinetic parameters. This observed stereotolerance is consistent with a proposed evolution of both natural products from a common ancestral resorcylic acid lactone.

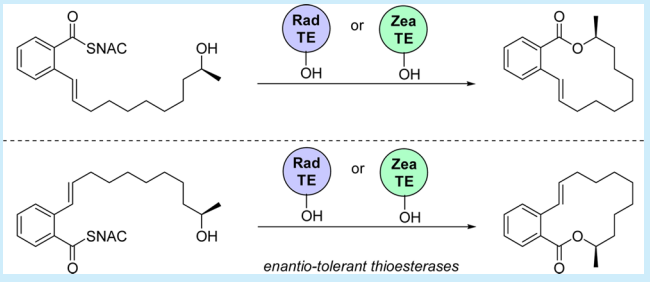

Resorcylic acid lactones (RALs) are a class of macrocyclic fungal polyketides all containing a resorcylate (2,4-dihydroxybenzoate) typically embedded into a 14-member ring lactone.[1,2] Zearalenone **1**, an estrogen receptor agonist,[3] and radicicol **2**, a HSP90 inhibitor,[4] are archetypical examples of the class (Figure 1). Unusual among closely related

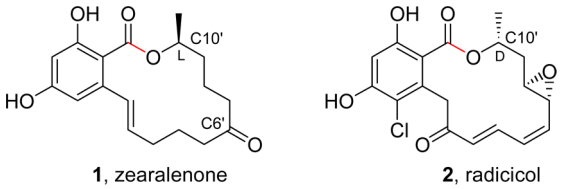

Figure 1. Fungal polyketides zearalenone **1** and radicicol **2** have the opposite configurations at C10′. Lactone bond formed by the TE is highlighted in red.

macrocyclic polyketides are the opposing configurations of the lactone alcohol group seen in zearalenone with the L (*S*) configuration and in radicicol, with the D (*R*) configuration. Apart from the RALs, this phenomenon is only observed in the mixed nonribosomal peptide-polyketide depsipeptides, the turnagainolides.[5] From a biosynthetic perspective this unusual feature provides a unique glimpse into the evolutionary process of accessing new structural features from an ancestral compound. Herein we show that the thioesterases (TEs) responsible for macrocyclizing these RALs are stereotolerant making them ideal as potential biocatalysts and showing the unique plasticity of fungal polyketide biosynthetic pathways.

RAL biosynthesis (Figure 2) is catalyzed by two iterative polyketide synthase (PKS) proteins, a highly reducing PKS (hrPKS) and a nonreducing PKS (nrPKS).[6−17] The hrPKS has a full complement of reductive domains and generates the alkyl portion of the RALs. The alcohol required for macrocyclization

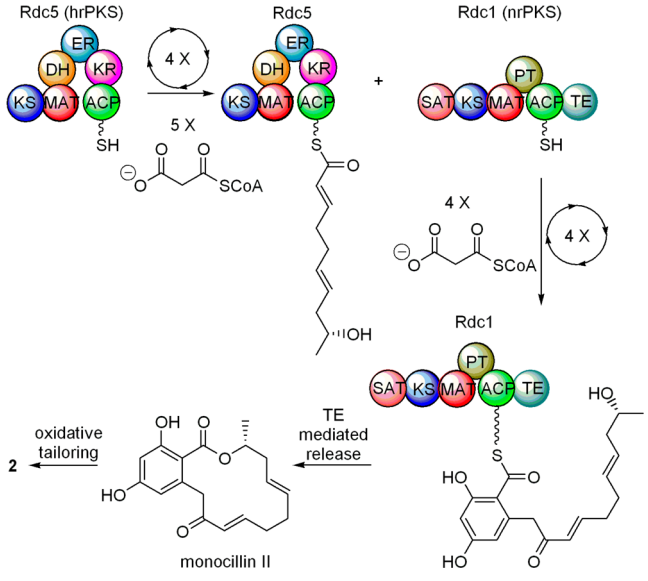

Figure 2. Biosynthesis of the polyketide precursor of radicicol, monocillin II by Rdc5 and Rdc1 is typical of RAL biosynthesis.

as well as other functional groups such as the oxygenation in **1** or the olefins in **2** are introduced by cryptic programming that enables the hrPKS to skip various reductive domains based on the length of the growing chain. The nrPKS, which lacks all reductive domains, takes the hrPKS product and adds additional malonate units generating a poly β-keto intermediate that is cyclized by a product template domain[18,19] into the resorcylate group. The completed polyketide chain is then

Received: September 17, 2014
Published: November 5, 2014

   dx.doi.org/10.1021/ol502747t | *Org. Lett.* 2014, 16, 5858−5861

released via macrocylization from the nrPKS by a thioesterase (TE) domain.[20]

The iterative nature of the hrPKS coupled with its cryptic programming enables the alkyl chains of the highly related RALs to differ substantially. For example, recent work by Vederas and Tang on the RAL pathway for hypothemycin biosynthesis shows that the ketoreductase (KR) facial selectivity for hydride delivery changes based on overall chain length.[17] This observation explains why a single KR from the hrPKS of the hypothemycin and by analogy zearalenone biosynthetic pathways can generate alcohols at C10′ and C6′ (which is ultimately oxidized to a ketone) with L and D stereochemistry, respectively. The first reduction by the hrPKS sets the chemistry at C10′, and this configuration can be inverted to that seen in radicicol by replacement of the $\beta_5\alpha_5\alpha_6$ motif in the KR active site with the sequence from the radicicol hrPKS KR. This is of particular relevance to macrocyclization as this alcohol is involved in formation of the macrolactone in these natural products.

Characterization of full length nrPKS proteins from RAL pathways suggests that the TEs embedded into these proteins are capable of macrocyclizing both L and D configured substrates.[12,14,17] *In vivo* and *in vitro* work with Hpm3, the nrPKS from hypothemycin biosynthesis, shows that both the native D and epimeric L configured macrocycles can be obtained.[14,17] Similarly *in vivo* characterization of Rdc1, the nrPKS from radicicol biosynthesis, showed that both the native D and enantiomeric L macrocycle could be generated.[12] This stereotolerant activity would be in stark contrast to their bacterial analogues[21,22] and represent unique activity for TE domains. However, as the TE has only been characterized in the context of the full length nrPKS, it is unclear if the TE is stereotolerant or stereoselective but much faster than the other steps in nrPKS substrate processing. To resolve this issue, *in vitro* biochemical characterization of isolated RAL TEs is required.

While the structural similarities between **1** and **2** indicate that the biosynthetic pathways are highly related, analysis of the entire PKS protein sequence shows that they share less than 29% identity and thus must have diverged from a common ancestor long ago. This ancient divergence is supported by the differences in gene cluster synteny.[23,24] The orientation of the PKS genes is maintained in the zearalenone and radicicol clusters; however, additional tailoring genes are inserted between the two PKS genes in the radicicol cluster. With substantial time for divergent evolution, it is reasonable to hypothesize that the TEs (47% identity) from the pathways for **1** and **2** could have specialized to macrocyclize their substrates stereoselectively. We thus expected to observe substantial kinetic stereoselectivity for the TE domains from zearalenone biosynthesis (Zea TE) and radicicol biosynthesis (Rad TE).

To examine the stereoselectivity of the Zea TE and Rad TE, we synthesized enantioenriched substrates mimicking the native linear completed polyketide intermediates. The substrates were designed to be synthetically tractable and differ only in the absolute stereochemistry of the lactone oxygen. The synthesis of these substrates is shown in Scheme 1. The key step was the use of a MacMillan diastereoselective α-chlorination[25] followed by reduction and epoxidation with inversion of configuration to generate the terminal epoxide, which could be reductively opened to deliver alcohols **3** and **4** in reasonable yield and excellent *ee* (94% *ee*, Scheme 1). This methodology represents a significant advantage over other methodologies used in the

Scheme 1. Synthesis of Eneantioenriched Substrate 8[a]

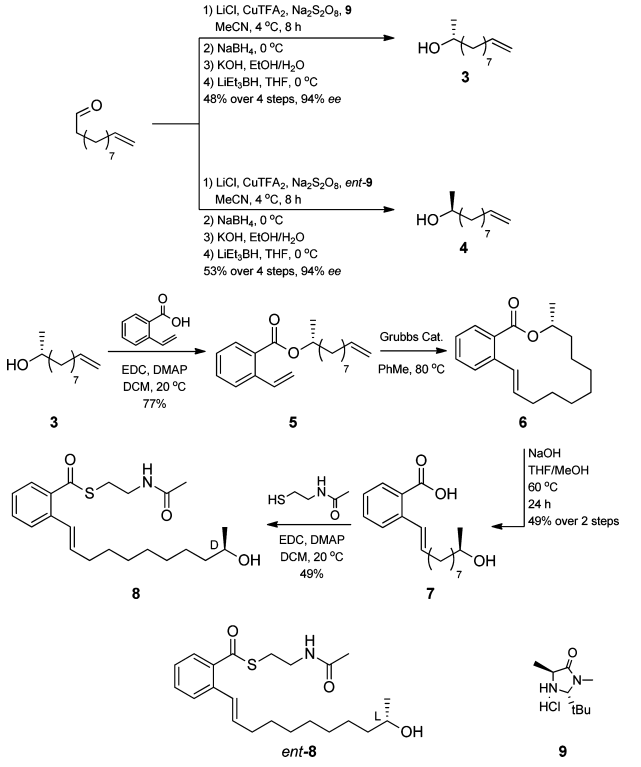

[a] *ent*-**8** was synthesized in an analogous manner from **4**, see the Supporting Information.

synthesis of RAL natural products[1,2] such as the Jacobsen hydrolytic kinetic resolution (HKR)[26] or the use of expensive asymmetric epoxides, such as enantioenriched propylene oxides.[27]

The enantioenriched alcohols were coupled to vinylbenzoic acid, which can be readily accessed from ethyl 2-bromobenzoate through a Hiyama coupling[28] and subsequent hydrolysis (see the Supporting Information). The resulting ester, **5**, was macrocyclized by treatment with Grubbs second generation metathesis catalyst. The resulting alkene containing macrocycle was found to be entirely *E*-configured (>95:5) as the *Z*-configured macrocyle is strongly disfavored due to transannular ring strain in the 14-member macrocycle. Hydrolysis followed by coupling with *N*-acetylcysteamine generates the two enantioenriched thioester substrates, **8** and *ent*-**8**. The *N*-acetylcysteamine thioester is employed to activate the carboxylate for reaction with the active site Ser of the TE and to mimic the phosphopantetheine arm of the ACP domain which delivers the linear polyketide to the TE *in vivo*.[11,21,22,29−39] While the *N*-acetyl cysteamine group does not provide the hydrogen bond interaction seen between the native phosphopantetheine arm and the TE,[40] it has been demonstrated to be effective *in vitro*.[11,21,22,29−39]

The excised Zea TE was recombinantly expressed and purified as previously described.[11] The Rad TE was generated by PCR amplification of the TE domain of *rdc1* from *Pochonia chlamydosporia*.[9] The excised Rad TE gene was cloned into an *Escherichia coli* expression vector under the control of the T7 promoter. Rad TE was overexpressed and purified by metal-affinity chromatography to high purity (>90%, see the Supporting Information).

dx.doi.org/10.1021/ol502747t | *Org. Lett.* 2014, 16, 5858−5861

Treatment of **8** and *ent*-**8** with recombinant, purified Zea TE and Rad TE showed that both TEs are stereotolerant, effectively macrocyclizing the L and D configured substrates (Figure 3). Kinetic analysis of macrocycle formation was performed by a discontinuous HPLC-based assay. TEs (5 μM except 2 μM for Rad TE with **8**) were incubated at room temperature with **8** or *ent*-**8** at concentrations between 0.1−5.0 mM in 50 mM phosphate buffer (pH 7.4) with 10% *v*/*v* DMSO. Aliquots were taken during the first 15 min of the reaction and analyzed by HPLC for macrocycle production. A standard curve based on authentic macrocycle was used to quantify production. All time points were within the linear range of initial velocities for product formation. Rad TE macrocyclized both substrates (**8**, k_{cat} = 0.180 ± 0.003 s^{-1}, K_M = 0.19 ± 0.02 mM, k_{cat}/K_M = 970 ± 180 M^{-1} s^{-1}; *ent*-**8**, k_{cat} = 0.15 ± 0.01 s^{-1}, K_M = 0.14 ± 0.03 mM, k_{cat}/K_M = 1100 ± 400 M^{-1} s^{-1}, K_i = 4.5 ± 0.9 mM). Zea TE macrocyclized both substrates at slower rates (**8**, k_{cat} = 0.088 ± 0.001 s^{-1}, K_M = 0.39 ± 0.02 mM, k_{cat}/K_M = 230 ± 70 M^{-1} s^{-1}; *ent*-**8**, k_{cat} = 0.06 ± 0.01 s^{-1}, K_M = 1.4 ± 0.6 mM, k_{cat}/K_M = 40 ± 20 M^{-1} s^{-1}). Macrocycle formation was confirmed in all cases by MS analysis. Little hydrolysis of either substrate to the seco acid was observed (Figure 3 and Figure S3), which is in agreement with our previous study of macrocyclization of a primary alcohol substrate by Zea TE.[11] In contrast *in vitro* studies of macrocyclization by bacterial PKS TEs from the picromycin[35] and epothilone C[32] pathways showed significant hydrolysis even when presented the SNAC thioester of their native substrates. Intriguingly, Rad TE generated substantial glycerol ester when incubated for prolonged periods with *ent*-**8** (Figure 3D).

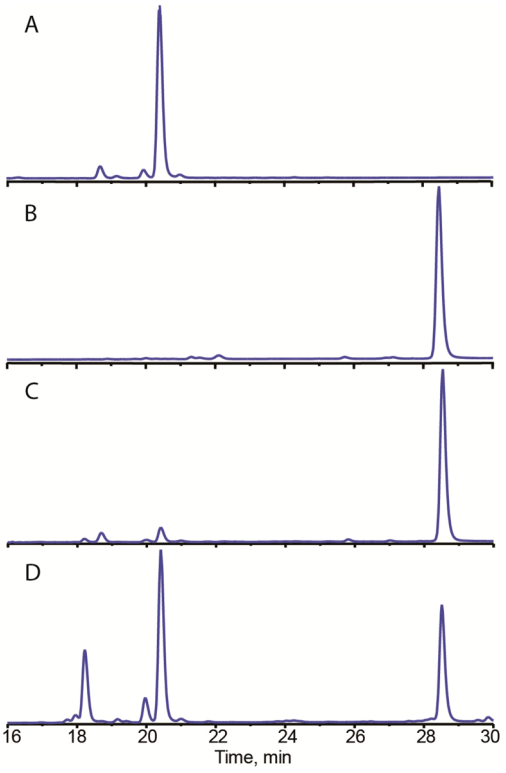

Figure 3. HPLC traces for incubations of **8** and *ent*-**8** with Rad TE. Incubations of Zea TE with substrates are in the Supporting Information. (A) No enzyme blank (5 mM **8**, 50 mM phosphate buffer pH 7.4, 24 h, rt); boiled enzyme blank showed a comparable result. (B) Racemic macrocycle, **6** (see the Supporting Information for synthesis). (C) **8** with Rad TE (5 mM **8**, 5 μM Rad TE, 50 mM phosphate buffer pH 7.4, 24 h, rt). (D) *ent*-**8** with Rad TE (5 mM *ent*-**8**, 5 μM Rad TE, 50 mM phosphate buffer, pH 7.4, 24 h, rt). The peak at 18 min is the glycerol ester of *ent*-**8**. *ent*-**8** concentration is at K_i leading to lower conversion than seen for **8**.

We also noted that with increasing concentration of the L substrate, *ent*-**8**, the rate of macrocyclization with the Rad TE decreased. Our data was modeled exceptionally well (R^2 = 0.9807) by Copeland's model for substrate inhibition (Equation S1).[41] This model assumes a second molecule of substrate binds, allosterically, to the substrate-enzyme complex. One other allosteric interaction with a polyketide TE was previously reported by Scaglione et al. in the tautomycetin pathway.[39] Unlike the Rad TE's inhibitory interaction, this study found a cooperative allosteric interaction. These findings should be interpreted with care as they are the result of *in vitro* assays with the TE removed from the context of its native pathway and treated with non-native levels of substrates.[42]

A working hypothesis in the field has been that nucleophile stereochemistry plays an important role in controlling TE-mediated macrocyclization. While this hypothesis is supported for bacterial PKS TEs,[21,22] it does not appear to hold true for fungal RAL TEs. This study provides clear *in vitro* kinetic characterization of stereotolerant PKS TEs. The relaxed substrate selectivity of these RAL TEs makes them appealing candidates for use in engineered combinatorial PKS pathways.[43] In addition, this activity warrants further study of the substrate scope of these TEs, as they may function as general macrocyclization catalysts for chemoenzymatic syntheses.

The screening hypothesis, an evolutionary model for describing the chemical diversity of natural products, predicts that there is an evolutionary cost to having high selectivity in the late stage of natural product biosynthesis.[44,45] The low stereoselectivity of RAL TEs is thus consistent with minimizing this evolutionary cost. Furthermore, by viewing the biosynthetic pathway as a series of logic gates where each enzymatic step asks a different "question" about the structure of the substrate, a stereoselective TE would be asking a redundant "question" since the stereochemistry of the nucleophilic alcohol is tightly controlled by an upstream process, the KR domain of the hrPKS. We propose that this substrate flexibility increases fitness and adaptability of the pathway as it enables the overall pathway to accommodate changes to the linear polyketide product brought about by mutations that impact the cryptic programming of the hrPKS and thus the configuration as well as steric and electronic environment of the nucleophilic alcohol. This TE stereotolerance may have facilitated the divergent evolution of the oppositely configured macrolactones from a common RAL ancestor.

In summary, we have kinetically characterized *in vitro* two fungal RAL PKS TEs for their ability to macrocyclize substrates with D and L nucleophile stereochemistry. We show that these RAL TEs are stereotolerant and macrocyclize either enantio-configured substrate with very little competing hydrolysis. This stereotolerance is in accordance with the prediction of the screening hypothesis and enables the RAL pathways to adapt to changes in the polyketide substrate due to the cryptic programming of the hrPKS. In comparison bacterial PKS TEs are highly stereoselective even though the screening hypothesis prediction should be equally true for them. Resolving the discrepancy between these two types of TEs will give much

dx.doi.org/10.1021/ol502747t | *Org. Lett.* 2014, 16, 5858−5861

needed insight into the different evolutionary pressures shaping iterative and modular PKS pathway evolution.

■ ASSOCIATED CONTENT

Supporting Information

Synthetic protocols, experimental procedure, and characterization data. This material is available free of charge via the Internet at http://pubs.acs.org.

■ AUTHOR INFORMATION

Corresponding Author

*E-mail: cboddy@uottawa.ca.

Notes

The authors declare no competing financial interest.

■ ACKNOWLEDGMENTS

This work was supported by NSERC, CFI, and the University of Ottawa. G.W.H. was supported by NSERC-CREATE

■ REFERENCES

(1) Bräse, S.; Gläser, F.; Kramer, C. S.; Lindner, S.; Linsenmeier, A. M.; Masters, K.-S.; Meister, A. C.; Ruff, B. M.; Zhong, S. *Prog. Chem. Org. Nat. Prod.* **2013**, *97* (v−xv), 1−300.
(2) Winssinger, N.; Barluenga, S. *Chem. Commun.* **2007**, 22−36.
(3) Kuiper, G. G.; Lemmen, J. G.; Carlsson, B.; Corton, J. C.; Safe, S. H.; Van der Saag, P. T.; Van der Burg, B.; Gustafsson, J. A. *Endocrinology* **1998**, *139*, 4252−63.
(4) Winssinger, N.; Fontaine, J.-G.; Barluenga, S. *Curr. Topics Med. Chem.* **2009**, *9*, 1419−35.
(5) Li, D.; Carr, G.; Zhang, Y.; Williams, D. E.; Amlani, A.; Bottriell, H.; Mui, A. L.-F.; Andersen, R. J. *J. Nat. Prod.* **2011**, *74*, 1093−9.
(6) Kim, Y.-T.; Lee, Y.-R.; Jin, J.; Han, K.-H.; Kim, H.; Kim, J.-C.; Lee, T.; Yun, S.-H.; Lee, Y.-W. *Mol. Microbiol.* **2005**, *58*, 1102−13.
(7) Gaffoor, I.; Trail, F. *Appl. Environ. Microbiol.* **2006**, *72*, 1793−9.
(8) Wang, S.; Xu, Y.; Maine, E. A.; Wijeratne, E. M. K.; Espinosa-Artiles, P.; Gunatilaka, A. A. L.; Molnár, I. *Chem. Biol.* **2008**, *15*, 1328−38.
(9) Reeves, C. D.; Hu, Z.; Reid, R.; Kealey, J. T. *Appl. Environ. Microbiol.* **2008**, *74*, 5121−9.
(10) Zhou, H.; Zhan, J.; Watanabe, K.; Xie, X.; Tang, Y. *Proc. Natl. Acad. Sci. U. S. A.* **2008**, *105*, 6249−54.
(11) Wang, M.; Zhou, H.; Wirz, M.; Tang, Y.; Boddy, C. N. *Biochemistry* **2009**, *48*, 6288−90.
(12) Zhou, H.; Qiao, K.; Gao, Z.; Vederas, J. C.; Tang, Y. *J. Biol. Chem.* **2010**, *285*, 41412−21.
(13) Zhou, H.; Qiao, K.; Gao, Z.; Meehan, M. J.; Li, J. W.-H.; Zhao, X.; Dorrestein, P. C.; Vederas, J. C.; Tang, Y. *J. Am. Chem. Soc.* **2010**, *132*, 4530−1.
(14) Gao, Z.; Wang, J.; Norquay, A. K.; Qiao, K.; Tang, Y.; Vederas, J. C. *J. Am. Chem. Soc.* **2013**, *135*, 1735−8.
(15) Xu, Y.; Zhou, T.; Zhou, Z.; Su, S.; Roberts, S. A.; Montfort, W. R.; Zeng, J.; Chen, M.; Zhang, W.; Lin, M.; Zhan, J.; Molnár, I. *Proc. Natl. Acad. Sci. U. S. A.* **2013**, *110*, 5398−403.
(16) Xu, Y.; Zhou, T.; Espinosa-Artiles, P.; Tang, Y.; Zhan, J.; Molnár, I. *ACS Chem. Biol.* **2014**, *9*, 1119−27.
(17) Zhou, H.; Gao, Z.; Qiao, K.; Wang, J.; Vederas, J. C.; Tang, Y. *Nat. Chem. Biol.* **2012**, *8*, 331−3.
(18) Crawford, J. M.; Korman, T. P.; Labonte, J. W.; Vagstad, A. L.; Hill, E. A.; Kamari-Bidkorpeh, O.; Tsai, S.-C.; Townsend, C. A. *Nature* **2009**, *461*, 1139−43.
(19) Li, Y.; Image, I. I.; Xu, W.; Image, I.; Tang, Y. *J. Biol. Chem.* **2010**, *285*, 22764−73.
(20) Cox, R. J. *Org. Biomol. Chem.* **2007**, *5*, 2010−26.
(21) Pinto, A.; Wang, M.; Horsman, M.; Boddy, C. N. *Org. Lett.* **2012**, *14*, 2278−81.
(22) Hari, T. P. A.; Boileau, M.; Labana, P.; Boddy, C. N. *ChemBioChem* **2014**, DOI: 10.1002/cbic.201402475, [Ahead of print].
(23) Campbell, M. A.; Rokas, A.; Slot, J. C. *Genome Biol. Evol.* **2012**, *4*, 289−93.
(24) Inglis, D. O.; Binkley, J.; Skrzypek, M. S.; Arnaud, M. B.; Cerqueira, G. C.; Shah, P.; Wymore, F.; Wortman, J. R.; Sherlock, G. *BMC Microbiol.* **2013**, *13*, 91.
(25) Amatore, M.; Beeson, T. D.; Brown, S. P.; MacMillan, D. W. C. *Angew. Chem., Int. Ed.* **2009**, *48*, 5121−4.
(26) Schaus, S. E.; Brandes, B. D.; Larrow, J. F.; Tokunaga, M.; Hansen, K. B.; Gould, A. E.; Furrow, M. E.; Jacobsen, E. N. *J. Am. Chem. Soc.* **2002**, *124*, 1307−15.
(27) Thirupathi, B.; Mohapatra, D. K. *RSC Adv.* **2014**, *4*, 8027.
(28) Denmark, S. E.; Butler, C. R. *Org. Lett.* **2006**, *8*, 63−6.
(29) Aggarwal, R. *J. Chem. Soc., Chem. Commun.* **1995**, 1519−1520.
(30) Gokhale, R. S.; Hunziker, D.; Cane, D. E.; Khosla, C. *Chem. Biol.* **1999**, *6*, 117−25.
(31) Lu, H.; Tsai, S.-C.; Khosla, C.; Cane, D. E. *Biochemistry* **2002**, *41*, 12590−7.
(32) Boddy, C. N.; Schneider, T. L.; Hotta, K.; Walsh, C. T.; Khosla, C. *J. Am. Chem. Soc.* **2003**, *125*, 3428−9.
(33) Beck, Z. Q.; Aldrich, C. C.; Magarvey, N. A.; Georg, G. I.; Sherman, D. H. *Biochemistry* **2005**, *44*, 13457−66.
(34) Aldrich, C. C.; Venkatraman, L.; Sherman, D. H.; Fecik, R. A. *J. Am. Chem. Soc.* **2005**, *127*, 8910−1.
(35) He, W.; Wu, J.; Khosla, C.; Cane, D. E. *Bioorg. Med. Chem. Lett.* **2006**, *16*, 391−4.
(36) Sharma, K. K.; Boddy, C. N. *Bioorg. Med. Chem. Lett.* **2007**, *17*, 3034−7.
(37) Wang, M.; Boddy, C. N. *Biochemistry* **2008**, *47*, 11793−803.
(38) Wang, M.; Opare, P.; Boddy, C. N. *Bioorg. Med. Chem. Lett.* **2009**, *19*, 1413−5.
(39) Scaglione, J. B.; Akey, D. L.; Sullivan, R.; Kittendorf, J. D.; Rath, C. M.; Kim, E.-S.; Smith, J. L.; Sherman, D. H. *Angew. Chem., Int. Ed.* **2010**, *49*, 5726−30.
(40) Liu, Y.; Zheng, T.; Bruner, S. D. *Chem. Biol.* **2011**, *18*, 1482−8.
(41) Copeland, R. A. In *Enzymes: A Practical Introduction to Structure, Mechanism, and Data Analysis*; Copeland, R. A., Ed.; Wiley-VCH, Inc.: 2000; Vol. 7, pp 109−145.
(42) Reed, M. C.; Lieb, A.; Nijhout, H. F. *BioEssays* **2010**, *32*, 422−9.
(43) Wong, F. T.; Khosla, C. *Curr. Opin. Chem. Biol.* **2012**, *16*, 117−23.
(44) Firn, R. D.; Jones, C. G. *Nat. Prod. Rep.* **2003**, *20*, 382−91.
(45) Firn, R. D.; Jones, C. G. *J. Exp. Bot.* **2009**, *60*, 719−26.

2.5 Supporting Information

This chapter uses Fischer–Rosanoff convention (D and L notation) throughout. This absolute stereochemical nomenclature defines descriptors based on the orientation of a substituent on a directional chain, such as a carbohydrate backbone or polyketide chain. Fischer-Rosanoff priorities and descriptors do not change as the polyketide intermediates are elongated and tailored, as can often be the case with the Cahn-Ingold-Prelog (CIP) priority system. The titles of the stereo-enriched substrates (**8** and *ent*-**8**) will have both the CIP IUPAC name followed by the Fischer–Rosanoff name in the supporting information.

General synthetic protocols

All reagents were purchased from Sigma-Aldrich at highest available purity and used without further purification. Solvents were purchased from Fischer. All reactions were performed with dried solvents except where noted. NMR analysis was performed on a Bruker Avance II, operating at 400 MHz for ^{1}H spectra, and 100 MHz for ^{13}C spectra. High-resolution mass spectroscopy (HR-MS) was conducted on a Micromass Q-TOF I (John L. Holmes Mass Spectroscopy Facility). HPLC-MS analysis was conducted with a Shimadzu Prominence 20A Modular HPLC using a Hypersil 3µm C18 100 mm reverse phase column coupled with an Applied Biosciences API 2000 Triple Quad in positive mode. Preparatory TLC was performed using Merck Millipore 20x20 cm silica gel 60 F_{254} plates.

Synthetic Protocols

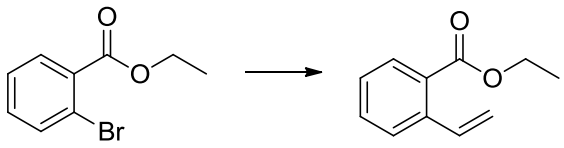

Ethyl 2-vinylbenzoate (S1). Based on procedure reported by Denmark et al[4]. To a 50 mL round bottom flask is added, under argon, 94 mg JohnPhos (0.15 mmol, 10 mol%), 42 mg palladium (II) bromide (0.15 mmol, 5 mol%), 7.0 mL tetrabutylammonium fluoride (1.0 M in THF, 7.0 mmol) , and 545 mg 2,4,6,8-tetramethyl-2,4,6,8-tetravinylcyclotetrasiloxane (1.58 mmol), and the mixture is stirred for 10 minutes. 721 mg ethyl 2-bromobenzoate (3.15 mmol) is then added and the reaction was stirred for 8 hours at 50 ˚C. At completion the reaction was cooled to room temperature and 15 mL of ether was added and the reaction stirred for an additional 15 minutes. The biphasic mixture was passed through a plug of silica gel with 100 mL additional ether, the flow through was concentrated *in vacuo* and the product was purified by column chromatography (5% EtOAc:Hex) yielding 551 mg (>99%) of the product as a slightly yellow oil. Characterization is consistent with values reported in the literature.[4] R_f = 0.35 (silica gel, 9:1 hexanes/EtOAc). ^{1}H NMR (400 MHz, $CDCl_3$) δ 7.88 (dd, *J* = 7.8, 1.4 Hz, 1H), 7.60 – 7.56 (m, 1H), 7.51 – 7.42 (m, 2H), 7.32 (td, *J* = 7.7, 1.2 Hz, 1H), 5.65 (dd, *J* = 17.5, 1.3 Hz, 1H), 5.35 (dd, *J* = 11.0, 1.3 Hz, 1H), 4.37 (q, *J* = 7.1 Hz, 2H), 1.40 (t, *J* = 7.1 Hz, 3H).

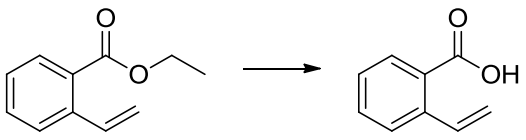

2-vinylbenzoic acid (S2). 550 mg of **S1** was dissolved in 35 mL of methanol to which was added 1.25 g of lithium hydroxide hydrate which was previously dissolved in 12 mL of water. The reaction was stirred overnight at room temperature, the reaction was quenched by the addition of 10% HCl to pH 2, and extracted (3x30 mL) with EtOAc. The combined organic extracts were washed with brine, dried over Na_2SO_4, and concentrated *in vacuo*. Yielded 437 mg (95%) of the expected product as a white solid. Characterization is consistent with values reported in the literature.[5] Rf = 0.18 (silica gel, 1:1 hexanes/ EtOAc). ^{1}H NMR (400 MHz, $CDCl_3$) δ 8.03 (dd, *J* = 7.9, 1.3 Hz, 1H), 7.64 – 7.51 (m, 3H), 7.41 – 7.33 (m, 1H), 5.68 (dd, *J* = 17.4, 1.3 Hz, 1H), 5.39 (dd, *J* = 11.0, 1.3 Hz, 1H).

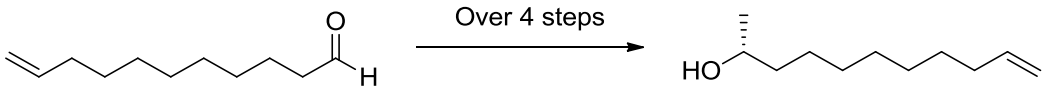

(*R*)-undec-10-en-2-ol (3). In a 100 mL round bottom flask 175 mg (2R,5S)-2-(tert-butyl)-3,5-dimethylimidazolidin-4-one hydrochloride (0.85 mmol, 20 mol%), 270 mg lithium chloride (6.37 mmol), 612 mg copper(II) trifluoroacetate (2.11 mmol), and 1.06g sodium persulfate (4.46 mmol) was combined in 34 mL acetonitrile and 180 μL water and cooled to 4 ˚C. After stirring for 10 minutes 750 mg of undecylenic aldehyde (4.46 mmol) was added and the mixture stirred for 8 hours. After 4 hours the reaction was supplemented with an additional 0.5 eq of lithium chloride and sodium persulfate. After 8 hours the reaction was cooled to 0 ˚C on ice and 400 mg of sodium borohydride (10.6 mmol) was added and continued stirring for 10 minutes after which the reaction was warmed to room temperature. After reaching room temperature 16.5 mL of aq. KOH in EtOH (25g KOH dissolved in 50 mL water, added to 24 mL EtOH) was added to the reaction mixture and stirred for an additional 30 minutes, generating the intermediate epoxide.

The reaction was then diluted with 90 mL water and extracted (3x100 mL) diethyl ether. The combined organic extracts were dried over Na_2SO_4 and carefully concentrated *in vacuo*, flash chromatography (5% EtOAc:Hex) was used to remove bulk impurities. Approximately 600 mg of partially purified epoxide product was dissolved in 35 mL THF and added to a dried 100 mL round bottom and chilled to 0 ˚C on ice. To this 17.83 mL of "Super Hydride" ($LiEt_3BH$) (1.0M in THF, 5eq) was slowly added and the reaction allowed to stir for 1 hour at 0 ˚C. After 1 hour the reaction was quenched by ***slow*** addition of 18 mL of water. This was extracted (3x25 mL) with DCM, the combined organic extracts were combined, dried over Na_2SO_4, and concentrated *in vacuo*. Purified by column chromatography 40% EtOAc:Hex yielding 369 mg (48%) of product as a colorless oil. Characterization is consistent with values reported in the literature.[6] R_f = 0.35 (silica gel, 4:1 hexanes/EtOAc). ^{1}H NMR (400 MHz, $CDCl_3$) δ 5.79 (ddt, *J* = 16.9, 10.1, 6.7 Hz, 1H), 4.97 (ddd, *J* = 17.1, 3.6, 1.6 Hz, 1H), 4.93 – 4.88 (m, 1H), 3.82 – 3.72 (m, 1H), 2.02 (dd, *J* = 14.3, 6.8 Hz, 2H), 1.44 – 1.26 (m, 14H), 1.17 (d, *J* = 6.2 Hz, 3H).

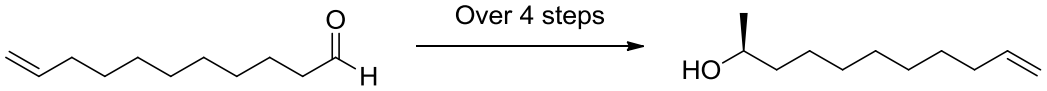

(*S*)-undec-10-en-2-ol (4). As described above for **3**, with the following exception: (2S,5R)-2-(tert-butyl)-3,5-dimethylimidazolidin-4-one hydrochloride is used as the catalyst. Yielded 404 mg (53%) as a colorless oil. Characterization is consistent with values reported in the literature.[6] R_f = 0.35 (silica gel, 4:1 hexanes/EtOAc). ^{1}H NMR (400 MHz, $CDCl_3$) δ 5.79 (ddt, *J* = 16.9,

10.1, 6.7 Hz, 1H), 4.97 (ddd, *J* = 17.1, 3.6, 1.6 Hz, 1H), 4.93 – 4.88 (m, 1H), 3.82 – 3.72 (m, 1H), 2.02 (dd, *J* = 14.3, 6.8 Hz, 2H), 1.44 – 1.26 (m, 14H), 1.17 (d, *J* = 6.2 Hz, 3H).

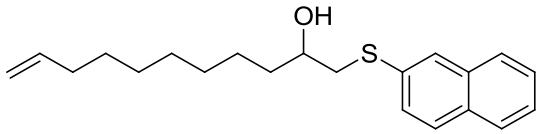

Analysis of enantiopurity. To determine the level of stereo control approximately 5 mg (0.03 mmol) of the partially purified epoxide intermediate was added to 5 mg 2-naphthalenethiol (0.031 mmol) and 3.75 mg triethylamine (0.037 mmol) in 200 μL methanol cooled to 0 ˚C on ice. The resulting mixture was stirred at room temp for 16 hours, the reaction was concentrated *in vacuo* and purified by preparatory TLC (1:4 EtOAc:Hexanes), the UV active band was removed and eluted with EtOAc. Stereochemical purity was determined by analyzing the UV active band by chiral HPLC, using a Chiracel OD-H column with isocratic mobile phase (5% isopropanol/Hexanes) at 1 mL/min; detection at 220 and 254nm. 94%*ee* for **3** and **4** determined by area under curve. ^{1}H NMR (300 MHz, $CDCl_3$) δ 7.86 – 7.74 (m, 4H), 7.54 – 7.43 (m, 3H), 5.81 (ddt, *J* = 16.9, 10.2, 6.7 Hz, 1H), 5.05 – 4.90 (m, 2H), 3.80 – 3.67 (m, 1H), 3.27 (dd, *J* = 13.7, 3.4 Hz, 1H), 2.95 (dd, *J* = 13.7, 8.7 Hz, 1H), 2.09 – 1.98 (m, 3H), 1.59 – 1.27 (m, 12H). See **Supplementary Figure 1** for traces.

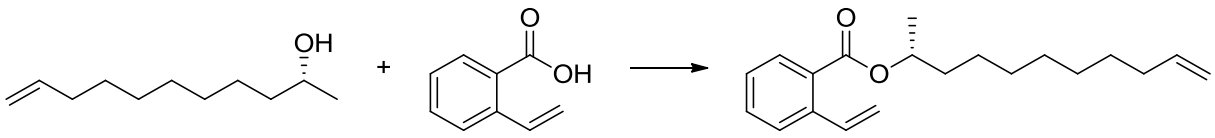

(*R*)-undec-10-en-2-yl 2-vinylbenzoate (5). In a 10 mL round bottom flask charged with 5 mL dry DCM was added 150 mg **3** (0.88 mmol), 196 mg 2-vinylbenzoic acid (1.36 mmol), 253 mg

1-Ethyl-3-(3-dimethylaminopropyl)carbodiimide (EDC) (1.32 mmol), and 161 mg 4-(Dimethylamino)pyridine (DMAP) (1.32 mmol). The reaction was stirred under N_2 overnight, the reaction was then quenched by the addition of 5 mL sat. aq. NH_4Cl, extracted (3x15 mL) DCM, the combined organic extracts were dried over Na_2SO_4 and concentrated *in vacuo*. Purification by column chromatography 10% EtOAc:Hexanes, yielded 203 mg product as colorless oil (81%). R_f = 0.52 (silica gel, 9:1 Hexanes:EtOAc). IR (NaCl) νmax = 2926, 2855, 1726, 1245, 1126 cm^{-1}; ^1H NMR (400 MHz, $CDCl_3$) δ 7.83 (d, *J* = 7.7 Hz, 1H), 7.56 (d, *J* = 7.3 Hz, 1H), 7.48 – 7.39 (m, 2H), 7.30 (t, *J* = 7.7 Hz, 1H), 5.78 (dq, *J* = 10.2, 6.6 Hz, 1H), 5.62 (d, *J* = 17.4 Hz, 1H), 5.32 (d, *J* = 11.0 Hz, 1H), 5.13 (dd, *J* = 12.8, 6.3 Hz, 1H), 4.96 (d, *J* = 17.1 Hz, 1H), 4.90 (d, *J* = 10.8 Hz, 1H), 2.01 (dd, *J* = 14.0, 7.1 Hz, 2H), 1.77– 1.25 (m, 15H). ^{13}C NMR (100 MHz, $CDCl_3$) δ 167.12, 139.37, 139.18, 135.97, 131.80, 130.06, 129.54, 127.35, 127.14, 116.20, 114.16, 71.94, 36.03, 33.78, 29.43, 29.37, 29.03, 28.89, 25.46, 20.05. HRMS (+ESI) Calculated for $C_{20}H_{28}O_2Na$ (M) 323.1987, observed 323.1985.

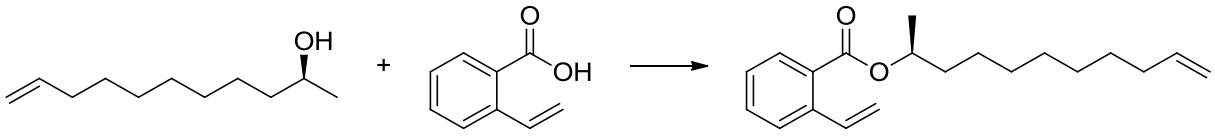

(*S*)-undec-10-en-2-yl 2-vinylbenzoate (*ent*-5). As described above for **5.** Yielded 177 mg product as a colorless oil (71%). %). R_f = 0.52 (silica gel, 9:1 Hexanes:EtOAc). IR (NaCl) νmax = 2926, 2855, 1726, 1245, 1126 cm^{-1}; ^1H NMR (400 MHz, $CDCl_3$) δ 7.83 (d, *J* = 7.7 Hz, 1H), 7.56 (d, *J* = 7.3 Hz, 1H), 7.48 – 7.39 (m, 2H), 7.30 (t, *J* = 7.7 Hz, 1H), 5.78 (dq, *J* = 10.2, 6.6 Hz, 1H), 5.62 (d, *J* = 17.4 Hz, 1H), 5.32 (d, *J* = 11.0 Hz, 1H), 5.13 (dd, *J* = 12.8, 6.3 Hz, 1H), 4.96 (d, *J* = 17.1 Hz, 1H), 4.90 (d, *J* = 10.8 Hz, 1H), 2.01 (dd, *J* = 14.0, 7.1 Hz, 2H), 1.80 – 1.25 (m,

15H). ^{13}C NMR (100 MHz, $CDCl_3$) δ 167.12, 139.37, 139.18, 135.97, 131.80, 130.06, 129.54, 127.35, 127.14, 116.20, 114.16, 71.94, 36.03, 33.78, 29.43, 29.37, 29.03, 28.89, 25.46, 20.05. HRMS (+ESI) Calculated for $C_{20}H_{28}O_2Na$ 323.1987 M, observed 323.2044.

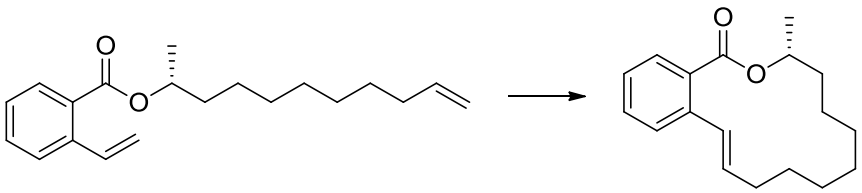

(*R*,E)-3-methyl-3,4,5,6,7,8,9,10-octahydro-1H-benzo[c]-1-oxacyclotetradecin-1-one (6). 120 mg **5** (0.40 mmol) was dissolved in 100 mL dry toluene and placed in a flame dried 250 mL round bottom flask equipped with a stir bar. 17 mg of Grubbs 2nd Generation catalyst (0.02 mmol, 5 mol%) was added with stirring and the reaction was heated to 80 ˚C and continued stirring for 24 hours under an N_2 atmosphere. At completion the reaction was concentrated *in vacuo* and partially purified by column chromatography (silica, 9:1 Hexanes:EtOAc). Yields 203 mg product as colorless oil. As the R_f of the product and the starting material were so similar the product was isolated as a mix with the starting material. This mixture was taken without further purification into the next step. R_f = 0.49 (silica gel, 9:1 Hexanes:EtOAc). ^{1}H NMR (400 MHz, CDCl3) δ 7.80 (dd, *J* = 7.8, 1.3 Hz, 1H), 7.52 – 7.46 (m, 1H), 7.41 (td, *J* = 7.7, 1.2 Hz, 1H), 7.30 – 7.24 (m, 1H), 7.00 (d, *J* = 15.7 Hz, 1H), 5.91 (dt, *J* = 15.6, 7.2 Hz, 1H), 5.22 (dt, *J* = 12.2, 6.1 Hz, 1H), 2.30 (td, *J* = 7.1, 1.3 Hz, 2H), 1.71 – 1.65 (m, 2H), 1.53 (dt, *J* = 10.3, 5.1 Hz, 2H), 1.39 – 1.26 (m, 11H). ^{13}C NMR (100 MHz, $CDCl_3$) δ 168.83, 138.14, 133.72, 131.40, 130.18, 130.13, 130.04, 127.30, 126.63, 72.37, 34.61, 30.70, 26.90, 26.51, 23.97, 23.83, 21.75, 20.13

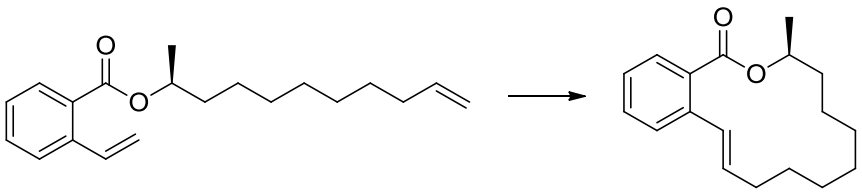

(*S*,E)-3-methyl-3,4,5,6,7,8,9,10-octahydro-1H-benzo[c]-1-oxacyclotetradecin-1-one (*ent*-6). As described above for **6**. Yielded 177 mg of product as a colorless oil. R_f = 0.49 (silica gel, 9:1 Hexanes:EtOAc). ^{1}H NMR (400 MHz, CDCl3) δ 7.80 (dd, *J* = 7.8, 1.3 Hz, 1H), 7.52 – 7.46 (m, 1H), 7.41 (td, *J* = 7.7, 1.2 Hz, 1H), 7.30 – 7.24 (m, 1H), 7.00 (d, *J* = 15.7 Hz, 1H), 5.91 (dt, *J* = 15.6, 7.2 Hz, 1H), 5.22 (dt, *J* = 12.2, 6.1 Hz, 1H), 2.30 (td, *J* = 7.1, 1.3 Hz, 2H), 1.71 – 1.65 (m, 2H), 1.53 (dt, *J* = 10.3, 5.1 Hz, 2H), 1.39 – 1.26 (m, 11H). ^{13}C NMR (100 MHz, $CDCl_3$) δ 168.83, 138.14, 133.72, 131.40, 130.18, 130.13, 130.04, 127.30, 126.63, 72.37, 34.61, 30.70, 26.90, 26.51, 23.97, 23.83, 21.75, 20.13

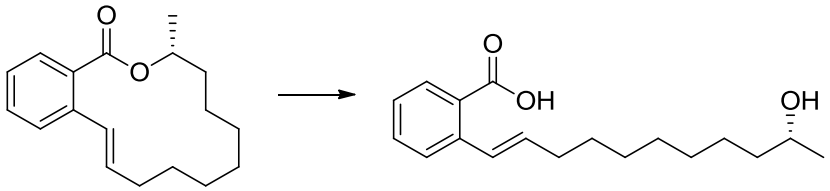

(*R*,E)-2-(10-hydroxyundec-1-en-1-yl)benzoic acid (7). 80 mg of **6** was dissolved in 1 mL of THF and to this was added 176 mg NaOH (15eq.) that was previously dissolved in 1 mL of water forming a biphasic system. Methanol and THF were added drop wise until a homogeneous solution was obtained, this was refluxed at 76 ˚C for 12 hours. The reaction was quenched by the addition of 1M HCl to a pH of 2. This was extracted (3x10 mL) with EtOAc, the combined organic extracts were dried over Na_2SO_4 and concentrated *in vacuo*. The residue was purified by column chromatography 1:3 EtOAc:Hexanes supplemented with a drop of glacial acetic acid per 250 mL of running solvent. Yielded 55 mg product as a colorless oil (47% over two steps). R_f =

0.55 (1:1 EtOAc:Hexanes). IR (NaCl) νmax = 3372 (br), 2920, 2855, 1707, 1249, 1090 cm^{-1}; ^{1}H NMR (400 MHz, $CDCl_3$) δ 7.93 (dd, *J* = 7.8, 1.0 Hz, 1H), 7.51 (d, *J* = 6.5 Hz, 1H), 7.47 – 7.42 (m, 1H), 7.27 (dd, *J* = 11.0, 4.5 Hz, 1H), 7.18 (d, *J* = 15.7 Hz, 1H), 6.06 (dt, *J* = 15.7, 7.0 Hz, 1H), 3.84 (dd, *J* = 11.6, 5.4 Hz, 1H), 2.24 (qd, *J* = 6.9, 1.4 Hz, 2H), 1.50 – 1.30 (m, 12H), 1.19 (d, *J* = 6.2 Hz, 3H). ^{13}C NMR (100 MHz, $CDCl_3$) δ 171.21, 140.41, 134.15, 132.50, 130.94, 129.11, 127.57, 127.37, 126.53, 68.54, 39.01, 32.69, 29.39, 29.01, 28.67, 28.33, 25.35, 23.51. HRMS (-ESI) Calculated for $C_{18}H_{25}O_3$ 289.1804, found 289.1808.

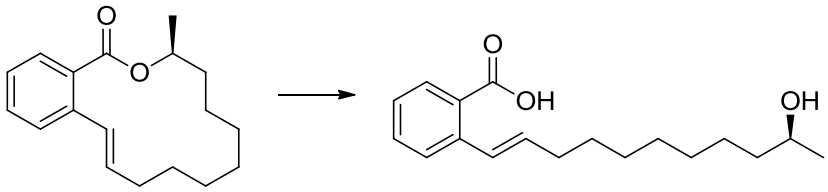

(*S*,E)-2-(10-hydroxyundec-1-en-1-yl)benzoic acid (*ent*-7). Prepared as for **7** starting with 40 mg of **ent-6** (0.147 mmol) and 88 mg of NaOH, dissolved in 700 μL THF. Yielded 26 mg of product as a colorless oil (23% over two steps). R_f = 0.55 (1:1 EtOAc:Hexanes). IR (NaCl) νmax = 3372 (br), 2920, 2855, 1707, 1249, 1090 cm^{-1}; ^{1}H NMR (400 MHz, $CDCl_3$) δ 7.93 (dd, *J* = 7.8, 1.0 Hz, 1H), 7.51 (d, *J* = 6.5 Hz, 1H), 7.47 – 7.42 (m, 1H), 7.27 (dd, *J* = 11.0, 4.5 Hz, 1H), 7.18 (d, *J* = 15.7 Hz, 1H), 6.06 (dt, *J* = 15.7, 7.0 Hz, 1H), 3.84 (dd, *J* = 11.6, 5.4 Hz, 1H), 2.24 (qd, *J* = 6.9, 1.4 Hz, 2H), 1.50 – 1.30 (m, 12H), 1.19 (d, *J* = 6.2 Hz, 3H). ^{13}C NMR (100 MHz, $CDCl_3$) δ 171.21, 140.41, 134.15, 132.50, 130.94, 129.11, 127.57, 127.37, 126.53, 68.54, 39.01, 32.69, 29.39, 29.01, 28.67, 28.33, 25.35, 23.51. HRMS (-ESI) Calculated for $C_{18}H_{25}O_3$ 289.1804, found 289.1813.

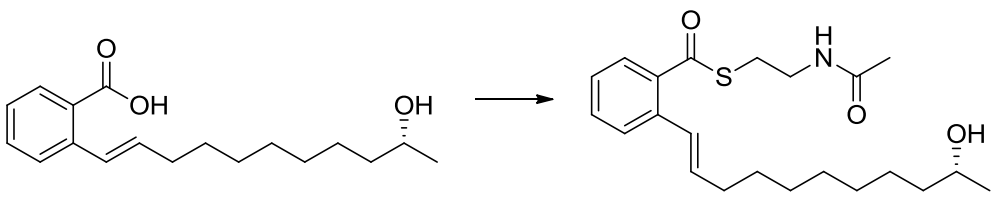

(*R*,E)-S-(2-acetamidoethyl) 2-(10-hydroxyundec-1-en-1-yl)benzothioate (8). **D-(E)-S-(2-acetamidoethyl) 2-(10-hydroxyundec-1-en-1-yl)benzothioate.** 46 mg of **7** (0.158 mmol) was dissolved in 400 μL DCM in a 2 mL round bottom flask equipped with a stir bar. 24.5 mg *N*-acetylcysteamine (22 μL, 0.206 mmol) and 39.5 mg EDC (0.206 mmol). The reaction was stirred at room temperature for 4 hours. The reaction was quenched with the addition of 0.5 mL of sat. aq. NH_4Cl and extracted with 3x2 mL portions of DCM. The combined organic extracts were dried over Na_2SO_4 and concentrated *in vacuo*. The compound was purified by preparatory TLC (40% Acetone:Hexanes), the product band was cut and eluted into a clean vial using DCM and acetone. Yielded the expected product as colorless oil, 30 mg (49%). R_f = 0.19, 2:3 Acetone:Hexanes; ^{1}H NMR (400 MHz, $CDCl_3$) δ 7.70 (dd, *J* = 7.8, 1.1 Hz, 1H), 7.54 (d, *J* = 7.6 Hz, 1H), 7.43 (dd, *J* = 10.9, 4.3 Hz, 1H), 7.28 – 7.21 (m, 1H), 6.76 (d, *J* = 15.7 Hz, 1H), 6.16 (dt, *J* = 15.7, 7.0 Hz, 1H), 6.06 (s, 1H), 3.77 (dt, *J* = 12.5, 6.2 Hz, 1H), 3.52 (dd, *J* = 12.4, 6.3 Hz, 2H), 3.18 (t, *J* = 6.5 Hz, 2H), 2.24 – 2.15 (m, 2H), 1.97 (s, 3H), 1.48 – 1.28 (m, 12H), 1.17 (d, *J* = 6.2 Hz, 3H). ^{13}C NMR (100 MHz, $CDCl_3$) δ 194.81, 170.38, 136.66, 135.74, 134.85, 131.98, 128.44, 127.15, 126.99, 126.64, 68.17, 39.78, 39.36, 33.12, 29.56, 29.36, 29.30, 29.06, 28.99, 25.70, 23.51, 23.23. Low Resolution Mass Spectroscopy (LRMS) (+ESI) found 392.3 (M); HRMS (+ESI) calculated for $C_{22}H_{33}NO_3SNa$ 414.2079, found 414.2047. HPLC retention time: 20.45min using method described below.

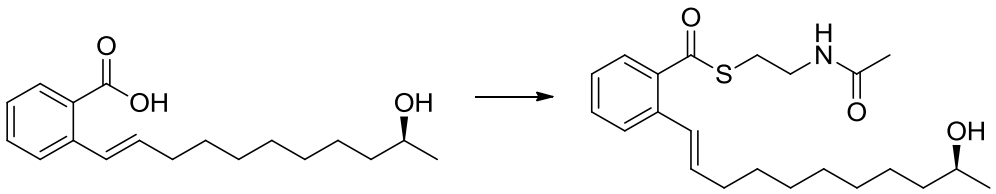

(*S*,E)-S-(2-acetamidoethyl) 2-(10-hydroxyundec-1-en-1-yl)benzothioate (*ent*-8). L-(E)-S-(2-acetamidoethyl) 2-(10-hydroxyundec-1-en-1-yl)benzothioate. Prepared as described above for **8** starting with 15 mg of *ent*-**7** (0.052 mmol) dissolved in 150 μL of DCM and combined with 8 mg *N*-acetylcysteamine (7.1 μL, 0.067 mmol) and 13 mg EDC (0.067 mmol) in a 2 mL pear-shape flask fitted with a stir bar. Yielded product as a colorless oil, 9 mg (44%). R_f = 0.19, 2:3 Acetone:Hexanes; ^{1}H NMR (400 MHz, $CDCl_3$) δ 7.70 (dd, *J* = 7.8, 1.1 Hz, 1H), 7.54 (d, *J* = 7.6 Hz, 1H), 7.43 (dd, *J* = 10.9, 4.3 Hz, 1H), 7.28 – 7.21 (m, 1H), 6.76 (d, *J* = 15.7 Hz, 1H), 6.16 (dt, *J* = 15.7, 7.0 Hz, 1H), 6.06 (s, 1H), 3.77 (dt, *J* = 12.5, 6.2 Hz, 1H), 3.52 (dd, *J* = 12.4, 6.3 Hz, 2H), 3.18 (t, *J* = 6.5 Hz, 2H), 2.24 – 2.15 (m, 2H), 1.97 (s, 3H), 1.48 – 1.28 (m, 12H), 1.17 (d, *J* = 6.2 Hz, 3H). ^{13}C NMR (100 MHz, $CDCl_3$) δ 194.81, 170.38, 136.66, 135.74, 134.85, 131.98, 128.44, 127.15, 126.99, 126.64, 68.17, 39.78, 39.36, 33.12, 29.56, 29.36, 29.30, 29.06, 28.99, 25.70, 23.51, 23.23. LRMS (+ESI) found 392.3 HRMS (+ESI) calculated for $C_{22}H_{33}NO_3SNa$ 414.2079, found 414.2101. HPLC retention time: 20.45min using method described below.

Racemic Macrocycle Synthesis

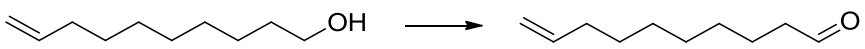

Dec-9-enal (S3). To a dry 100 mL round bottom charged with 35 mL dry DCM was added 1.0g 9-decenol (6.4 mmol) and 3.45g pyridinium chlorochromate (PCC) (16.0 mmol, 2.5eq) and an equal mass of silica gel. The mixture was stirred for 3hours after which the reaction was

concentrated *in vacuo* and the resulting black power was applied directly to the top of silica gel column and was purified with 95:5 Hexanes:EtOAc. Yielded 945 mg of the title compound as a colorless oil (96%). Characterization was consistent with reported values in the literature.[7] R_f=0.55 (EtOAc:Hexanes 1:4) ^{1}H NMR (400 MHz, $CDCl_3$) δ 9.76 (t, *J* = 1.9 Hz, 1H), 5.80 (ddt, *J* = 17.0, 10.2, 6.7 Hz, 1H), 4.99 (ddd, *J* = 17.1, 3.6, 1.6 Hz, 1H), 4.96 – 4.91 (m, 1H), 2.42 (td, *J* = 7.4, 1.9 Hz, 2H), 2.04 (dd, *J* = 14.2, 6.9 Hz, 2H), 1.62 (dd, *J* = 14.6, 7.3 Hz, 2H), 1.41 – 1.30 (m, 8H). ^{13}C NMR (101 MHz, $CDCl_3$) δ 202.90, 139.08, 114.24, 43.91, 33.74, 29.19, 29.11, 28.88, 28.82, 22.06.

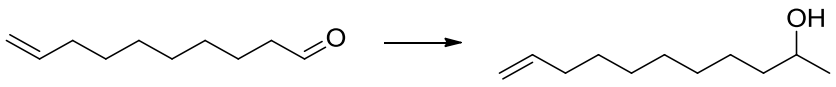

Undec-10-en-2-ol (S4). A 50 mL flame dried round bottom was charged with 13 mL dry ether and a stir bar. This was cooled to -78 ˚C (dry ice/acetone) and 2.16 mL of a 1.5M methyllithium (MeLi) solution (3.24 mmol, 1 eq) was added and stirred for several minutes. With stirring, 500 mg of **S3** (3.24 mmol) was added dropwise, after full addition the reaction was allowed to slowly warm to room temperature, and was quenched with 10 mL 10% HCl. The reaction mixture was extracted 3x10 mL with ether, the combined organic extracts were dried over Na_2SO_4 and concentrated *in vacuo*, then the tile compound was purified using column chromatography (2:3 EtOAc:Hexanes) yielding 390 mg product as a colorless oil (77%). Characterization was consistent with **3** and **4**. R_f = 0.35 (silica gel, 4:1 hexanes/EtOAc). ^{1}H NMR (400 MHz, $CDCl_3$) δ 5.79 (ddt, *J* = 16.9, 10.1, 6.7 Hz, 1H), 4.97 (ddd, *J* = 17.1, 3.6, 1.6 Hz, 1H), 4.93 – 4.88 (m, 1H), 3.82 – 3.72 (m, 1H), 2.02 (dd, *J* = 14.3, 6.8 Hz, 2H), 1.44 – 1.26 (m, 14H), 1.17 (d, *J* = 6.2 Hz, 3H).

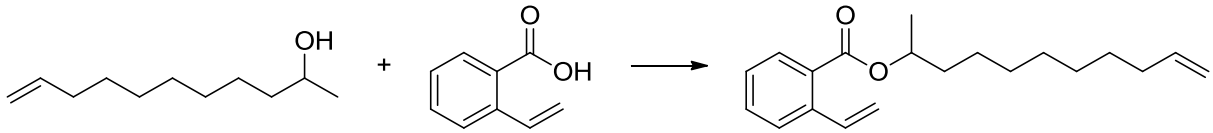

Undec-10-en-2-yl 2-vinylbenzoate (*racemic*-5). As described above for **5**, yielded 175 mg of the title compound as a colorless oil (66%). Characterization was consistent with **5**. R_f = 0.52 (silica gel, 9:1 Hexanes:EtOAc). ^{1}H NMR (400 MHz, $CDCl_3$) δ 7.83 (d, *J* = 7.7 Hz, 1H), 7.56 (d, *J* = 7.3 Hz, 1H), 7.48 – 7.39 (m, 2H), 7.30 (t, *J* = 7.7 Hz, 1H), 5.78 (dq, *J* = 10.2, 6.6 Hz, 1H), 5.62 (d, *J* = 17.4 Hz, 1H), 5.32 (d, *J* = 11.0 Hz, 1H), 5.13 (dd, *J* = 12.8, 6.3 Hz, 1H), 4.96 (d, *J* = 17.1 Hz, 1H), 4.90 (d, *J* = 10.8 Hz, 1H), 2.01 (dd, *J* = 14.0, 7.1 Hz, 2H), 1.77– 1.25 (m, 15H).

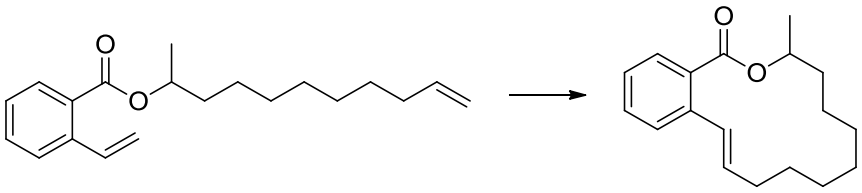

(E)-3-methyl-3,4,5,6,7,8,9,10-octahydro-1H-benzo[c]-1-oxacyclotetradecin-1-one (*racemic*-6). As described above for **6**. Starting with 160 mg **racemic 5** (0.533 mmol), and 22.6 mg Grubbs 2nd Gen catalyst (0.027, 5mol%) in 133 mL dry toluene. yielded 24 mg product as a colorless oil (17%). Characterization is consistent with **6**. R_f = 0.49 (silica gel, 9:1 Hexanes:EtOAc). ^{1}H NMR (400 MHz, CDCl3) δ 7.80 (dd, *J* = 7.8, 1.3 Hz, 1H), 7.52 – 7.46 (m, 1H), 7.41 (td, *J* = 7.7, 1.2 Hz, 1H), 7.30 – 7.24 (m, 1H), 7.00 (d, *J* = 15.7 Hz, 1H), 5.91 (dt, *J* = 15.6, 7.2 Hz, 1H), 5.22 (dt, *J* = 12.2, 6.1 Hz, 1H), 2.30 (td, *J* = 7.1, 1.3 Hz, 2H), 1.71 – 1.65 (m, 2H), 1.53 (dt, *J* = 10.3, 5.1 Hz, 2H), 1.39 – 1.26 (m, 11H).

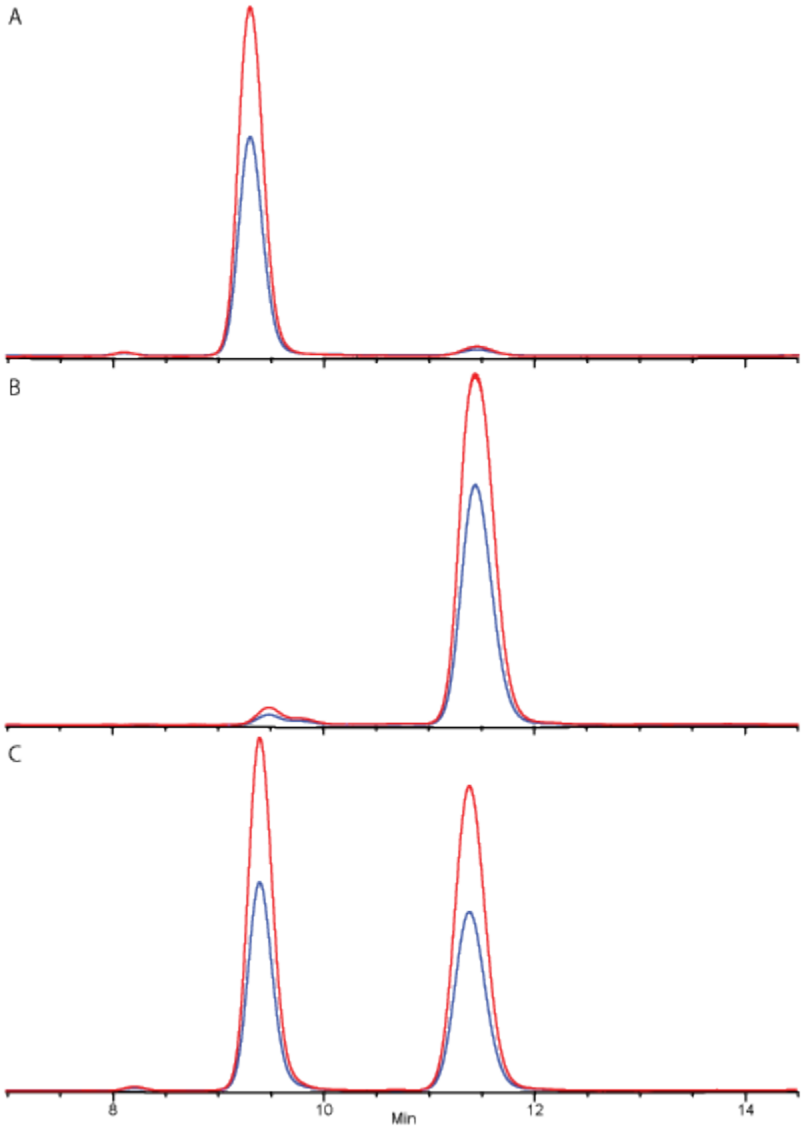

Figure S1. Chiral HPLC traces of **A:** 2-naphthalenethiol derivative of **3; B:** 2-naphthalenethiol derivative of **4**; **C:** Racemic standard. The blue line is the trace for 254 nm and the red is 220 nm.

Enzymatic Assays

Expression and purification of Rad TE.

Rad TE was amplified from pKJ31[8] by PCR (forward primer 5'-TCATACATATGCAGTTGACGCCCATGTT-3'; reverse primer 5'-TACCGGAATTCCGTCCAAAGTGCTCAA-3') and cloned into NdeI, EcoRI linearized pET28b, generating pMW29. pMW29 was confirmed by sequencing (Genome Quebec, Montreal QC).

The Expression vector encoding Rad TE (pMW29) was transformed into chemical competent *E. coli* BL21(DE3) for protein expression. 400 mL of standard Luria-Bertani media supplemented with 50 μg/mL of kanamycin was inoculated with 0.5 % *v*/*v* of a dense overnight culture of *E. coli* BL21(DE3)/pMW29 and the culture was grown at 37 °C to OD600 of 0.5. Protein expression was induced by adding isopropyl thiogalactoside (IPTG) to a final concentration of 0.1 mM. The culture was incubated at 20 °C with shaking at 200 rpm for 12 h.

All protein purification procedures were performed at 4 °C. The cells were harvested by centrifugation at 4000 g and resuspended in 10 mL of lysis buffer (100 mM sodium phosphate, 300 mM NaCl, 10% (*v*/*v*) glycerol, 1 mg/mL lysozyme, 1 μg/mL pepstatin A, 1 μg/mL leupeptin, pH 8.0). The cells were disrupted by sonication on ice and cell debris was removed by centrifugation at 15000 g at 4 °C. After adding imidazole to a final concentration of 10 mM, the cleared lysate was incubated for 1 h with 400 μL of nickel-nitrotriacetic acid (Ni-NTA) resin

(QIAGEN, Valenica, CA) and loaded onto a column. The resin was first washed with wash buffer (100 mM Tris, 300 mM NaCl, 20 mM imidazole, pH 8.0) and the protein was eluted with wash buffer supplemented with 250 mM imidazole. The purified protein was exchanged into dialysis buffer (100 mM Tris, 300 mM NaCl, pH 7.43) and concentrated by centrifugation (Amicon 5000 MWCO). The concentrated protein was flash frozen and stored at –78 °C. Protein concentration was determined by the Bradford assay (Bio-rad). Approximately 5.4 mg of purified protein was obtained per L of cell culture.

Figure S2. SDS-PAGE analysis of purified recombinant Rad TE and Zea TE. Expected molecular weights are 47kDa and 45kDa. Left to Right: Fischer Rec-Protein ladder (50kDa reference band) , Rad TE, Zea TE.

Kinetic Analysis of Macrocycle Formation

Discontinuous enzymatic assays were carried out in 50 mM phosphate buffer (pH 7.4), with 5 μM Zea TE (both substrates) and Rad TE for the L-substrate (*ent*-**8**) and 2 μM for Rad TE with the D-substrate (**8**). Substrate concentrations between 0.1 mM and 5 mM (from 10 mM or 50 mM

stock solutions in DMSO), and DMSO up to 10% solution volume if necessary. Assays were quenched with an equal volume of 0.5% formic acid in acetonitrile before analysis by HPLC. Analysis was performed using a BDS Hypersil C18 100x2.1 mm reverse phase column, using a gradient elution of 0 to 100% B over 30 minutes (A: 95% H_2O, 5% MeCN, 0.05% formic acid; B: 95% MeCN, 5% H_2O, 0.05% formic acid). Amount of macrocycle produced was determined by comparison to a standard curve of authentic macrocycle. Non-linear regression analysis was performed in GraphPad Prism 5.

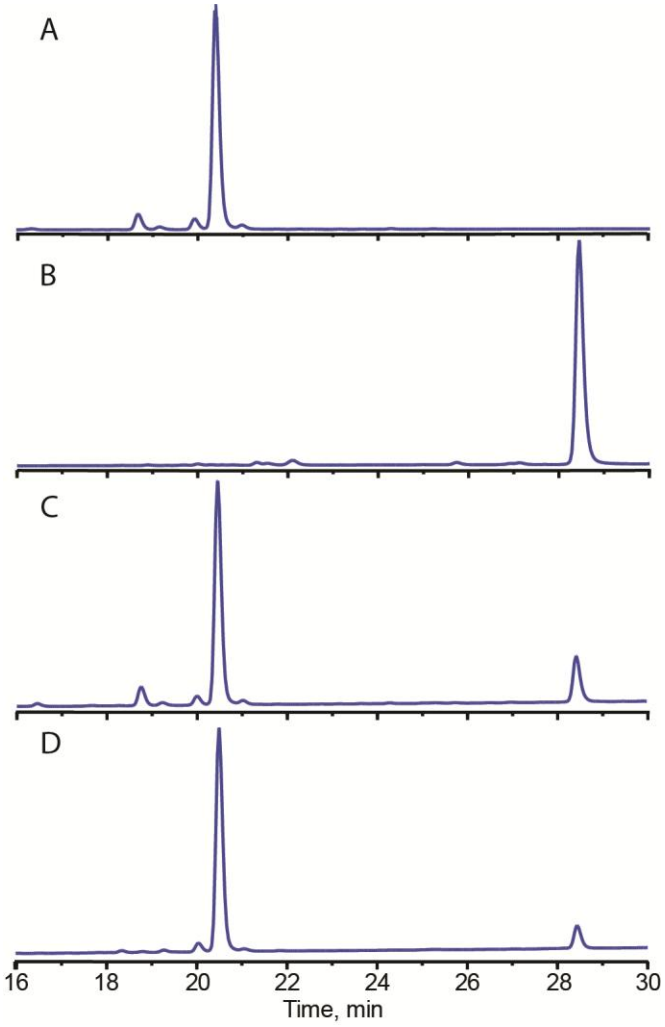

Figure S3. HPLC traces for incubations of **8** and *ent*-**8** with ZeaTE. A, no enzyme blank (5 mM **8**, 50 mM phosphate buffer pH 7.4, 24 h, rt). B, Racemic macrocycle, *racemic*-**6** . C, **8** with Zea

TE (3 mM **8**, 5 μM Zea TE, 50 mM phosphate buffer pH 7.4, 0.5 h, rt). D *ent*-**8** with Zea TE (3 mM *ent*-**8**, 5 μM Zea TE, 50 mM phosphate buffer, pH 7.4, 0.5 h, rt). Small peak at 20 min is the hydrolysis product.

Fitting of rate data

$$v = \frac{V_{Max}}{1 + \frac{K_M}{[S]} + \frac{[S]}{K_i}}$$

Equation S1. Equation, as described by Copeland[9], used to model substrate inhibition of Rad TE by *ent*-**8**, based on allosteric binding of a second molecule of substrate to the enzyme-substrate complex. Used to generate Figure S5.

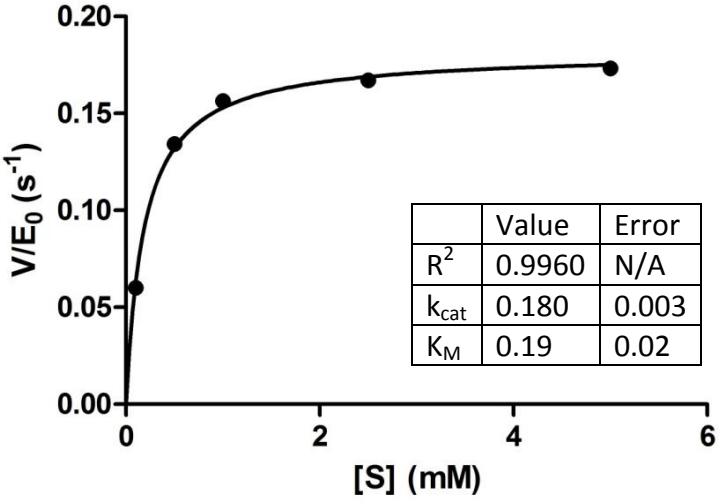

Figure S4. Initial reaction rates (s^{-1}) plotted against substrate concentration (mM) for conversion to macrocycle by Rad TE with **8**. These data was fit to the Michaelis-Menten model.

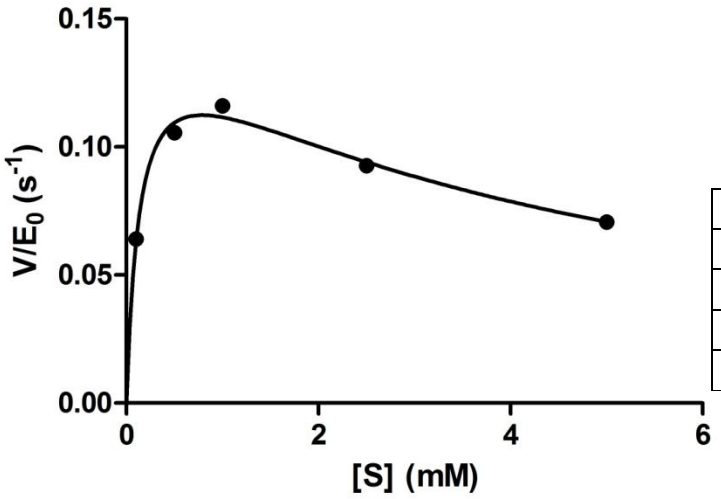

	Value	Error
R^2	0.9807	N/A
k_{cat}	0.15	0.01
K_M	0.14	0.03
K_I	4.5	0.9

Figure S5. Initial reaction rates (s^{-1}) plotted against substrate concentration (mM) for conversion to macrocycle by Rad TE with *ent*-**8** . These data were fit to Equation S1.

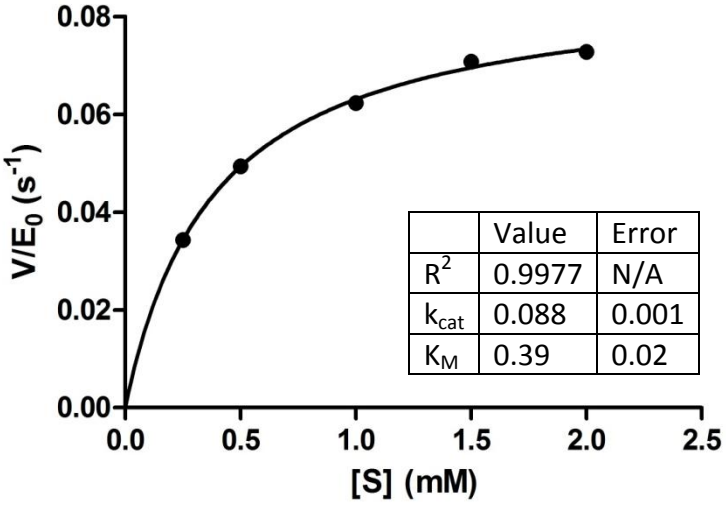

	Value	Error
R^2	0.9977	N/A
k_{cat}	0.088	0.001
K_M	0.39	0.02

Figure S6. Initial reaction rates (s^{-1}) plotted against substrate concentration (mM) for conversion to macrocycle by Zea TE with **8**. These data were fit to the Michaelis-Menten model.

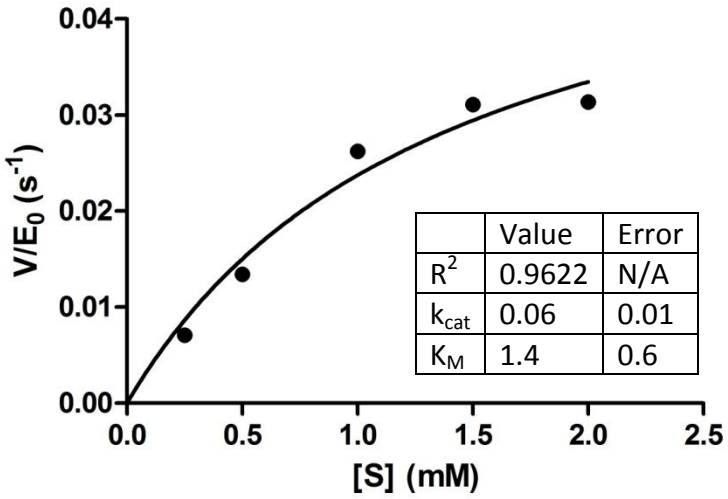

Figure S5. Initial reaction rates (s^{-1}) plotted against substrate concentration (mM) for conversion to macrocycle by ZeaTE with *ent*-**8**. These data were fit to the Michaelis-Menten model.

Selected NMR Spectra

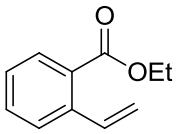

S1

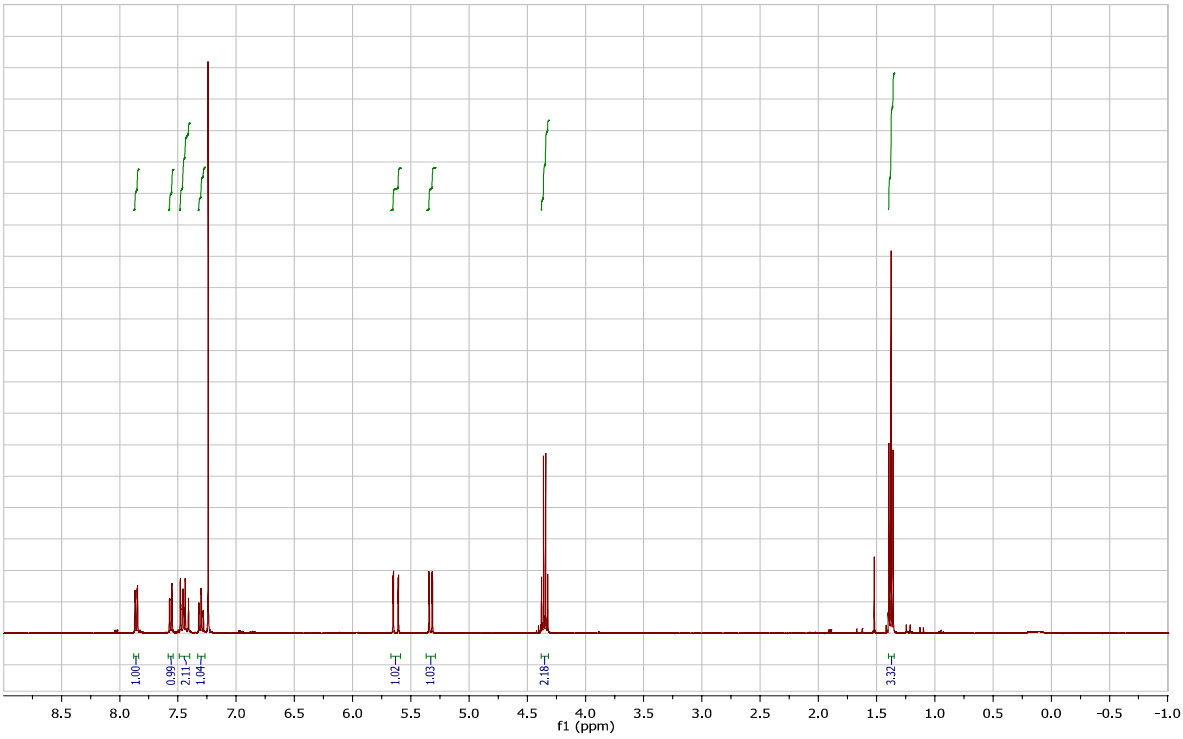

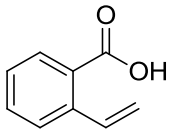
O
OH

S2

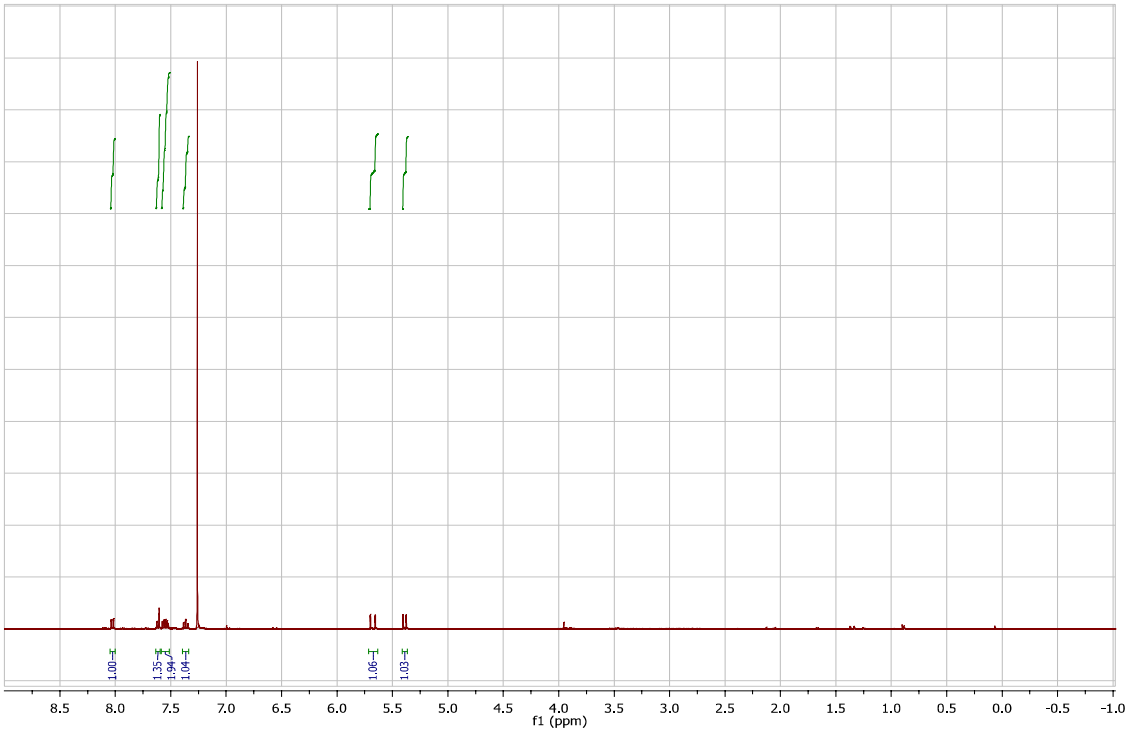
1.00
1.35
1.94
1.04
1.06
1.03
8.5
8.0
7.5
7.0
6.5
6.0
5.5
5.0
4.5
4.0
3.5
3.0
2.5
2.0
1.5
1.0
0.5
0.0
-0.5
-1.0
f1 (ppm)

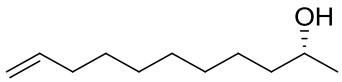
OH

3

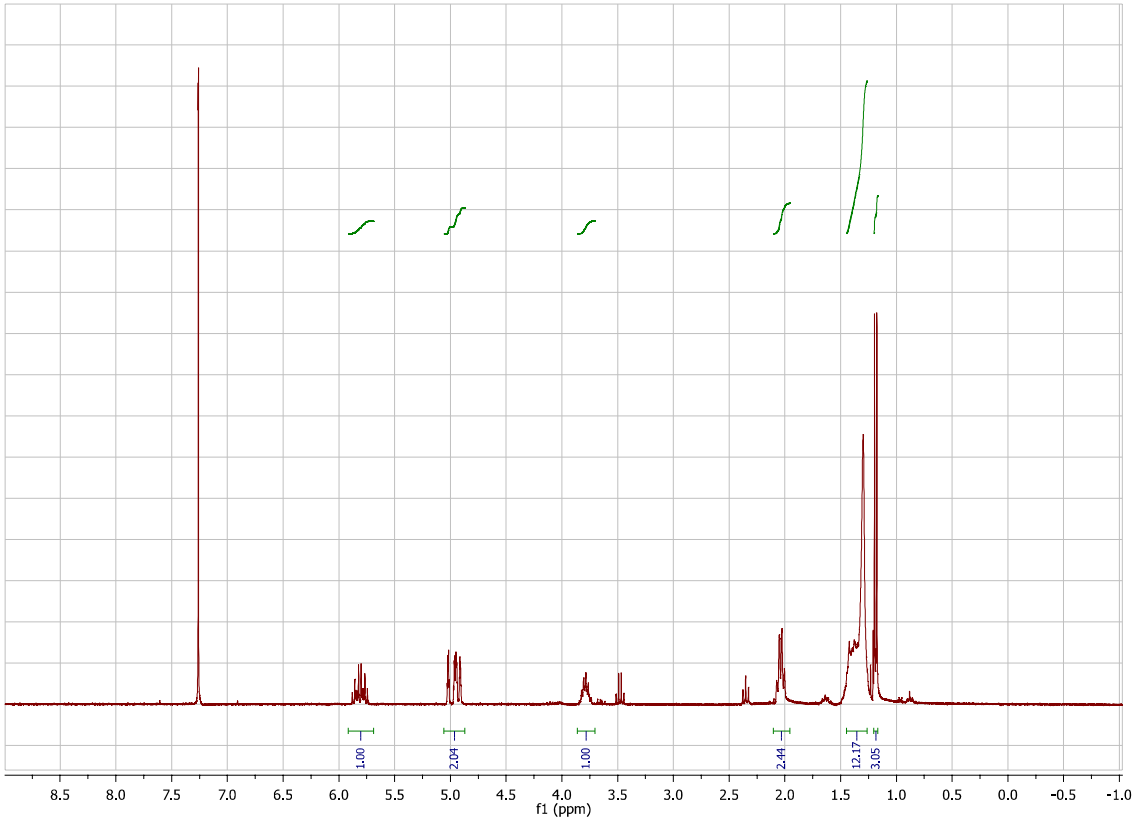
1.00
2.04
1.00
2.44
12.17
3.05
8.5
8.0
7.5
7.0
6.5
6.0
5.5
5.0
4.5
4.0
3.5
3.0
2.5
2.0
1.5
1.0
0.5
0.0
-0.5
-1.0
f1 (ppm)

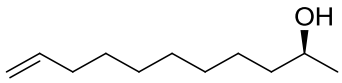
OH

4

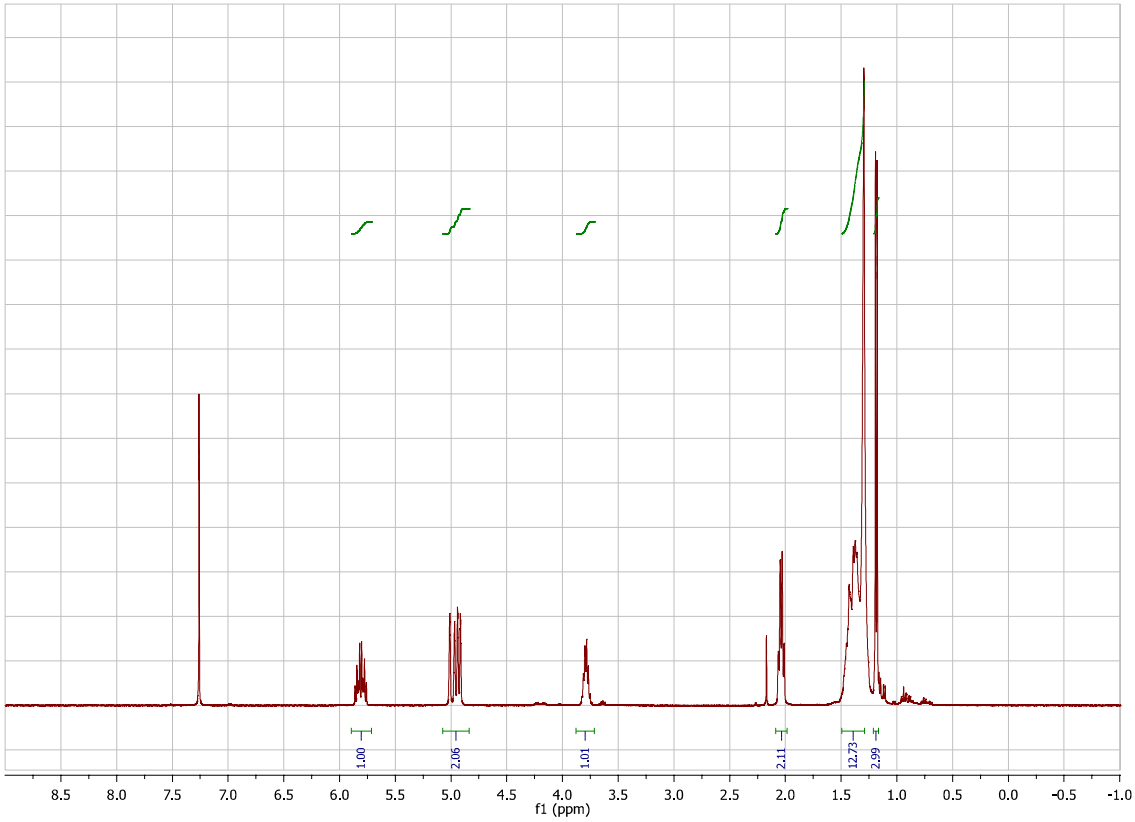
1.00
2.06
1.01
2.11
12.73
2.99
8.5
8.0
7.5
7.0
6.5
6.0
5.5
5.0
4.5
4.0
3.5
3.0
2.5
2.0
1.5
1.0
0.5
0.0
-0.5
-1.0
f1 (ppm)

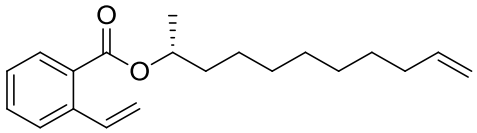

5

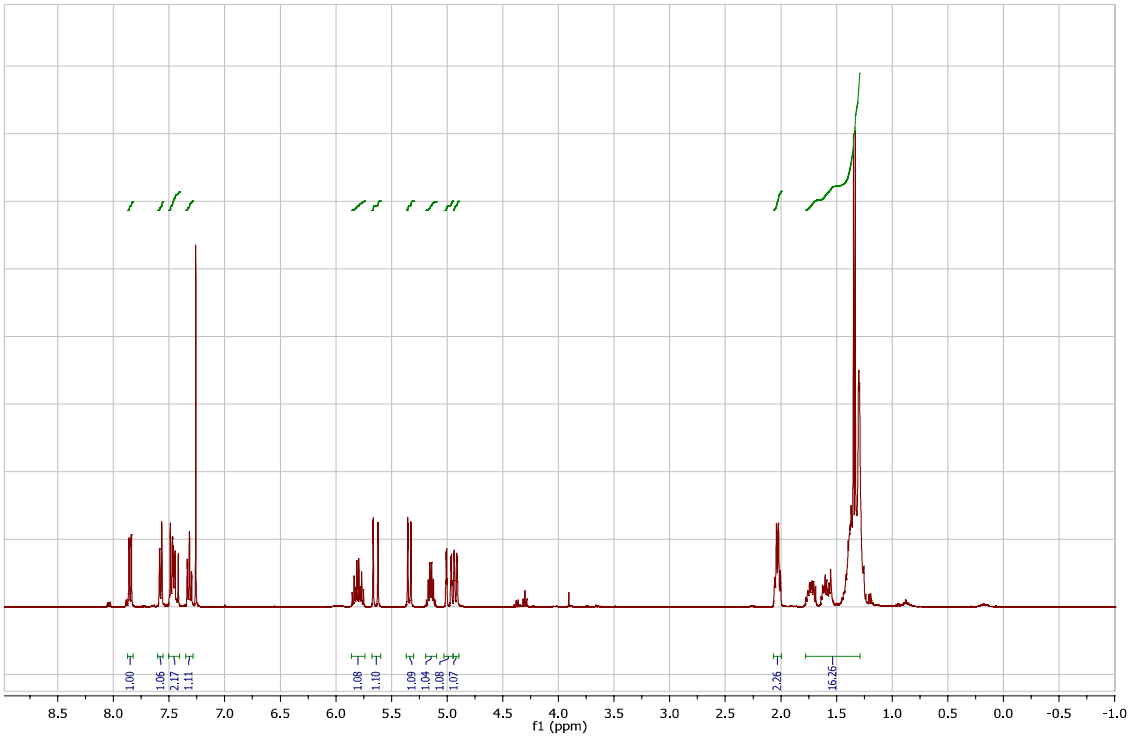
1.00
1.06
2.17
1.11
1.08
1.10
1.09
1.04
1.08
1.07
2.26
16.26
f1 (ppm)

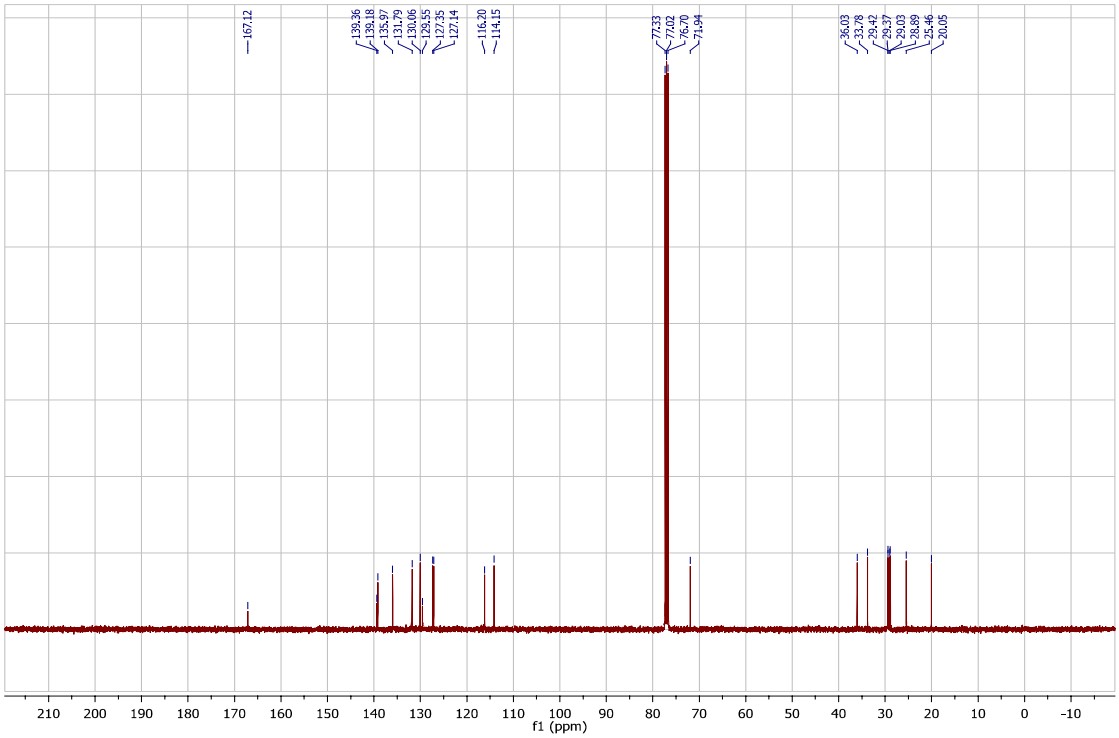
167.12
139.36
139.18
135.97
131.79
130.06
129.55
127.35
127.14
116.20
114.15
77.33
77.02
76.70
71.94
36.03
33.78
29.42
29.37
29.03
28.89
25.46
20.05
f1 (ppm)

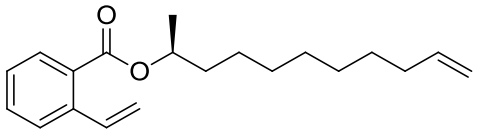

ent-**5**

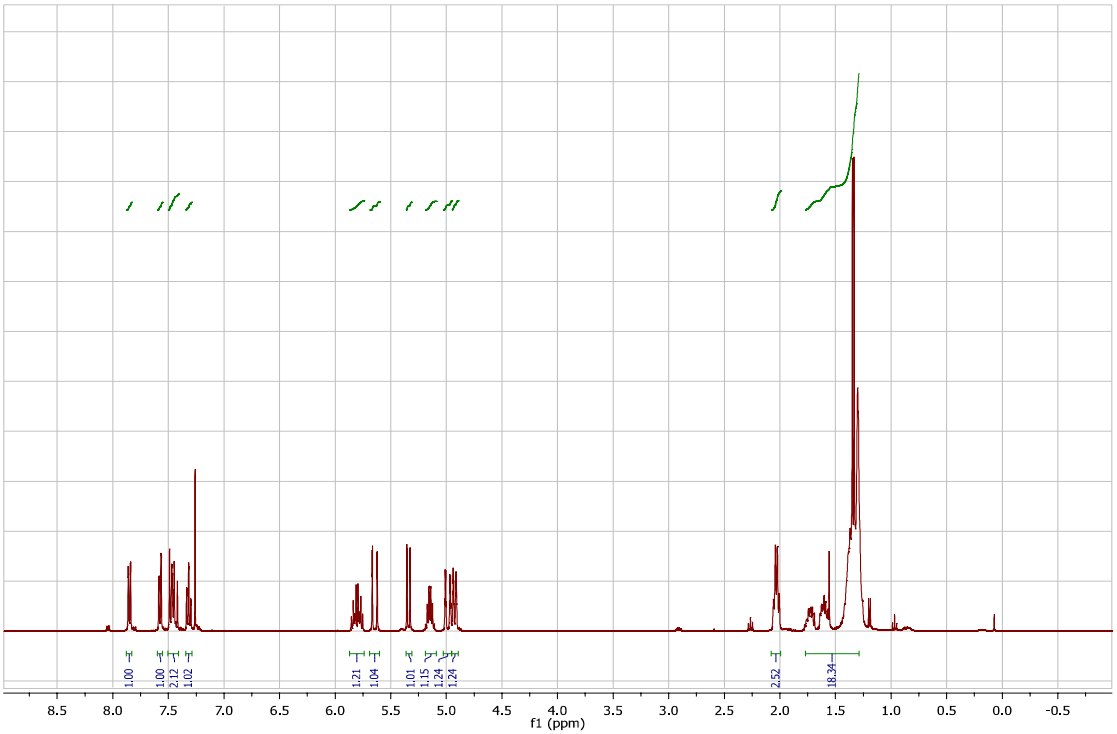
1.00
1.00
2.12
1.02
1.21
1.04
1.01
1.15
1.24
1.24
2.52
18.34
f1 (ppm)

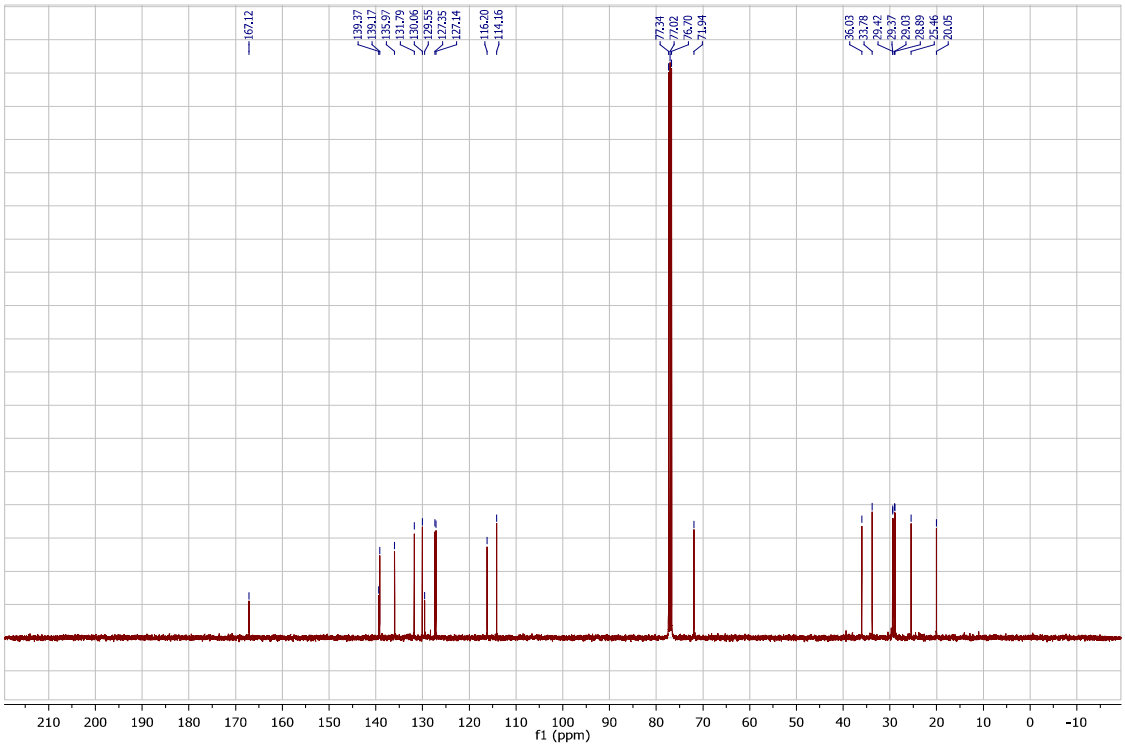
167.12
139.37
139.17
135.97
131.79
130.06
129.55
127.35
127.14
116.20
114.16
77.34
77.02
76.70
71.94
36.03
33.78
29.42
29.37
29.03
28.89
25.46
20.05
f1 (ppm)

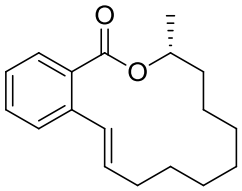

6

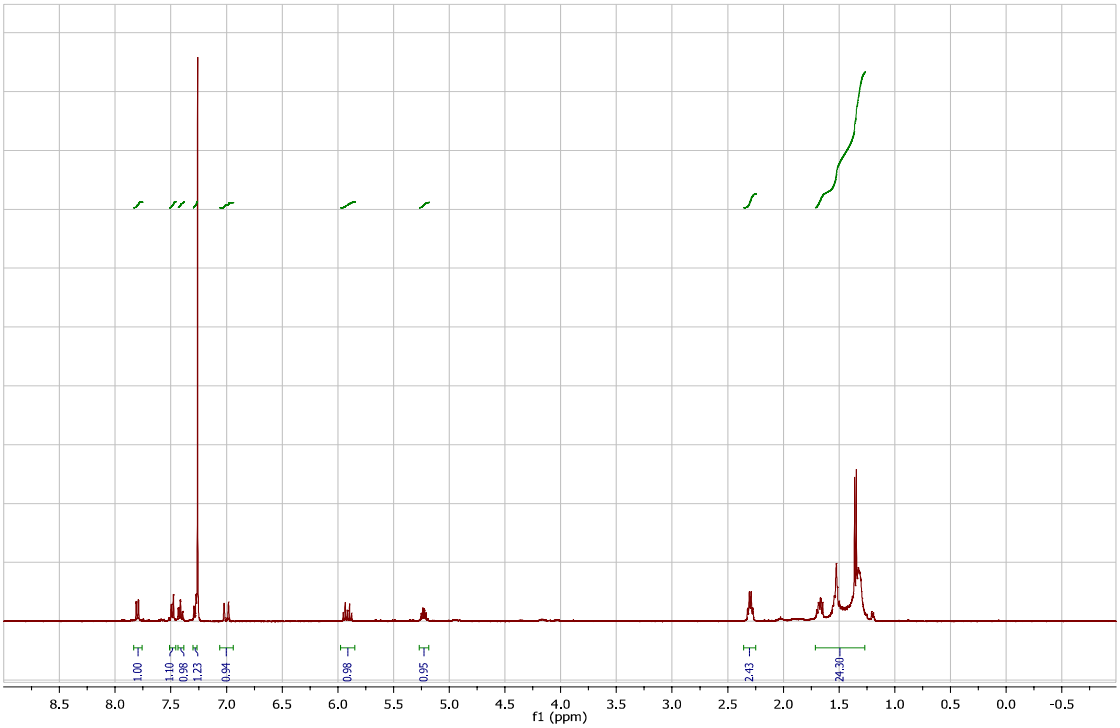
1.00
1.10
0.98
1.23
0.94
0.88
0.95
2.43
24.30
8.5 8.0 7.5 7.0 6.5 6.0 5.5 5.0 4.5 4.0 3.5 3.0 2.5 2.0 1.5 1.0 0.5 0.0 -0.5
f1 (ppm)

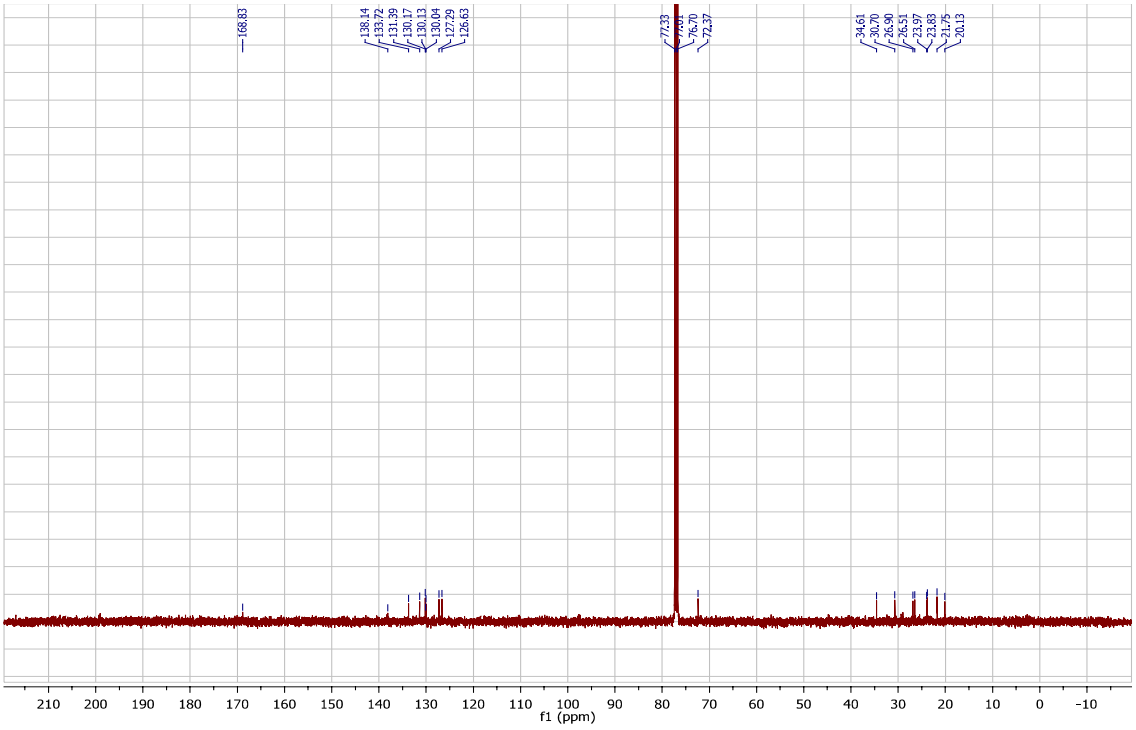
168.83
138.14
133.72
131.39
130.17
130.13
130.04
127.29
126.63
77.33
77.00
76.70
72.37
34.61
30.70
26.90
26.51
23.97
23.83
21.75
20.13
210 200 190 180 170 160 150 140 130 120 110 100 90 80 70 60 50 40 30 20 10 0 -10
f1 (ppm)

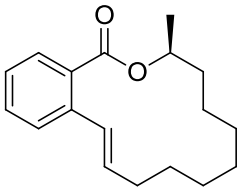

ent-**6**

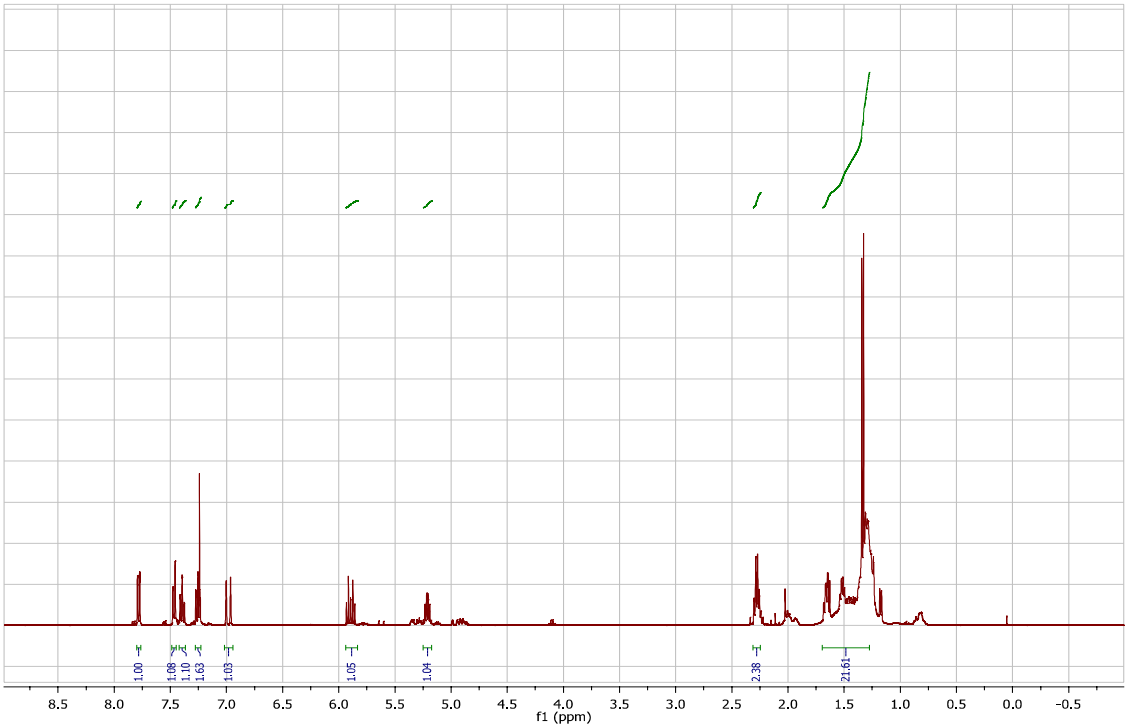
1.00
1.08
1.10
1.63
1.03
1.05
1.04
2.38
21.61
f1 (ppm)

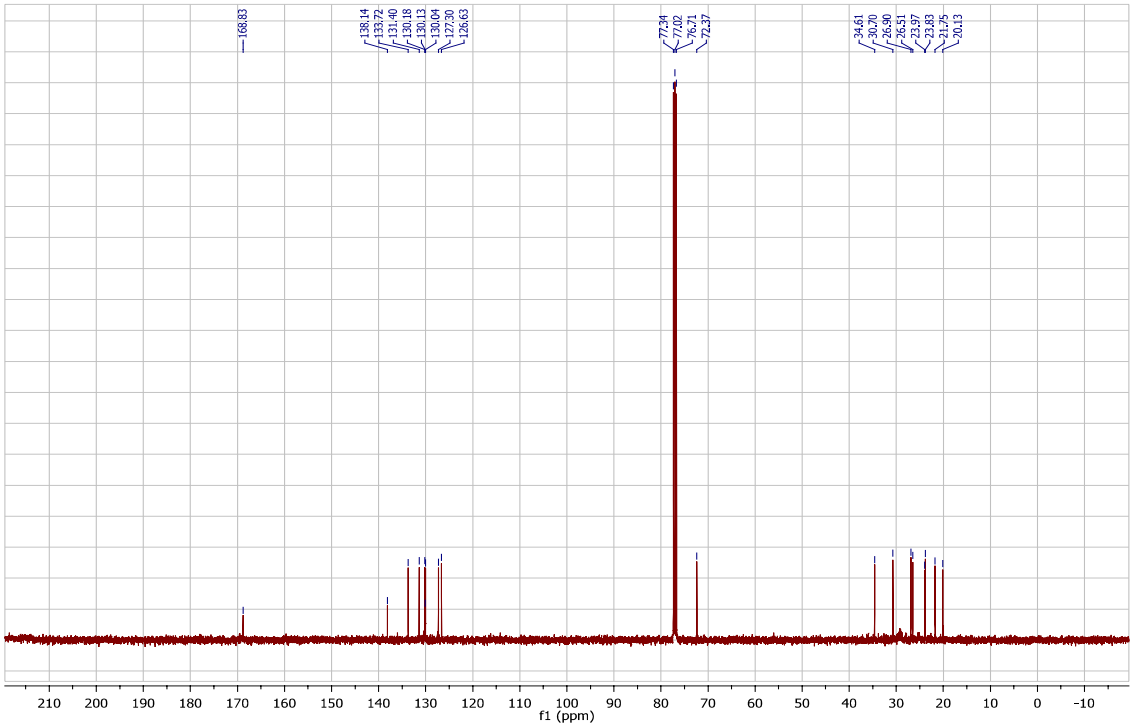
168.83
138.14
133.72
131.40
130.18
130.13
130.04
127.30
126.63
77.34
77.02
76.71
72.37
34.61
30.70
26.90
26.51
23.97
23.83
21.75
20.13
f1 (ppm)

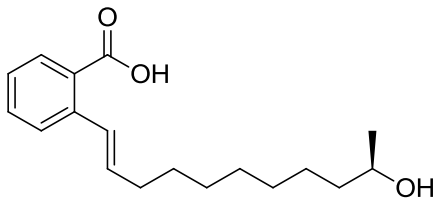
O
OH
OH

7

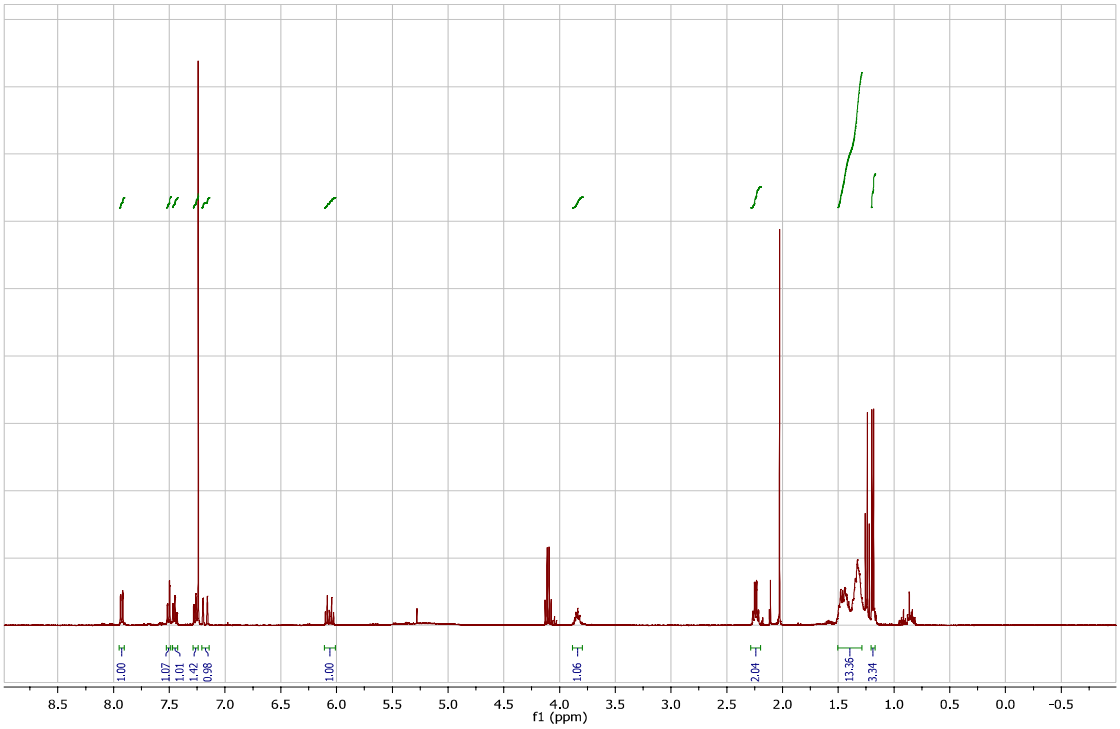
1.00
1.07
1.01
1.42
0.98
1.00
1.06
2.04
13.36
3.34
8.5 8.0 7.5 7.0 6.5 6.0 5.5 5.0 4.5 4.0 3.5 3.0 2.5 2.0 1.5 1.0 0.5 0.0 -0.5
f1 (ppm)

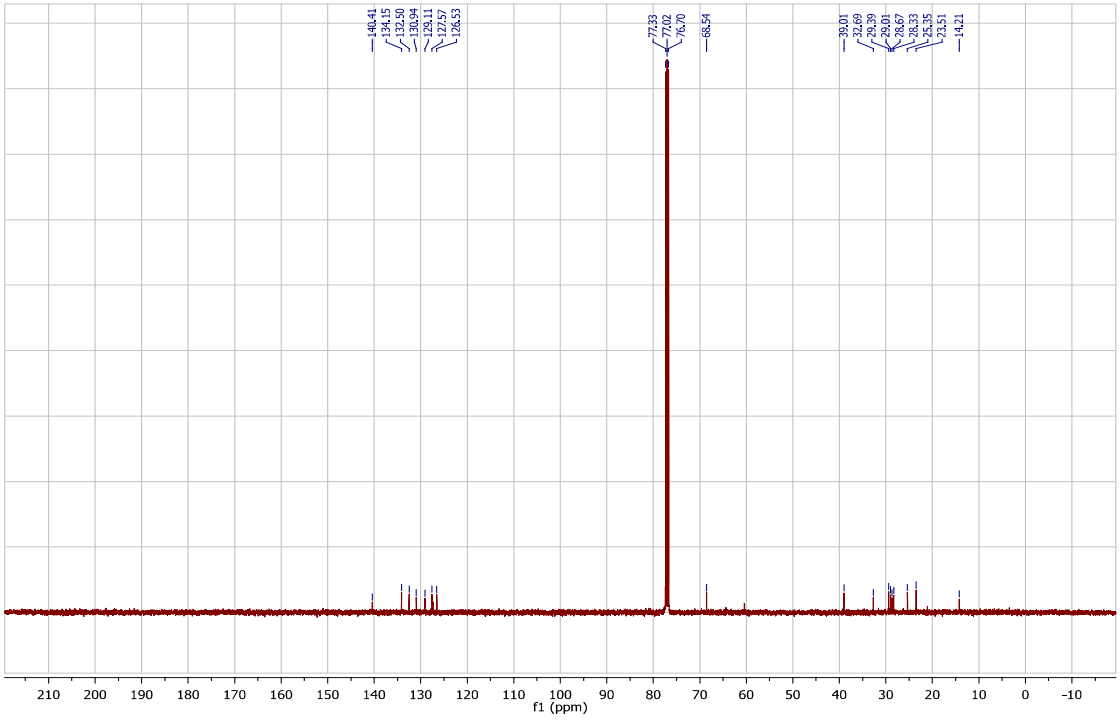
140.41
134.15
132.50
130.94
129.11
127.57
126.53
77.33
77.02
76.70
68.54
39.01
32.69
29.39
29.01
28.67
28.33
25.35
23.51
14.21
210 200 190 180 170 160 150 140 130 120 110 100 90 80 70 60 50 40 30 20 10 0 -10
f1 (ppm)

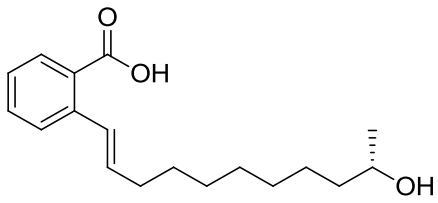
O
OH
OH

ent-**7**

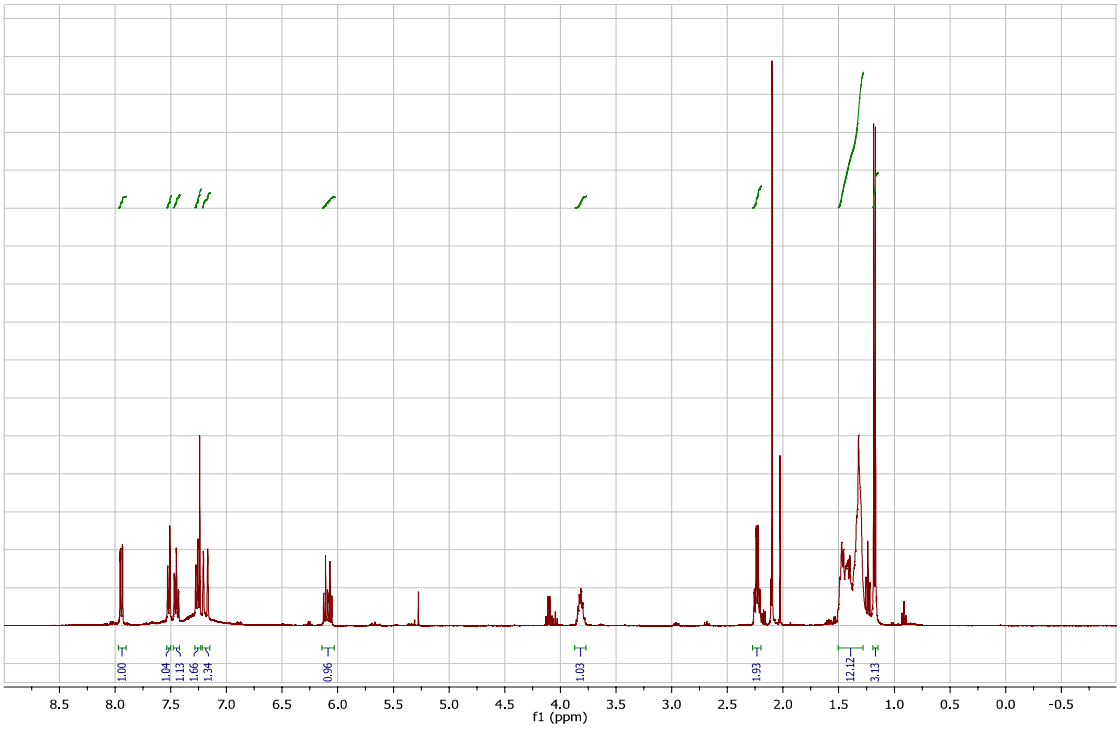
1.00
1.04
1.13
1.66
1.34
0.96
1.03
1.93
12.12
3.13
8.5 8.0 7.5 7.0 6.5 6.0 5.5 5.0 4.5 4.0 3.5 3.0 2.5 2.0 1.5 1.0 0.5 0.0 -0.5
f1 (ppm)

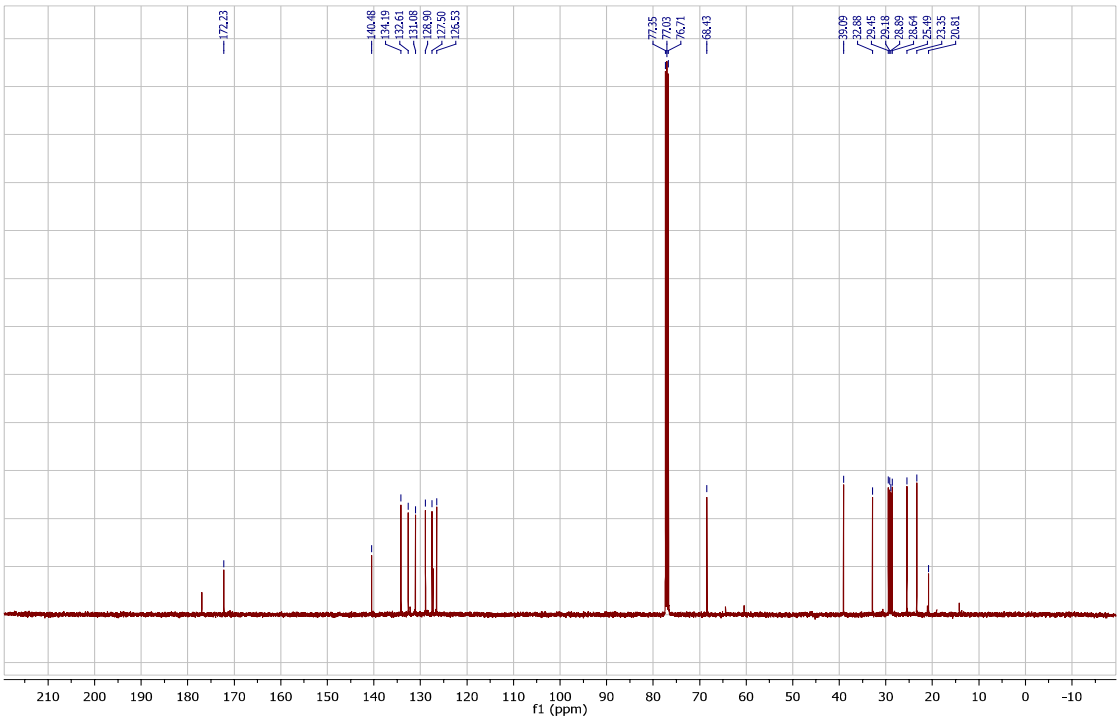
172.23
140.48
134.19
132.61
131.08
128.30
127.50
126.53
77.35
77.03
76.71
68.43
39.09
32.88
29.45
29.18
28.89
28.64
25.49
23.35
20.81
210 200 190 180 170 160 150 140 130 120 110 100 90 80 70 60 50 40 30 20 10 0 -10
f1 (ppm)

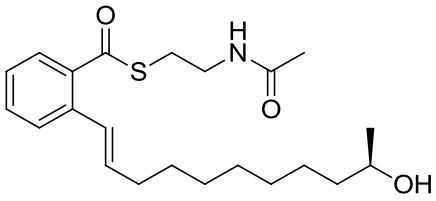
O
H
N
S
O
OH

8

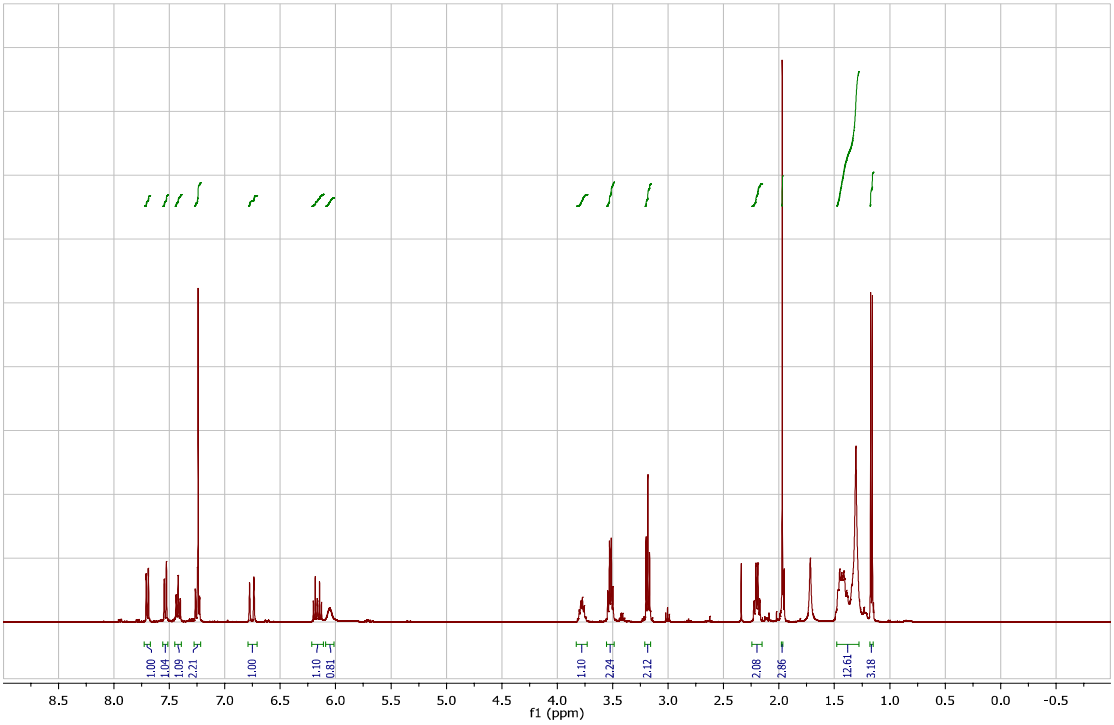
1.00
1.04
1.09
2.21
1.00
1.10
0.81
1.10
2.24
2.12
2.08
2.86
12.61
3.18
8.5
8.0
7.5
7.0
6.5
6.0
5.5
5.0
4.5
4.0
3.5
3.0
2.5
2.0
1.5
1.0
0.5
0.0
-0.5
f1 (ppm)

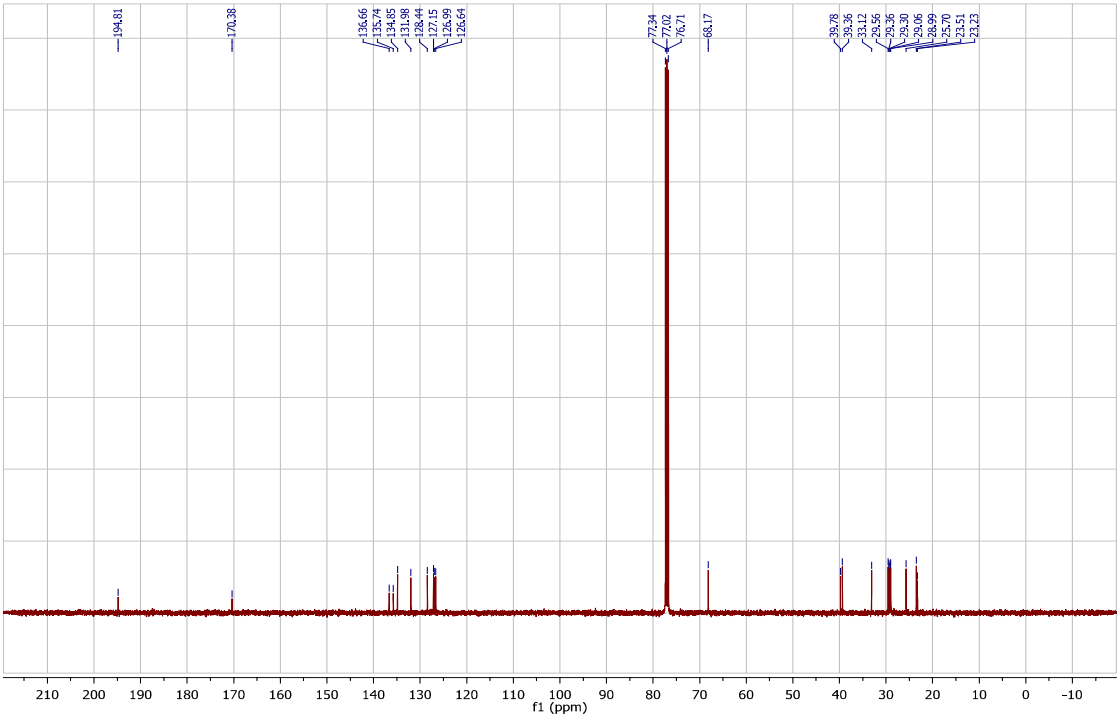
194.61
170.38
136.66
135.74
134.85
131.98
128.44
127.15
126.99
126.64
77.34
77.02
76.71
68.17
39.78
39.36
33.12
29.56
29.36
29.30
29.06
28.99
25.70
23.51
23.23
210
200
190
180
170
160
150
140
130
120
110
100
90
80
70
60
50
40
30
20
10
0
-10
f1 (ppm)

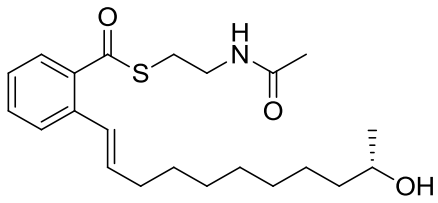
O
H
N
S
O
OH

ent-**8**

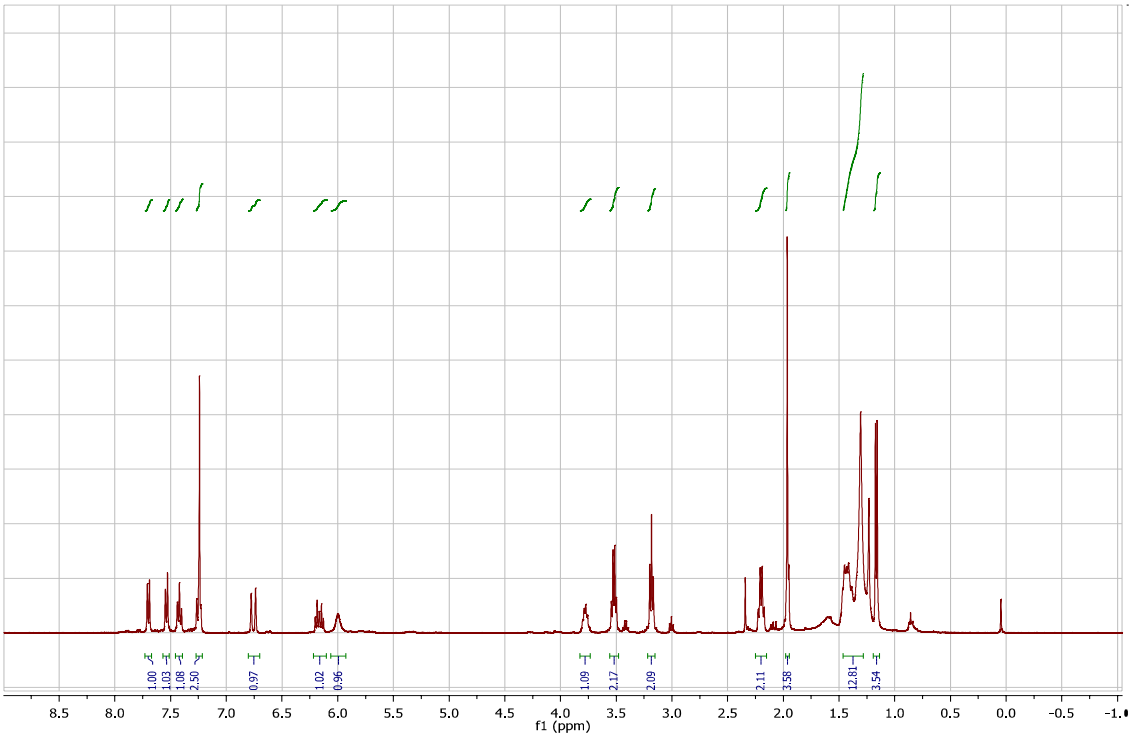
1.00
1.03
1.08
2.50
0.97
1.02
0.96
1.09
2.17
2.09
2.11
3.58
12.81
3.54
8.5 8.0 7.5 7.0 6.5 6.0 5.5 5.0 4.5 4.0 3.5 3.0 2.5 2.0 1.5 1.0 0.5 0.0 -0.5
f1 (ppm)

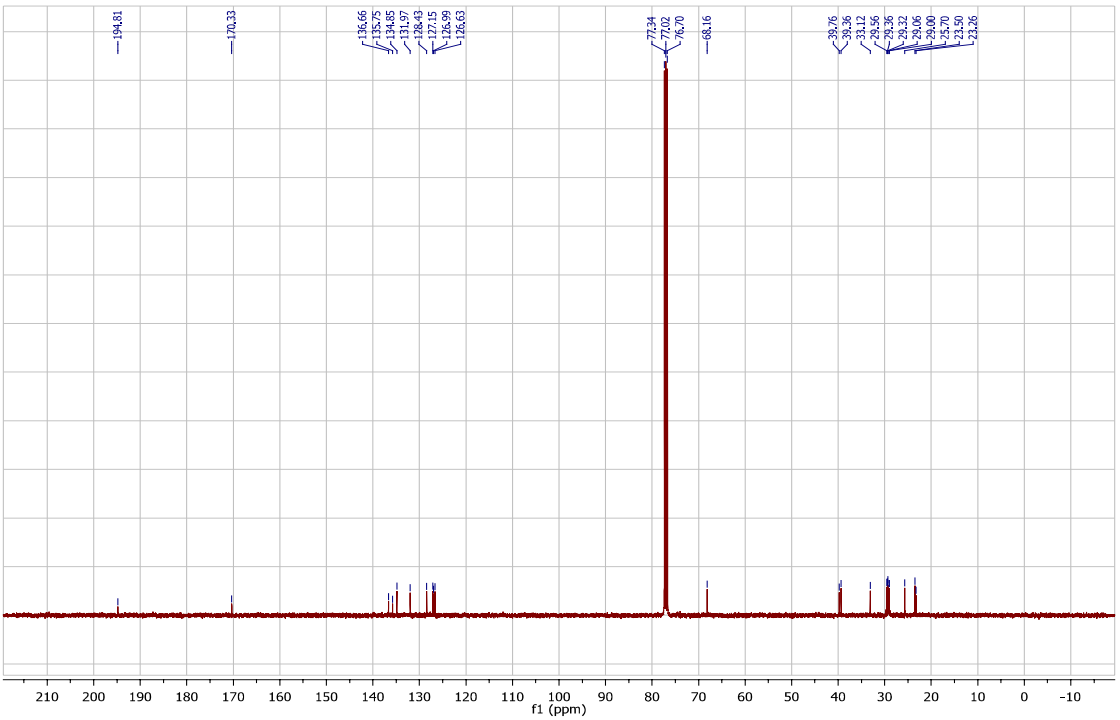
194.61
170.33
136.66
135.75
134.85
131.97
128.43
127.15
126.99
126.63
77.24
77.02
76.70
68.16
39.76
39.36
33.12
29.56
29.36
29.32
29.06
29.00
25.70
23.50
23.26
210 200 190 180 170 160 150 140 130 120 110 100 90 80 70 60 50 40 30 20 10 0 -10
f1 (ppm)

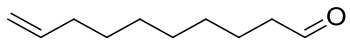

S3

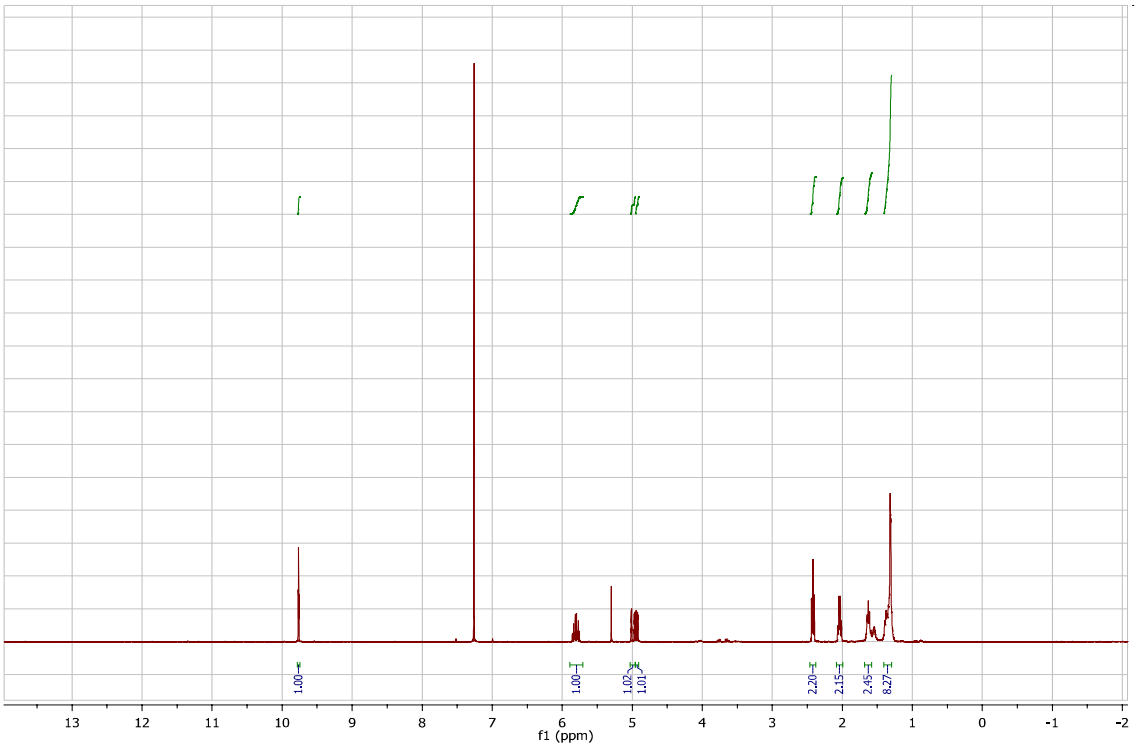
1.00
1.00
1.02
1.01
2.20
2.15
2.45
8.27
f1 (ppm)

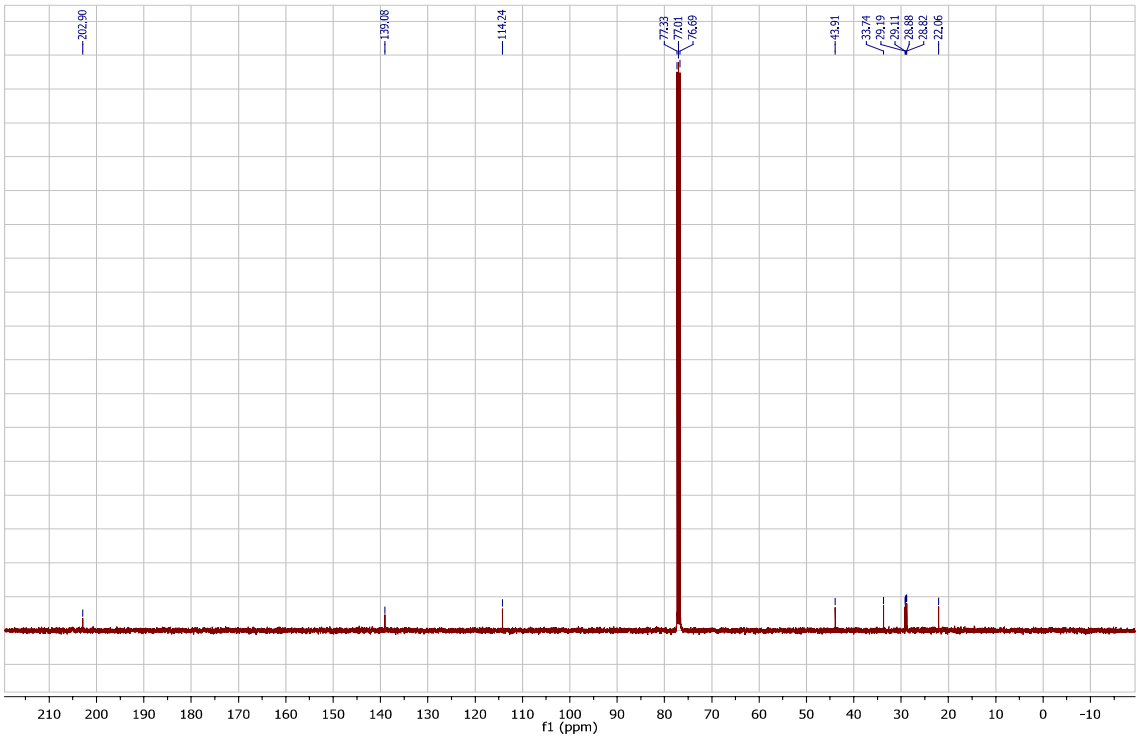
202.90
139.08
114.24
77.33
77.01
76.69
43.91
33.74
29.19
29.11
28.88
28.82
22.06
f1 (ppm)

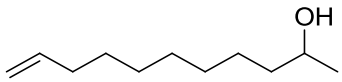
OH

S4

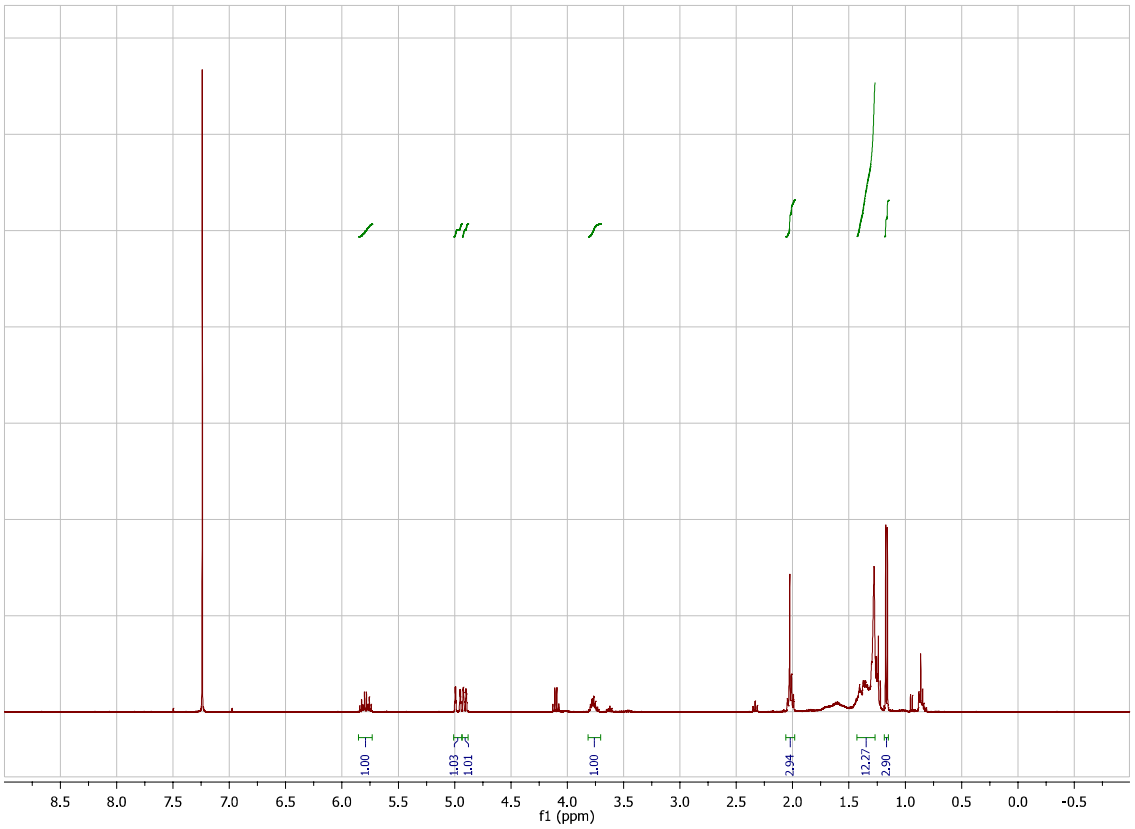
1.00
1.03
1.01
1.00
2.94
12.27
2.90
8.5
8.0
7.5
7.0
6.5
6.0
5.5
5.0
4.5
4.0
3.5
3.0
2.5
2.0
1.5
1.0
0.5
0.0
-0.5
f1 (ppm)

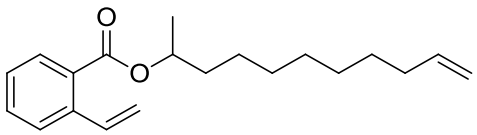

racemic-**5**

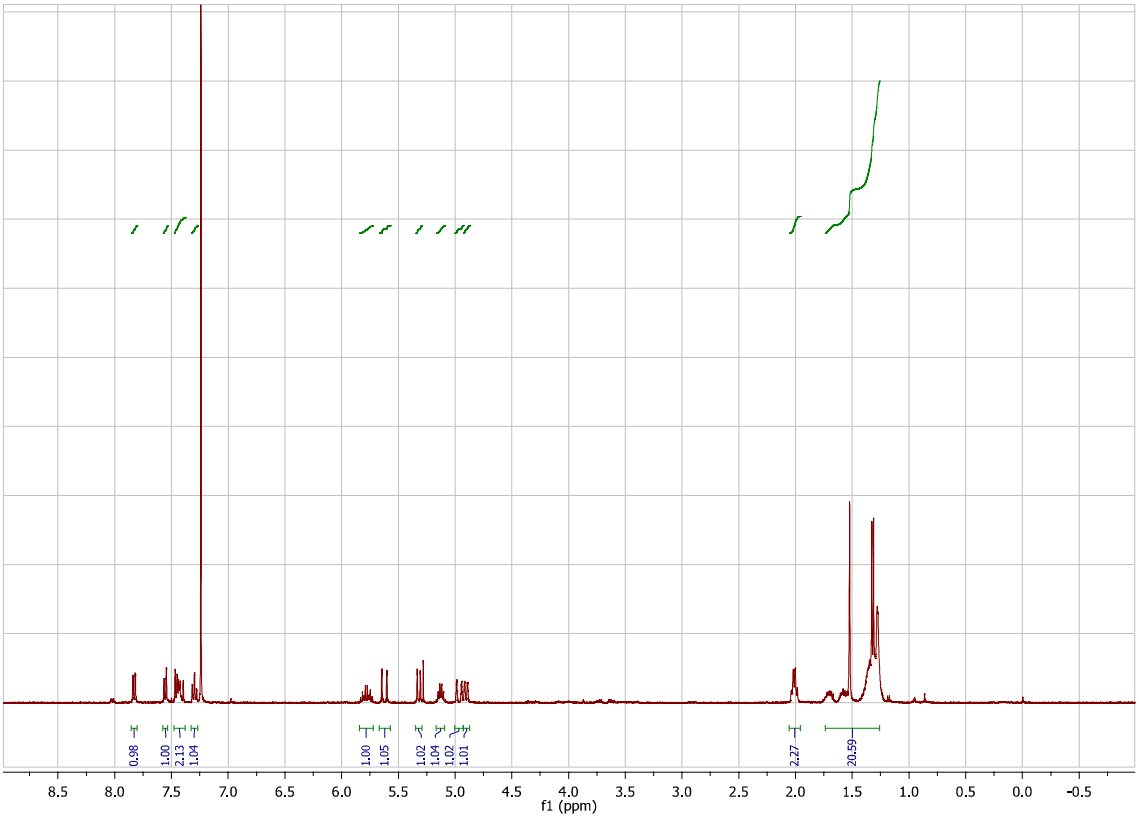
0.98
1.00
2.13
1.04
1.00
1.05
1.02
1.04
1.02
1.01
2.27
20.59
8.5
8.0
7.5
7.0
6.5
6.0
5.5
5.0
4.5
4.0
3.5
3.0
2.5
2.0
1.5
1.0
0.5
0.0
-0.5
f1 (ppm)

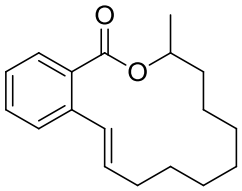
O
O

racemic-**6**

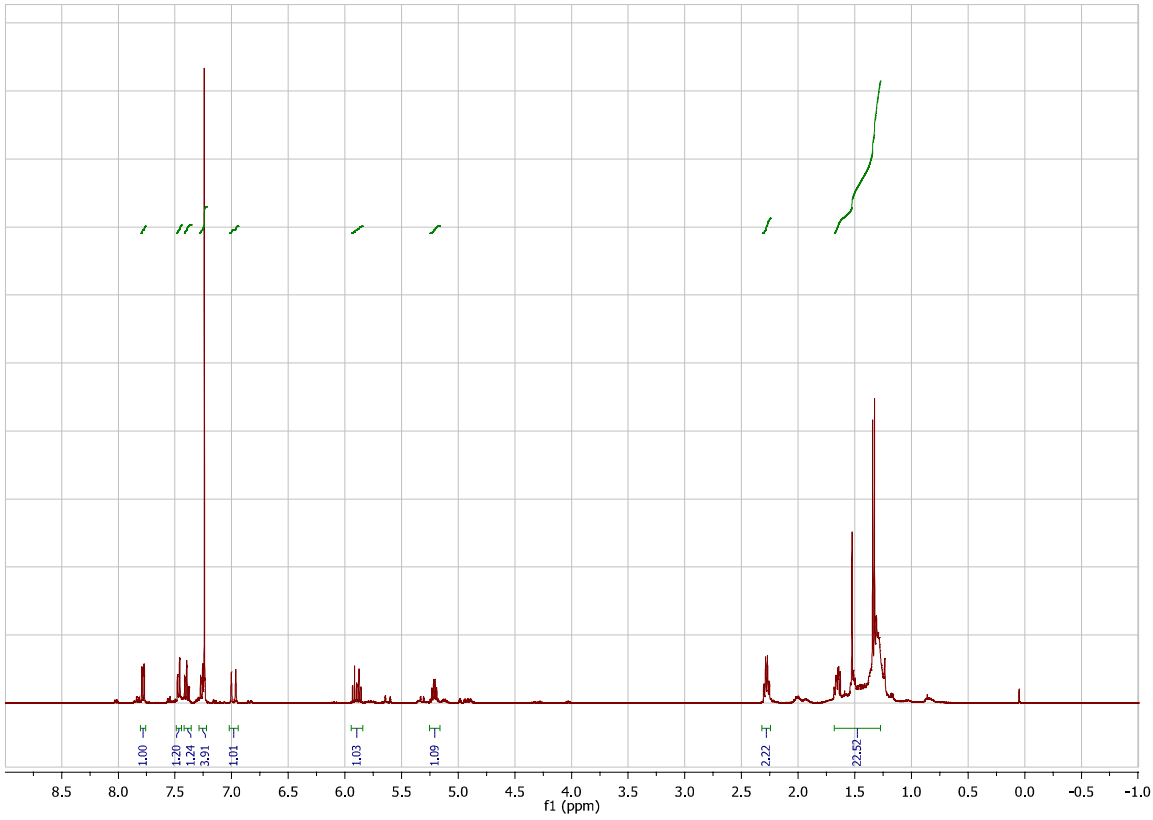
1.00
1.20
1.24
3.91
1.01
1.03
1.09
2.22
22.52
8.5
8.0
7.5
7.0
6.5
6.0
5.5
5.0
4.5
4.0
3.5
3.0
2.5
2.0
1.5
1.0
0.5
0.0
-0.5
-1.0
f1 (ppm)

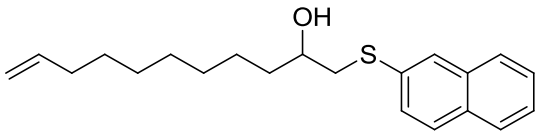
OH
S

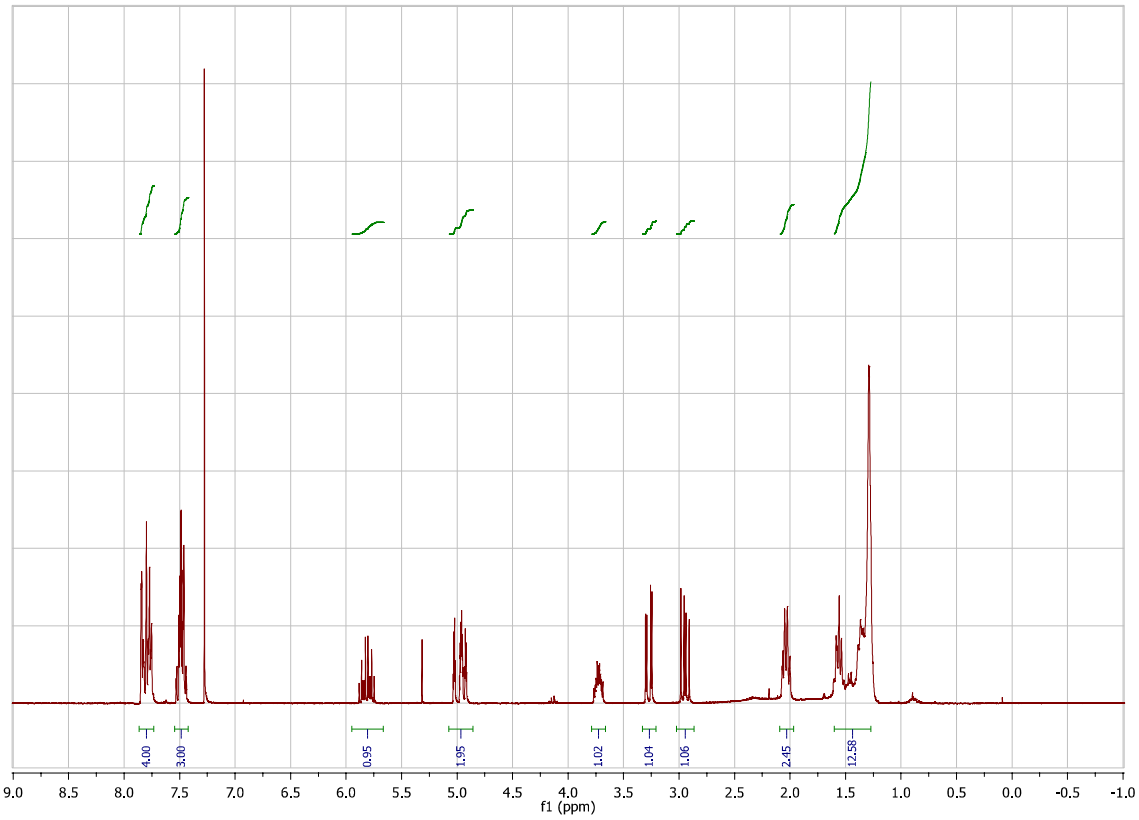
4.00
3.00
0.95
1.95
1.02
1.04
1.06
2.45
12.58
9.0
8.5
8.0
7.5
7.0
6.5
6.0
5.5
5.0
4.5
4.0
3.5
3.0
2.5
2.0
1.5
1.0
0.5
0.0
-0.5
-1.0
f1 (ppm)

References

[1] M. Wang, C. N. Boddy, *Biochemistry* **2008**, *47*, 11793–11803.
[2] T. P. A. Hari, P. Labana, M. Boileau, C. N. Boddy, *ChemBioChem* **2014**, *15*, 2656–2661.
[3] A. Pinto, M. Wang, M. Horsman, C. N. Boddy, *Org. Lett.* **2012**, *14*, 2278–2281.
[4] S. E. Denmark, C. R. Butler, *Org. Lett.* **2006**, *8*, 63–6.
[5] M. Matos, P. V Murphy, *J. Org. Chem.* **2007**, *72*, 1803–1806.
[6] F. Bracher, J. Krauß, *Eur. J. Org. Chem.* **2001**, *2001*, 4701.
[7] M. Uyanik, M. Akakura, K. Ishihara, *J. Am. Chem. Soc.* **2009**, *131*, 251–62.
[8] H. Zhou, K. Qiao, Z. Gao, J. C. Vederas, Y. Tang, *J. Biol Chem.* **2010**, *285*, 41412–21.
[9] Robert A. Copeland, in *Enzymes: A Practical Introduction to Structure, Mechanism, and Data Analysis* (Ed.: Robert A. Copeland), Wiley-VCH, Inc., **2000**, pp. 109–145.

Chapter 3. Chemoenzymatic macrolactone synthesis using resorcylic acid lactone thioesterase domains

3.1 Introduction

Having established that the thioesterases (TEs) from radicicol and zearalenone biosynthesis were stereotolerant, we wanted to expand the scope of macrolactone formation reactions these enzyme could catalyze.[1] We chose ring size as our starting point for this follow-up study as macrocyclic lactone natural products come in a variety of sizes (**Fig 1.4**). We believed these macrocycles would be accessible since similar 12-member resorcyclic acid lactones, such as lasiodiplodin, are known.[2,3] Expanding the scope of the Zea and Rdc TEs to access to 12-18 member systems would capture over 50% of macrocyclic lactone natural products.[4] While the DEBS TE is tolerant of various ring sizes *in vivo*[5–10] its capacity to access the same diversity *in vitro* has not been determined. This lack of demonstrated *in vitro* diversity coupled with the strict stereochemistry requirement on the nucleophile for cyclization[11,12] this would establish these fungal TEs (Rdc and Zea) as enzyme of choice for macrolactone formation.[13]

Expanding the scope of these TEs to include amine nucleophiles to generate macrolactams would capture an additional group of known natural products (approximately 700).[4] Further access to peptide containing substrates would give these potential biocatalysts an exceptionally broad scope and make them ideal platforms for protein engineering efforts.

3.2 References

[1] G. W. Heberlig, M. Wirz, M. Wang, C. N. Boddy, *Org. Lett.* 2014, *16*, 5858–5861.

[2] Y. Xu, T. Zhou, P. Espinosa-Artiles, Y. Tang, J. Zhan, I. Molnár, *ACS Chem. Biol.* 2014, *9*, 1119–1127.
[3] J. Xu, C. Jiang, Z. Zhang, W. Ma, Y. Guo, *Acta Pharmacol. Sin.* 2014, *35*, 316–330.
[4] L. A. Wessjohann, E. Ruijter, D. Garcia-Rivera, W. Brandt, *Mol. Divers.* 2005, *9*, 171–186.
[5] J. R. Jacobsen, C. R. Hutchinson, D. E. Cane, C. Khosla, *Science* 1997, *277*, 367–369.
[6] C. M. Kao, L. Katz, C. Khosla, *Science* 1994, *265*, 509–512.
[7] C. M. Kao, G. Luo, L. Katz, D. E. Cane, C. Khosla, *J. Am. Chem. Soc.* 1995, *117*, 9105–9106.
[8] C. M. Kao, G. Luo, L. Katz, D. E. Cane, C. Khosla, *J. Am. Chem. Soc.* 1996, *118*, 9184–9185.
[9] C. M. Kao, M. McPherson, R. N. McDaniel, H. Fu, D. E. Cane, C. Khosla, *J. Am. Chem. Soc.* 1997, *119*, 11339–11340.
[10] R. McDaniel, A. Thamchaipenet, C. Gustafsson, H. Fu, M. Betlach, M. Betlach, G. Ashley, *Proc. Natl. Acad. Sci. U.S.A* 1999, *96*, 1846–1851.
[11] A. Pinto, M. Wang, M. Horsman, C. N. Boddy, *Org. Lett.* 2012, *14*, 2278–2281.
[12] T. P. A. Hari, P. Labana, M. Boileau, C. N. Boddy, *ChemBioChem* 2014, *15*, 2656–2661.
[13] G. W. Heberlig, J. T. C. Brown, R. D. Simard, M. Wirz, W. Zhang, M. Wang, L. I. Susser, M. E. Horsman, C. N. Boddy, *Org. Biomol. Chem.* 2018, *16*, 5771–5779.

3.3 Author Contributions

GWH synthesized all compounds except **14-19**, expressed protein, and carried out and analyzed all TE reactions except for those involving **17-19**, and performed the kinetic analyses for all except **17-19**. **JTCB** synthesized and carried out all analysis on **17-19** and expressed protein. **RDS** also synthesized **14-16**. **M. Wirz** and **WZ** carried out initial synthetic studies. **M. Wang** cloned the expression vectors for the TEs used. **LIS** and **MEH** carried out the lyophilization stability study. **GWH, JTCB,** and **CNB** wrote the manuscript with input from all authors.

Copyright

Organic & Biomolecular Chemistry

PAPER

View Article Online
View Journal | View Issue

Cite this: *Org. Biomol. Chem.*, 2018, **16**, 5771

Chemoenzymatic macrocycle synthesis using resorcylic acid lactone thioesterase domains†

Graham W. Heberlig,[a] Jesse T. C. Brown,[a] Ryan D. Simard,[a] Monica Wirz,[a] Wei Zhang,[a] Meng Wang,[b] Leah I. Susser,[a] Mark E. Horsman[a] and Christopher N. Boddy*[a]

A key missing tool in the chemist's toolbox is an effective biocatalyst for macrocyclization. Macrocycles limit the conformational flexibility of small molecules, often improving their ability to bind selectively and with high affinity to a target, making them a privileged structure in drug discovery. Macrocyclic natural product biosynthesis offers an obvious starting point for biocatalyst discovery *via* the native macrocycle forming biosynthetic mechanism. Herein we demonstrate that the thioesterase domains (TEs) responsible for macrocyclization of resorcylic acid lactones are promising catalysts for the chemoenzymatic synthesis of 12- to 18-member ring macrolactones and macrolactams. The TE domains responsible for zearalenone and radicicol biosynthesis successfully generate resorcylate-like 12- to 18-member macrolactones and a 14-member macrolactam. In addition these enzymes can also macrolactonize a non-resorcylate containing depsipeptide, suggesting they are versatile biocatalysts. Simple saturated omega-hydroxy acyl chains are not macrocyclized, nor are the alpha-beta unsaturated derivatives, clearly outlining the scope of the substrate tolerance. These data dramatically expand our understanding of substrate tolerance of these enzymes and are consistent with our understanding of the role of TEs in iterative polyketide biosynthesis. In addition this work shows these TEs to be the most substrate tolerant polyketide macrocyclizing enzymes known, accessing resorcylate lactone and lactams as well as cyclicdepsipeptides, which are highly biologically relevant frameworks.

Received 26th June 2018,
Accepted 20th July 2018

DOI: 10.1039/c8ob01512k

rsc.li/obc

Introduction

Enzymatic reactions are increasingly important in chemical synthesis and small molecule manufacturing.[1–6] They are particularly effective at accessing high purity stereogenic elements in the early stages of synthetic routes but have rarely been applied in the late stages of complex molecule formation. Their enormous rate enhancements and high levels of chemo-, regio- and stereoselectivity under mild reaction conditions are well suited for late stage chemistry such as macrocyclization. The use of enzymes to construct these systems is even more relevant given that the chemical synthesis of macrocycles continues to be a significant challenge.[7–11]

Macrocyclic natural product biosynthesis provides an obvious starting place for identification of an enzyme for late stage enzymatic macrocyclization. In polyketide biosynthesis macrolactones are generated from linear precursors by the C-terminal thioesterase (TE) domain of polyketide synthases (PKSs).[12] This enzyme releases the completed acyl chain, which is covalently linked through a thioester bond to the PKS, through macrolactonization,[12] hydrolysis[13,14] or in rare cases transesterification.[15]

Herein we identify two promising macrolactonizing TEs from resorcylic acid lactone (RAL) biosynthesis that can affect macrocyclization of benzoate containing substrates, which mimic the native resorcylate group, generating 12- to 18-member macrolactones and a 14-member macrolactam. In addition, these TEs macrocyclize a substrate lacking the resorcylate mimic and instead possessing an amino acid residue. The tolerance of these TEs for diverse carboxylate and nucleophile termini of the substrates is the broadest of known polyketide TE domains and suggest they may serve as platforms for the future development of macrocylization biocatalysts.

Results

RALs are a class of fungal polyketide natural products that contain the 2,4-dihydroxybenzoate moiety fused typically with

[a]*Department of Chemistry and Biomolecular Sciences, Centre for Catalysis Research and Innovation, University of Ottawa, Ottawa, ON, K1N 6N5, Canada. E-mail: cboddy@uottawa.ca*
[b]*Key Laboratory of Systems Microbial Biotechnology, Tianjin Institute of Industrial Biotechnology, Chinese Academy of Sciences, Tianjin, 300308 China*

†Electronic supplementary information (ESI) available: Additional HPLC traces, kinetic characterization, additional synthetic protocols, and characterization data of selected compounds. See DOI: 10.1039/c8ob01512k

a 14-member macrolactone. Radicicol **1**, an HSP90 inhibitor, and zearalenone **2**, an estrogen receptor agonist (Fig. 1), are typical examples of this class of compounds[16] and we have previously shown that the TEs from both of these pathways (Rdc TE and Zea TE) are stereo-tolerant[17] and highly efficient.[18]

To further evaluate the ring size substrate scope of these enzymes, we synthesized precursors of 10 through 18-member lactones. A representative synthesis of the 14-member ring substrate **6** is shown in Scheme 1. These syntheses relied on a convergent ring closing metathesis (RCM) based route that concomitantly provided a synthetic standard of the macrolactone product. **7**–**9** were synthesized following a similar route with comparable yields. RCM failed to produce any macrocycle in the case of the 10-member ring substrate **11**, thus the route was revised to rely on an intermolecular cross metathesis as shown in Scheme 1. All of the substrates were activated as *N*-acetyl cysteamine (SNAC) thioesters, which act as a mimic of the native phosphopantetheine linker.

Kinetic analysis of 14-member macrolactone formation was monitored by discontinuous HPLC-based assays of recombinant purified Rdc TE[17] treated with **6** (pH 7.4 phosphate buffer 10% v/v DMSO). All time points were within the linear range of initial velocities for macrolactone formation and the HPLC traces showed negligible by-products, such as hydrolysis and glycerolysis (Fig. 2). The no enzyme control and boiled enzyme controls showed no reaction. Rdc TE macrolactonized **6** with k_{cat} = 1.14 ± 0.11 s^{-1}, K_M = 0.71 ± 0.18 mM, and k_{cat}/K_M = 1.61 × 10^3 ± 0.61 × 10^3 M^{-1} s^{-1}. The k_{cat}/K_M compares well to the value previously reported for Zea TE with **6** (2.92 × 10^3 ± 0.16 × 10^3 M^{-1} s^{-1}).[18]

The reactions of 16-member ring substrate **8** and 18-member ring substrate **9** with Rdc TE and Zea TE proceeded with similar efficiency as the 14-member ring substrate **6**

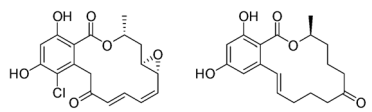

Fig. 1 The structures of two resorcylic acid lactones.

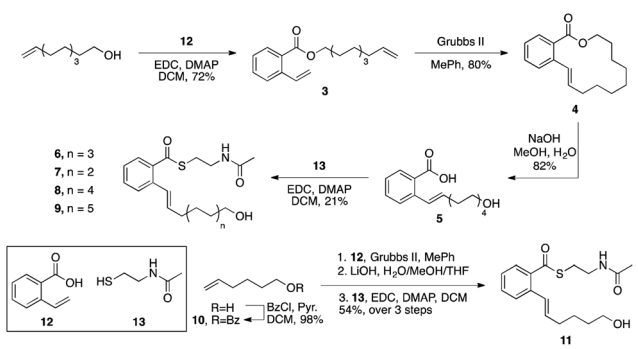

Scheme 1 The structures and representative syntheses of substrates used to probe the ring size selectivity of RAL TEs.

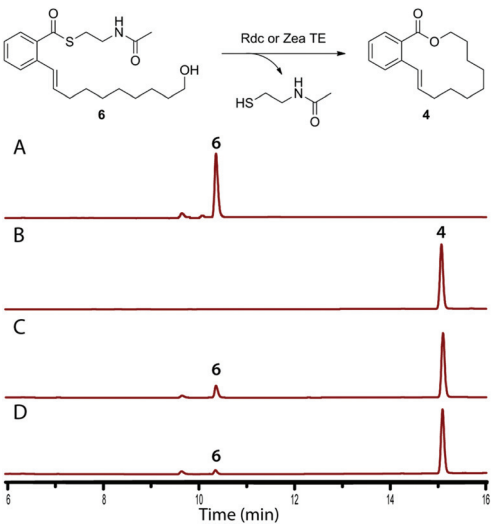

Fig. 2 Thioesterase reaction converting **6** into macrolactone **4**. HPLC traces demonstrating that RAL TEs can macrocyclize **6**, generating **4**. A 1 mM **6** with no-enzyme for 2 h. B. Authentic **4** standard. C. 5 μM Rdc TE incubated with 1 mM **6** for 2 h. D. 5 μM Zea TE incubated with 1 mM **6** for 2 h. HPLC conditions: Zorbax C18 column (50 × 2.1 mm) with a gradient elution 15% B to 95% B over 18 min (A: water, B: acetonitrile) and a flow rate of 0.2 mL min^{-1}.

(Fig. S5, Fig. S6†). The fidelity of macrolactonization with 12-member ring substrate **7** was less than that with 14- and larger macrolactones. While 12-member ring macrocycle was generated, the predominant product was a linear dimer with the SNAC thioester still attached (**S15**) (Fig. S4, S11, and S12†). However, no macrodiolide product was observed. The concentration of substrate was varied to determine if linear dimer formation was an artifact of the high substrate concentrations used in the enzymatic reaction however the product profile was identical at both 1.0 mM and 0.2 mM **7**. Non-native dimer formation was previously observed with the 6-deoxyerythronolide B thioesterase (DEBS TE)[19] and is consistent with the mechanism for dimer formation.[20,21]

Macrolactonization of the 10-member ring substrate **11** was not observed with either Rdc TE or Zea TE. This is not surprising as our attempts to generate a macrolactone standard were unsuccessful using the Grubbs II RCM strategy.

Similarly, attempts to cyclize the seco-acid *via* Keck, Yamaguchi, Corey-Nicolaou, and Mitsunobu conditions all failed. The primary product of the reaction of **11** with Rdc and Zea TE was the hydrolysis product. However, some of the substrate was converted to unidentified multimeric products.

To compare the enzymatic activity of the two TEs across the various ring size substrate, v_{rel} values were obtained by incubating the substrates with the TEs and quantifying the amount of SNAC released with Ellman's reagent. The results are summarized in Table 1.

The slow processing of the 10-member substrate **11**, coupled with the enzymes' inability to form the macrolactone establishes a clear lower limit to the ring size these enzymes can generate. The 12-member substrate **7** was processed less

Table 1 Relative initial velocities for macrocylization with 1 mM substrate and 5 μM RAL and Zea TE

Substrate	Ring size	v_{rel} Rdc TE	v_{rel} Zea TE
11	10	$\sim 10^{-4} \pm 10^{-4}$	$\sim 10^{-4} \pm 10^{-4}$
7	12	0.19 ± 0.06	0.88 ± 0.01
6	14	0.66 ± 0.02	1.00 ± 0.03
8	16	3.13 ± 0.01	1.89 ± 0.05
9	18	0.22 ± 0.05	0.55 ± 0.17
16	*Aza*-14	0.32 ± 0.06	0.11 ± 0.01
17	*unsat*-14	0.02 ± 0.01	0.04 ± 0.03
18	*sat*-14	0.02 ± 0.01	0.05 ± 0.01
19	*gly*-14	0.65 ± 0.09	0.39 ± 0.03

efficiently than the 14-member substrate **6**, which coupled with the unwanted dimer formation, limits the use of these TEs for 12-member rings. Macrolactones with ring sizes of 14 and larger would appear to be promising candidates for macrolactonization with either of these TEs.

To assess the ability of these TEs to function on a synthetically relevant scale, reactions with **8** and **9** were carried out on 2 mg of substrate with both Rdc and Zea TE. The reaction progress was monitored by HPLC. **8** was quantitatively converted to macrocycle within 5 hours, while **9** required 24 hours with an additional aliquot of TE to achieve quantitative conversion. The 16- and 18-member macrolactones were recovered and isolated in 65% and 71% yield respectively for Rdc TE and 88% and 90% yield respectively for Zea TE.

A TE capable of also generating macrolactams would be of significantly expanded utility. To assess the ability of the Zea and Rdc TEs to form macrolactams, the amine containing analog of the 14-member substrate **16** was generated from intermediate **5** (Scheme 2). The ability of the Rdc and Zea TEs to macrolactamize substrate **16** was assayed by incubation with the TEs under typical reaction conditions (Fig. 3). Both TEs were able to macrolactamize this substrate, generating the amide containing product with lower v_{rel} values as compared to macrolactonization of **6** (Table 1, Line 6).

While the Zea and Rdc TEs were very similar in respect to macrolactone formation, the Rdc TE was a better catalyst with respect to macrolactam formation. The Zea TE required higher catalyst loadings to achieve the same processivity as the Rdc TE. The ability to form both macrolactones and macrolactams is a rare feature previously observed only for TEs from the non-ribosomal peptide synthetase biosynthetic pathways for tyrocidine and A54145.[22,23]

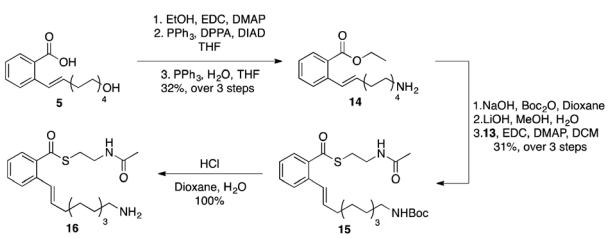

Scheme 2 Synthesis of the aza substrate analog **16**.

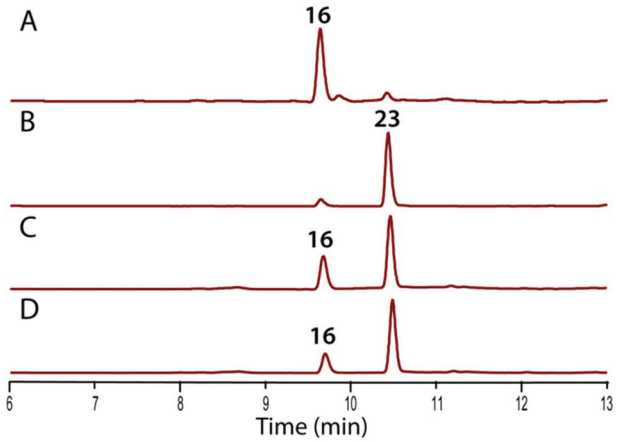

Fig. 3 HPLC traces demonstrating that RAL TEs can macrolactamize **16**, generating **S13**. A 1 mM **16** with no-enzyme, 2 h. B. Authentic macrolactam standard (**23**). C. 5 μM Rdc TE incubated with 1 mM **16** for 2 h. D. 25 μM Zea TE incubated with 1 mM **16** for 2 h. HPLC conditions: Zorbax C18 column (50 × 2.1 mm) with a gradient elution 15% B to 95% B over 18 min (A: water, B: acetonitrile) and a flow rate of 0.2 mL min^{-1}.

To investigate the ability of Zea and Rdc TEs to accept non-benzoate-based substrates, a panel of three 14-member ring forming substrates was generated, **17**, **18**, and **19** (Fig. 4). Incubation of each substrate for 18 h with each TE followed by HPLC analysis showed that **19** was converted to the expected

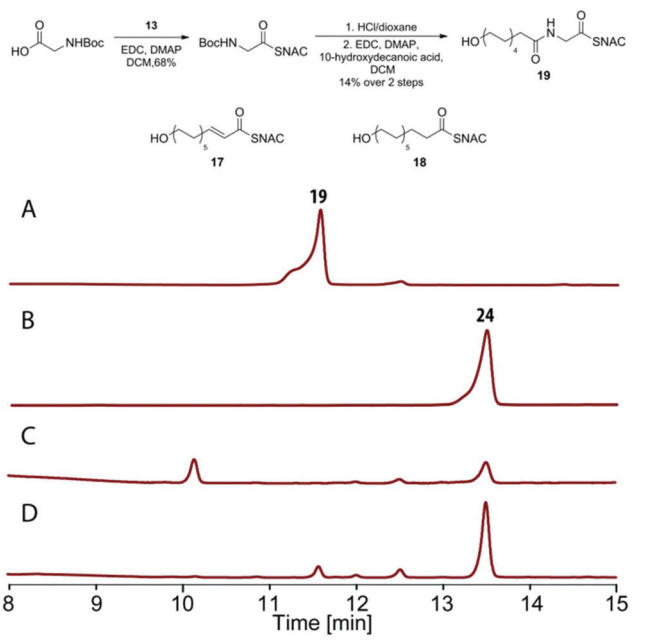

Fig. 4 Substrates **17**, **18**, and **19** and the conversion of **19** into macrocycle by Zea and Rdc TEs. A. 1 mM **19** with no-enzyme, 18 h. B. Authentic macrolactone standard (**24**). C. 5 μM Rdc TE incubated with 1 mM **19** for 18 h. D. 5 μM Zea TE incubated with 1 mM **19** for 18 h. HPLC conditions: Leapsil C18 column (100 × 2.1 mm) with a gradient of 0% B to 100% B over 35 minutes (A: water, B: acetonitrile) with a flow rate of 0.4 mL min^{-1}.

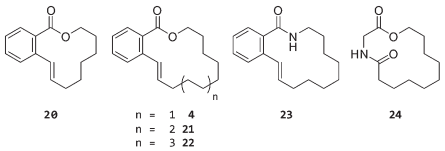

Fig. 5 Currently described macrocylization scope of the resorcylic acid lactone thioesterase domains Rdc TE and Zea TE.

macrocycle **24** (90% and 55% conversion with Zea TE and Rdc TE respectively, Fig. 5), whereas **17** and **18** generated no detectable macrocycle (Fig. 4). Similarly, v_{rel} data showed **19** was effectively processed by the TEs in a thiol release assay whereas **17** and **18** were poor substrates (Table 1). These data confirm that both RAL TEs are tolerant to some non-benzoate based substrates, such as a substrate with a C-terminal glycine residue, significantly expanding the potential scope of these catalysts to cyclic depsipeptide formation. However both TEs are unable to process simple saturated and α,β-unsaturated thioester substrates consistent with the role of these TEs as gatekeepers in fungal polyketide biosynthesis.[12]

In addition to the ring size tolerance, nucleophile tolerance, and ability to macrocyclize non-benzoate based substrates, the RAL TEs show excellent stability and tolerance to organic solvent, both important features for use as a biocatalyst. For example, lyophilized Rdc TE stored at room temperature for >10 weeks could be resuspended in reaction buffer and retain macrocyclization activity (Fig. S8†). Similarly, fresh Rdc TE could function with little impact on activity in up to 40% DMSO by volume (Fig. S2†). This stability is in stark contrast to DEBS TE, a bacterial macrocyclizing TE, that is known to have a surprisingly low T_m.[24]

In this work we identify the Zea TE and Rdc TE from the fungal biosynthetic pathways for zearaleneone and radicicol, which in their native pathways catalyze 14-member macrolactone formation, as promising, substrate tolerant macrocyclization biocatalysts. There are limited examples of macrocyclizing biocatalysts, particularly for non-peptidic compounds. While lipases have been shown to affect macrolactonization,[25–29] these catalysts are plagued by low reactivity (2–7 day reaction times), and sensitivity to external nucleophiles.[28] Macrocyclizing enzymes from natural product biosynthesis have proven to be promising macrocyclizing biocatalysts. For example, the TE from non-ribosomal peptide (NRP) biosynthetic pathway for tyrocidine can load and cyclize over 100 tyrocidine analogs.[30,31] While this catalyst is broadly substrate tolerant, it relies on hydrogen-bond mediated substrate preorganization to ensure macrocyclization that is unlikely to be applicable for non-peptide based substrates.[12]

Discussion

TEs from bacterial polyketide biosynthetic pathways have been investigated for their macrocycle forming capability.[19,32–35] The TEs responsible for macrocyclization of epothilone, deoxyerythronolide, and pikromycin have been characterized *in vitro* and been shown to be moderately efficient catalysts (k_{cat}/K_M 1–30 M^{-1} s^{-1})[19,32–36] with high and capricious substrate selectivity. Even with a growing high-resolution understanding of the enzyme–substrate interactions in TE-mediated macrocyclization, no clear model has yet emerged to rationalize and predict the reactivity of these TEs.[24,37–40]

Our work demonstrates that the fungal RAL TEs possess key properties needed for a macrocyclization catalyst. They are efficient TEs (k_{cat}/K_M 1–3 × 10^3 M^{-1} s^{-1}) and relatively insensitive to external nucleophiles, enabling their use in aqueous conditions while limiting dimer and higher order oligomer formation. They show high substrate tolerance to absolute stereochemistry[17] and ring sizes between 12 to 18-member macrolactones. In addition the Rdc TE is flexible enough to accommodate macrolactamization, demonstrating an expanded range of chemistries is possible.

Intriguingly these TEs can accommodate replacement of the conserved benzoate moiety from RALs with a glycine. Zea TE has been shown to load benzyol thioesters significantly faster than alkyl thioesters.[24] This is proposed to prevent premature off-loading of incomplete β-ketothioester substrates prior to resorcylate formation.[12] While the results from the saturated (**18**) and α,β-unsaturated (**17**) substrates are consistent with this hypothesis, the glycyl thioester substrate (**19**) is not. As these TE and their evolutionary ancestors have not been challenged with glycyl-based substrates, there would have been no need to screen against reactivity with these substrate types. Presumably the amide is able to avoid or overcome the unfavorable interactions that limit reactivity of β-keto, α,β-unsaturated, and saturated substrates. Regardless as both TEs can accommodate the glycyl substitution, the scope of these TEs can be significantly expanded to include cyclic depsipeptide formation.

Conclusions

These RAL TEs are the most substrate tolerant polyketide TEs identified to date. Coupled with their ability to retain activity after lyophilization and function with a high level of organic co-solvent, these enzymes appear very well suited for biocatalysis applications. Using modern protein engineering approaches, these lead enzymes should be amenable to engineering for macrocyclization of a wide range of substrates for natural product synthesis and medicinal chemistry studies.

Experimental section

General synthetic protocols

All reagents were purchased from Sigma-Aldrich at the highest available purity and used without further purification. All solvents were purchased from Fisher Scientific. All reactions were conducted using dry solvents under an argon atmosphere

unless otherwise noted. NMR spectroscopy, with the exception of LC-SPE-NMR, was performed with a Bruker Avance II, operating at 400 MHz for ^{1}H spectra, and 100 MHz for ^{13}C spectra. HPLC analysis was conducted with an Agilent 1260 Modular system using an Agilent Zorbax C18 100 × 2.1 mm column. LC-SPE-NMR experiments were conducted using the same Agilent 1260 HPLC system and column with a Prospekt 2 (Spark Holland) solid-phase extraction module using HySphere Resin GP cartridges. Compounds were eluted off the cartridges with d_3-acetonitrile and analyzed by mass spectroscopy and ^{1}H NMR using a Bruker Avance III, with cryoprobe operating at 600 MHz. High-resolution mass spectroscopy (HRMS) was conducted on a Micromass Q-TOF I for ESI measurements and a Kratos Concept 1S High Resolution Mass Spectrometer for EI measurements (John L. Holmes Mass Spectroscopy Facility).

(*E*)-3,4,5,6,7,8,9,10-Octahydro-1*H*-benzo[*c*][1] oxacyclotetradecin-1-one (4)

To 105 mL dry toluene was added 120 mg **3** (0.42 mmol) under argon, to this stirred solution 18 mg of Grubbs 2nd Gen. catalyst (0.02 mmol, 5 mol%) was added. The reaction was stirred at 80 °C for 24 hours. At completion the reaction was concentrated and purified by column chromatography (95 : 5 hexanes : EtOAc), yielding 96 mg (89%) of the title compound as a colorless oil. R_f = 0.78 (9 : 1 hexanes : EtOAc) IR (NaCl) ν_{max} = 2930, 2853, 1705, 1200, 1254 cm^{-1}. ^{1}H NMR (400 MHz, $CDCl_3$) δ 7.82 (dd, J = 7.8, 1.1 Hz, 1H), 7.48 (dd, J = 4.3, 3.6 Hz, 1H), 7.41 (ddd, J = 7.9, 7.3, 1.0 Hz, 1H), 7.26 (dt, J = 5.6, 2.9 Hz, 1H), 6.91 (d, J = 15.7 Hz, 1H), 5.93 (dt, J = 15.6, 7.1 Hz, 1H), 4.36–4.32 (m, 2H), 2.28 (ddd, J = 12.1, 7.2, 1.4 Hz, 2H), 1.79–1.69 (m, 2H), 1.57–1.31 (m, 10H). ^{13}C NMR (100 MHz, $CDCl_3$) δ 169.16, 138.35, 133.24, 131.65, 130.55, 130.10, 129.43, 127.33, 126.67, 65.49, 30.72, 27.19, 26.65, 26.56, 24.15, 23.89, 23.21. HRMS (+EI): calcd for $C_{17}H_{22}O_2$ (M) 258.1620, obsd 258.1618.

(*E*)-2-(10-Hydroxydec-1-en-1-yl)benzoic acid (5)

In a 10 mL round bottom 96 mg **4** (0.371 mmol) was dissolved in 4 : 1 : 3 methanol : water : THF (8 mL total) and to this 156 mg of LiOH (3.71 mmol, 10 eq.) was added. The reaction was stirred over night at 50 °C. At completion the reaction was diluted with water and the pH was adjusted to 2 using 10% HCl. This was extracted 3 × 10 mL with EtOAc and the organic fractions were combined, dried over Na_2SO_4, and concentrated *in vacuo*. This yielded 83 mg seco-acid **5** (80%) as a clear oil. R_f = 0.22 (1 : 1 EtOAc : hexanes). ^{1}H NMR (400 MHz, $CDCl_3$) δ 7.94 (dd, J = 7.9, 0.9 Hz, 1H), 7.52 (d, J = 7.4 Hz, 1H), 7.48–7.43 (m, 1H), 7.27 (dd, J = 10.3, 3.6 Hz, 1H), 7.18 (d, J = 15.8 Hz, 1H), 6.08 (dt, J = 15.6, 7.0 Hz, 1H), 3.66 (t, J = 6.4 Hz, 2H), 2.28–2.20 (m, 2H), 1.61–1.31 (m, 10H). ^{13}C NMR (100 MHz, $CDCl_3$) δ 171.67, 140.45, 134.22, 132.59, 131.03, 128.94, 127.52, 127.26, 126.54, 63.03, 32.81, 32.45, 29.18, 29.08, 28.79, 28.53, 25.46. HRMS (+EI): calcd for $C_{17}H_{24}O_3$ (M) 276.1725, obsd 276.1719.

(*E*)-*S*-(2-Acetamidoethyl) 2-(10-hydroxydec-1-en-1-yl) benzothioate (6)

In 4 mL of dry DCM, 101 mg of **5** (0.365 mmol) was added with stirring. To this mixture 42.6 μL of HSNAC (0.401 mmol, 1.1 eq.), 91 mg of EDC (0.475 mmol, 1.3 eq.), and 4.5 mg DMAP (0.037 mmol, 0.1 eq.) were added under an argon atmosphere. The reaction mixture was stirred overnight at room temperature. At completion the reaction was quenched by the addition of sat. NH_4Cl, the organic layer was separated and the remaining aqueous layer was extracted 3 × 10 mL DCM. The combined organic fractions were pooled, dried with Na_2SO_4 and concentrated *in vacuo* and purified by column chromatography (1 : 1 acetone : hexanes) to yield 29 mg (21%) of **6** as a slightly yellow oil. R_f = 0.23 (1 : 1 hexanes : acetone) IR (NaCl) ν_{max} = 2930, 2853, 1705, 1200, 1254 cm^{-1}. ^{1}H NMR (400 MHz, $CDCl_3$) δ 7.71–7.66 (m, 1H), 7.53 (d, J = 7.8 Hz, 1H), 7.41 (t, J = 7.3 Hz, 1H), 7.27–7.21 (m, 1H), 6.75 (d, J = 15.7 Hz, 1H), 6.16 (dt, J = 15.6, 7.0 Hz, 1H), 6.13 (s, 1H), 3.61 (t, J = 6.6 Hz, 2H), 3.51 (q, J = 6.3 Hz, 2H), 3.17 (t, J = 6.5 Hz, 2H), 2.18 (dt, J = 7.7, 4.0 Hz, 2H), 1.95 (s, 3H), 1.57–1.27 (m, 10H). ^{13}C NMR (100 MHz, $CDCl_3$) δ 194.78, 170.43, 136.64, 135.75, 134.84, 131.96, 128.41, 127.13, 126.98, 126.63, 62.97, 39.73, 33.12, 32.77, 29.34 (2C), 29.30, 29.05, 28.99, 25.69, 23.22. HRMS (ESI+): calcd for $C_{21}H_{31}NO_3S$ 400.1922 (M + Na), obsd 400.1920.

(*E*)-*S*-(2-Acetamidoethyl) 2-(8-hydroxyoct-1-en-1-yl)benzothioate (7)

In 2 mL of dry DCM 86 mg of **S3** (0.346 mmol) was added with stirring. To this mixture 40.5 μL of HSNAC (0.381 mmol, 1.1 eq.), 87 mg of EDC (0.450 mmol, 1.3 eq.), and 4 mg DMAP (0.035 mmol, 0.1 eq.) were added under an argon atmosphere. The reaction mixture was stirred overnight at room temperature. At completion the reaction was quenched by the addition of sat. NH_4Cl, the organic layer was separated and the remaining aqueous layer was extracted 3 × 10 mL DCM. The combined organic fractions were pooled, dried with Na_2SO_4 and concentrated *in vacuo* and purified by column chromatography (6 : 4 acetone : hexanes) to yield 80 mg (66%) of **7** as a slightly yellow oil. R_f = 0.44 (1 : 1 hexanes : acetone) IR (NaCl) ν_{max} = 3282 (br), 3066, 2931, 2858, 1653, 1191 cm^{-1}. ^{1}H NMR (400 MHz, $CDCl_3$) δ 7.71 (dd, J = 7.8, 0.9 Hz, 1H), 7.53 (d, J = 6.6 Hz, 1H), 7.43 (dd, J = 10.8, 4.3 Hz, 1H), 7.30–7.22 (m, 2H), 6.75 (d, J = 15.8 Hz, 1H), 6.31 (s, 1H), 6.14 (dt, J = 15.7, 6.9 Hz, 1H), 3.65 (t, J = 6.5 Hz, 2H), 3.56–3.47 (m, 2H), 3.18 (t, J = 6.5 Hz, 2H), 2.27–2.17 (m, 2H), 1.99 (s, 3H), 1.62–1.33 (m, 8H). ^{13}C NMR (100 MHz, $CDCl_3$) δ 194.77, 170.44, 136.72, 135.70, 134.55, 132.02, 128.44, 127.46, 127.08, 126.67, 62.89, 39.69, 32.84, 32.79, 29.25, 28.84, 28.67, 25.45, 23.23. HRMS (+EI): calcd for $C_{15}H_{19}O_2$ (M − $SC_2H_4NHCOCH_3$) 231.1385, obsd 231.1365.

(*E*)-*S*-(2-Acetamidoethyl) 2-(12-hydroxydodec-1-en-1-yl) benzothioate (8)

In a 10 mL round bottom flask was combined 200 mg **S6** (0.33 mmol, 1 eq.), 52 μL HSNAC (0.5 mmol, 1.5 eq.), 96 mg

EDC (0.5 mmol, 1.5 eq.), and 4 mg DMAP (0.033 mmol, 0.1 eq.) in 2 mL anhydrous DCM. The reaction was stirred under argon, overnight at room temperature. The reaction was quenched by the addition of sat. NH_4Cl, and the organic layer was removed. The aqueous remainder was extracted with DCM. The combined organic fractions were washed with brine, dried over Na_2SO_4, and concentrated. The compound was purified by column chromatography (100% EtOAc) yielding 76 mg of **8** (30%) as a thick oil. R_f = 0.48 (1 : 1 hexanes : acetone) IR (NaCl) ν_{max} = 3755, 3285 (br), 2928, 2856, 1662, 1189, 1098 cm^{-1}. ^1H NMR (400 MHz, $CDCl_3$) δ 7.70 (ddd, J = 7.8, 1.4, 0.6 Hz, 1H), 7.54 (ddd, J = 7.9, 0.7, 0.5 Hz, 1H), 7.42 (dddd, J = 7.8, 7.4, 1.4, 0.6 Hz, 1H), 7.25 (ddd, J = 7.7, 7.5, 1.3 Hz, 1H), 6.77 (d, J = 15.7 Hz, 1H), 6.17 (dt, J = 15.7, 7.0 Hz, 1H), 5.92 (bs, 1H), 3.62 (t, J = 6.6 Hz, 2H), 3.53 (dt, J = 6.5, 6.2 Hz, 2H), 3.19 (t, J = 6.2 Hz, 2H), 2.25–2.15 (m, 2H), 1.97 (s, 3 H), 1.64–1.49 (m, 4H), 1.49–1.39 (m, 2H), 1.38–1.24 (m, 10H). ^{13}C NMR (75 MHz, $CDCl_3$) δ 194.8 170.3, 136.7, 135.7, 135.0, 132.0, 128.4, 127.0, 127.0, 126.6, 63.1, 39.8, 33.2, 32.8, 31.6, 29.5, 29.5, 29.4, 29.4, 29.2, 25.7, 22.7, 14.1 HRMS (+EI): calcd for $C_{23}H_{35}NO_3S$ (M) 405.2338, obsd 405.2356.

(*E*)-*S*-(2-Acetamidoethyl) 2-(14-hydroxytetradec-1-en-1-yl) benzothioate (9)

In a 10 mL round bottom flask was combined 105 mg **S8** (0.31 mmol, 1 eq.), 50 μL HSNAC (0.47 mmol, 1.5 eq.), 91 mg EDC (0.47 mmol, 1.5 eq.), and 4 mg DMAP (0.033 mmol, 0.1 eq.) in 2 mL anhydrous DCM. The reaction was stirred under argon, overnight at room temperature. The reaction was quenched by the addition of sat. NH_4Cl, and the organic layer was removed. The aqueous remainder was extracted with DCM. The combined organic fractions were washed with brine, dried over Na_2SO_4, and concentrated. The compounds was purified by column chromatography (100% EtOAc) yielding 104 mg of **9** (77%) as a waxy solid. R_f = 0.51 (1 : 1 hexanes : acetone) IR (NaCl) ν_{max} = 3287 (br), 3072, 2926, 2853, 1655, 1187 cm^{-1}. ^1H NMR (400 MHz, $CDCl_3$) δ 7.70 (dd, J = 7.8, 1.0 Hz, 1H), 7.53 (d, J = 7.8 Hz, 1H), 7.41 (t, J = 7.2 Hz, 1H), 7.26–7.21 (m, 2H), 6.76 (d, J = 15.7 Hz, 1H), 6.17 (dt, J = 15.6, 6.9 Hz, 1H), 6.00 (s, 1H), 3.61 (t, J = 6.6 Hz, 2H), 3.52 (dd, J = 12.4, 6.1 Hz, 2H), 3.18 (t, J = 6.4 Hz, 2H), 2.19 (dt, J = 8.0, 4.1 Hz, 2H), 1.96 (s, 3H), 1.58–1.49 (m, 2H), 1.47–1.40 (m, 2H), 1.32–1.23 (m, 16H). ^{13}C NMR (100 MHz, $CDCl_3$) δ 194.78, 170.36, 136.69, 135.70, 135.00, 131.97, 128.43, 127.02, 126.99, 126.61, 63.04, 39.79, 33.26, 32.81, 29.60, 29.58 (2C), 29.55, 29.47, 29.41, 29.35, 29.23, 29.22, 25.74, 23.24. HRMS (+EI): calcd for $C_{21}H_{32}O_2$ (M − $SC_2H_4NHCOCH_3$) 314.2246, obsd 314.2247.

Hex-5-en-1-yl benzoate (10)

To a 25 mL round bottom flask charged with 7.5 mL of DCM was added 360 μL of 5-hexen-1-ol (3 mmol), 544 μL of triethylamine (TEA, 3.9 mmol, 1.3 eq.), and 73 mg of 4-(dimethylamino)pyridine (DMAP, 0.6 mmol, 0.2 eq.). This mixture was cooled to 0 °C in an ice bath. To this 522 μL of benzoyl chloride was added dropwise with stirring. The reaction mixture was allowed to come to room temperature and stirring was continued overnight. Upon completion the reaction mixture was concentrated *in vacuo* and purified by column chromatography, hexanes (hex) : ethyl acetate (EtOAc) 9 : 1. Yielding 613 mg (98%) of the expected product. Characterization consistent with previously reported data.[41] R_f = 0.66 9 : 1 Hex : EtOAc. ^1H NMR (400 MHz, $CDCl_3$) δ 8.07–7.99 (m, 2H), 7.57–7.49 (m, 1H), 7.46–7.38 (m, 2H), 5.80 (ddt, J = 16.9, 10.2, 6.7 Hz, 1H), 5.02 (ddd, J = 17.1, 3.6, 1.6 Hz, 1H), 4.96 (ddt, J = 10.2, 2.1, 1.2 Hz, 1H), 4.31 (t, J = 6.6 Hz, 2H), 2.16–2.07 (m, 2H), 1.82–1.72 (m, 2H), 1.59–1.49 (m, 2H).

(*E*)-*S*-(2-Acetamidoethyl) 2-(6-hydroxyhex-1-en-1-yl) benzothioate (11)

To a 50 ml round bottom flask, 600 mg **10** (2.93 mmol, 5 eq.) and 104 mg **12** (ethyl 2-vinyl benzoate)[17] (0.59 mmol, 1 eq.) was added to 3 ml dichloromethane (DCM), under argon atmosphere. 25 mg of Grubbs 2nd generation catalyst (0.03 mmol, 5 mol%) was then added and the reaction was heated to reflux with stirring for 12 hours. The dark solution was passed through a plug of silica to remove solid impurities and evaporated. From combined reactions 600 mg (1.7 mmol, 1 eq.) of crude cross metathesis product was combined with 713 mg LiOH (17 mmol, 10 eq.) in a methanol/THF/water blend (23 mL total volume) and stirred at room temperature for 4 hours. The reaction was diluted with water and adjusted to pH = 2 with 10% HCl. This mixture was extracted 3 times with EtOAc and the combined organic fractions were combined, dried over Na_2SO_4, and concentrated *in vacuo*. Yielding 110 mg crude seco-acid which was added to 3 mL DCM, to which was added 59 μL *N*-acetylcysteamine (**13**, HSNAC, 0.55 mmol, 1.1 eq.), 125 mg 1-ethyl-3-(3-dimethylaminopropyl)carbodiimide (EDC, 0.65 mmol, 1.3 eq.), and 6 mg DMAP (0.05 mmol, 0.1 eq.). The reaction was stirred overnight at room temperature. The reaction was quenched by the addition of sat. NH_4Cl and the organic layer was separated. The residual aqueous layer was extracted 3 × 10 mL DCM and the combined organic fractions were combined, dried over Na_2SO_4, and concentrated *in vacuo*. The title compound was purified by column chromatography (6 : 4 acetone : hexanes) yielding 87 mg as a slightly yellow oil (54%). R_f = 0.17 (1 : 1 hexanes : acetone) IR (NaCl) ν_{max} = 3745, 3286 (br), 2920, 2854, 1655, 1195, 1090 cm^{-1}. ^1H NMR (400 MHz, $CDCl_3$) δ 7.69 (dd, J = 7.8, 1.2 Hz, 1H), 7.52 (d, J = 7.5 Hz, 1H), 7.45–7.40 (m, 1H), 7.28–7.23 (m, 1H), 6.78 (d, J = 15.7 Hz, 1H), 6.15 (dt, J = 15.7, 6.8 Hz, 1H), 6.02 (s, 1H), 3.66 (t, J = 6.3 Hz, 2H), 3.53 (dd, J = 12.4, 6.2 Hz, 2H), 3.19 (t, J = 6.4 Hz, 2H), 2.25 (qd, J = 7.0, 1.4 Hz, 2H), 1.97 (s, 3H), 1.67–1.51 (m, 4H). ^{13}C NMR (100 MHz, $CDCl_3$) δ 194.85, 170.47, 136.55, 135.85, 134.22, 131.98, 128.35, 127.61, 127.06, 126.75, 62.75, 39.75, 32.72, 32.14, 29.36, 25.13, 23.21. HRMS (+EI): calcd for $C_{17}H_{23}NO_3S$ (M − $SC_2H_4NHCOCH_3$) 202.0993, obsd 202.0978.

(*E*)-Ethyl 2-(10-aminodec-1-en-1-yl)benzoate (14)

To a 100 mL round bottom 413 mg **5** (1.49 mmol) was added to 9 mL anhydrous DCM and 3.47 mL absolute ethanol

(5.94 mmol, 4 eq.). With stirring, 313 mg EDC (1.65 mmol, 1.1 eq.) and 22 mg DMAP (0.15 mmol, 0.1 eq.) was added. The reaction was at room temperature for 3 hours, then quenched by the addition of sat. NH_4Cl, the organic layer was removed and the aqueous remainder was extracted with DCM. The combined organic fractions were washed with brine, dried over Na_2SO_4, and concentrated to an oil. To a 10 mL round bottom flask charged with 3 mL anhydrous THF and equipped with a stir bar was added 354 mg triphenylphosphine (1.35 mmol, 1.5 eq.). The solution was cooled to −20 °C (salt/ice bath) and 266 μL diisopropyl azodicarboxylate (1.35 mmol, 1.5 eq.) was added dropwise. This was stirred at −20 °C for 10 minutes after which 275 mg of the crude ester (0.9 mmol) dissolved in 3 mL THF was added dropwise. The reaction was stirred for 30 minutes then allowed to warm to 0 °C, then 290 μL diphenylphosphoryl azide (1.35 mmol, 1.5 eq.) was added slowly with stirring. The reaction was stirred for an additional 5 minutes, followed by the addition of additional THF until a precipitate formed. The precipitate was removed, and the remaining liquid was subjected to a standard aqueous workup. The crude product was dissolved in 4 mL THF followed by 200 μL water. To the stirred solution was added 241 mg triphenylphosphine (0.92 mmol, 1.05 eq.) at room temperature, the reaction was stirred overnight, and quenched with sat. NH_4Cl. The organic layer was removed and the aqueous layer was extracted with THF. The combined organic fractions were washed with brine, over Na_2SO_4, and concentrated. The compound was purified by column chromatography (80 : 20 : 0.5 DCM : methanol : NH_4OH) yielding 154 mg **14** (32%, 3 steps). R_f = 0.5 (8 : 2 : 0.5 DCM : methanol : NH_4OH). ^{1}H NMR (400 MHz, $CDCl_3$) δ 8.27 (s, 2H), 7.81 (dd, J = 7.8, 1.2 Hz, 1H), 7.50 (d, J = 7.2 Hz, 1H), 7.43–7.36 (m, 1H), 7.24–7.20 (m, 1H), 7.09 (d, J = 15.7 Hz, 1H), 6.09 (dt, J = 15.7, 6.9 Hz, 1H), 4.34 (q, J = 7.1 Hz, 2H), 2.99–2.91 (m, 2H), 2.20 (q, J = 6.9 Hz, 2H), 1.78–1.70 (m, 2H), 1.49–1.28 (m, 13H). ^{13}C NMR (100 MHz, $CDCl_3$) δ 167.74, 139.50, 133.77, 131.77, 130.19, 128.55, 128.50, 127.14, 126.44, 60.92, 39.96, 33.19, 29.25, 29.23, 29.13, 28.93, 27.67, 26.48, 14.34. HRMS (+ESI): calcd for $C_{19}H_{29}NO_2Na$ (M + Na) 326.2096, obsd 326.2066

(*E*)-*S*-(2-Acetamidoethyl) 2-(10-((*tert*-butoxycarbonyl)amino) dec-1-en-1-yl)benzothioate (15)

To a 15 mL round bottom flask charged with 2 : 1 dioxane : water (7 mL total) was added 134 mg **14** (0.46 mmol) and the solution was cooled to 0 °C. With stirring 2.4 mL of a 5 N NaOH solution was added followed by 138 mg of di-*tert*-butyl dicarbonate (0.63 mmol, 1.35 eq.). The solution was warmed to room temperature and the reaction was stirred for 4 hours. Upon completion the reaction was concentrated to remove dioxane, the remaining aqueous portion was extracted with EtOAc, dried over Na_2SO_4, and concentrated. The residue was dissolved in 4 : 3 : 1 methanol : THF : water (6.5 mL total) and 196 mg LiOH (4.7 mmol, 10 eq.) was added, the reaction was stirred at 50 °C overnight. At completion the organic solvents were removed by rotary evaporation and the remaining aqueous fraction was carefully acidified to pH = 4 with citric acid. This was extracted 3 × 10 mL with EtOAc, the organic fractions were combined were washed with brine, over Na_2SO_4, and concentrated. In a 10 mL round bottom flask was combined 100 mg crude acid (0.27 mmol), 32 μL HSNAC (0.30 mmol, 1.1 eq.), 67 mg EDC (0.35 mmol, 1.3 eq.), and 4 mg DMAP (0.033 mmol, 0.1 eq.) in 2 mL anhydrous DCM. The reaction was stirred under argon, overnight at room temperature. The reaction was quenched by the addition of sat. NH_4Cl, and the organic layer was removed. The aqueous remainder was extracted with DCM. The combined organic fractions were washed with brine, dried over Na_2SO_4, and concentrated. The compound was purified by column chromatography (100% EtOAc) yielding 83 mg of **15** (31%, 3 steps) as a colorless oil. R_f = 0.43 (EtOAc). ^{1}H NMR (400 MHz, $CDCl_3$) δ 7.70 (dd, J = 7.8, 1.1 Hz, 1H), 7.54 (d, J = 7.9 Hz, 1H), 7.42 (t, J = 7.2 Hz, 1H), 7.27–7.22 (m, 1H), 6.76 (d, J = 15.7 Hz, 1H), 6.16 (dt, J = 15.7, 7.0 Hz, 1H), 5.97 (s, 1H), 4.50 (s, 1H), 3.53 (dd, J = 12.4, 6.3 Hz, 2H), 3.19 (t, J = 6.5 Hz, 2H), 3.13–3.04 (m, 2H), 2.20 (q, J = 6.9 Hz, 2H), 1.97 (s, 3H), 1.59–1.54 (m, 2H), 1.47–1.41 (m, 10H), 1.29 (s, 9H). ^{13}C NMR (100 MHz, $CDCl_3$) δ 194.75, 170.32, 136.64, 135.73, 134.86, 131.97, 128.44, 127.11, 126.99, 126.63, 40.64, 39.76, 33.17, 30.06, 29.33 (2C), 29.24, 29.11, 29.06, 28.44 (3C), 26.77, 23.26. HRMS (ESI+) calcd for $C_{26}H_{40}N_2O_4SNa$ (M + Na) 499.2606, obsd 499.2644.

(*E*)-*S*-(2-Acetamidoethyl) 2-(10-aminodec-1-en-1-yl) benzothioate (16)

In a 5 mL round bottom flask charged with 300 μL 4 N HCl/dioxane was added 30 mg **15** (0.06 mmol) at 0 °C. The reaction was allowed to warm to room temperature and was stirred for an additional 30 minutes. The reaction was evaporated and purified by preparatory TLC (80 : 20 : 2.5 DCM : methanol : NH_4OH) yielding 24 mg **16** (100%) as an oil. R_f = 0.21 (8 : 2 : 2.5 DCM : methanol : NH_4OH). ^{1}H NMR (400 MHz, MeOD) δ 7.69 (dd, J = 7.8, 0.9 Hz, 1H), 7.60 (d, J = 7.8 Hz, 1H), 7.47 (t, J = 7.2 Hz, 1H), 7.30 (dd, J = 10.9, 4.3 Hz, 1H), 6.75 (d, J = 15.7 Hz, 1H), 6.22 (dt, J = 15.7, 7.0 Hz, 1H), 3.44 (t, J = 6.6 Hz, 2H), 3.18 (t, J = 6.6 Hz, 2H), 2.78–2.73 (m, J = 13.0, 5.4 Hz, 2H), 2.26–2.16 (m, J = 6.9 Hz, 2H), 1.94 (s, 3H), 1.59–1.47 (m, 4H), 1.43–1.31 (m, J = 9.7 Hz, 11H). ^{13}C NMR (100 MHz, MeOD) δ 195.61, 173.49, 137.65, 137.50, 135.45, 132.90, 129.20, 128.34, 127.76 (2C), 41.69, 40.13, 34.15, 31.26, 30.39, 30.37, 30.16, 30.14, 30.12, 27.71, 22.57. HRMS (ESI+) calcd for $C_{21}H_{33}N_2O_2S$ (M + H) 377.2263, obsd 377.2292.

S-(2-Acetamidoethyl) (*E*)-13-hydroxytridec-2-enethioate (17)

102 mg compound **S19** (0.232 mmol) was dissolved in acetonitrile, 331 μl HF (28.0 M, 40 eq.) was slowly added and the solution was stirred for 10 minutes. The reaction was quenched with sat. NH_4Cl, extracted with EtOAc, dried over $MgSO_4$ and concentrated to yield 63 mg pure **17** (87%) as a white solid. R_f = 0.14 (3 : 1 EtOAc/hexanes). ^{1}H NMR (400 MHz, DMSO-d_6) δ 8.03 (s, 1H), 6.88–6.73 (dt, J = 15.6, 7.0 Hz, 1H), 6.18 (d, J = 15.6 Hz, 1H), 3.32 (t, J = 6.6 Hz, 2H), 3.14 (dd, J = 12.8, 6.5 Hz, 2H), 2.91 (t, J = 6.8 Hz, 2H), 2.15 (q, J = 7.0 Hz, 2H), 1.75 (s, 3H), 1.36 (m, 4H), 1.20 (m, 12H). ^{13}C NMR

(100 MHz, CD_3OD) δ 189.62, 172.12, 146.17, 128.12, 61.60, 38.87, 32.26, 31.72, 29.29, 29.19, 29.17, 29.05, 28.85, 27.74, 27.46, 25.54, 21.02. HRMS (ESI+) calc. for $C_{17}H_{31}NO_3SNa$ (M + Na) 352.1922; obsd 352.1917.

S-(2-Acetamidoethyl) 13-hydroxytridecanethioate (18)

40 mg **S20** (0.174 mmol) was dissolved in dry DCM under argon and cooled to 0 °C. 50 mg EDC (0.26 mmol 1.5 eq.) and 2.6 mg DMAP (0.017 mmol, 0.1 eq.) was added and the solution stirred at 0 °C for 10 minutes. 25 mg of **13** (0.21 mmol, 1.2 eq.) was added and the solution was stirred at room temperature for 20 h. The reaction was quenched with NH_4Cl, extracted with DCM, washed with Brine, dried over $MgSO_4$, and concentrated. The crude product was purified by column chromatography (3 : 97 MeOH/DCM) to yield 25 mg of pure **18** (44%) as a grey solid. R_f = 0.21 (3 : 97 MeOH/DCM). ^{1}H NMR (400 MHz, $CDCl_3$) δ 5.86–5.71 (m, 1H), 3.67–3.57 (m, 2H), 3.41 (q, J = 6.4 Hz, 2H), 3.00 (t, J = 6.4 Hz, 2H), 2.59–2.50 (m, 2H), 1.94 (s, 3H), 1.67–1.60 (m, 2H), 1.54 (m, 2H), 1.24 (m, 16H). ^{13}C NMR (100 MHz, CD_3OD) δ 199.21, 172.03, 61.61, 43.40, 38.78, 32.27, 29.33, 29.28, 29.26, 29.19, 29.11, 28.94, 28.54, 27.68, 25.54, 25.30, 21.08. HRMS (ESI+) calc. for $C_{17}H_{33}NO_3SNa$ (M + Na) 354.2079; obsd 354.2058.

S-(2-Acetamidoethyl) 2-(10-hydroxydecanamido)ethanethioate (19)

0.5 g **S21** (1.923 mmol) was dissolved in dioxane under argon and cooled to 0 °C. 4 ml of 4.0 HCl/dioxane was added to the solution on ice. The solution was stirred for 30 minutes and the precipitated pure salt was filtered and suspended in dry DCM and cooled to 0 °C. 244 mg EDC (1.27 mmol, 1.5 eq.), 350 μl NEt_3 (2.51 mmol, 3 eq.), and 160 mg 10-hydroxydecanoic acid (0.955 mmol) was added and the solution was stirred at room temperature for 3 h. NH_4Cl was added, and the solution was extracted with DCM, washed with $NaHCO_3$, Brine, dried over $MgSO_4$, and concentrated. The crude product was purified by column chromatography (1 : 1 EtOAc/hexanes) to yield 40 mg **19** (14%) as a white powder. R_f = 0.11 (1 : 1 EtOAc/hexanes). ^{1}H NMR (400 MHz, DMSO-d_6) δ 8.46 (t, J = 5.1 Hz, 1H), 8.00 (s, 1H), 4.29 (t, J = 5.1 Hz, 1H), 3.92 (d, J = 6.0 Hz, 2H), 3.36–3.31 (m, 2H), 3.15–3.05 (m, 2H), 2.83 (t, J = 7.0 Hz, 2H), 2.11 (t, J = 7.4 Hz, 2H), 1.74 (s, 3H), 1.47 (m, 2H), 1.36 (m, 2H), 1.21 (m, 10H). ^{13}C NMR (100 MHz, CD_3OD) δ 197.50, 175.53, 172.06, 61.60, 48.62, 38.58, 35.38, 32.26, 29.19, 29.12, 28.96, 28.86, 27.34, 25.52, 25.32, 21.09. HRMS (ESI+) calc. for $C_{16}H_{30}N_2O_4SNa$ (M + Na) 369.1824; obsd 369.1805.

General TE assay protocols

TE assays for product distribution analysis. TE assays were performed in 50 mM phosphate buffer at pH 7.4, with 10% v/v DMSO, 1 mM SNAC activated substrate, and 5 μM TE with the exception of the 10-member substrate (**11**), which used 20 μM of both TEs, and the 14-member lactam substrate (**16**), which used 25 μM Zea TE. Assays were incubated at 20 °C for the indicated amount of time and were quenched by the addition of an equal volume of 0.5% formic acid in acetonitrile. HPLC analysis was performed using a Zorbax C18 column (50 × 2.1 mm) with a gradient elution 15% B to 95% B over 18 min (A: water, B: acetonitrile) and a flow rate of 0.2 mL min^{-1} with the exception of assays for substrates **17**, **18**, and **19**, where a Leapsil C18 column (100 × 2.1 mm) with a gradient of 0% B to 100% B over 35 minutes with a flow rate of 0.4 mL min^{-1} was used.

TE assays for v_{rel} determination. Initial velocity was determined from an assay containing 50 mM phosphate buffer at pH 7.4 with 10% v/v DMSO, 1 mM substrate, and 5 μM Rdc or Zea TE. Assays were incubated at 20 °C for the indicated amount of time and were quenched by the addition of an equal volume of 8% saturated aqueous Ellman's reagent in acetonitrile to generate a final concentration of 4% Ellman's reagent in approximately 1 : 1 acetonitrile water. Absorbance was measured at 412 nm in a UV/Vis spectrophotometer. All kinetic measurements were collected in triplicate.

Conflicts of interest

There are no conflicts to declare.

Notes and references

1 G. Grogan and N. J. Turner, *Chem. – Eur. J.*, 2016, **22**, 1900–1907.
2 J. H. Schrittwieser, S. Velikogne and W. Kroutil, *Adv. Synth. Catal.*, 2015, **357**, 1655–1685.
3 S. K. Ma, J. Gruber, C. Davis, L. Newman, D. Gray, A. Wang, J. Grate, G. W. Huisman and R. A. Sheldon, *Green Chem.*, 2010, **12**, 81–86.
4 C. K. Savile, J. M. Janey, E. C. Mundorff, J. C. Moore, S. Tam, W. R. Jarvis, J. C. Colbeck, A. Krebber, F. J. Fleitz, J. Brands, P. N. Devine, G. W. Huisman and G. J. Hughes, *Science*, 2010, **329**, 305–309.
5 D. Ghislieri, A. P. Green, M. Pontini, S. C. Willies, I. Rowles, A. Frank, G. Grogan and N. J. Turner, *J. Am. Chem. Soc.*, 2013, **135**, 10863–10869.
6 T. Hudlicky and J. W. Reed, *Chem. Soc. Rev.*, 2009, **38**, 3117.
7 A. Parenty, X. Moreau and J.-M. Campagne, *Chem. Rev.*, 2006, **106**, 911–939.
8 A. Parenty, X. Moreau, G. Niel and J.-M. Campagne, *Chem. Rev.*, 2013, **113**, PR1–P40.
9 A. K. Yudin, *Chem. Sci.*, 2015, **6**, 30–49.
10 J. R. Donald and W. P. Unsworth, *Chemistry*, 2017, **23**, 8780–8799.
11 E. Marsault and M. L. Peterson, *J. Med. Chem.*, 2011, **54**, 1961–2004.
12 M. E. Horsman, T. P. A. Hari and C. N. Boddy, *Nat. Prod. Rep.*, 2016, **33**, 183–202.
13 J. Young, D. C. Stevens, R. Carmichael, J. Tan, S. Rachid, C. N. Boddy, R. Müller and R. E. Taylor, *J. Nat. Prod.*, 2013, **76**, 2269–2276.
14 L. Shao, J. Zi, J. Zeng and J. Zhan, *Appl. Environ. Microbiol.*, 2012, **78**, 2034–2038.

15 L. Ray, K. Yamanaka and B. S. Moore, *Angew. Chem., Int. Ed.*, 2016, **55**, 364–367.
16 N. Winssinger and S. Barluenga, *Chem. Commun.*, 2007, **171**, 22–36.
17 G. W. Heberlig, M. Wirz, M. Wang and C. N. Boddy, *Org. Lett.*, 2014, **16**, 5858–5861.
18 M. Wang, H. Zhou, M. Wirz, Y. Tang and C. N. Boddy, *Biochemistry*, 2009, **48**, 6288–6290.
19 T. P. A. Hari, P. Labana, M. Boileau and C. N. Boddy, *ChemBioChem*, 2014, **15**, 2656–2661.
20 Y. Zhou, A. C. Murphy, M. Samborskyy, P. Prediger, L. C. Dias and P. F. Leadlay, *Chem. Biol.*, 2015, **22**, 745–754.
21 Y. Zhou, P. Prediger, L. C. Dias, A. C. Murphy and P. F. Leadlay, *Angew. Chem., Int. Ed.*, 2015, **54**, 5232–5235.
22 J. W. Trauger, R. M. Kohli and C. T. Walsh, *Biochemistry*, 2001, **40**, 7092–7098.
23 F. Kopp, J. Grünewald, C. Mahlert and M. A. Marahiel, *Biochemistry*, 2006, **45**, 10474–10481.
24 M. Wang and C. N. Boddy, *Biochemistry*, 2008, **47**, 11793–11803.
25 I. L. Gatfield, *Ann. N. Y. Acad. Sci.*, 1984, **434**, 569–572.
26 A. Makita, T. Nihira and Y. Yamada, *Tetrahedron Lett.*, 1987, **28**, 805–808.
27 Z. W. Guo and C. J. Sih, *J. Am. Chem. Soc.*, 1988, **110**, 1999–2001.
28 M. Lobell and M. P. Schneider, *Tetrahedron: Asymmetry*, 1993, **4**, 1027–1030.
29 G. K. Robinson, M. J. Alston, C. J. Knowles, P. S. J. Cheetham and K. R. Motion, *Enzyme Microb. Technol.*, 1994, **16**, 855–863.
30 C. T. Walsh, J. W. Trauger, R. M. Kohli, H. D. Mootz and M. A. Marahiel, *Nature*, 2000, **407**, 215–218.
31 R. M. Kohli, C. T. Walsh and M. D. Burkart, *Nature*, 2002, **418**, 658–661.
32 A. Pinto, M. Wang, M. Horsman and C. N. Boddy, *Org. Lett.*, 2012, **14**, 2278–2281.
33 C. C. Aldrich, L. Venkatraman, D. H. Sherman and R. A. Fecik, *J. Am. Chem. Soc.*, 2005, **127**, 8910–8911.
34 W. He, J. Wu, C. Khosla and D. E. Cane, *Bioorg. Med. Chem. Lett.*, 2006, **16**, 391–394.
35 C. N. Boddy, T. L. Schneider, K. Hotta, C. T. Walsh and C. Khosla, *J. Am. Chem. Soc.*, 2003, **125**, 3428–3429.
36 A. A. Koch, D. A. Hansen, V. V. Shende, L. R. Furan, K. N. Houk, G. Jiménez-Osés and D. H. Sherman, *J. Am. Chem. Soc.*, 2017, **139**, 13456–13465.
37 P. Argyropoulos, F. Bergeret, C. Pardin, J. M. Reimer, A. Pinto, C. N. Boddy and T. M. Schmeing, *Biochim. Biophys. Acta, Gen. Subj.*, 2016, **1860**, 486–497.
38 S.-C. Tsai, L. J. W. Miercke, J. Krucinski, R. Gokhale, J. C.-H. Chen, P. G. Foster, D. E. Cane, C. Khosla and R. M. Stroud, *Proc. Natl. Acad. Sci. U. S. A.*, 2001, **98**, 14808–14813.
39 D. L. Akey, J. D. Kittendorf, J. W. Giraldes, R. A. Fecik, D. H. Sherman and J. L. Smith, *Nat. Chem. Biol.*, 2006, **2**, 537–542.
40 J. W. Giraldes, D. L. Akey, J. D. Kittendorf, D. H. Sherman, J. L. Smith and R. A. Fecik, *Nat. Chem. Biol.*, 2006, **2**, 531–536.
41 S. Mizuta, S. Verhoog, K. M. Engle, T. Khotavivattana, M. O. Duill, K. Wheelhouse, G. Rassias and M. Me, *J. Am. Chem. Soc.*, 2013, **135**, 2505–2508.

3.5 Supporting Information

General Synthetic Protocols

All reagents were purchased from Sigma-Aldrich at the highest available purity and used without further purification. All solvents were purchased from Fisher Scientific. All reactions were conducted using dry solvents under an argon atmosphere unless otherwise noted. NMR spectroscopy, with the exception of LC-SPE-NMR, was performed with a Bruker Avance II, operating at 400 MHz for ^{1}H spectra, and 100 MHz for ^{13}C spectra. HPLC analysis was conducted with an Agilent 1260 Modular system using an Agilent Zorbax C18 100x2.1 mm column. LC-SPE-NMR experiments were conducted using the same Agilent 1260 HPLC system and column with a Prospekt 2 (Spark Holland) solid-phase extraction module using HySphere Resin GP cartridges. Compounds were eluted off the cartridges with *d3*-acetonitrile and analyzed by mass spectroscopy and ^{1}H NMR using a Bruker Avance III, with cryoprobe operating at 600 MHz. High-resolution mass spectroscopy (HRMS) was conducted on a Micromass Q-TOF I for ESI measurements and a Kratos Concept 1S High Resolution Mass Spectrometer for EI measurements (John L. Holmes Mass Spectroscopy Facility).

Synthetic Protocols

Oct-7-en-1-yl 2-vinylbenzoate (S1).

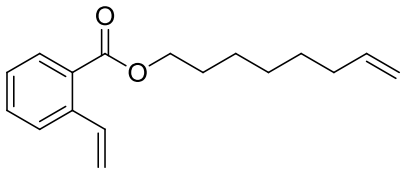

A 15 mL round bottom flask equipped with a stir bar was charged with 7 mL dry DMF, to which was added 200 mg 2-vinylbenzoic acid[1] (1.37 mmol, 1 eq.), 668 mg cesium carbonate (2.05 mmol, 1.5 eq.), and 275 mg 8-bromooctene (1.44 mmol, 1.05 eq.). The reaction was stirred overnight at room temperature. The reaction mixture was diluted with 50 ml water, and extracted 3x10 mL Et_2O. The combined organic extracts were washed sequentially with 25 mL 1/2 sat. NaCl, 3/4 sat. NaCl, and finally brine. The organic layer was dried with Na_2SO_4 and concentrated *in vacuo* and purified by column chromatography 5% EtOAc/Hex. Yielded 283 mg **S1** (80%).

R_f = 0.5 (5:95 EtOAc:Hexanes)

IR (NaCl) ν_{max} = 2945, 2871, 1718, 1286 cm^{-1}

^{1}H NMR (400 MHz, $CDCl_3$) δ 7.88 – 7.83 (m, 1H), 7.58 – 7.54 (m, 1H), 7.48 – 7.40 (m, 2H), 7.30 (td, *J* = 7.6, 1.2 Hz, 1H), 5.79 (ddt, *J* = 16.9, 10.2, 6.7 Hz, 1H), 5.63 (dd, *J* = 17.5, 1.3 Hz, 1H), 5.33 (dd, *J* = 11.0, 1.3 Hz, 1H), 4.98 (ddd, *J* = 17.1, 3.7, 1.6 Hz, 1H), 4.92 (ddt, *J* = 10.2, 2.2, 1.2 Hz, 1H), 4.28 (t, *J* = 6.7 Hz, 2H), 2.04 (q, *J* = 6.8 Hz, 2H), 1.79 – 1.70 (m, 2H), 1.50 – 1.22 (m, 8H)

^{13}C NMR (100 MHz, $CDCl_3$) δ 167.53, 139.51, 138.96, 135.97, 131.98, 130.23, 129.03, 127.38,

127.21, 116.33, 114.35, 65.19, 33.68, 28.78, 28.73, 28.65, 25.96.

HRMS (+EI) : calcd for $C_{15}H_{18}O_2$ (M) 230.1307, obsd 230.1302.

(E)-3,4,5,6,7,8-hexahydro-1H-benzo[c][1]oxacyclododecin-1-one (20).

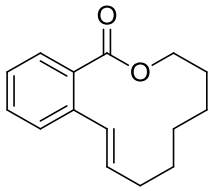

To 192 mL dry toluene was added 200 mg **S1** (0.77 mmol) under argon, to this stirred solution 33 mg of Grubbs 2nd Gen. catalyst (0.04 mmol, 5 mol%) was added. The reaction was stirred at 88˚C for 4 days. At completion the reaction was concentrated and purified by column chromatography (95:5 Hexanes:EtOAc), yielding 79 mg (45%) of the title compound as a colorless oil.

R_f = 0.47 (9:1 hexanes:EtOAc)

IR (NaCl) ν_{max} = 2924, 2867, 1720, 1288, 1249 cm^{-1}

^{1}H NMR (400 MHz, $CDCl_3$) δ 7.73 (dd, *J* = 7.7, 1.2 Hz, 1H), 7.41 (td, *J* = 7.5, 1.3 Hz, 1H), 7.32 – 7.24 (m, 2H), 6.69 (d, *J* = 15.8 Hz, 1H), 5.69 (dt, *J* = 15.8, 7.1 Hz, 1H), 4.34 – 4.27 (m, 2H), 2.27 (dt, *J* = 7.2, 3.6 Hz, 2H), 1.76 – 1.68 (m, 2H), 1.64 – 1.41 (m, 8H)

^{13}C NMR (100 MHz, $CDCl_3$) δ 169.53, 139.30, 132.29, 131.52, 131.49, 130.53, 129.79, 127.84, 126.59, 66.09, 30.90, 26.71, 26.21, 25.45, 23.78.

HRMS (+EI) : calcd for $C_{15}H_{18}O_2$ (M) 230.1307, obsd 230.1302.

(E)-2-(8-hydroxyoct-1-en-1-yl)benzoic acid (S3).

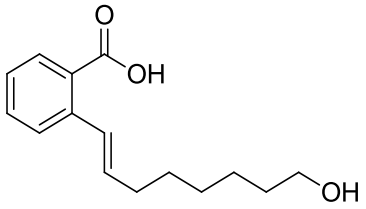

In a 10 mL round bottom 79 mg **S2** (0.343 mmol) was dissolved in 2:1 methanol:water (3 mL total) and to this 144 mg of LiOH (3.43 mmol, 10 eq.) was added. Several drops of THF were added until the solution became clear. The reaction was stirred over night at room temperature. At completion the reaction was diluted with water and the pH was adjusted to 2 using 10% HCl. This was extracted 3x 10 mL with EtOAc and the organic fractions were combined, dried over Na_2SO_4, and concentrated *in vacuo*. This yielded 86 mg of seco-acid **S3** (100%) as a clear oil.

R_f = 0.19 (1:1 EtOAc:hexanes)

IR (NaCl) ν_{max} = 3859, 2936, 2863, 1692, 1260 cm^{-1}

^{1}H NMR (400 MHz, $CDCl_3$) δ 7.96 (dd, *J* = 7.9, 1.1 Hz, 1H), 7.53 – 7.49 (m, 1H), 7.46 (td, *J* = 7.6, 1.1 Hz, 1H), 7.29 – 7.24 (m, 1H), 7.19 (d, *J* = 15.8 Hz, 1H), 6.08 (dt, *J* = 15.7, 6.9 Hz, 1H), 3.66 (t, *J* = 6.4 Hz, 2H), 2.26 (qd, *J* = 7.0, 1.4 Hz, 2H), 1.61 – 1.36 (m, 8H)

^{13}C NMR (100 MHz, $CDCl_3$) δ 171.65, 140.63, 133.79, 132.67, 131.05, 129.11, 127.55, 127.18, 126.58, 62.73, 32.61, 28.71, 28.40, 25.29.

HRMS (+EI) : calcd for $C_{15}H_{20}O_3$ (M) 248.1412, obsd 248.1405.

Dec-9-en-1-yl 2-vinylbenzoate (3).

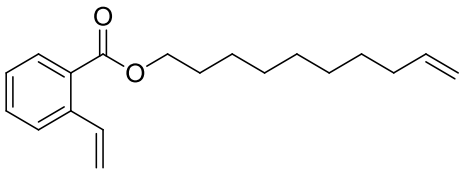

Prepared according to our previously reported conditions.[2] (72%)

R_f = 0.74 (9:1 hexanes:EtOAc).

^{1}H NMR (400 MHz, CDCl3) δ 7.86 (dd, *J* = 7.9, 1.3 Hz, 1 H), 7.56 (d, *J* = 7.9 Hz, 1 H), 7.50-7.38 (m, 2 H), 7.30 (ddd, *J* = 7.7, 7.4, 0.9 Hz, 1 H), 5.79 (ddt, *J* = 17.1, 10.3, 6.5 Hz, 1 H), 5.63 (dd, *J* = 17.4, 1.3 Hz, 1 H), 5.33 (dd, *J* = 10.9, 1.3 Hz, 1 H), 4.98 (ddt, *J* = 17.1, 2.0, 1.7 Hz, 1 H), 4.92 (ddt, *J* = 10.3, 1.1, 1.1 Hz, 1 H), 4.29 (t, *J* = 6.8 Hz, 2 H), 2.08-1.97 (m, 2 H), 1.80-1.62 (m, 2 H), 1.48-1.21 (m, 10 H)

^{13}C NMR (100 MHz, CDCl3) δ 167.5, 139.5, 139.1, 136.0, 132.0, 130.2, 129.1, 127.4, 127.2, 116.3, 114.2, 65.2, 33.8, 29.4, 29.2, 29.0, 28.9, 28.7, 26.1.

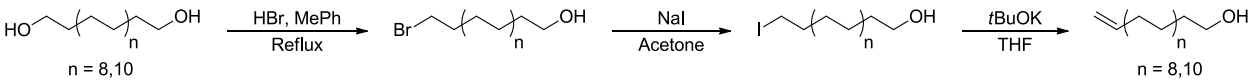

Scheme S1. General synthetic strategy for the synthesis of the olefin terminated alcohols used to generate **8** and **9** from commercially available diols.

Dodec-11-en-1-ol (S4).

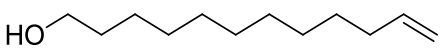

To 5 mL of toluene in a 25 mL round bottom flask was added 300 mg of 1,12-dodecanediol (1.48 mmol), to this was added 268 μL of 48% HBr (2.37 mmol, 1.6 eq.). The mixture was stirred overnight at reflux, at completion the aqueous layer was removed and the organic layer was washed with 1 N NaOH, brine, dried over Na_2SO_4 and concentrated *in vacuo*. The crude product was then dissolved in 8 mL of acetone to which was added 794 mg of NaI (5.3 mmol, 3.5 eq.) followed by 4A molecular sieves. The reaction was stirred at reflux overnight, then diluted with brine and extracted with Et_2O. The combined organic extracts were dried over Na_2SO_4 and concentrated. The iodide was dissolved in 12 mL of anhydrous THF and 364 mg of solid potassium *t*-butoxide (3.24 mmol, 2.2 eq.) was added as a single portion. The reaction was stirred for a further 20 minutes then slowly quenched by the addition of water until the solution became clear. This was further diluted with brine and extracted with EtOAc, the combined organic extracts were dried over Na_2SO_4 and concentrated *in vacuo* to yield 270 mg **S4** (89%, over three steps) as a clear oil. Characterization data is consistent with reported values.[3]

R_f = 0.5 (7:3 hexanes:EtOAc)

^{1}H NMR (400 MHz, $CDCl_3$) δ 5.79 (ddt, *J* = 16.9, 10.2, 6.7 Hz, 1H), 4.97 (ddd, *J* = 17.1, 3.6, 1.7 Hz, 1H), 4.93 – 4.87 (m, 1H), 3.62 (t, *J* = 6.6 Hz, 2H), 2.08 – 1.97 (m, 2H), 1.60 – 1.49 (m, 2H), 1.25 (m, 14H).

Dodec-11-en-1-yl 2-vinylbenzoate (S5).

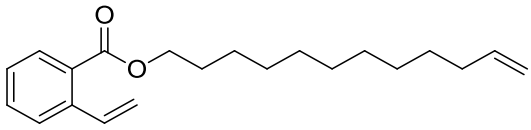

2-vinyl benzoic acid (180 mg, 1.22 mmol) was dissolved in 7 mL anhydrous DCM, to this solution was added 270 mg **S4** (1.46 mmol, 1.2 eq.), 350 mg of EDC (1.83 mmol, 1.5 eq.), and 224 mg DMAP (1.83 mmol, 1.5 eq.). The reaction was stirred under argon at room temperature overnight. The reaction was quenched by the addition of sat. NH_4Cl, and the organic layer was removed. The aqueous layer was extracted with DCM, and combined organic extracts were washed with brine, dried over Na_2SO_4, and concentrated. The product was purified by column chromatography (98:2 hexanes:EtOAc) yielding 230 mg of **S5** (60%) as a colorless oil.

R_f = 0.55 (9:1 hexanes:EtOAc)

IR (NaCl) ν_{max} = 2925, 2853, 1712, 1260 cm^{-1}

^{1}H NMR (400 MHz, $CDCl_3$) δ 7.85 (dd, *J* = 7.8, 1.2 Hz, 1H), 7.58 – 7.54 (m, 1H), 7.44 (ddd, *J* = 14.2, 10.2, 8.6 Hz, 2H), 7.30 (td, *J* = 7.6, 1.2 Hz, 1H), 5.79 (ddt, *J* = 16.9, 10.2, 6.7 Hz, 1H), 5.63 (dd, *J* = 17.4, 1.3 Hz, 1H), 5.32 (dd, *J* = 11.0, 1.3 Hz, 1H), 4.97 (ddd, *J* = 17.1, 3.7, 1.6 Hz, 1H), 4.91 (ddt, *J* = 10.2, 2.3, 1.2 Hz, 1H), 4.28 (t, *J* = 6.7 Hz, 2H), 2.06 – 1.98 (m, 2H), 1.78 – 1.69 (m, 2H), 1.46 – 1.21 (m, 14H).

^{13}C NMR (100 MHz, $CDCl_3$) δ 167.5, 139.5, 139.2, 136.0, 132.0, 130.2, 129.1, 127.4, 127.2, 116.3, 114.1, 64.7, 33.8, 29.5, 29.5, 29.3, 29.1, 28.9, 28.6, 26.1, 25.9

HRMS (+EI) : calcd for $C_{21}H_{30}O_2$ (M) 314.2246, obsd 314.2248.

(E)-2-(12-hydroxydodec-1-en-1-yl)benzoic acid (S6).

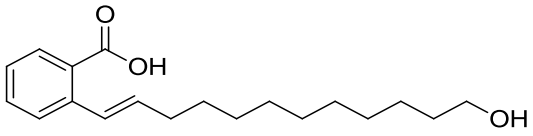

A 250 mL flame-dried round bottom flask was charged with 160 mL of anhydrous toluene, 205 mg **S5** (0.65 mmol), and 28 mg of Grubbs 2nd Generation catalyst (5 mol%). The reaction was stirred at 80˚C for 24 hours, at which the reaction was concentrated and passed through a plug of silica to remove the catalyst. This crude product was dissolved in a 4:3:1 methanol:THF: water (14.5 mL total volume) solution and 273 mg of LiOH (6.5 mmol, 10 eq.) was added the reaction was stirred at 50˚C overnight. At completion the reaction was acidified to pH=2 with 10% HCl, and then was extracted with EtOAc. The combined organic fractions were combined, dried over Na_2SO_4, and concentrated. To yield 149 mg **S6** (75%, over two steps) as a colorless oil.

R_f = 0.41 (1:1 EtOAc:hexanes)

IR (NaCl) ν_{max} = 3861 2925, 2853, 1717 cm^{-1}

^{1}H NMR (400 MHz, $CDCl_3$) δ 7.97 (dd, *J* = 7.9, 1.2 Hz, 1H), 7.54 (d, *J* = 6.9 Hz, 1H), 7.49 – 7.43 (m, 1H), 7.27 (dd, *J* = 10.8, 4.3 Hz, 1H), 7.22 (d, *J* = 15.7 Hz, 1H), 6.13 (dt, *J* = 15.7, 6.9 Hz, 1H), 3.66 – 3.61 (m, 2H), 2.28 – 2.20 (m, 2H), 1.59 – 1.44 (m, 4H), 1.37 – 1.24 (m, 14H).

^{13}C NMR (100 MHz, $CDCl_3$) δ 172.2, 140.6, 134.4, 132.7, 131.2, 128.6, 127.4, 127.1, 126.5, 63.1, 33.1, 32.6, 29.4, 29.3, 39.3, 29.3, 29.1, 29.0, 25.6

HRMS (+EI) : calcd for $C_{19}H_{28}O_3$ (M) 304.2038, obsd 304.2048.

Tetradec-13-en-1-ol (S7).

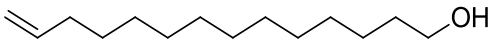

To 6 mL of toluene in a 25 mL round bottom flask was added 200 mg of 1,14-tetradecanediol (0.868 mmol), to this was added 160 μL of 48% HBr (1.40 mmol, 1.6 eq.). The mixture was stirred overnight at reflux, at completion the aqueous layer was removed and the organic layer was washed with 1 N NaOH, brine, dried over Na_2SO_4 and concentrated *in vacuo*. The crude product was then dissolved in 7 mL of acetone to which was added 601 mg of NaI (4.00 mmol, 3.5 eq.) followed by 4Å molecular sieves. The reaction was stirred at reflux overnight, then diluted with brine and extracted with Et_2O. The combined organic extracts were dried over Na_2SO_4 and concentrated. The iodide was dissolved in 7 mL of anhydrous THF and 218 mg of solid potassium *t*-butoxide (1.94 mmol, 2.2 eq.) was added as a single portion. The reaction was stirred for a further 20 minutes then slowly quenched by the addition of water until the solution became clear. This was further diluted with brine and extracted with EtOAc, the combined organic extracts were dried over Na_2SO_4 and concentrated *in vacuo* to yield 270 mg **S7** (71%, over three steps) as a clear oil. Characterization is consistent with previously reported values.[4]

R_f = 0.37 (1:1 hexanes:EtOAc)

^{1}H NMR (400 MHz, $CDCl_3$) δ 5.79 (ddt, *J* = 16.9, 10.2, 6.7 Hz, 1H), 5.01 – 4.93 (m, 1H), 4.91 (ddt, *J* = 10.2, 2.3, 1.2 Hz, 1H), 3.62 (t, *J* = 6.6 Hz, 2H), 2.05 – 1.98 (m, 2H), 1.59-1.49 (m, 2H), 1.35 – 1.23 (m, 20H).

(E)-2-(14-hydroxytetradec-1-en-1-yl)benzoic acid (S8).

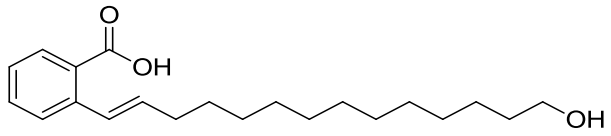

2-Vinyl benzoic acid (75 mg, 0.51 mmol) was dissolved in 3 mL anhydrous DCM, to this solution was added 130 mg **S7** (0.61 mmol, 1.2 eq.), 147 mg of EDC (0.77 mmol, 1.5 eq.), and 93 mg DMAP (0.77 mmol, 1.5 eq.). The reaction was stirred under argon at room temperature overnight. The reaction was quenched by the addition of sat. NH_4Cl, and the organic layer was removed. The aqueous layer was extracted with DCM, and combined organic extracts were washed with brine, dried over Na_2SO_4, and concentrated. A 250 ml flame-dried round bottom flask was charged with 60 mL of anhydrous toluene, the crude esterification product, and 10 mg of Grubbs 2nd Generation catalyst (5 mol%). The reaction was stirred at 80˚C for 24 hours, at which the reaction was concentrated and passed through a plug of silica to remove the catalyst. This crude product was dissolved in a 4:3:1 methanol:THF: water (5.5 mL total volume) solution and 100 mg of LiOH (2.4 mmol, 10 eq.) was added the reaction was stirred at 50˚C overnight. At completion the reaction was acidified to pH 2 with 10% HCl, and then was extracted with EtOAc. The combined organic fractions were combined, dried over Na_2SO_4, and concentrated. To yield 75 mg **S8** (44%, over three steps) as a colorless oil.

R_f = 0.43 (1:1 EtOAc:hexanes)

IR (NaCl) ν_{max} = 3460(br), 2930, 2857, 1694, 1261 cm^{-1}

^{1}H NMR (400 MHz, $CDCl_3$) δ 7.99 (dd, *J* = 7.9, 1.1 Hz, 1H), 7.56 (d, *J* = 7.6 Hz, 1H), 7.51 – 7.45 (m, 1H), 7.31 – 7.26 (m, 1H), 7.24 (d, *J* = 15.6 Hz, 1H), 6.16 (dt, *J* = 15.6, 6.9 Hz, 1H), 3.65 (t, *J* = 6.6 Hz, 2H), 2.26 (td, *J* = 8.1, 1.2 Hz, 2H), 1.61 – 1.45 (m, 4H), 1.38 – 1.26 (m, 16H).

^{13}C NMR (100 MHz, $CDCl_3$) δ 172.28, 140.58, 134.43, 132.69, 131.16, 128.55, 127.43, 127.04, 126.52, 63.10, 33.18, 32.65, 29.53, 29.50, 29.49 (2C), 29.41, 29.36, 29.17, 29.14, 25.69.

HRMS (+EI) : calcd for $C_{21}H_{32}O_3$ (M) 332.2351, obsd 332.2343.

10-azidodec-1-ene (S9).

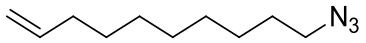

A 50 mL round bottom equipped with a stir bar was charged with 21 mL of anhydrous THF and 2.52 g triphenylphosphine (9.6 mmol, 1.5 eq.) then chilled to -20˚C. To this stirred solution was added 1.94 g diisopropyl azodicarboxylate (9.6 mmol, 1.5 eq.) then stirred for 10 additional minutes after which 1.0 g of 9-decen-1-ol (6.4 mmol) was added dropwise. After stirring for 30 minutes the reaction was warmed to 0˚C and 2.64 g diphenylphosphoryl azide (9.6 mmol, 1.5 eq.) was added dropwise then stirred for 10 minutes. THF was added until a yellow precipitate was formed, the precipitate was removed by filtration and the reaction mixture was concentrated and purified by column chromatography eluting with 5% EtOAc in hexanes. Yielded 902 mg **S9** (78%) as a slightly yellow oil. Characterization data are consistent with reported values.[5]

R_f = 0.87 (95:5 Hexanes:EtOAc)

^{1}H NMR (400 MHz, $CDCl_3$) δ 5.79 (ddt, *J* = 16.9, 10.2, 6.7 Hz, 1H), 4.97 (ddd, *J* = 17.1, 3.7, 1.6 Hz, 1H), 4.91 (ddt, *J* = 10.2, 2.3, 1.2 Hz, 1H), 3.24 (t, *J* = 7.0 Hz, 2H), 2.07 – 1.96 (m, 2H), 1.62 – 1.54 (m, 2H), 1.39 – 1.26 (m, 10H).

Dec-9-en-1-amine (S10).

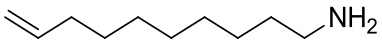

To 50 mL round bottom flask charged with 20 mL of THF and 1 mL water was added 900 mg **S9** (4.97 mmol) and 1.37 g triphenylphosphine (5.22 mmol, 1.05 eq.) at room temperature. The reaction mixture was stirred overnight and quenched with sat. NH_4Cl. The organic layer was removed and the aqueous layer was extracted with THF. The combined organic fractions were washed with brine, over Na_2SO_4, and concentrated. The compound was purified by column chromatography (80: 25: 0.5 DCM:methanol: NH_4OH) yielding 700 mg **S10** (91%) as a slightly yellow oil. Characterization data are consistent with reported values.[6]

R_f = 0.38 (80: 25: 0.5 DCM:methanol: NH_4OH)

^{1}H NMR (400 MHz, $CDCl_3$) δ 5.79 (ddt, *J* = 17.0, 10.2, 6.7 Hz, 1H), 4.97 (ddd, *J* = 17.1, 3.7, 1.6 Hz, 1H), 4.91 (ddt, *J* = 10.2, 2.3, 1.2 Hz, 1H), 2.67 (t, *J* = 7.0 Hz, 2H), 2.06 – 1.97 (m, 2H), 1.44 – 1.25 (m, 12H).

Tert-butyl dec-9-en-1-yl(2-vinylbenzoyl)carbamate (S11).

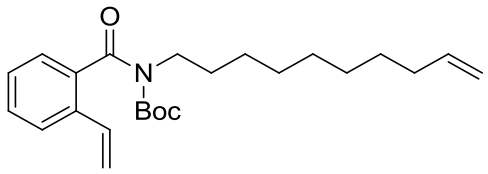

2-vinyl benzoic acid (120 mg, 0.81 mmol) was dissolved in 5 mL anhydrous dimethylformamide (DMF), to this solution was added 138 mg **S10** (0.89 mmol, 1.1 eq.), 171 mg of EDC (0.89 mmol, 1.1 eq.), 300 μL Hünig's base (1.70 mmol, 2.1 eq.), and 137 mg HOBt (0.89 mmol, 1.1 eq.). The reaction was stirred under argon at room temperature overnight. The reaction was quenched by the addition of sat. NH_4Cl, and the organic layer was removed. The aqueous layer was extracted with DCM, and combined organic extracts were washed with brine, dried over Na_2SO_4, and concentrated. This was dissolved in 6 mL THF to which was added 306 mg of di-*tert*-butyl dicarbonate (1.4 mmol, 2 eq.) and 94 mg DMAP (0.77 mmol, 1.1 eq.). The reaction was stirred at room temperature overnight, concentrated *in vacuo* and purified by column chromatography (8:2 hexanes:acetone) yielding 243 mg **S11** (78%, over 2 steps) as a slightly yellow oil.

R_f = 0.51 (8:2 hexanes:acetone)

^{1}H NMR (400 MHz, $CDCl_3$) δ 7.55 – 7.51 (m, 1H), 7.37 – 7.31 (m, 1H), 7.26 – 7.21 (m, 1H), 7.17 (dd, *J* = 7.6, 1.1 Hz, 1H), 6.78 (dd, *J* = 17.4, 11.0 Hz, 1H), 5.79 (ddt, *J* = 16.9, 10.2, 6.7 Hz, 1H), 5.68 (dd, *J* = 17.4, 1.0 Hz, 1H), 5.30 (dd, *J* = 11.0, 1.0 Hz, 1H), 4.97 (ddd, *J* = 17.1, 3.7, 1.6 Hz, 1H), 4.91 (ddt, *J* = 10.2, 2.3, 1.2 Hz, 1H), 3.84 – 3.76 (m, 2H), 2.06 – 1.98 (m, 2H), 1.72 – 1.61 (m, 2H), 1.39 – 1.26 (m, 10H), 1.07 (s, 9H);

^{13}C NMR (100 MHz, $CDCl_3$) δ 172.11, 152.87, 139.22, 138.02, 134.89, 133.76, 129.26, 127.27, 126.00, 125.56, 116.55, 114.14, 82.96, 45.04, 33.81, 29.42, 29.28, 29.06, 28.91, 28.59, 27.31, 26.96.

HRMS (ESI+) calc. for $C_{24}H_{35}NO_3Na$ (M+Na) 408.2515, obsd. 408.2532

(E)-tert-butyl 1-oxo-3,4,5,6,7,8,9,10-octahydrobenzo[c][1]azacyclotetradecine-2(1H)-carboxylate (S12)

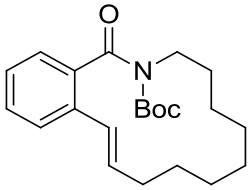

To 52 mL dry toluene was added 80 mg **S11** (0.21 mmol) under argon, to this stirred solution 9 mg of Grubbs 2nd Gen. catalyst (0.01 mmol, 5 mol%) was added. The reaction was stirred at 80˚C for 24 hours. At completion the reaction was concentrated and purified by column chromatography (90:10 Hexanes:EtOAc), yielding 37 mg (49%) of the title compound as a colorless oil.

R_f = 0.37 (90:10 Hexanes:EtOAc)

^{1}H NMR (400 MHz, $CDCl_3$) δ 7.39 (d, *J* = 7.8 Hz, 1H), 7.30 – 7.25 (m, 1H), 7.17 (td, *J* = 7.5, 1.2 Hz, 1H), 7.07 (dd, *J* = 7.6, 1.0 Hz, 1H), 6.53 (d, *J* = 15.8 Hz, 1H), 5.99 (dt, *J* = 15.8, 6.6 Hz, 1H), 2.23 (dd, *J* = 10.3, 6.4 Hz, 2H), 1.53 – 1.46 (m, 2H), 1.40 – 1.21 (m, 10H), 1.06 (s, 9H)

^{13}C NMR (100 MHz, $CDCl_3$) δ 171.62, 153.21, 138.07, 135.11, 133.30, 128.58, 127.44, 126.19, 125.95, 124.42, 83.08, 44.44, 30.45, 29.71, 27.55, 27.21, 27.14, 26.04, 24.81, 24.04, 23.58.

HRMS (ESI+) calc. for $C_{22}H_{31}NO_3Na$ (M+Na) 380.2202, obsd. 380.2228

(E)-3,4,5,6,7,8,9,10-octahydrobenzo[c][1]azacyclotetradecin-1(2H)-one (23).

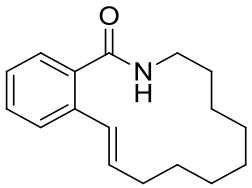

To a solution of 9.7 mg **S12** (0.03 mmol) in DCM at 0˚C was added 49 μL TMSOTf (0.27 mmol, 10 eq.). The reaction was stirred at 0˚C until complete as determined by TLC, at completion 38 μL of 2,6-lutidine (0.32 mmol, 12 eq.) was added and the reaction stirred 5 minutes. The reaction was then quenched with the addition of sat. $NaHCO_3$ and was extracted 3x 5 mL with DCM. The combined organic fractions were washed sequentially with $NaHCO_3$, $NaHSO_4$, and brine. Finally the organic fractions were dried with Na_2SO_4, and concentrated giving 6.6 mg **23** (95%) as a slightly yellow solid.

R_f = 0.20 (9:1 Hexanes:EtOAc)

HPLC 10.5 min

^{1}H NMR (400 MHz, $CDCl_3$) δ 7.46 (d, *J* = 7.8 Hz, 1H), 7.38 – 7.30 (m, 2H), 7.21 (t, *J* = 7.5 Hz, 1H), 6.64 (d, *J* = 15.7 Hz, 1H), 6.02 (dt, *J* = 15.7, 7.0 Hz, 1H), 5.81 (s, 1H), 3.46 (dd, *J* = 10.8, 5.9 Hz, 2H), 2.26 (dd, *J* = 11.4, 6.3 Hz, 2H), 1.61 – 1.26 (m, 12H).

^{13}C NMR (100 MHz, $CDCl_3$) δ 169.96, 135.94, 135.23, 133.75, 129.66, 128.03, 126.87, 125.97, 124.60, 39.45, 30.64, 28.10, 27.04, 26.47, 24.56, 24.35, 24.01.

HRMS (ESI+) calc. for $C_{17}H_{23}NONa$ (M+Na) 280.1677; obsd. 280.1656

(E)-8-(2-(((2-acetamidoethyl)thio)carbonyl)phenyl)oct-7-en-1-yl 2-((E)-8-hydroxyoct-1-en-1-yl)benzoate (S14).

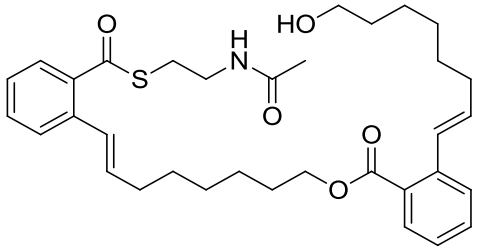

The title compound was isolated by LC-SPE trapping of the peak at 14.2 min in **Figure S4 D**, NMR characterization of the eluted peak can be found in **Figure S8** and **Figure S9**. Tabulated ^{1}H NMR data for the visible peaks is located below.

^{1}H NMR (600 MHz, CD_3CN) δ 7.78 (d, *J* = 7.9 Hz, 1H), 7.70 (d, *J* = 7.7 Hz, 1H), 7.64 (d, *J* = 8.1 Hz, 1H), 7.62 (d, *J* = 7.8 Hz, 1H), 7.50 (q, *J* = 6.2 Hz, 2H), 7.38 – 7.29 (m, 2H), 7.05 (d, *J* = 15.9 Hz, 1H), 6.75 (d, *J* = 15.8 Hz, 1H), 6.64 (s, 1H), 6.29 (dt, *J* = 15.6, 6.9 Hz, 1H), 6.23 (dt, *J* = 15.7, 6.9 Hz, 1H), 4.31 (t, *J* = 6.5 Hz, 2H), 3.50 (dd, *J* = 12.0, 6.5 Hz, 2H), 3.42 (q, *J* = 6.4 Hz, 2H), 3.16 (t, *J* = 6.6 Hz, 2H), 1.87 (s, *J* = 2.9 Hz, 3H), 1.81 – 1.75 (m, 2H), 1.54 – 1.44 (m, 10H), 1.40 – 1.29 (m, 11H).

HRMS (ESI+) calc. for $C_{34}H_{45}NO_5SNa$ (M+Na) 602.2916; obsd. 602.2959

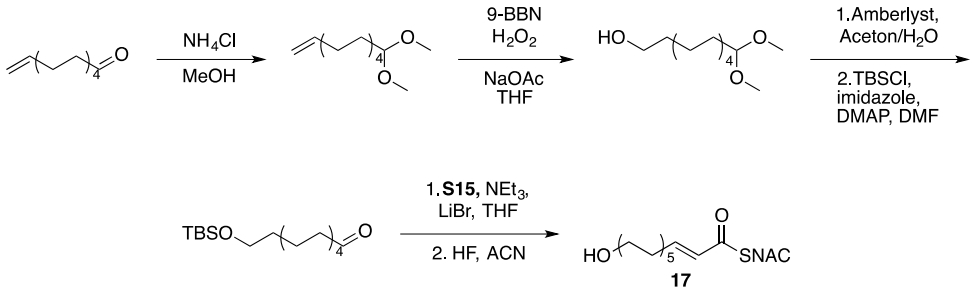

Scheme S2. General synthetic strategy for the synthesis of compound **17**.

S-(2-acetamidoethyl) 2-(diethoxyphosphoryl)ethanethioate (S15)

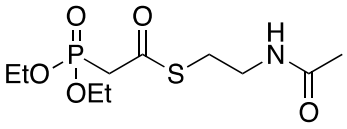

To a solution of 1.22 g diethyl phosphonoacetic acid (6.22 mmol) in DCM at 0˚C was added 1.48 mg EDC (7.74 mmol, 1.3 eq.), 82 mg DMAP (0.672 mmol 0.1 eq.), and 888 mg of **13**. The reaction was stirred overnight at room temperature. Upon completion the reaction was quenched with sat. NH_4Cl. The organic layer was separated and the aqueous layer extracted with DCM. The organic layers were washed with sat. $NaHCO_3$, Brine, dried over $MgSO_4$, and concentrated. The crude product was purified by column chromatography (5:95 MeOH/DCM) yielding 422 mg of **S15** (23%) as a colorless oil. Characterization is consistent with previously reported values.[7]

R_f = 0.17 (5:95 methanol/DCM)

^{1}H NMR (400 MHz, $CDCl_3$) δ 6.15 – 5.99 (s, 1H), 4.15 (q, *J* = 7.1, 4H), 3.45 (dd, *J* = 12.2, 6.1 Hz, 2H), 3.22 (s, 2H), 3.14 – 3.02 (m, 2H), 1.95 (s, 3H), 1.34 (t, *J* = 7.1 Hz, 6H).

11,11-dimethoxyundec-1-ene (S16)

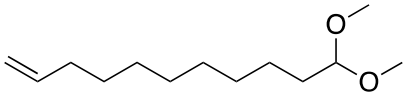

To a solution of 1.68 g undec-10-enal (10 mmol) in dry methanol was added 50 mg NH_4Cl (0.5 mmol, 0.05 eq.) The solution was heated to reflux for 18 h. The solution was quenched with sat. $NaHCO_3$, extracted with EtOAc, dried over $MgSO_4$, and concentrated to yield 1.97 g **S16** (92%) as a colorless oil. Characterization is consistent with previously reported data.[8]

^{1}H NMR (400 MHz, $CDCl_3$) δ 5.84 – 5.73 (m, 1H), 4.99 – 4.87 (m, 2H), 4.34 (t, *J* = 5.7 Hz, 1H), 3.29 (s, 6H), 2.03 – 1.98 (m, 2H), 1.60 – 1.53 (m, 2H), 1.37 – 1.26 (m, 12H).

11,11-dimethoxyundecan-1-ol (S17)

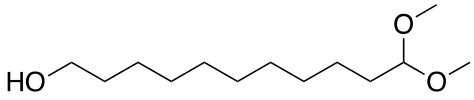

To a solution of 1.15 g **S16** (5.37 mmol) in dry THF was added 11 ml of 9-BBN THF solution (0.5 M, 5.5 mmol, 1.1 eq.). The solution was stirred for 1 h at room temperature followed by the addition of 5.5 ml NaOAc solution (3 M, 16.5 mmol, 3 eq.) and 1 ml of water. The solution was cooled to 0˚C and 2.25 ml of 30% H_2O_2 in water (20 mmol, 4 eq.) was slowly added over 30 minutes and stirred for 16 h. The solution was extracted with Et_2O, dried over $MgSO_4$ and concentrated. The crude product was purified by column chromatography (20:80 EtOAc/hexanes) to yield 450 mg **S17** (37%) as a colorless oil. Characterization is consistent with previously reported data.[9]

R_f = 0.1 (20:80 EtOAc/hexanes)

^{1}H NMR (400 MHz, $CDCl_3$) δ 4.34 (t, *J* = 5.7 Hz, 1H), 3.62 (t, *J* = 6.7 Hz, 2H), 3.29 (s, 6H), 1.61 – 1.49 (m, 4H), 1.26 (s, 14H).

11-((*tert*-butyldimethylsilyl)oxy)undecanal (S18)

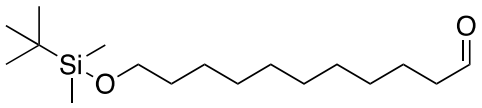

400 mg of Amberlyst cation exchange resin was added to 900 mg of **S17** (3.88 mmol) in an Acetone/water solution (60:1) and stirred overnight. The solution was filtered, dried over $MgSO_4$ and concentrated to yield 720 mg of 11-hydroxyundecanal. The crude product was dissolved in DMF, followed by the addition of 310 mg imidazole (4.55 mmol, 1.2 eq.), 31 mg DMAP (0.254 mmol, 0.05 eq.), and 800 mg TBSCl (5.3 mmol, 1.4 eq.). The solution was stirred for 18 h and quenched with sat. NH_4Cl. The aqueous mixture was extracted with Et_2O, dried over $MgSO_4$ and concentrated. The crude mixture was purified by column chromatography (5:95 EtOAc/hexanes) to yield 900 mg **S18** (77% over 2 steps) as a colorless oil. Characterization is consistent with previously reported data.[10]

R_f = 0.45 (5:95 EtOAc/hexanes)

^{1}H NMR (400 MHz, $CDCl_3$) δ 9.74 (t, *J* = 1.9 Hz, 1H), 3.57 (t, *J* = 6.7 Hz, 2H), 2.40 (td, *J* = 7.3, 1.9 Hz, 2H), 1.60 (m, 2H), 1.48 (m, 2H), 1.26 (m, 12H), 0.89 – 0.85 (s, 9H), 0.10 – -0.06 (s, 6H).

S-(2-acetamidoethyl) (E)-13-((tert-butyldimethylsilyl)oxy)tridec-2-enethioate (S19)

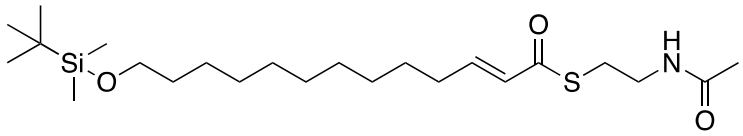

To a solution of 104 mg LiBr (1.2 mmol, 5 eq.) in dry THF was added 144 mg **S15** (0.485 mmol, 2 eq.) under argon, the solution was stirred for 10 minutes at room temperature. 210 µl NEt_3 (1.5 mmol, 6 eq.) was slowly added and the solution was stirred 10 more minutes. 97 mg **S18** (0.323 mmol) was added over 30 minutes and the solution was stirred for 16 h. The solution was quenched with NH_4Cl, extracted with EtOAc, dried over $MgSO_4$ and concentrated. The crude product was purified by column chromatography (50:50 EtOAc/hexanes) to yield 109 mg **S19** (76%) as a colorless oil.

R_f = 0.14 (50:50 EtOAc/hexanes)

^{1}H NMR (400 MHz, $CDCl_3$) δ 6.91 (dt, *J* = 15.6, 7.0 Hz, 1H), 6.11 (d, *J* = 15.6 Hz, 1H), 5.91 – 5.77 (m, 1H), 3.57 (t, *J* = 6.6 Hz, 2H), 3.45 (q, *J* = 6.5 Hz, 2H), 3.07 (t, *J* = 6.3 Hz, 2H), 2.18 (q, *J* = 6.6 Hz, 2H), 1.94 (s, 3H), 1.46 (m, 4H), 1.25 (m, 12H), 0.87 (s, 9H), 0.02 (s, 6H).

^{13}C NMR (100 MHz, $CDCl_3$) δ 170.26, 146.91, 128.29, 63.35, 39.90, 32.92, 32.31, 29.61, 29.43, 29.38, 29.34, 29.20, 28.29, 27.95, 25.99, 25.83, 23.28, -5.25

HRMS (ESI+) calc. for $C_{23}H_{45}NO_3SSiNa$ (M+Na) 466.2787; obsd. 466.2766

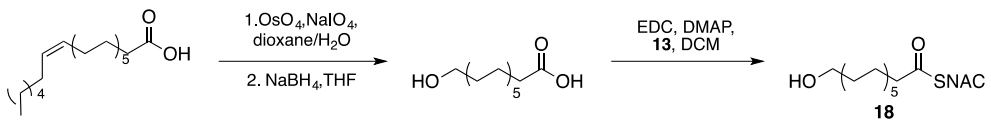

Scheme S3. General synthetic strategy for the synthesis of compound **18**.

13-hydroxytridecanoic acid (S20)

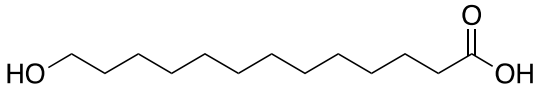

To a solution of 2 g of erucic acid (5.9 mmol) in dioxane/water 3:1, was added 1.4 ml 2,6-lutidine (11.8 mmol, 2 eq.), 53 mg potassium osmate dihydrate (0.59 mmol, 0.1 eq.), and 5 g sodium periodate (23.6 mmol, 4 eq.).The solution was stirred at room temperature for 16 h. The solution was diluted with water, extracted with EtOAc, washed with $NaHCO_3$, Brine, dried over $MgSO_4$ and concentrated. The crude product was dissolved in dry THF and cooled to 0˚C. 70 mg of $NaBH_4$ (1.10 mmol, 0.5 eq.) was added slowly over 15 minutes under argon. The solution was stirred for 3 h at room temperature, at completion 1.0 M HCl was added and the solution was extracted with EtOAc, dried over $MgSO_4$, and concentrated. The crude product was purified by column chromatography (40:60 EtOAc/hexanes) to yield 1.1 g of pure **S20** (81%) as a grey solid. Characterization is consistent with previously reported data.[11]

R_f = 0.19 (40:60 EtOAc/hexanes)

^{1}H NMR (400 MHz, $CDCl_3$) δ 3.63 (t, *J* = 6.6 Hz, 2H), 2.33 (t, *J* = 7.4 Hz, 2H), 1.55 (m, 4H), 1.25 (m, 16H).

S-(2-acetamidoethyl) 2-((tert-butoxycarbonyl)amino)ethanethioate (S21)

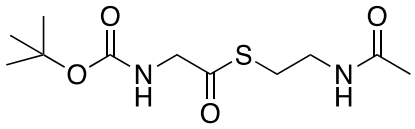

To a solution of 450 mg Boc-Gly-OH (2.83 mmol) in dry DCM at 0˚C was added 755 mg EDC (3.95 mmol, 1.5 eq.) and 29 mg DMAP (0.28 mmol, 0.1 eq.), the solution was then stirred for 10 min. 350 mg **13** (2.93, 1.1 eq.) was added, and the solution was stirred for 22 h at room temperature. The solution was quenched with NH_4Cl, extracted with DCM, washed with Brine, dried over $MgSO_4$, and concentrated. The crude product was purified by column chromatography (40:60 EtOAc/hexanes) to yield 500 mg **20** (68%) as colorless oil. Characterization is consistent with previously reported data.[12]

R_f = 0.15 (40:60 EtOAc/hexanes)

^{1}H NMR (400 MHz, $CDCl_3$) δ 5.96 (s, 1H), 5.20 (s, 1H), 4.00 (d, *J* = 6.1 Hz, 2H), 3.40 (q, *J* = 6.2 Hz, 2H), 3.02 (t, *J* = 13.6 Hz, 2H), 1.93 (s, 3H), 1.43 (s, 9H).

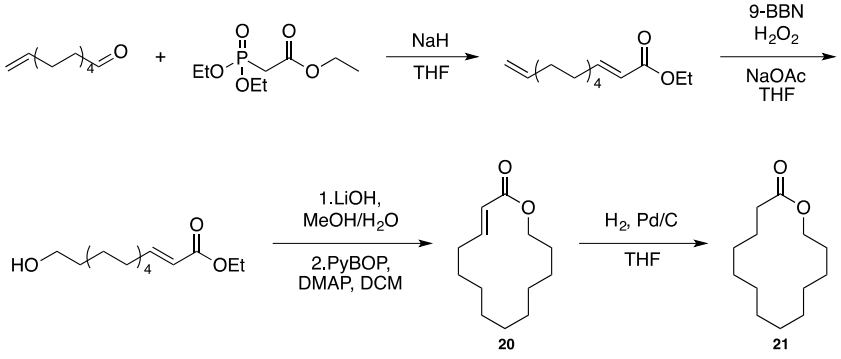

Scheme S4. General synthetic strategy for the synthesis of compound **20** and **21**.

Ethyl (E)-trideca-2,12-dienoate (S22)

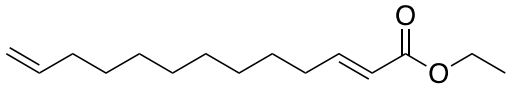

To a solution of 9 g triethyl phosphonacetate (40 mmol, 1.5 eq.) cooled to 0˚C in dry THF, was added 1.9 g NaH (40 mmol 1.5 eq.) slowly over 10 minutes. The solution was stirred 20 minutes followed by the addition of 6 g undec-10-enal (27 mmol) over 3 h. The solution was stirred for 5 h and quenched with NH_4Cl. The aqueous layer was extracted with ether, washed with brine, dried over $MgSO_4$ and concentrated. The crude product was purified by column chromatography (5:95 EtOAc/hexanes) to yield 6.67 g of **S22** (93%) as a colorless oil. Characterization is consistent with previously reported data.[13]

R_f = 0.5 (5:95 EtOAc/hexanes)

^{1}H NMR (400 MHz, $CDCl_3$) δ 6.94 (dt, *J* = 15.6, 7.0 Hz, 1H), 5.84 – 5.73 (m, 2H), 5.00 – 4.88 (m, 2H), 4.16 (q, *J* = 7.1 Hz, 2H), 2.17 (q, *J* = 7.3 Hz, 2H), 2.02 (q, *J* = 6.8 Hz, 2H), 1.47 – 1.20 (m, 15H).

ethyl (E)-13-hydroxytridec-2-enoate (S23)

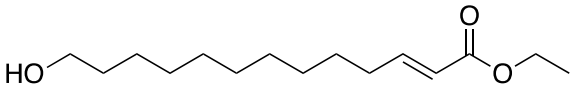

To a solution of 3.04 g **S22** (10.7 mmol) in dry THF was added 20 ml of 9-BBN THF solution (0.5 M, 10.7 mmol, 1.1 eq.). The solution was stirred for 1 h at room temperature followed by

the addition of 15 ml NaOAc solution (3 M, 32.1 mmol, 3 eq.) and 2.5 ml of water. The solution was cooled to 0˚C and 7.5 ml of 30% H_2O_2 in water (42.8 mmol, 4 eq.) was slowly added over 30 minutes and stirred for 16 h. The solution was extracted with Et_2O, dried over $MgSO_4$ and concentrated. The crude product was purified by column chromatography (50:50 EtOAc/hexanes) to yield 2.0 g **S23** (61%) as a colorless oil. Characterization is consistent with previously reported data.[14]

R_f = 0.45 (50:50 EtOAc/hexanes)

^{1}H NMR (400 MHz, $CDCl_3$) δ 6.94 (dt, *J* = 15.6, 7.0 Hz, 1H), 5.78 (d, *J* = 15.6 Hz, 1H), 4.20 – 4.13 (m, 2H), 3.62 (t, *J* = 6.6 Hz, 2H), 2.16 (q, *J* = 7.2 Hz, 2H), 1.53 (m, 2H), 1.42 (m, 2H), 1.30 – 1.24 (m, 15H).

(E)-oxacyclotetradec-3-en-2-one (S24)

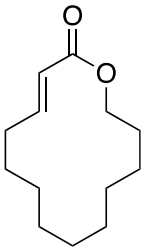

63 mg of **S23** (0.424 mmol) was dissolved in a MeOH/THF/H_2O (4:3:1) mix, followed by 80 mg LiOH (4.2 mmol). The solution was heated to 50˚C and stirred for 12 hours. Upon completion the solution was acidified to pH 2, extracted with EtOAc, dried over $MgSO_4$ and concentrated. The seco acid was dissolved in dry DCM and added to a solution of 705 g DMAP (5.8 mmol, 30

eq.) and 407 mg PyBOP (0.8 mmol, 4 eq.), over a 10-hour period at room temperature to final concentration 0.004 M. The solution was stirred an additional 2 h, quenched with NH_4Cl, extracted with EtOAc, dried over $MgSO_4$ and concentrated. The crude product was purified by column chromatography (3:97 EtOAc/hexanes) to yield 24 mg **S24** (52%) as a colorless oil. Characterization is consistent with previously reported data.[15]

R_f = 0.3 (5:95 EtOAc/hexanes)

^{1}H NMR (400 MHz, $CDCl_3$) δ 7.05 – 6.92 (dt, *J* = 15.6, 7.0 Hz, 1H), 5.79 (d, *J* = 15.7 Hz, 1H), 4.29 – 4.18 (m, 2H), 2.24 (m, 2H), 1.66 (m, 2H), 1.57 (m, 2H), 1.26 (m, 12H).

oxacyclotetradecan-2-one (S25)

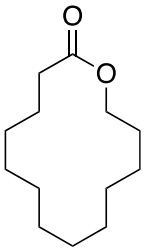

12 mg **S24** (0.06 mmol) was dissolved in a mixture of THF/MeOH (1:1), containing 5 mg Pd/C catalyst. The flask was stirred for 24 h under 1 atm of H_2. The solution was diluted with THF, filtered through celite and concentrated. The crude product was purified by column chromatography (3:97 EtOAc/hexanes) to yield 9 mg **S25** (75%) as a colorless oil. Characterization is consistent with previously reported data.[16]

R_f = 0.1 (3:97 EtOAc/hexanes)

^{1}H NMR (400 MHz, $CDCl_3$) δ 4.17 – 4.09 (m, 2H), 2.39 – 2.30 (m, 2H), 1.62 (dd, *J* = 11.7, 6.2 Hz, 4H), 1.42 – 1.21 (m, 16H).

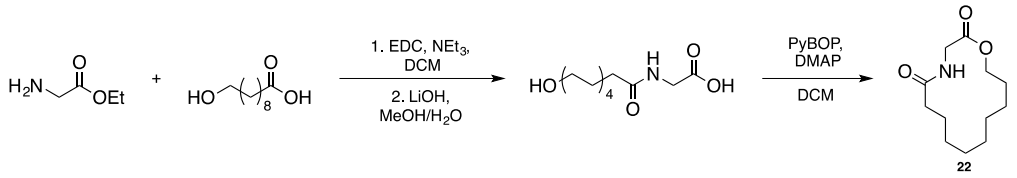

Scheme S4. General synthetic strategy for the synthesis of compound **22**.

(10-hydroxydecanoyl)glycine (S26)

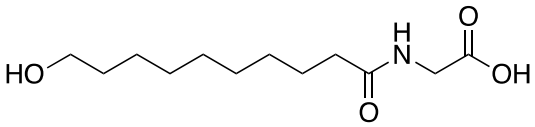

To a solution of 685 mg ethyl glycinate (4.91 mmol, 1.5 eq.) in DCM was added 1.1 g EDC (3.19 mmol, 1.6 eq.) and 1.37 mL NEt_3 (9.8 mmol, 3 eq.), the solution was then stirred for 10 minutes. 600 mg 10-hydroxydecanoic acid (3.19 mmol) was added to the solution at 0˚C and stirred for 14 h at room temperature. The solution was quenched with NH_4Cl, extracted with EtOAc, dried over $MgSO_4$, and concentrated. The crude product was dissolved in MeOH/THF/H_2O (6:10:6), followed by the addition of 845 mg LiOH (36.7 mmol, 10 eq.) and subsequently stirred at 60˚C for 4 h. The solution was acidified to pH 2, extracted with EtOAc, dried over $MgSO_4$, and concentrated. The crude product was purified by column chromatography (80:20 EtOAc) to yield 600 mg **S26** (77%) as a white powder.

R_f = 0.2 (80:20 EtOAc/hexanes)

^{1}H NMR (400 MHz, DMSO-d_6) δ 8.02 (s, 1H), 3.66 (d, *J* = 5.9 Hz, 2H), 3.33 (m, 2H), 2.06 (t, *J* = 7.4 Hz, 2H), 1.50 – 1.30 (m, 4H), 1.20 (m, 10H).

^{13}C NMR (100 MHz, DMSO-d_6) δ 173.02, 171.92, 61.18, 40.99, 35.52, 33.01, 29.46, 29.39, 29.25, 29.07, 25.96, 25.65.

HRMS (ESI+) calc. for $C_{12}H_{23}NO_4Na$ (M+Na) 268.1525; obsd. 268.1536

1-oxa-4-azacyclotetradecane-2,5-dione (24)

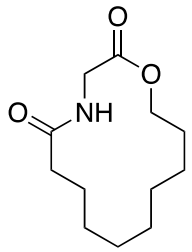

100 mg **S26** (0.41 mmol) was dissolved in dry DCM and added to a solution of 705 g DMAP (5.8 mmol, 30 eq.) and 407 mg PyBOP (0.8 mmol, 4 eq.), over a 10-hour period at room temperature to a final concentration of 0.004 M. The solution was stirred an additional 2 h, quenched with NH_4Cl, extracted with EtOAc, dried over $MgSO_4$ and concentrated. The crude product was purified by column chromatography (30:70 EtOAc/hexanes) to yield 56 mg **24** (56%) as a white solid.

R_f = 0.3 (30:70 EtOAc/hexanes)

^{1}H NMR (400 MHz, $CDCl_3$) δ 5.92 – 5.76 (s, 1H), 4.22 – 4.15 (m, 2H), 4.08 (d, *J* = 6.3 Hz, 2H), 2.30 – 2.22 (m, 2H), 1.73 – 1.59 (m, 4H), 1.36 (m, 10H).

^{13}C NMR (100 MHz, CD_3OD) δ 172.91, 169.16, 64.57, 41.86, 35.50, 26.76, 26.30, 26.01, 25.85, 25.25, 24.89, 23.16.

HRMS (ESI+) calc. for $C_{12}H_{21}NO_3Na$ (M+Na)250.1419; obsd. 250.1407

Enzymatic Assays

Rdc TE and Zea TE were expressed from pMW29[1] and pMW14[2] respectively. The proteins were purified to homogeneity according to our previously reported method[1]. The enzymes were stored at -80˚C in a 30% glycerol solution until immediately before use, where they were diluted to 100 μM stock solutions in 50 mM phosphate buffer (pH 7.4). The lyophilized Rdc TE was expressed and purified in an identical manner as the freezer stocks; however, it was freeze dried prior to the addition of glycerol. The powdered enzyme was reconstituted in 50 mM phosphate buffer (pH 7.4) and diluted to a working concentration of 100 μM in 50 mM phosphate buffer (pH 7.4). All TE assays where HPLC was used to characterize product distribution were carried out with 1.0 mM of the SNAC substrate, 50 mM phosphate buffer at pH 7.4, DMSO up to 10% by volume, and 5 μM thioesterase with the exception of the 10-member substrate (**11**) which used 20 μM of both thioesterases, and the 14-member lactam substrate (**16**) which used 25 μM for the Zea TE assay. Assays were quenched by the addition of an equal volume of 0.5% formic acid in acetonitrile. HPLC analysis was conducted using a gradient from 15% B to 95% B over 18 minutes and held at 95% B for 1 minute (A: Water, B: Acetonitrile) with the exception of 14-

membered substrates **17, 18,** and **19**, that used a gradient of 0% B to 100% B over 35 minutes and held at 100% B for 2 minutes (A: Water, B: Acetonitrile).

Macrocyclization kinetics for the Rdc TE with the 14-member substrate (**6**) were studied in a discontinuous manner in 50 mM phosphate buffer (pH 7.4), substrate concentrations ranging from 0.5 mM to 2.0 mM (from a 50 mM stock solution), 5 μM of Rdc TE, and DMSO up to 10% solution volume. The assays were quenched with an equal volume of 0.5% formic acid in acetonitrile before being analyzed by HPLC. HPLC analysis was conducted in an identical manner as above. Amount of macrocycle produced was determined by comparison to a standard curve of authentic, synthetic macrocycle. Non-linear regression was performed with GraphPad Prism 6.

Activity was assayed discontinuously with reaction aliquots mixed with saturated Ellman's reagent. Rdc TE has been shown to inactivate in real-time assays in the presence of DTNB. 1 μL of saturated DTNB in 50 mM potassium phosphate was mixed with 24 μL of reaction mixture at its endpoint to reach a final 4 % volume as shown in previous assay conditions. 2 μL of this mixture was loaded onto a Nanodrop 2000 podium and recorded at 412 nm. A standard curve using *N*-acetyl cysteamine in assay conditions was used to generate a standard curve (0, 5, 10, 25, 50, 75, 100, 500, 1000 μM in triplicate).

The effect of DMSO concentration on lyophilized Rdc TE activity was assayed on the 100 μL scale with 5 μM enzyme, 2.5 mM *S*-(2-acetamidoethyl) benzothioate[2], 10-50% (v/v) DMSO, and 50 mM potassium phosphate (pH 7.4). Conversion was measured after 10 minutes of reaction.

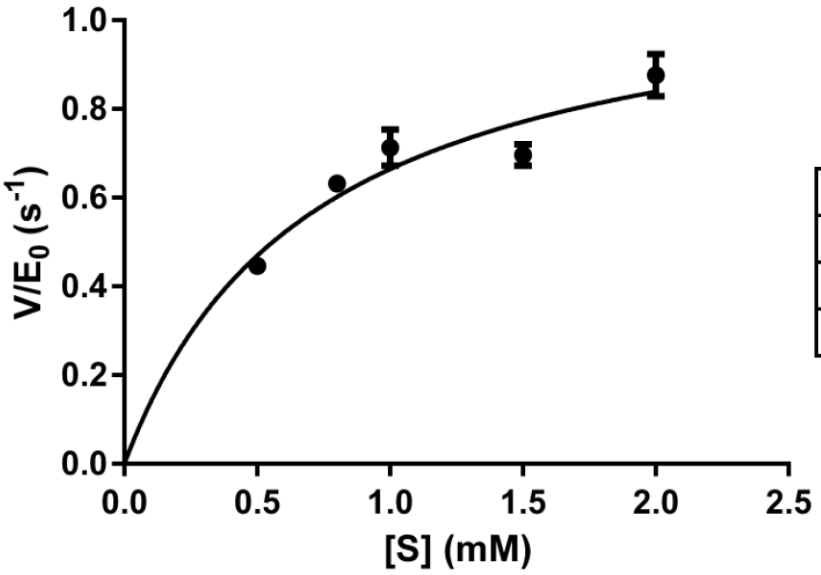

	Value	Error
R^2	0.846	N/A
k_{cat}	1.14	0.11
K_M	0.71	0.18

Figure S1. Initial reaction rates (s^{-1}) plotted against substrate concentration (mM) for conversion to macrocycle for Rdc TE with substrate **6**. These data were fit with the Michaelis-Menten model.

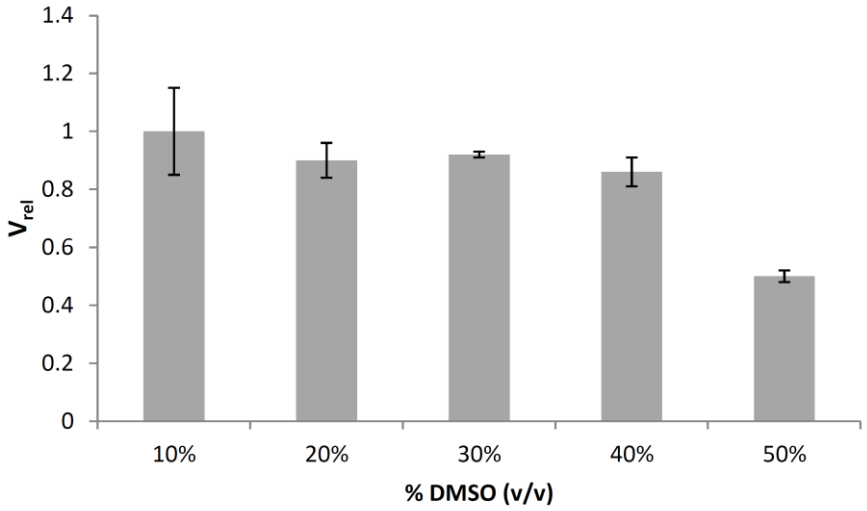

Figure S2. Initial reaction rates for *S*-(2-acetamidoethyl) benzothioate with Rdc TE with varying concentrations of DMSO. Rates are relative to the standard reaction conditions at 10% (v/v) DMSO. Duplicate data for 20% and 30% DMSO, triplicate for all others.

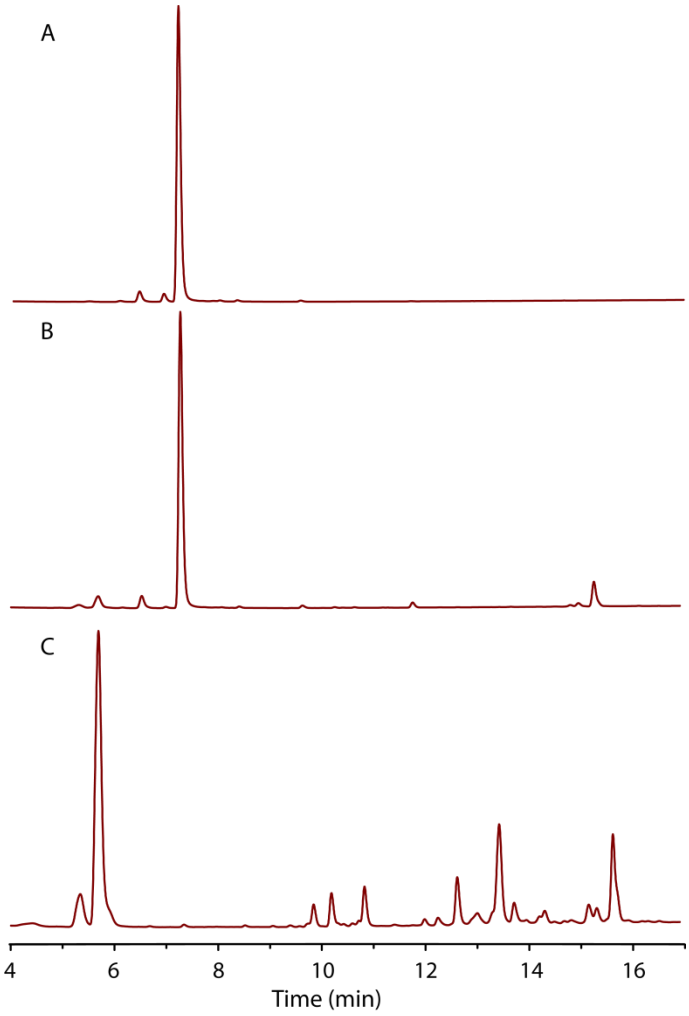

Figure S3. Summary trace for the enzymatic reaction of **11** with Radicicol and Zearalenone TEs. A: No enzyme blank containing 1 mM **11**, 50 mM phosphate buffer (pH 7.4) and 10% v/v DMSO, 12 hours. B: 1 mM **11** incubated with 20 µM Rdc TE, 50 mM phosphate buffer (pH 7.4), 10% v/v DMSO, 12 hours. C: 1 mM **11**, incubated with 20 µM Zea TE, 50 mM phosphate buffer (pH 7.4), 10% v/v DMSO, 12 hours.

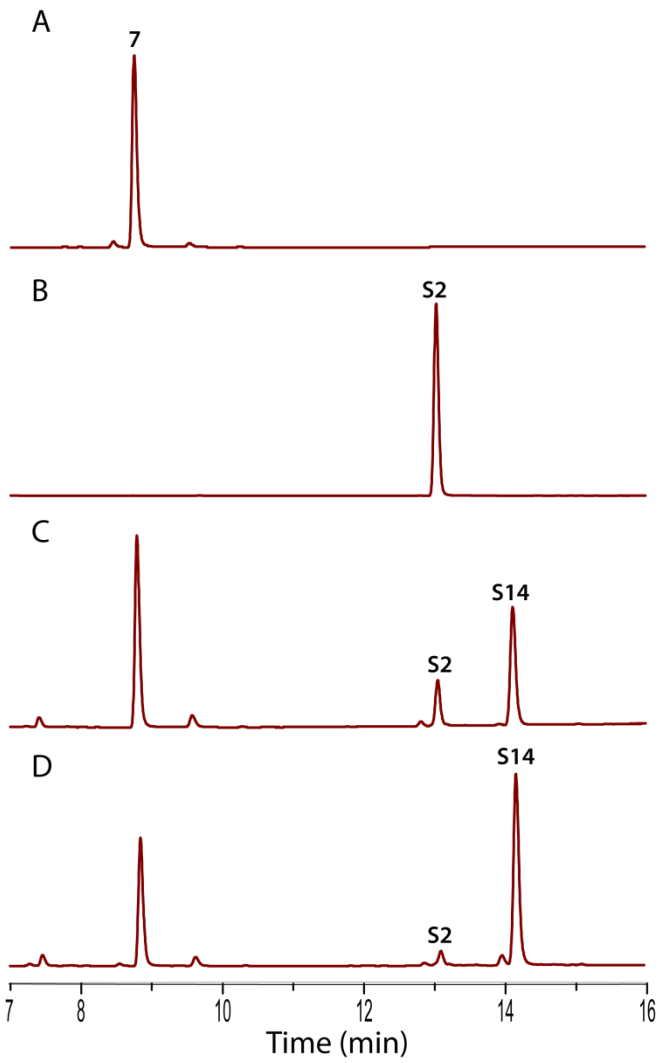

Figure S4. Summary trace for the enzymatic reaction of **7** with Radicicol and Zearalenone TEs. A: No enzyme blank containing 1 mM **7**, 50 mM phosphate buffer (pH 7.4) and 10% v/v DMSO, 2 hours. B: Macrocycle authentic standard **S2**. C: 1 mM **7** incubated with 5 µM Rdc TE, 50 mM phosphate buffer (pH 7.4), 10% v/v DMSO, 2 hours. D: 1 mM **7**, incubated with 5 µM Zea TE, 50 mM phosphate buffer (pH 7.4), 10% v/v DMSO, 2 hours. Peak at 14.2 min is linear-SNAC dimer **S14**

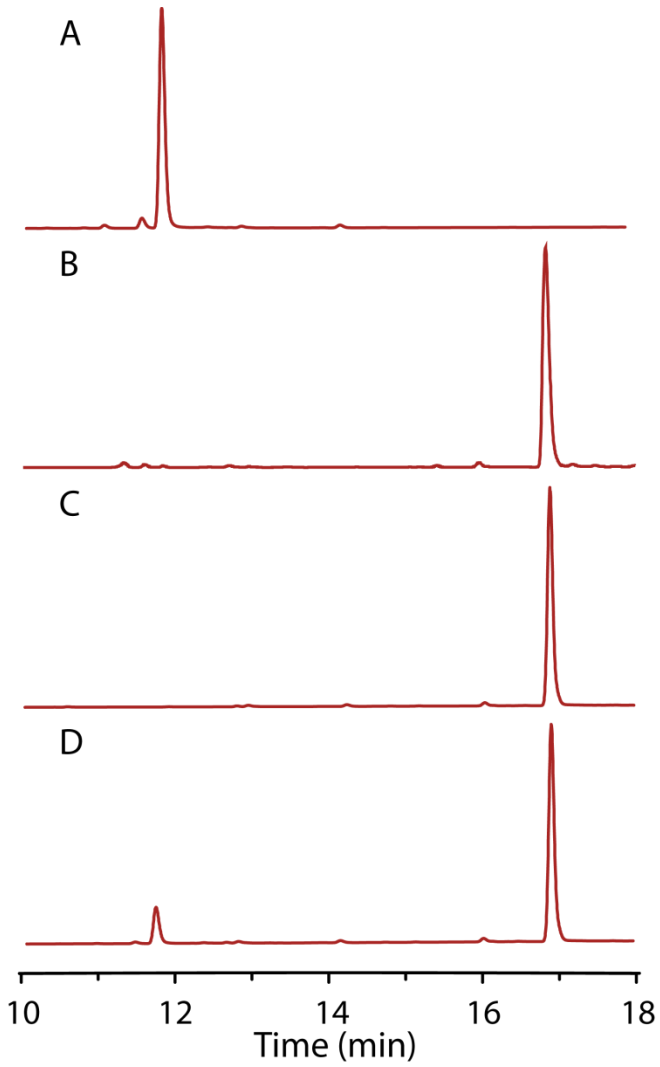

Figure S5. Summary trace for the enzymatic reaction of **8** with Radicicol and Zearalenone TEs. A: No enzyme blank containing 1 mM **8**, 50 mM phosphate buffer (pH 7.4) and 10% v/v DMSO, 2 hours. B: Authentic macrocycle standard. C: 1 mM **8** incubated with 5 µM Rdc TE, 50 mM phosphate buffer (pH 7.4), 10% v/v DMSO, 2 hours. D: 1 mM **8**, incubated with 5 µM Zea TE, 50 mM phosphate buffer (pH 7.4), 10% v/v DMSO, 2 hours.

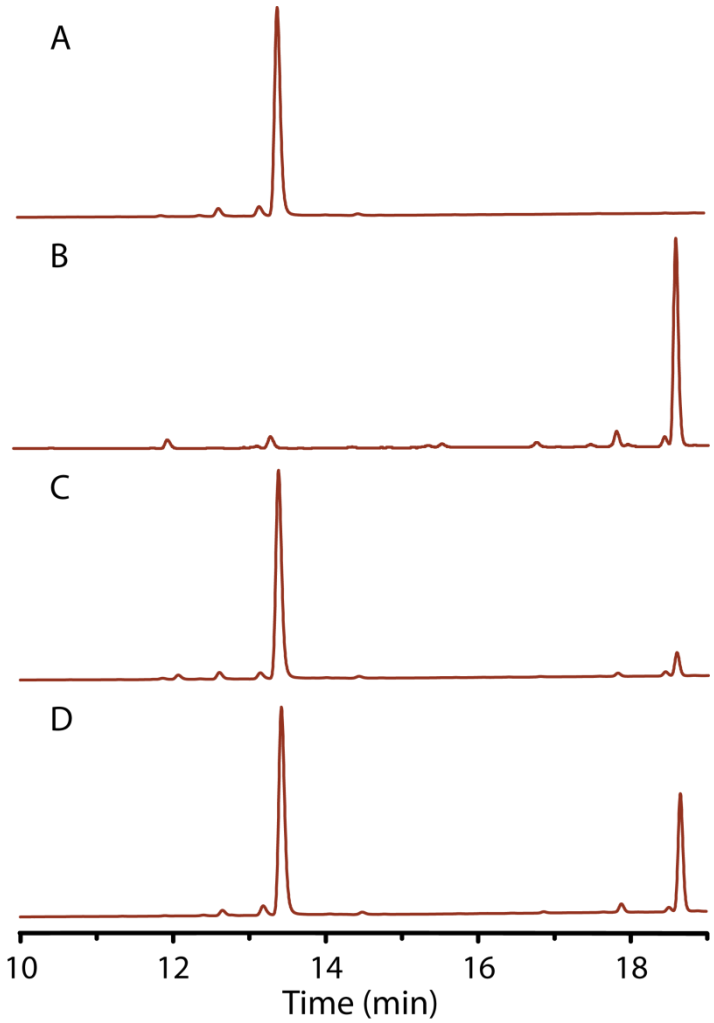

Figure S6. Summary trace for the enzymatic reaction of **9** with Radicicol and Zearalenone TEs. A: No enzyme blank containing 1 mM **9**, 50 mM phosphate buffer (pH 7.4) and 10% v/v DMSO, 2 hours. B: Authentic macrocycle standard. C: 1 mM **9** incubated with 5 µM Rdc TE, 50 mM phosphate buffer (pH 7.4), 10% v/v DMSO, 2 hours. D: 1 mM **9**, incubated with 5 µM Zea TE, 50 mM phosphate buffer (pH 7.4), 10% v/v DMSO, 2 hours.

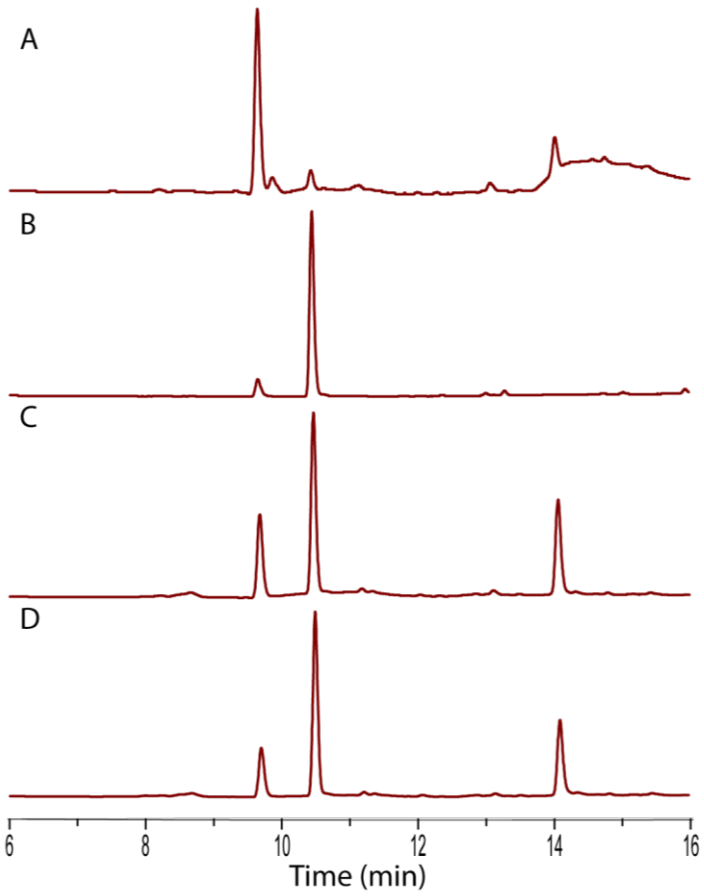

Figure S7. Summary HPLC traces for macrolactam substrate **16** showing production of macrocycle **S13** as well as dimer formation. A: No enzyme blank containing 1 mM **16**, 50 mM phosphate (pH 7.4) and 10% DMSO v/v, 3 h. B: Macrocycle standard **S12**. C: 1 mM **16** incubated with 5 µM Rdc TE, 50 mM phosphate buffer (pH 7.4), 10% v/v DMSO, 3 h. D: 1 mM **16**, incubated with 25 µM Zea TE, 50 mM phosphate buffer (pH 7.4), 10% v/v DMSO, 3 h.

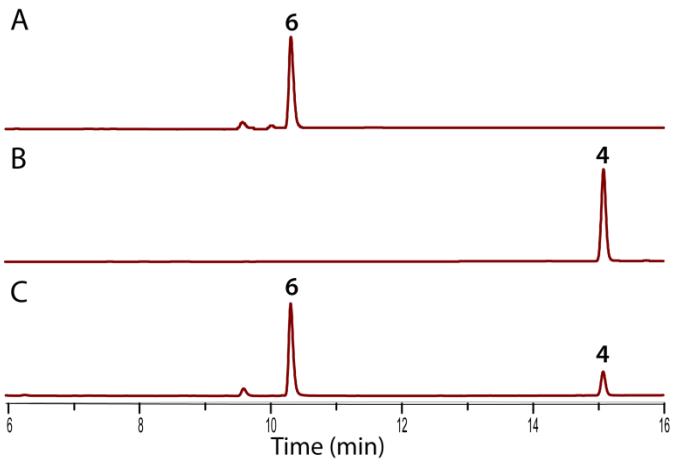

Figure S8. HPLC traces demonstrating that Rdc TE retains activity after lyophylization and prolonged room temperature storage. A. No enzyme blank containing 1 mM **6**, 50 mM phosphate (pH 7.4) and 10% DMSO v/v, 3 h. B: Macrocycle standard **4**. C: 1 mM **6** incubated with lyophilized 5 µM Rdc TE, 50 mM phosphate buffer (pH 7.4), 10% v/v DMSO, 3 h. D: 1 mM **6**, incubated with lyophilized 25 µM Zea TE, 50 mM phosphate buffer (pH 7.4), 10% v/v DMSO, 3 h

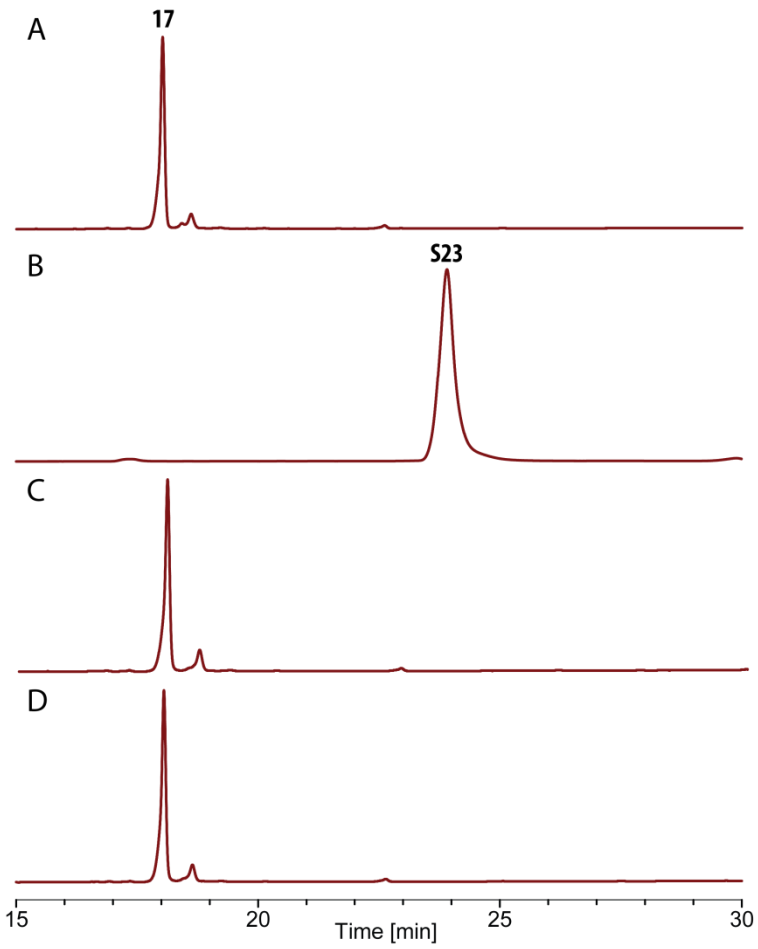

Figure S9. Summary trace for the enzymatic reaction of **17** with Radicicol and Zearalenone TEs. A. No enzyme blank containing 1 mM **17**, 50 mM phosphate (pH 7.4) and 10% DMSO v/v, 16 h. B: Macrocycle standard **S23**. C: 1 mM **17** incubated with 5 µM Rdc TE, 50 mM phosphate buffer (pH 7.4), 10% v/v DMSO, 16 h. D: 1 mM **17**, incubated with 5 µM Zea TE, 50 mM phosphate buffer (pH 7.4), 10% v/v DMSO, 16 h

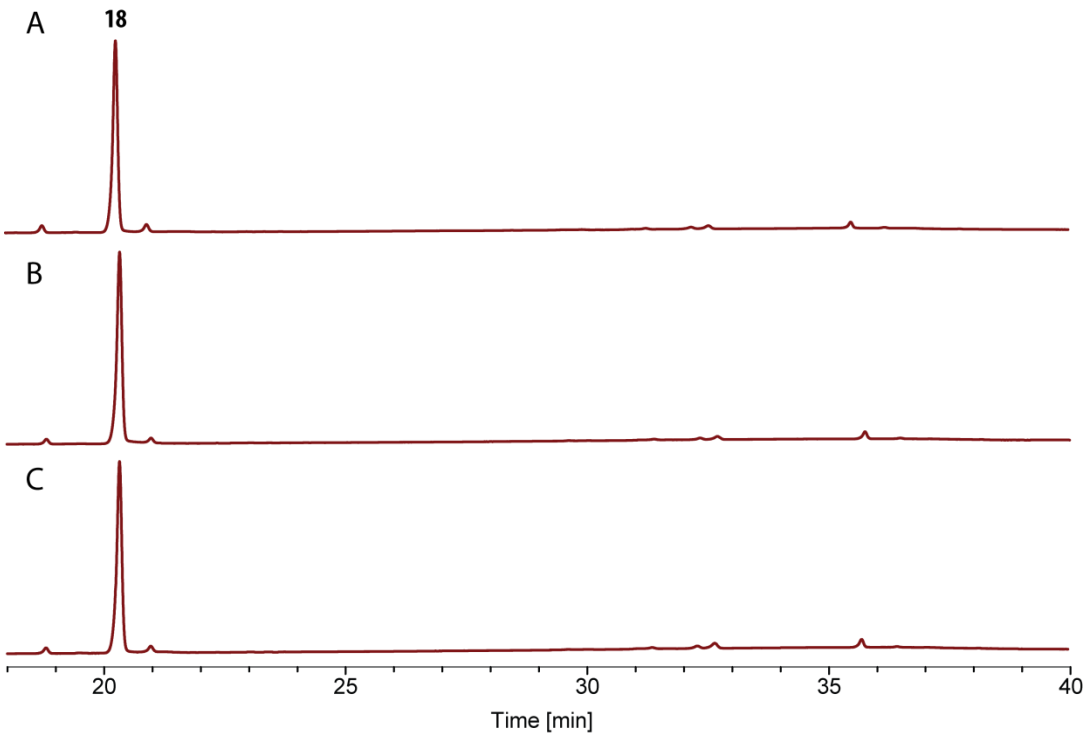

Figure S10. Summary trace for the enzymatic reaction of **18** with Radicicol and Zearalenone TEs. A. No enzyme blank containing 1 mM **18**, 50 mM phosphate (pH 7.4) and 10% DMSO v/v, 16 h. B: 1 mM **18** incubated with 5 µM Rdc TE, 50 mM phosphate buffer (pH 7.4), 10% v/v DMSO, 16 h. C: 1 mM **18**, incubated with 5 µM Zea TE, 50 mM phosphate buffer (pH 7.4), 10% v/v DMSO, 16 h

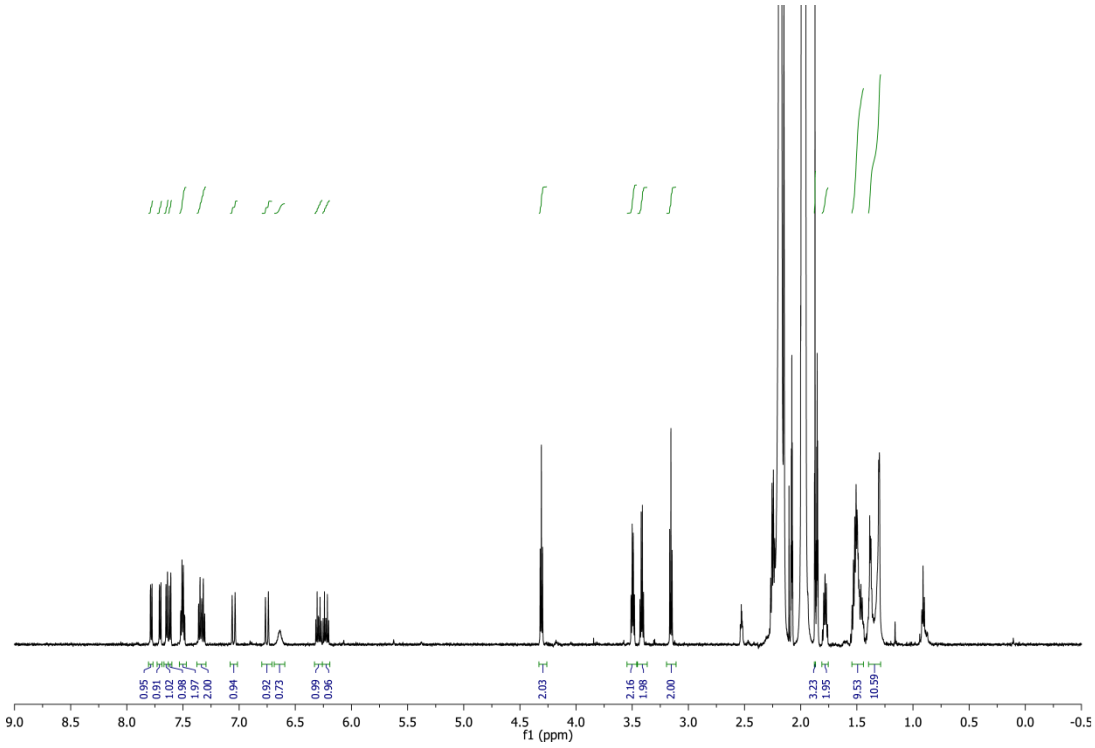

Figure S11. 600 MHz ^{1}H spectra of the enzymatically generated linear SNAc dimer of **7, S14**. The spectrum shows characteristic doubling of peaks in the aromatic region as well as characteristic peaks for the -C**H**$_2$C**H**$_2$- methylenes and broad -N**H**- singlet of the SNAc thioester.

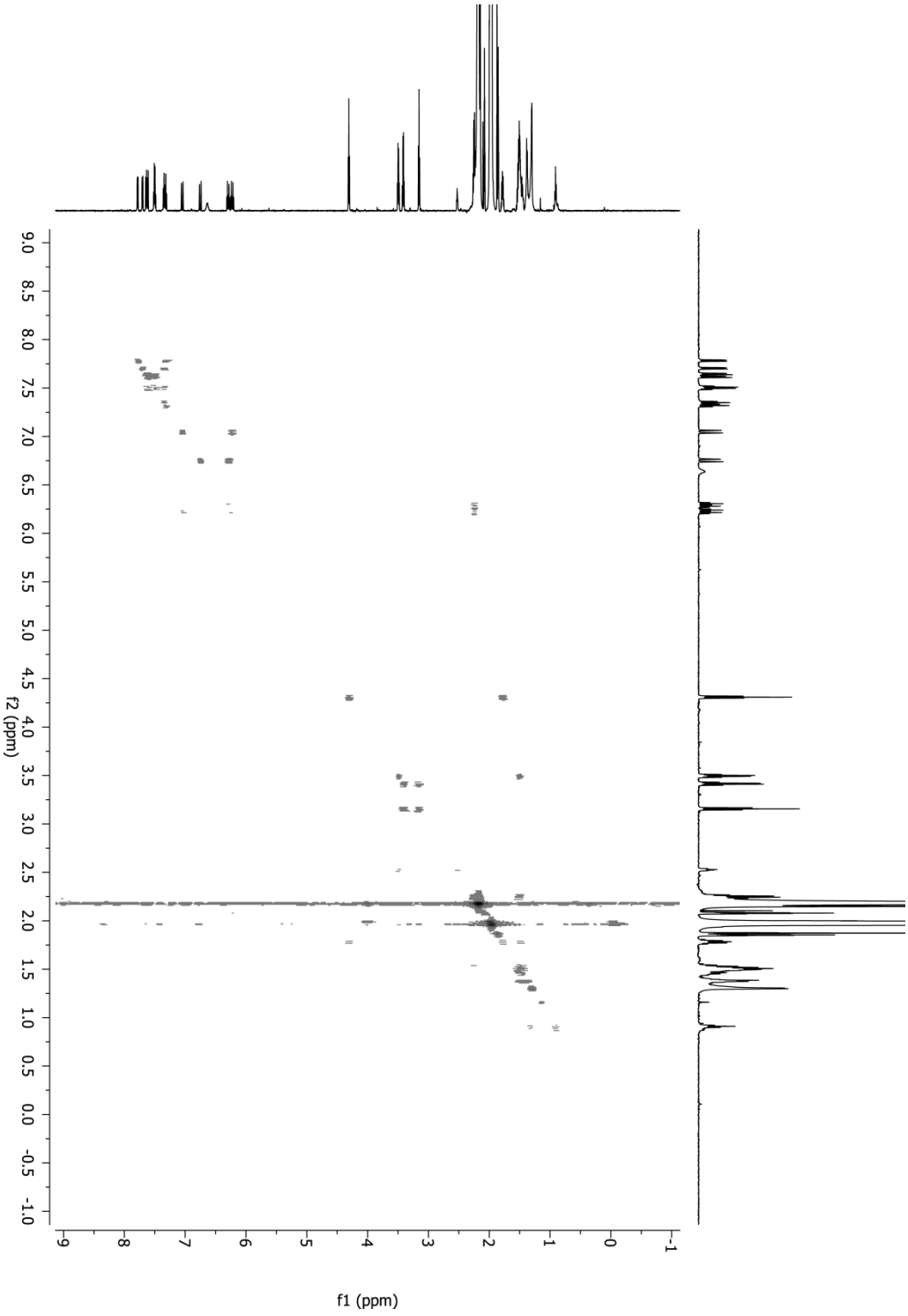

Figure S12. 2D COSY spectrum of the enzymatically generated linear SNAc dimer of **7, S14**

Selected NMR Spectra

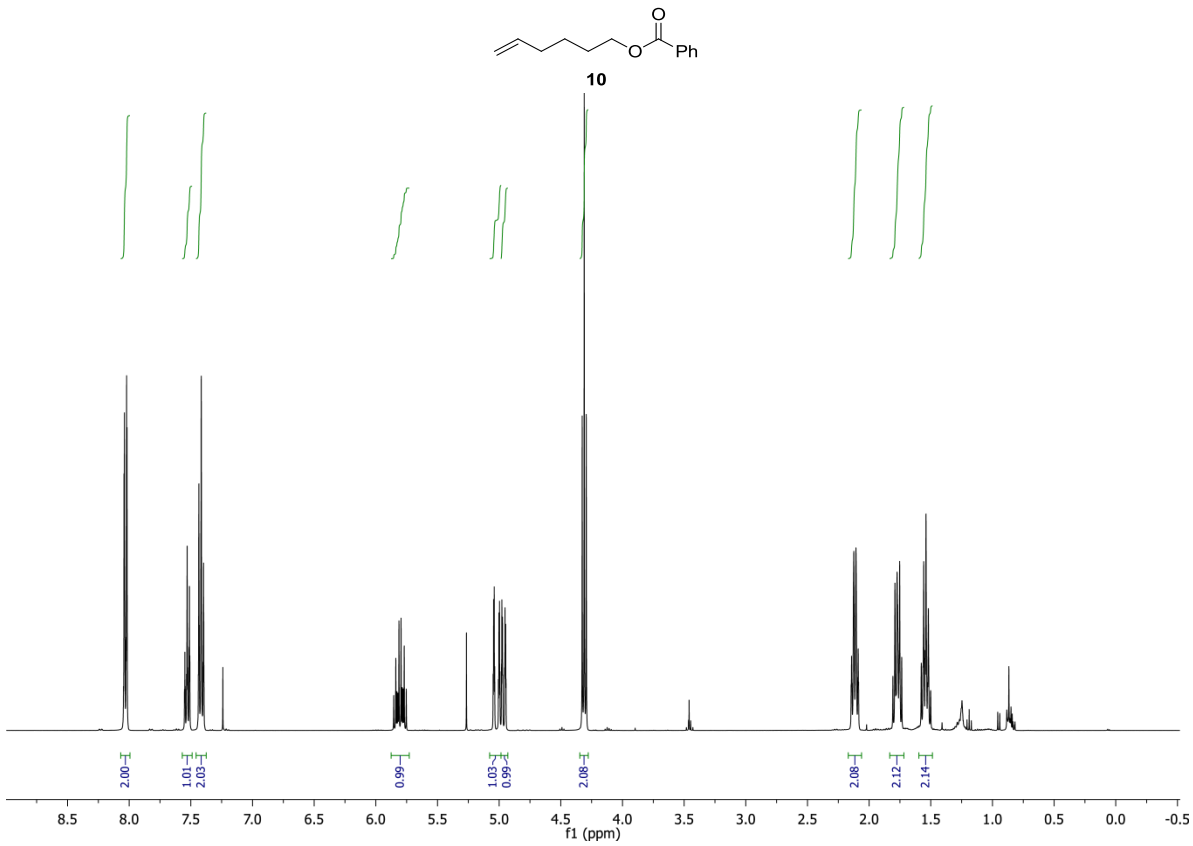

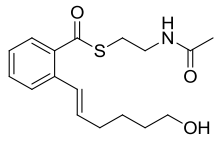
O
S
H
N
O
OH

11

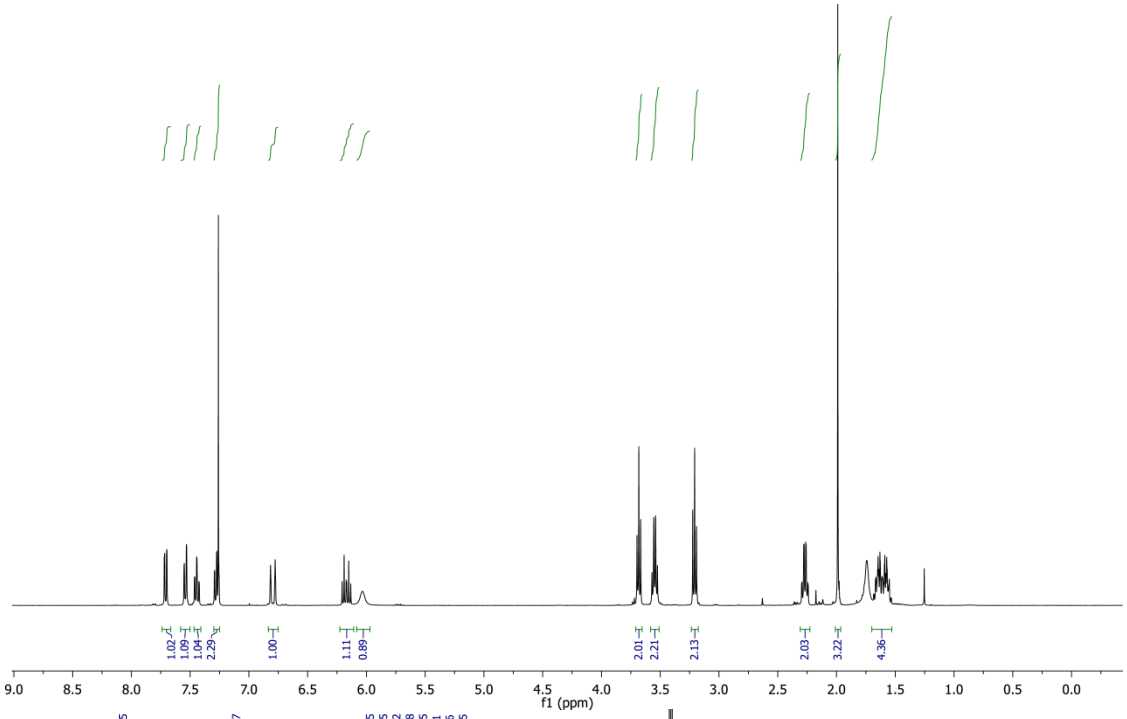
1.02
1.09
1.04
2.29
1.00
1.11
0.89
2.01
2.21
2.13
2.03
3.22
4.36
9.0 8.5 8.0 7.5 7.0 6.5 6.0 5.5 5.0 4.5 4.0 3.5 3.0 2.5 2.0 1.5 1.0 0.5 0.0
f1 (ppm)

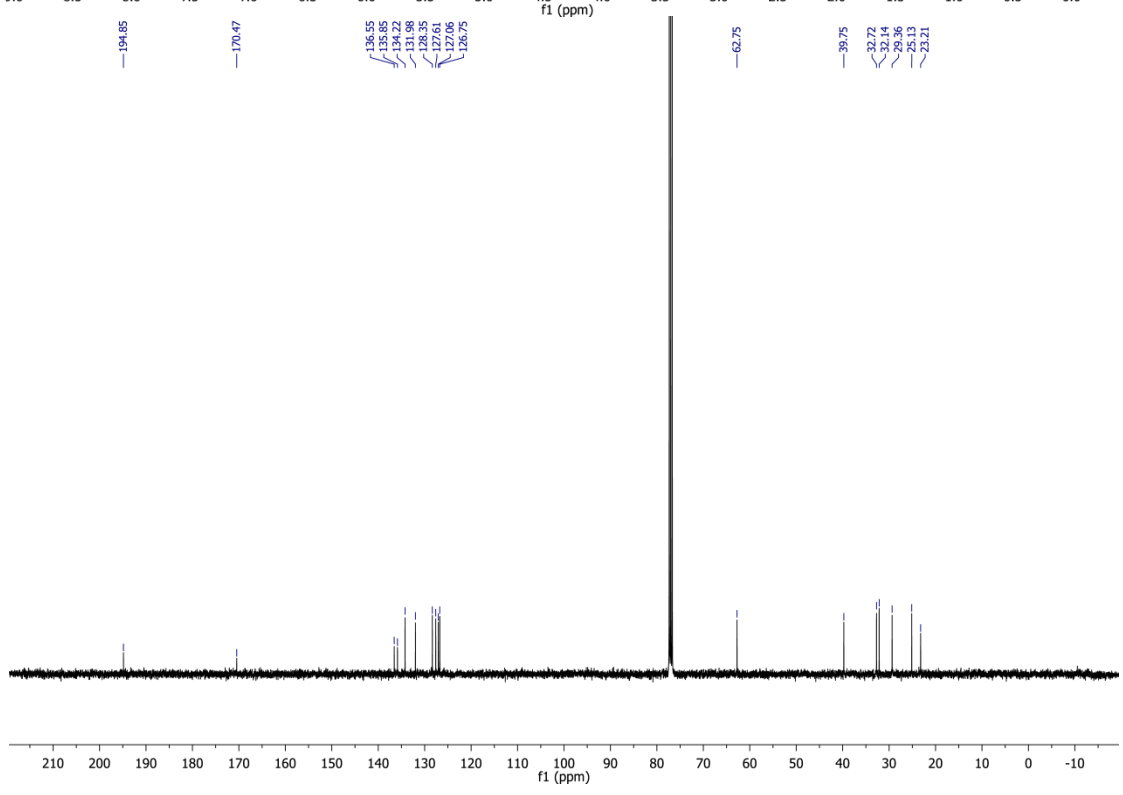
194.85
170.47
136.55
135.85
134.22
131.98
128.35
127.61
127.06
126.75
62.75
39.75
32.72
32.14
29.36
25.13
23.21
210 200 190 180 170 160 150 140 130 120 110 100 90 80 70 60 50 40 30 20 10 0 -10
f1 (ppm)

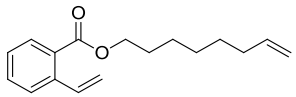

S1

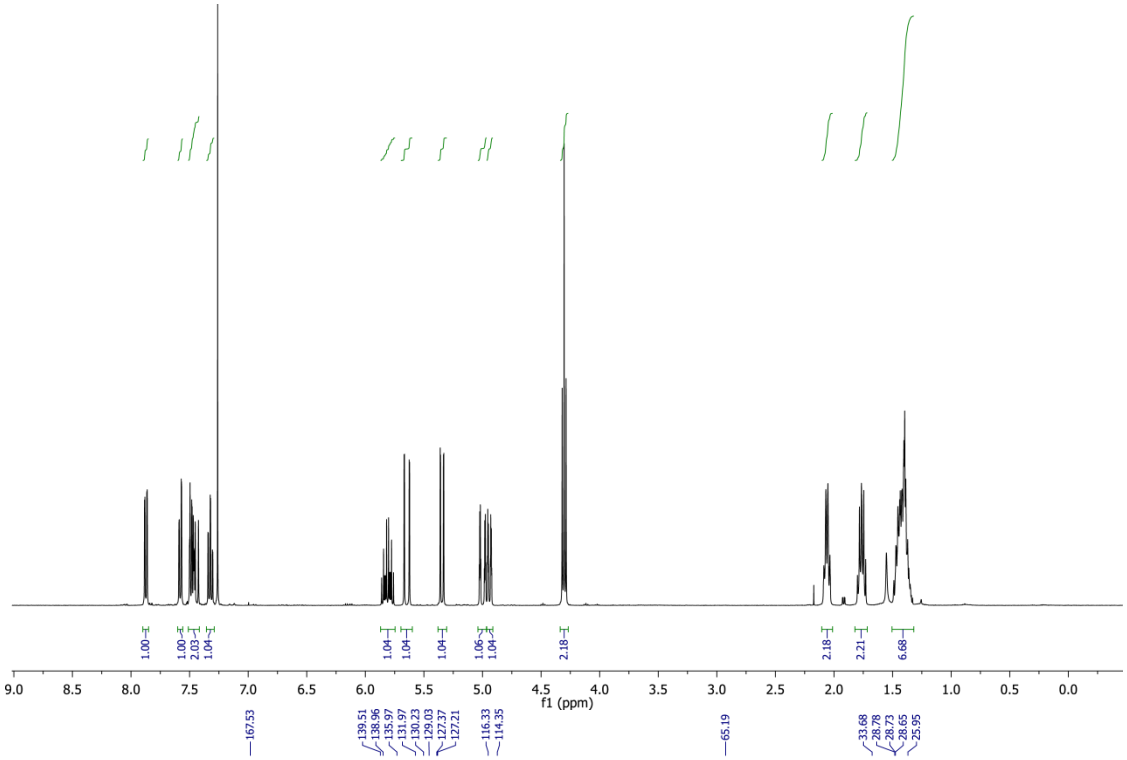
1.00
1.00
2.03
1.04
1.04
1.04
1.04
1.06
1.04
2.18
2.18
2.21
6.68
9.0 8.5 8.0 7.5 7.0 6.5 6.0 5.5 5.0 4.5 4.0 3.5 3.0 2.5 2.0 1.5 1.0 0.5 0.0
f1 (ppm)

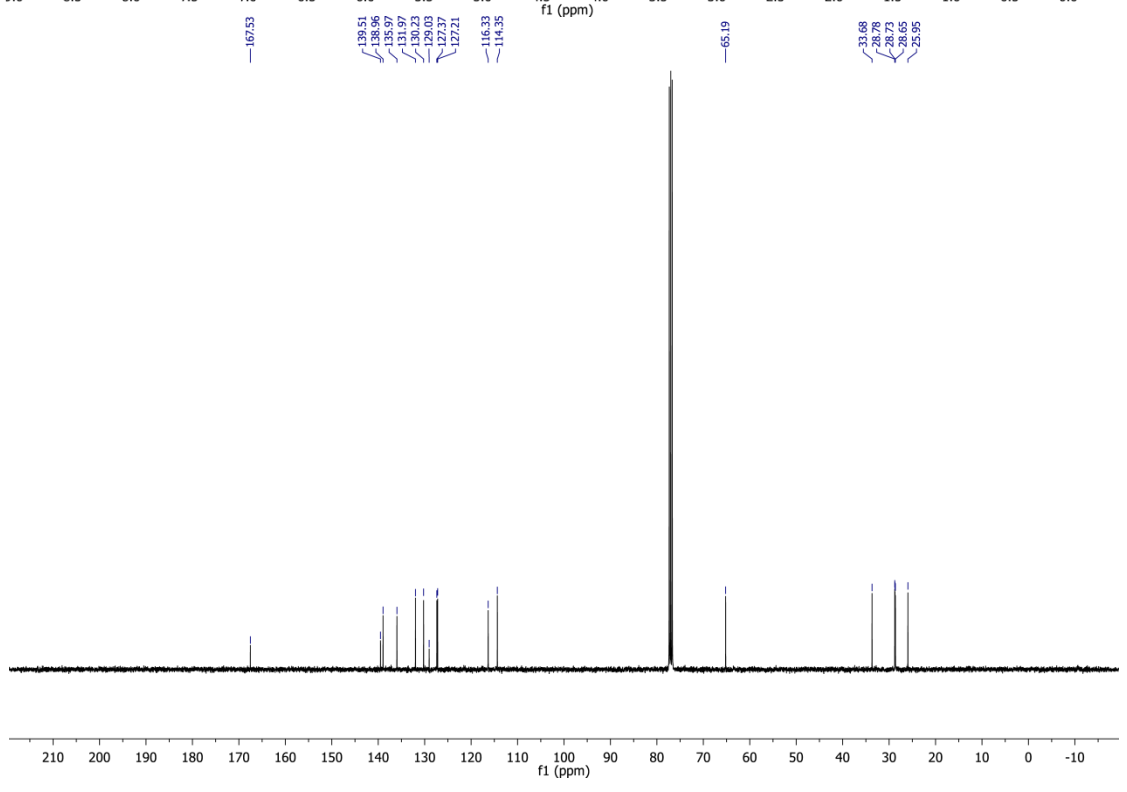
167.53
130.51
138.96
135.97
131.97
130.23
129.03
127.37
127.21
116.33
114.35
65.19
33.68
28.78
28.73
28.65
25.95
210 200 190 180 170 160 150 140 130 120 110 100 90 80 70 60 50 40 30 20 10 0 -10
f1 (ppm)

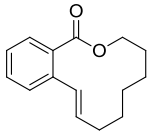

20

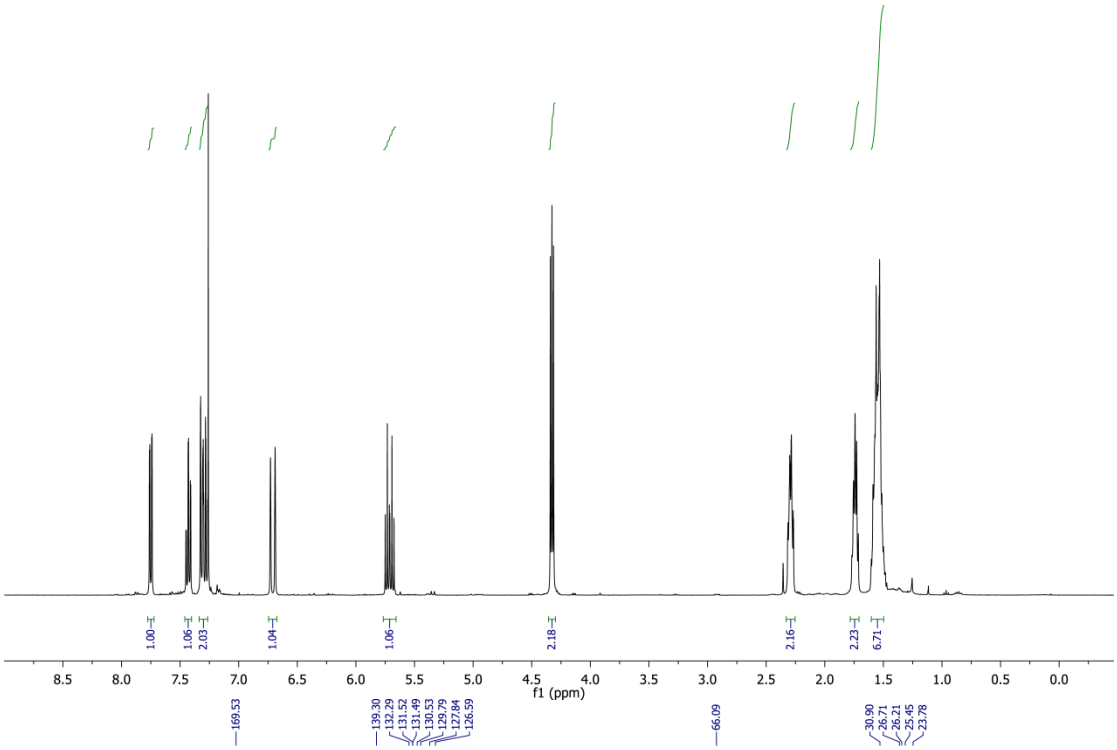
1.00
1.06
2.03
1.04
1.06
2.18
2.16
2.23
6.71
f1 (ppm)

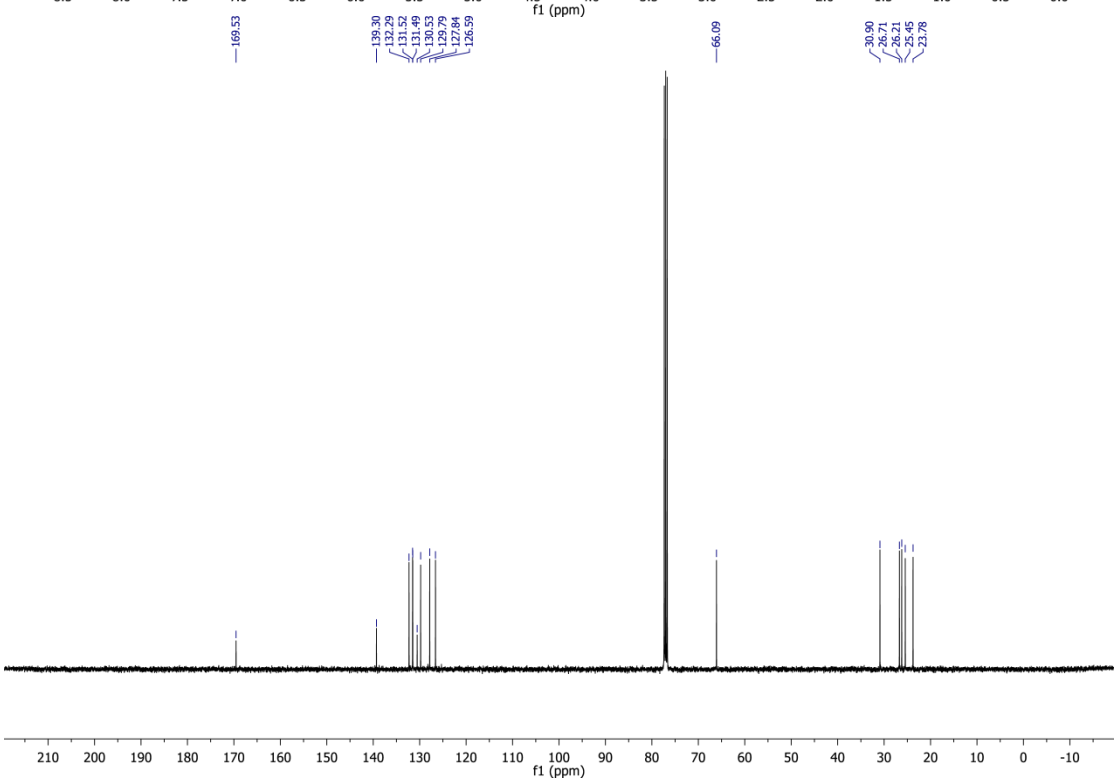
169.53
139.30
132.29
131.52
131.49
130.53
129.79
127.84
126.59
66.09
30.90
26.71
26.21
25.45
23.78
f1 (ppm)

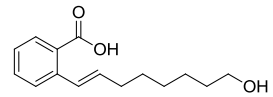
O
OH
OH

S5

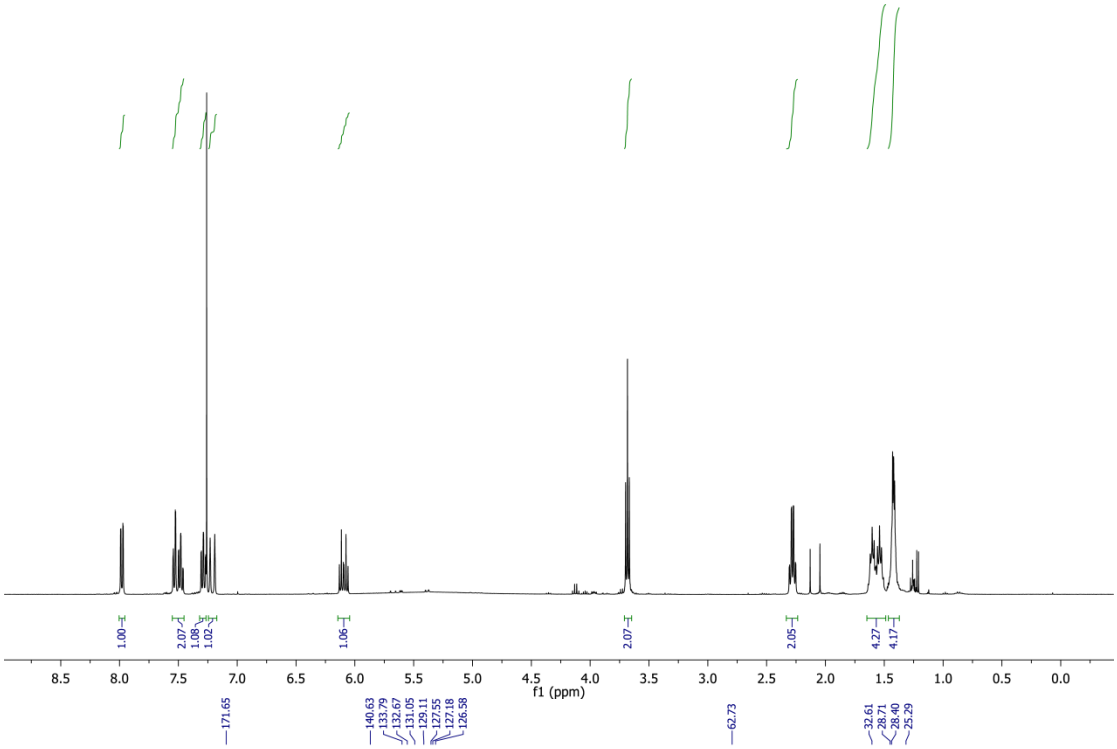
1.00
2.07
1.08
1.02
1.06
2.07
2.05
4.27
4.17
8.5 8.0 7.5 7.0 6.5 6.0 5.5 5.0 4.5 4.0 3.5 3.0 2.5 2.0 1.5 1.0 0.5 0.0
f1 (ppm)

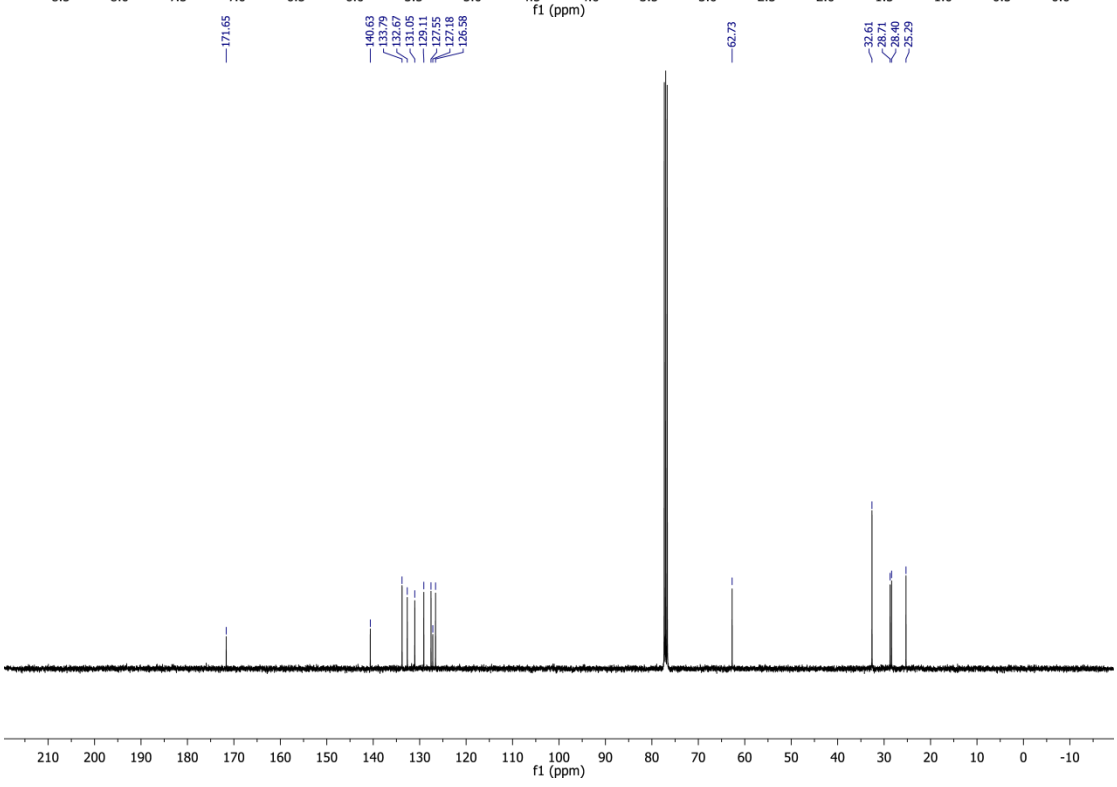
171.65
140.63
133.79
132.67
131.05
129.11
127.55
127.18
126.58
62.73
32.61
28.71
28.40
25.29
210 200 190 180 170 160 150 140 130 120 110 100 90 80 70 60 50 40 30 20 10 0 -10
f1 (ppm)

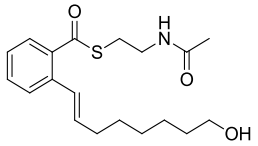
O
H
N
S
O
OH

7

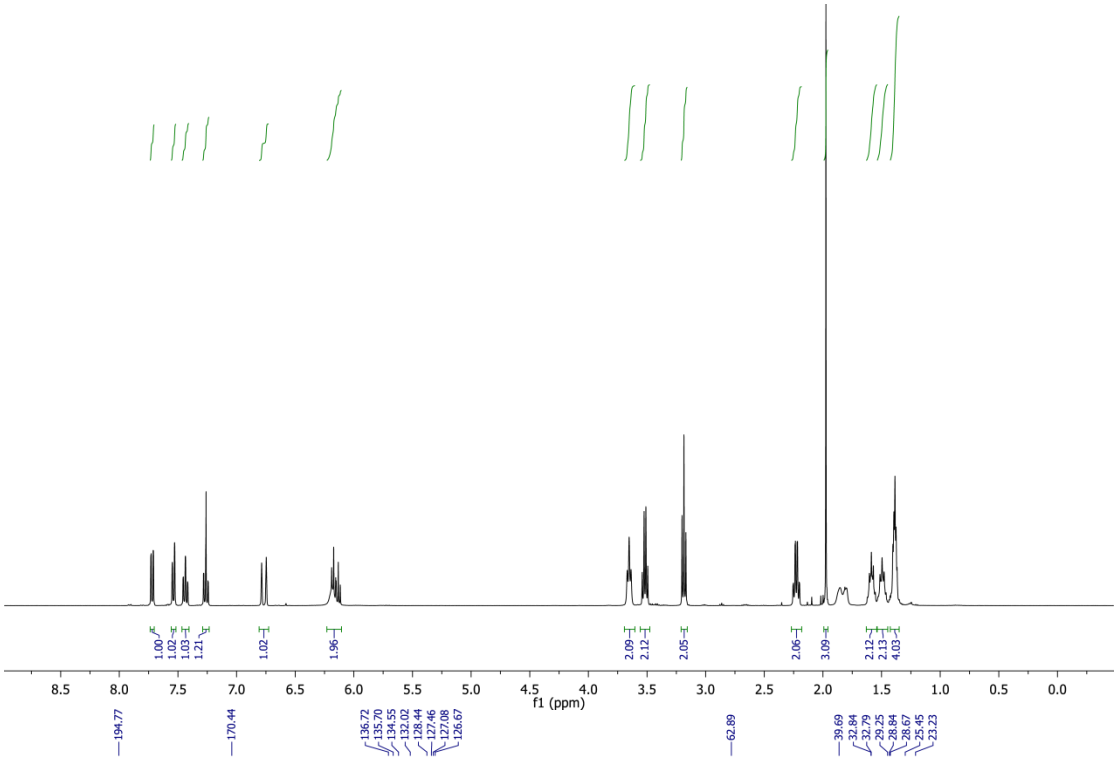
1.00
1.02
1.03
1.21
1.02
1.96
2.09
2.12
2.05
2.06
3.09
2.12
2.13
4.03
8.5 8.0 7.5 7.0 6.5 6.0 5.5 5.0 4.5 4.0 3.5 3.0 2.5 2.0 1.5 1.0 0.5 0.0
f1 (ppm)

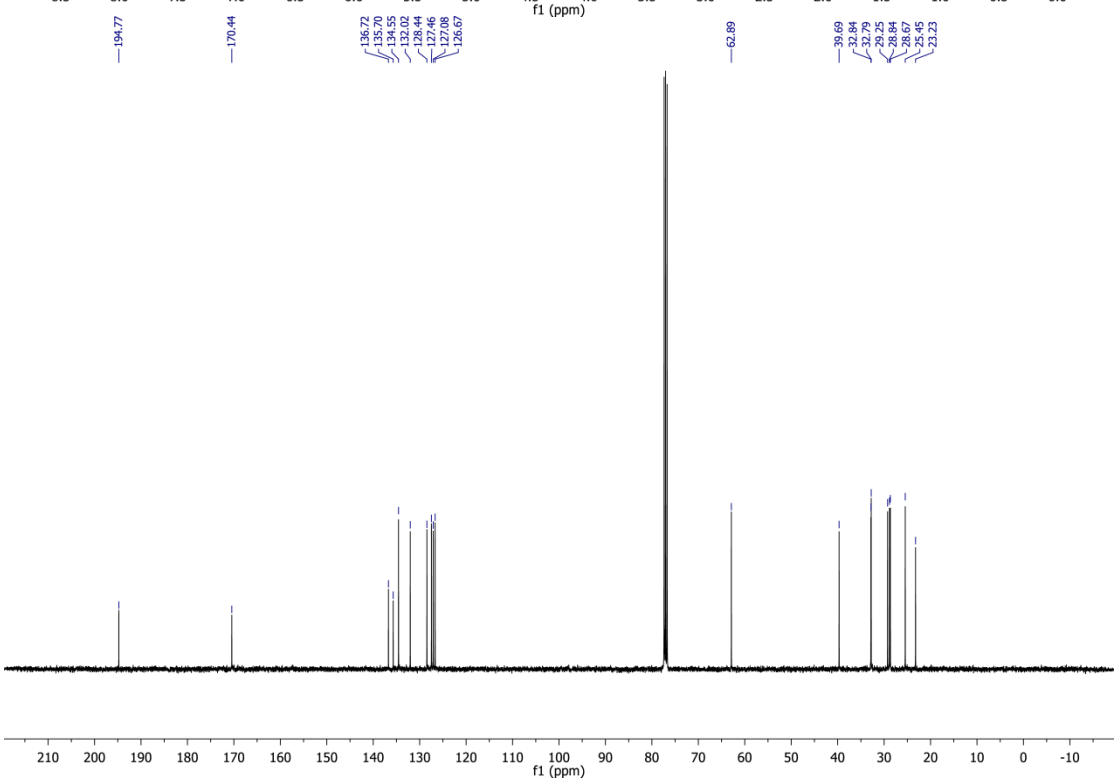
194.77
170.44
136.72
135.70
134.55
132.02
128.44
127.46
127.08
126.67
62.89
39.69
32.84
32.79
29.25
28.84
28.67
25.45
23.23
210 200 190 180 170 160 150 140 130 120 110 100 90 80 70 60 50 40 30 20 10 0 -10
f1 (ppm)

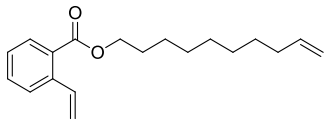

3

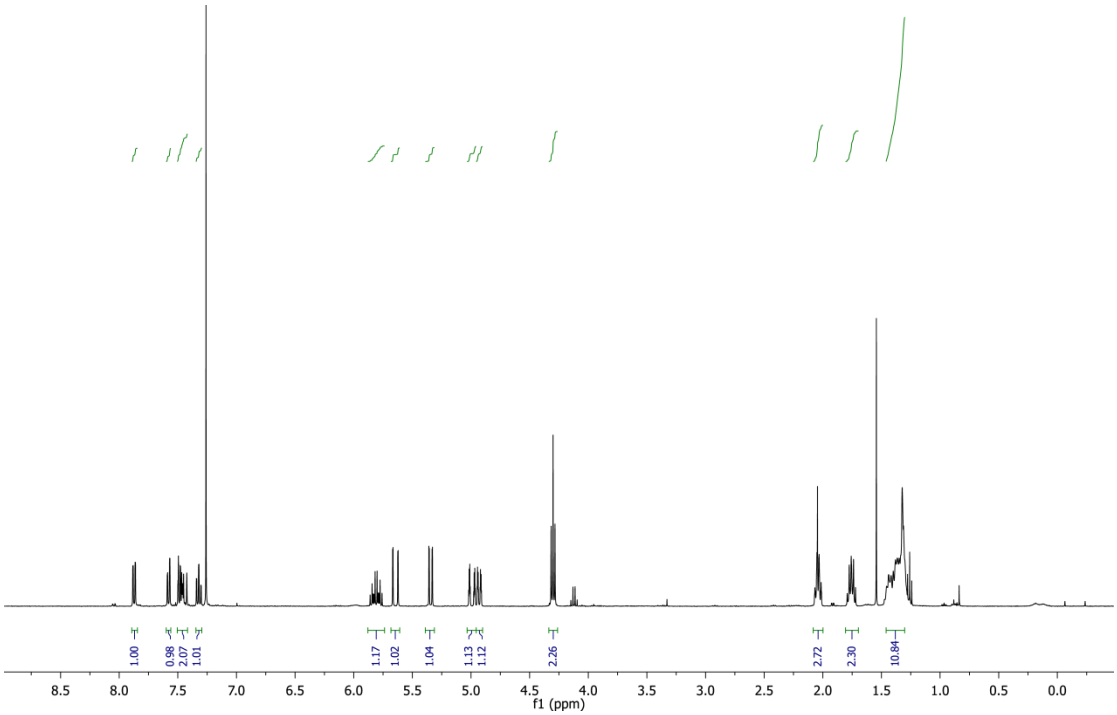
1.00
0.98
2.07
1.01
1.17
1.02
1.04
1.13
1.12
2.26
2.72
2.30
10.84
8.5
8.0
7.5
7.0
6.5
6.0
5.5
5.0
4.5
4.0
3.5
3.0
2.5
2.0
1.5
1.0
0.5
0.0
f1 (ppm)

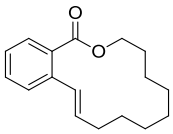

4

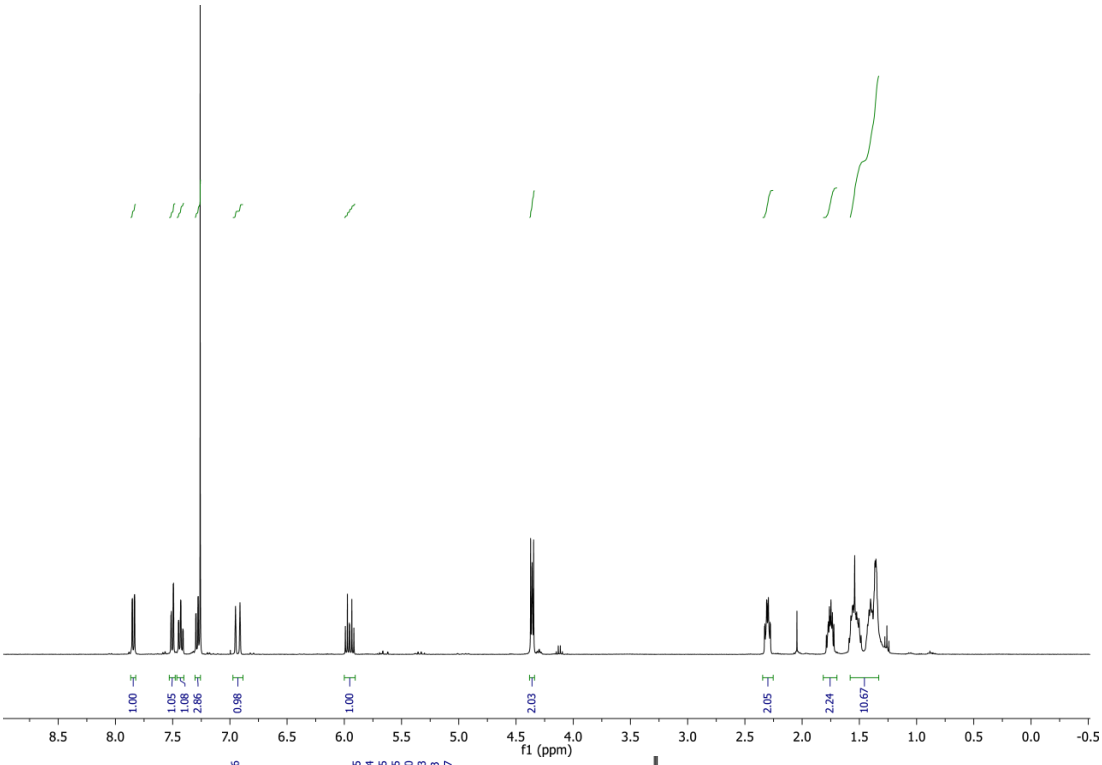
1.00
1.05
1.08
2.86
0.98
1.00
2.03
2.05
2.24
10.67
f1 (ppm)

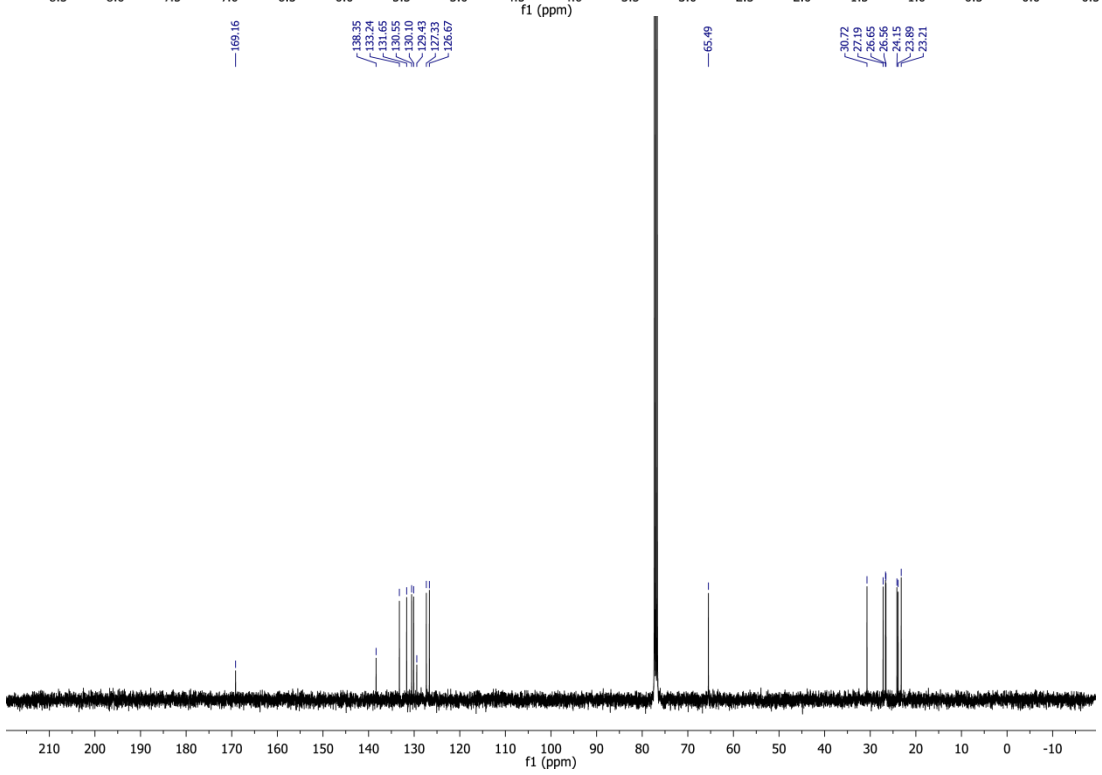
169.16
138.35
133.24
131.65
130.55
130.10
129.43
127.33
126.67
65.49
30.72
27.19
26.65
26.56
24.15
23.89
23.21
f1 (ppm)

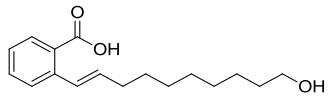
O
OH
OH

5

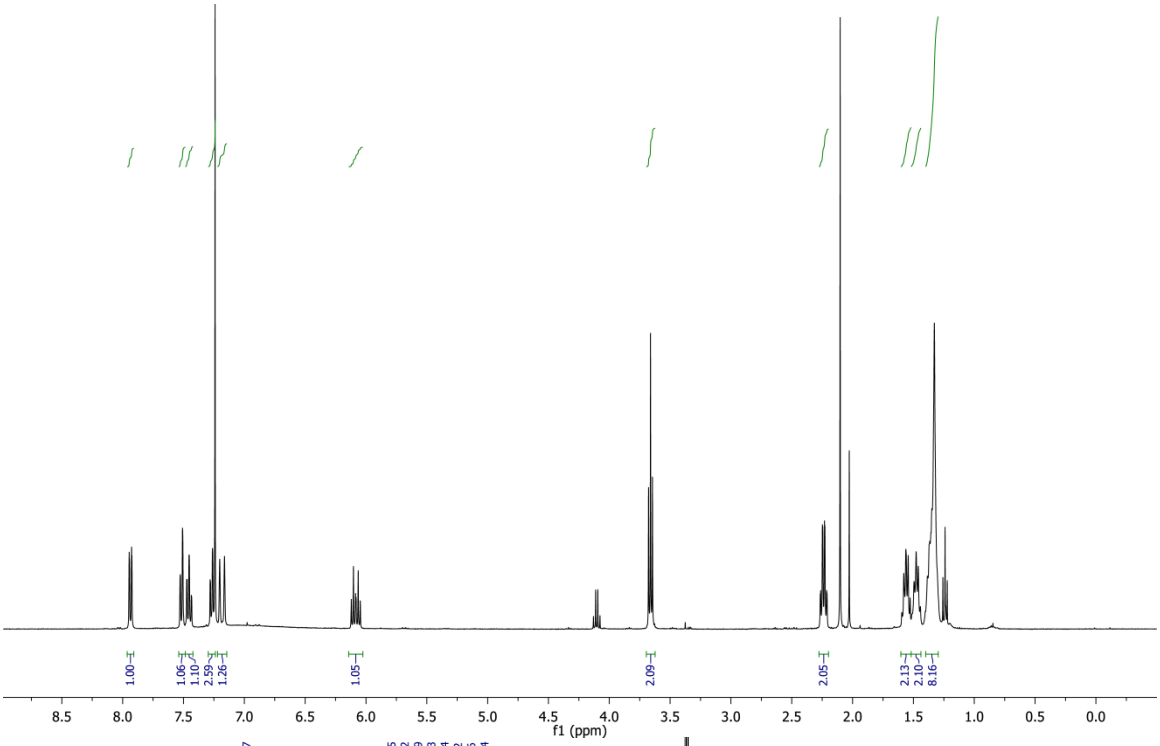
1.00
1.06
1.10
2.59
1.26
1.05
2.09
2.05
2.13
2.10
8.16
8.5 8.0 7.5 7.0 6.5 6.0 5.5 5.0 4.5 4.0 3.5 3.0 2.5 2.0 1.5 1.0 0.5 0.0
f1 (ppm)

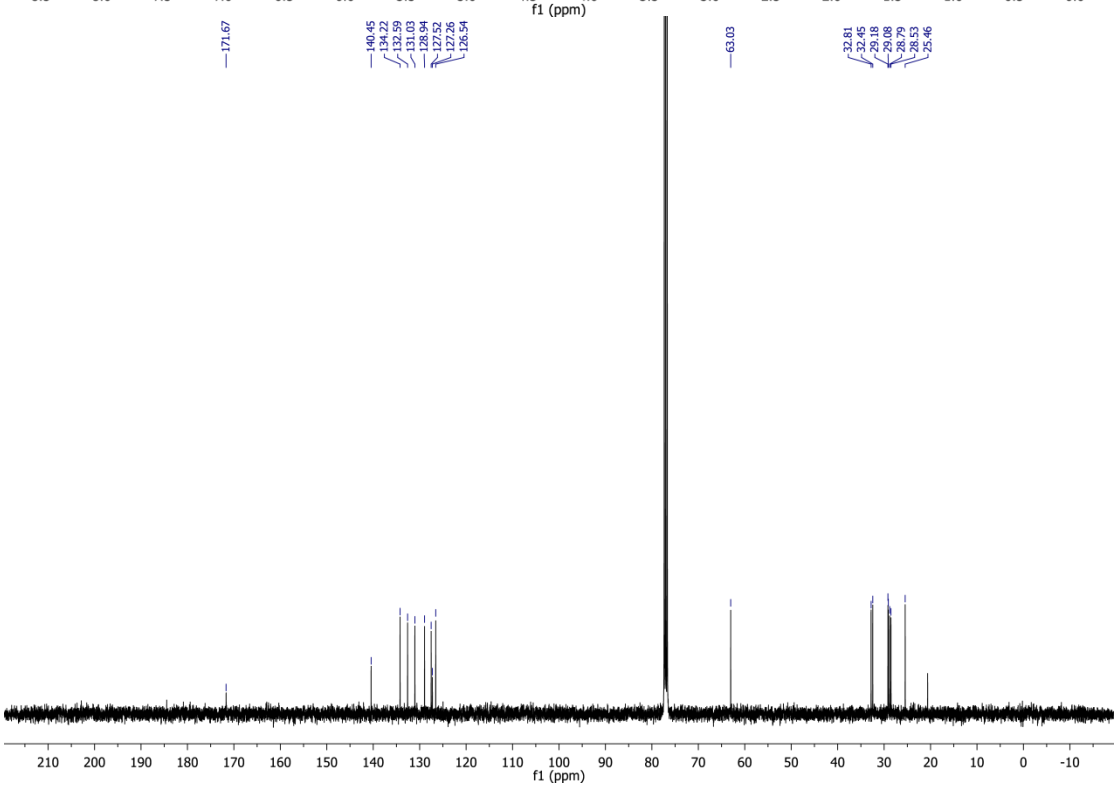
171.67
140.45
134.22
132.59
131.03
128.94
127.52
127.26
126.54
63.03
32.81
29.45
29.18
29.08
28.79
28.53
25.46
210 200 190 180 170 160 150 140 130 120 110 100 90 80 70 60 50 40 30 20 10 0 -10
f1 (ppm)

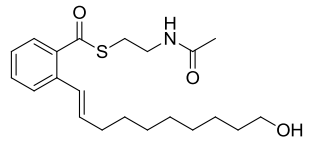
O
S
H
N
O
OH

6

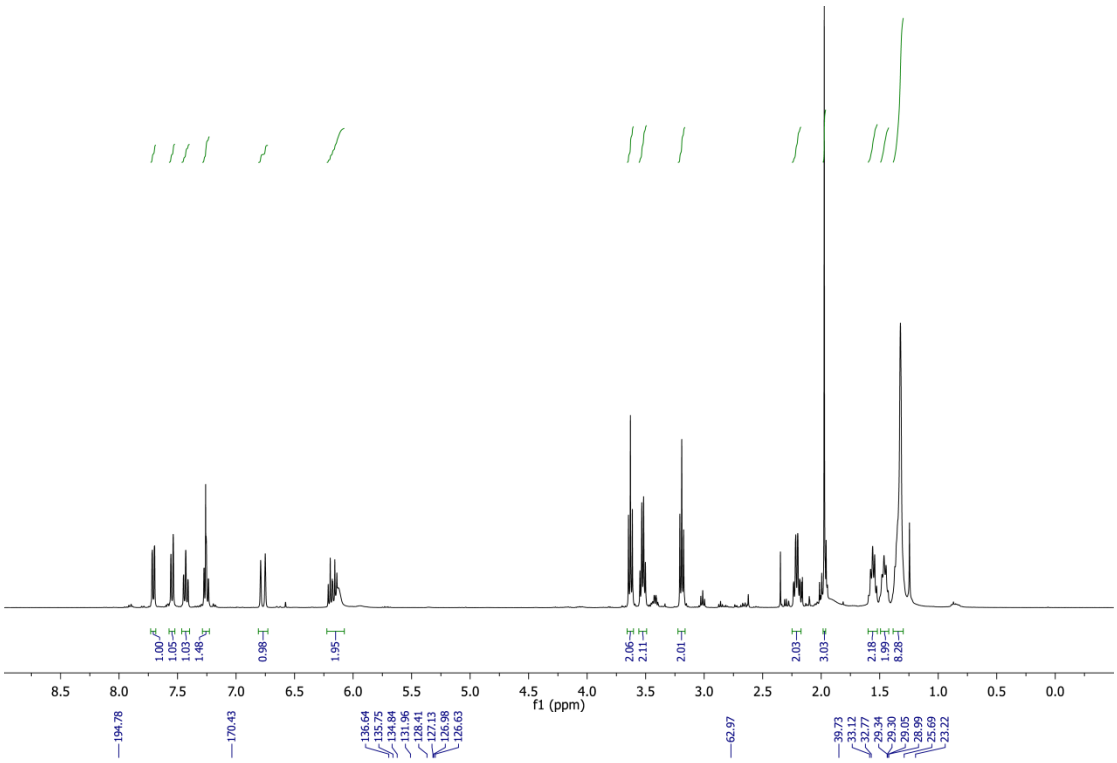
1.00
1.05
1.03
1.48
0.98
1.95
2.06
2.11
2.01
2.03
3.03
2.18
1.99
8.28
8.5 8.0 7.5 7.0 6.5 6.0 5.5 5.0 4.5 4.0 3.5 3.0 2.5 2.0 1.5 1.0 0.5 0.0
f1 (ppm)
194.78
170.43
136.64
135.75
134.84
131.96
128.41
127.13
126.98
126.63
62.97
39.73
33.12
32.77
29.34
29.30
29.05
28.99
25.69
23.22

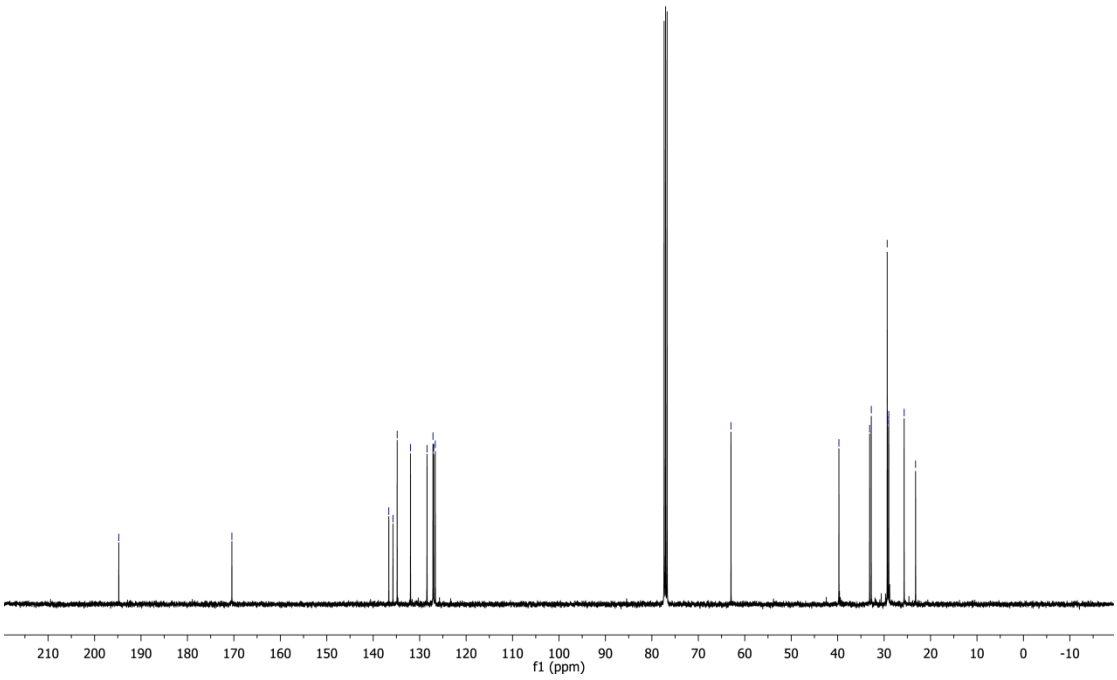
210 200 190 180 170 160 150 140 130 120 110 100 90 80 70 60 50 40 30 20 10 0 -10
f1 (ppm)

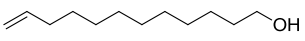
OH

S4

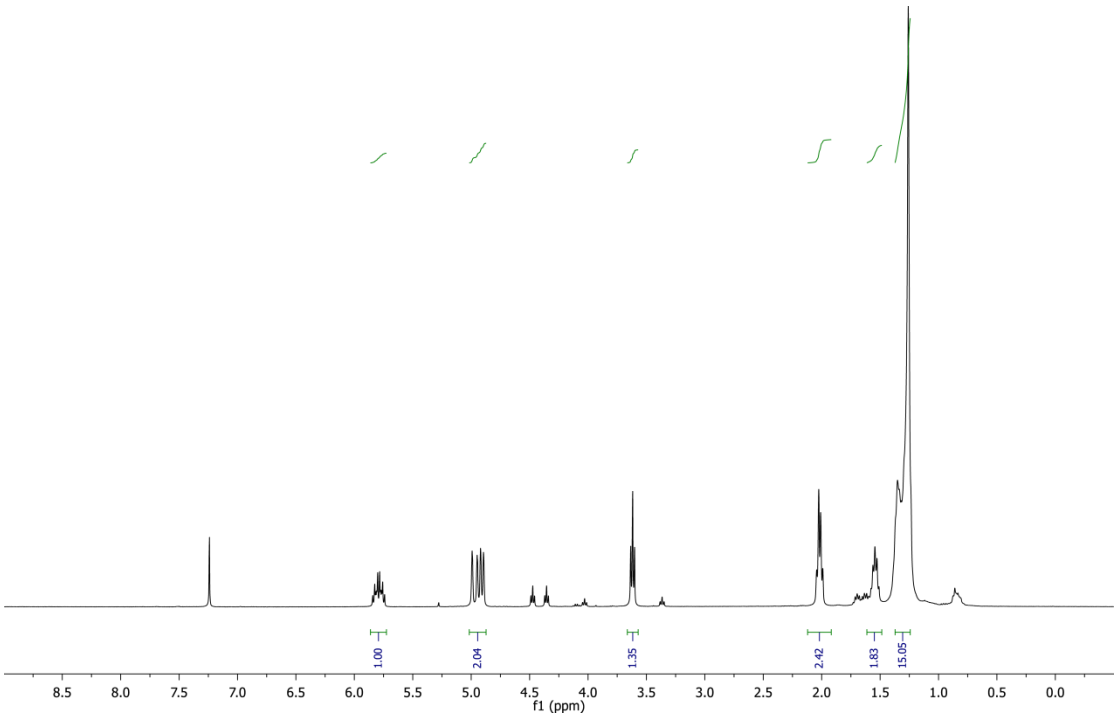
1.00
2.04
1.35
2.42
1.83
15.05
8.5
8.0
7.5
7.0
6.5
6.0
5.5
5.0
4.5
4.0
3.5
3.0
2.5
2.0
1.5
1.0
0.5
0.0
f1 (ppm)

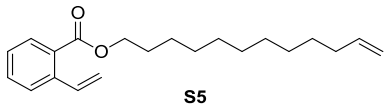

S5

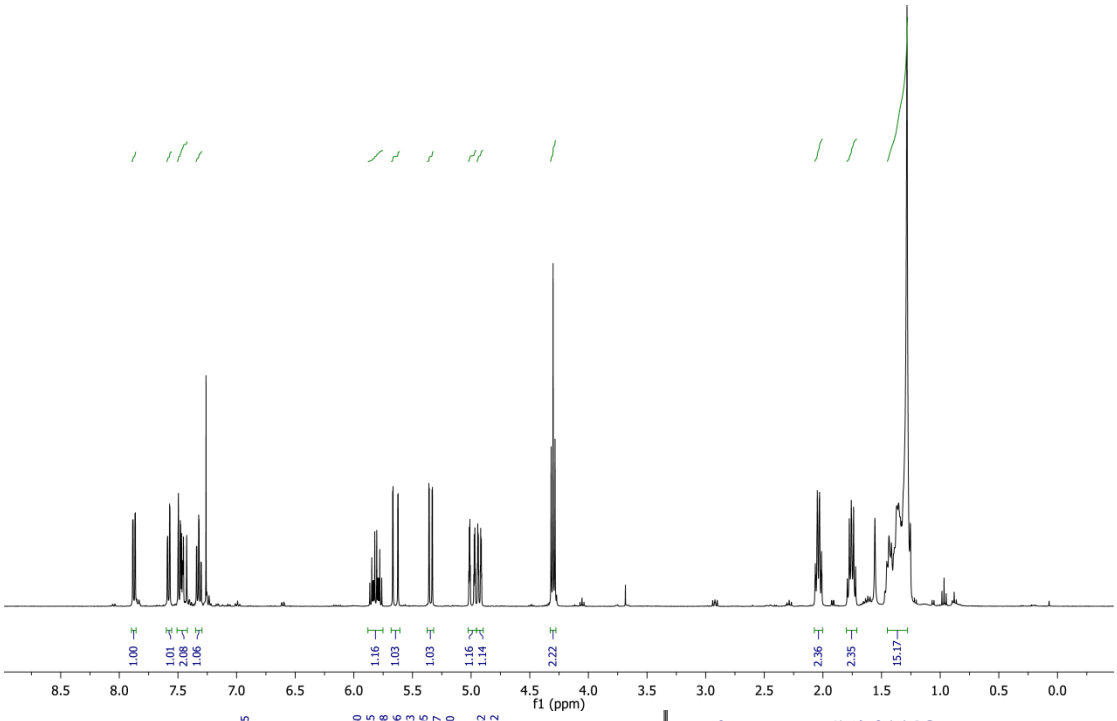
1.00
1.01
2.08
1.06
1.16
1.03
1.03
1.16
1.14
2.22
2.36
2.35
15.17
8.5
8.0
7.5
7.0
6.5
6.0
5.5
5.0
4.5
4.0
3.5
3.0
2.5
2.0
1.5
1.0
0.5
0.0
f1 (ppm)

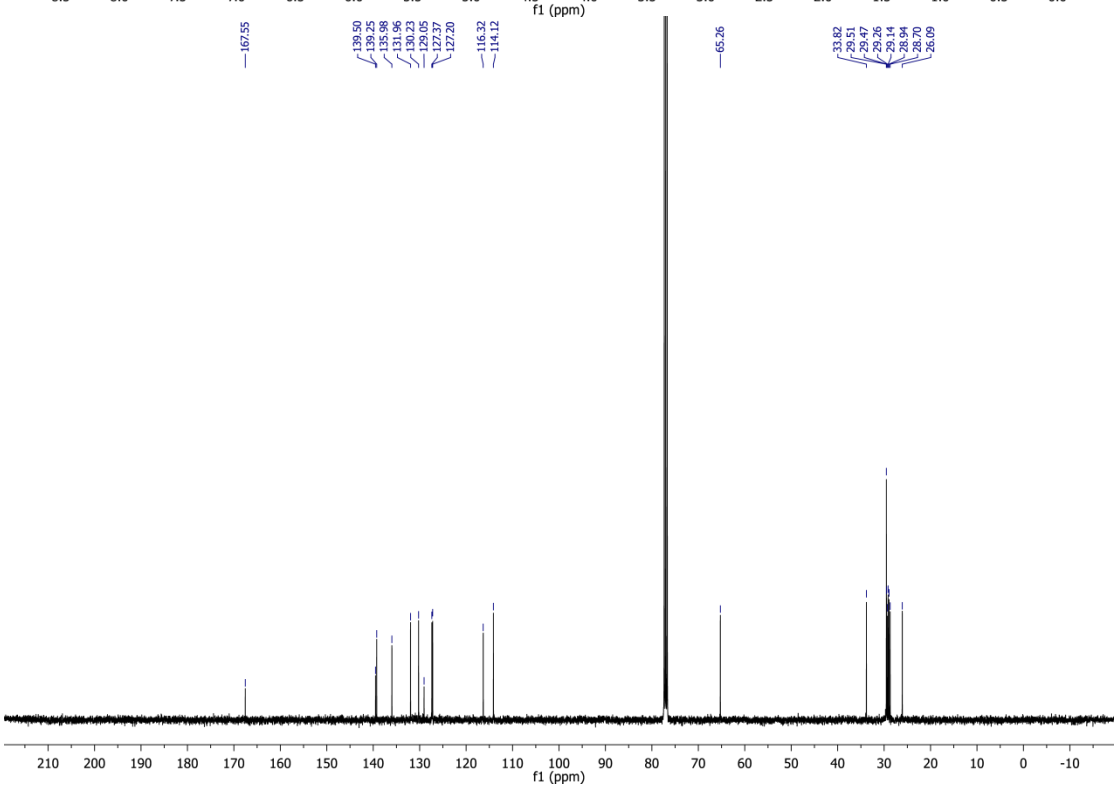
167.55
130.50
130.25
135.98
131.96
130.23
129.05
127.37
127.20
116.32
114.12
65.26
33.82
29.51
29.47
29.26
29.14
28.94
28.70
26.09
210
200
190
180
170
160
150
140
130
120
110
100
90
80
70
60
50
40
30
20
10
0
-10
f1 (ppm)

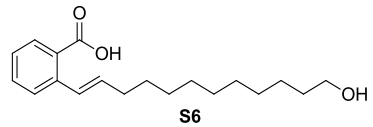
O
OH
OH

S6

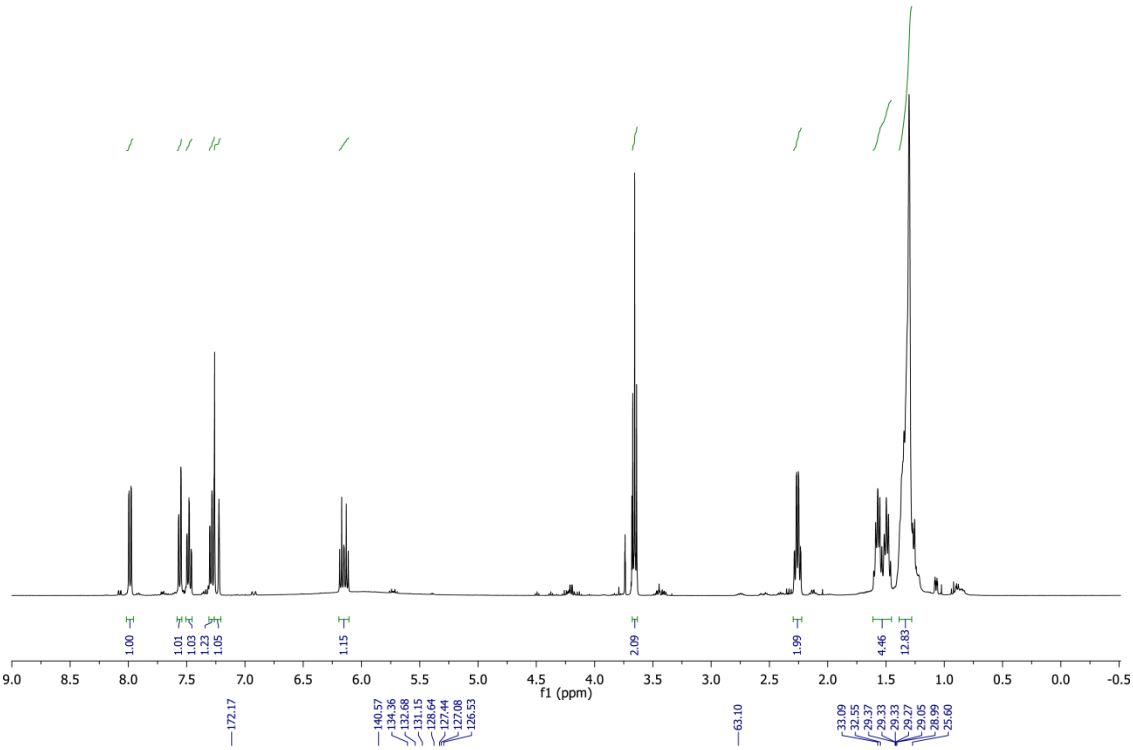
1.00
1.01
1.03
1.23
1.05
1.15
2.09
1.99
4.46
12.83
f1 (ppm)
172.17
140.57
134.36
132.68
131.15
128.64
127.44
127.08
126.53
63.10
33.09
32.55
29.37
29.33
29.33
29.27
29.05
28.99
25.60

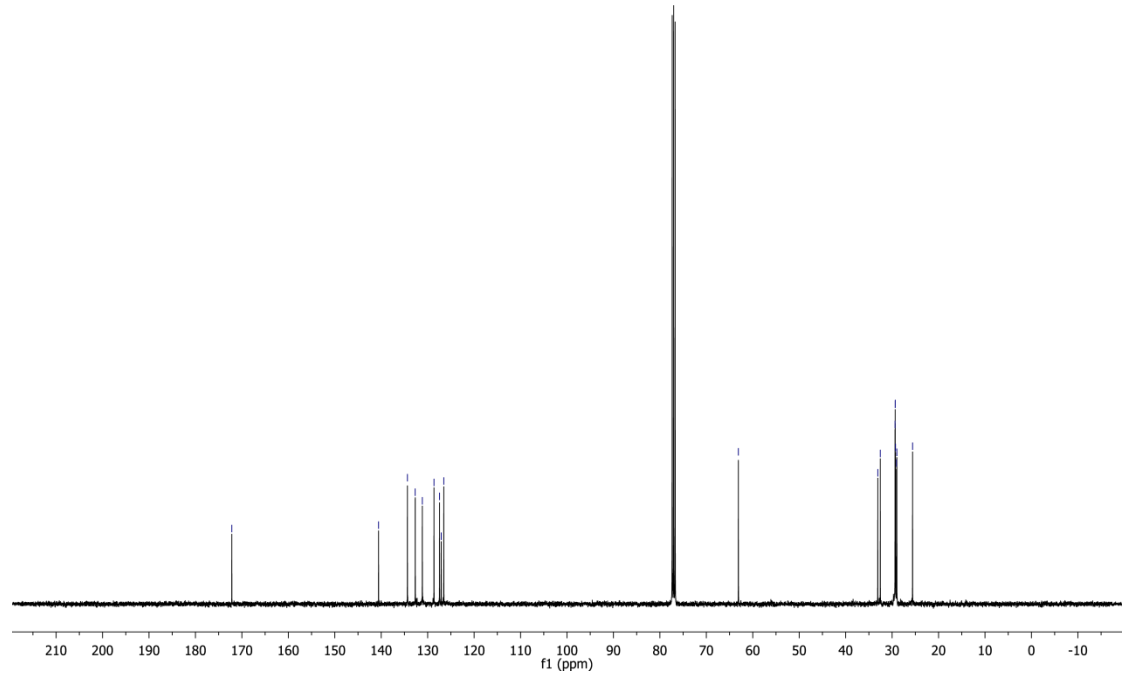
f1 (ppm)

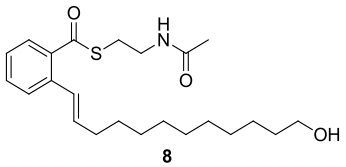
O
H
N
S
O
OH

8

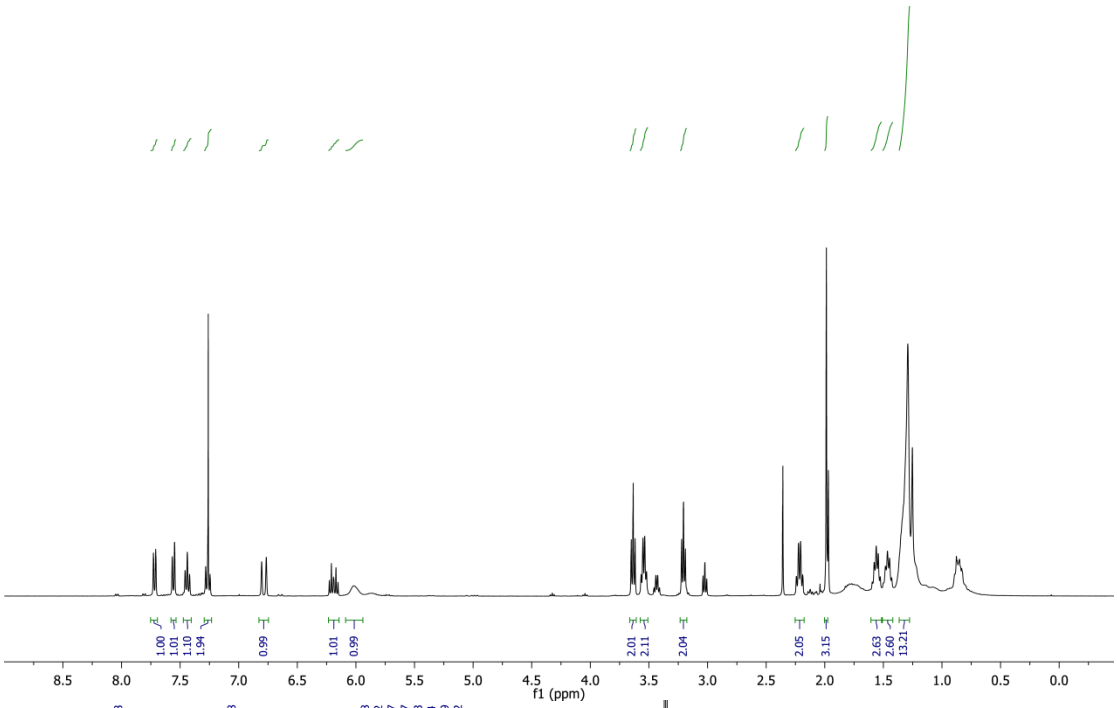
1.00
1.01
1.10
1.94
0.99
1.01
0.99
2.01
2.11
2.04
2.05
3.15
2.63
2.60
13.21
8.5 8.0 7.5 7.0 6.5 6.0 5.5 5.0 4.5 4.0 3.5 3.0 2.5 2.0 1.5 1.0 0.5 0.0
f1 (ppm)

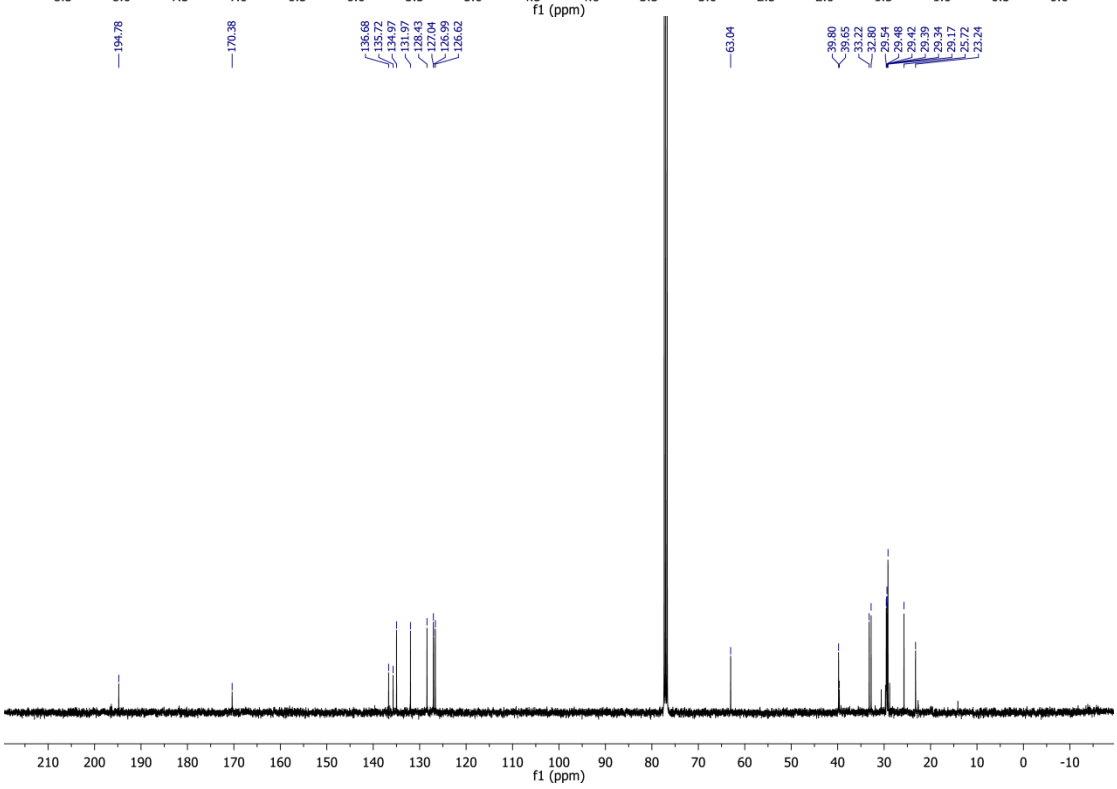
194.78
170.38
136.68
135.72
134.97
131.97
128.43
127.04
126.99
126.62
63.04
39.80
39.65
33.22
32.80
29.54
29.48
29.42
29.39
29.34
29.17
25.72
23.24
210 200 190 180 170 160 150 140 130 120 110 100 90 80 70 60 50 40 30 20 10 0 -10
f1 (ppm)

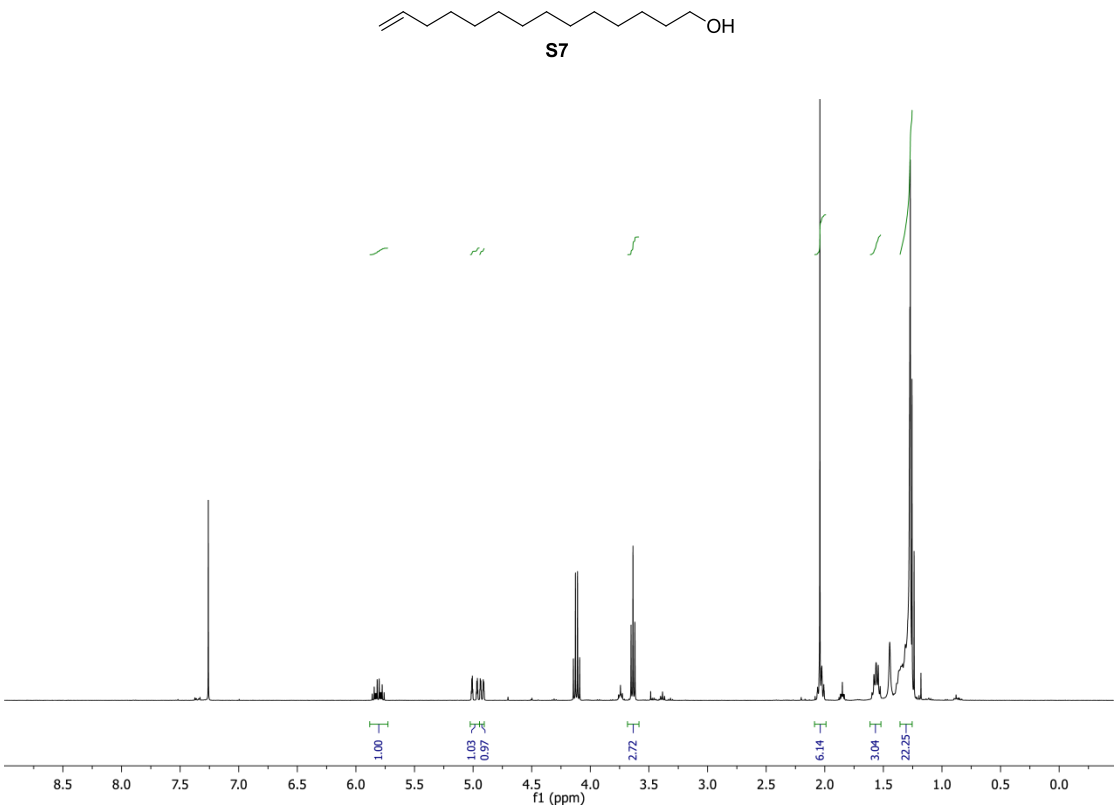
OH
S7
1.00
1.03
0.97
2.72
6.14
3.04
22.25
8.5
8.0
7.5
7.0
6.5
6.0
5.5
5.0
4.5
4.0
3.5
3.0
2.5
2.0
1.5
1.0
0.5
0.0
f1 (ppm)

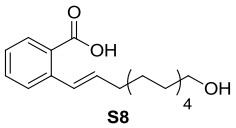
O
OH
OH
4

S8

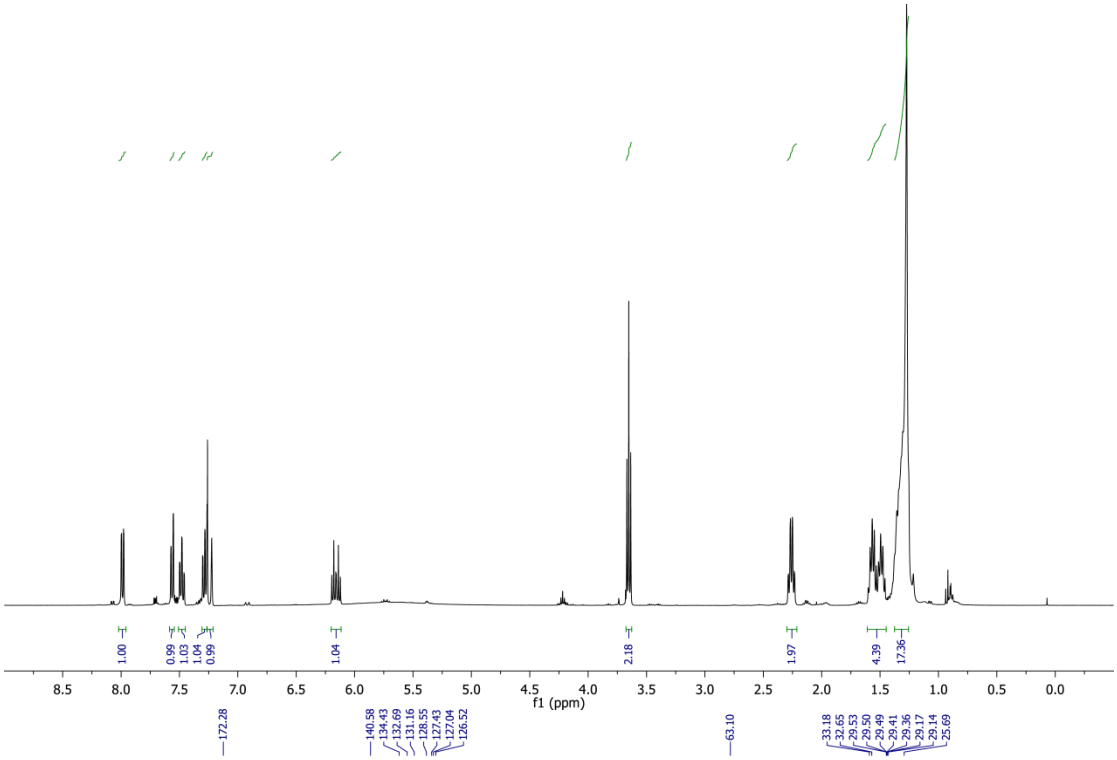
1.00
0.99
1.03
1.04
0.99
1.04
2.18
1.97
4.39
17.36
8.5 8.0 7.5 7.0 6.5 6.0 5.5 5.0 4.5 4.0 3.5 3.0 2.5 2.0 1.5 1.0 0.5 0.0
f1 (ppm)
172.28
140.58
134.43
132.69
131.16
128.55
127.43
127.04
126.52
63.10
33.18
32.65
29.53
29.50
29.49
29.41
29.36
29.17
29.14
25.69

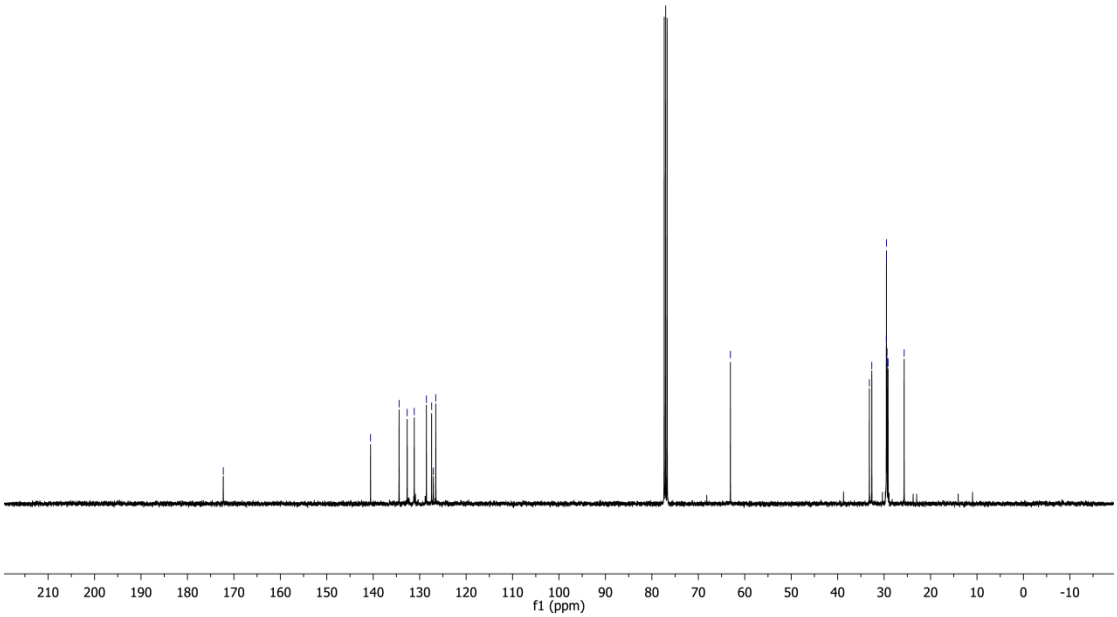
210 200 190 180 170 160 150 140 130 120 110 100 90 80 70 60 50 40 30 20 10 0 -10
f1 (ppm)

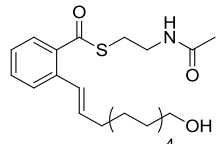
O
S
H
N
O
OH
4

9

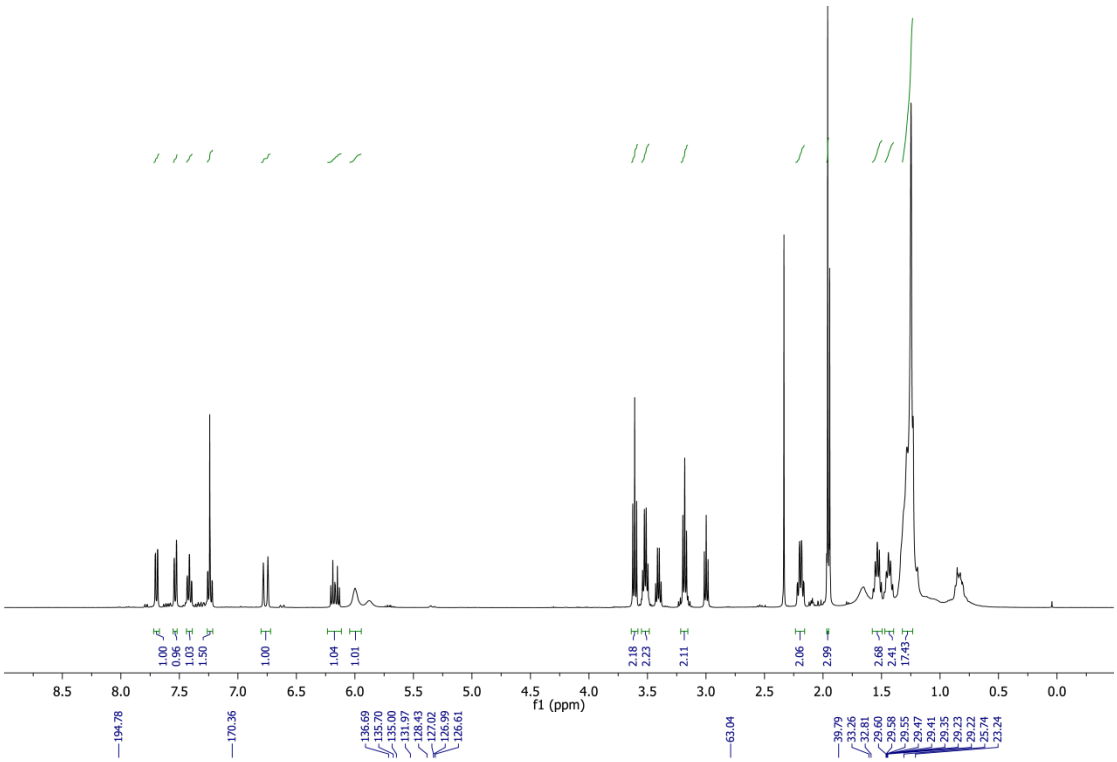
1.00
0.96
1.03
1.50
1.00
1.04
1.01
2.18
2.23
2.11
2.06
2.99
2.68
2.41
17.43
8.5 8.0 7.5 7.0 6.5 6.0 5.5 5.0 4.5 4.0 3.5 3.0 2.5 2.0 1.5 1.0 0.5 0.0
f1 (ppm)

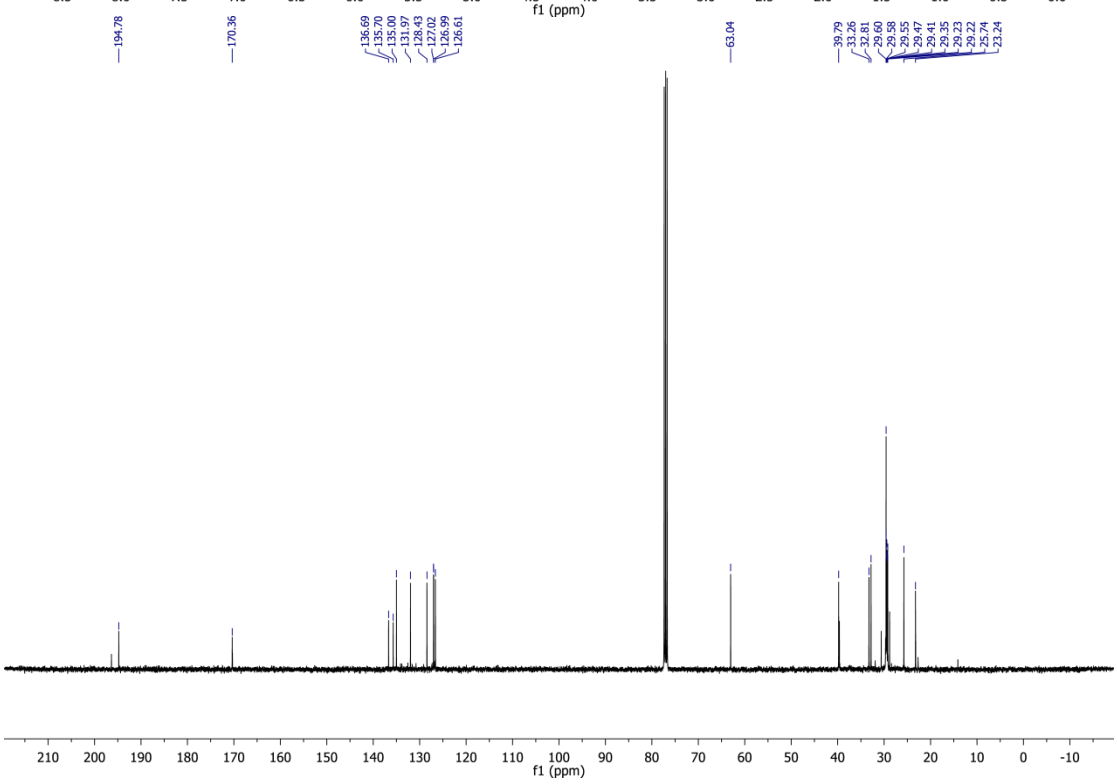
194.78
170.36
136.69
135.70
135.00
131.97
128.43
127.02
126.99
126.61
63.04
39.79
33.26
32.81
29.60
29.58
29.55
29.47
29.41
29.35
29.23
29.22
25.74
23.24
210 200 190 180 170 160 150 140 130 120 110 100 90 80 70 60 50 40 30 20 10 0 -10
f1 (ppm)

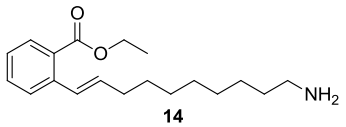
O
O
NH2

14

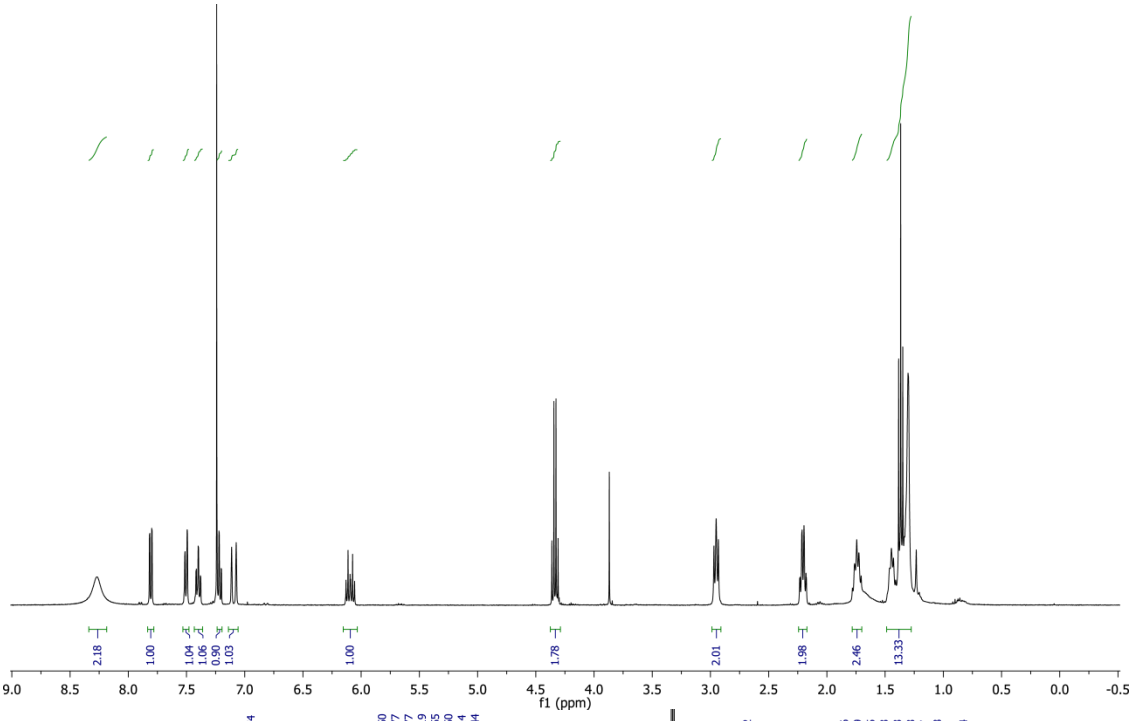
2.18
1.00
1.04
1.06
0.90
1.03
1.00
1.78
2.01
1.98
2.46
13.33
9.0 8.5 8.0 7.5 7.0 6.5 6.0 5.5 5.0 4.5 4.0 3.5 3.0 2.5 2.0 1.5 1.0 0.5 0.0 -0.5
f1 (ppm)

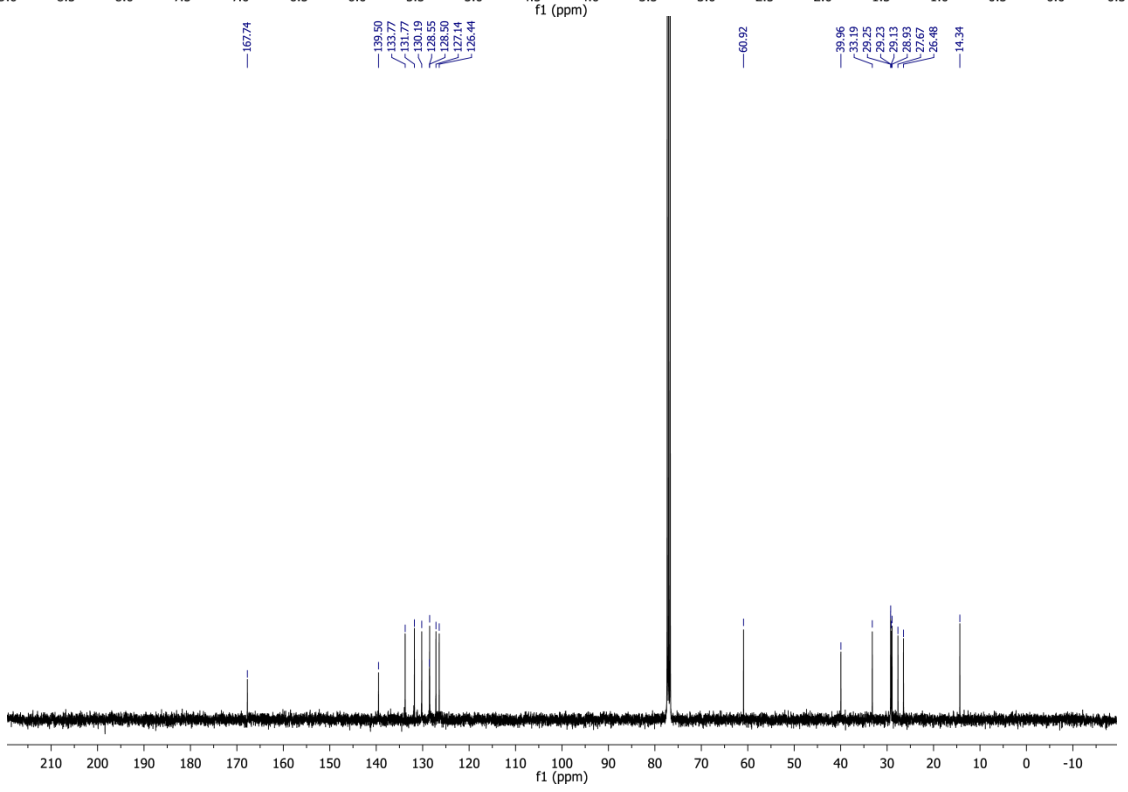
167.74
139.50
133.77
131.77
130.19
128.55
128.50
127.14
126.44
60.92
39.96
33.19
29.25
29.23
29.13
28.93
27.67
26.48
14.34
210 200 190 180 170 160 150 140 130 120 110 100 90 80 70 60 50 40 30 20 10 0 -10
f1 (ppm)

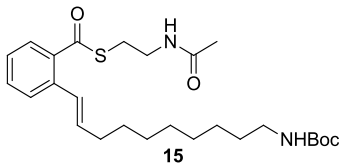
O
H
N
S
O
NHBoc

15

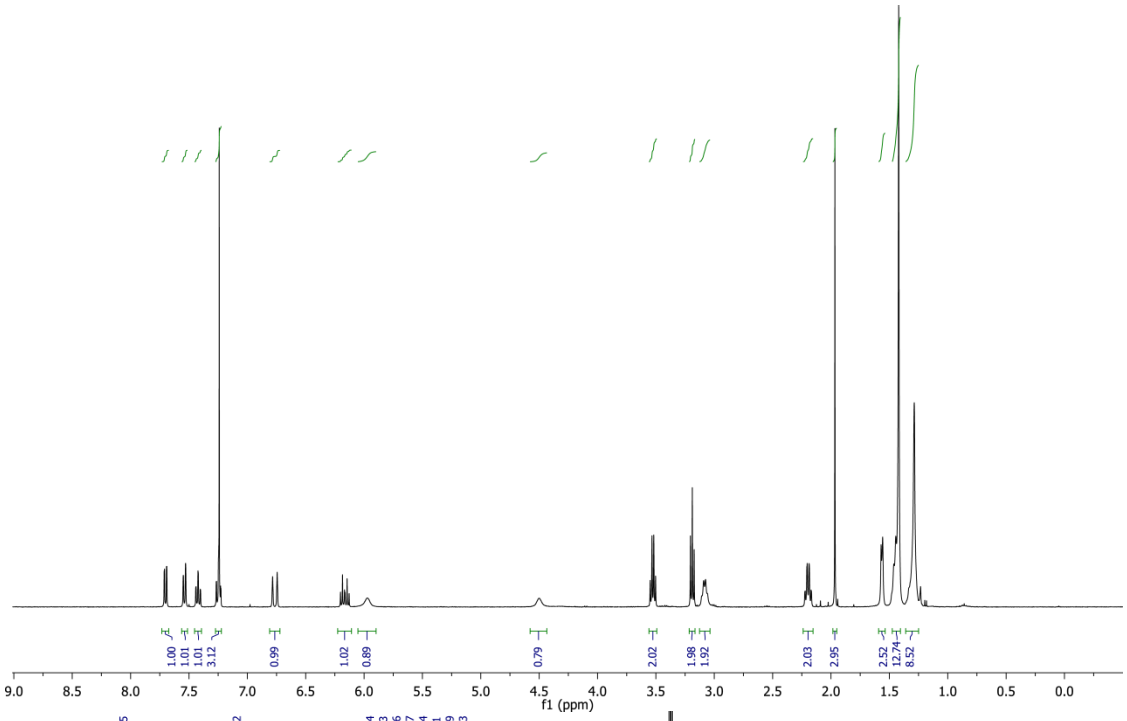
1.00
1.01
1.01
3.12
0.99
1.02
0.89
0.79
2.02
1.98
1.92
2.03
2.95
2.52
12.74
8.52
f1 (ppm)

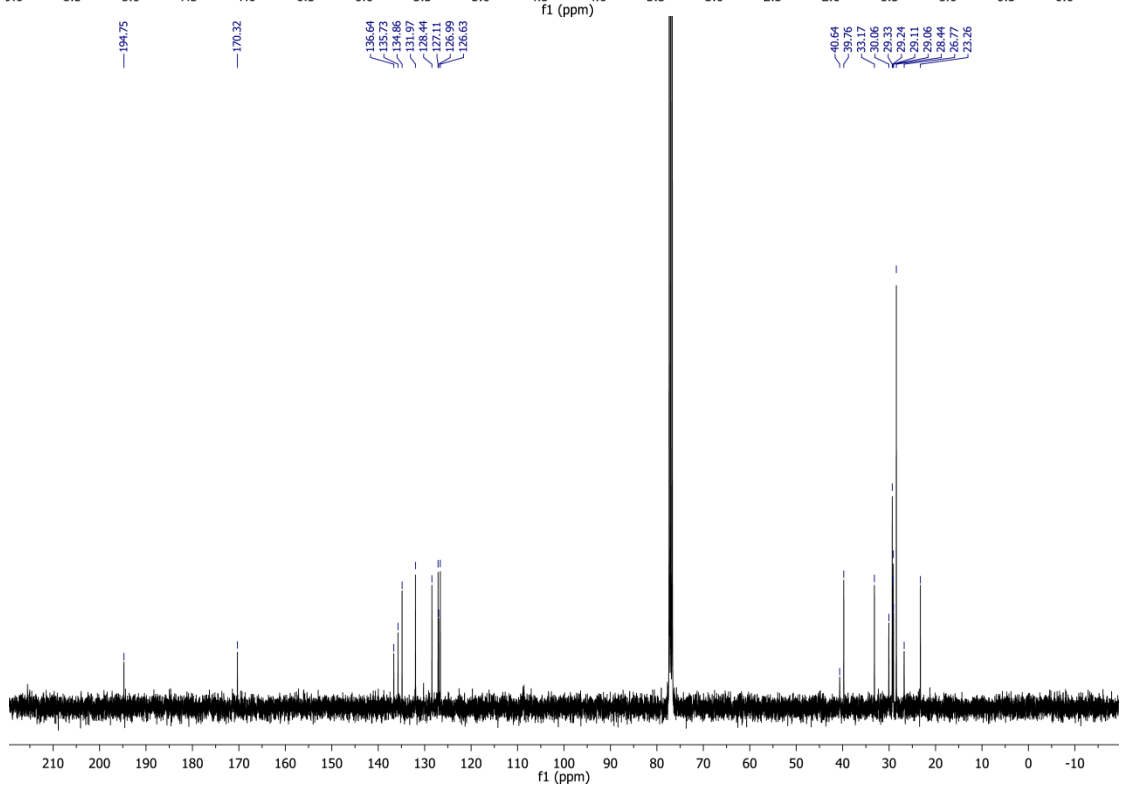
194.75
170.32
136.64
135.73
134.86
131.97
128.44
127.11
126.99
126.63
40.64
39.76
33.17
30.06
29.33
29.24
29.11
29.06
28.44
26.77
23.26
f1 (ppm)

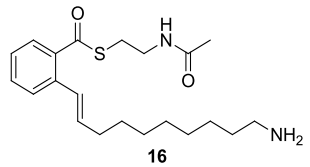
O
H
N
S
O
NH2

16

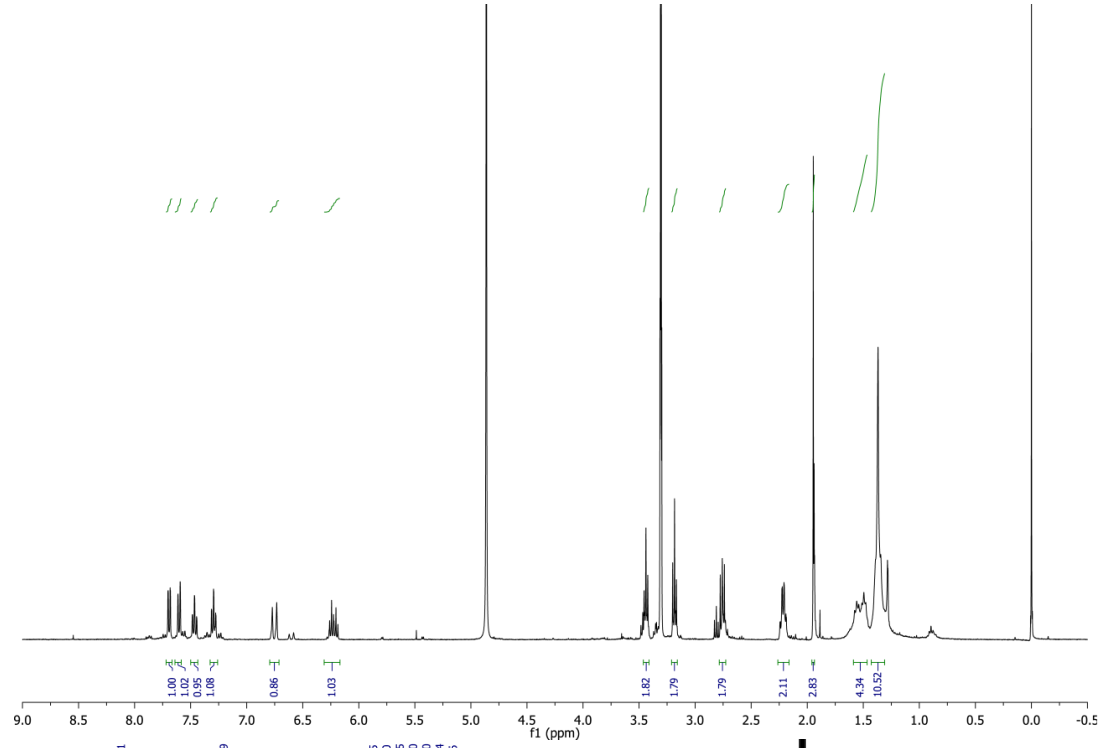
1.00
1.02
0.95
1.08
0.86
1.03
1.82
1.79
1.79
2.11
2.83
4.34
10.52
9.0 8.5 8.0 7.5 7.0 6.5 6.0 5.5 5.0 4.5 4.0 3.5 3.0 2.5 2.0 1.5 1.0 0.5 0.0 -0.5
f1 (ppm)

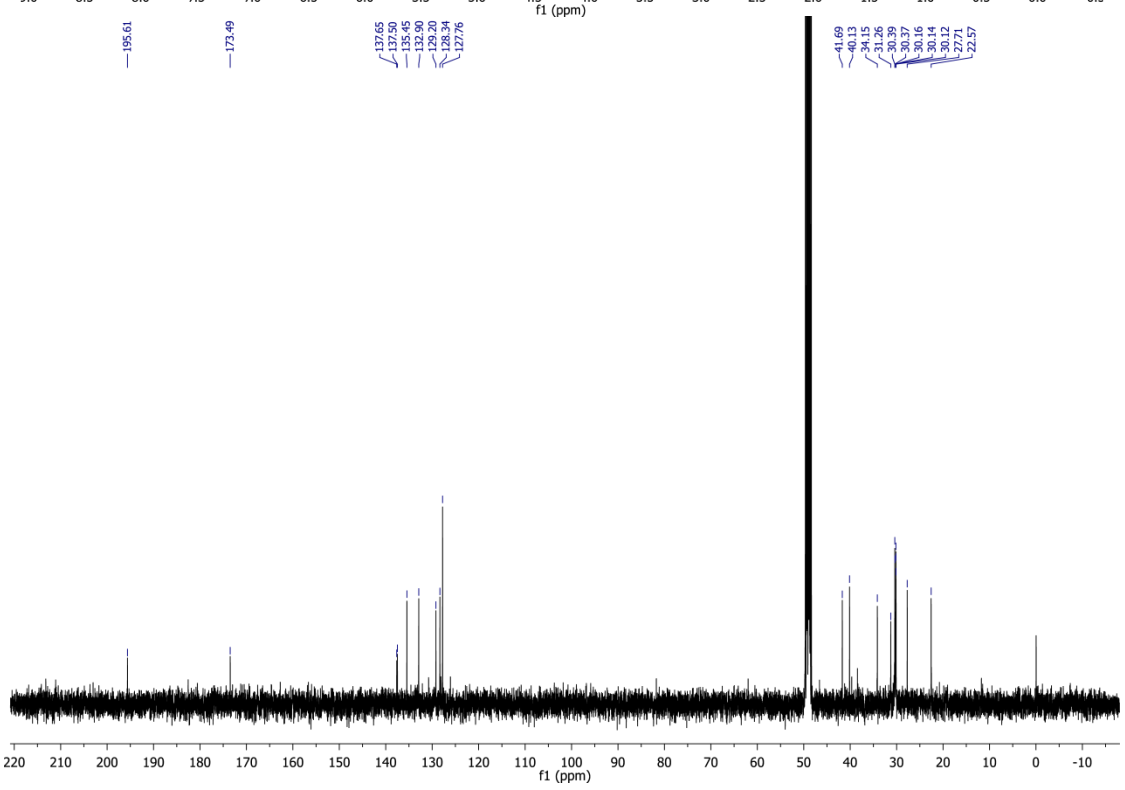
195.61
173.49
137.65
137.50
135.45
132.90
129.20
128.34
127.76
41.69
40.13
34.15
31.26
30.39
30.37
30.16
30.14
30.12
27.71
22.57
220 210 200 190 180 170 160 150 140 130 120 110 100 90 80 70 60 50 40 30 20 10 0 -10
f1 (ppm)

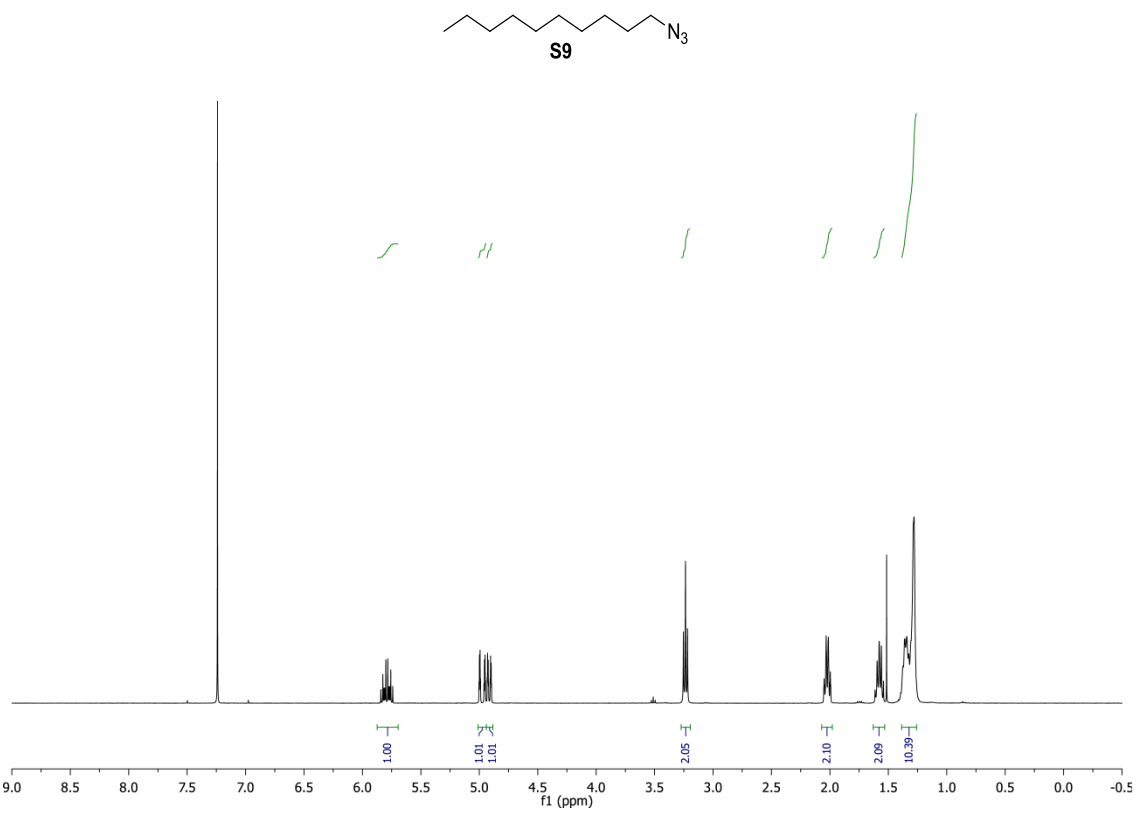
N3
S9
1.00
1.01
1.01
2.05
2.10
2.09
10.39
9.0 8.5 8.0 7.5 7.0 6.5 6.0 5.5 5.0 4.5 4.0 3.5 3.0 2.5 2.0 1.5 1.0 0.5 0.0 -0.5
f1 (ppm)

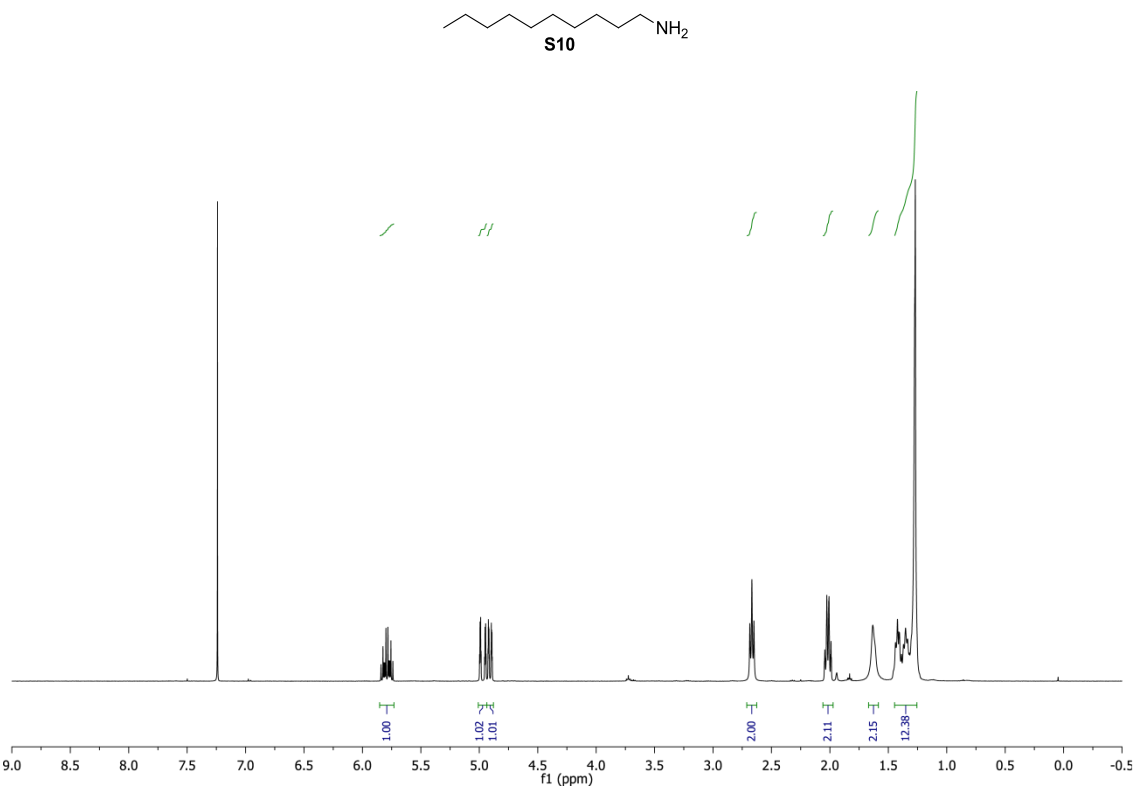
NH2
S10
1.00
1.02
1.01
2.00
2.11
2.15
12.38
9.0 8.5 8.0 7.5 7.0 6.5 6.0 5.5 5.0 4.5 4.0 3.5 3.0 2.5 2.0 1.5 1.0 0.5 0.0 -0.5
f1 (ppm)

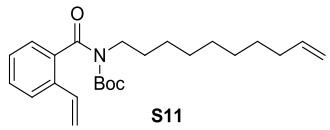
O
N
Boc

S11

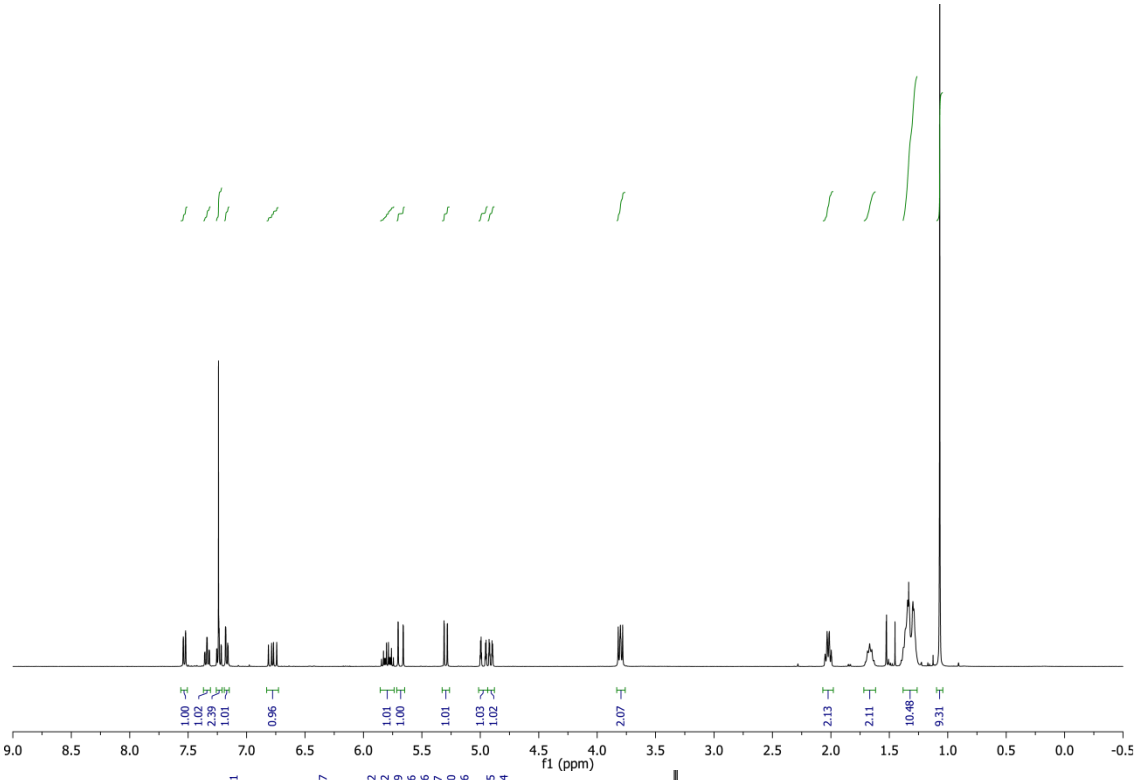
1.00
1.02
2.39
1.01
0.96
1.01
1.00
1.01
1.03
1.02
2.07
2.13
2.11
10.48
9.31
f1 (ppm)

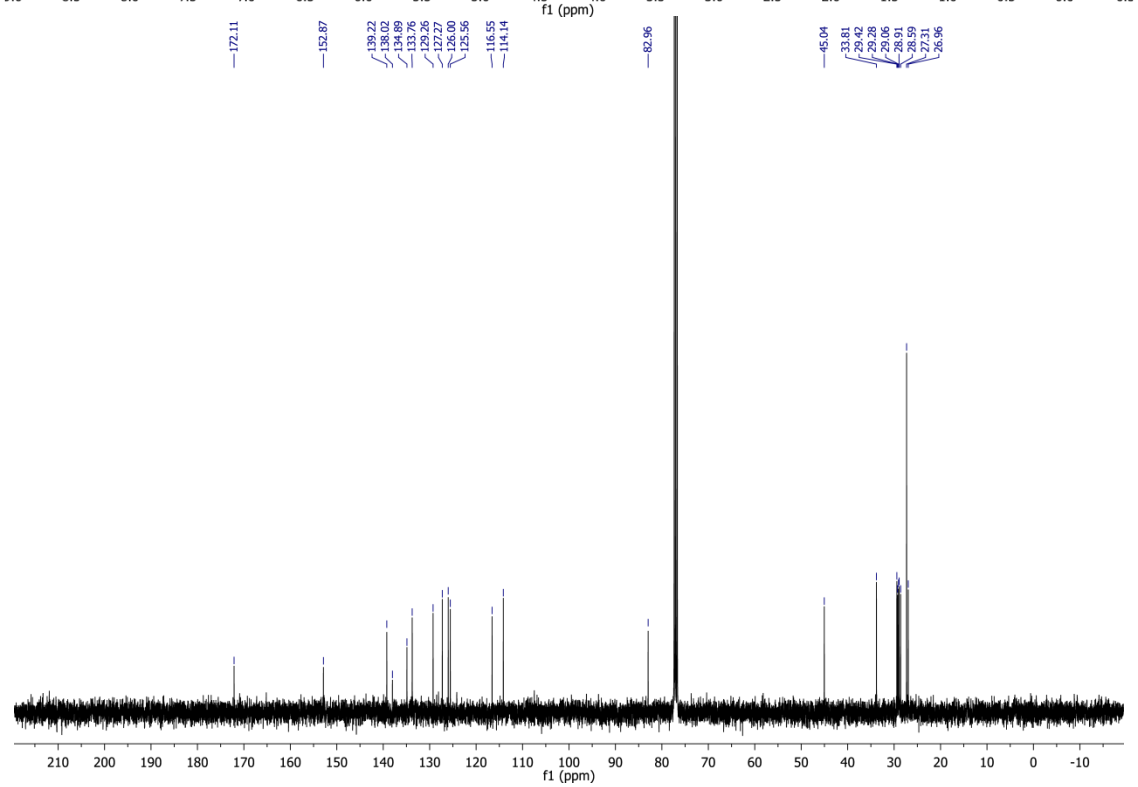
172.11
152.87
139.22
138.02
134.89
133.76
129.26
127.27
126.60
125.56
116.55
114.14
82.96
45.04
33.81
29.42
29.28
29.06
28.91
28.59
27.31
26.96
f1 (ppm)

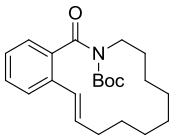
O
N
Boc

S12

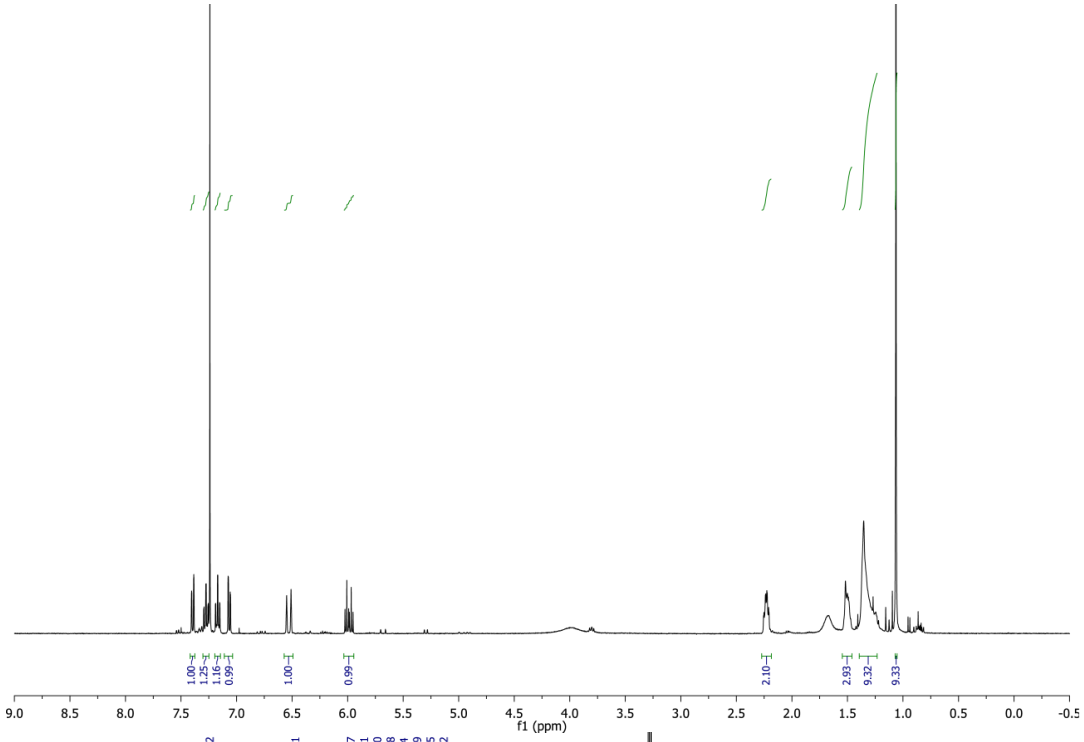
1.00
1.25
1.16
0.99
1.00
0.99
2.10
2.93
9.32
9.33
9.0 8.5 8.0 7.5 7.0 6.5 6.0 5.5 5.0 4.5 4.0 3.5 3.0 2.5 2.0 1.5 1.0 0.5 0.0 -0.5
f1 (ppm)

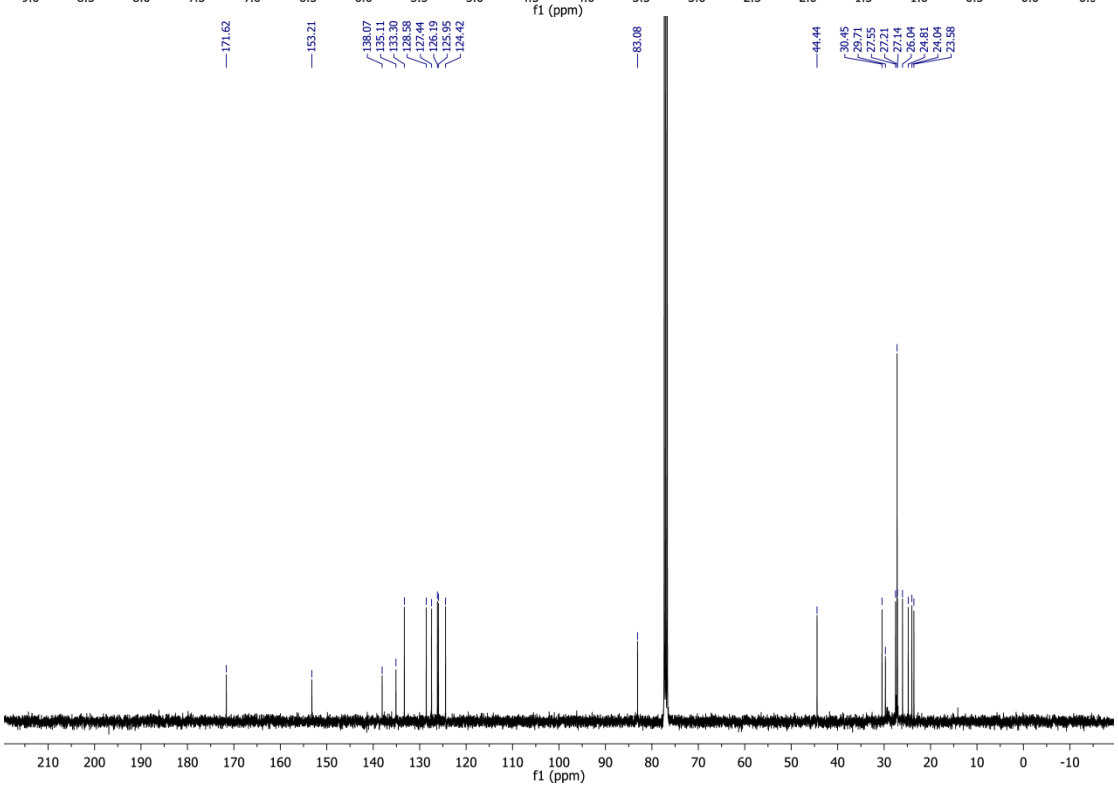
171.62
153.21
138.07
135.11
133.30
128.58
127.44
126.19
125.95
124.42
83.08
44.44
30.45
29.71
27.55
27.21
27.14
26.04
24.81
24.04
23.58
210 200 190 180 170 160 150 140 130 120 110 100 90 80 70 60 50 40 30 20 10 0 -10
f1 (ppm)

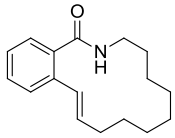
O
N
H

23

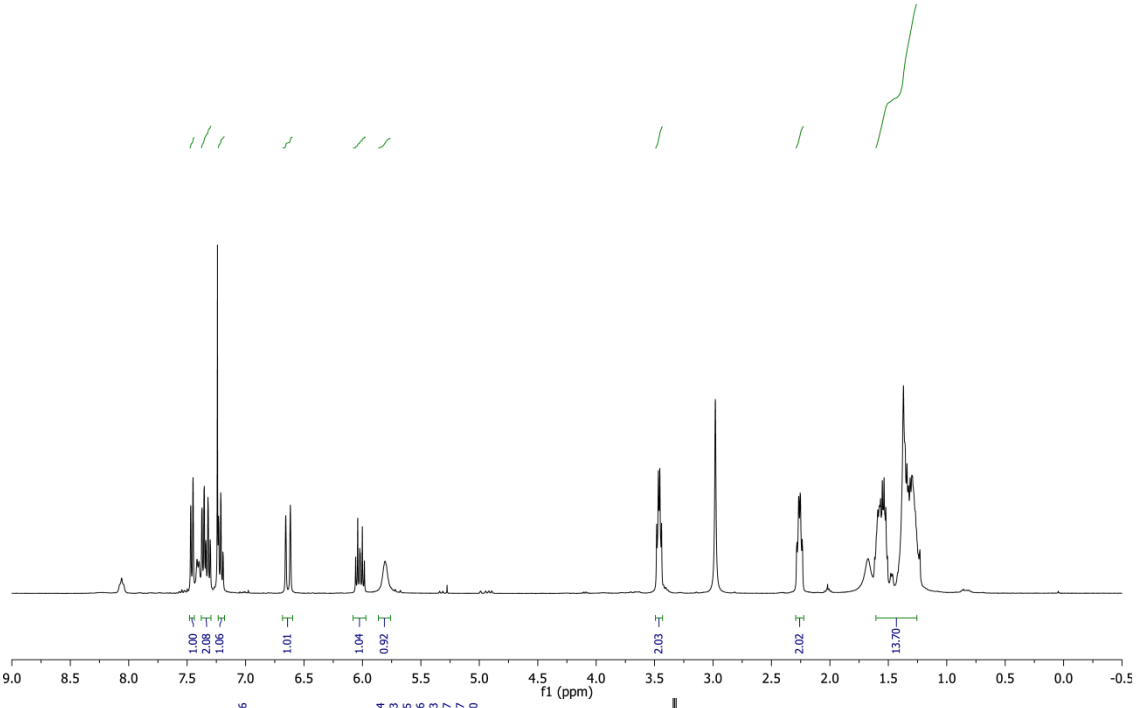
1.00
2.08
1.06
1.01
1.04
0.92
2.03
2.02
13.70
9.0 8.5 8.0 7.5 7.0 6.5 6.0 5.5 5.0 4.5 4.0 3.5 3.0 2.5 2.0 1.5 1.0 0.5 0.0 -0.5
f1 (ppm)

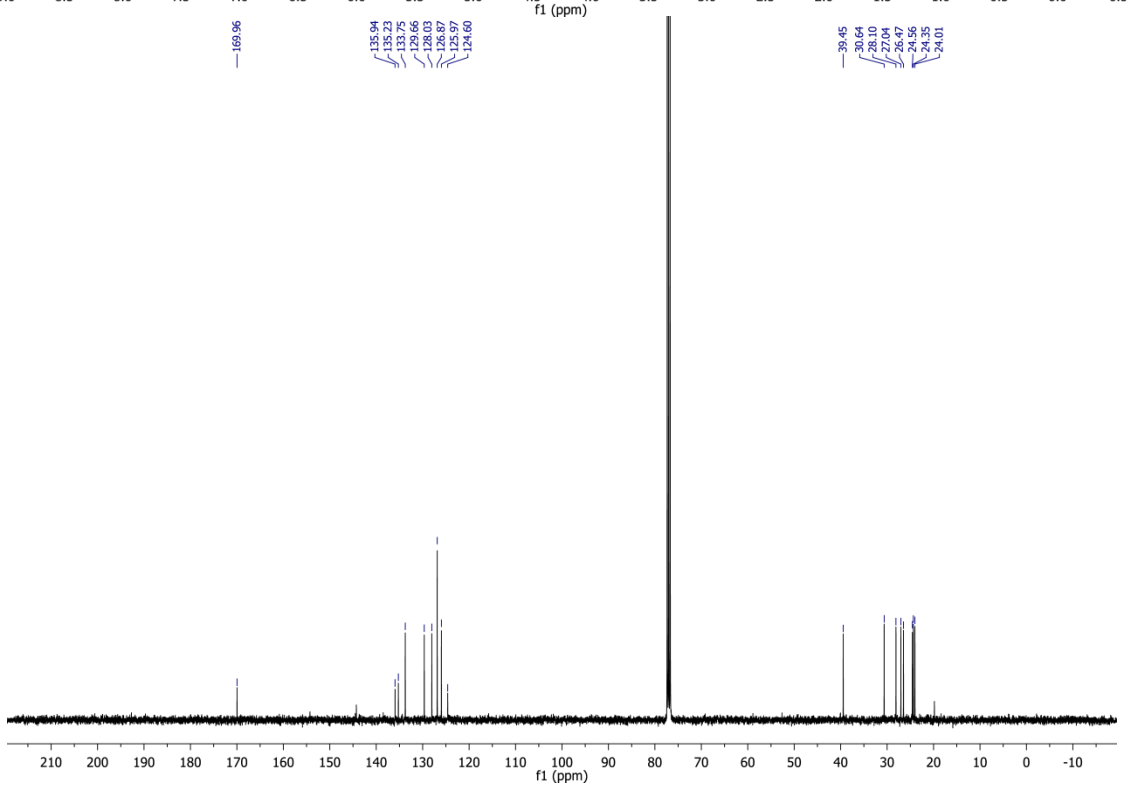
169.96
135.94
135.23
133.75
129.66
128.03
126.87
125.97
124.60
39.45
30.64
28.10
27.04
26.47
24.56
24.35
24.01
210 200 190 180 170 160 150 140 130 120 110 100 90 80 70 60 50 40 30 20 10 0 -10
f1 (ppm)

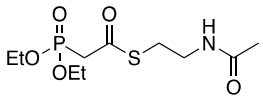

S15

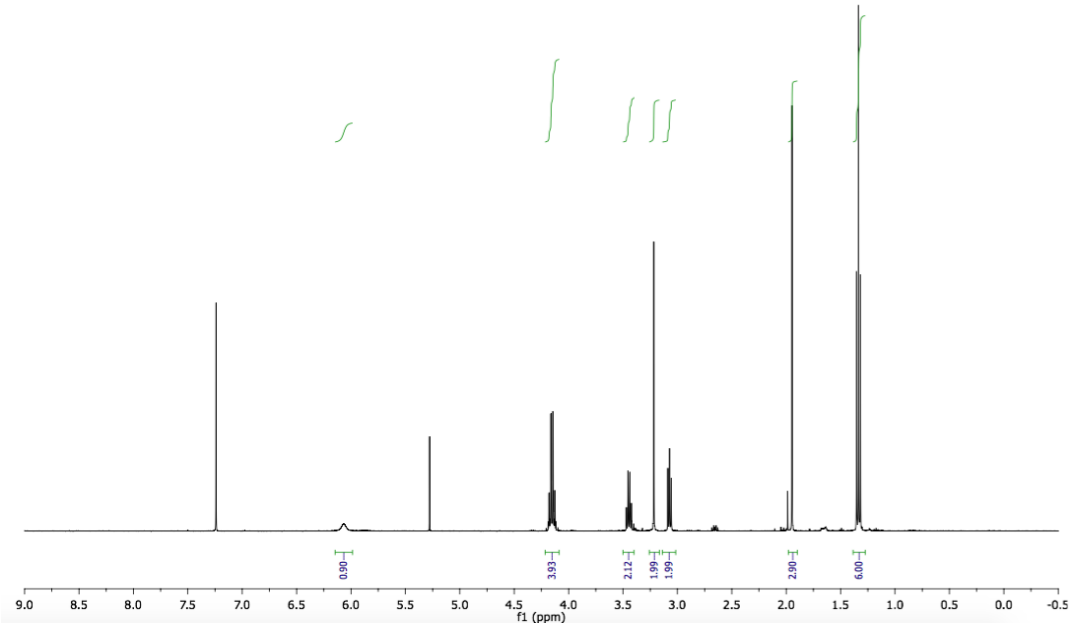
0.90
3.93
2.12
1.99
1.99
2.90
6.00
9.0 8.5 8.0 7.5 7.0 6.5 6.0 5.5 5.0 4.5 4.0 3.5 3.0 2.5 2.0 1.5 1.0 0.5 0.0 -0.5
f1 (ppm)

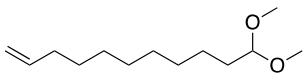

S16

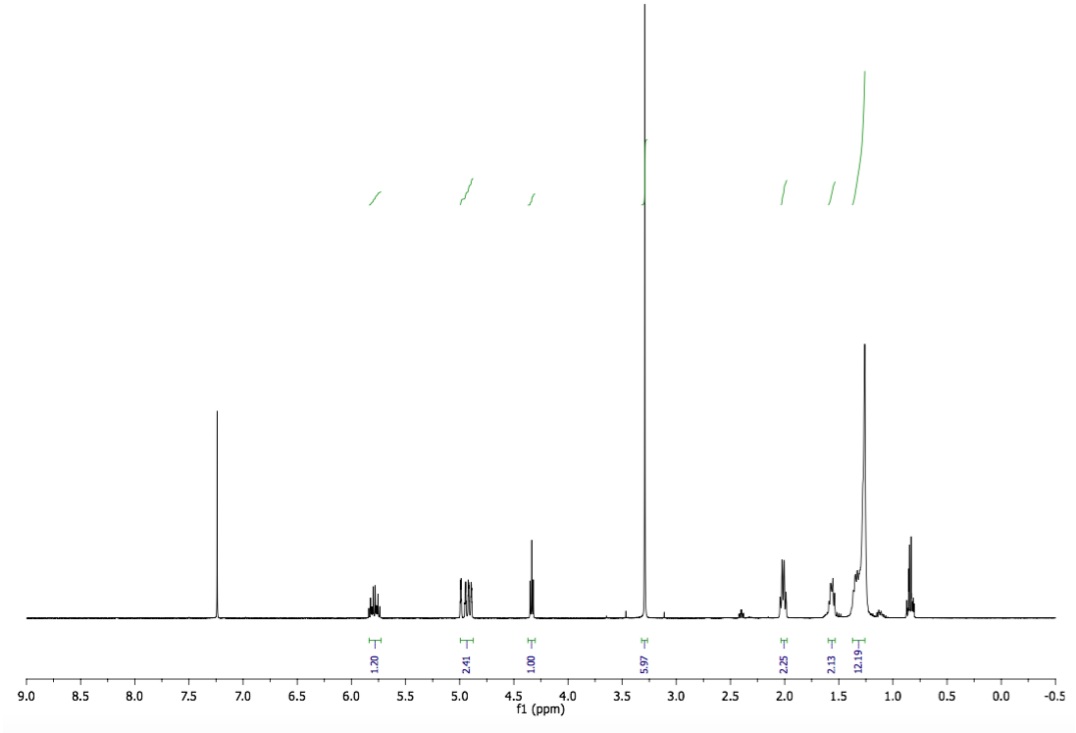
1.20
2.41
1.00
5.97
2.25
2.13
12.19
9.0
8.5
8.0
7.5
7.0
6.5
6.0
5.5
5.0
4.5
4.0
3.5
3.0
2.5
2.0
1.5
1.0
0.5
0.0
-0.5
f1 (ppm)

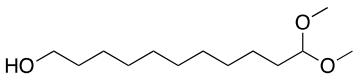
HO
O
O

S17

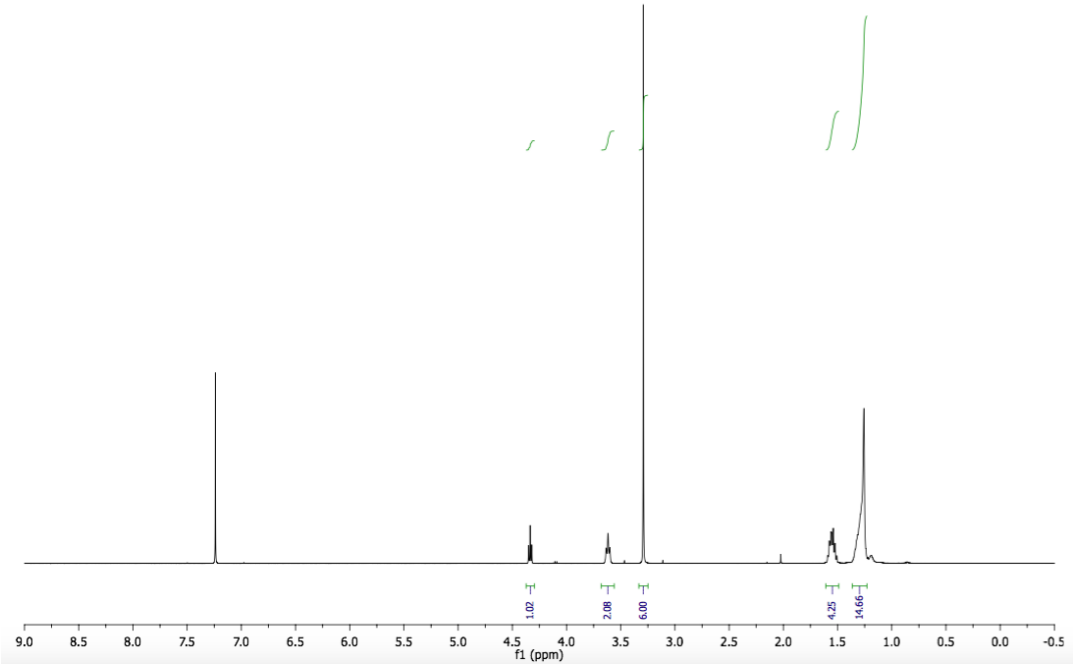
1.02
2.08
6.00
4.25
14.66
9.0
8.5
8.0
7.5
7.0
6.5
6.0
5.5
5.0
4.5
4.0
3.5
3.0
2.5
2.0
1.5
1.0
0.5
0.0
-0.5
f1 (ppm)

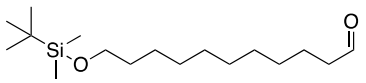
Si
O
O

S18

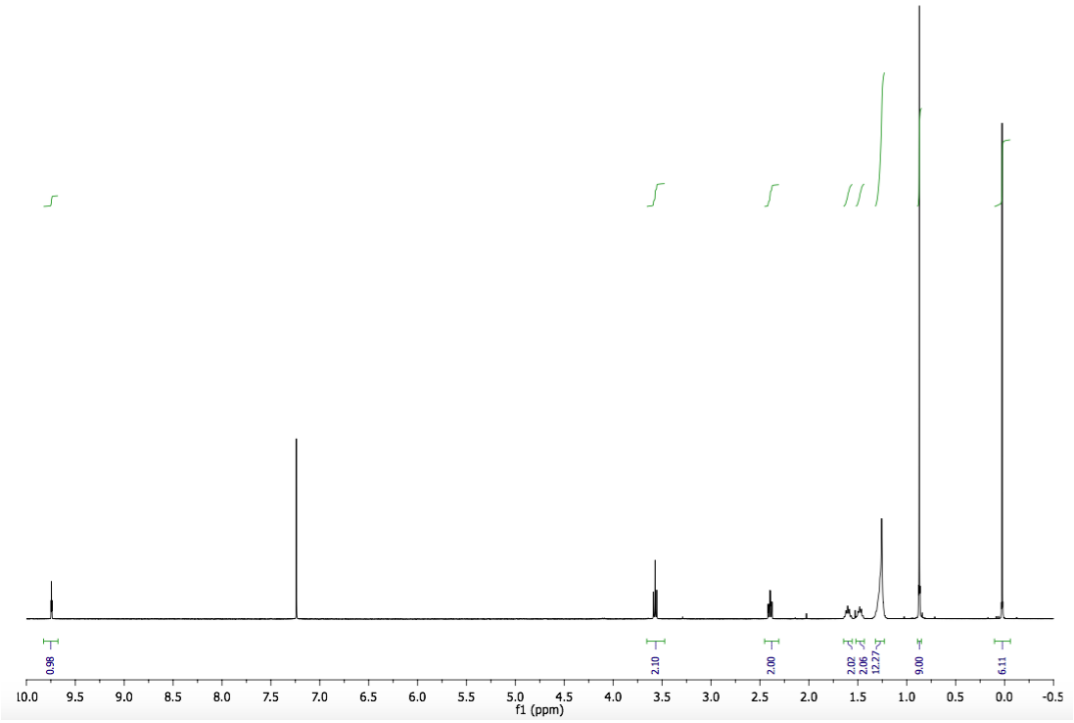
0.98
2.10
2.00
2.02
2.06
12.27
9.00
6.11
10.0
9.5
9.0
8.5
8.0
7.5
7.0
6.5
6.0
5.5
5.0
4.5
4.0
3.5
3.0
2.5
2.0
1.5
1.0
0.5
0.0
-0.5
f1 (ppm)

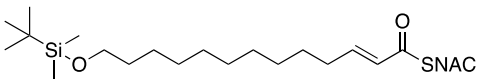
O
Si
O
SNAC

S19

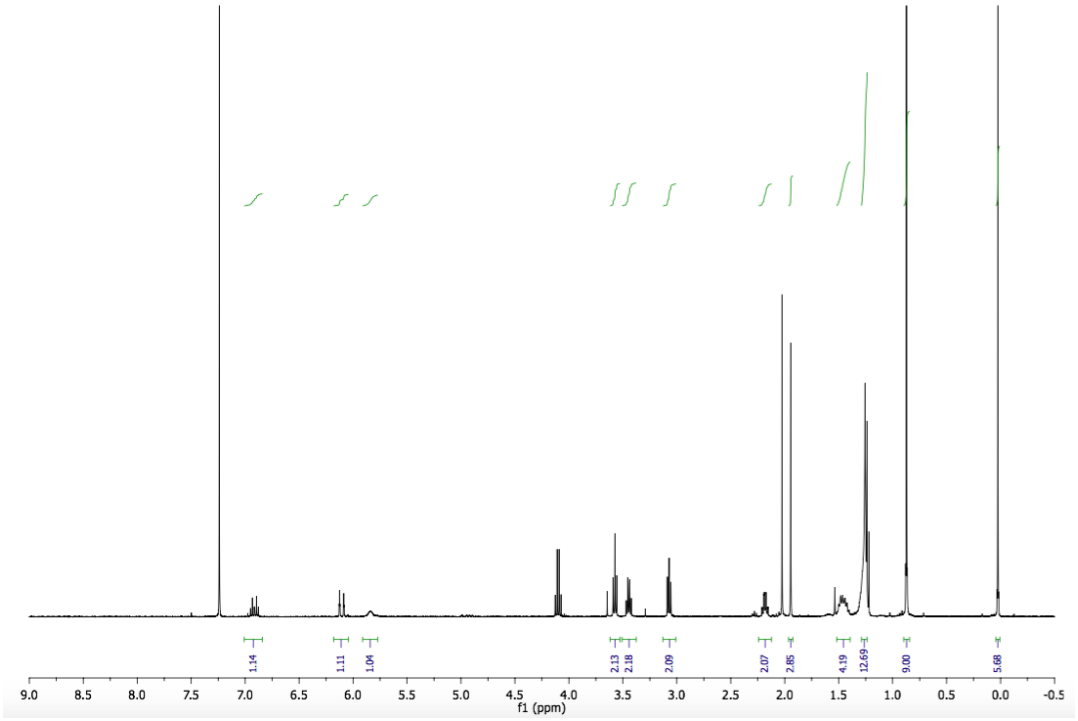
1.14
1.11
1.04
2.13
2.18
2.09
2.07
2.85
4.19
12.69
9.00
5.68
9.0 8.5 8.0 7.5 7.0 6.5 6.0 5.5 5.0 4.5 4.0 3.5 3.0 2.5 2.0 1.5 1.0 0.5 0.0 -0.5
f1 (ppm)

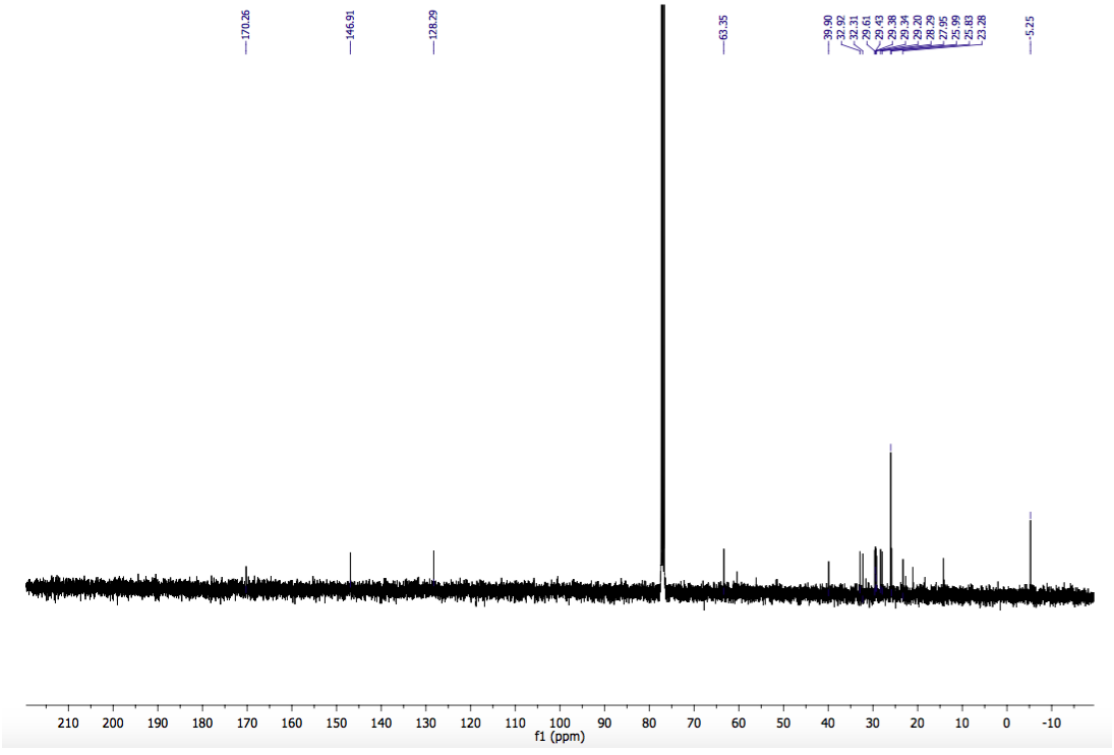
170.26
146.91
128.29
63.35
39.90
32.92
32.31
29.61
29.43
29.38
29.34
29.20
29.09
27.95
25.99
25.83
23.28
5.25
210 200 190 180 170 160 150 140 130 120 110 100 90 80 70 60 50 40 30 20 10 0 -10
f1 (ppm)

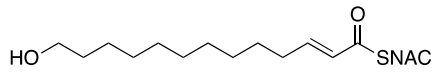
HO
O
SNAC

17

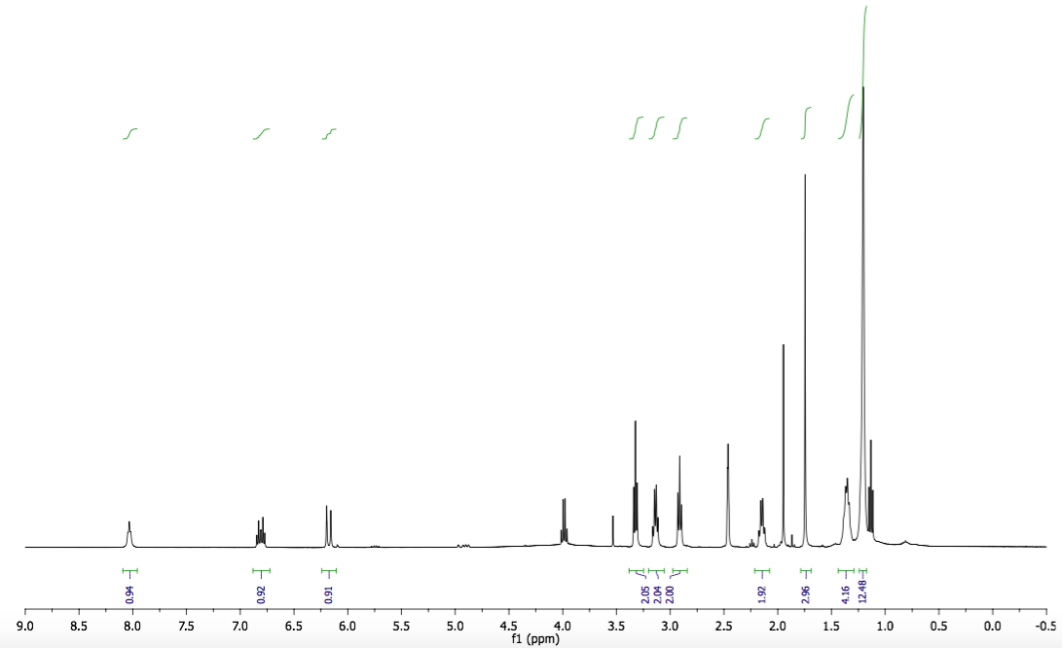
0.94
0.92
0.91
2.05
2.04
2.00
1.92
2.96
4.16
12.48
9.0 8.5 8.0 7.5 7.0 6.5 6.0 5.5 5.0 4.5 4.0 3.5 3.0 2.5 2.0 1.5 1.0 0.5 0.0 -0.5
f1 (ppm)

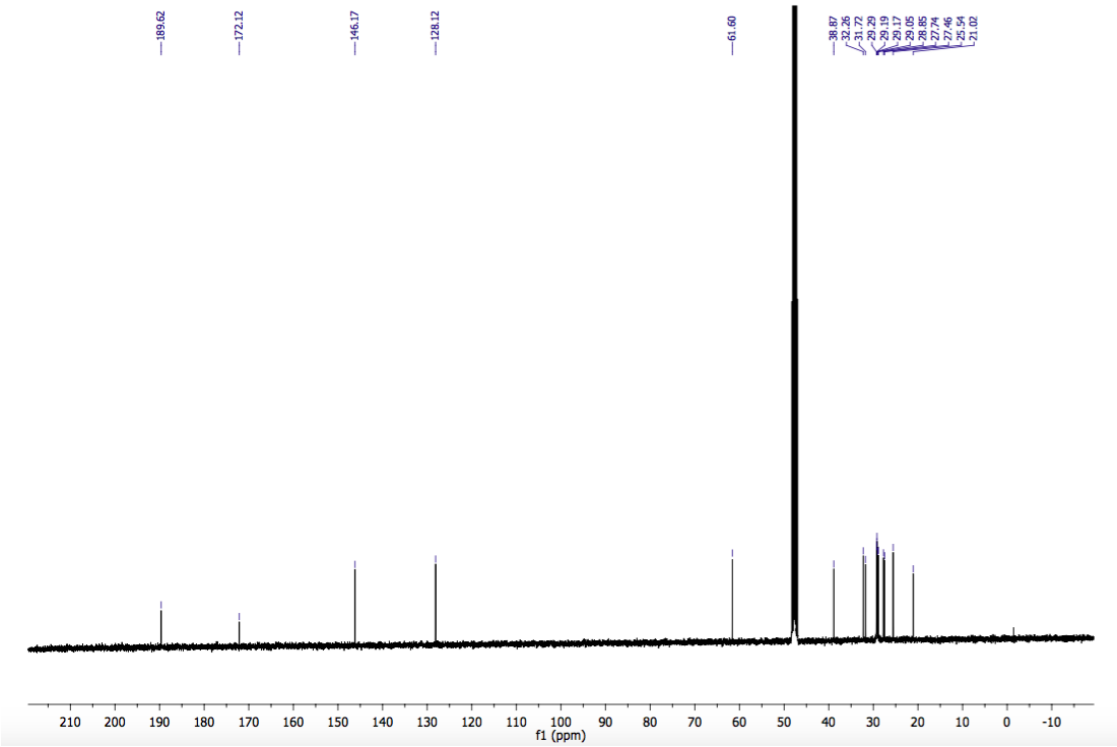
189.62
172.12
146.17
128.12
61.60
38.87
32.26
31.72
29.29
29.19
29.17
29.05
28.85
27.74
27.46
25.54
21.02
210 200 190 180 170 160 150 140 130 120 110 100 90 80 70 60 50 40 30 20 10 0 -10
f1 (ppm)

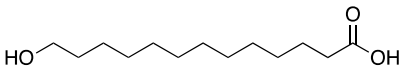
HO
O
OH

S20

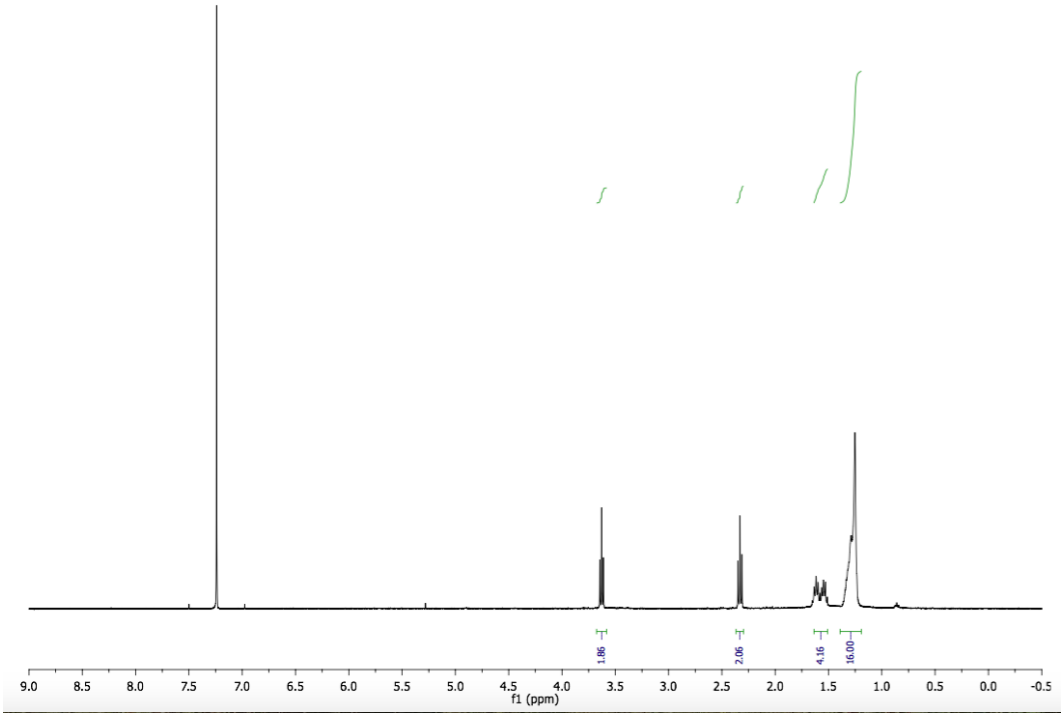
1.86
2.06
4.16
16.00
9.0
8.5
8.0
7.5
7.0
6.5
6.0
5.5
5.0
4.5
4.0
3.5
3.0
2.5
2.0
1.5
1.0
0.5
0.0
-0.5
f1 (ppm)

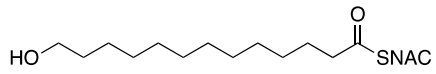
HO
O
SNAC

18

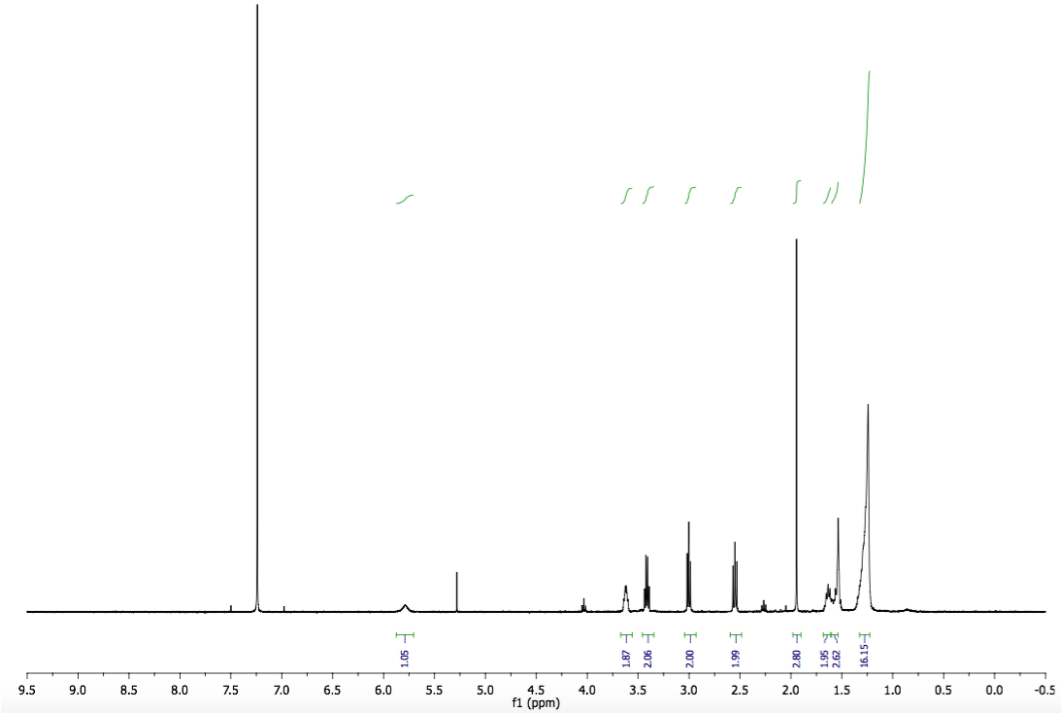
1.05
1.87
2.06
2.00
1.99
2.80
1.95
2.62
16.15
9.5 9.0 8.5 8.0 7.5 7.0 6.5 6.0 5.5 5.0 4.5 4.0 3.5 3.0 2.5 2.0 1.5 1.0 0.5 0.0 -0.5
f1 (ppm)

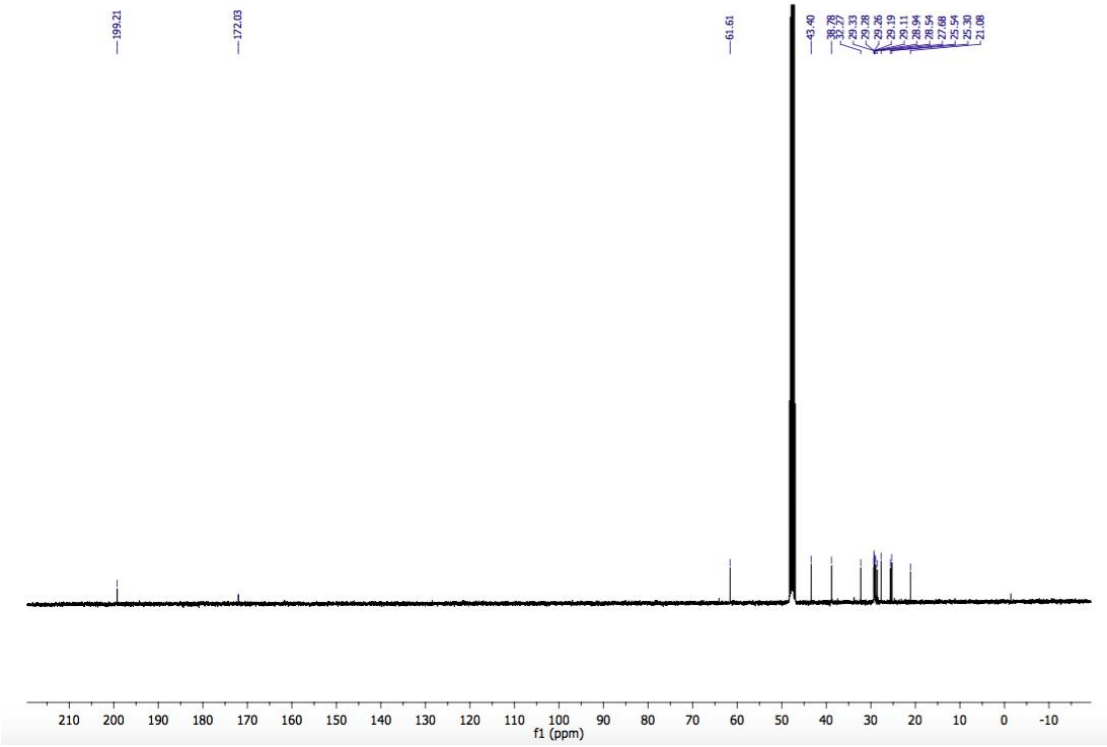
199.21
172.03
61.61
43.40
38.78
38.27
29.33
29.28
29.26
29.19
29.11
28.94
28.54
25.68
25.54
25.30
21.08
210 200 190 180 170 160 150 140 130 120 110 100 90 80 70 60 50 40 30 20 10 0 -10
f1 (ppm)

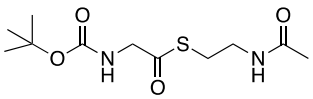

S21

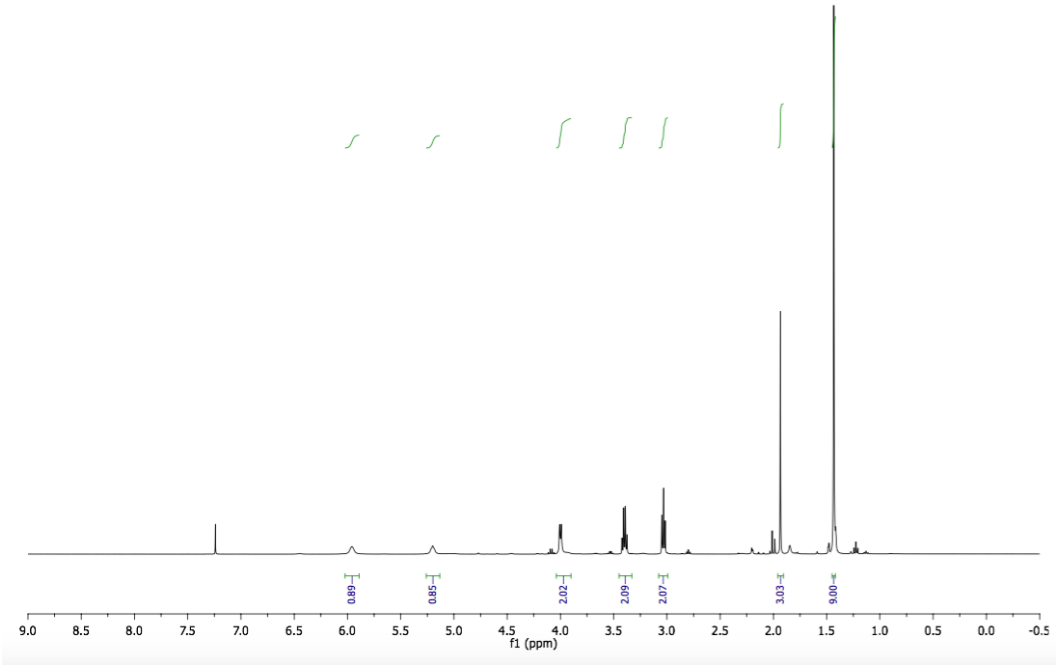
0.89
0.85
2.02
2.09
2.07
3.03
9.00
9.0 8.5 8.0 7.5 7.0 6.5 6.0 5.5 5.0 4.5 4.0 3.5 3.0 2.5 2.0 1.5 1.0 0.5 0.0 -0.5
f1 (ppm)

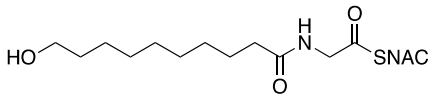
HO
H
N
O
O
SNAC
O

19

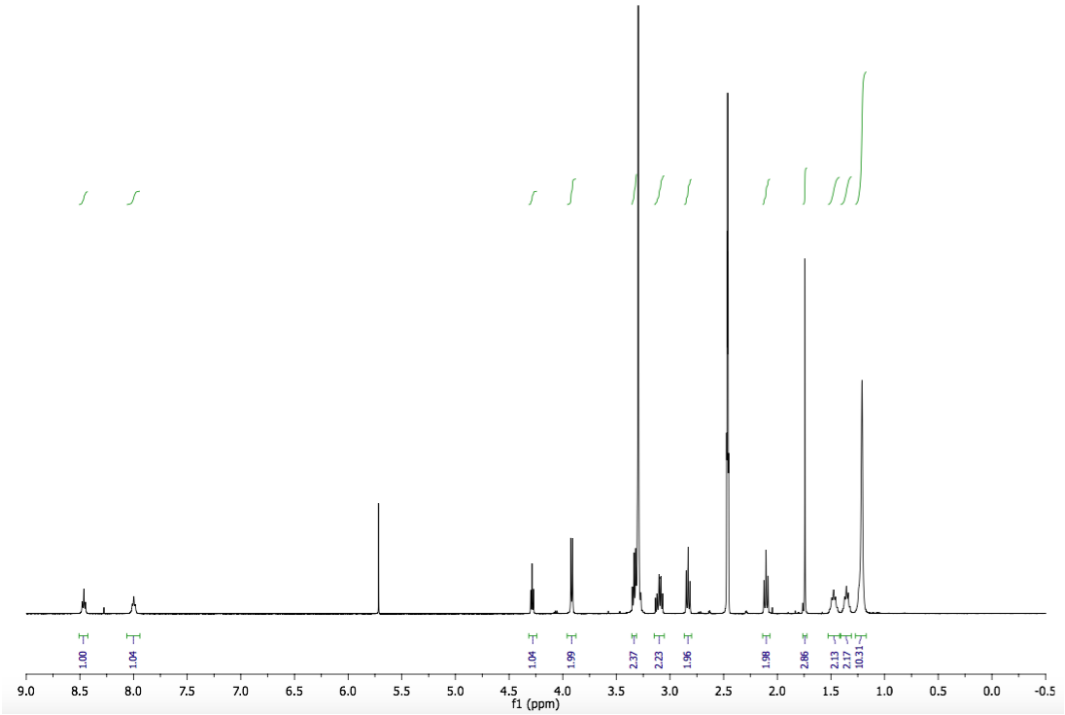
1.00
1.04
1.04
1.99
2.37
2.23
1.96
1.98
2.86
2.13
2.17
10.31
9.0 8.5 8.0 7.5 7.0 6.5 6.0 5.5 5.0 4.5 4.0 3.5 3.0 2.5 2.0 1.5 1.0 0.5 0.0 -0.5
f1 (ppm)

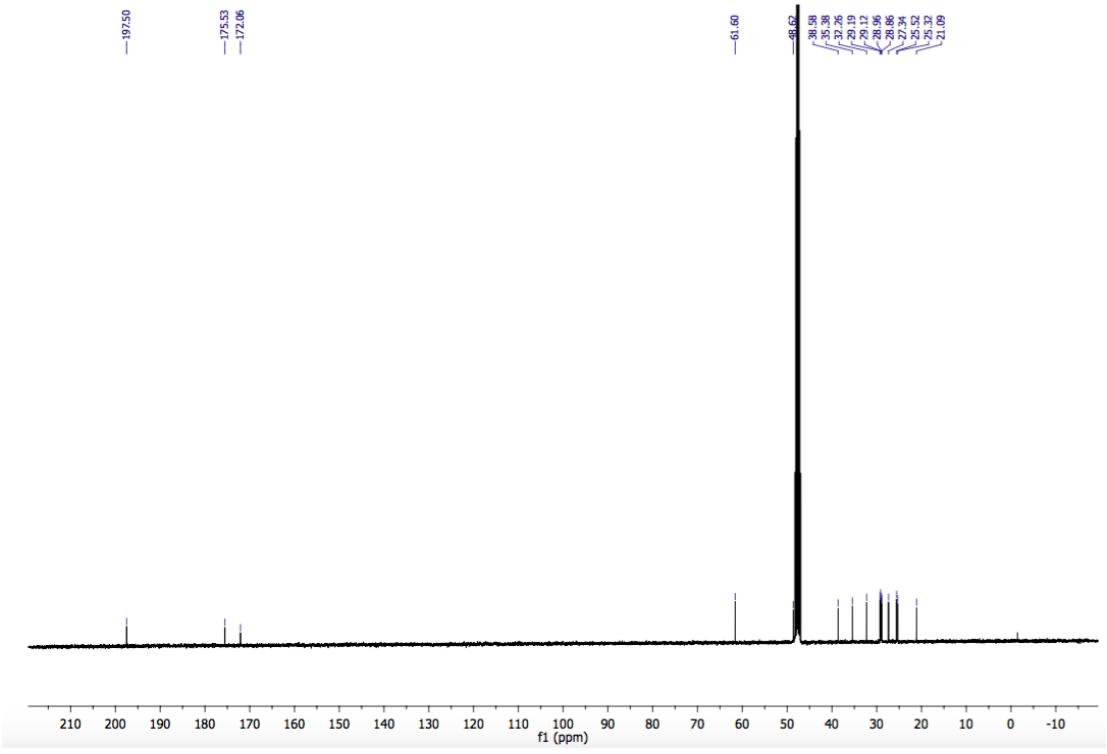
197.50
175.53
172.06
61.60
48.62
38.58
35.38
32.26
29.19
29.12
28.96
28.86
27.34
25.52
25.33
21.09
210 200 190 180 170 160 150 140 130 120 110 100 90 80 70 60 50 40 30 20 10 0 -10
f1 (ppm)

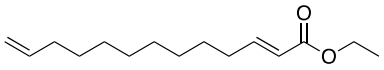

S22

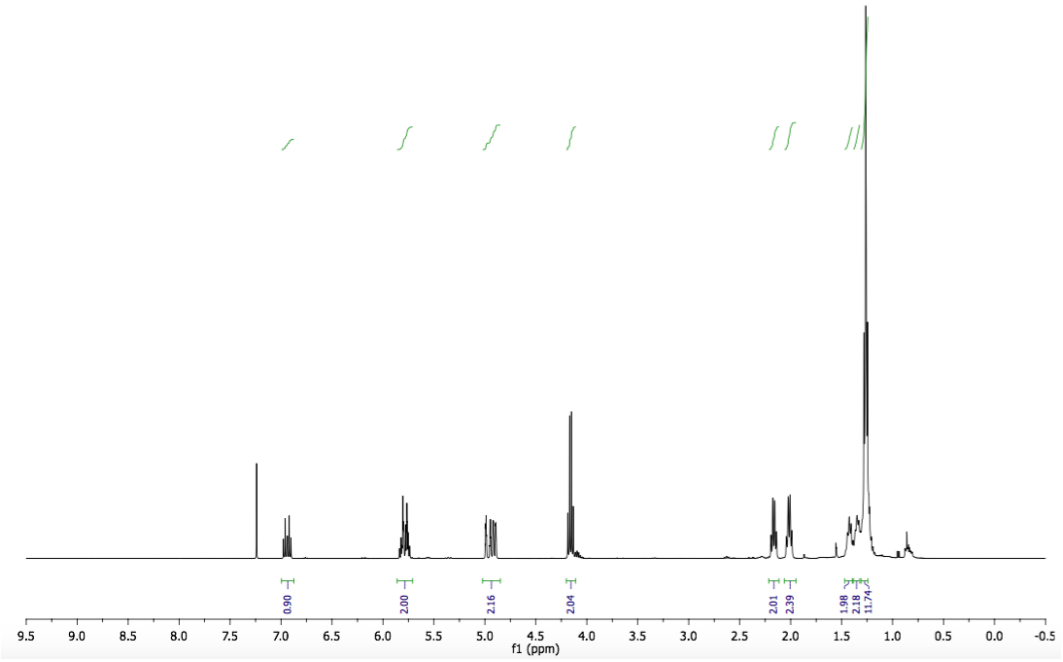
0.90
2.00
2.16
2.04
2.01
2.39
1.98
2.18
11.74
9.5 9.0 8.5 8.0 7.5 7.0 6.5 6.0 5.5 5.0 4.5 4.0 3.5 3.0 2.5 2.0 1.5 1.0 0.5 0.0 -0.5
f1 (ppm)

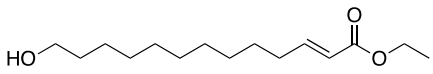
HO
O
O

S23

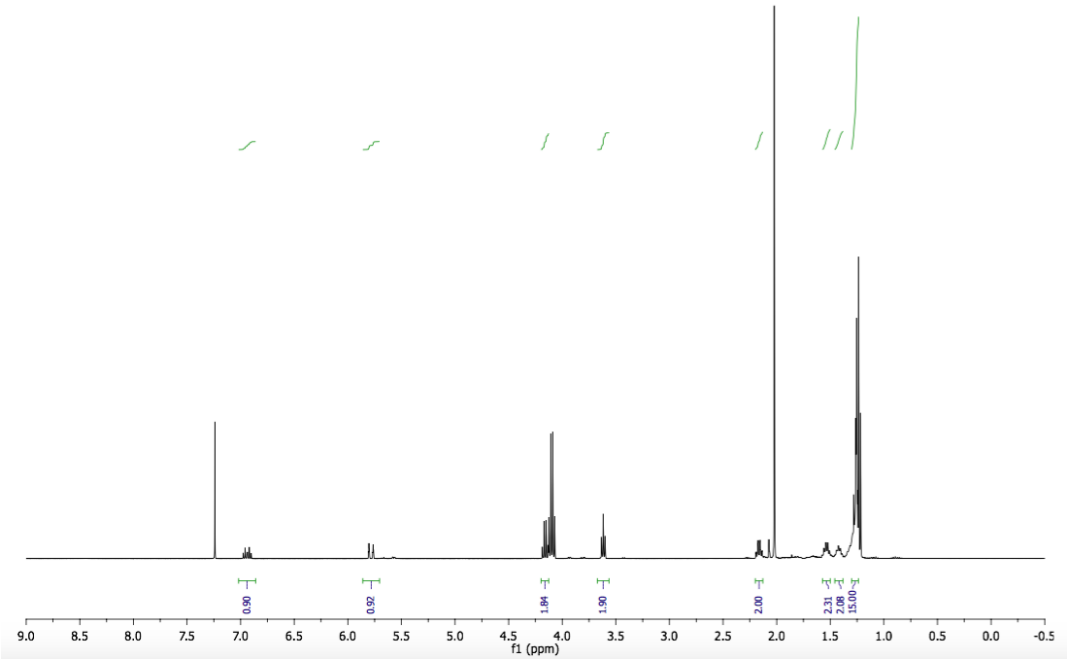
0.90
0.92
1.84
1.90
2.00
2.31
2.08
15.00
9.0
8.5
8.0
7.5
7.0
6.5
6.0
5.5
5.0
4.5
4.0
3.5
3.0
2.5
2.0
1.5
1.0
0.5
0.0
-0.5
f1 (ppm)

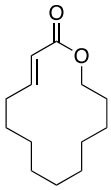
O
O

S24

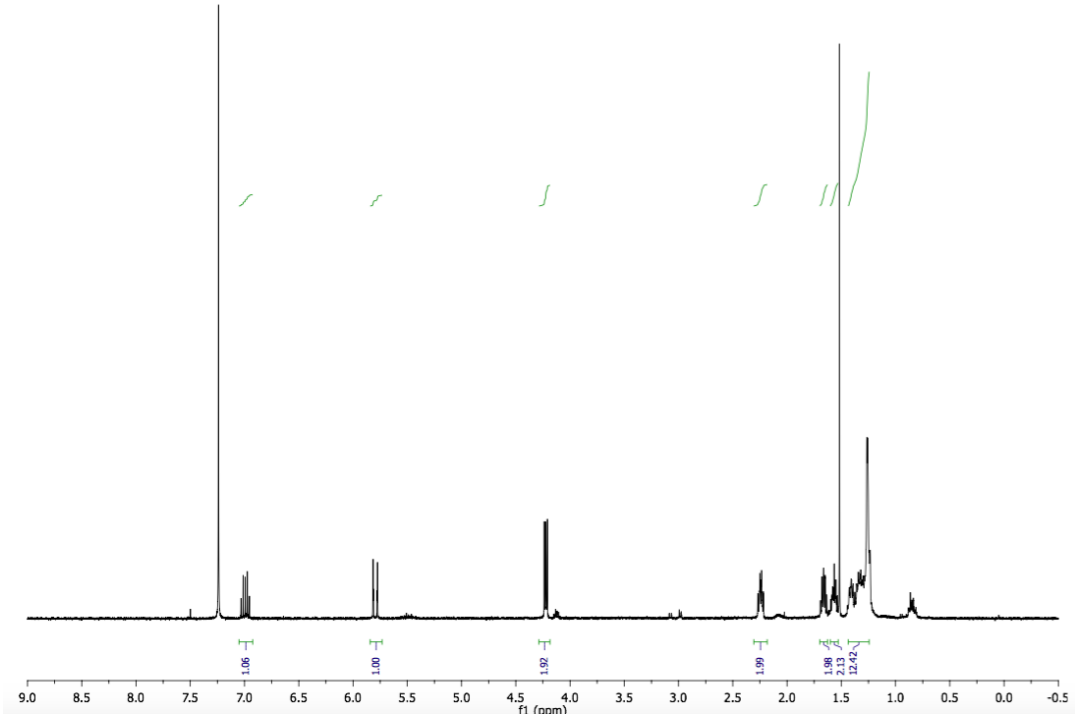
1.06
1.00
1.92
1.99
1.98
2.13
12.42
9.0
8.5
8.0
7.5
7.0
6.5
6.0
5.5
5.0
4.5
4.0
3.5
3.0
2.5
2.0
1.5
1.0
0.5
0.0
-0.5
f1 (ppm)

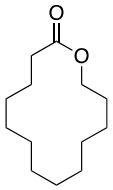
O
O

S25

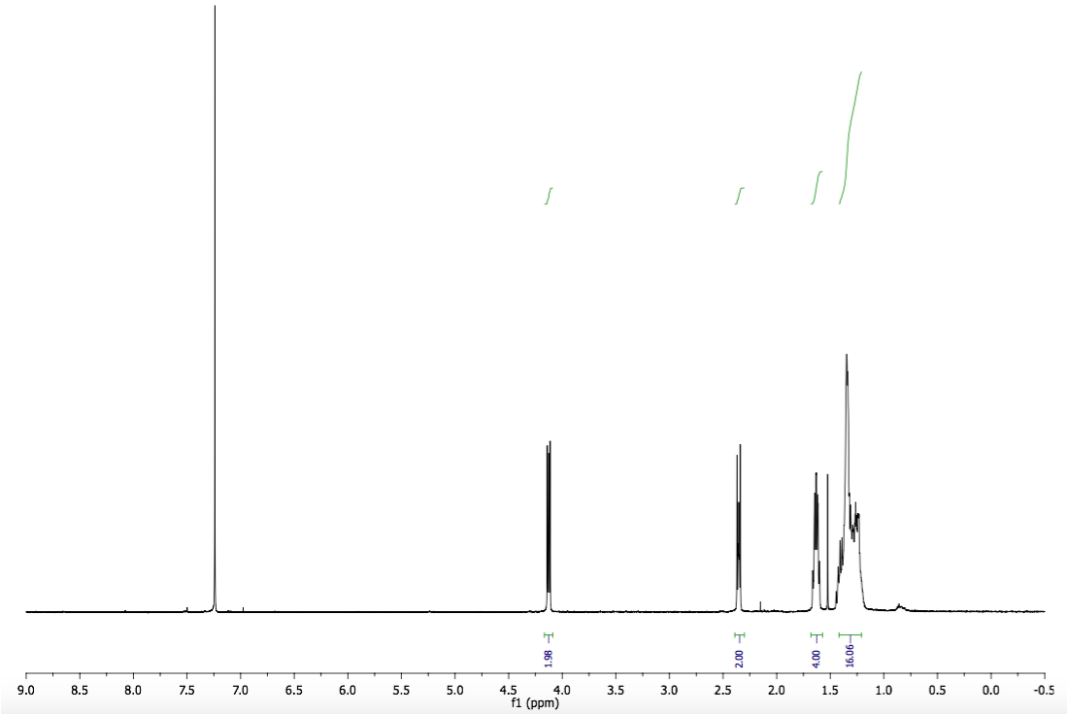
1.98
2.00
4.00
16.06
9.0
8.5
8.0
7.5
7.0
6.5
6.0
5.5
5.0
4.5
4.0
3.5
3.0
2.5
2.0
1.5
1.0
0.5
0.0
-0.5
f1 (ppm)

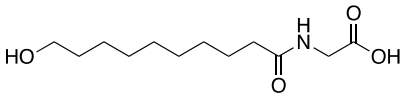
HO
H
N
O
O
OH
O

S26

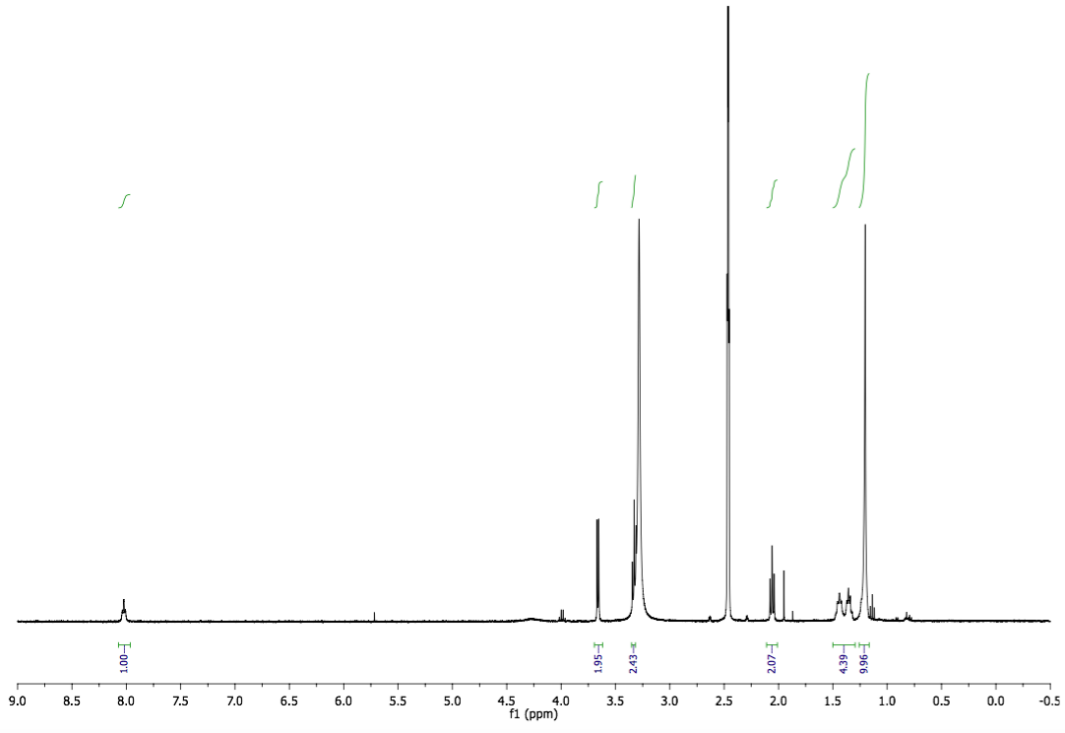
1.00
1.95
2.43
2.07
4.39
9.96
9.0 8.5 8.0 7.5 7.0 6.5 6.0 5.5 5.0 4.5 4.0 3.5 3.0 2.5 2.0 1.5 1.0 0.5 0.0 -0.5
f1 (ppm)

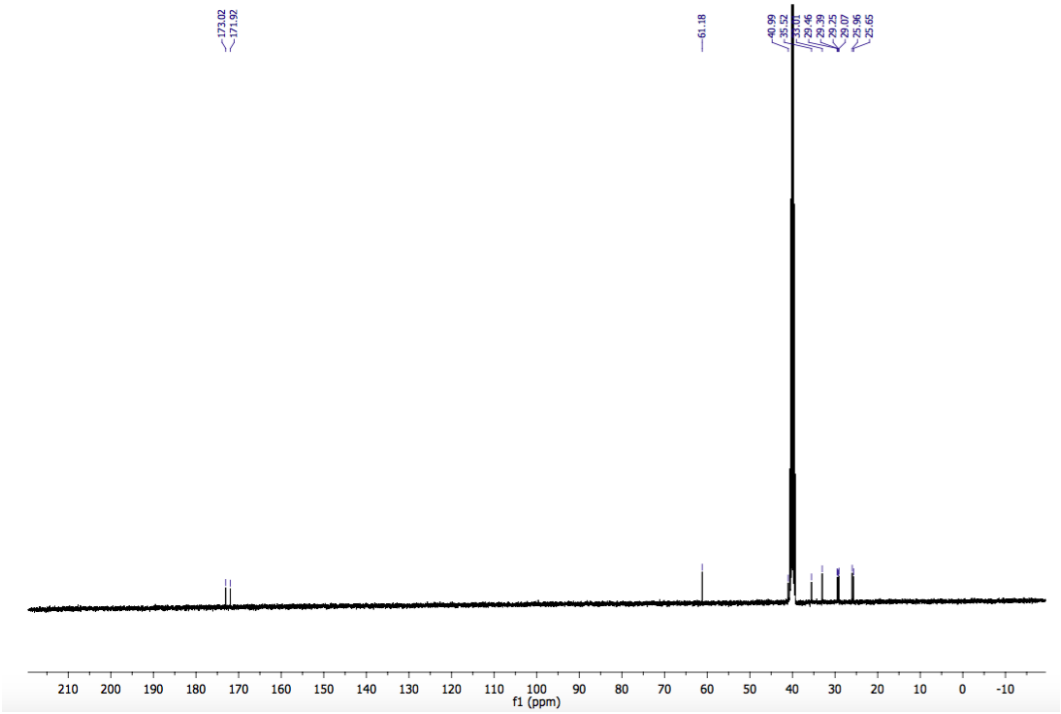
173.02
171.92
61.18
40.99
35.52
33.01
29.46
29.39
29.35
29.07
25.96
25.65
210 200 190 180 170 160 150 140 130 120 110 100 90 80 70 60 50 40 30 20 10 0 -10
f1 (ppm)

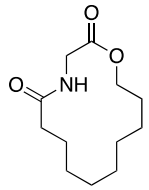
O
O
O
NH

24

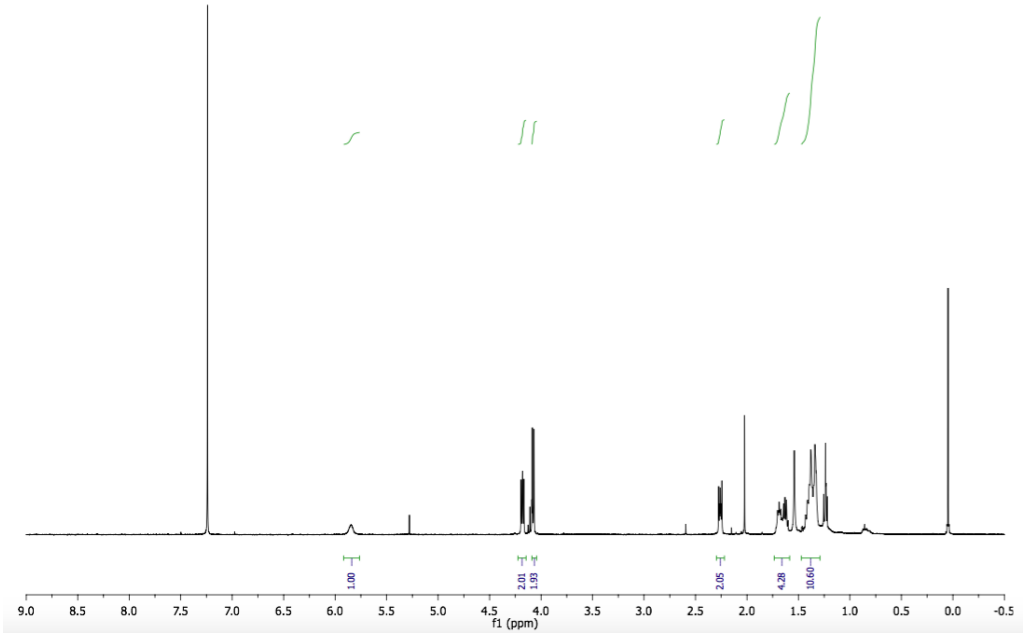
1.00
2.01
1.93
2.05
4.28
10.60
9.0 8.5 8.0 7.5 7.0 6.5 6.0 5.5 5.0 4.5 4.0 3.5 3.0 2.5 2.0 1.5 1.0 0.5 0.0 -0.5
f1 (ppm)

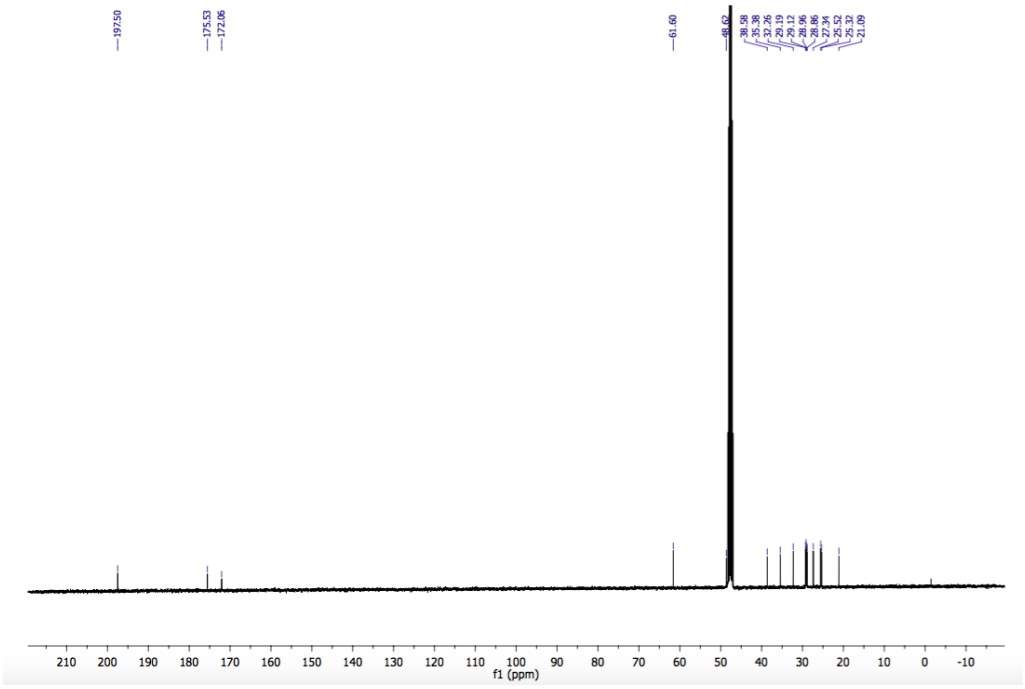
197.50
175.53
172.06
61.60
46.62
38.58
35.38
32.26
29.19
29.12
28.96
28.86
27.34
25.52
25.32
21.09
210 200 190 180 170 160 150 140 130 120 110 100 90 80 70 60 50 40 30 20 10 0 -10
f1 (ppm)

References

1 G. W. Heberlig, M. Wirz, M. Wang and C. N. Boddy, *Org. Lett.*, 2014, **16**, 5858–5861.
2 M. Wang, H. Zhou, M. Wirz, Y. Tang and C. N. Boddy, *Biochemistry*, 2009, **48**, 6288–6290.
3 G. Kumaraswamy, K. Sadaiah and N. Raghu, *Tetrahedron: Asymmetry*, 2012, **23**, 587–593.
4 Y.-S. Hon, Y.-C. Wong, C.-P. Chang and C.-H. Hsieh, *Tetrahedron*, 2007, **63**, 11325–11340.
5 H. Yun, J. Sim, H. An, J. Lee, H. S. Lee, Y. K. Shin, S.-M. Paek and Y.-G. Suh, *Org. Biomol. Chem.*, 2014, **12**, 7127–35.
6 V. N. Tsarev, Y. Morioka, J. Caner, Q. Wang, R. Ushimaru, A. Kudo, H. Naka and S. Saito, *Org. Lett.*, 2015, **17**, 2530–2533.
7 J. M. Winter, D. Cascio, D. Dietrich, M. Sato, K. Watanabe, M. R. Sawaya, J. C. Vederas and Y. Tang, *J. Am. Chem. Soc.*, 2015, **137**, 9885–9893.
8 S. T. Kemme, T. Šmejkal and B. Breit, *Adv. Synth. Catal.*, 2008, **350**, 989–994.
9 B. M. Trost and M. Lautens, *J. Am. Chem. Soc.*, 1987, **109**, 1469–1478.
10 G. Makado, T. Morimoto, Y. Sugimoto, K. Tsutsumi, N. Kagawa and K. Kakiuchi, *Adv. Synth. Catal.*, 2010, **352**, 299–304.
11 J. Jose, G. Pourfallah, D. Merkley, S. Li, L. Bouzidi, A. L. Leao and S. S. Narine, *Polym. Chem.*, 2014, **5**, 3203–3213.
12 M. Wang, P. Opare and C. N. Boddy, *Bioorg. Med. Chem. Lett.*, 2009, **19**, 1413–5.
13 I. G. Molnár and R. Gilmour, *J. Am. Chem. Soc.*, 2016, **138**, 5004–5007.
14 V. D. Kadam and G. Sudhakar, *Tetrahedron*, 2015, **71**, 1058–1067.
15 M. Nagarajan, V. S. Kumar and B. V. Rao, *Tetrahedron*, 1999, **55**, 12349–12360.

Chapter 4. Trapping biosynthetic acyl-enzyme intermediates with encoded 2,3-diaminopropionic acid

4.1 Introduction

The previous two chapters have dealt with thioesterases (TEs) that catalyze macrocyclization by loading a substrate from the upstream acyl-carrier protein onto the active site serine and then directly releasing it again, through hydrolysis or macrocyclization.[1–3] There is an additional class of TEs that load the substrate, forming the acyl-TE intermediate, which is retained until another monomer unit is available on the ACP. The TE then catalyzes a transesterification reaction linking the two monomer units together and then reloads the dimeric product. This may then result in release of a dimeric product, such as elaiolide/elaiophylin,[4,5] or the cycle can be repeated again generating a trimeric product such as enterobactin or valinomycin.[6,7] These natural products are shown in **Figure 4.1**.

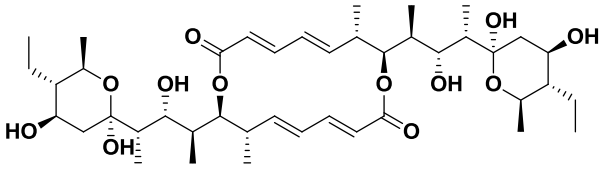

Elaiolide

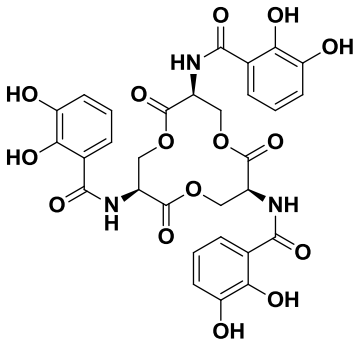

Enterobactin

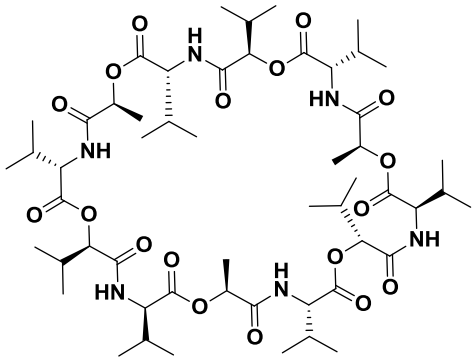

Valinomycin

Figure 4.1 Several natural product oligomeric macrocycles.

Compared to the typical TE release chemistry of hydrolysis or macrocyclization this release mechanism is uncommon.[5] This is not surprising considering the exquisite selectivity that must be exercised by a TE performing this chemistry. Distinguishing between hydrolysis and macrocyclization requires the TE to distinguish between water and an alcohol or amine as the correct nucleophile. Whether undergoing transesterification to add a monomer or releasing the product as a macrocycle the presented nucleophile is chemically identical. Understanding the key structural features that control this incredible selectivity is of great importance to the field of natural product biosynthesis.[8]

Valinomycin, a potent ionophore,[9] is an example of a natural product that is produced by TE-mediated trimerization and macrocyclization. It was first isolated and reported in 1955[10]; however, the cyclic dimer shunt product, montanastatin, would not be isolated until over 40 years later and even then only in tiny amounts (**Fig. 4.2**).[11] Interestingly, montanastatin is a rare case of a natural product being made synthetically before being discovered as a natural product.[12] This is clearly related to the biological activities of the two molecules, while valinomycin is quite toxic, montanastatin is largely benign.[11] Clearly the trimeric valinomycin is the privileged structure and this large difference in activity contributes to a strong evolutionary pressure to only generate cyclic trimer.

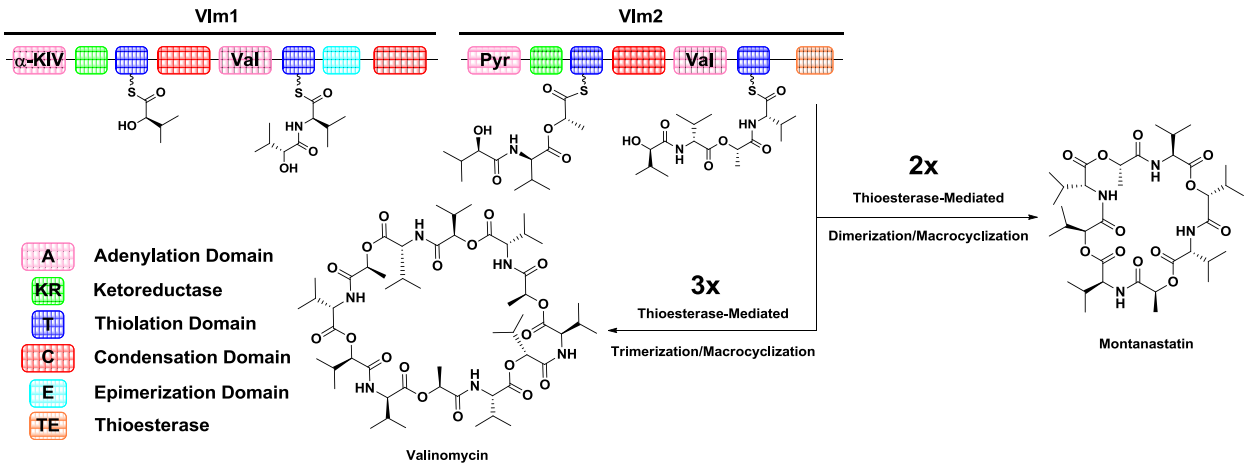

Figure 4.2 Biosynthesis of the cyclic trimer valinomycin and cyclic dimer montanastatin. The abbreviations in the adenylation (A) domains indicates the selected monomer unit. α-KIV = alpha-keto isovalerate, Val = L-valine, and Pyr = pyruvate.

To understand how the valinomycin TE (Vlm TE) could exert such selectivity we set out to synthesize linear monomer, dimer, and trimer-SNAC activated substrates. Structural characterization of the TE loaded with each of these would provide snapshots of the TE's conformation at each stage of valinomycin growth and provide insight to mechanism of selective trimer release. Unfortunately the dimer and trimer substrates underwent attack, not only at the desired activated thioester, but at the ester linkage between monomer units. This degraded the substrates and ultimately lead to formation of valinomycin. While a disappointing result, it supported my suggestion that the reverse reaction using commercially available valinomycin may provide an avenue to loading trimer on the enzyme (**Fig. 4.3**).[8]

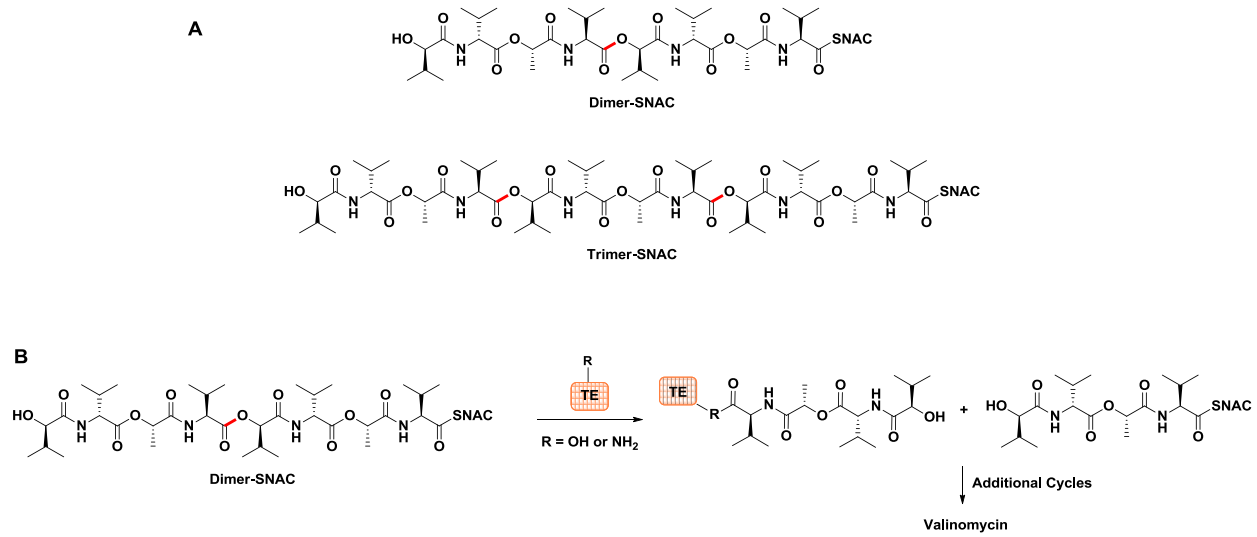

Figure 4.3 A) Linear dimer and trimer-SNAC substrates. **B)** Vlm TE catalyzed decomposition reaction of multimer substrates (dimer shown here) to monomer and eventual assembly to valinomycin. Non-native ester linkage attacked by thioesterase is highlighted in red.

4.2 References

[1] M. E. Horsman, T. P. A. Hari, C. N. Boddy, *Nat. Prod. Rep.* 2016, *33*, 183–202.
[2] G. W. Heberlig, M. Wirz, M. Wang, C. N. Boddy, *Org. Lett.* 2014, *16*, 5858–5861.
[3] G. W. Heberlig, J. T. C. Brown, R. D. Simard, M. Wirz, W. Zhang, M. Wang, L. I. Susser, M. E. Horsman, C. N. Boddy, *Org. Biomol. Chem.* 2018, *16*, 5771–5779.
[4] S. F. Haydock, T. Mironenko, H. I. Ghoorahoo, P. F. Leadlay, *J. Biotechnol.* 2004, *113*, 55–68.
[5] Y. Zhou, P. Prediger, L. C. Dias, A. C. Murphy, P. F. Leadlay, *Angew. Chem. Int. Edit.* 2015, *54*, 5232–5235.
[6] Z. L. Reitz, M. Sandy, A. Butler, *Metallomics* 2017, *9*, 824–839.
[7] J. Jaitzig, J. Li, R. D. Süssmuth, P. Neubauer, *ACS Synth. Biol.* 2014, *3*, 432–438.
[8] N. Huguenin-Dezot, D. A. Alonzo, G. W. Heberlig, M. Mahesh, D. P. Nguyen, M. H. Dornan, C. N. Boddy, T. M. Schmeing, J. W. Chin, *Nature* 2019, *565*, 112.
[9] W. C. McMurray, R. W. Begg, *Arch. Biochem.Biophys.* 1959, *84*, 546–548.
[10] H. Brockmann, G. Schmidt-Kastner, *Ber. Dtsch. Chem. Ges.* 1955, *88*, 57–61.
[11] G. R. Pettit, R. Tan, N. Melody, J. M. Kielty, R. K. Pettit, D. L. Herald, B. E. Tucker, L. P. Mallavia, D. L. Doubek, J. M. Schmidt, *Bioorg. Med. Chem.* 1999, *7*, 895–899.
[12] M. Rothe, W. Kreiss, *Angew. Chem. Int. Edit.* 1973, *12*, 1012–1013.

4.3 Author Contributions

N.H.-D. and D.A.A. contributed equally. M.M and **G.W.H.** contributed equally. N.H.-D. and D.P.N. selected the synthetases for **2**–**6**. N.H.-D. characterized the incorporation of **6** and its deprotection to produce DAP, and performed the TEV conjugation. D.P.N and M.M. designed, and M.M. synthesized **2**–**6**. T.M.S. and D.A.A. designed, and D.A.A. performed, the biochemistry and crystallography with Vlm TE_{wt}. D.A.A. and N.H.-D. performed biochemistry and crystallography with Vlm TE_{DAP}. **G.W.H.** and M.H.D. synthesized Vlm TE substrates. J.W.C. supervised N.H.-D., D.P.N. and M.M. T.M.S. supervised D.A.A. C.N.B. supervised G.W.H. and M.H.D. T.M.S., D.A.A., N.H.-D. and J.W.C. wrote the paper with input from all authors.

G.W.H. also synthesized linear octadepsipeptide-SNAC (dimer-SNAC) and dodecadepsipeptide-SNAC (trimer-SNAC). These substrates were unable to be used in the presented study do to instability on the TE_{DAP}. This allowed **G.W.H.** to design the experiment to incubate Vlm TE_{DAP} with natural valinomycin to generate a stable dodecadepsipeptide bound complex without the generation of tetradepsipeptide or octadepsipeptide.

Copyright

Supplementary videos are available online at: nature.com/articles/s41586-018-0781-z

4.4 Abstract

Many enzymes catalyse reactions that proceed through covalent acyl-enzyme (ester or thioester) intermediates.[1] These enzymes include serine hydrolases[2,3] (encoded by one per cent of human genes, and including serine proteases and thioesterases), cysteine proteases (including caspases), and many components of the ubiquitination machinery.[4,5] Their important acyl-enzyme intermediates are unstable, commonly having half-lives of minutes to hours.[6] In some cases, acyl-enzyme complexes can be stabilized using substrate analogues or active-site mutations but, although these approaches can provide valuable insight,[7–10] they often result in complexes that are substantially non-native. Here we develop a strategy for incorporating 2,3-diaminopropionic acid (DAP) into recombinant proteins, via expansion of the genetic code.[11] We show that replacing catalytic cysteine or serine residues of enzymes with DAP permits their first-step reaction with native substrates, allowing the efficient capture of acyl-enzyme complexes that are linked through a stable amide bond. For one of these enzymes, the thioesterase domain of valinomycin synthetase,[12] we elucidate the biosynthetic pathway by which it progressively oligomerizes tetradepsipeptidyl substrates to a dodecadepsipeptidyl intermediate, which it then cyclizes to produce valinomycin. By trapping the first and last acyl-thioesterase intermediates in the catalytic cycle as DAP conjugates, we provide structural insight into how conformational changes in thioesterase domains of such nonribosomal peptide synthetases control the oligomerization and cyclization of linear substrates. The encoding of DAP will facilitate the characterization of diverse acyl-enzyme complexes, and may be extended to capturing the native substrates of transiently acylated proteins of unknown function.

4.5 Main

We proposed that selectively replacing the sulfhydryl or hydroxyl groups in catalytic cysteine or serine residues with an amino group, making 2,3-diaminopropionic acid (DAP, **1**), would enable the trapping of acyl-enzyme intermediates that are linked through an amide bond (**Fig. 4.4a, b**). Within peptides, the conjugate acid of the β-amino group of DAP has a reported pK_a value of between 6.3 and 7.5 (compared with the conjugate acid of the ε-amino group of free lysine, which has a pK_a of 10.5).[13] This suggests that the β-amino group of DAP could act as a nucleophile, and may form amide bonds with the substrates of enzymes. The half-life of amides in aqueous solution is about 500 years,[14] so the amide analogues of labile thioester and ester intermediates should be substantially stabilized, such that subsequent reactions with nucleophiles or solvent should be severely attenuated or abolished (**Fig. 4.4b**).

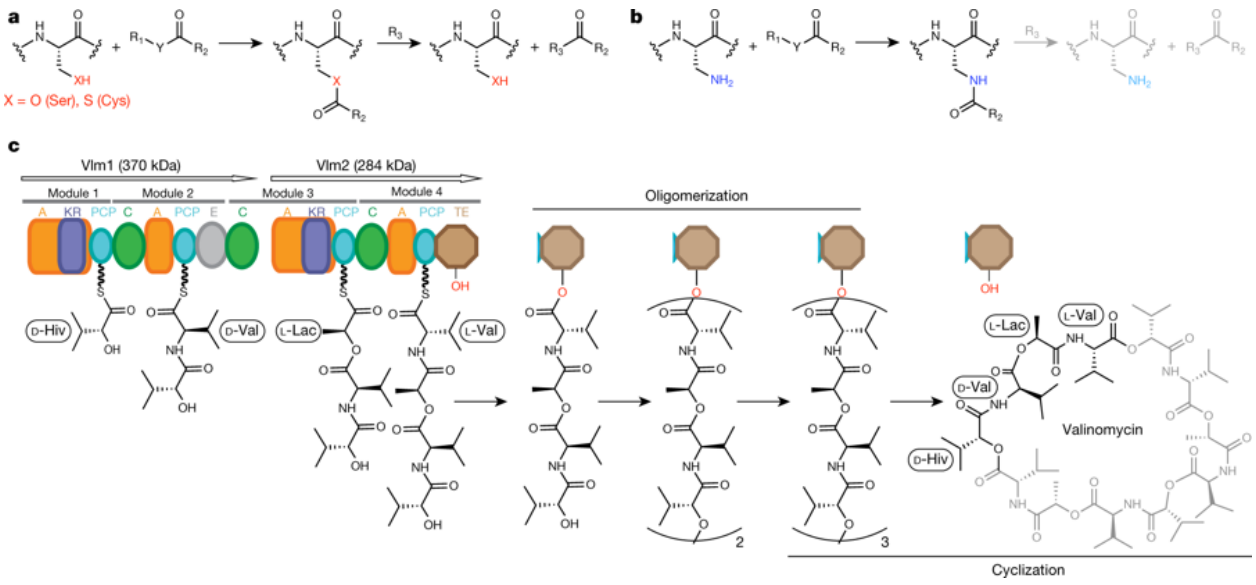

Figure 4.4) a, Active-site serine or cysteine residues react with carbonyl groups to form tetrahedral intermediates (not shown) that collapse to acyl-enzyme intermediates by loss of R_1–YH. Attack by nucleophilic R_3 groups (commonly a hydroxyl, amine or thiol) releases the

bound substrate fragment and regenerates the enzyme. R_1, R_2 and Y represent the diverse chemical groups that may be found in distinct reactants. **b**, Replacing cysteine or serine with DAP may result in a first acyl-enzyme intermediate that is resistant to cleavage. **c**, Valinomycin synthetase (Vlm) condenses D-α-hydroxyisovaleric acid (D-α-hiv), D-valine (D-val), L-lactic acid (L-lac) and L-valine (L-val) to form the tetradepsipeptidyl (D-hiv–D-val–L-lac–L-val) intermediate. D-α-hiv and L-lac arise from the reduction of precursor ketoacyl moieties by ketoreductase (KR) domains. Tetradepsipeptidyl intermediates are oligomerized to a dodecadepsipeptidyl intermediate that is cyclized, by the terminal TE domain, to produce valinomycin. Vlm1 and Vlm2 are the two protein subunits that form valinomycin synthetase. A module is a set of domains that work together to add one monomer to the growing depsipeptide. A, adenylation domain; C, condensation domain; PCP, peptidyl carrier protein domain. See App. 1, Fig. 1 for a synthetic cycle of an NRPS.

The secondary-metabolite-producing nonribosomal peptide synthetases (NRPSs) and polyketide synthases (PKSs) generate complex acyl-enzyme intermediates during their synthetic cycles.[15] These megaenzymes use thio-templated pathways to assemble small acyl molecules into a broad array of biologically active natural products, including antitumour compounds, antibiotics, antifungals and immunosuppressants (App. 1, Fig. 1). Unravelling their molecular mechanisms has been hampered by the challenge of characterizing their multiple acyl-enzyme intermediates at high resolution.

This challenge is exemplified by the thioesterase (TE) domains[16] from NRPS pathways that oligomerize and cyclize linear peptidyl substrates,[17] including the TE domain from valinomycin synthetase[12] (**Fig. 4.4c**). This enzyme—a two-protein, four-module NRPS—alternatively links hydroxy acids (from in situ reduction of α-keto acids) and amino acids into a

tetradepsipeptide intermediate, which the thioesterase domain (Vlm TE) oligomerizes up to, but not beyond, the dodecadepsipeptide. Vlm TE then cyclizes the dodecadepsipeptide to release valinomycin[12,18] (a potassium ionophore with antimicrobial, antitumoural and cytotoxic properties; **Fig. 4.4c**). The oligomerizations and cyclization must be rapid enough to prevent substantial spontaneous hydrolysis to linear depsipeptides, which are useless side products.

High-resolution structures of acyl-TE intermediates in valinomycin biosynthesis could provide mechanistic insight into how thioesterases control substrate fate. A handful of high-resolution acyl-TE structures have been obtained, most notably with the polyketide pikromycin-forming TE and non-native substrate analogues.[19] These have helped to identify the putative oxyanion hole and demonstrated the interaction of the 'lid' element of the TE domain with the substrate. However, structural studies of TE domains have been hampered by several factors, especially the hydrolysis rates of acyl-TE intermediates,[20,21] which are high by comparison with the crystallographic timescale.

Here we develop a strategy for the site-specific incorporation of DAP into recombinant proteins, and demonstrate the efficient capture of acyl-enzyme intermediates for a cysteine protease and Vlm TE. We elucidate the biosynthetic pathway for converting tetradepsipeptides to valinomycin, and structurally characterize deoxy-tetradepsipeptidyl–*N*-TE_{DAP} and dodecadepsipeptidyl–*N*-TE_{DAP} conjugates to provide insights into the first and last acyl-TE intermediates in the catalytic cycle of Vlm TE. Our results reveal how the fate of substrates may be determined by conformational changes in the TE domains of NRPSs that oligomerize and cyclize linear precursors.

The structural similarity of DAP (**1**) to cysteine and serine makes it challenging to discover an aminoacyl-tRNA synthetase that is selective for DAP in vivo. We therefore created five protected versions of DAP (**2**–**6**; App. 1, Fig. 2a), for which we anticipated that the successful discovery of specific aminoacyl-tRNA synthetase/$tRNA_{CUA}$ pairs would enable site-specific incorporation into proteins. The subsequent post-translational deprotection[22,23] would reveal DAP. We found that **2**–**5** accumulated in *Escherichia coli* at low concentrations (less than 10 μM; App. 1, Fig. 4.2b–e) and we were unable to evolve a synthetase for these noncanonical amino acids using several libraries of the orthogonal *Methanosarcina barkeri* (*Mb*) pyrrolysyl-tRNA synthetase (PylRS)/$tRNA^{Pyl}_{CUA}$ pair.[11] By contrast, **6** accumulated in *E. coli* at millimolar concentrations and we were able to evolve an *Mb*PylRS variant (named DAPRS, containing mutations Y271C, N311Q, Y349F and V366C) for the site-specific incorporation of **6** (App. 1, Fig. 2f–h). The DAPRS/$tRNA^{Pyl}_{CUA}$ pair enabled the synthesis of green fluorescent protein (GFP) containing **6** at position 150 (GFP150(**6**); **Fig. 4.5a**) in good yield.[24] Photo-deprotection of GFP150(**6**) and subsequent incubation converted **6** to **1** in GFP (**Fig. 4.5b, c**).

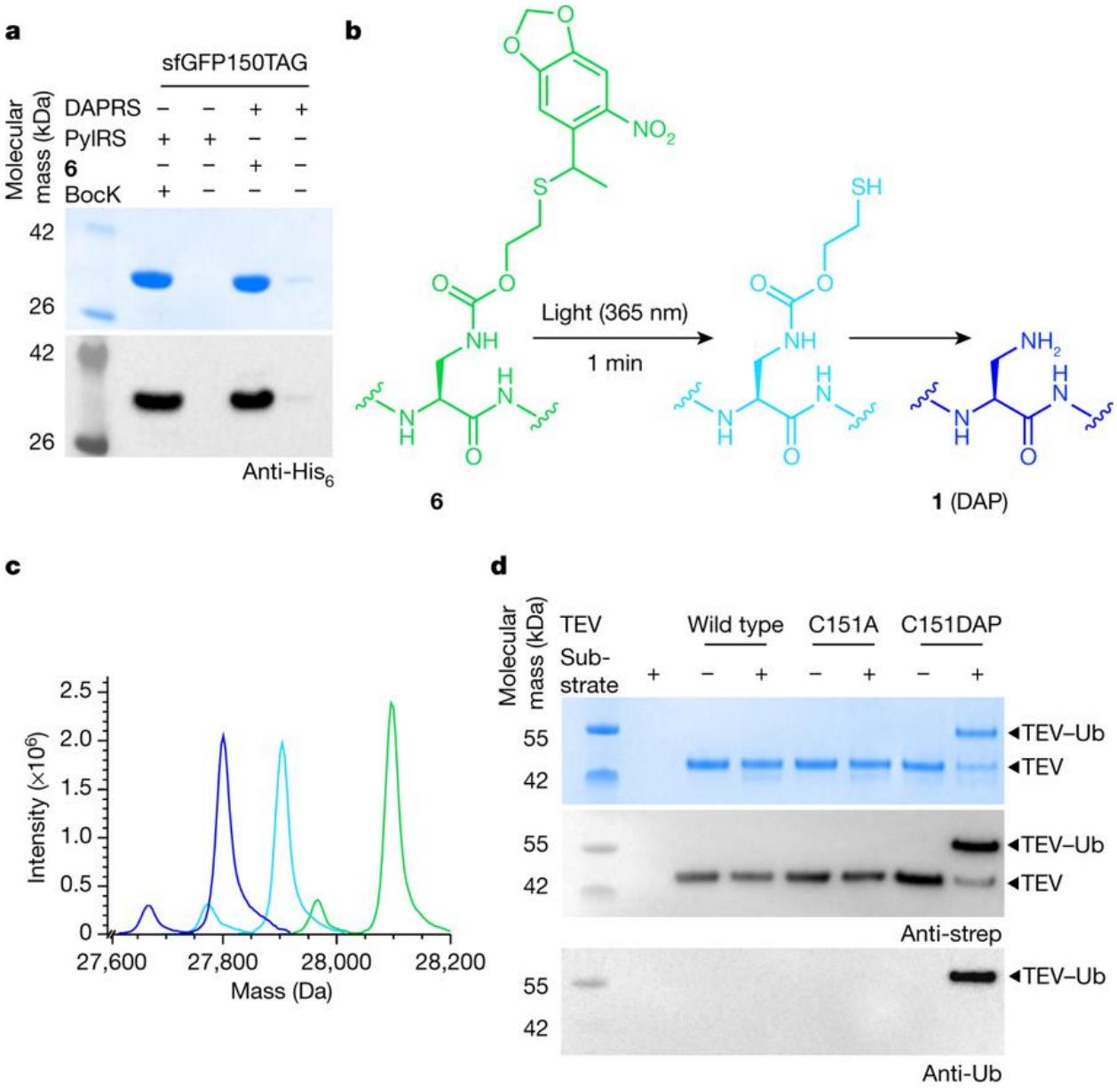

Figure 4.5) a, SDS–PAGE gels of GFP150 (**6**) and GFP150 (BocK), with protein detected by Coomassie staining (top gel) or anti-His_6antibody (bottom gel); the experiment was performed in two biological replicates with similar results. We used the indicated enzymes (DAPRS and PylRS) with their cognate $tRNA_{CUA}$ and amino acids (**6** and BocK (*N*ε-[(tert-butoxy)carbonyl]-L-lysine) together with an sfGFP150TAG reporter construct. **b**, Encoded **6** was photo-deprotected, leading to an intermediate, which spontaneously fragments to reveal DAP. **c**,

Deprotection of **6** in sfGFP followed by electrospray ionization mass spectroscopy (ESI-MS) analysis. Green trace, purified GFP150(**6**): expected molecular mass 28,096.27 Da; observed 28,097.21 Da. Light blue trace, intermediate: expected 27,902.22 Da; observed 27,904.14 Da. Dark blue trace, incubation (10 h, 37 °C) converts the intermediate to DAP (**1**): expected 27,798.23 Da; observed 27,800.88 Da. Minor peaks resulting from loss of the N-terminal methionine are also observed. The experiment was performed in two biological replicates with similar results. **d**, TEV protease variants were incubated with Ub–tev–His. TEV(C151DAP)–Ub is the amide-bond-linked complex. Anti-Ub and anti-strep western blots confirm the identity of the complex (TEV constructs contain a streptavidin tag). The experiment was performed in two biological replicates with similar results.

Cysteine proteases, including the tobacco etch virus (TEV) protease, react with substrates through a catalytic cysteine to generate an intermediate in which the protease is linked to the amino-terminal portion of its substrate through a thioester.[4] We replaced the active-site cysteine 151 of TEV protease with DAP, by genetically encoding **6** and deprotecting it, creating TEV(C151DAP). Incubating TEV(C151DAP) with Ub–tev–His_6, a model substrate in which the cleavage site recognized by TEV protease (tev) is flanked by ubiquitin (Ub) and a hexahistidine tag (His_6), led to cleavage of the His_6 tag from ubiquitin and formation of a covalently linked TEV(C151DAP)–Ub conjugate (**Fig. 4.5d** and Appendix (App.) 1, Fig. 3a–c). Control experiments demonstrated that the stable conjugate was dependent on DAP incorporation. Tandem mass spectrometry (MS/MS) demonstrated amide-bond formation between DAP and ubiquitin (App. 1, Fig. 3d). These results demonstrate that substitution of the catalytic cysteine in TEV with DAP creates a protease that performs the first step of the protease cycle, releasing the

carboxy-terminal fragment of the substrate and leaving the amino-terminal fragment covalently attached to the protease through a stable amide bond that is resistant to hydrolysis.

To gain insight into the function of the TE domain and to prepare it for use with the DAP system, we expressed and purified wild-type Vlm TE (TE_{wt}). We found that Vlm TE can use an *N*-acetylcysteine (SNAC) derivative of the native depsipeptide (tetradepsipeptidyl–SNAC, **7**; App. 1, Fig. 4) to complete all stages of its catalytic cycle and yield valinomycin (**Figs. 4.4c, 4.6a** and App. 1, Fig. 5). Thus, **7** can mimic the natural phosphopantetheine–peptidyl carrier protein (PCP)-linked substrate, consistent with previous observations of other TE domains and substrates.[17,21,25]

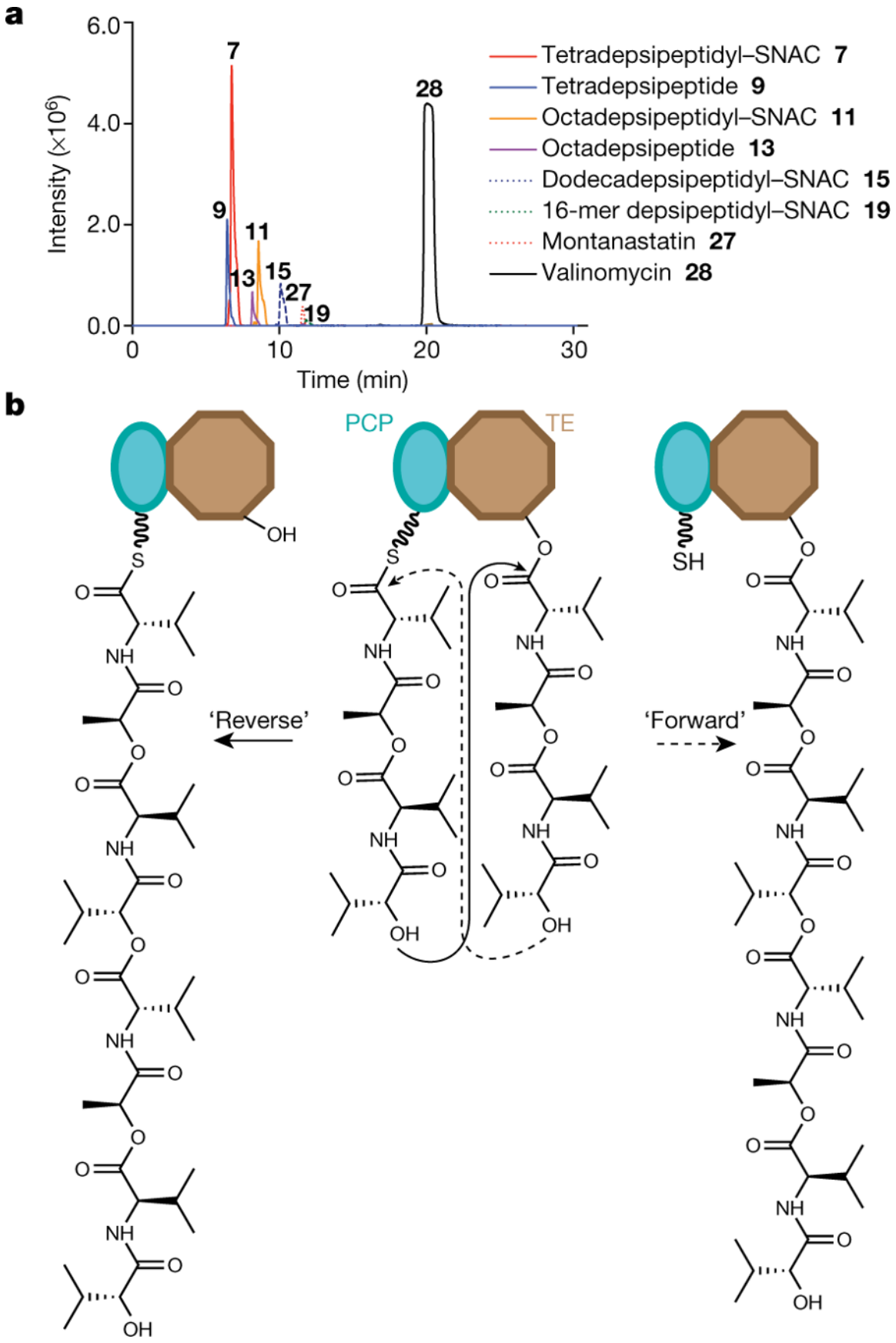
a
6.0
4.0
2.0
0.0
Intensity (×10^6)
0
10
20
30
Time (min)
7
9
11
13
15
27
19
28
Tetradepsipeptidyl–SNAC 7
Tetradepsipeptide 9
Octadepsipeptidyl–SNAC 11
Octadepsipeptide 13
Dodecadepsipeptidyl–SNAC 15
16-mer depsipeptidyl–SNAC 19
Montanastatin 27
Valinomycin 28
b
PCP
TE
'Reverse'
'Forward'
OH
SH
NH
O
S

Figure 4.6) a, Extracted ion chromatograms (EICs) from high-resolution (HR) liquid chromatography (LC)–ESI-MS of reactions of tetradepsipeptidyl–SNAC (**7**; 1.7 mM) and Vlm TE (6.5 μM); TE_{wt} produces valinomycin as its major product. The experiment was performed two independent times with similar results. **b**, Two scenarios for oligomerization.[17,26] In the 'forward transfer' scenario, the distal hydroxyl group of tetradepsipeptidyl–*O*-TE (TE) attacks (dotted line) the thioester group in tetradepsipeptidyl–*S*-PCP (PCP), directly forming octadepsipeptidyl–*O*-TE (right). In the 'reverse' scenario, the distal hydroxyl group of tetradepsipeptidyl–*S*-PCP attacks the ester group in tetradepsipeptidyl–*O*-TE, forming octadepsipeptidyl–*S*-PCP (left), which would later be transferred onto the TE domain serine. Our data are consistent with the 'reverse' oligomerization scenario; see also App. 1, Fig. 5.

There are two possible pathways for the oligomerization of NRPS intermediates by TE domains, and analysis of the synthetic intermediates detected in valinomycin synthesis revealed that Vlm TE_{wt}catalyses oligomerization via a 'reverse transfer' pathway (**Fig. 4.6b**, App. 1, Fig. 5). This pathway is analogous to that used by the more canonical gramicidin S synthetase[17,26] and we suggest that nearly all oligomerizing–cyclizing NRPSs (or PKSs[27]) will use this synthetic scheme.

We next obtained the structure of Vlm TE_{wt} (App. 1, Fig. 6 and App. 1, Table 1). It adopts the α/β-hydrolase fold typical of type I TE domains, with a canonical serine–histidine–aspartate catalytic triad[16] covered by the TE 'lid'. The lid is a mobile element with proposed roles that include substrate positioning and solvent exclusion.[21,28,29] The lid of Vlm TE is large, composed of an extended loop, three helices (Lα1–3, seen here as a bundle), a five-residue helix (Lα4), a long helix (Lα5) and another short helix (Lα6) (App. 1, Fig. 6a, b). We obtained another structure of TE_{wt} that differs only in the lid. In the first, the lid is nearly completely ordered,

although the B factors are markedly higher for the Lα1–4 region, which makes almost no contact with the rest of the domain (App. 1, Fig. 6b). In the second structure, Lα4–5 have similar positions to those in the first structure, whereas Lα3 is rotated 10° towards the active site and Lα1–2 are too disordered to model.

Incubating Vlm TE with depsipeptidyl–SNACs did not yield stable conjugates (App. 1, Fig. 6c), and attempts to soak TE_{wt} crystals with depsipeptidyl–SNACs failed to reveal interpretable ligand electron density in the active site or conformational changes. Others have reported similar setbacks when attempting to visualize acyl-enzyme complexes from SNAC molecules.[20,21] We conclude that acyl intermediates in valinomycin biosynthesis are not stable, and that it is exceptionally challenging to use wild-type Vlm TE to visualize biosynthetic intermediates.

We therefore produced Vlm TE in which the active-site serine 2463 was replaced by DAP (TE_{DAP}; App. 1, Fig. 7a–c) in order to capture stable acyl-TE conjugates (**Fig. 4.7**). To provide insight into the first acyl-thioesterase intermediate in the catalytic cycle of Vlm TE, we captured tetradepsipeptidyl–*N*-TE_{DAP}: incubation of TE_{DAP} with tetradepsipeptidyl–SNAC (**7**) led to production of a stable depsipeptidyl–TE_{DAP} intermediate in greater than 60% yield (App. 1, Fig. 7d), and we did not observe valinomycin synthesis. However, remarkably, we did observe a small amount of octadepsipeptidyl–SNAC (**11**; App. 1, Fig. 5f, h). **11** is probably formed by enzyme-catalysed attack of the tetradepsipeptidyl–SNAC's hydroxyl group on the amide bond that links the tetradepsipeptide to TE_{DAP}. The attack of a hydroxyl on an amide is analogous to the first reaction used by related serine proteases,[30] but it is surprising that this TE domain is capable of catalysing a more demanding chemical reaction (amide cleavage) than the reaction (ester hydrolysis) it evolved to perform. In an effort to enhance conjugate yield, we optimized

the conditions for conjugating deoxy-tetradepsipeptidyl–SNAC **8** with TE_{DAP}, which produced (in about 70% yield) the deoxy-depsipeptidyl–TE_{DAP} conjugate (**Fig. 4.7a**). The marginal solubility of these hydrophobic SNACs may limit the conjugation efficiency.

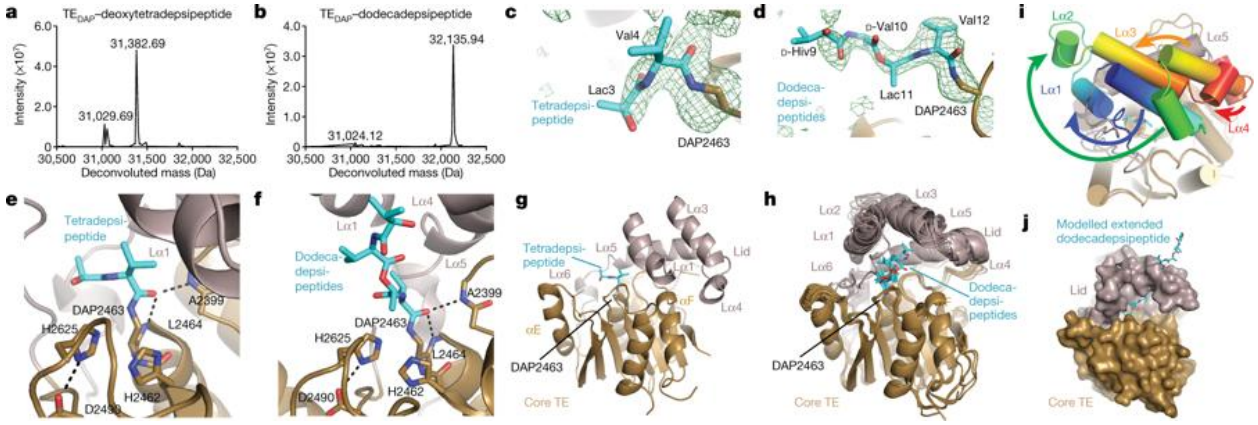

Figure 4.7) a, **b**, Deconvoluted mass spectra. **a**, TE_{DAP} incubated with deoxy-tetradepsipeptidyl–SNAC (**8**). Expected molecular masses 31,027.24 Da (unmodified) and 31,383.70 Da (modified); observed 31,029.69 Da and 31,382.69 Da. **b**, TE_{DAP} incubated with valinomycin. Expected molecular masses 31,027.24 Da (unmodified) and 32,139.11 Da (modified); observed 31,024.12 Da and 32,135.94 Da. The experiments were repeated independently five times with similar results. **c**, **d**, Unbiased electron-density ($mF_o - DF_c$) maps (green mesh, 2.5σ) for depsipeptide residues of tetradepsipeptidyl–TE_{DAP} (**c**, Protein Data Bank (PDB) accession number 6ECD) and dodecadepsipeptidyl–TE_{DAP} (**d**; 6ECE and 6ECF). An amide bond links DAP (brown) and depsipeptide residues (cyan). **e**, **f**, The active sites of tetradepsipeptidyl–TE_{DAP} (**e**) and dodecadepsipeptidyl–TE_{DAP} (**f**). The carbonyl oxygen of the amide formed by DAP and valine 4 (**e**) or valine 12 (**f**) is positioned close to the oxyanion hole formed by the main chain of A2399 and L2464. Catalytic triad residues H2625 and D2490 are shown as sticks. **g**, The lid of tetradepsipeptidyl–TE_{DAP} (6ECD) is in a similar position to that seen in TE_{wt} (6ECB; not shown). **h**, All crystallographically independent molecules of the dodecadepsipeptidyl–

TE_{DAP} (6ECE and 6ECF) are in a set of similar conformations, distinct from that seen in TE_{wt}. **i**, Substantial conformational changes occur in lid helices Lα1–Lα4 between the conformations of tetradepsipeptidyl–TE_{DAP} (**g**) and dodecadepsipeptidyl–TE_{DAP} (**h**). See also Supplementary Videos 1 and 2. **j**, In the dodecadepsipeptidyl–TE_{DAP} structure, the lid sterically prevents the dodecadepsipeptide from extending out in a linear fashion, instead favouring it curling back through this steric block and forming largely hydrophobic, non-specific interactions with the lid.

To determine the structure of the deoxy-tetradepsipeptidyl–*N*-TE_{DAP}conjugate, we incubated TE_{DAP} crystals with the deoxy-tetradepsipeptidyl–SNAC (**8**). The resulting electron density shows somewhat weak but unambiguous density for an amide bond between DAP 2463 and L-valine 4 of the deoxy-tetradepsipeptide (**Fig. 4.7c** and App. 1, Fig. 8a). The carbonyl oxygen of the L-valine 4 is close to backbone amides of residues alanine 2399 and leucine 2464—the putative oxyanion hole[25] (**Fig. 4.7e**). There is also density for the next residue, L-lactic acid 3 (L-lac3), but it is insufficient to reliably model D-valine 2 and D-α-hydroxyisovaleric acid 1 (D-hiv1) as the deoxy-tetradepsipeptide arcs out, indicating substrate flexibility. The deoxy-tetradepsipeptide does not make any interactions with the lid, which is in a conformation nearly identical to that in the first TE_{wt} (apo) structure (**Fig. 4.7g** and App. 1, Fig. 6d).

Next, we sought insight into the last acyl-TE intermediate in the catalytic cycle. Upon incubation of valinomycin and TE_{DAP}, we captured dodecadepsipeptidyl–*N*-TE_{DAP} in 65–100% yield, formed through a ring-opening reaction analogous to the reverse of the natural cyclization (**Fig. 4.7b**). This reaction is thermodynamically favoured by virtue of amide-bond formation. Dodecadepsipeptidyl–TE_{DAP} produced crystals in similar conditions to those of TE_{wt}, but with a different morphology and belonging to two different space groups (*H*3 and *P*1, with two and six molecules per asymmetric unit, respectively; App. 1, Table 1). All eight crystallographically

independent molecules of dodecadepsipeptidyl–TE_{DAP} showed some density for the dodecadepsipeptide. Molecules P1_A–F and H3_A–B show strong density for four, three, two, two, two, three and one dodecadepsipeptide residues respectively (**Fig. 4.7d** and App. 1, Fig. 8b–i). Additional weaker density is present in some molecules, which could accommodate up to the full 12 residues (App.1, Fig. 8j–l); in others, weaker density suggests multiple conformations for the distal residues, but they were not possible to definitively model. The modelled depsipeptides all follow a similar trajectory away from the active site. There is no consistent interaction between the depsipeptide beyond the L-valine residue attached to DAP and the TE domain (**Fig. 4.7f, h**). Rather, each depsipeptide makes different contacts with the lid. The lid forms a semi-sphere-like pocket/steric barrier made up of helices Lα1, 3, 4 and 5, and the strand amino-terminal to Lα1. The lid of each crystallographically independent molecule of dodecadepsipeptidyl–TE_{DAP} is in a similar but nonidentical position, and the loops between lid helices are disordered in most molecules (**Fig. 4.7h**). This again highlights the mobility of the lid and explains why the conformation and extent of order of dodecadepsipeptides differ between molecules (**Fig. 4.7h**). The semi-sphere-like barrier occurs only because of a major rearrangement of the lid in the dodecadepsipeptidyl–TE_{DAP} structures with respect to the conformation of the lid seen in both the apo and tetradepsipeptidyl-bound structures of Vlm TE.

Comparing the position of the Vlm TE lid in the apo and tetradepsipeptide-bound structures with the position of the lid in the dodecadepsipeptide-bound structures demonstrates and emphasizes its extreme mobility. To transition from one lid conformation to the other, helices Lα5–6 maintain their position, Lα3–4 rotate by about 45° and translocate roughly 13 Å, Lα2 translocates roughly 25 Å, and Lα1 shortens, translocates about 13 Å and rotates more than 90° in the opposite direction to Lα3–4 (**Fig. 4.7i** and Supplementary Videos 1, 2). This dramatic

rearrangement means that the lid helices pack together in a markedly different manner in the apo/tetradepsipeptidyl-bound structure and in dodecadepsipeptidyl-bound conformations.

The distinct lid conformations directly influence the possible location of the depsipeptide. In the apo/tetradepsipeptide-bound conformation of the lid, the carboxyl terminus of Lα1 comes within 10 Å of serine/DAP 2463, leading the tetradepsipeptide to extend towards the TE core helix αE. In the dodecadepsipeptide-bound conformations of the lid, the loop adjacent to Lα1 blocks the location occupied by the tetradepsipeptide in the tetradepsipeptide-bound structure. Moreover, in the dodecadepsipeptide-bound structure the amino terminus of Lα1 forms part of the semi-sphere-like pocket. This pocket probably helps to curl the dodecadepsipeptide back towards serine/DAP 2463, entropically controlling cyclization as part of the oligomerization/cyclization pathway (**Fig. 4.7j**, App. 1, Fig. 9).

In summary, we have genetically encoded DAP in place of catalytic cysteine and serine residues to capture unstable thioester or ester intermediates as stable amide analogues. We have exemplified the utility of this approach for a cysteine protease and a thioesterase, and provided unique insight into intermediates in the synthesis of valinomycin: a massive lid rearrangement that is associated with the dodecadepsipeptidyl-bound Vlm TE reorients the substrate from its position during oligomerization and places it into a pocket that entropically controls cyclization. Importantly, the DAP system enables the formation of near-native acyl-enzyme complexes with widely used, reaction-competent substrates (for example, native proteins containing protease sites), substrate analogues (here SNACs), and commercially available natural products (here valinomycin, and probably other cyclic products).[25] We anticipate that the approach will be broadly applicable and may be extended to capturing native substrates of transiently acylated proteins of unknown function.

The models and structure factors for the crystal structures are deposited in the Protein Data Bank with accession numbers 6ECB, 6ECC, 6ECD, 6ECE and 6ECF.

4.6 References

[1] G. L. Holliday, J. B. O. Mitchell, J. M. Thornton, *J. Mol. Biol.* **2009**, *390*, 560–577.
[2] L. Hedstrom, *Chem. Rev.* **2002**, *102*, 4501–4524.
[3] J. Z. Long, B. F. Cravatt, *Chem. Rev.* **2011**, *111*, 6022–6063.
[4] H.-H. Otto, T. Schirmeister, *Chem. Rev.* **1997**, *97*, 133–172.
[5] K. N. Swatek, D. Komander, *Cell Research* **2016**, *26*, 399–422.
[6] W. Yang, D. G. Drueckhammer, *J. Am. Chem. Soc.* **2001**, *123*, 11004–11009.
[7] B. Liu, C. J. Schofield, R. C. Wilmouth, *J. Biol. Chem.* **2006**, *281*, 24024–24035.
[8] J. B. Scaglione, D. L. Akey, R. Sullivan, J. D. Kittendorf, C. M. Rath, E.-S. Kim, J. L. Smith, D. H. Sherman, *Angew. Chem. Int. Edit.* **2010**, *49*, 5726–5730.
[9] L. Cappadocia, C. D. Lima, *Chem. Rev.* **2018**, *118*, 889–918.
[10] A. Plechanovová, E. G. Jaffray, M. H. Tatham, J. H. Naismith, R. T. Hay, *Nature* **2012**, *489*, 115–120.
[11] J. W. Chin, *Annu. Rev. Biochem.* **2014**, *83*, 379–408.
[12] N. A. Magarvey, M. Ehling-Schulz, C. T. Walsh, *J. Am. Chem. Soc.* **2006**, *128*, 10698–10699.
[13] Y. Lan, B. Langlet-Bertin, V. Abbate, L. S. Vermeer, X. Kong, K. E. Sullivan, C. Leborgne, D. Scherman, R. C. Hider, A. F. Drake, et al., *ChemBioChem* **2010**, *11*, 1266–1272.
[14] A. Radzicka, R. Wolfenden, *J. Am. Chem. Soc.* **1996**, *118*, 6105–6109.
[15] J. M. Reimer, A. S. Haque, M. J. Tarry, T. M. Schmeing, *Curr. Opin. Struc. Biol.* **2018**, *49*, 104–113.
[16] M. E. Horsman, T. P. A. Hari, C. N. Boddy, *Nat. Prod. Rep.* **2016**, *33*, 183–202.
[17] K. M. Hoyer, C. Mahlert, M. A. Marahiel, *Chem. Biol.* **2007**, *14*, 13–22.
[18] J. Jaitzig, J. Li, R. D. Süssmuth, P. Neubauer, *ACS Synth. Biol.* **2014**, *3*, 432–438.
[19] D. L. Akey, J. D. Kittendorf, J. W. Giraldes, R. A. Fecik, D. H. Sherman, J. L. Smith, *Nat. Chem. Biol.* **2006**, *2*, 537–542.
[20] S. D. Bruner, T. Weber, R. M. Kohli, D. Schwarzer, M. A. Marahiel, C. T. Walsh, M. T. Stubbs, *Structure* **2002**, *10*, 301–310.
[21] S. A. Samel, B. Wagner, M. A. Marahiel, L.-O. Essen, *J. Mol. Biol.* **2006**, *359*, 876–889.
[22] J. Li, J. Yu, J. Zhao, J. Wang, S. Zheng, S. Lin, L. Chen, M. Yang, S. Jia, X. Zhang, et al., *Nat. Chem.* **2014**, *6*, 352–361.
[23] A. S. Baker, A. Deiters, *ACS Chem. Biol.* **2014**, *9*, 1398–1407.
[24] S. Virdee, Y. Ye, D. P. Nguyen, D. Komander, J. W. Chin, *Nat. Chem. Biol.* **2010**, *6*, 750–757.
[25] C. C. Tseng, S. D. Bruner, R. M. Kohli, M. A. Marahiel, C. T. Walsh, S. A. Sieber, *Biochemistry* **2002**, *41*, 13350–13359.
[26] J. W. Trauger, R. M. Kohli, H. D. Mootz, M. A. Marahiel, C. T. Walsh, *Nature* **2000**, *407*, 215–218.

[27] Y. Zhou, P. Prediger, L. C. Dias, A. C. Murphy, P. F. Leadlay, *Angew. Chem. Int. Edit.* **2015**, *54*, 5232–5235.
[28] D. P. Frueh, H. Arthanari, A. Koglin, D. A. Vosburg, A. E. Bennett, C. T. Walsh, G. Wagner, *Nature* **2008**, *454*, 903–906.
[29] J. R. Whicher, G. Florova, P. K. Sydor, R. Singh, M. Alhamadsheh, G. L. Challis, K. A. Reynolds, J. L. Smith, *J. Biol. Chem.* **2011**, *286*, 22558–22569.
[30] Ö. D. Ekici, M. Paetzel, R. E. Dalbey, *Protein Sci.* **2008**, *17*, 2023–2037.

4.7 Supplementary Material

Supplementary Discussion 1: The direction of the oligomerization pathway catalyzed by Vlm TE_{wt}

There are two possible pathways for oligomerization of NRPS intermediates by TE domains such as Vlm TE, as illustrated in **Figure 4.6b** and **App. 1, Fig. 5a-d**. Vlm TE_{wt} could oligomerize tetradepsipetidyl *D*-hiv–*D*-val-*L*-lac–*L*-val moieties by ester bond formation between the distal hydroxyl of *D*-hiv in tetradepsipeptidyl-O-TE and the carbonyl of *L*-val from tetradepsipeptidyl-S-PCP ("forward transfer"; **App. 1, Fig. 5a,c**), or else by ester bond formation between the distal hydroxyl of *D*-hiv in tetradepsipeptidyl-S-PCP and the carbonyl of *L*-val from tetradepsipeptidyl-O-TE ("reverse transfer" (**App. 1, Fig. 5b,d)**. The reverse transfer pathway is so called because the intermediate is passed from a more C-terminal domain of the NRPS (TE domain) to a more N-terminal domain (PCP domain), whereas typically in NRPS synthesis intermediates are progressively elongated and transferred from more N- to more C- terminal domains (**Figure 4.4c, App. 1, Fig. 1)**. In addition, the octadepsipeptide would later be transferred again to the TE domain, as seen in the far right of panels and **App. 1, Fig. 5a-d**.

The synthetic intermediates detected in the Vlm TE_{wt}-mediated synthesis of valinomycin differentiate between two possible oligomerization pathways[17,26]. LC-MS analysis of Vlm TE_{wt} reactions with tetradepsipeptidyl-SNAC **7** showed formation of valinomycin, as well as the octadepsipeptidyl-SNAC **11** and dodecadepsipeptidyl-SNAC **15**, (**Figure 4.6a, App. 1, Fig. 5g**). Intermediates **11** and

15 are only produced in the reverse transfer oligomerization pathway (**App. 1, Fig. 5b,d**) and not the forward transfer pathway, indicating Vlm TE catalyzes the reverse transfer pathway. Consistent with the reverse pathway, experiments using a mixture of tetradepsipeptidyl-SNAC **7** and tetradepsipeptidyl-SNAC missing the terminal hydroxyl (deoxy-tetradepsipeptidyl-SNAC **8**), showed peaks for deoxy-octadepsipeptidyl-SNAC **12** and deoxy-dodecadepsipeptidyl-SNAC **16** (**App. 1, Fig.5j**). In addition, the valinomycin synthesis assay also shows small peaks corresponding to the 16-mer depsipeptidyl-SNAC **19**, the 20-mer depsipeptidyl-SNAC **23** and the cyclic 16-mer depsipeptide **29,** (**Figure 4.6a, App. 1, Fig. 5i**) indicating that a small percentage of the time, the oligomerization (again, by the reverse pathway) by Vlm TE domain proceeds past the dodecadepsipeptidyl intermediate, and that Vlm TE has somewhat more flexibility in final product than previously thought.

Our biochemical experiments with TE_{DAP} also supports the conclusion that synthesis occurs via the reverse transfer pathway. As discussed in the main text, incubation of tetradepsipeptidyl-SNAC with TE_{DAP} produces tetradepsipeptidyl-*N*-TE_{DAP}, where the tetradepsipeptidyl is attached to TE by a stable amine bond (**Figure 4.7**), but all other atoms are the same as in the native transient tetradepsipeptidyl-*O*-TE_{wt} intermediate. If the synthesis occurs by the forward transfer pathway, the distal hydroxyl of *D*-hiv in tetradepsipeptidyl-*N*-TE_{DAP} should attack the carbonyl of *L*-val from the next tetradepsipeptidyl-SNAC molecule, making octadepsipeptidyl-*N*-TE_{DAP} (like **App. 1, Fig. 5a,c**). This should then undergo the next oligomerization step analogously, producing dodecadepsipeptidyl-*N*-TE_{DAP}. This dodecadepsipeptidyl-*N*-TE_{DAP} intermediate should accumulate because the amide link will stall cyclization.

Thus, in the forward transfer case, incubation of tetradepsipeptidyl-SNAC with TE_{DAP} should result in dodecadepsipeptidyl-*N*-TE_{DAP} (with smaller amounts of tetradepsipeptidyl-*N*-TE_{DAP} and octadepsipeptidyl-*N*-TE_{DAP}). In contrast, if the synthesis occurs by the reverse transfer pathway, the distal hydroxyl of *D*-hiv in tetradepsipeptidyl-SNAC will attempt to attack the carbonyl of *L*-val in the amide group of tetradepsipeptidyl-*N*-TE, but will be stalled by the enhanced stability of the amide bond. Thus, in the reverse transfer case, incubation of tetradepsipeptidyl-SNAC with TE_{DAP} should result in tetradepsipeptidyl-*N*-TE_{DAP}, and negligible amounts of other acyl-TE species. Our data shows formation of tetradepsipeptidyl-*N*-TE_{DAP}, with no octadepsipeptidyl-*N*-TE_{DAP} or dodecadepsipeptidyl-*N*-TE_{DAP} detected, fully consistent with the reverse transfer pathway.

That this oligomerizing-cyclizing depsipeptide synthetases uses an analogous reverse pathway to the more canonical gramicidin S synthetase [17,26] and the dimerizing-cyclizing elaiophylin synthase [27] suggests that all oligomerizing-cyclizing NRPSs and PKSs will use this synthetic scheme.

Supplementary Discussion 2: Putative model of oligomerization and cyclization catalyzed by Vlm TE

Several NRPS pathways feature TE domains that oligomerize and cyclize linear peptidyl or depsipeptidyl substrates. They are involved in biosynthesis of the antibiotic gramicidin S [17], the emetic toxin cereulide [12,31], the siderophores enterobactin and bacillibactin [32,33], the anticancer conglobatin [34], the DNA bis-intercalator thiocoraline [35] and valinomycin, a potassium ionophore depsipeptide with antimicrobial, antitumoral and cytotoxic properties[12,18]. These TE domains perform a challenging synthetic task: They oligomerize their (depsi)peptidyl intermediates up to, but not beyond, the number of copies found in the biologically active compound, and then change their reactivity mode to catalyse cyclization and release of the completed product.

The structures of TE_{wt}, tetradepsipeptidyl-TE_{DAP} and dodecadepsipeptidyl-TE_{DAP} can provide insight into the oligomerization steps, change in reactivity, and cyclization step. While the rest of the TE domain does not alter its conformation substantially between any of our structures, there is a major difference in lid conformations of the early (apo TE_{wt}, tetradepsipeptidyl-TE_{DAP}) and late (dodecadepsipeptidyl-TE_{DAP}) stage structures (**Figure 4.7h-i**). We do not believe the crystal packing environment unduly influences the conformation of the lid because all the structures are derived from crystallization in very similar conditions, and because the dodecadepsipeptidyl-TE_{DAP} conformation is seen in several different crystal packing environments. However, it is likely that the presence of a particular length of depsipeptidyl- moiety does not "lock" the lid into one particular conformation.

Rather, the lid will remain dynamic throughout the catalytic cycle, with the presence of the various substrates influencing which conformations predominate. Indeed, the dodecadepsipeptidyl-TE_{DAP} structures are actually a clustered of similar conformations, rather than one single conformation (**Fig. 4.7h**). When for simplicity and clarity only one dodecadepsipeptidyl-TE_{DAP} (or tetradepsipeptidyl-TE_{DAP}) structure is shown (**Fig. 4.7c-g,j,i, App. 1, Fig. 9,** Supplementary Video 1, 2) it is meant to be representative of the family of similar conformations, rather than "the dodecadepsipeptidyl-TE_{DAP} conformation".

As described in the main text, to transition from the early type of lid conformation (apo TE_{wt}, tetradepsipeptidyl-TE_{DAP}) to the late (dodecadepsipeptidyl-TE_{DAP}), the lid undergoes a dramatic, non-rigid body movement where some helices rotate >90° and others translocate by ~25Å (**Fig. 4.7j,** Supplementary Video 1, 2). The mobility of the lid has been observed in other studies (often because of disorder and lack of electron density), but the conformational changes observed with TE_{DAP} are substantially more dramatic and more informative. Lid conformations vary between apo TE structures from open conformations, suggesting ease of access of the incoming substrate to the active site pocket, to closed conformation, presumably restricting access to the active sites, and lastly to a channel, restricting but not eliminating access to the active site. Examination of the few TEs with apo and holo structures show little change in lid conformation upon formation of the acyl-enzyme intermediate. For example the structure of pikromycin TE with a non-hydrolyzable phosphonate based analog of the polyketide acyl chain shows the lid in a channel conformation very similar to the channel seen in the apo TE structure. Similarly, the deoxyerythronolide B TE domain shows subtle movement of the lid upon formation

of a phosphonate ester. This underscores the significant changes seen in the lid conformation of the Vlm TE upon formation of the dodecodepsipeptidyl-intermediate.

In dodecadepsipeptidyl-TE_{DAP}, the lid helices form a concave pocket, which seems likely to be important during the cyclization step in the thioesterase cycle. This pocket is mainly made up of hydrophobic residues, and it provides a steric barrier that prevents a dodecadepsipeptide attached to Ser/DAP2463 from extending out in a linear fashion (**Figure 4.7j)**. Rather, this lid conformation favours curling back of the substrate's free end towards the acyl linkage between TE and the substrate**.** Thus, cyclization of the dodecadepsipeptide to valinomycin may be thought of as entropically controlled by the pocket, with the dodecapeptide conformations dictated by partial confinement in the pocket and TE domain active site.

The PCP domain, a key player in the TE domain catalytic cycle, is absent from the structures we have determined. Its binding site can be inferred from the informative dead-end inhibitor trapped PCP-TE structure of EntF [36] (**App. 1, Fig. 9a**). The PCP domain docks at αE of the TE, and the PPE extends the ~15 Å to position the thiol near Ser/DAP2463 (**App. 1, Fig. 9a,b-iii**). The position of the PPE in the EntF structure is compatible with the dodecapeptide-bound conformation of the lid, but not with the apo/tetrapeptide-bound conformation in our Vlm TE structures. (The lid in the EntF structure is partially disordered.) This EntF structure showed how the PCP and TE domains can position the thioester of the depsipeptidyl-PPE near Ser/DAP2463, but in Vlm, these domains must also be able to position the terminal hydroxyl of tetradepsipeptidyl-PPE near Ser/DAP2463 for the oligomerization step. To do so, another ~15 Å of length of tetradepsipeptide (between terminal hydroxyl

and PPE sulphur) must be accommodated in the TE domain (compare **App. 1, Fig. 9b**). The lid likely facilities this, perhaps using a pocket similar to the one we observe in the dodecapeptidyl-TE_{DAP} structures.

One can thus assemble the known structures into a hypothetical pathway for oligomerization and cyclization (**App. 1, Fig. 9b**). When in the observed apo/tetradepsipeptide-bound conformation, Lα1 of Vlm TE may inhibit any attached depsipeptide from curling around for cyclization (**App. 1, Fig. 9b-i**). PCP binding could induce a TE conformation similar to those we observe for the dodecadepsipeptide-bound TE, which could accommodate the ~30 Å tetradepsipeptidyl-PPE bound to the PCP domain and guide it towards the active site (**App. 1, Fig. 9b-ii**). A transition to an open / largely disordered lid (as seen in EntF PCP-TE) could allow the PCP to present the thioester for transfer back to the Ser2463 (**App. 1, Fig. 9b-iii**). Finally, the lid conformation observed in the dodecadepsipeptide-TE_{DAP} structures, with its semi-sphere-like pocket, could help curl the dodecadepsipeptide back towards Ser2463 for cyclization. (**E App. 1, Fig. 9b-iv**).

The observation that there are multiple similar conformations of Vlm TE even when it is covalently bound with bona fide substrates, and the paucity of specific interactions between the lid and the rest of the TE domain make it unlikely that there is a single, fully defined conformation at any of these steps of the synthetic cycle. Formation of a pre-defined / templated conformation of the cyclization substrate has been proposed to facilitate cyclization in tyrocidine synthetase [26,37], while specific interaction between the lid and the polyketide substrate was proposed to do this in

pikromycin synthase, but there is no evidence for these mechanisms in Vlm TE. Indeed, specific and strong binding interactions could slow the synthetic cycle, as the tetradepsipeptide must transition back and forth between being ligated to the PCP domain and to the TE domain, and the same tetradepsipeptide must assume multiple different positions in the course of a cycle. Rather, the lid conformation likely fluctuates rapidly through the cycle, "breathing" and transiently visiting reaction-competent conformations. Interestingly, a novel inhibitor to a *Mycobacterium tuberculosis* polyketide synthase TE domain binds between the cluster of lid helices [38]. It is proposed to compete with substrate binding, but such an inhibitor could also act by preventing structural rearrangements in the lid similar to those we observe here.

Supplementary Methods

Supplementary Table 1: List of primers used in this study. Mutated residues are depicted in uppercase.

Primer name	Primers sequence
MbY271f	ggaaaggtctcgaccctgNNKaactatctgcgtaaactggatcgtattc
MbY271r	ggaaaggtctcagggtcggggccagcatcggacgcag
MbN311f	ggaaaggtctccatggttNNKttttgccaaatgggcagcggctgcacc
MbN311r	ggaaaggtctcaccatggtgaattcttccaggtgttctttgc
MbY349f	ggaaaggtctccatggtgNNKggcgataccctggatattatgcatgg
MbY349r	ggaaaggtctcaccatgcagctatcgcccacaatttcgaagtc
MbV366f	ggaaaggtctccagcgcgNNKgtgggtccggttagcctggatcgtg
MbV366r	ggaaaggtctcgcgctgctcagttccagatcgccatgc
MbW382f	ggaaaggtctctaaaccgNNKattggcgcgggttttggcctggaacg
MbW382r	ggaaaggtctcggtttatcaatgccccattcacgatcc
TEV_Amb_fw	ggaaaggtctcgTAGggcagtccattagtatcaactagagatgg
TEV_Amb_rev	ggaaaggtctcccCTActgcccatccttggtttgaatccaatgc
TEV_Ala_fw	ggaaaggtctcgGCTggcagtccattagtatcaactagagatgg
TEV_Ala_rev	ggaaaggtctcccAGCctgcccatccttggtttgaatccaatgc
TE_for_pNHD_fw	ttattacatatgcatcatcatcaccaccatc
TE_for_pNHD_rev	ataataactcgagttagccacgcg
Vlm2_TE_Amb_Fw	gtgtatatcggtggtcacTAGctgggtggccatat
Vlm2_TE_Amb_Rev	atatggccacccagCTAgtgaccaccgatatacac

Creation of DAPRSlib library by inverse PCR

Using the plasmid pBK-*pylS* as a template[39], the library (DAPRSlib) for amino acid **6** was generated by five consecutive rounds of inverse PCR reactions using the PrimeSTAR HS DNA Polymerase (Takara Bio) following manufacturer's guidelines. Primers randomised the codons for positions Y271, N311, Y349, V366 and W382 of the *pylS* gene to the codons for all 20 natural amino acids (All primer are listed in **Supplementary Table 1**). The resulting PCR products were digested with BsaI-HF and DpnI, and circularised with T4 DNA ligase. DNA was transformed into Eletrocompetent MegaX DH10B™ T1R Electrocomp™ *E.coli* cells (Invitrogen) following the manufacturer's instructions and inoculated into overnight culture with appropriate antibiotic to prepare plasmid DNA. Diversity was estimated by plating serial dilutions of the transformation rescue culture on LB-agar plates with appropriate antibiotic. A library of 10^8 transformants that was isolated covered the theoretical diversity of the library with 97% confidence.

Selections of active aaRS with DAP derivatives

Selections of synthetase mutants specific for amino acids **2**-**6** were carried out as previously reported[39] using the following libraries: DAPRSlib (Y271, N311, Y349, V366, W382), D3 (L270, Y271, L274, N311, C313), PylS fwd (A267, Y271, L274, C313, M315), Susan 1(A267, Y271, Y349, V366, W382), Susan 2 (N311, C313, V366, W382, G386), Susan 4 (A267, Y349, S364, V366, G386). Briefly, *Mb*PylRS libraries in pBK vectors were subjected to five rounds of alternating positive and negative selection. The positive selections were performed in the presence of the desired ncAA (1 mM) using a chloramphenicol acetyl transferase reporter with an amber codon at a permissive position (codon 112) and expressing the cognate tRNA.

Cells that survived the positive selection on chloramphenicol (typically 50 μg/mL) LB agar are predicted to use either a natural amino acid that is constitutively present in the cell or the ncAA added to the cell. The negative selection used a barnase reporter containing amber codons and providing the cognate tRNA, in the absence of ncAA, to remove synthetase variants that use natural amino acids.

***GFP(150TAG)His6* expression and purification**

Superfolder green fluorescent protein (sfGFP) with **6** incorporated at position 150 was expressed from pSF-sfGFP150TAG in MegaX DH10B T1R cells containing pBK_DAP5RS or pBK_PylRS vector. LB broth supplemented with 12.5 μg/mL tetracycline, 25 μg/mL kanamycin and 1 mM of **6** or N^{ϵ}-*tert*-butyloxycarbonyl-lysine (BocK) was inoculated with the transformed cells. Expression was induced with 0.2% (w/v) L-(+)-arabinose (Sigma) for 16 h at 37˚C whilst shaking at 220 rpm. Bacteria were then harvested and the protein purified by polyhistidine affinity chromatography.

His6-lipoyl-TEV-Strep expression and purification

BL21 (DE3) cells were transformed with pNHD-His6-lipoyl-TEV$_{wt}$-Strep, pNHD-His6-lipoyl-TEV$_{Ala}$-Strep (gene is a gift from Mark Allen) [40] or co-transformed with pSF-DAP5RS-PylT[41] pNHD-His6-lipoyl-TEV$_{Amber}$-Strep and grown on TB-agar plates containing 25 μg/mL tetracycline and (and 50 μg/mL kanamycin for co-transformed cells) overnight at 37˚C (TB media containing 25 μg/mL tetracycline (and 50 μg/mL kanamycin for co-transformed cells) was inoculated with some transformed colonies. The cultures were diluted 1:100 into TB media containing 12.5 μg/mL tetracycline (and 25 μg/mL kanamycin and 100 μM of **6** for co-transformed

cells) and incubated at 37˚C; once the OD_{600} reached 0.5-0.7, the cultures were moved to 20˚C. After 30 min of further incubation, the cultures were induced using 250 μM isopropyl β-D-1-thiogalactopyranoside (IPTG) and protein expression was carried out at 20˚C for 16 h. Cells were harvested by centrifugation and resuspended in 50 mM tris-HCl pH 7.5, 150 mM NaCl, 2 mM β-Mercaptoethanol, 1 Roche Inhibitor Cocktail tablet / 50 mL, 0.5 mg/mL lysozyme (Sigma), 50 μg/mL DNase (Sigma) and lysed by sonication. The lysate was clarified by centrifugation at 39'000 × *g* for 30 min and filtered through a 0.4 μm polyethersulfone (PES) membrane. His6-lipoyl-TEV-Strep was purified using nickel affinity chromatography (HisTrap HP column, GE Healthcare) with a linear gradient of imidazole (0 mM to 500 mM). Fractions containing the protein were further purified by Strep-tag affinity purification using a 5 mL StrepTrap HP column (GE Healthcare). After sample loading, the column was washed with strep binding buffer (50 mM 4-(2-hydroxyethyl)-1-piperazineethanesulfonic acid [HEPES] pH 8.0, 150 mM NaCl, 1 mM ethylenediaminetetraacetic acid [EDTA], 5 mM dithiothreitol [DTT]). The protein was eluted using a linear gradient of desthiobiotin (0 mM to 1.25 mM). For His6-lipoyl-TEV_{Amber}-Strep, the protein was irradiated with UV light (365 nm, 35 $mWcm^{-2}$, 1 min) at the end of the purification.

Ub_{tev} expression and purification

BL21 (DE3) cells were transformed with pNHD-Ub-tev-His6 and grown on LB-agar plates containing 25 μg/mL tetracycline overnight at 37˚C. LB media containing 25 μg/mL tetracycline was inoculated with the some colonies resulting from the transformation. The culture was diluted 1:100 into fresh LB media containing 12.5 μg/mL tetracycline; once the OD_{600} reached 0.5, the cultures were induced using 1

mM IPTG and protein expression was carried out at 37˚C for 6 h. Cells were harvested by centrifugation and resuspended 50 mM tris-HCl pH 7.5, 150 mM NaCl, 2 mM β-Mercaptoethanol, 1 Roche Inhibitor Cocktail tablet / 50 mL, 0.5 mg/mL lysozyme (Sigma), 50 µg/mL DNase (Sigma) and lysed by sonication. The lysate was clarified by centrifugation at 39'000 × *g* for 30 min and filtration through a 0.4 µm PES membrane. Ub was purified using nickel affinity chromatography (HisTrap HP column, GE Healthcare) with a linear gradient of imidazole (30 mM to 500 mM). The protein was dialysed overnight against 10 mM tris-HCl at 4˚C and Ub was further purified by ion exchange chromatography (HiTrapS 5mL column, GE Healthcare) using a NaCl gradient (0-1 M mM) in 50 mM ammonium acetate, pH 4.5. Pure fractions were pooled before overnight dialysis against 20 mM tris-HCl pH 7.4. The sample was then concentrated to ~15 mg/mL using an Amicon Ultra-15 (3 kDa MWCO) centrifugal filter device (Millipore).

Reactions of TEV with Ub_{tev}

15 µg of His6-lipoyl-TEV-Strep were incubated at 30˚C with 60 µg of Ub_{tev} and allowed to react overnight in 150 µL of 50 mM HEPES pH 8.0, 150 mM NaCl, 1 mM EDTA, 5 mM DTT. 20 µL of the reaction were loaded on a 4-12% NuPAGE Bis-Tris gel (Invitrogen) and allowed to run for 45 min in 2-(n-morpholino)-ethanesulfonic acid (MES) buffer. Protein was transferred on a polyvinylidene fluoride (PVSF) membrane (Roche) using 25 mM Tris pH 8.2, 192 mM glycine, 10% (v/v) methanol. Membranes were subsequently blocked for 1h in TBST buffer (25 mM Tris pH pH 7.4, 150 mM NaCl, 0.05% [v/v] Tween 20) containing 5% (w/v) milk powder at room temperature. Antibodies (Strep-Tactin-HRP conjugate (α Strep) [IBA Lifesciences] or P4D1 antibody (α Ub) [Enzo Life Sciences]) were added in 5% TBST-Milk and

incubated at 4˚C overnight. Secondary antibody (for α Ub antibody) was added in 5% TBST-Milk and incubated at room temperature for 1 h. Blots were developed using Amersham enhanced chemiluminescence (ECL) (GE Healthcare) and a ChemiDoc XRS+ gel imaging system (Bio-Rad).

Analysis of intracellular concentration of DAP derivatives

The analysis of intracellular concentration of DAP derivatives was performed as previously described[41]. In short, DAP derivatives were added to a 5 mL solution of LB media to a final concentration of 1 mM. A control sample was also prepared with 5 mL of unsupplemented LB media. Each solution was inoculated with DH10B cells. The cultures were agitated at 220 rpm in the dark at 37˚C for 12 h. The OD_{600} of each sample was determined, and the cells from each culture were harvested. The cell pellets were washed three times with 1 mL of fresh ice-cold LB media by cycles of resuspension and centrifugation. The washed cell pellets were resuspended in a methanol:water solution (60:40). Zirconium beads (0.1 mm) were added to each suspension. The suspensions were vortexed for 12 min to lyse the cells. The lysate was centrifuged at 21000 x *g* for 30 min at 4˚C. The supernatant was carefully removed, and placed into a fresh 1.5 mL Eppendorf tube. The solutions were centrifuged again at 21000 x *g* for 2 h at 4˚C. A 100 µl aliquot of the supernatant from the resulting sample was analyzed by LC-ESI-MS. A gradient of 0.5% to 95% acetonitrile in water was applied to elute the clarified lysates from a Zorbax C18 (4.6 x 150 mm) column. The concentrations were estimated using an estimate of 8×10^8 cells per 1 OD_{600} unit and a cell volume of 0.6×10^{-15} L.

Synthesis of amino acids

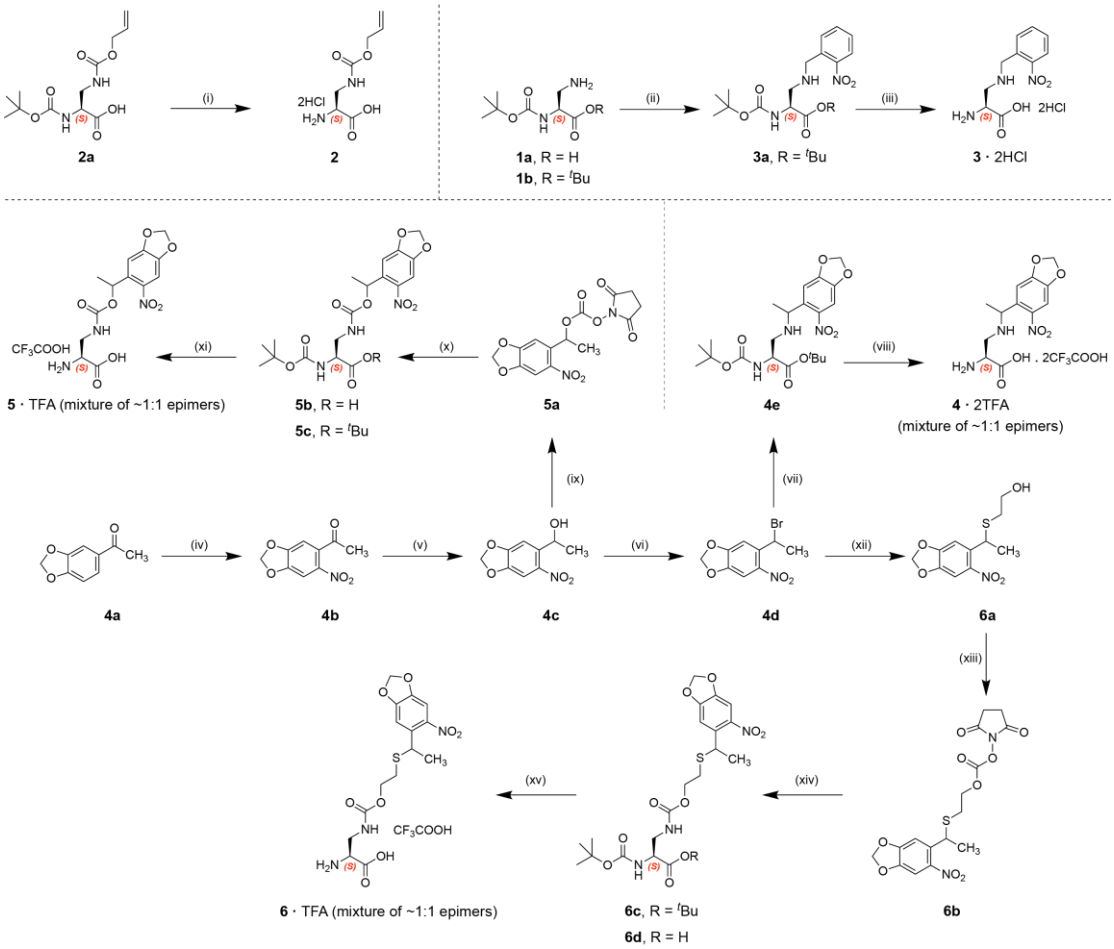

Supplementary Scheme 1: Synthesis scheme of amino acids presented in this study.

Reagents and Conditions: (i) **2a** (10.0 mmol), HCl (4M in 1,4-dioxane) (8.0 eq.), Et_3SiH (2 eq.), r.t., 1 h, 90% (**2**); (ii) **1b** (19.2 mmol), 2-nitrobenzyl bromide (1.2 eq.), DIPEA (2.0 eq.), dry THF, r.t., 10 h, 67% (**3a**); (iii) **3a** (11.6 mmol), HCl (4M in 1,4-dioxane) (8.62 eq.), Et_3SiH (2.7 eq.), r.t., 24 h, 99% (**3** • 2HCl); (iv) **4a** (20.0 mmol) in glacial CH_3COOH (1.563 M), dropwise addition to conc. HNO_3 (70%), 0 °C, 1 h of dropwise addition, then 40 °C, 2.5 h, 58% (**4b**); (v) **4b** (209.0 mmol), $NaBH_4$ (0.9 eq.), portion-wise addition (8 × 15 min), r.t., CH_3OH-C_2H_5OH-CH_2Cl_2 (44:29:27), then 4 h (total time = 6 h), r.t., 99% (**4c**); (vi) **4c** (75.0 mmol), PBr_3 (0.4 eq., dropwise addition), dry CH_2Cl_2, 0 °C, then dry pyridine (cat.), 0 °C, 15 min, then r.t., 1.5 h, 89% (**4d**); (vii) Boc-L-Dap-O^{t}Bu **1b** (15.0 mmol), 13 (1.2 eq.), DIPEA (3.0 eq.), dry THF, r.t., 64 h, 82% (**4e**); (viii) **4e** (9.49 mmol), TFA (20.64 eq.), Et_3SiH (6.60 eq.), dry CH_2Cl_2, 73% (**4** • $2CF_3COOH$); (ix) **4c** (100.0 mmol), Su_2O (1.5 eq.), DIPEA (3.0 eq.), dry CH_3CN, r.t., 16 h, 92% (**5a**); (x) *Method 1*: Boc-L-Dap-O^{t}Bu **1b** (14.05 mmol), **5a** (1.2 eq.), DIPEA (3.0 eq.), dry CH_2Cl_2 / dry THF (2:1), r.t. 20 h, 94% (**5c**); *Method 2*: **5a** (12.5 mmol), Boc-L-Dap-OH **1a** (1.25 eq.), DIPEA (3.0 eq.), dry THF / dry CH_3CN (9:1), r.t., 24 h, 99% (**5b**); (xi) **5b** (9.2 mmol), TFA (21.3 eq.), dry

CH_2Cl_2, r.t., 99% (**5**•CF_3COOH); (xii) **4d** (21.0 mmol), 2-mercaptoethanol (1.05 eq.), 1,4-dioxane (degassed), aq. NaOH (0.5 M in degassed H_2O, 1.0 eq.), r.t., 12 h, dark, argon atm., 95% (**6a**); (xiii) **6a** (61.0 mmol), Su_2O (1.4 eq.), dry DIPEA (4.0 eq.), dry CH_3CN, r.t., dark, argon atm., 14 h, quant. conv. (**6b**); (xiv) *Method 1*: **6b** (18.0 mmol), Boc-L-Dap-O^{t}Bu.HCl **1b** (1.6 eq.), dry DIPEA (3.0 eq.), dry CH_3CN, r.t., 10 h, dark, argon atm., 94% (**6c**); *Method 2*: **6b** (60.0 mmol), Boc-L-Dap-OH.HCl **1a** (1.1 eq.), dry DIPEA (4.0 eq.), dry CH_3CN, r.t., 14 h, dark, argon atm., 96% (**6d**); (xv) *Method 1*: **6c** (12.066 mmol), TFA (21.647 eq.), dry Et_3SiH (10.378 eq.), dry CH_2Cl_2, r.t., dark, 24 h, monitored by LC-MS instrument (reverse phase, H_2O-CH_3CN as mobile phase), product purified by trituration (CH_3OH/Et_2O), 64% (**6**•TFA); *Method 2*: **6d** (57.626 mmol), TFA (9.065 eq.), dry Et_3SiH (2.173 eq.), dry CH_2Cl_2, r.t., dark, 5 h, monitored by LC-MS instrument (reverse phase, H_2O-CH_3CN as mobile phase), if reaction was incomplete it was left stirring longer with additional TFA (up to 2 eq.), product purified by trituration (dry CH_3OH/Et_2O), 63% (**6**•TFA);

Abbreviations: M = Molarity; conc. = concentrated; mol = moles; mmol = millimoles; ^oC = degree Celsius; eq. = equivalents; h = hour; min = minutes; r.t. = room temperature; cat. = catalytic, aq. = aqueous; Su = succinimidyl; DIPEA = diisopropylethylamine; atm = atmosphere, Boc = *tert*-butoxycarbonyl; ^{t}Bu = *tert*-butyl; Et = ethyl; TFA = trifluoroacetic acid; THF = tetrahydrofuran; LC-MS = liquid chromatography-mass spectrometry; ELS = evaporative light scattering.

(*S*)-3-{[(Allyloxy)carbonyl]amino}-2-aminopropanoic acid (2)

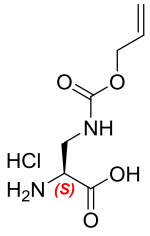

Chemical Formula: $C_7H_{12}N_2O_4$. HCl
Exact Mass: 188.07971 (without HCl)
Molecular Weight: 224.64100 (with HCl)

2

Boc-Dap(Alloc)-OH **2a** (4.325 g, 15.0 mmol, 1.0 eq., procured from Bachem Ltd.) was loaded onto a dry 250 mL single-necked round-bottomed flask and dissolved in HCl (4M in 1,4-dioxane, 60.0 mL, 240.0 mmol, 16.0 eq.). Dry Et_3SiH (10.0 mL, 62.6075 mmol, 4.174 eq.) was added to the solution at r.t. and a faint white precipitate appeared immediately, which intensified with time upon stirring at r.t. under a nitrogen atmosphere. After 24 h, an intense white precipitate was observed and the reaction was judged to be complete by LC-MS analysis (C18 reverse phase column,

H_2O-CH_3CN as mobile phase, gradient). The mixture was then evaporated under reduced pressure and the product was dissolved in dry CH_3OH (100 mL) followed by evaporation to dryness under reduced pressure. This was repeated thrice to remove bulk of 1,4-dioxane by azeotropic evaporation. The residue was re-dissolved in dry CH_3OH (10 mL) and triturated with dry Et_2O (500 mL) to precipitate the product. This was filtered and washed with further Et_2O (2 ×125 mL) and dried in high vacuum (<0.1 mbar) overnight to obtain (*S*)-3-{[(allyloxy)carbonyl]amino}-2-aminopropanoic acid HCl salt **2** as a bright white powder (3.03 g, 90%); ^{1}H NMR (400.13 MHz, DMSO-d_6) δ 3.42-3.56 (m, 2H), 4.48 (d, J = 5.3 Hz, 2H), 5.15-5.36 (m, 2H), 5.80-5.98 (m, 1H), 7.44-7.60 (m, 1H), 8.24-8.70 (broad s, 3H); ^{13}C NMR (100.61 MHz, DMSO-d_6) δ 40.4 (CH_2), 52.4 (CH), 64.7 (CH_2), 117.2 (CH_2), 133.4 (CH), 156.2 (C), 169.1 (C); MS (ESI+) *m/z* (rel intensity) 189 [$(M+H)^+$, 100], 134 (4), 81 (9); HRMS (ESI +) *m/z* calc'd for $C_7H_{13}O_4N_2$ $[M+H]^+$: 189.0870, found 189.0866 (Δ = -2.19 ppm)

tert-Butyl (*S*)-2-[(_tert_-butoxycarbonyl)amino]-3-[(2-nitrobenzyl)amino]propanoate (3a)

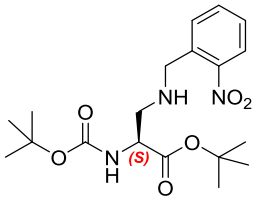

Chemical Formula: $C_{19}H_{29}N_3O_6$
Exact Mass: 395.20564
Molecular Weight: 395.45600

3a

Boc-L-Dap-O^{t}Bu·HCl **1b** (5.0 g, 19.206 mmol, 1.0 eq.) was loaded into a dry 500 mL 2-neck round-bottomed flask and dry THF (75 mL) was added to it, followed by dry DIPEA (6.69 mL, 38.412 mmol, 2.0 eq.). The contents were left stirring under an argon atmosphere at 0˚C. 2-nitrobenzyl bromide (4.979 g, 23.048 mmol, 1.2 eq.) was

loaded on to a separate 250 mL dry single-neck round bottomed flask, dissolved in dry THF (125 mL), and the resulting solution then transferred to the main flask containing Boc-L-Dap-O^{t}Bu by cannula under a positive pressure of argon over 5 min at 0˚C. The mixture was then warmed to r.t. and left stirring at r.t. for 10 h. The reaction mixture was then concentrated under reduced pressure and the crude mixture extracted with EtOAc (200 mL) and washed with brine solution (3 × 250 mL). The organic layer was separated, dried over anhydrous Na_2SO_4, filtered and evaporated to dryness to obtain a brown viscous oil. Product was purified by flash chromatography on SiO_2 (gradient; eluent: EtOAc/*n*-hexane = 1:9 → 1:4) to obtain the desired product, *tert-butyl (S)-2-[(tert-butoxycarbonyl)amino]-3-[(2-nitrobenzyl)amino]propanoate* **3a** as a faint yellow viscous oil (5.05 g, 67%): R_f = 0.27 (SiO_2 plate, EtOAc/*n*-hexane = 1:4); ^{1}H NMR (400.13 MHz, $CDCl_3$ with TMS as internal standard) δ 1.44 (s, 9H), 1.46 (s, 9H), 2.85-3.40 (m, 2H), 4.02 (d, *J* = 14.5 Hz, 1H), 4.07 (d, *J* = 14.5 Hz, 1H), 4.22-4.35 (m, 1H), 5.20-5.55 (m, 1H), 7.41 (ddd, *J* = 8.4, 8.4, 2.0 Hz, 1H), 7.50-7.67 (m, 2H), 7.94 (d, *J* = 8.0 Hz, 1H); ^{13}C NMR (100.61 MHz, $CDCl_3$ with TMS as internal standard) δ 28.1 (CH_3), 28.5 (CH_3), 50.7 (CH_2), 50.9 (CH_2), 54.4 (CH), 79.9 (C), 82.3 (C), 124.9 (CH), 128.2 (CH), 131.3 (CH), 133.3 (CH), 135.5 (C), 149.2 (C), 155.7 (C), 170.9 (C).

(*S*)-2-Amino-3-[(2-nitrobenzyl)amino]propanoic acid 3

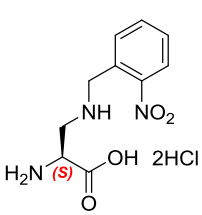

3. 2HCl

Chemical Formula: $C_{10}H_{13}N_3O_4$. 2HCl
Exact Mass: 239.09061
Molecular Weight: 312.14700 (as 2HCl salt)

A 100 mL dry single necked round-bottomed flask was charged with tert-butyl (*S*)-2-[(tert-butoxycarbonyl)amino]-3-[(2-nitrobenzyl)amino]propanoate **3a** (4.59 g, 11.607 mmol, 1.0 eq.). HCl (25 mL, 4 M in 1,4-dioxane, 100.0 mmol, 8.615 eq.) was added, followed by dry Et_3SiH (5.0 mL, 31.304 mmol, 2.697 eq.). The contents were stirred in the dark under an argon atmosphere. The progress of the reaction was periodically monitored by TLC analysis (SiO_2 plate, EtOAc/*n*-hexane = 3:7). After 48 h, an intense white precipitate was formed and the reaction was judged to be complete by TLC and LC-MS analysis (C18 reverse phase column, H_2O-CH_3CN as mobile phase, gradient). The contents were evaporated to dryness under reduced pressure. Remaining 1,4-dioxane was removed by azeotropic evaporation 3x dry CH_3OH (25 mL). The contents were then re-dissolved in dry CH_3OH (25 mL), cooled to 0˚C, triturated with dry Et_2O (400 mL) and vigorously stirred in the dark at room temperature to obtain an intense precipitate. The precipitate was filtered, washed with further dry Et_2O (150 mL), followed by dry *n*-hexane (50 mL), and then evaporated to dryness under high vacuum (<0.1 mbar) for 14 h in dark to obtain the desired product, *(S)-2-amino-3-[(2-nitrobenzyl)amino]propanoic acid HCl salt* **3**, as an off-white powder (3.575 g, 99%): ^{1}H NMR (400.13 MHz, CD_3OD) δ 3.68 (dd, *J* = 13.2, 5.6 Hz, 1H), 3.81 (dd, *J* = 13.2, 7.7 Hz, 1H); 4.48 (dd, *J* = 7.7, 5.6 Hz, 1H), 4.65 (d, *J* = 13.2 Hz, 1H), 4.69 (d, *J* = 13.2 Hz, 1H), 7.74-7.82 (m, 1H), 7.84-7.95 (m, 2H), 8.30 (app. d, *J* = 8.1 Hz, 1H); ^{13}C NMR (100.61 MHz, CD_3OD) δ 47.8 (CH_2), 50.2 (CH), 50.7 (CH_2), 127.1 (CH), 127.3 (C), 132.8 (CH), 135.3 (CH), 136.0 (CH), 150.3 (C), 169.0 (C); MS (ESI+, LC-MS) *m/z* (rel intensity) 240 [$(M+H)^+$, 100%].

4',5'-Methylenedioxy-2'-nitroacetophenone (4b)

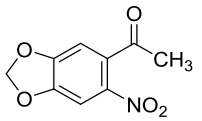

Chemical Formula: $C_9H_7NO_5$
Exact Mass: 209.03242
Molecular Weight: 209.15700

4b

Following a slightly modified procedure described by McGall *et al.*[42], a solution of 3',4'-(methylenedioxy)acetophenone **4a** (16.416 g, 0.1 mol) in glacial CH_3COOH (64 mL) was added drop-wise to a 2 litre three-necked round-bottomed flask containing conc. HNO_3 (136 mL, 70% strength) at 0˚C over 1 h. The reaction mixture was maintained at 0˚C during addition and for a further 1 h with stirring under an argon atmosphere. The mixture was then warmed to 40˚C and stirred for additional 2.5 h. Finally, the mixture was cooled to r.t. and poured slowly into crushed ice (1 litre) in a beaker. A yellow precipitate appeared which was stirred for 15 min and then filtered. The yellow solid was washed with water (3 × 200 mL) and dried in vacuum. The crude yellow solid was then purified by recrystallization (THF/*n*-hexane) and then by flash chromatography on SiO_2 [eluent: CH_2Cl_2/*n*-hexane (1:1) to 100%CH_2Cl_2] to obtain 4',5'-methylenedioxy-2'-nitroacetophenone[42-44] **4b** as yellow crystals (12.141 g, 58%): R_f = 0.52 (CH_2Cl_2); m.p. 122.8-124.0˚C([44] m.p. 112 ^oC); ^1H NMR (400.13 MHz, $CDCl_3$) δ 2.45 (s, 3H), 6.16 (s, 2H), 6.71 (s, 1H), 7.48 (s, 1H); ^{13}C NMR (100.61 MHz, $CDCl_3$) δ 30.2 (CH_3), 103.8 (CH_2), 104.8 (CH), 106.2 (CH), 135.1 (C), 140.1 (C), 148.9 (C), 152.8 (C), 199.3 (C); IR (CH_2Cl_2) ν_{max} 2980, 1708, 1525, 1506, 1484, 1424, 1362, 1338, 1271, 1152, 1038, 932, 875, 819 cm^{-1}; MS (ESI+) *m/z* (rel intensity) 232 [$(M+Na)^+$, 10%], 210 (2), 209 (7), 194 (100), 171 (45), 130 (32), 111 (9).

(*R*,*S*)-1-[4',5'-(Methylenedioxy)-2'-nitrophenyl]ethanol (4c)

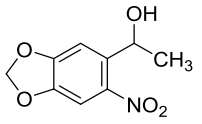

Chemical Formula: $C_9H_9NO_5$
Exact Mass: 211.04807
Molecular Weight: 211.17300

4c

4',5'-Methylenedioxy-2'-nitroacetophenone **4b** (43.714 g, 0.209 mol, 1.0 eq.) was suspended in CH_2Cl_2 (400 mL), CH_3OH (650 mL) and absolute CH_3CH_2OH (425 mL) in a 2 litre, single-necked, round-bottomed flask. The mixture was sonicated for 10 min at r.t. to dissolve the majority of the yellow solid. $NaBH_4$ granules (7.116 g, 0.188 mol, 0.9 eq.) were added in 8 portions (each 0.890 g) to the yellow suspension every 15 min (total time = 2 h addition) at 15 °C, NOTE: effervescence appeared as $NaBH_4$ dissolved and the reaction mixture became a homogeneous yellow solution. After the addition was complete, the reaction mixture was stirred at r.t. for a further 4 h. After this time the reaction was judged complete by TLC analysis (SiO_2, TLC eluent: 100% CH_2Cl_2), and the reaction quenched by addition of dry acetone (100 mL) stirring at r.t. for a further 2 h. The mixture was then evaporated to dryness under reduced pressure to obtain a yellow solid. The solid was subsequently re-dissolved in CH_2Cl_2 (800 mL) and washed sequentially with saturated aq. NH_4Cl solution (3 × 500 mL) and finally with saturated aq. NaCl solution (6 × 800 mL) The organic layer was separated, dried over anhydrous Na_2SO_4, filtered, and evaporated to dryness in high vacuum to obtain (*R*,*S*)-1-[4',5'-(methylenedioxy)-2'-nitrophenyl]ethanol[42,43] **4c** as a yellow solid (43.563 g, 99%): R_f = 0.19 (CH_2Cl_2); m.p. 76.5-77.5 ^oC; ^1H NMR (400.13 MHz, $CDCl_3$) δ 1.50 (d, J = 6.3 Hz, 3H), 2.54 (d, J = 3.0 Hz, 1H), 5.42 (qd, J = 6.3, 3.0 Hz, 2H), 6.096 (app. d, $^2J_{HH}$ = 3.5 Hz, 1 H, diastereotopic OCH_2O), 6.104 (app. d, $^2J_{HH}$ = 3.5 Hz, 1 H, diastereotopic OCH_2O), 7.24 (s, 1H), 7.42 (s, 1H); ^{13}C NMR (100.61 MHz, $CDCl_3$) δ 24.3 (CH_3), 65.8 (CH), 103.1 (CH_2), 105.2 (CH), 106.4 (CH), 139.2 (C), 141.5 (C), 147.0 (C), 152.5 (C); IR (CH_2Cl_2) ν_{max} 3649, 2980, 2889,

2360, 2343, 1521, 1506, 1482, 1393, 1340, 1253, 1135, 1090, 1038, 934, 819 cm^{-1}; MS (ESI+) *m/z* (rel intensity) 234 [$(M+Na)^+$, 1%], 194 [$(M-OH)^+$, 100], 130 (20); HRMS (ESI +) *m/z* calc'd for $C_9H_9NO_5$ $[M+Na]^+$: 234.0373, found 234.0364 (Δ = -3.95 ppm).

(*R*,*S*)-1-Bromo-1-[4',5'-(methylenedioxy)-2'-nitrophenyl]ethane (4d)

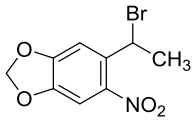

Chemical Formula: $C_9H_8BrNO_4$
Exact Mass: 272.96367
Molecular Weight: 274.07000

4d

A 1 litre, 3-necked round-bottomed flask was dried *in vacuo* for 15 min at >100˚C using a heat gun and purged with dry argon gas and allowed to cool to room temperature. To this was added (*R*,*S*)-1-[4',5'-(methylenedioxy)-2'-nitrophenyl]ethanol, **4c** (15.838 g, 75.0 mmol, 1.0 eq.). **4c** was dissolved in dry CH_2Cl_2 (375 mL, sonication required for complete solubility), cooled to 0˚C under an argon atmosphere, and the round-bottomed flask was wrapped with aluminium foil to shield it from light. After 20 min, PBr_3 (2.82 mL, 30.0 mmol, 0.4 eq.) was added dropwise for 10 min using a syringe pump at 0 °C, followed by addition of dry pyridine (0.5 mL). The yellow reaction mixture was stirred at 0˚C for 15 min, then brought to r.t. and stirred continuously for 1.5 h. The reaction was judged to be complete by TLC analysis (SiO_2, TLC eluent: 100% CH_2Cl_2), cooled to 0 °C, quenched by the addition of dry CH_3OH (15 mL), warmed to r.t. and stirred for 30 min under an argon atmosphere. After the quenching was complete, the reaction mixture was evaporated to dryness under reduced pressure using a rotary evaporator. The resulting yellow gum was dissolved in CH_2Cl_2 (300 mL) and saturated aq. $NaHCO_3$ solution (300 mL). The contents were loaded into a separating funnel, the

aqueous phase was discarded and the organic phase was washed sequentially with further saturated aq. $NaHCO_3$ solution (1 × 300 mL) and saturated aq. NaCl solution (3 × 300 mL). The organic layer was separated, dried over anhydrous Na_2SO_4, filtered and evaporated to dryness to obtain a yellow solid. The crude product was purified by flash chromatography on SiO_2 [eluent: CH_2Cl_2/*n*-hexane (1:1), then 100%CH_2Cl_2] to obtain a pure sample of (*R*,*S*)-1-bromo-1-[4',5'-(methylenedioxy)-2'-nitrophenyl]ethane[43] **4d** (18.330 g, 89%) as shining yellow crystals. The sample was stored in a freezer at -20˚C in a dry atmosphere and in the dark for several months without any significant decomposition: R_f = 0.17 (CH_2Cl_2/*n*-hexane, 1:4); m.p. 76.1-77.8 ^{o}C; ^{1}H NMR (400.13 MHz, $CDCl_3$) δ 2.04 (d, J = 6.8 Hz, 3H), 5.89 (q, J = 6.8 Hz, 1H), 6.13 (s, 2H), 7.27 (s, 1H), 7.35 (s, 1H); ^{13}C NMR (100.61 MHz, $CDCl_3$) δ 27.6 (CH_3), 42.9 (CH), 103.3 (CH_2), 105.1 (CH), 108.8 (CH), 134.8 (C), 141.6 (C), 147.7 (C), 152.1 (C); IR (CH_2Cl_2) ν_{max} 2981, 2970, 2930, 1615, 1504, 1481, 1420, 1395, 1385, 1328, 1305, 1257, 1156, 1141, 1057, 1028, 1014, 957, 925, 872, 815, 752, 730, 719, 698 cm^{-1}; HRMS (ESI+) *m/z* calc'd for $C_9H_8{}^{79}BrNO_4$ $[M+Na]^+$: 295.9529, found 295.9519 (Δ = -3.45ppm)

tert-Butyl (2*S*)-2-[(_tert_-butoxycarbonyl)amino]-3-{[1-(6-nitrobenzo[*d*][1,3]dioxol-5-yl)ethyl] amino}propanoate (4e)

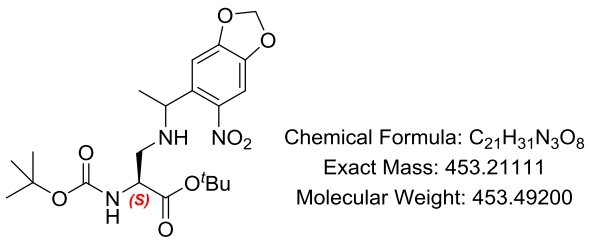

Chemical Formula: $C_{21}H_{31}N_3O_8$
Exact Mass: 453.21111
Molecular Weight: 453.49200

4e

Boc-L-Dap-O^{t}Bu·HCl **1b** (6.233 g, 21.0 mmol, 1.1 eq.) was suspended in dry THF (275 mL) in a dry 1 litre 3-neck round-bottomed flask and dry DIPEA (9.98 mL,

57.273 mmol, 3.0 eq.) was added. The contents were stirred for 10 min at r.t. under a nitrogen atmosphere. The flask was wrapped with aluminium foil and the contents were kept in the dark. (*R,S*)-1-bromo-1-[4',5'-(methylenedioxy)-2'-nitrophenyl]ethane **4d** (5.232 g, 19.091 mmol, 1.0 eq.) was then added to the reaction mixture. The homogeneous yellow solution and was left stirring in the dark at r.t. under a nitrogen atmosphere for a period of 68 h. The reaction was judged to be complete by TLC analysis (SiO_2 plate; CH_2Cl_2/*n*-hexane = 3:7) and evaporated to dryness under reduced pressure to obtain a dark brown oil. The crude reaction oil was dissolved in CH_2Cl_2 (250 mL) and washed with saturated brine solution (3 × 500 mL). The organic layer was separated, dried over anhydrous Na_2SO_4, filtered and evaporated to dryness to obtain a dark brown viscous oil. This was then purified by flash chromatography on SiO_2 (gradient; eluent: 100% CH_2Cl_2, then CH_2Cl_2/CH_3OH/NEt_3 = 94:5:1) to afford the desired product, *tert-butyl (2S)-2-[(tert-butoxycarbonyl)amino]-3-{[1-(6-nitrobenzo[d][1,3]dioxol-5-yl) ethyl]amino}propanoate* **4e,** as a yellow-brown sticky gum (7.49 g, 87%): R_f = 0.13 (SiO_2 plate, CH_2Cl_2); ^{1}H NMR (400.13 MHz, $CDCl_3$ with TMS as internal standard) δ 1.34 and 1.36 (2 × d, *J* = 3.6 and 3.6 Hz, 3H), 1.42 and 1.450 (2 × s, 9H), 1.454 and 1.47 (2 × s, 9H), 2.54-2.74 (m, 1H), 2.75-2.89 (m, 1H), 4.03-4.27 (m, 1H), 4.28-4.53 (m, 1H), 5.15-5.43 (m, 1H), 6.05-6.10 (m, 2H), 7.21 (app. broad s, 1H), 7.345 and 7.352 (2 × s, 1H); ^{13}C NMR (100.61 MHz, $CDCl_3$ with TMS as internal standard) δ (mixture of diastereoisomers) 23.9 (CH_3), 24.0 (CH_3), 28.12 (CH_3), 28.15 (CH_3), 28.41 (CH_3), 28.46 (CH_3), 49.3 (CH_2), 49.4 (CH_2), 53.1 (CH), 53.2 (CH), 54.3 (CH), 54.5 (CH), 79.9 (C), 80.1 (C), 82.3 (C), 82.4 (C), 102.8 (2 × CH_2), 105.2 (2 × CH), 106.77 (CH), 106.83 (CH), 138.1 (C), 143.30 (C), 143.37 (C), 146.7 (C), 152.1 (C), 152.2 (C), 155.5 (C), 155.6 (C), 170.7 (C), 170.8 (C); MS (ESI+) *m/z* (rel intensity)

454 [$(M+H)^+$, 86%], 301 (70), 261 (100), 205 (7), 203 (10), 186 (7), 147 (10); HRMS (ESI+) *m/z* calc'd for $C_{21}H_{32}O_8N_3$ $[M+H]^+$: 454.2184, found 454.2201 (Δ = 3.65 ppm).

(2*S*)-2-Amino-3-{[1-(6-nitrobenzo[*d*][1,3]dioxol-5-yl)ethyl]amino}propanoic acid (4)

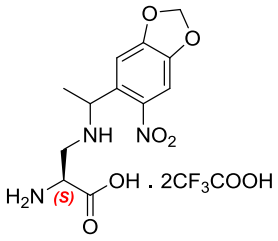

4. 2TFA
(mixture of ~1:1 epimers)

Chemical Formula: $C_{12}H_{15}N_3O_6$. $2CF_3COOH$
Exact Mass: 297.09609
Molecular Weight: 525.31342 (as disalt of CF_3COOH)

tert-Butyl (2*S*)-2-[(*tert*-butoxycarbonyl)amino]-3-{[1-(6-nitrobenzo[*d*][1,3]dioxol-5-yl) ethyl]amino} propanoate **4e** (4.303 g, 9.489 mmol, 1.0 eq.) was dissolved in dry CH_2Cl_2 (30 mL) in a dry 250 mL round-bottomed flask wrapped with aluminium foil to exclude light. Freshly distilled CF_3COOH (15 mL, 195.887 mmol, 20.644 eq.) was added and the yellow solution turned brown. Dry Et_3SiH (10.0 mL, 62.608 mmol, 6.598 eq.) was added and the reaction mixture stirred at r.t. in the dark. The reaction was periodically monitored by LC-MS analysis. After 48 h, the reaction was judged to be complete by LC-MS analysis (C18 reverse phase column, H_2O-CH_3CN as mobile phase, gradient), and the mixture then evaporated to dryness to obtain a dark brown gum. The gum was dissolved in anhydrous CH_3OH (10 mL) and cooled to 0˚C under an argon atmosphere in a dry 2 L round-bottomed flask. This was triturated by addition of dry Et_2O (900 mL) at 0˚C and then stirred vigorously at r.t. for 1 h to obtain a pale-yellow precipitate. The precipitate was filtered, washed with additional dry Et_2O (2 × 200 mL), followed by *n*-hexane (150 mL). The pale yellow powder was

transferred to a 100 mL round-bottomed flask and dried in high vacuum (<0.1 mbar) for 40 h in the dark. *(2S)-2-Amino-3-{[1-(6-nitrobenzo[d][1,3]dioxol-5-yl)ethyl]amino} propanoic acid* **4** was obtained as a free-flowing pale yellow powder (3.646 g, 73%). The product is a salt of CF_3COOH and a ~1:1 mixture of epimers. The product was stored under argon in the dark at -20 °C: ^{1}H NMR (400.13 MHz, DMSO-d_6 with TMS as internal standard) δ 1.36 and 1.38 (2 × d, J = 3.8 and 3.8 Hz, 3H), 2.65-2.95 and 2.96-3.20 (2 × m, 1H), 3.07-3.25 (m, 1H), 3.60-3.70 (m, 1H), 3.71-3.85 and 4.18-4.44 (2 × m, 1H), 6.21 and 6.23 (2 × d, J = 3.5 and 2.9 Hz, 2H), 7.41 and 7.42 (2 × s, 1H), 7.52 and 7.53 (2 × s, 1H); ^{13}C NMR (100.61 MHz, DMSO-d_6 with TMS as internal standard) δ (mixture of diastereoisomers) 22.6 (CH_3), 22.7 (CH_3), 38.5 (CH_2), 45.8 (CH_2), 51.6 (CH), 51.8 (CH), 52.3 (CH), 52.6 (CH), 103.2 (CH_2), 103.3 (CH_2), 104.5 (CH), 104.6 (CH), 106.4 (CH), 106.6 (CH), 117.1 (C, q, $^1J_{C\text{-}F}$ = 299.0 Hz), 135.4 (C), 135.6 (C), 142.96 (C), 143.01 (C), 146.61 (C), 146.66 (C), 151.93 (C), 151.96 (C), 158.56 (C, q, $^2J_{C\text{-}F}$ = 31.5 Hz), 168.7 (2 × C), 169.6 (2 × C); MS (ESI+) *m/z* (rel intensity) 298 [$(M+H)^+$, 100%], 261 (10), 225 (10), 211 (4), 147 (12), 144 (9), 134 (6), 105 (9), 82 (31); HRMS (ESI+) *m/z* calc'd for $C_{12}H_{16}O_6N_3$ $[M+H]^+$: 298.1034, found 298.1039 (Δ = 1.74 ppm).

2,5-Dioxopyrrolidin-1-yl (1-(6-nitrobenzo[*d*][1,3]dioxol-5-yl)ethyl) carbonate (5a)

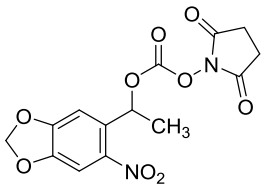

Chemical Formula: $C_{14}H_{12}N_2O_9$
Exact Mass: 352.05428
Molecular Weight: 352.25500

5a

(*R*,*S*)-1-[4',5'-(Methylenedioxy)-2'-nitrophenyl]ethanol **4c** (42.234 g, 200.0 mmol, 1.0 eq.) was charged onto a dry 2 litre 3-neck round-bottomed flask and dissolved in dry

CH_3CN (1 L). Dry DIPEA (104.5 mL, 600.0 mmol, 3.0 eq.) was added to the solution, followed by *N,N*-disuccinimidyl carbonate (80.896 g of ≥ 95% purity, 300 mmol, 1.5 eq.). The flask was wrapped with aluminium foil to keep the contents in the dark. The yellow heterogeneous reaction mixture was stirred at r.t. under an argon atmosphere in the dark. After 16 h, the reaction mixture was homogeneous and reaction was judged to be complete by TLC analysis (SiO_2 plate, CH_3CN/CH_2Cl_2 = 1:19). The yellow reaction mixture was then adsorbed on to Biotage® Isolute HM-N sorbent and dried under reduced pressure. This was then quickly subjected to flash chromatography on SiO_2 [eluent: CH_2Cl_2, then CH_3CN/CH_2Cl_2 = 1:19] in the dark to obtain the desired product, *2,5-dioxopyrrolidin-1-yl-(1-(6-nitrobenzo[d][1,3]dioxol-5-yl)ethyl) carbonate* **5a** as yellow crystalline needles (65.051 g, 92%) [NOTE: The flash column must be performed quickly to avoid decomposition of the product on prolonged exposure to SiO_2]. The product **5a** was used for the subsequent step immediately. It can be stored in the dark at -20˚C in a freezer: R_f = 0.6 (SiO_2 plate, CH_3CN/CH_2Cl_2 = 1:19); ^{1}H NMR (400.13 MHz, $CDCl_3$ with TMS as internal standard) δ 1.75 (d, *J* = 6.4 Hz, 3H), 2.81 (s, 4H), 6.15 (d, *J* = 3.0 Hz, 2H), 6.42 (q, *J* = 6.4 Hz, 1H), 7.11 (s, 1H), 7.51 (s, 1H); ^{13}C NMR (100.61 MHz, $CDCl_3$ with TMS as internal standard) δ 22.2 (CH_3), 25.6 (CH_2), 76.4 (CH), 103.5 (CH_2), 105.5 (CH), 105.8 (CH), 133.1 (C), 141.6 (C), 148.0 (C), 150.7 (C), 153.0 (C), 168.6 (C).

(2*S*)-2-[(*tert*-Butoxycarbonyl)amino]-3-({[1-(6-nitrobenzo[*d*][1,3]dioxol-5-yl)ethoxy]carbonyl}- amino)propanoic acid (5b)

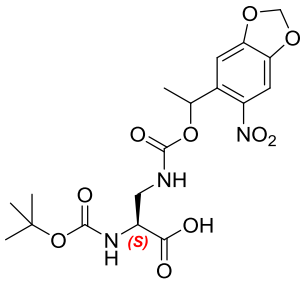

Chemical Formula: $C_{18}H_{23}N_3O_{10}$
Exact Mass: 441.13834
Molecular Weight: 441.39300

5b

Boc-L-Dap-OH **1a** (2.553 g, 12.5 mmol, 1.25 eq.) was suspended in dry THF (180 mL) and dry CH_3CN (20 mL) in a dry 1 litre single-necked round-bottomed flask wrapped with aluminium foil to exclude light. Dry DIPEA (5.23 mL, 30.0 mmol, 3.0 eq.) was added to the mixture and the contents were stirred for 20 min at r.t. under an argon atmosphere, after which 2,5-dioxopyrrolidin-1-yl-(1-(6-nitrobenzo[*d*][1,3]dioxol-5-yl)ethyl) carbonate **5a** (3.523 g, 10.0 mmol, 1.0 eq.) was added. The heterogeneous mixture was stirred at r.t. under an argon atmosphere in the dark and the progress of the reaction was periodically monitored by LC-MS analysis. After a few hours the heterogeneous mixture started to be a homogeneous yellow solution. After 24 h, the reaction was judged to be complete and the contents were adsorbed onto Biotage® Isolute HM-N sorbent and dried under reduced pressure. This was then quickly subjected to flash chromatography on SiO_2 [eluent: CH_2Cl_2, then $CH_2Cl_2/CH_3OH/CH_3COOH$ = 94:5:1] in the dark to obtain the desired product, *(2S)-2-[(tert-butoxycarbonyl)amino]-3-({[1-(6-nitrobenzo[d][1,3]dioxol-5-yl)ethoxy]carbonyl}amino) propanoic acid* **5b** as a brown-yellow gum. This was subjected to azeotropic evaporation using CH_2Cl_2 / cyclohexane (1:1) under reduced pressure to remove residual CH_3COOH from the product **5b**. The product was dried in high vacuum to obtain a pure sample of **5b** as a yellow solid (4.360 g, 99%) and a ~1:1 mixture of epimers; R_f = 0.41 (SiO_2 plate, $CH_2Cl_2/CH_3OH/CH_3COOH$ = 94:5:1); MS (ESI-, LC-MS) *m/z* (rel intensity) 440 [$(M-H)^-$, 100%].

(2*S*)-2-Amino-3-({[1-(6-nitrobenzo[*d*][1,3]dioxol-5-yl)ethoxy]carbonyl}amino)propanoic acid (5)

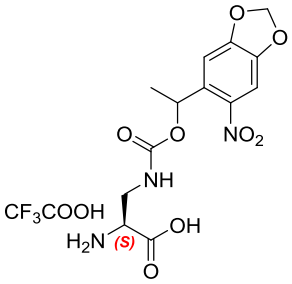

Chemical Formula: $C_{13}H_{15}N_3O_8$. CF_3COOH
Exact Mass: 341.08591
Molecular Weight: 455.29921 (with TFA)

5.TFA (mixture of ~1:1 epimers)

Freshly distilled CF_3COOH (15 mL, 195.894 mmol, 21.293 eq.) was added to a solution of (2*S*)-2-[(*tert*-butoxycarbonyl)amino]-3-({[1-(6-nitrobenzo[*d*][1,3]dioxol-5-yl)ethoxy] carbonyl}amino)propanoic acid **5b** (4.061 g, 9.2 mmol, 1.0 eq.) in dry CH_2Cl_2 (50 mL) in a dry 1 L single-necked round-bottomed flask wrapped with aluminium foil. Upon addition of CF_3COOH the yellow solution turned to dark brown, the reaction was stirred at r.t. in the dark and monitored by TLC analysis. After 2 h, the reaction was judged to be complete by both TLC (SiO_2 plate; $CH_2Cl_2/CH_3OH/CH_3COOH$ = 94:5:1) and LC-MS analysis (C18 reverse phase column, H_2O-CH_3CN as mobile phase, gradient). The reaction mixture was evaporated to dryness under reduced pressure to obtain a dark brown gum. The gum was dissolved in dry CH_3OH (5 mL), cooled to 0˚C and triturated with dry Et_2O (0.9 L) to obtain a pale yellow precipitate. The mixture was left stirring vigorously in the dark under an atmosphere of argon at r.t. The pale yellow precipitate was then filtered and washed with Et_2O (2 × 100 mL) and dry hexane (50 mL). This was dried in vacuo (<0.1 mbar) for 2 days in the dark to obtain the desired *(2S)-2-amino-3-({[1-(6-nitrobenzo[d][1,3]dioxol-5-yl)ethoxy]carbonyl}amino)propanoic acid* TFA salt **5** as a fine, pale yellow powder (4.132 g, 99%) and a ~1:1 mixture of epimers as observed

by ^{1}H and ^{13}C NMR spectroscopic analysis: ^{1}H NMR (400.13 MHz, CD_3OD) δ 1.57 (d, J = 6.2 Hz, 3H), 2.68 (s, 2H), 3.41-3.58 (m, 1H), 3.59-3.74 (m, 1H), 3.78-4.15 (m, 1H), 6.14 (s, 2H), 6.22 (q, J = 6.2 Hz, 1H), 7.12 (app. d, J = 5.2 Hz, 1H), 7.47 (s, 1H); ^{13}C NMR (100.61 MHz, CD_3OD) δ 22.4 (CH_3), 22.5 (CH_3), 42.1 (CH_2), 42.3 (CH_2), 55.6 (CH), 55.9 (CH), 70.4 (2 × CH), 104.8 (2 × CH_2), 105.7 (2 × CH), 106.7 (CH), 106.9 (CH), 118.2 (C, q, $^{1}J_{C\text{-}F}$ = 292.6 Hz), 136.8 (C), 137.1 (C), 142.8 (C), 142.9 (C), 148.8 (C), 154.0 (C), 158.5 (C), 158.6 (C), 163.1 (C, q, $^{2}J_{C\text{-}F}$ = 34.4 Hz), 170.9 (2 × C), 174.9 (2 × C); MS (ESI+) *m/z* (rel intensity) 342 [$(M+H)^+$, 100%], 311 (10), 233 (5), 189 (9), 130 (19); HRMS (ESI+) *m/z* calc'd for $C_{13}H_{16}O_8N_3$ $[M+H]^+$: 342.0932, found 342.0923 (Δ = -2.63 ppm).

2-{[1-(6-Nitrobenzo[*d*][1,3]dioxol-5-yl)ethyl]thio}ethan-1-ol (6a)

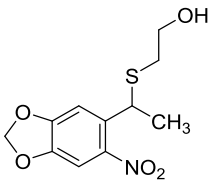

Chemical Formula: $C_{11}H_{13}NO_5S$
Exact Mass: 271.05144
Molecular Weight: 271.28700

6a

A freshly prepared solution of NaOH (0.5 M, 8 g in 40 mL of deionized H_2O, 20.0 mmol, 1 eq.) was loaded onto a 500 mL round 3-necked round-bottomed flask and the solution was degassed by bubbling through a stream of argon gas at r.t. After 30 min, mercaptoethanol (1.47 mL, 21.0 mmol, 1.05 eq.) was added to the flask and degassing was continued for a further 15 min. Separately, freshly (*R*,*S*)-1-bromo-1-[4',5'-(methylenedioxy)-2'-nitrophenyl]ethane **13** (5.481 g, 20.0 mmol, 1.0 eq) was dissolved in 1,4-dioxane (20 mL) in a 100 mL round-bottomed flask wrapped with

aluminium foil and degassed by bubbling a stream of argon gas for 15 min in the dark. The degassed solution of **13** in 1,4-dioxane was transferred onto the flask containing aq. NaOH and mercaptoethanol solution, dropwise, for a period of 90 min at r.t. using a cannula under a positive pressure of argon gas. A yellow precipitate formed, which was then dissolved by addition of degassed 1,4-dioxane (60 mL), followed by sonication for 30 min until a homogenous clear yellow solution was obtained. The contents were then left stirring for 12 h at r.t. in the dark under an argon atmosphere, after which time the reaction was judged to be complete by TLC and LC-MS analysis (C18 reverse phase column, H_2O-CH_3CN as mobile phase, gradient). The mixture was then evaporated under reduced pressure to remove the volatile organic components. The yellow aqueous content was then extracted with EtOAc (2 × 175 mL) and the combined organic phase was washed with saturated NH_4Cl solution (1 × 500 mL), followed by brine solution (3 × 500 mL). The organic layer was then separated, dried over anhydrous Na_2SO_4, filtered and evaporated to dryness to obtain a yellow oil. The product was purified by flash chromatography on SiO_2 (eluent: EtOAc/*n*-hexane = 3:7) in the dark to obtain *2-{[1-(6-nitrobenzo[d][1,3]dioxol-5-yl)ethyl]thio}ethan-1-ol* **6a** as a sticky yellow oil (5.179 g, 95%): R_f = 0.33 (SiO_2 plate, EtOAc/*n*-hexane = 3:7); ^{1}H NMR (400.13 MHz, $CDCl_3$) δ 1.55 (d, *J* = 7.0 Hz, 3H), 1.96 (t, J = 5.9 Hz, 1H), 2.44-2.65 (m, 2H), 3.52-3.74 (m, 2H), 4.78 (q, *J* = 7.0 Hz, 1H), 6.10 (dd, *J* = 3.8, 1.0 Hz, 2H), 7.27 (s, 1H), 7.28 (s, 1H); ^{13}C NMR (100.61 MHz, $CDCl_3$) δ 23.2 (CH_3), 34.9 (CH_2), 38.4 (CH), 60.9 (CH_2), 103.1 (CH_2), 104.8 (CH), 108.0 (CH), 136.1 (C), 143.3 (C), 146.9 (C), 152.0 (C); IR (neat) ν_{max} 3393, 2980, 1617, 1518, 1503, 1480, 1418, 1375, 1332, 1252, 1156, 1031, 928, 872, 817, 759; *m*/*z* (ESI-, LC-MS) 270.1 [$(M-H)^-$, 100%].

2,5-Dioxopyrrolidin-1-yl-(2-{[1-(6-nitrobenzo[d][1,3]dioxol-5-yl)ethyl]thio}ethyl) carbonate (6b)

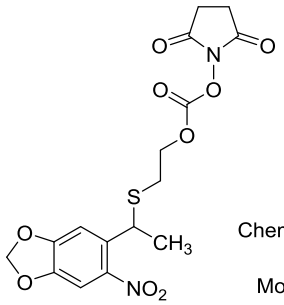

Chemical Formula: $C_{16}H_{16}N_2O_9S$
Exact Mass: 412.05765
Molecular Weight: 412.36900

6b

Intermediate **6b** used for the subsequent reaction for the synthesis of DAP derivatives **6c** and **6d** was synthesised *in situ* starting from the alcohol **6a**. A 3-necked 500 mL round-bottomed flask was dried *in vacuo* using a heat gun and purged with argon gas; this procedure was repeated three times prior to use. The dry flask was charged with 2-{[1-(6-nitrobenzo[*d*][1,3]dioxol-5-yl)ethyl]thio}ethan-1-ol **6a** (4.883 g, 18.0 mmol, 1.0 eq.) dissolved in dry CH_3CN (90 mL). Dry DIPEA (9.41 mL, 54.0 mmol, 3.0 eq.), followed by *N*,*N*'-disuccinimidyl carbonate (6.796 g of ≥95% purity, 25.2 mmol, 1.4 eq.), was added to the reaction mixture at r.t. in the dark under an argon atmosphere. The reaction mixture turned to turbid yellow and a white precipitate began to form, and after 1 h, the reaction mixture became a homogeneous yellow-brown solution. The reaction was left stirring at r.t. for 12 h and was judged to be complete by TLC analysis (SiO_2 plate, EtOAc/*n*-hexane = 3:7) after this time. The *2,5-dioxopyrrolidin-1-yl-(2-{[1-(6-nitrobenzo[d][1,3]dioxol-5-yl)ethyl]thio}ethyl) carbonate* **6b** was immediately carried to the next step without further purification: R_f = 0.12 (SiO_2 plate, EtOAc/*n*-hexane = 3:7).

***tert*-Butyl (2*S*)-2-[(*tert*-Butoxycarbonyl)amino]-3-{[(2-{[1-(6-nitrobenzo[*d*][1,3]dioxol-5-yl)ethyl]thio}ethoxy)carbonyl]amino}propanoate (6c)**

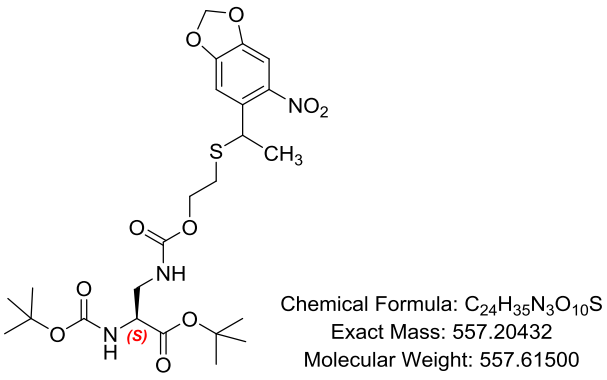

6c

Boc-L-Dap-O^{t}Bu·HCl (8.548 g, 28.8 mmol, 1.6 eq.) was added in one portion to a solution of **6b**, prepared as described above. The yellow reaction mixture turned homogeneous in few minutes and the contents were stirred in dark under an argon atmosphere at After 10 h the reaction was judged to be complete by both TLC (SiO_2 plate, R_f = 0.39, EtOAc/n-hexane = 3:7) and LC-MS analysis (C18 reverse phase column, H_2O-CH_3CN as mobile phase), confirming consumption of **6b**. The reaction mixture was then adsorbed onto Biotage® Isolute HM-N sorbent and dried under reduced pressure. This was then subjected to flash chromatography on SiO_2 [eluent: EtOAc/*n*-hexane = 3:7] in the dark to obtain the desired *tert-butyl (2S)-2-[(tert-butoxycarbonyl)amino]-3-{[(2-{[1-(6-nitrobenzo[d][1,3]dioxol-5-yl)ethyl]thio}ethoxy)carbonyl] amino}propanoate* **6c** as a thick yellow gum (9.405 g, 94%) and a mixture of ~1:1 epimers: R_f = 0.39 (EtOAc/*n*-hexane = 3:7); ^{1}H NMR (400.13 MHz, $CDCl_3$) δ (Mixture of epimers) 1.44 (s, 9H), 1.46 (s, 9H), 1.54 (d, *J* = 6.8 Hz, 3H), 2.36-2.61 (m, 2H), 3.41-3.68 (m, 2H), 4.00-4.18 (m, 2H), 4.24 (broad s, 1H), 4.85 (q, *J* = 6.8 Hz, 1H), 5.15 (broad s, 1H), 5.41 (broad s, 1 H), 6.10 (d, *J* = 6.8,

2H), 7.27 (s, 1H), 7.29 (s, 1H); ^{13}C NMR (100.61 MHz, $CDCl_3$) δ 23.1 (CH_3), 28.1 (CH_3), 28.4 (CH_3), 30.5 (CH_2), 39.0 (CH), 43.2 (CH_2), 54.6 (CH), 65.2 (CH_2), 80.1 (C), 82.9 (C), 103.0 (CH_2), 104.7 (CH), 108.2 (CH), 136.3 (C), 143.5 (C), 146.9 (C), 152.1 (C), 155.6 (C), 156.4 (C), 169.7 (C); *m*/*z* (ESI+, LC-MS) 558.2 [$(M+H)^+$, 100%]

(2*S*)-2-[(*tert*-Butoxycarbonyl)amino]-3-{[(2-{[1-(6-nitrobenzo[*d*][1,3]dioxol-5-yl)ethyl] thio}ethoxy)carbonyl]amino}propanoic acid (6d)

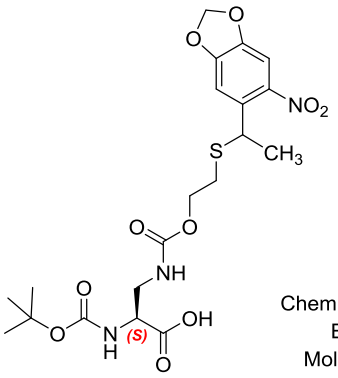

Chemical Formula: $C_{20}H_{27}N_3O_{10}S$
Exact Mass: 501.14171
Molecular Weight: 501.50700

6d

Boc-L-Dap-OH (13.479 g, 66.0 mmol, 1.082 eq.) was added in one portion to a solution of **6b** (26.70 g, prepared as described above) in dry CH_3CN (305 mL) under argon and stirred for 12 h at r.t. After this time the reaction was judged to be complete by LC-MS (C18 reverse phase column, H_2O-CH_3CN as mobile phase) and the contents were adsorbed on to Biotage® Isolute HM-N sorbent and dried under reduced pressure. This was then subjected to flash chromatography on spherical SiO_2 [Supelco®, procured from Sigma Aldrich Ltd., 40-75 μm particle size; gradient; eluent: EtOAc/*n*-hexane = 1:1 → 7:3 → 1:0] in the dark to obtain the desired *(2S)-2-[(tert-butoxycarbonyl)amino]-3-{[(2-{[1-(6-nitrobenzo[d][1,3]dioxol-5-*

yl)ethyl]thio}ethoxy)- carbonyl]amino}propanoic acid **6d** as a thick yellow gum (28.995 g, 95%) and a mixture of ~1:1 epimers: ^{1}H NMR [400.13 MHz, $CDCl_3$ with 0.1% v/v TMS as internal standard] δ (Mixture of epimers) 1.43 (s, 9H), 1.52 (d, J = 6.8 Hz, 3H), 2.30-2.95 (m, 2H), 3.33-3.82 (broad m, 2H), 3.86-4.18 (m, 2H), 4.20-4.48 (m, 1H), 4.64-4.97 (m, 1H), 5.34-5.58 (broad s, 1H), 5.60-5.84 (broad s, 1H), 6.20 (d, J = 8.3 Hz, 2H), 7.10-7.39 (m, 2H), 8.47 (broad s, 1H); ^{13}C NMR [100.61 MHz, $CDCl_3$ with 0.1% v/v TMS as internal standard] δ 23.1 (CH_3), 28.4 (3 × CH_3), 30.5 (CH_2), 39.0 (CH), 42.7 (CH_2), 54.4 (CH), 65.3 (CH_2), 80.8 (C), 103.1 (CH_2), 104.7 (CH), 108.1 (CH), 136.2 (C), 143.4 (C), 146.9 (C), 152.1 (C), 156.3 (C), 157.2 (C), 173.5 (C); *m*/*z* (ESI-, LC-MS) 500.1 [$(M-H)^-$, 100%]

(2*S*)-2-Amino-3-{[(2-{[1-(6-nitrobenzo[*d*][1,3]dioxol-5-yl)ethyl]thio}ethoxy)carbonyl] amino}propanoic acid (6)

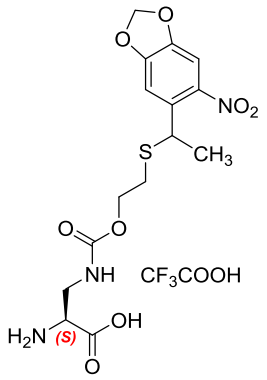

Chemical Formula: $C_{15}H_{19}N_3O_8S$. CF_3COOH
Exact Mass: 401.08929 (without TFA)
Molecular Weight: 515.41321 (with TFA)

6.TFA (mixture of ~1:1 epimers)

Method I (prepared from 6c):

A dry sample of (2*S*)-2-[(*tert*-butoxycarbonyl)amino]-3-{[(2-{[1-(6-nitrobenzo[*d*][1,3]dioxol-5-yl)ethyl]thio}-ethoxy)carbonyl]amino}propanoate **6c** (6.728 g, 12.066 mmol, 1.0 eq.) was loaded to a dry 250 mL single-necked round-

bottomed flask and dissolved in dry CH_2Cl_2 (50 mL), the flask was wrapped in foil to exclude light. Dry Et_3SiH (20 mL, 125.215 mmol, 10.378 eq.) was added to the solution followed by the drop-wise addition of freshly distilled CF_3COOH (20 mL, 261.182 mmol, 21.647 eq.) using a syringe over 15 min at r.t. The reaction mixture turned from yellow to a brown-green colour and was left stirring at r.t. in the dark. After 24 h, the reaction was judged to be complete by TLC (SiO_2 plate, EtOAc/*n*-hexane = 3:7) and LC-MS analysis (C18 reverse phase column, H_2O-CH_3CN as mobile phase). The reaction mixture was concentrated under reduced pressure in the dark to obtain a yellow-brown gum. This was dissolved in anhydrous CH_3OH (20 mL) and evaporated to dryness under reduced pressure; this was repeated three times and dried in high vacuum (<0.1 mbar) to remove any residual CF_3COOH, Et_3SiH and H_2O. The yellow-brown gum was then dissolved in dry CH_3OH (40 mL) and transferred to a dry 2 L round-bottomed flask under an argon atmosphere and cooled to 0˚C. Dry Et_2O (2 L) was added to the solution *via* cannula under a positive pressure of argon gas in the dark and the contents were vigorously stirred. A yellow precipitate formed and the contents stirred vigorously at 0˚C for 15 min, then at r.t. for a further 2 h. The pale yellow precipitate was filtered and washed with dry Et_2O (3 × 250 mL) and finally with dry *n*-hexane (50 mL). The product was dried in vacuum (<0.1 mbar) overnight for 14 h in the dark to obtain *(2S)-2-amino-3-{[(2-{[1-(6-nitrobenzo[d][1,3]dioxol-5-yl)ethyl]thio}ethoxy)carbonyl]amino}propanoic acid TFA salt* **6** as a pale yellow powder (3.940 g, 63%) and a 1:1 mixture of epimers: ^{1}H NMR [400.13 MHz, CD_3OD/CF_3COOD (5:1) with 1% v/v TMS as internal standard] δ (Mixture of epimers) 1.55 (d, J = 7.0 Hz, 3H), 2.49-2.73 (m, 2H), 3.63 (dd, J = 15.0, 6.4 Hz, 1H), 3.78 (ddd, J = 15.0, 3.6, 2.3 Hz, 1H), 4.0-4.24 (m, 3H), 4.81 (q, J = 7.0 Hz, 1H), 6.11 and 6.13 (2 × s, 1 H), 6.40 (s, 1H), 7.29 and 7.33 (2 × s, 1H); ^{13}C NMR

[100.61 MHz, CD_3OD/CF_3COOD (5:1) with 1% v/v TMS as internal standard] δ 23.2 (CH_3), 31.4 (CH_2), 40.0 (CH), 42.1 (CH_2), 55.1 (CH), 65.8 (CH_2), 104.8 (CH_2), 105.6 (CH), 109.0 (CH), 117.0 (C, $^1J_{C\text{-}F}$ = 286.5 Hz), 137.1 (C), 144.9 (C), 148.7 (C), 153.7 (C), 160.7 (C), 160.8 (C, $^1J_{C\text{-}F}$ = 38.1 Hz), 170.2 (C); MS (ESI+) *m/z* (rel intensity) 402 [$(M+H)^+$, 100%], 386 (20), 224 (9), 208 (11), 151 (11); HRMS (ESI+) *m/z* calc'd for $C_{15}H_{20}N_3O_8S$ $[M+H]^+$: 402.0971, found 402.0974 (Δ = 0.7 ppm).

Storage: The dry sample of DAP amino acid **6**·TFA was stored in air-tight dark glass vials in a cold, dry and dark environment and was stable for over 3 years without decomposition.

Handling: DAP amino acid **6**·TFA is light sensitive and slightly hygroscopic upon exposure to moist air, hence the sample of it in a vial was always handled in a dark and dry atmosphere. It is noteworthy that the vial containing **6**·TFA taken out from the fridge or freezer was always allowed to warm to r.t. prior to opening and handling.

Method II (prepared from 6d):

A dry sample of (2*S*)-2-[(*tert*-butoxycarbonyl)amino]-3-{[(2-{[1-(6-nitrobenzo[*d*][1,3] dioxol-5-yl)ethyl]thio}ethoxy)carbonyl]amino}propanoic acid **6d** (26.70 g, 53.2395 mmol, 1.0 eq.) was loaded on to a dry 1 litre single-necked round-bottomed flask and dissolved in dry CH_2Cl_2 (300 mL). The flask was wrapped with aluminium foil to exclude light, and dry Et_3SiH (84.69 mL, 530.24 mmol, 10.0 eq.) was added to the solution. After 5 min, freshly distilled CF_3COOH (81.54 mL, 1.0648 mol, 20.0 eq.) was added to the solution drop-wise for 15 min. The solution turned yellow-brown and was left stirring at r.t. in the dark. After 5 h, the reaction was judged to be complete by TLC (SiO2 plate, EtOAc/CH_3COOH = 98:2) and LC-MS

analysis (C18 reverse phase column, H_2O-CH_3CN as mobile phase) and the solution was concentrated to dryness under reduced pressure to obtain a yellow-brown gum. This was dissolved in dry CH_3OH (40 mL) and evaporated to dryness under reduced pressure; this was repeated three times and product dried in high vacuum (<0.1 mbar) to remove any residual CF_3COOH, Et_3SiH and H_2O. The yellow-brown gum was dissolved in dry CH_3OH (40 mL), transferred to a dry 3 L round-bottomed flask under an argon atmosphere and cooled to 0 ^oC. Dry Et_2O (2.5 L) was added to the flask *via* cannula under a positive pressure of argon gas while the contents were vigorously stirred. A pale yellow precipitate was formed and the contents stirred vigorously at 0˚C for 15 min and then at r.t. for 2 h. The precipitate was then filtered and washed with dry Et_2O (3 × 500 mL), followed by dry *n*-hexane (150 mL). The product was dried in high vacuum (<0.1 mbar) overnight for 14 h in the dark to obtain *(2S)-2-amino-3-{[(2-{[1-(6-nitrobenzo[d][1,3]dioxol-5-yl)ethyl]thio}ethoxy)carbonyl]amino}propanoic acid TFA salt* **6** as a pale-yellow powder (20.465 g, 75%) and a mixture of ~1:1 epimers.

VlmTE substrate syntheses

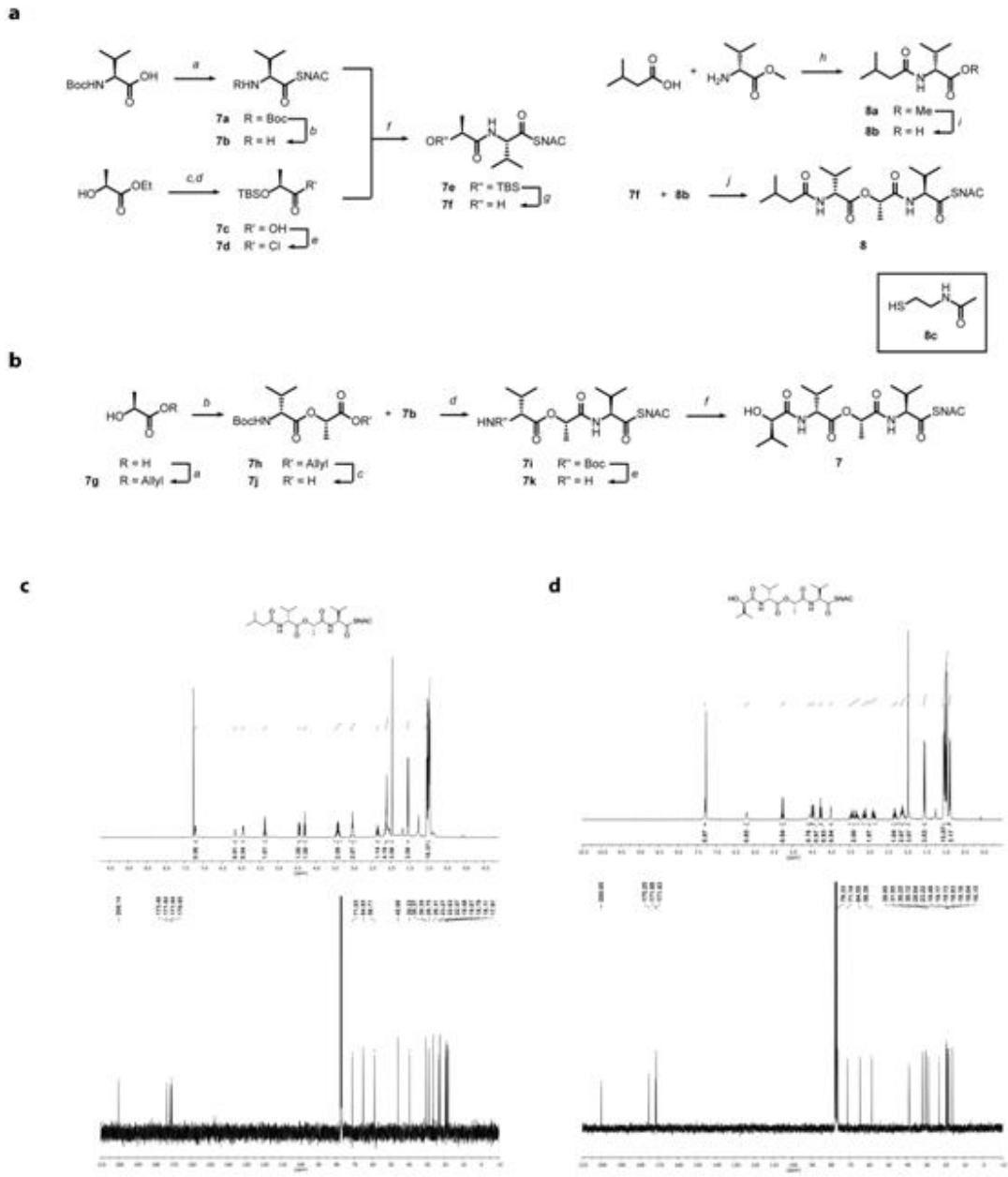

Supplementary Scheme 2: Synthesis scheme for depsipeptidyl-SNAC compounds 7 and 8.

a, Synthesis of deoxytetradepsipeptidyl-SNAC **8**. *a)* **8c**, EDC, DMAP, 72%; *b)* TFA, DCM, 99%; *c)* TBSCl, Imid., DCM; *d)* LiOH, THF, 78%, 2 steps; *e)* $(COCl)_2$, DMF, DCM; *f)* TEA, DCM, 53%; *g)* HF, Pyr., MeCN, 84%; *h)* EDC, DMAP, TEA, DCM, 60%; *i)* LiOH, MeOH, THF, 60%; *j)* EDC, DMAP, DMF, 5:4 *dr*, 92%

b, Synthesis of tetradepsipeptidyl-SNAC **7.** *a)* AllylBr, Cs_2CO_3, DMF, 95%; *b)* Boc-d-Val, EDC, DMAP, DCM, 84%; *c)* $Pd(PPh_3)_4$, Morpholine, DCM; *d)* EDC, HOBt, DIPEA, DCM, 94%; *e)* HCl, Dioxane; *f)* d-HIV, EDC, HOBt, DIPEA, DCM, 95%.

c and d, ^1H (top) and ^{13}C (bottom) NMR spectra for deoxytetradepsipeptidyl-SNAC **8 (c) and** tetradepsipeptidyl-SNAC **7 (d).**

General Synthetic Procedures.

All reagents were purchased from Sigma-Aldrich with the following exceptions: L-lactic acid was purchased from Fisher Scientific, EDC was purchased from Oakwood Chemicals (Estill, SC) at the highest available purity and used without further purification. Valinomycin was purchased from Sigma-Aldrich and BioShop Canada. All solvents were purchased from Fisher Scientific. All reactions were conducted using dry solvents under an argon atmosphere unless otherwise noted. NMR spectroscopy was performed with a Bruker AVANCE II, operating at 400 MHz for ^1H spectra, and 100 MHz for ^{13}C spectra and a Bruker AVANCE 300, operating at 300 MHz for ^1H spectra, and 75 MHz for ^{13}C spectra. High-resolution mass spectroscopy (HRMS) was conducted on a Micromass Q-TOF I for ESI measurements (John L. Holmes Mass Spectroscopy Facility).

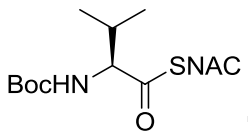

7a

(*S*)-*S*-(2-acetamidoethyl) 2-((*tert*-butoxycarbonyl)amino)-3-methylbutanethioate (7a). Boc-L-Valine (7.29 g, 33.56 mmol, 1.0 equiv.) was dissolved in CH_2Cl_2. *N*-Acetylcysteamine (4.00 g, 33.56 mmol, 1.0 equiv.). *N*-(3-dimethylaminopropyl)-*N*′-

ethylcarbodiimide hydrochloride (EDC, 7.72 g, 40.27 mmol, 1.2 equiv.) and 4-(dimethylamino)pyridine (DMAP, 410 mg, 3.36 mmol, 0.1 equiv.) were added to the mixture. The reaction was stirred for 16 h at ambient temperature. The reaction was quenched with NH_4Cl(aq) and extracted 3 × with EtOAc. The organic fractions were combined, washed with brine, dried over Na_2SO_4 and concentrated. The desired product (7.69 g, 24.16 mmol, 72 % yield) was purified with silica column chromatography (5 % MeOH in CH_2Cl_2). R_f = 0.37 (2:3 acetone:hexanes). ^{1}H NMR (400 MHz, $CDCl_3$) δ 5.95 (s, 1H), 4.97 (d, *J* = 8.8 Hz, 1H), 4.21 (dd, *J* = 8.9, 4.8 Hz, 1H), 3.48 – 3.30 (m, 2H), 3.08 – 2.94 (m, 2H), 2.22 (td, *J* = 13.4, 6.7 Hz, 1H), 1.43 (s, 9H), 0.96 (d, *J* = 6.9 Hz, 3H), 0.85 (d, *J* = 6.9 Hz, 3H). ^{13}C NMR (100 MHz, $CDCl_3$) δ 201.74, 170.35, 155.66, 80.42, 65.68, 39.38, 30.77, 28.38, 28.33, 23.16, 19.40, 17.01. HRMS (ESI+) Calculated Mass ($C_{14}H_{26}N_2O_4SNa$) 341.1511, found 341.1512..

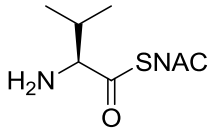

7b

(*S*)-*S*-(2-acetamidoethyl) 2-amino-3-methylbutanethioate (7b). In a round-bottom flask, **7a** (0.5 g, 1.57 mmol, 1.0 equiv.) was dissolved in CH_2Cl_2 (3 mL). The solution was cooled to 0˚C using an ice bath and trifluoroacetic acid (3 mL) was added. The reaction was allowed to proceed at ambient temperature for 45 min. The reaction mixture was concentrated and the desired product (341 mg, 1.56 mmol, >99 % yield) was purified by silica column chromatography (5 % to 10 % MeOH in CH_2Cl_2). ^{1}H NMR (300 MHz, DMSO) δ 8.45 (s, 157 2H), 8.10 (t, J = 5.5 Hz, 1H), 4.15 (d, J = 4.8 Hz, 1H), 3.27 – 3.17 (m, 2H), 3.13 – 2.98 (m, 2H), 2.28 – 2.09 (m, 1H), 0.99 (d, J =

6.9 Hz, 3H), 0.95 (d, J = 7.0 Hz, 3H). ^{13}C NMR (75 MHz, DMSO) δ 196.18, 169.35, 63.48, 37.78, 30.10, 28.40, 22.50, 18.03, 17.26.

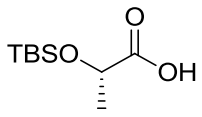

7c

(*S*)-2-((tert-butyldimethylsilyl)oxy)propanoic acid (7c). In a round-bottom flask, ethyl L-lactate (5.08 g, 43.0 mmol, 1.0 equiv.) was dissolved in CH_2Cl_2 (55 mL) and the solution was cooled to 0˚C using an ice bath. *tert*-Butyldimethylsilyl chloride (6.48 g, 45.15 mmol, 1.05 equiv.) and imidazole (3.51 g, 51.6 mmol, 1.2 equiv.) was added to this mixture, after which the reaction was allowed to proceed at ambient temperature for 2 h. The reaction mixture was then diluted with H_2O and extracted 3 × with CH_2Cl_2. The organic fractions were combined, washed with ice cold 5 % HCl(aq), washed with brine, dried over Na_2SO_4 and concentrated. The crude intermediate (*S*)-ethyl 2-(*tert*-butyldimethylsilyloxy)propanoate was dissolved in THF (215 mL). The mixture was cooled to 0˚C using an ice bath, and a cooled solution of LiOH (0.4 M, 215 mL) was added dropwise over 20 min. The reaction mixture was stirred for 4 h at ambient temperature. The resulting reaction mixture was concentrated to half its original volume, and the resulting aqueous solution was extracted 3 × with Et_2O. The organic fractions were combined and extracted 3 × with a saturated solution of $NaHCO_3$(aq). The aqueous fractions were combined, acidified to pH 4 with 1 M $KHSO_4$(aq) and extracted 3 × with Et_2O. The organic fractions were combined, dried over Na_2SO_4 and concentrated. The desired product (6.88 g, 33.7 mmol, 78 % yield over two steps) was obtained and used without further purification.

The NMR data were consistent with literature values[45]. ^{1}H NMR (300 MHz, $CDCl_3$) δ 4.36 (q, J = 6.8 Hz, 1H), 1.45 (d, J = 6.8 Hz, 3H), 0.92 (s, 9H), 0.13 (s, 6H).

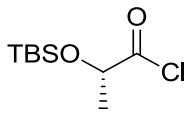

7d

(*S*)-2-((*tert*-butyldimethylsilyl)oxy)propanoyl chloride (7d). In a round-bottom flask, **7c** (3.7 g, 18 mmol, 1.0 equiv.) was dissolved in DMF (45 mL) and the solution was cooled to 0˚C using an ice bath. Oxalyl chloride (13.6 mL of a 2.0 M solution in DCM, 10.0 equiv.) and a catalytic amount of DMF were added. The reaction proceeded for 2 h from 0˚C to ambient temperature. The reaction mixture was concentrated and the crude oil was used in subsequent reactions without purification.

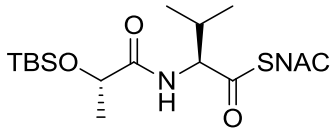

7e

TBSO-L-Lac-L-Val-SNAC (7e). In a round-bottom flask, **7b** (1.95 g, 9 mmol, 1.0 equiv.) was dissolved in CH_2Cl_2 (40 mL). The crude oil **7d** (18 mmol, 2.0 equiv.) was dissolved in CH_2Cl_2 (5 mL) and added to the mixture. Et_3N (2.5 mL, 18 mmol, 2.0 equiv.) was added and the reaction was allowed to proceed for 4 h. The reaction mixture was quenched with NH_4Cl(aq), extracted 3 × with EtOAc, washed with brine and concentrated. The desired product (1.93 g, 4.77 mmol, 53 % yield) was purified from the crude mixture by silica column chromatography (50 % to 90 % EtOAc in hexanes). ^{1}H NMR (300 MHz, $CDCl_3$) δ 7.22 (d, J = 9.3 Hz, 1H), 6.03 (s, 1H), 4.53 (dd, J = 9.3, 4.5 Hz, 1H), 4.25 (q, J = 6.7 Hz, 1H), 3.38 (q, J = 6.2 Hz, 2H), 3.07 – 2.98 (m, 2H), 2.40 – 2.21 (m, 1H), 1.93 (s, 3H), 1.38 (d, J = 159 6.7 Hz, 3H), 1.01 –

0.82 (m, 15H), 0.13 (s, 3H), 0.12 (s, 3H). ^{13}C NMR (75 MHz, $CDCl_3$) δ 200.34, 174.90, 170.47, 70.03, 63.48, 39.47, 31.04, 28.51, 25.82, 23.23, 22.04, 19.47, 18.00, 16.83, -4.54, -5.03.

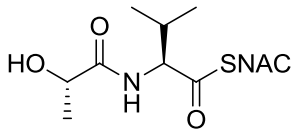

7f

HO-L-Lac-L-Val-SNAC (7f). Compound **7e** (250 mg, 0.617 mmol, 1.0 equiv.) was dissolved in acetonitrile (20 mL) in a 50 mL polypropylene Falcon tube. Pyridine (249 μL, 3.09 mmol, 5 equiv.) and HF (48 wt. % aq. 533 μL, 30.9 mmol, 50 equiv.) were added. The reaction was stirred at ambient temperature for 16 h. The reaction mixture was quenched with NH_4Cl(aq), extracted 3 × with EtOAc, washed with brine, dried over Na_2SO_4 and concentrated. The desired product (150.1 mg, 0.517 mmol, 84 % yield) was purified with silica column chromatography (2 % to 8 % MeOH in CH_2Cl_2). ^{1}H NMR (400 MHz, $CDCl_3$) δ 7.21 (d, J = 9.2 Hz, 1H), 6.20 (s, 1H), 4.54 (dd, J = 9.2, 5.4 Hz, 1H), 4.30 (q, J = 6.8 Hz, 1H), 4.15 (s, 1H), 3.52 – 3.32 (m, 2H), 3.12 – 2.94 (m, 2H), 2.36 – 2.21 (m, 1H), 1.95 (s, 3H), 1.44 (t, J = 6.3 Hz, 3H), 0.97 (d, J = 6.8 Hz, 3H), 0.91 (d, J = 6.8 Hz, 3H). ^{13}C NMR (100 MHz, $CDCl_3$) δ 200.20, 175.47, 170.94, 68.66, 63.77, 39.24, 30.90, 28.71, 23.25, 21.28, 19.45, 17.27.

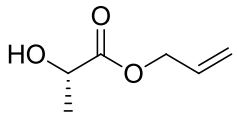

7g

(*S*)-allyl 2-hydroxypropanoate (7g). In a round bottom flask, 1 g L-lactic acid (11.11 mmol, 1 equiv.), and 3.8 g caesium carbonate (11.67 mmol, 1.05 equiv.) were

dissolved in 13 mL DMF. Allyl bromide (3.75 mL, 5.37 g, 44.44 mmol, 4 equiv.) was added dropwise at ambient temperature. Upon complete addition the reaction was stirred at ambient temperature for 48 h. At completion the excess allyl bromide was removed by rotary evaporation and the remaining solution diluted with water then extracted 3 x with Et_2O. The combined organic fractions were washed twice with water, once with brine, dried over Na_2SO_4 and concentrated to the title compound (1.47 g, 95 %) as a pale yellow oil. Characterization data is consistent with reported values[46]. ^{1}H NMR (400 MHz, $CDCl_3$) δ 5.99 – 5.82 (m, 1H), 5.40 – 5.18 (m, 2H), 4.71 – 4.59 (m, 2H), 4.29 (q, *J* = 6.9 Hz, 1H), 2.75 (s, 1H), 1.42 (d, *J* = 6.9 Hz, 3H).

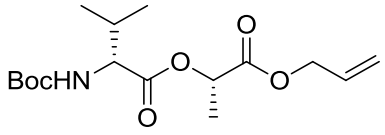

7h

(*R*)-(*S*)-1-(allyloxy)-1-oxopropan-2-yl 2-((*tert*-butoxycarbonyl)amino)-3-methylbutanoate (7h). In a round bottom flask, 1 g of **7g** (7.69 mmol, 1 equiv.) and 1.67 g of Boc-D-Val (8.46 mmol, 1.1 equiv.) were dissolved in 39 mL of CH_2Cl_2. To this solution 2.21 g EDC (11.54 mmol, 1.5 equiv.) and 1.03 g DMAP (8.46 mmol, 1 equiv.) were added at ambient temperature. The resulting solution was stirred for 20 h at ambient temperature. The reaction was quenched with NH_4Cl(aq), extracted 3 × with CH_2Cl_2, washed with $NaHCO_3$(aq), washed with brine, dried over Na_2SO_4, and concentrated. The title compound (2.12 g, 84 %) was purified by silica column chromatography (20 % EtOAc in hexanes). R_f = 0.41 (1:3 EtOAc:Hexanes) ^{1}H NMR (400 MHz, $CDCl_3$) δ 5.95 – 5.81 (m, 1H), 5.29 (dddd, *J* = 21.3, 11.7, 6.6, 1.3 Hz, 2H), 5.13 (q, *J* = 7.0 Hz, 1H), 4.97 (d, *J* = 8.9 Hz, 1H), 4.67 – 4.59 (m, 2H), 4.28 (dd, *J* = 8.9, 4.8 Hz, 1H), 2.25 – 2.11 (m, 1H), 1.50 (d, *J* = 7.1 Hz, 3H), 1.43 (s, 9H), 0.97 (d, *J* = 6.9 Hz, 3H), 0.91 (d, *J* = 6.9 Hz, 3H). ^{13}C NMR (100 MHz, $CDCl_3$) δ 171.50,

169.95, 155.56, 131.43, 118.83, 79.77, 69.17, 65.93, 58.60, 31.28, 28.32, 18.99, 17.49, 17.00. HRMS (ESI+): Exact mass calculated for $C_{16}H_{27}NNaO_6$: 352.1736. Found: 352.1721

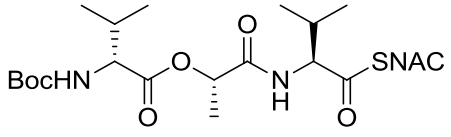

7i

Boc-D-Val-L-Lac-L-Val-SNAC (7i). In a round bottom flask, 250 mg of **7h** (0.76 mmol, 1 equiv.) was dissolved in 4 mL of CH_2Cl_2 under a nitrogen atmosphere. To this solution 86 μL of morpholine (87 mg, 0.99 mmol, 1.3 equiv.) and 62 mg of $Pd(PPh_3)_4$ was added in a single portion. The reaction was stirred at ambient temperature and monitored by TLC. At completion the reaction was quenched by the addition of 10 % aq. HCl, the organic layer was removed and the remaining aqueous fraction was extracted 3 x with CH_2Cl_2. The combined organic fractions were washed with brine, dried over Na_2SO_4 and concentrated, this intermediate, **7j**, was used immediately in the subsequent reaction. To a flame dried round bottom flask was added 194 mg of **7b** (as HCl salt, 0.76 mmol, 1 equiv.) and the crude **7j** (0.76 mmol, 1 equiv.) in 4 mL of CH_2Cl_2. To the resulting solution was added 400 μL of Hünig's base (295 mg, 2.28 mmol, 3 equiv.), 154 mg HOBt (1.14 mmol, 1.5 equiv.) and 220 mg EDC (1.14 mmol, 1.5 equiv.). The reaction was stirred under argon at ambient temperature for 20 h. The reaction was quenched with NH_4Cl(aq), extracted 3 × with CH_2Cl_2, washed with $NaHCO_3$(aq), then with brine, dried over Na_2SO_4, and concentrated. The title compound (350 mg, 94 % over 2 steps) was purified by silica column chromatography (40 % acetone in hexanes). R_f = 0.35 (2:3 acetone:hexanes) ^{1}H NMR (400 MHz, $CDCl_3$) δ 7.08 (d, *J* = 8.2 Hz, 1H), 6.07 (s, 1H), 5.38 (q, *J* = 6.8

Hz, 1H), 5.02 (d, *J* = 7.0 Hz, 1H), 4.46 – 4.39 (m, 1H), 3.99 (t, *J* = 6.9 Hz, 1H), 3.45 – 3.30 (m, 2H), 3.11 – 2.89 (m, 2H), 2.30 (dq, *J* = 13.4, 6.7 Hz, 1H), 2.11 – 2.01 (m, 1H), 1.92 (s, 3H), 1.49 (d, *J* = 6.9 Hz, 3H), 1.39 (s, 9H), 1.01 – 0.91 (m, 12H). ^{13}C NMR (100 MHz, $CDCl_3$) δ 200.14, 171.72, 170.89, 170.48, 155.92, 80.45, 70.58, 64.74, 59.74, 39.30, 30.47, 30.27, 28.46, 28.26, 23.10, 19.33, 18.90, 18.49, 17.85, 17.53. HRMS (ESI+): Exact mass calculated for $C_{22}H_{39}N_3NaO_7S$: 512.2406. Found: 512.2391

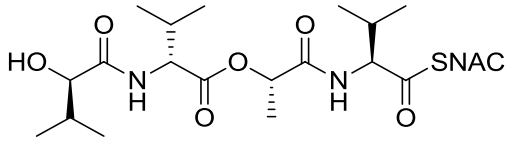

7

HO-D-Hiv-D-Val-L-Lac-L-Val-SNAC (7). To a round bottom flask was added 118 mg **7i** (0.24 mmol, 1 equiv.) in a minimal amount of THF and this was cooled to 0˚C. To this was added 1 mL of 4 M HCl in dioxane (Sigma), and the reaction allowed to warm to ambient temperature. The reaction was monitored by TLC and at completion all solvent was removed by rotary evaporation. The unpurified intermediate **7k** was used immediately in the subsequent reaction. Intermediate **7k** was dissolved in 2 mL of CH_2Cl_2 and to this was added sequentially 125 μL of Hünig's base (93 mg, 0.72 mmol, 3 equiv.), 32 mg of D-α-hydroxyisovaleric acid (0.27 mmol, 1.1 equiv.), 49 mg HOBt (0.36 mmol, 1.5 equiv.), and 70 mg EDC (0.36 mmol, 1.5 equiv.). The reaction was stirred at ambient temperature for 24 h and at completion was quenched with NH_4Cl(aq), extracted 5 × with CH_2Cl_2, washed with $NaHCO_3$(aq), then with brine, dried over Na_2SO_4, and concentrated. The title compound (111 mg, 95%) was purified by silica column chromatography (50 % Acetone in hexanes). ^{1}H NMR (300 MHz, $CDCl_3$) δ 7.29 (s, 1H), 6.20 (t, J = 5.7 Hz, 1H), 5.26 (q, J = 7.0 Hz, 1H), 4.55 (br, 1H),

4.47 (dd, J = 9.0, 6.5 Hz, 1H), 4.26 (t, J = 7.7 Hz, 1H), 3.99 (d, J = 2.9 Hz, 1H), 3.52 – 3.25 (m, 2H), 2.99 (ddt, J = 20.4, 13.3, 6.5 Hz, 2H), 2.39 – 2.25 (m, 1H), 2.20 – 2.06 (m, 2H), 1.97 (s, 3H), 1.54 (d, J = 7.0 Hz, 3H), 1.06 – 0.93 (m, 15H), 0.88 (d, J = 6.9 Hz, 3H). ^{13}C NMR (75 MHz, $CDCl_3$) δ 200.05, 175.25, 171.69, 171.43 (2C), 76.33, 71.14, 64.55, 58.39, 38.95, 31.95, 30.25, 30.12, 28.64, 23.22, 19.49, 19.17, 19.13, 18.83, 18.18, 18.04, 16.15. HRMS (ESI+): Exact mass calculated for $C_{22}H_{39}N_3NaO_7S$: 512.2401. Found: 512.2406

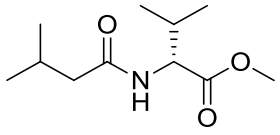

8a

(*R*)-methyl 3-methyl-2-(3-methylbutanamido)butanoate (8a). In a round-bottom flask, D-valine methyl ester hydrochloride (250 mg, 1.5 mmol, 1.0 equiv.) was dissolved in CH_2Cl_2 (15 mL). Isovaleric acid (230 mg, 2.25 mmol, 1.5 equiv.), EDC (430 mg, 2.25 mmol, 1.5 equiv.), DMAP (276 mg, 2.25 mmol, 1.5 equiv.), and Et_3N (420 μL, 3.00 mmol, 2.0 equiv.) were added and the reaction was allowed to mix at ambient temperature for 16 h. The reaction was quenched with NH_4Cl(aq), extracted 3 × with CH_2Cl_2, washed with $NaHCO_3$(aq), washed with brine, dried over Na_2SO_4, and concentrated. The desired compound (193.7 mg, 0.90 mmol, 60 % yield) was purified by silica column chromatography (20 to 50 % EtOAc in hexanes). ^{1}H NMR (400 MHz, $CDCl_3$) δ 5.96 (d, J = 8.0 Hz, 1H), 4.57 (dd, J = 8.8, 4.9 Hz, 1H), 3.71 (s, 3H), 2.19 – 2.04 (m, 4H), 0.97 – 0.86 (m, 12H). ^{13}C NMR (100 MHz, $CDCl_3$) δ 172.85, 172.49, 56.91, 52.19, 46.14, 31.35, 26.29, 22.56, 22.53, 19.07, 17.93

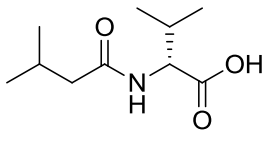

8b

(*R*)-3-methyl-2-(3-methylbutanamido)butanoic acid (8b). In a round-bottom flask, **8a** (180 mg, 1.2 mmol, 1.0 equiv.) was dissolved in MeOH (24 mL) and THF (24 mL) and the solution was cooled to 0˚C using an ice bath. LiOH (1 M, 24 mL) was added dropwise and the solution was allowed to proceed from 0˚C to ambient temperature over 4 h. The solution was concentrated to one-third volume and the resulting aqueous solution was acidified to pH 3 with 10 % HCl. The solution was extracted 3 × with CH_2Cl_2, dried over Na_2SO_4 and concentrated. The desired product (145 mg, 0.72 mmol, 60 % yield) was purified by silica column chromatography (5 % MeOH in CH_2Cl_2 + 0.5 % acetic acid). ^{1}H NMR (300 MHz, MeOD) δ 4.32 (d, J = 5.8 Hz, 1H), 2.23 – 2.01 (m, 4H), 1.01 – 0.92 (m, 12H). ^{13}C NMR (75 MHz, MeOD) δ 175.84, 174.93, 59.00, 45.90, 31.53, 27.50, 22.76, 22.72, 19.65, 18.41.

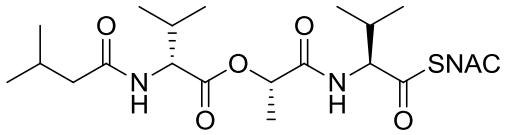

A

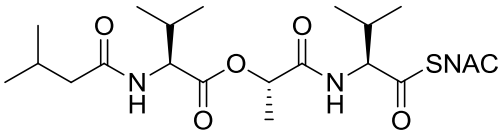

B

8(A) and 8c (B)

(*R*)-(*S*)-1-(((*S*)-1-((2-acetamidoethyl)thio)-3-methyl-1-oxobutan-2-yl)amino)-1-oxopropan-2-yl 3-methyl-2-(3-methylbutanamido)butanoate (8). In a round bottom flask, the alcohol **7f** (25.2 mg, 0.087 mmol, 1.0 equiv.) and carboxylic acid **8b** (35 mg, 0.174 mmol, 2.0 equiv.) were dissolved in DMF (1 mL). The solution was

cooled to –20˚C using a dry ice / acetone bath and EDC (67 mg, 0.35 mmol, 4.0 equiv.) and DMAP (21 mg, 0.174 mmol, 2.0 equiv.) were added. The mixture was allowed to warm to ambient temperature and the reaction proceeded for 16 h. The reaction was quenched with NH_4Cl(aq) and extracted 3 × with EtOAc. The organic fractions were combined, washed with brine, dried over Na_2SO_4 and concentrated. A mixture of C-2.2 diastereomers (37.9 mg, 0.08 mmol, 92 % yield) in a 5:4 ratio (A : B) was purified from the crude residue by silica column chromatography (1 % to 5 % MeOH in CH2Cl2). The diastereomers were separated with preparatory-TLC. **8 (A)** ^{1}H NMR (400 MHz, $CDCl_3$) δ 7.21 (d, J = 8.2 Hz, 1H), 6.15 (s, 1H), 5.93 (d, J = 6.8 Hz, 1H), 5.35 (q, J = 7.0 Hz, 1H), 4.44 167 (dd, J = 8.3, 6.4 Hz, 1H), 4.29 (t, J = 7.0 Hz, 1H), 3.50 – 3.32 (m, 2H), 3.08 – 2.95 (m, 2H), 2.41 – 2.29 (m, 1H), 2.19 – 2.00 (m, 4H), 1.96 (s, 3H), 1.53 (d, J = 6.9 Hz, 3H), 1.05 – 0.92 (m, 18H). ^{13}C NMR (100 MHz, $CDCl_3$) δ 200.14, 173.48, 171.62, 171.04, 170.65, 71.03, 64.93, 58.71, 45.66, 39.33, 30.37, 30.35, 28.75, 26.31, 23.27, 22.63, 22.57, 19.48, 19.07, 18.79, 18.11, 17.91. **8c (B)** ^{1}H NMR (400 MHz, $CDCl_3$) δ 6.95 (d, J = 8.7 Hz, 1H), 6.04 (s, 1H), 5.81 (d, J = 7.2 Hz, 1H), 5.25 (q, J = 6.8 Hz, 1H), 4.54 (dd, J = 8.8, 5.9 Hz, 1H), 4.49 (dd, J = 7.3, 4.7 Hz, 1H), 3.47 – 3.36 (m, 2H), 3.11 – 2.98 (m, 2H), 2.38 – 2.26 (m, 2H), 2.20 – 2.09 (m, 3H), 1.95 (s, 3H), 1.51 (d, J = 6.9 Hz, 3H), 1.04 (d, J = 6.9 Hz, 3H), 0.99 (dd, J = 6.7, 2.5 Hz, 12H), 0.94 (d, J = 6.8 Hz, 3H). ^{13}C NMR (100 MHz, $CDCl_3$) δ 199.74, 173.66, 170.84, 170.68, 170.49, 71.63, 64.29, 57.90, 46.06, 39.32, 30.72, 30.55, 28.91, 26.35, 23.30, 22.64, 22.57, 19.42 (2C), 18.16, 17.94, 17.70. HRMS (ESI+): Exact mass calculated for $C_{22}H_{39}N_3NaO_6S$: 496.2452. Found: 496.2457

Cloning, expression and purification of Vlm TE constructs

A codon-optimized construct containing *vlm2*$_{PCP4\text{-}TE}$(encoding residues 2290-2655 of Vlm2 from *Streptomyces tsusimaensis*, GenBank: ABA59548.1) was synthesized by ATUM (formerly DNA 2.0) in a *pJExpress411* vector, with an N-terminal hexahistidine tag followed by a tobacco etch virus protease (TEV) cleavage recognition sequence (*pJExpress411-vlm2-PCP4-TE*$_{wt}$). Two BamHI recognition sequences were included in *pJExpress411-vlm2-PCP4-TE*$_{wt}$, at nucleotide positions 2024-2025 and 2267-2268. Digestion with BamHI followed by ligation with T4 DNA ligase (New England Biolabs) excised the PCP4 domain sequence, yielding the plasmid *pJExpress411-vlm2-TE*$_{wt}$ which encodes residues 2368-2655 of Vlm2. To generate an expression vector for $TE_{DAP,}$ the TE_{wt} coding sequence was PCR-amplified from *pJExpress411-vlm2-TE*$_{wt}$ with primers TE_for_pNHD_fw and TE_for_pNHD_rev. The PCR product was digested with *NdeI* and *XhoI* and ligated into similarly digested pNHD plasmid using T4 DNA ligase, generating plasmid *pNHD-vlm2-TE*$_{wt}$. Next, an amber stop codon was introduced in place of the codon for serine 2463 by site-directed mutagenesis using primers Vlm2_TE_Amb_Fw and Vlm2_TE_Amb_Rev, generating *pNHD-vlm2-TE*$_{amber2463}$.

TE domains were heterologously expressed in *E. coli* BL21(DE3) cells transformed with *pJExpress411-vlm2-TE*$_{wt}$ (TE_{wt}) or co-transformed with *pNHD-Vlm2-TE*$_{amber2463}$ and pSF-DAP5RS-PylT (TE_{DAP}). Cultures expressing TE_{wt} were grown in LB media supplemented with 17 mg L^{-1} of kanamycin. Those expressing TE_{DAP} were grown in TB media supplemented with 25 mg L^{-1} of kanamycin, 12.5 mg L^{-1} of tetracycline, 0.1 mM of **6** (a 100 mM stock solution of **6** was prepared in 0.4 M NaOH, added to the culture and neutralised using 5 M HCl). Cultures were incubated at 37˚C, with agitation at 220 r.p.m, until they reached an OD_{600nm} = 0.6, after which they were

incubated at 16˚C for 30 min, and then expression was induced with 100 μM IPTG. Cultures were incubated for an additional 16 hours at 16˚C before harvesting by centrifugation at 5000 *g* for 20 min. Cell pellets were stored at -80˚C.

For protein purification, cell pellets of TE_{wt} were resuspended in 5 mL of buffer wt-A (50 mM TRIS pH 7.4, 150 mM NaCl, 50 mM imidazole, 2 mM β-mercaptoethanol [βME]) plus DNAseI (Bioshop) per g of wet cells, and lysed by sonication. Lysate was clarified by centrifugation at 40 000 *g* for 20 min. Clarified lysate was applied to two 5 mL HiTrap IMAC FF (GE Healthcare Life Sciences) columns connected in series on an AKTA Prime system (GE Healthcare Life Sciences). Bound protein was eluted with buffer wt-B (buffer wt-A plus 150 mM imidazole). Fractions containing TE_{wt} (as determined by SDS-PAGE analysis) were pooled and incubated with TEV protease in a 1:100 (Te:TEV) mass/mass ratio and dialyzed against buffer wt-C (50 mM TRIS pH 7.4, 10 mM NaCl, 2 mM βME) for 16 hours at 4˚C. The dialyzed sample was applied to two 5 mL HiTrap IMAC FF columns connected in series, pre-equilibrated in buffer wt-A. Cleaved protein was recovered from the flow through and applied to two 5 mL HiTrap Q HP columns connected in series, pre-equilibrated in buffer Q-A (50 mM TRIS pH 7.4, 10 mM NaCl, 2 mM βME). Protein was eluted by a gradient of 0 to 100% buffer Q-B (50 mM TRIS pH 7.4, 500 mM NaCl, 2 mM βME) over 240 mL. TE_{wt}-containing fractions were concentrated in a 10 kDa molecular weight cut off Amicon® Ultra centrifugal filter (Millipore) and injected onto a Superdex S-200 16/60 PG column (GE-Healthcare) pre-equilibrated in SEC buffer (25 mM HEPES pH 7.4 or pH 8.0, 100 mM NaCl, 0.2 mM tris(2-carboxyethyl)phosphine [TCEP]). Fractions containing purified TE_{wt} were pooled, concentrated and flash frozen.

Cell resuspension, lysis, clarification and Ni-IMAC purification for TE_{DAP} were performed as described for Te_{wt}, except that prolonged exposure to light was avoided. After elution from the Ni-IMAC column, the sample was irradiated with UV light (365 nm, 35 $mWcm^{-2}$, 1 min). TEV cleavage and the subsequent IMAC column were performed as described for TE_{wt}, except that a 1:1 TE:TEV ratio was used. Anion exchange was performed as described for $Te_{wt,}$ except that 25 mM HEPES replaced TRIS as the buffer and 0.2 mM TCEP replaced βME as the reducing agent in the mobile phases. Relevant fractions were concentrated and injected onto a Superdex S-75 10/300 column pre-equilibrated in buffer T (25 mM HEPES pH 8.0, 100 mM NaCl, 0.2 mM TCEP). Fractions containing purified TE_{DAP} were pooled, concentrated, and immediately used for further experiments. The yield of purified TE_{wt} was 30-60 mg per L, the yield of purified TE_{DAP} was 0.1-0.5 mg per L.

Crystallography

Crystallization conditions for TE_{wt} structure 1 were found in vapour diffusion crystallization trials using commercially available screens (Qiagen) and a protein concentration of 10 mg mL^{-1}. Optimization of an initial crystallization hit in 24-well plates led to a final crystallization condition where 3.2 µL of 10 mg mL^{-1} TE_{wt}, 4.0 µL 1.65 M DL-malic acid pH 9.5, and 0.8 µL of 17 % m/v IPTG were incubated against a reservoir solution of 500 µL of 1.65 M DL-malic acid pH 9.5. TE_{wt} structure 2 crystals were grown in similar conditions, where 0.5 µL of purified TE_{wt} at 22.4 mg mL^{-1} and 0.5 µL of 1.65 M DL-malic acid pH 8.1 were incubated against a reservoir solution of 500 µL of DL-malic acid pH 8.1. Crystals appeared between 24 and 48 hours and reached their maximum size in approximately one week.

Crystals of unliganded TE_{DAP} were grown in similar conditions to TE_{wt}, with a reservoir solution of 1.65 M DL-malic acid pH 8.0. In order to obtain the tetradepsipeptidyl-TE_{DAP} complex structure, TE_{DAP} crystals were incubated with deoxytetradepsipeptidyl-SNAC **8** once they achieved their maximum size. The reservoir solution was exchanged to 2.66 M DL-malic acid, pH 9.5, and 32 μL of a solution of 1 mM deoxytetradepsipeptidyl-SNAC**,** 2.66 M DL-malic acid pH 9.5, 100 mM NaCl, 25 mM HEPES pH 9.2, 10% DMSO was added to the drop. Crystals were incubated in this condition for 9 days at room temperature.

For dodecadepsipeptidyl-TE_{DAP} complex crystals, TE_{DAP} (0.1 mg mL^{-1}) was incubated in a 1.1 mg mL^{-1} suspension of valinomycin in buffer T for 16 hours at room temperature. The sample was centrifuged at 20 000 *g* and applied to a Superdex S-75 10/300 column preequilibrated in buffer T to remove excess valinomycin. Relevant fractions were pooled and complex formation was evaluated by LC-ESI-MS (see below). The sample was concentrated to 13.4 mg mL^{-1} and diffraction-quality crystals, with a different morphology from the TE_{wt} crystals, were obtained in sitting drops consisting of 1 μL of dodecadepsipeptidyl-TE_{DAP} complex plus 1 μL reservoir solution (1.30 to 1.45 M DL-malic acid pH 8.1) equilibrated against 500 μL reservoir solution. In an attempt to improve the occupancy of the ligand, a subset of these crystals were further incubated with valinomycin, by addition of 20 μL of a solution containing 555 μM valinomycin, 2 M DL-malic acid pH 8.1, 11 mM HEPES pH 8.0, 44 mM NaCl, 0.088 mM TCEP for 24 hours.

TE_{wt} and dodecadepsipeptidyl-TE_{DAP} crystals were cryo-protected by addition of 10 μL (TE_{wt} structure 1 and dodecadepsipeptidyl-TE_{DAP}) or 20 μL (TE_{wt} structure 2) 3.6 M DL-malic acid pH 8.1 to the crystallization drop. For dodecadepsipeptidyl-Te_{DAP} crystals that had been incubated with valinomycin, the drop solution was removed and replaced by 10 μL of 3.6 M DL-malic acid. Crystals were equilibrated for at least two minutes and then flash cooled in liquid nitrogen. Tetradepsipeptidyl-TE_{DAP} complex crystals were looped and flash cooled directly from the incubating solution. TE_{wt} data were first collected at the Centre for Structural Biology at McGill University, Montreal, Canada, on a Rigaku RUH3R generator and a R-AXIS IV++ detector. Higher resolution data for TE_{wt} and depsipeptidyl-TE_{DAP} complexes were collected at the Canadian Light Source (CLS) 08ID-1 beamline or at the Advanced Photon Source (APS) NE-CAT 24-ID-C beamline using a Pilatus detector (**App. 1, Table 1**).

TE_{wt} structure determination

Diffraction data from TE_{wt} structure 1 crystals were indexed and integrated in the space group P432 using iMosflm [47] or DIALS [48]. Further space group determination and scaling were performed using the programs POINTLESS and SCALA [49]. The structure was solved by molecular replacement using PHASER [50], with a SCULPTOR [51] modified version of the TE domain of srfA-C (PDB ID 2VSQ) [52] as a search model. The structure was iteratively refined and built with the programs Phenix [53] and AUTOBUILD [54]. Coot [55] was used for iterative model building. Topology diagrams were generated using TopDraw [56] based on results from PDBsum generate (http://www.ebi.ac.uk/thornton-srv/databases/pdbsum/Generate.html) using the TE_{wt} structure as input.

Diffraction data sets collected from dodecadepsipeptidyl-TE_{DAP} complex crystals were indexed into either P1 or H3 space groups using iMosflm [47] or DIALS [48]. Most crystals belonging to the H3 group showed evidence of twinning, and only non-twinned diffraction data were used for structure determination. Structures in both the P1 and H3 space groups were solved by molecular replacement using PHASER[50], with the TE_{wt} structure lacking residues 2500-2647 used as a search model. The P1 structure had six molecules in the asymmetric unit whereas the H3 structure contained 2 molecules in the asymmetric unit. All depsipeptidyl-TE_{DAP} models were refined, and mF_o-F_c maps were generated before depsipeptide residues were built in the model (**Fig. 4.7c,d and App. 1, Fig. 8**). Depsipeptides were built from individual monomers of the PDB Chemical Component Dictionary (DPP, VAL, 2OP, DVA, VAD). Monomer libraries and restraints for the links between the monomers (namely DPP -> VAL, VAL -> 2OP, 2OP -> DVA, DVA -> VAD and VAD -> VAL) were calculated using AceDRG[57] and merged using LIBCHECK[58]. The resulting merged dictionary was then used for substrate building in Coot[55] and refinement in REFMAC5[59] and phenix.refine[53]. Final statistics are shown in **App. 1, Table 1**.

Depsipeptidyl-TE complex formation

TE_{DAP} or TE_{wt} at a final concentration of 0.2 mg mL^{-1} was incubated with tetradepsipeptidyl-SNAC **7** (1.7 mM), or valinomycin (50 μM) in buffer T containing 1.7% or 1% v/v DMSO for 16 hours. Reactions were concentrated in a 10 kDa molecular weight cut off Amicon® Ultra centrifugal filter (Millipore), clarified by centrifugation at 20 000 *g* and applied to a Superdex S-75 10/300 column pre-equilibrated in buffer T to remove excess depsipeptidyl-SNACs or valinomycin before final LC-ESI-MS analysis. To form the deoxytetradepsipeptidyl-TE_{DAP}

complex, TE_{DAP} at a final concentration of 8.7 mg mL^{-1} was incubated with deoxytetradepsipeptidyl-SNAC **8** (2.6 mM) in 25 mM HEPES pH 8.6, 100 mM NaCl, 3.8% v/v DMSO for 40 hours. The sample was diluted in 100 mM ammonium bicarbonate pH 8.0 before final LC-ESI-MS analysis. All incubations were performed at room temperature.

LC-ESI-MS analysis of intact proteins

For experiments shown in **Figure 4.5c**, **App. 1, Fig. 7c**, protein samples were subjected to a liquid chromatography (LC) system (Agilent 1200 series) followed by in-line electrospray ionization mass spectrometry (ESI-MS) on a 6130 Quadrupole spectrometer. Using a Jupiter 5µ C4 300A column, 150 mm x 2.00 mm (Phenomenex), proteins were run through the LC system using water with 0.1% (v/v) formic acid (solvent A) and a gradient (10% to 75% in 6 min and 75% to 95% in 1,5 min) of acetonitrile with 0.1% (v/v) formic acid (solvent B). Proteins were detected by monitoring UV absorbance at 200 and 280 nm. Protein masses were calculated by deconvolution from the MS acquisition in positive ion mode, using the OpenLAB CDS software (Agilent Technologies).

For experiments shown in **Figure 4.7a,b, App. 1, Fig. 6d, 7c,d,** protein concentration was adjusted to 0.1 mg mL^{-1} in buffer T, and 16 uL was injected onto an Agilent PLRP-S (1000 A 5 µM, 50 x 2.1 mm ID) column pre-equilibrated in 95% mobile phase A (0.1% formic acid in water) and 5% mobile phase B (0.1% formic acid in 100% acetonitrile) on an Agilent Technologies 1260 Infinity HPLC system coupled to a Bruker Amazon Speed ETD ion trap mass spectrometer. MS data was collected with ExtremeScan mass range mode in positive ion polarity, scan range from 50 to 3000

m/z, accumulation time of 1586 µs, RF level of 96%, trap drive 69.8, PSP target Mass 922 m/z, and averaging over 5 spectra. External instrument calibration was performed using the Agilent ESI tune mix. The column compartment temperature was set up at 80˚C throughout the run. After injection, the column was washed for 5 minutes in initial HPLC conditions with the sample compartment diversion valve in the waste position. Next, a 5-minute gradient from 5% to 100% mobile phase B was performed, followed by an isocratic step of 100% mobile phase B for 8 minutes. Proteins were detected by monitoring UV absorbance at 280 nm. Data was analyzed using the Bruker DataAnalysis software (Bruker). Mass spectra were integrated from 10.5 to 13 minutes, and deconvoluted using a window between 10 000 to 40 000 m/z.

Tandem MS/MS analysis

Proteins were run on 4-12% NuPAGE Bis-Tris gel (Invitrogen) with MES buffer and briefly stained using InstantBlue (Expedeon). The bands were excised and stored in 20 mM Tris pH 7.4. Tryptic digestion and tandem MS/MS analyses were performed by Kate Heesom (Proteomics Facility, University of Bristol).

LC-ESI-MS analysis of Vlm TE reaction products

Purified TE_{wt} or TE_{DAP} at 0.2 mg mL^{-1} (6.5 µM) was incubated with tetradepsipeptidyl-SNAC **7** (1.7 mM), or a mix of tetradepsipeptidyl-SNAC **7** and deoxytetradepsipeptidyl-SNAC **8** (1.7 mM each) in buffer T. Samples were incubated at room temperature for 24 hours, and then quenched with one volume of 0.1% formic acid in acetonitrile. Next, samples were centrifuged at 20,000 *g*, flash frozen in liquid nitrogen and stored at -80˚C before HPLC analysis. For HPLC-MS analysis, frozen samples were thawed at room temperature, vortexed and clarified by centrifugation at

20,000 *g* before injection. HR-LC-ESI-MS was performed at the Mass Spectroscopy Facility (Department of Chemistry, McGill University) with an Agilent XDB-C8 (5 μm, 4.6 x 150 mm) column in a Dionex Ultimate 3000 UHPLC system coupled to a Bruker maXis impact QTOF mass spectrometer in positive ESI mode. Ion-trap LC-ESI-MS analysis was performed in an Agilent Technologies 1260 Infinity HPLC system coupled to a Bruker Amazon Speed ETD ion trap mass spectrometer in positive ESI mode. The column compartment was set up at 40˚C throughout the runs. Starting HPLC conditions were 50% mobile phase A (0.1% formic acid in H_2O), 50% mobile phase B (0.1% formic acid in acetonitrile). After injection (1μL for HR-LC-ESI-MS and 5 μL for ion-trap LC-ESI-MS), a gradient from 50% to 98% mobile phase B in 5 minutes was performed, followed by an isocratic step of 98% mobile phase B, run for 20 minutes. For HR-LC-ESI-MS, internal calibration was performed with an intra-run infusion at the beginning of the first analysis using Na^+ formate, and the resulting calibration was used as an external calibration for subsequent analysis. Ion trap external calibration was performed using the Agilent ESI tune mix. Data was analyzed using the Bruker DataAnalysis software and the SmartFormula tool (Bruker).

Statistics and Reproducibility

Supplementary Table 2: Smart formula analysis of the reactions shown Fig. 4.6a (a) and App. 1, Fig. 5j (b). Experiment on Fig. 3a was replicated twice with similar results. HR-MS analysis of experiment **App. 1, Fig. 5j** was done once.

a. TE_{wt}+tetradepsipeptidyl-SNAC **7.**

Molecule	Adduct	Meas. m/z	#	Ion Formula	m/z	err [ppm]	Mean err [ppm]	rdb	N-Rule	eØ Conf	mSigma	Std I
tetradepsipeptidyl-SNAC **7**	H^+	490.2593	1	C22H40N3O7S	490.2581	-2.4	-3.4	4.5	ok	even	32.2	66.4
	$[NH_4]^+$	507.2878	1	C22H43N4O7S	507.2847	-6.1	1681	3.5	ok	even	50.2	108.7
	Na^+	512.2414	1	C22H39N3NaO7S	512.2401	-2.6	-4.4	4.5	ok	even	33.7	67.6
tetradepsipeptide **9**	H^+	389.2296	1	C18H33N2O7	389.2282	-3.5	-4.4	3.5	ok	even	32.5	59.9
	$[NH_4]^+$	406.2571	1	C18H36N3O7	406.2548	-5.7	1018	2.5	ok	even	24	48.7
	Na^+	411.2120	1	C18H32N2NaO7	411.2102	-4.6	-5.2	3.5	ok	even	21.6	38.1
octadepsipeptidyl-SNAC **11**	H^+	860.4695	1	C40H70N5O13S	860.4685	-1.1	-2.8	8.5	ok	even	35.4	55.8
	$[NH_4]^+$	877.4972	1	C40H73N6O13S	877.4951	-2.4	-0.7	7.5	ok	even	29.5	44
	Na^+	882.4508	1	C40H69N5NaO13S	882.4505	-0.4	-2.1	8.5	ok	even	32.9	52.4
octadepsipeptide **13**	H^+	759.4409	1	C36H63N4O13	759.4386	-3	-3.8	7.5	ok	even	30.4	44.7
	$[NH_4]^+$	776.4686	1	C36H66N5O13	776.4652	-4.5	-2.3	6.5	ok	even	19.4	26.7
	Na^+	781.4227	1	C36H62N4NaO13	781.4206	-2.7	-3.8	7.5	ok	even	28.1	42.1
dodecadepsipeptidyl-SNAC **15**	H^+	1230.6842	1	C58H100N7O19S	1230.6789	-4.3	-5.8	12.5	ok	even	38.3	44
	$[NH_4]^+$	1247.7096	1	C58H103N8O19S	1247.7055	-3.3	-4.4	11.5	ok	even	34.5	40.2
	Na^+	1252.6680	1	C58H99N7NaO19S	1252.6609	-5.7	-6.7	12.5	ok	even	44.5	49.8
16-mer depsipeptidyl-SNAC **19**	H^+	1600.9055	1	C76H130N9O25S	1600.8893	-10.1	799.8	16.5	ok	even	89.4	107.7
	$[NH_4]^+$	1617.9319	1	C76H133N10O25S	1617.9159	-9.9	790.7	15.5	ok	even	91.4	110.2
	Na^+	1622.8891	1	C76H129N9NaO25S	1622.8713	-11	788.5	16.5	ok	even	92	110.5
montanastatin **27**	H^+	741.4309	1	C36H61N4O12	741.4281	-3.8	644.9	8.5	ok	even	22.2	36.8
	$[NH_4]^+$	758.4574	1	C36H64N5O12	758.4546	-3.7	628.9	7.5	ok	even	25.7	41.9
	Na^+	763.4120	1	C36H60N4NaO12	763.4100	-2.6	-5.4	8.5	ok	even	29.3	43.7
valinomycin **28**	$[NH_4]^+$	1128.6673	1	C54H94N7O18	1128.6650	-2.1	0.7	11.5	ok	even	78.2	72.3

b. TE_{wt}+tetradepsipeptidyl-SNAC **7**+ deoxytetradepsipeptidyl-SNAC **8**

Molecule	Adduct	Meas. m/z	#	Ion Formula	m/z	err [ppm]	Mean err [ppm]	rdb	N-Rule	eØ Conf	mSigma	Std I
tetradepsipeptidyl-SNAC **7**	H^+	490.2607	1	C22H40N3O7S	490.2581	-5.2	-10.1	4.5	ok	even	17	35.1
	$[NH_4]^+$	507.2884	1	C22H43N4O7S	507.2847	-7.3	15.7	3.5	ok	even	25.7	38.4
	Na^+	512.2408	1	C22H39N3NaO7S	512.2401	-1.3	-3.5	4.5	ok	even	33.1	67
deoxytetradepsipeptidyl-SNAC **8**	H^+	474.2649	1	C22H40N3O6S	474.2632	-3.5	-7.9	4.5	ok	even	34.5	49.2
	$[NH_4]^+$	496.2462	1	C22H39N3NaO6S	496.2452	-2	-7	4.5	ok	even	29.9	61.8
tetradepsipeptide **9**	H^+	389.2307	1	C18H33N2O7	389.2282	-6.2	5.6	3.5	ok	even	7.6	12.1
	$[NH_4]^+$	406.2565	1	C18H36N3O7	406.2548	-4.1	19	2.5	ok	even	97	158.9
	Na^+	411.2126	1	C18H32N2NaO7	411.2102	-5.9	3.2	3.5	ok	even	7.9	12.8
deoxyoctadepsipeptide **10**	H^+	743.4482	1	C36H63N4O12	743.4437	-6	-7.5	7.5	ok	even	34.4	55.6
	$[NH_4]^+$	760.4719	1	C36H66N5O12	760.4702	-2.2	627.4	6.5	ok	even	39.4	52.3
	Na^+	765.4321	1	C36H62N4NaO12	765.4256	-6.6	622.1	7.5	ok	even	39.7	51.7
octadepsipeptidyl-SNAC **11**	H^+	860.4731	1	C40H70N5O13S	860.4685	-5.4	-21.3	8.5	ok	even	128.9	140.4
	$[NH_4]^+$	877.5009	1	C40H73N6O13S	877.4951	-6.6	-7	7.5	ok	even	26.4	37.9
	Na^+	882.4517	1	C40H69N5NaO13S	882.4505	-1.4	-4.1	8.5	ok	even	26.8	42
deoxyoctadepsipeptidyl-SNAC **12**	H^+	844.4781	1	C40H70N5O12S	844.4736	-5.2	-9.3	8.5	ok	even	28.4	46.5
	$[NH_4]^+$	861.5006	1	C40H73N6O12S	861.5002	-0.5	-7.1	7.5	ok	even	27.1	41.4
	Na^+	866.4591	1	C40H69N5NaO12S	866.4556	-4	-9.3	8.5	ok	even	30.1	48.4
octadepsipeptide **13**	H^+	759.4466	1	C36H63N4O13	759.4386	-10.5	-25.8	7.5	ok	even	354.4	364.2
	$[NH_4]^+$	776.4740	1	C36H66N5O13	776.4652	-11.4	0.1	6.5	ok	even	108.7	156.6
	Na^+	781.4250	1	C36H62N4NaO13	781.4206	-5.6	-0.7	7.5	ok	even	123.1	169.9
dodecadepsipeptidyl-SNAC **15**	H^+	1230.6992	1	C58H100N7O19S	1230.6789	-16.5	-28.4	12.5	ok	even	481.7	518
	$[NH_4]^+$	1247.7206	1	C58H103N8O19S	1247.7055	-12.1	719.1	11.5	ok	even	58.3	78.3
	Na^+	1252.6585	1	C58H99N7NaO19S	1252.6609	1.9	727.4	12.5	ok	even	51.6	64.5
deoxydodecadepsipeptidyl-SNAC **16**	H^+	1214.6971	1	C58H100N7O18S	1214.6840	-10.7	-19.9	12.5	ok	even	11.1	11.5
	$[NH_4]^+$	1231.7221	1	C58H103N8O18S	1231.7106	-9.4	-17.9	11.5	ok	even	29.4	34.6
	Na^+	1236.6816	1	C58H99N7NaO18S	1236.6660	-12.6	-13.1	12.5	ok	even	14.3	14.8
16-mer depsipeptidyl-SNAC **19**	$[NH_4]^+$	1617.9346	1	C76H133N10O25S	1617.9159	-11.6	683.6	15.5	ok	even	465.4	437.1
	Na^+	1622.8725	1	C76H129N9NaO25S	1622.8713	-0.8	994.2	16.5	ok	even	216	286.2
deoxy 16-mer depsipeptidyl-SNAC **20**	H^+	1584.9076	1	C76H130N9O24S	1584.8944	-8.3	794.8	16.5	ok	even	86	100
	$[NH_4]^+$	1601.9337	1	C76H133N10O24S	1601.9209	-8	288.2	15.5	ok	even	14.2	13.1
	Na^+	1606.8919	1	C76H129N9NaO24S	1606.8763	-9.7	554.5	16.5	ok	even	29	31
valinomycin **28**	$[NH_4]^+$	1128.6752	1	C54H94N7O18	1128.6650	-9	445.7	11.5	ok	even	24	29.7

Full Acknowledgments to Synchrotron Sources

CLS: Research described in this paper was performed using beamline 08ID-1 at the Canadian Light Source, which is supported by the Canada Foundation for Innovation, Natural Sciences and Engineering Research Council of Canada, the University of Saskatchewan, the Government of Saskatchewan, Western Economic Diversification Canada, the National Research Council Canada, and the Canadian Institutes of Health Research.

APS: This work is based upon research conducted at the Northeastern Collaborative Access Team beamlines, which are funded by the National Institute of General Medical Sciences from the National Institutes of Health (P41 GM103403). The Pilatus 6M detector on 24-ID-C beam line is funded by a NIH-ORIP HEI grant (S10 RR029205). This research used resources of the Advanced Photon Source, a U.S. Department of Energy (DOE) Office of Science User Facility operated for the DOE Office of Science by Argonne National Laboratory under Contract No. DE-AC02-06CH11357.

References (Continued from main paper)

31 Alonzo, D. A., Magarvey, N. A. & Schmeing, T. M. *PloS one* **10**, e0128569, (2015).

32 Shaw-Reid, C. A. *et al. Chem. Biol.* **6**, 385-400, (1999).

33 May, J. J., Wendrich, T. M. & Marahiel, M. A. *J Biol Chem* **276**, 7209-7217, (2001).

34 Zhou, Y. *et al. Chem. Biol.* **22**, 745-754, (2015).

35 Robbel, L., Hoyer, K. M. & Marahiel, M. A. *FEBS J* **276**, 1641-1653, (2009).

36 Liu, Y., Zheng, T. & Bruner, S. D. S *Chem. Biol.* **18**, 1482-1488, (2011).

37 Trauger, J. W., Kohli, R. M. & Walsh, C. T.. *Biochemistry* **40**, 7092-7098 (2001).

38 Aggarwal, A. *et al.* 13. *Cell* **170**, 249-259 e225, (2017).

39 Neumann, H., Peak-Chew, S. Y. & Chin, J. W. *Nat Chem Biol* **4**, 232-234, (2008).

40 Rogerson, D. T. *et al. Nat Chem Biol* **11**, 496-503, (2015).

41 Zhang, M. S. *et al. Nat Methods* **14**, 729-736, (2017).

42 McGall, G. H. *et al. J. Am. Chem. Soc.* **119**, 5081-5090, (1997).

43 Nguyen, D. P. *et al. J. Am. Chem. Soc.* **136**, 2240-2243, (2014).

44 Pendrak, I., Wittrock, R. & Kingsbury, W. D. S *J Org Chem* **60**, 2912-2915, (1995).

45 Mayer, S. C., Ramanjulu, J., Vera, M. D., Pfizenmayer, A. J. & Joullie, M. M. *J Org Chem* **59**, 5192-5205, (1994).

46 Faure, S. *et al. J Org Chem* **67**, 1061-1070, (2002).

47 Battye, T. G., Kontogiannis, L., Johnson, O., Powell, H. R. & Leslie, A. G.. *Acta crystallographica. Section D, Biological crystallography* **67**, 271-281, (2011).

48 Winter, G. *et al.*. *Acta Crystallogr.D* **74**, 85-97, (2018).

49 Evans, P.. *Acta Crystallogr.D* **62**, 72-82, (2006).

50 McCoy, A. J. *et al. J. Appl. Crystallogr.* **40**, 658-674, (2007).

51 Bunkoczi, G. & Read, R. J. I *Acta Crystallogr.D* **67**, 303-312, (2011).

52 Tanovic, A., Samel, S. A., Essen, L. O. & Marahiel, M. A.. *Science* **321**, 659-663, (2008).

53 Adams, P. D. *et al. Acta Crystallogr. D,* **66**, 213-221, (2010).

54 Terwilliger, T. C. *et al.* . *Acta Crystallogr. D* **64**, 61-69, (2008).

55 Emsley, P., Lohkamp, B., Scott, W. G. & Cowtan, K. *Acta Crystallogr. D* **66**, 486-501, (2010).

56 Bond, C. S. T *Bioinformatics* **19**, 311-312 (2003).

57 Long, F. *et al. A Acta Crystallogr. D* **73**, 112-122, (2017).

58 Vagin, A. A. *et al. A Acta Crystallogr. D* **60**, 2184-2195, (2004).

59 Murshudov, G. N. *et al.* R *A Acta Crystallogr. D* **67**, 355-367, (2011).

60 Korman, T. P. *et al. Proc. Nat. Acad. Sci. U.S.A.* **107**, 6246-6251, (2010).

61 Gehret, J. J. *et al.* . *J Biol Chem* **286**, 14445-14454, (2011).

62 Tsai, S. C. *et al.* . *Proc. Nat. Acad. Sci. U.S.A.* **98**, 14808-14813, (2001).

63 Tsai, S. C., Lu, H., Cane, D. E., Khosla, C. & Stroud, R. M. *Biochemistry* **41**, 12598-12606 (2002).

64 Argyropoulos, P. *et al. Biochim Biophys Acta* **1860**, 486-497, (2016).

65 Giraldes, J. W. *et al. Nat Chem Biol* **2**, 531-536, (2006).

66 Koglin, A. *et al.*. *Nature* **454**, 907-911, (2008).

67 Drake, E. J. *et al.*. *Nature* **529**, 235-238, (2016).

68 Gavalda, S. *et al.*. *Chem. Biol.* **21**, 1660-1669, (2014).

69 Guntaka, N. S., Healy, A. R., Crawford, J. M., Herzon, S. B. & Bruner, S. D. S *ACS Chem Biol* **12**, 2598-2608, (2017).

Chapter 5. Conclusions and Future Directions

5.1 Overview

The review in Chapter 1 established the synthetic difficulties in accessing macrocyclic lactones, requiring a diverse set of complementary reactions (C-C and C-O forming) to overcome this challenging reaction. Chapters 2 and 3 establish the exceptionally broad substrate tolerance of fungal thioesterases to access not only diverse ring sizes, but also stereotolerance, amine nucleophiles, and peptidic substrates. Further development of any thioesterase will require an understanding of what protein features are important for the desired release chemistry. The work presented in Chapter 4 opens the possibility of obtaining highly native-like acyl-enzyme intermediate structures through the incorporation of 2,3-diaminopropionate. All together this suite of experiments sets the stage for a variety of new studies, some of which are postulated below.

5.2 Perspective on fungal PKS thioesterases

The research presented in Chapters 2 and 3 firmly establish the radicicol and zearalenone (Rdc and Zea, respectively) thioesterases as the most flexible macrocyclic ester forming thioesterases.[1,2] They have proven tolerant to stereochemical changes, ring size changes, and replacement of the aromatic ring with an amino acid (**Figure 5.1**).

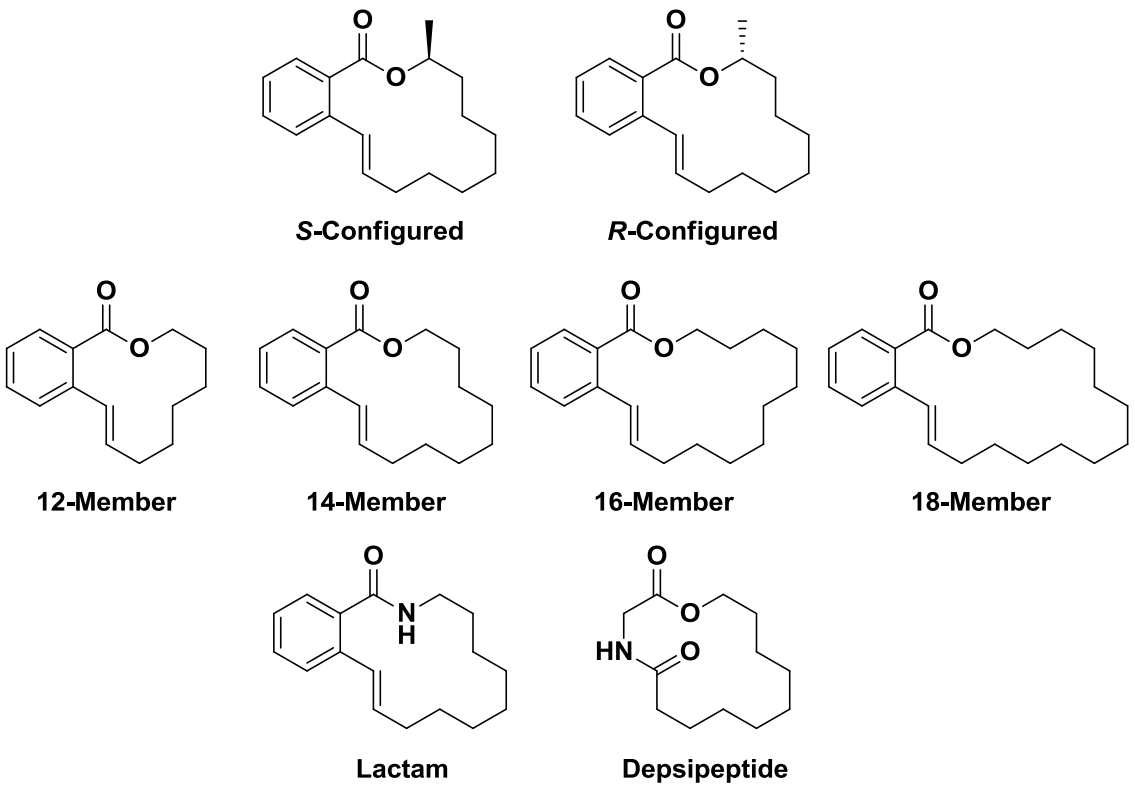

Figure 5.1 Current scope of *in vitro* accessible macrocycles by Rdc and Zea TEs

This is consistent with the screening hypothesis which states that enzymes that occur later in biosynthetic pathways should be more substrate tolerant than enzyme earlier in a pathway.[3,4] This lowers the evolutionary cost of the whole pathway by providing flexibility should an earlier enzyme in the pathway change its selectivity. However these TEs only represent one class of fungal non-reducing megasynthases. The penultimate step in these non-reducing (NR) systems is a product template (PT) domain mediated aromatization of the poly-β-keto product generated by the NR-PKS. This aromatic cyclization is either f-type (fungal) or s-type (streptomyces) and results in either the thioester in conjugation with the aromatic ring or separated from the aromatic system by a methylene spacer (**Figure 5.2**).[5]

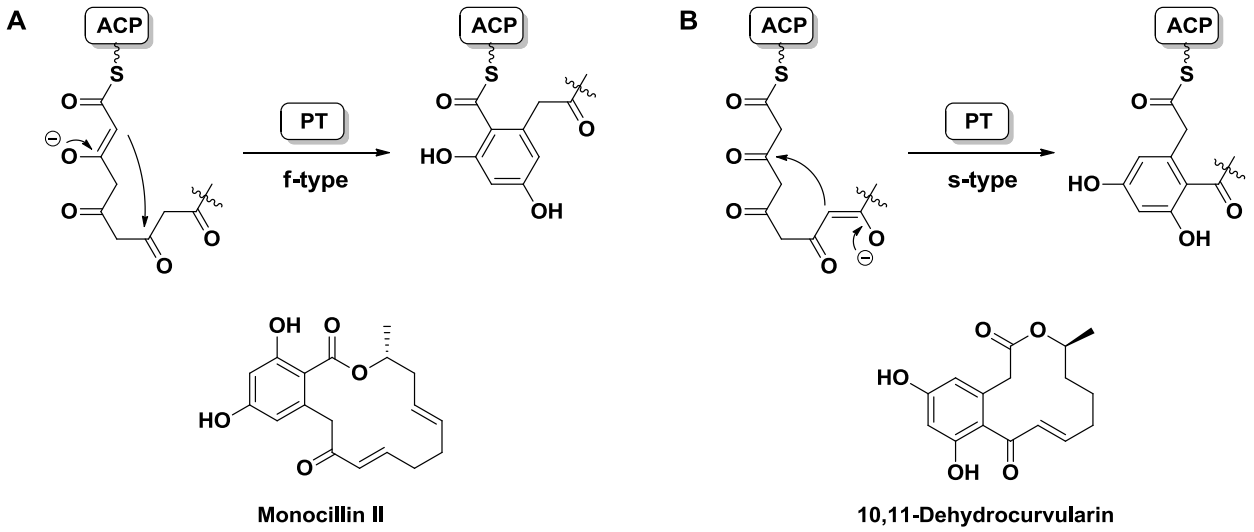

Figure 5.2 General mechanism for **A**. f-type aromatization chemistry and monocillin II which comes from this type of PT domain **B**. s-type aromatization chemistry and 10,11-dehydrocurvularin which comes from this type of PT domain.

Work by Molnár in 2013 indicated that chimeric NR-PKS proteins made by domain swapping between the 10,11-dehydrocurvularin (CurS2) and radicicol (RadS2) pathways could yield new macrocyclic compounds *in vivo* only when the PT and TE domains types were matched.[6] It is worth reexamining these experiments *in vitro* with simplified s-type substrates similar to those used in Chapters 2 and 3.

An additional question regarding the selectivity of fungal TEs was raised by later research in the group. While the glycine containing depsipeptide substrate could be macrocyclized a β-alanine analog could not (**Fig 5.3**).[7] Neither of these substrates were expected to cyclize as the thioesterases would have never been challenged by amino acid containing substrates in their native pathways. The origin of this selectivity may lie with the pre-PT substrate bound on the acyl-carrier protein (ACP), this poly β-keto intermediate needs to undergo multiple rounds of elongation before aromatization and final release by the TE. To maintain the fidelity of the final

product the TE should not accept any ACP-bound species containing a β-,δ-,or ζ-ketone as these will not have undergone aromatization. Shifting from an α-amino acid to a β-amino acid moves the amide carbonyl from the γ- to the δ-position and this may be chemically similar enough to the δ-keto ACP bound intermediate that the TE would have evolved sufficient selectivity to not load this compound. Work to examine the effect of carbonyl position on macrocyclization ability is ongoing.

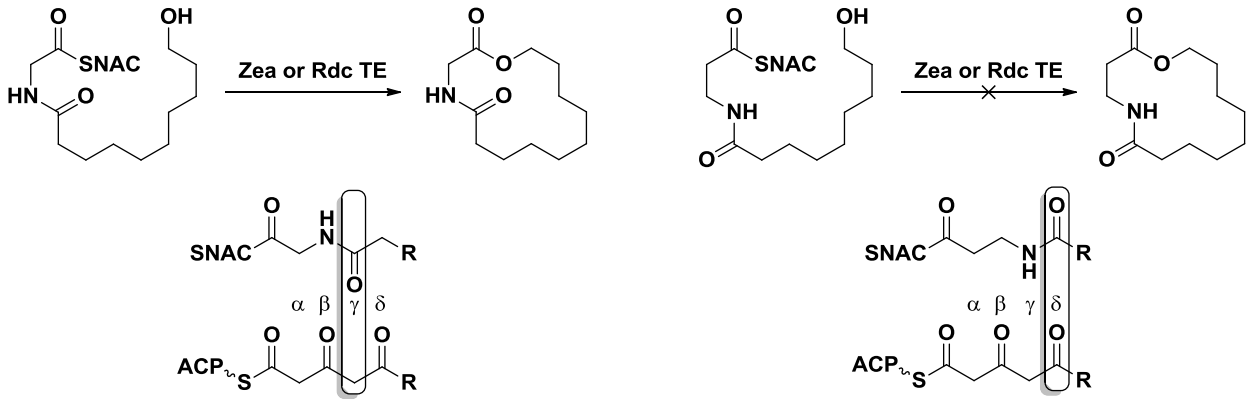

Figure 5.3 Macrocyclization scope of α-amino acid and β-amino acid substrates with the Zea and Rdc TEs. Amide carbonyl position relative to the native ACP bound δ-keto intermediate may drive this selectivity in non-native systems.

The characterization of the Rdc and Zea TEs covered in Chapters 2 and 3 combined with above experiments detailing the role of PT-domain mediated aromatization will provide the most complete picture to date of loading and release chemistry. Follow up of these experiments with the incorporation of 2,3-diaminopropionate (DAP) in place of the active site serine and structural characterization through crystallography would be a welcome addition to the fungal TE field.[8]

5.3 Future applications for DAP incorporation in TEs

The work on the valinomycin TE (Vlm TE) presented in Chapter 4 highlights the role of the lid in selecting between transesterification and macrocyclization to generate its trimeric structure. This exceptionally large lid undergoes a large translocation capping the active site and curling the trimeric substrate into a macrocyclization competent conformation. Other multimeric TEs with smaller substrates and smaller lids may also rely on lid translocation to ensure the correct macrocycles is generated. One candidate is the enterobactin pathway which trimerizes 2,3-dihydroxybenzoyl-L-serine monomer to generate the active siderophore (**Fig. 5.4**).[9]

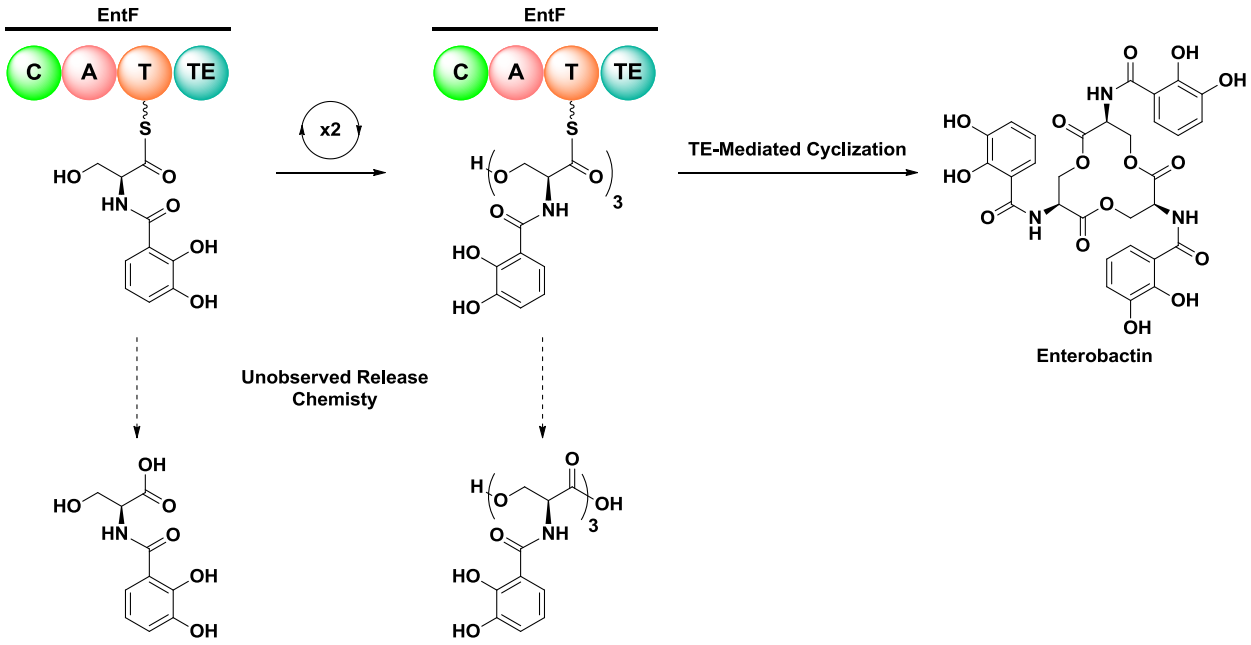

Figure 5.4 Enterobactin trimerization and macrocyclization on EntF. The selectivity of the TE for macrocyclizing release of the trimer over hydrolytic release of earlier biosynthetic intermediates.

The crystal structure of the EntF T-TE didomain (3TEJ)[10] reveals a typical two helix lid region; how this normal-sized lid participates in selection between transesterification and

macrocyclization would provide valuable sequence-to-function information and improve our ability to predict TE function.

Revisiting well studied and structurally characterized TEs with this DAP incorporation technique may yield new insight to their function and selectivity. A prime candidate for this type of experiment is the 6-desoxyerythronolide B (DEBS) TE as several solved crystal structures are known (1KEZ,[11] 1MO2,[12] 5D3K,[13] and 5D3Z[13]) and several *in vitro* substrates have already been tested for their ability to macrocyclize (**Fig 5.5**).

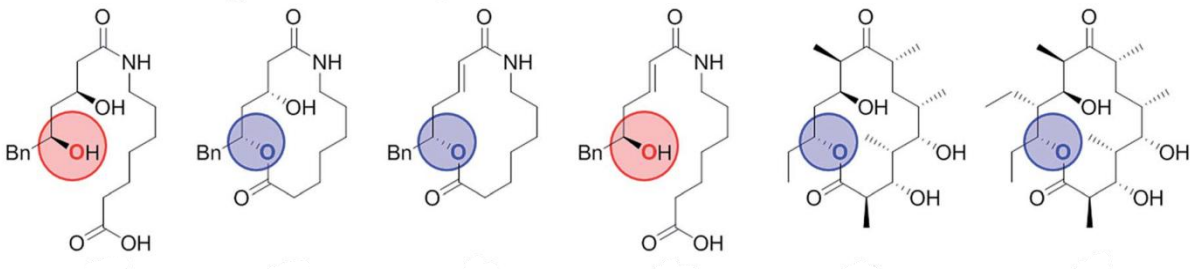

Figure 5.5 *In vitro* substrates that have been tested with the $DEBS_{WT}$ TE, blue circles indicate substrates that possess the necessary D-configured nucleophile for cyclization. These substrates would be ideal candidates to load on $DEBS_{DAP}$ TE. Adapted from Horsman et al.[14]

5.4 Conclusions

Overall the future is bright for the development of polyketide TEs as macrocyclization catalysts. The work presented in Chapters 2 and 3 describe and characterize the stand-alone TEs from fungal pathways and demonstrate their tolerance for a wide variety of substrates. The development of DAP incorporation to study substrate interactions with TEs will facilitate a new set of structural insights on how TEs bind substrates and determine release chemistry.

5.5 References

[1] G. W. Heberlig, M. Wirz, M. Wang, C. N. Boddy, *Org. Lett.* **2014**, *16*, 5858–5861.
[2] G. W. Heberlig, J. T. C. Brown, R. D. Simard, M. Wirz, W. Zhang, M. Wang, L. I. Susser, M. E. Horsman, C. N. Boddy, *Org. Biomol. Chem.* **2018**, *16*, 5771–5779.
[3] R. D. Firn, C. G. Jones, *Nat. Prod. Rep.* **2003**, *20*, 382–391.
[4] R. D. Firn, C. G. Jones, *J Exp. Bot.* **2009**, *60*, 719–726.
[5] R. Thomas, *ChemBioChem* **2001**, *2*, 612–627.
[6] Y. Xu, T. Zhou, S. Zhang, L.-J. Xuan, J. Zhan, I. Molnár, *J. Am. Chem. Soc.* **2013**, *135*, 10783–10791.
[7] J. Brown, Resorcylic Acid Lactone Thioesterases as Potential Biocatalysts, Thesis, Université d'Ottawa / University of Ottawa, **2019**.
[8] N. Huguenin-Dezot, D. A. Alonzo, G. W. Heberlig, M. Mahesh, D. P. Nguyen, M. H. Dornan, C. N. Boddy, T. M. Schmeing, J. W. Chin, *Nature* **2019**, *565*, 112.
[9] Z. L. Reitz, M. Sandy, A. Butler, *Metallomics* **2017**, *9*, 824–839.
[10] Y. Liu, T. Zheng, S. D. Bruner, *Chem. Biol.* **2011**, *18*, 1482–1488.
[11] S.-C. Tsai, L. J. W. Miercke, J. Krucinski, R. Gokhale, J. C.-H. Chen, P. G. Foster, D. E. Cane, C. Khosla, R. M. Stroud, *Proc. Nat. Acad. Sci. U.S.A.* **2001**, *98*, 14808–14813.
[12] S.-C. Tsai, H. Lu, D. E. Cane, C. Khosla, R. M. Stroud, *Biochemistry* **2002**, *41*, 12598–12606.
[13] P. Argyropoulos, F. Bergeret, C. Pardin, J. M. Reimer, A. Pinto, C. N. Boddy, T. M. Schmeing, *Biochim. Biophys. Acta* **2016**, *1860*, 486–497.
[14] M. E. Horsman, T. P. A. Hari, C. N. Boddy, *Nat. Prod. Rep.* **2016**, *33*, 183–202.

Appendix 1. Extended Figures for Chapter 4

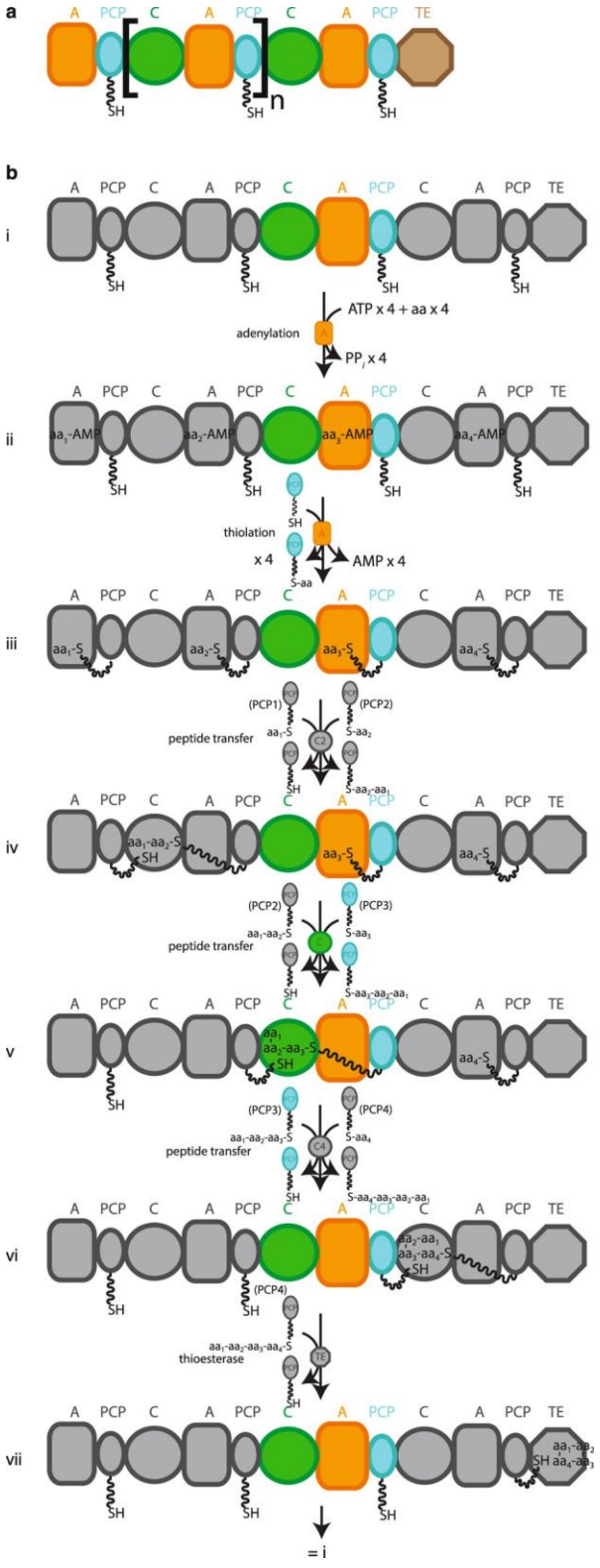

Figure 1. Schematic representation and reaction cycle of a canonical NRPS.

a, Schematic representation of a generic type I NRPS. The square brackets denote a single module. **b**, i–vii, Synthetic cycle of a canonical elongation module. NRPSs assemble peptides from amino acyl and other small acyl building blocks using a modular and thio-templated logic. A canonical NRPS is composed of one module for every residue in the peptide product. The initiation module contains an adenylation (A) domain, which binds cognate acyl substrate and performs adenylation and transfer of that substrate as a thioester on the phosphopantetheine arm (PPE, shown as a wavy line) of a peptidyl carrier protein (PCP) domain, for transport between active sites. Each elongation module contains an A and a PCP domain, and also a condensation (C) domain, which condenses aminoacyl and peptidyl substrates bound to PCP domains, thus progressively elongating the nascent chain. Termination modules contain C, A and PCP domains, and a specialized terminating/offloading domain responsible for the release of the peptide in its final form. The most common and most versatile terminating domain in NRPSs is the TE domain. Similar TE domains terminate synthesis in polyketide and fatty acid synthases. PP_i, diphosphate; aa, amino acid.

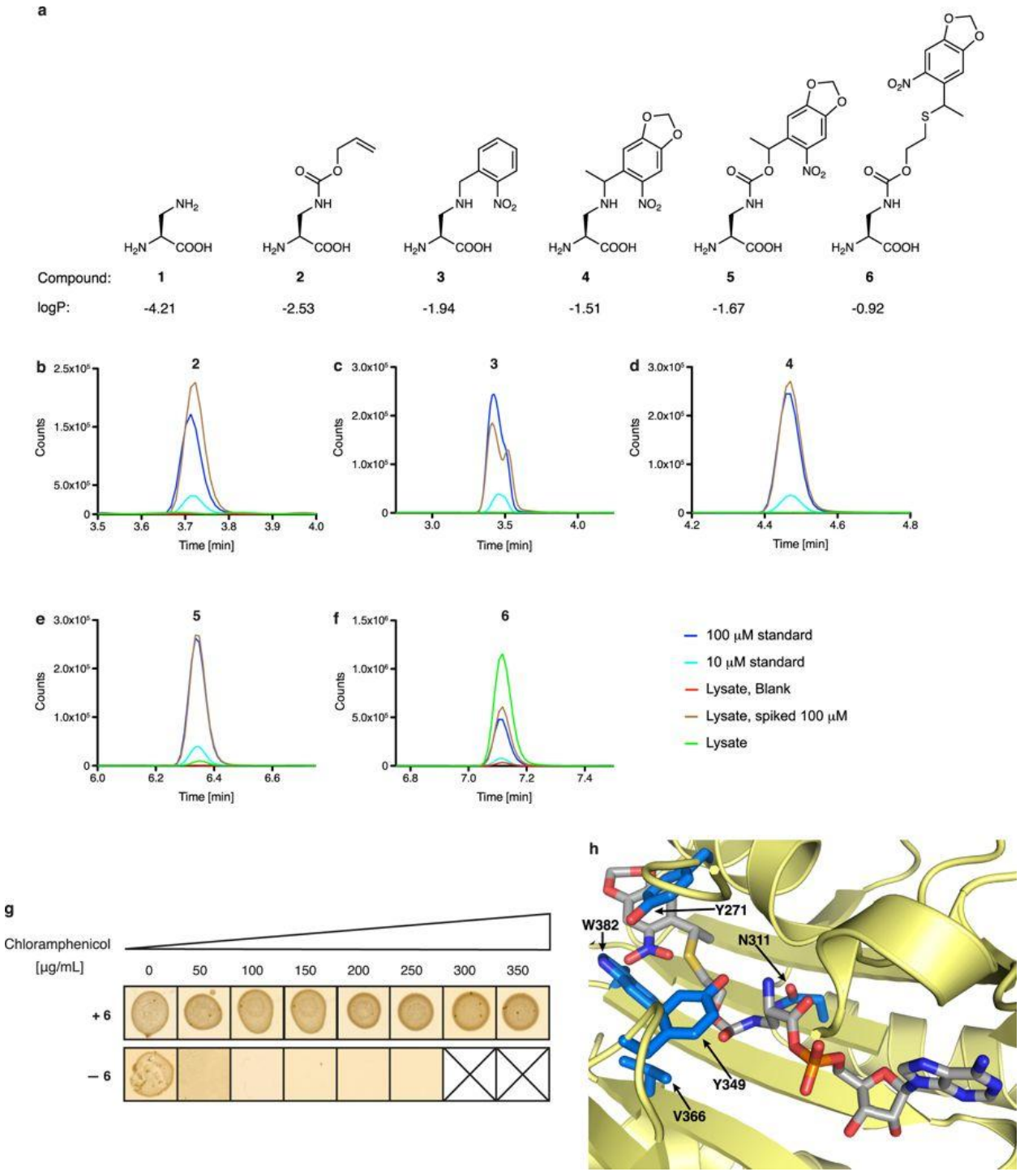

Figure 2. Genetically directing DAP incorporation in recombinant proteins.

a, Structure of DAP and the protected versions investigated herein. **1**, 2,3-diaminopropionic acid (DAP); **2**, (*S*)-3-(((allyloxy)carbonyl)amino)-2-aminopropanoic acid; **3**, (*S*)-2-amino-3-((2-nitrobenzyl)amino)propanoic acid; **4**, (2*S*)-2-amino-3-((1-(6-nitrobenzo[*d*][1,3]dioxol-5-yl)ethyl)amino)propanoic acid; **5**, (2*S*)-2-amino-3-(((1-(6-nitrobenzo[*d*][1,3]dioxol-5-

yl)ethoxy)carbonyl)amino)propanoic acid; **6**, (2*S*)-2-amino-3-(((2-((1-(6-nitrobenzo[*d*][1,3]dioxol-5-yl)ethyl)thio)ethoxy)carbonyl)amino)propanoic acid. Calculated log*P* values are indicated (calculated using the Molinspiration molecular property calculation services at www.molinspiration.com/cgi-bin/properties). **b**–**f**, Determining the intracellular concentration of compounds **2**–**6** by an LC–MS assay, performed on extracts. The dark-blue trace represents a 100 µM standard for each compound. The light-blue trace represents a 10 µM standard for each compound. The red trace results from cells grown in the absence of the compound. The brown trace results from cells grown in the absence of the compound, but spiked with the compound to 100 µM. The green trace results from cells grown in the presence of 1 mM compound. The experiments were repeated in two biological replicates with similar results. **g**, Phenotyping of the DAPRS/$tRNA_{CUA}$ pair. Cells containing the DAPRS/$tRNA_{CUA}$ pair and *cat*(*112TAG*) (encoding a chloramphenicol-resistance gene containing an amber stop codon (TAG) at codon 112) were plated in the presence or absence of **6** on the indicated concentrations of chloramphenicol. The experiment was performed in two biological replicates with similar results. **h**, The side chain of **6** (grey sticks) was modelled into the active site of PylRS using a co-crystal structure of PylRS and adenylated pyrrolysine (PDB accession number 2ZIM).[1] PylRS is displayed in pale yellow and amino-acid positions randomized in DAPRSlib are shown in marine blue.

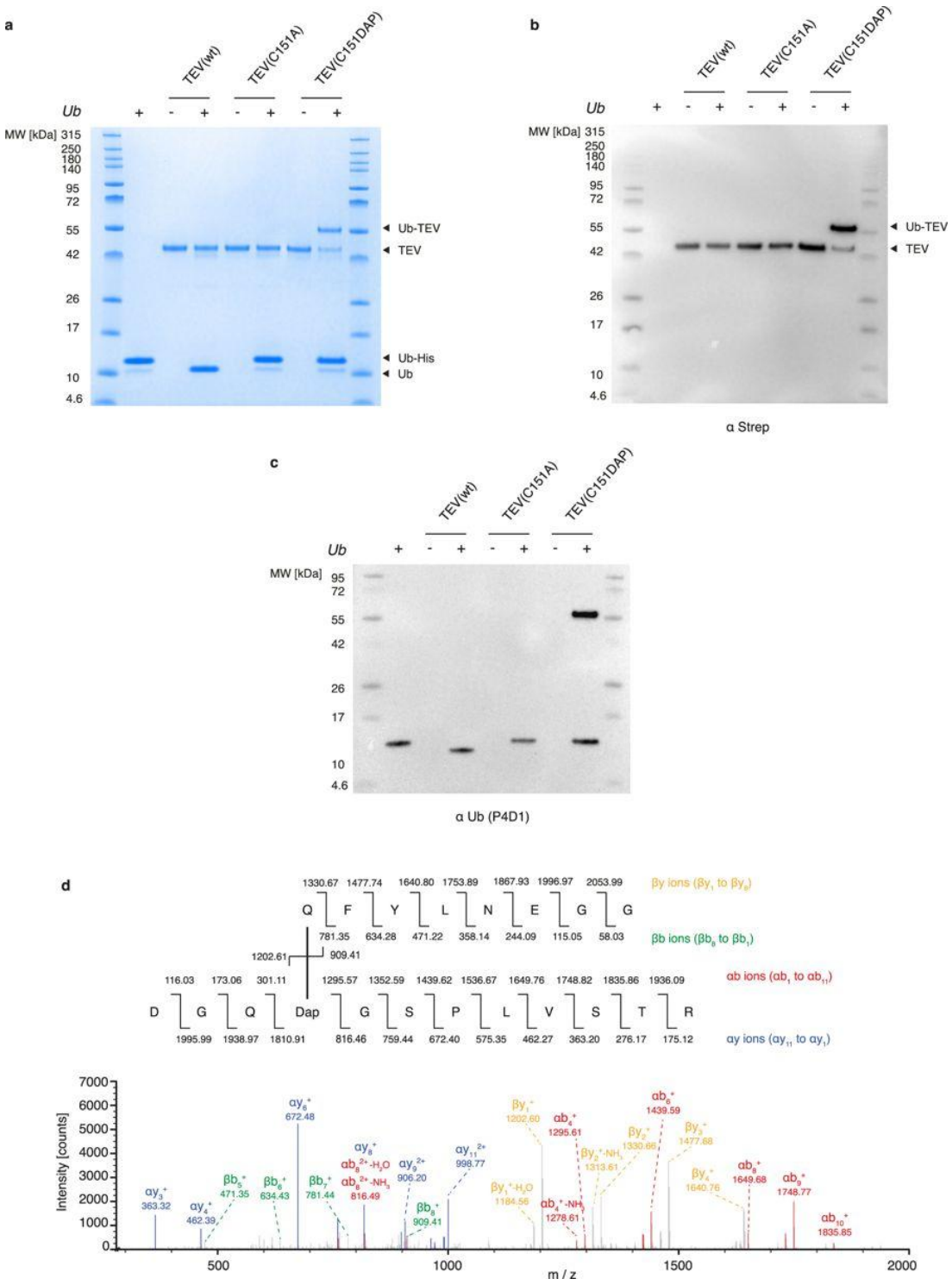

Figure 3. Stably trapping the acyl-enzyme intermediate of a cysteine protease.

a, Different variants of TEV protease (shown at the top) were reacted with Ub–tev–His. The use of TEV(wt) results in cleavage of the TEV cleavage sequence. The use of TEV(C151A) results in minimal cleavage. The presence of DAP in the active site of TEV results in the

presence of an extra band in the Coomassie gel, representing the isopeptide-linked TEV(C151DAP)–Ub complex. **b**, **c**, Anti-streptavidin (α-strep; **b**) and anti-Ub (α-Ub antibody P4D1; **c**) western blots of the reactions confirm the identity of the complex. For **a**–**c**, the experiment was repeated in two biological replicates with similar results. **d**, Tandem mass spectrometry following tryptic digest of the TEV(C151DAP)–Ub conjugate confirms amide-bond formation at the expected position. Top, the sequence of the branched peptide subject to fragmentation. Fragmentation of the substrate chain is predicted to lead to a series of y ions (yellow) and a series of b ions (green); the ions from this chain are labelled as 'β'. Fragmentation of the TEV(C151DAP)-derived chain is predicted to lead to a series of y ions (blue) and a series of b ions (red); the ions from this chain are labelled as 'α'. Bottom, MS/MS spectra with peak assignments. Ions in the α-chain were assigned by treating DAP and the β-chain as a modification of known mass. Ions in the β-chain were manually assigned. The mass-spectrometry analysis was performed once.

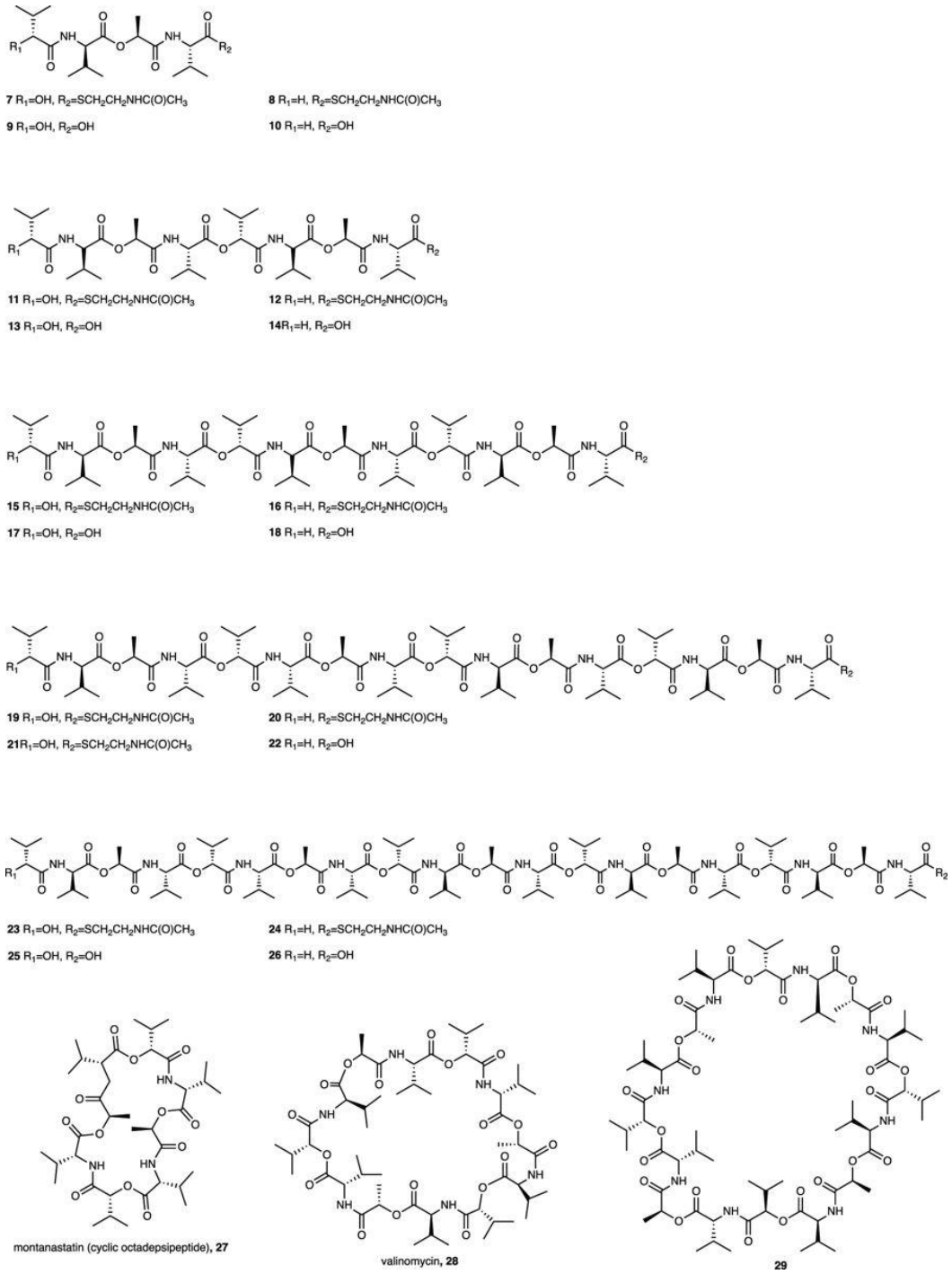

Figure 4. Chemical structures of key Vlm TE substrates and products.

The chemical structures and the numbers used to refer to them are shown.

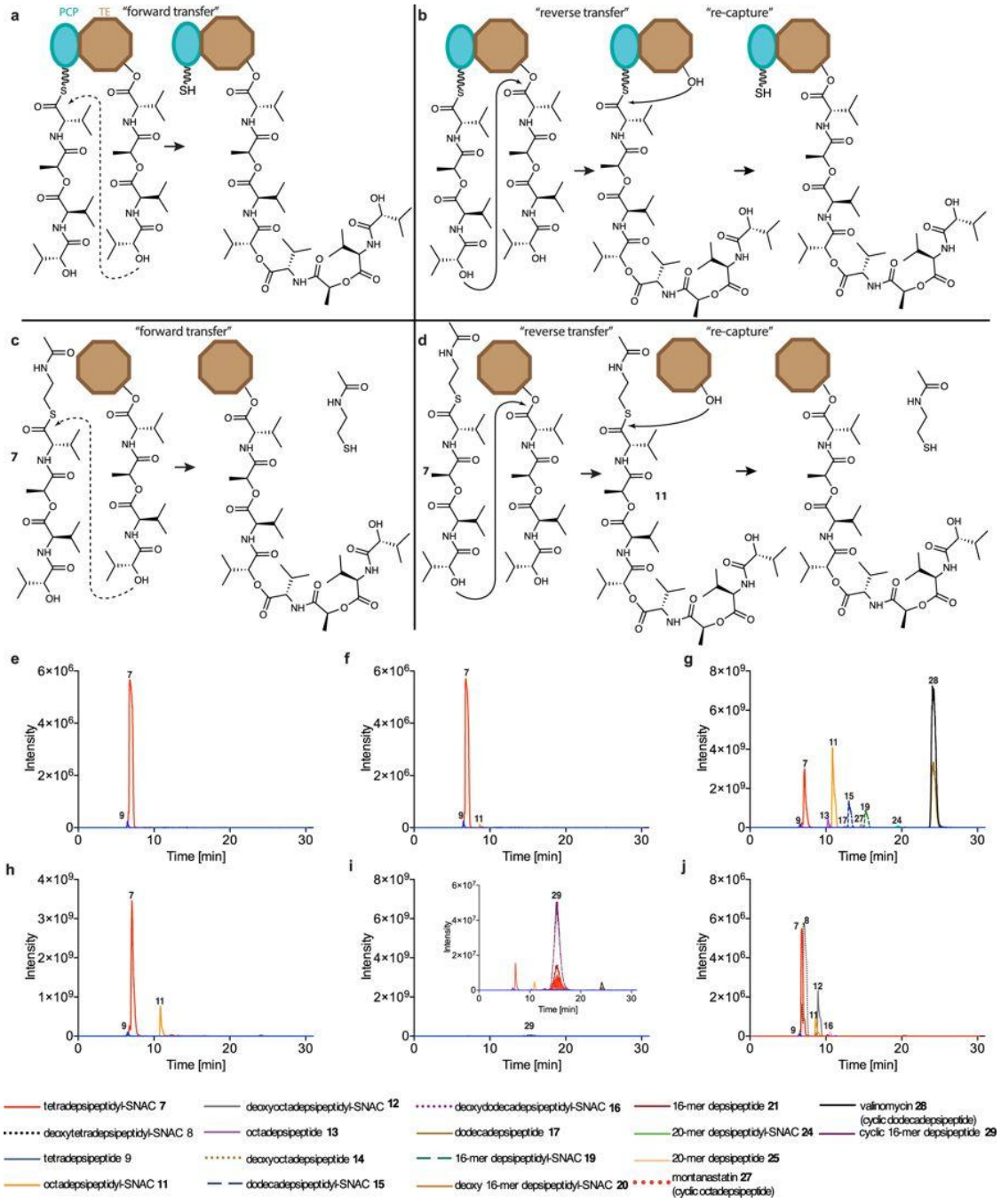

Figure 5. The mechanism by which by Vlm TE catalyses oligomerization.

Oligomerization could conceivably take place in two ways. **a**, In the first scenario, 'forward transfer', the distal hydroxyl group of the tetradepsipeptidyl–*O*-TE complex attacks the thioester group in the tetradepsipeptidyl–*S*-PCP enzyme intermediate, directly forming octadepsipeptidyl–*O*-TE as a product. **b**, In the second scenario, 'reverse transfer', the distal hydroxyl group of the tetradepsipeptidyl–*S*-PCP complex attacks the ester group in the tetradepsipeptidyl–*O*-TE enzyme intermediate, forming octadepsipeptidyl–*S*-PCP as a product,

which would then need to be transferred onto the TE-domain serine (here labelled as 're-capture'). **c**, **d**, Analogous scenarios involving tetradepsipeptidyl–SNAC (**7**) as the substrate instead of tetradepsipeptidyl–*S*-PCP. **e**, **f**, EICs (HR LC–ESI-MS) of a mix of **7** (1.7 mM) and buffer (**e**), or the products of a reaction between **7** (1.7 mM) and Vlm TE_{DAP} (6.5 μM) (**f**). **g**–**i**, EICs (low-resolution (LR) LC–ESI-MS) of reactions using a higher-volume injection into an ion-trap MS instrument. **g**, The higher-volume injection of a reaction of **7** (1.7 mM) and Vlm TE_{wt} (6.5 μM) enabled detection of a peak consistent with the 20-mer depsipeptidyl–SNAC (**24**). **h**, LC ion-trap MS of the reaction of **7** (1.7 mM) and Vlm TE_{DAP} (6.5 μM). **i**, Small amounts of the cyclic 16-mer depsipeptide **29** elute during post-run column clean-up of experiment shown in **g**. **j**, EICs (HR LC–ESI-MS) of products of reactions between Vlm TE_{wt} (6.5 μM) and a mix of **7** and deoxy-tetradepsipeptidyl–SNAC (**8**; 1.7 mM of each). TE_{wt} produces the intermediates deoxy-octadepsipeptidyl–SNAC (**12**), deoxy-dodecadepsipeptidyl–SNAC (**16**) and deoxy 16-mer depsipeptidyl–SNAC (**20**), confirming the reaction pathway shown in **b**. The experiments in **e**–**i** were repeated independently twice with similar results. Mass-spectrometry analysis of the experiment in **j** was performed once.

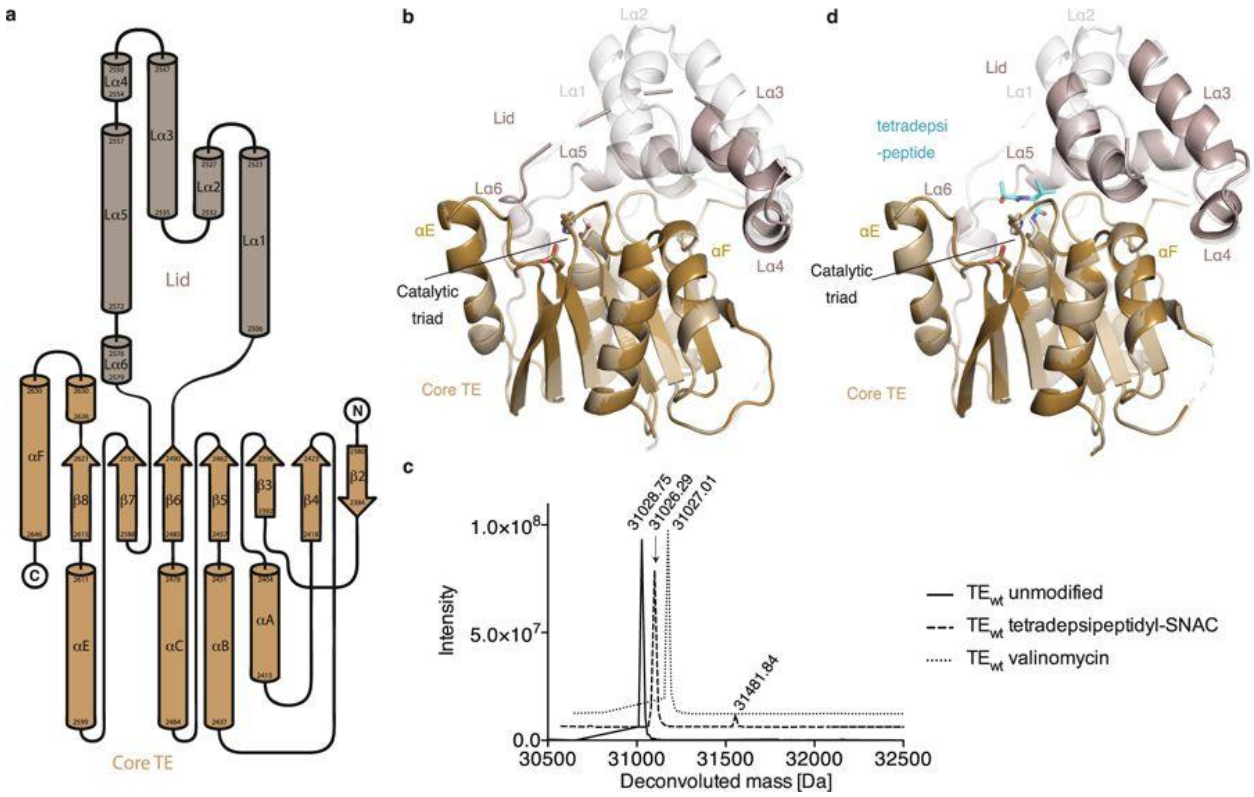

Figure 6. Structures of Vlm TE_{wt} and tetradepsipeptidyl–TE_{DAP}, and top-down LC–ESI-MS of Vlm TE_{wt}.

a, Secondary-structure elements of Vlm TE; the naming is based on the convention for α/β-hydrolase proteins. **b**, Comparison of two TE_{wt} structures (PDB accession numbers 6ECB and 6ECC). The active-site lid of the first structure (light grey) is nearly completely ordered, whereas the lid of second structure (dark grey) shows density for Lα3, Lα4 and Lα5 only. In the second structure, Lα3 is rotated 10° towards the active site. **c**, Deconvoluted mass spectra of TE_{wt} incubated with different substrates. Solid line, buffer control: expected molecular mass 31,028.22 Da; observed 31,028.75 Da. Dashed line, TE_{wt} incubated with tetradepsipeptidyl–SNAC: expected 31,028.22 Da (unmodified) and 31,399.44 Da (modified); observed 31,026.29 Da. Dotted line, TE_{wt}incubated with valinomycin: expected 31,028.22 Da (unmodified) and 32,139.86 Da (modified); observed 31,027.01 Da. Experiments were repeated independently twice with similar results. **d**, Comparison of near-identical conformations of TE_{wt} (light grey; 6ECB) and tetradepsipeptidyl–TE_{DAP} (tan and dark grey; 6ECD).

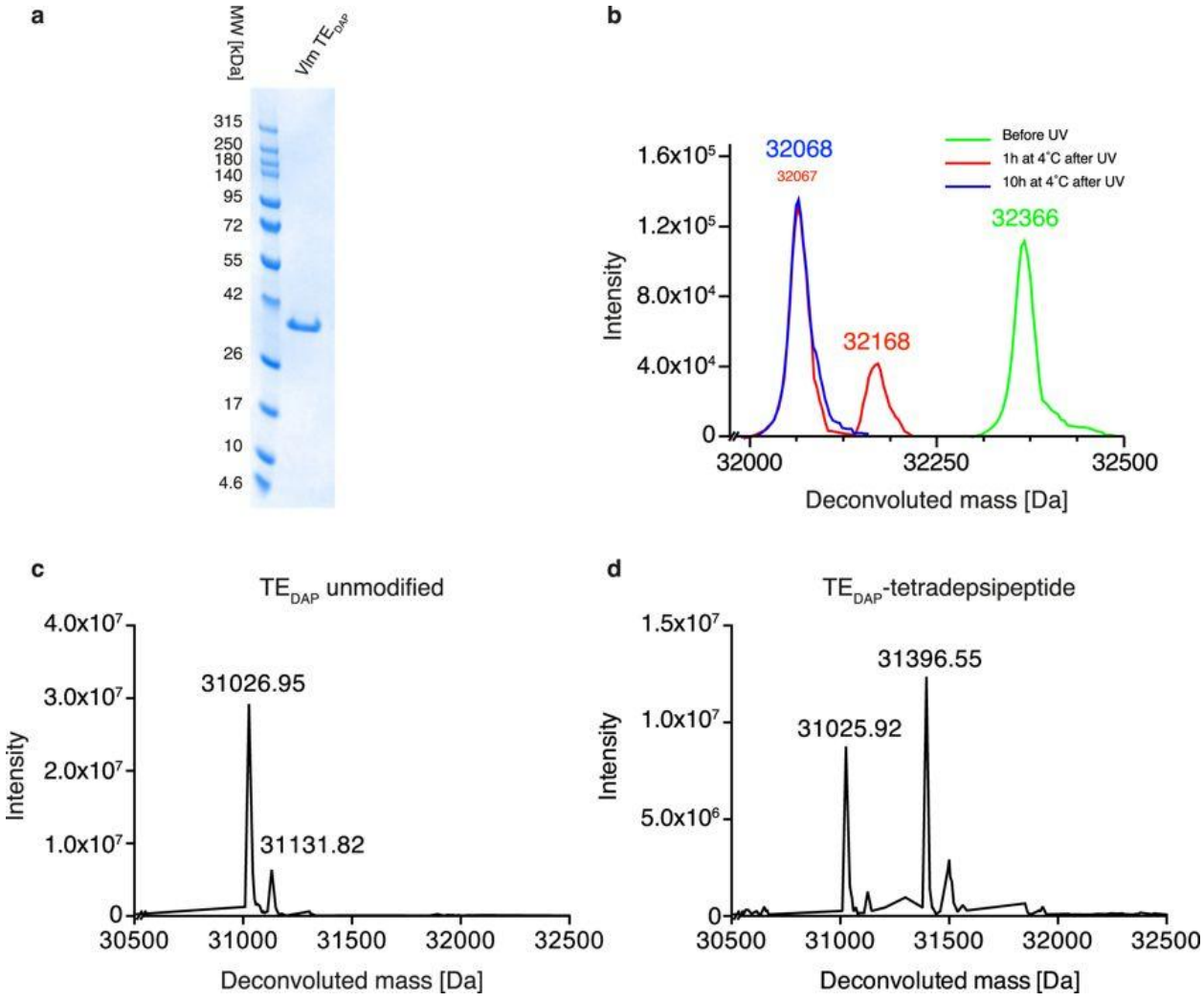

Figure 7. Expression and substrate conjugation to Vlm TE containing DAP at position 2463.

a, Following expression and purification of Vlm TE_{DAP}, the protein was loaded on an SDS–PAGE gel and Coomassie stained; the experiment was repeated in two biological replicates with similar results. **b**, The deprotection of **6** in TE_{DAP}–strep was followed by ESI-MS analysis. Green trace, purified TE_{DAP}–strep containing **6** at position 2463: expected mass 32,364.6 Da, observed 32,365.78 Da. Red trace, TE_{DAP}–strep containing **6**at position 2463 following illumination to convert **6** to the intermediate: expected 32,171.56 Da, observed 32,168.48 Da; and further incubation (1 h, 4 °C) to convert the intermediate to product: expected 32,067.62 Da, observed 32,068 Da). Blue trace, TE_{DAP}–strep containing **6** at position 2,463 following illumination (to convert **6** to the intermediate) and further incubation (10 h, 4 °C) to convert the intermediate to DAP (**1**): expected 32,067.62 Da; observed, 32,067.84 Da. The experiment was repeated in two biological replicates with similar results. **c**, Purified TE_{DAP} after illumination and intermediate fragmentation: expected 31,027.24 Da, observed 31,026.95 Da and 31,131.82 Da. **d**, TE_{DAP} incubated with tetradepsipeptidyl–SNAC **7**: expected 31,027.24 Da (unmodified) and 31,398.69 Da (modified); observed 31,025.92 Da and 31,396.55 Da. The experiments in **c**, **d** were repeated independently twice with similar results.

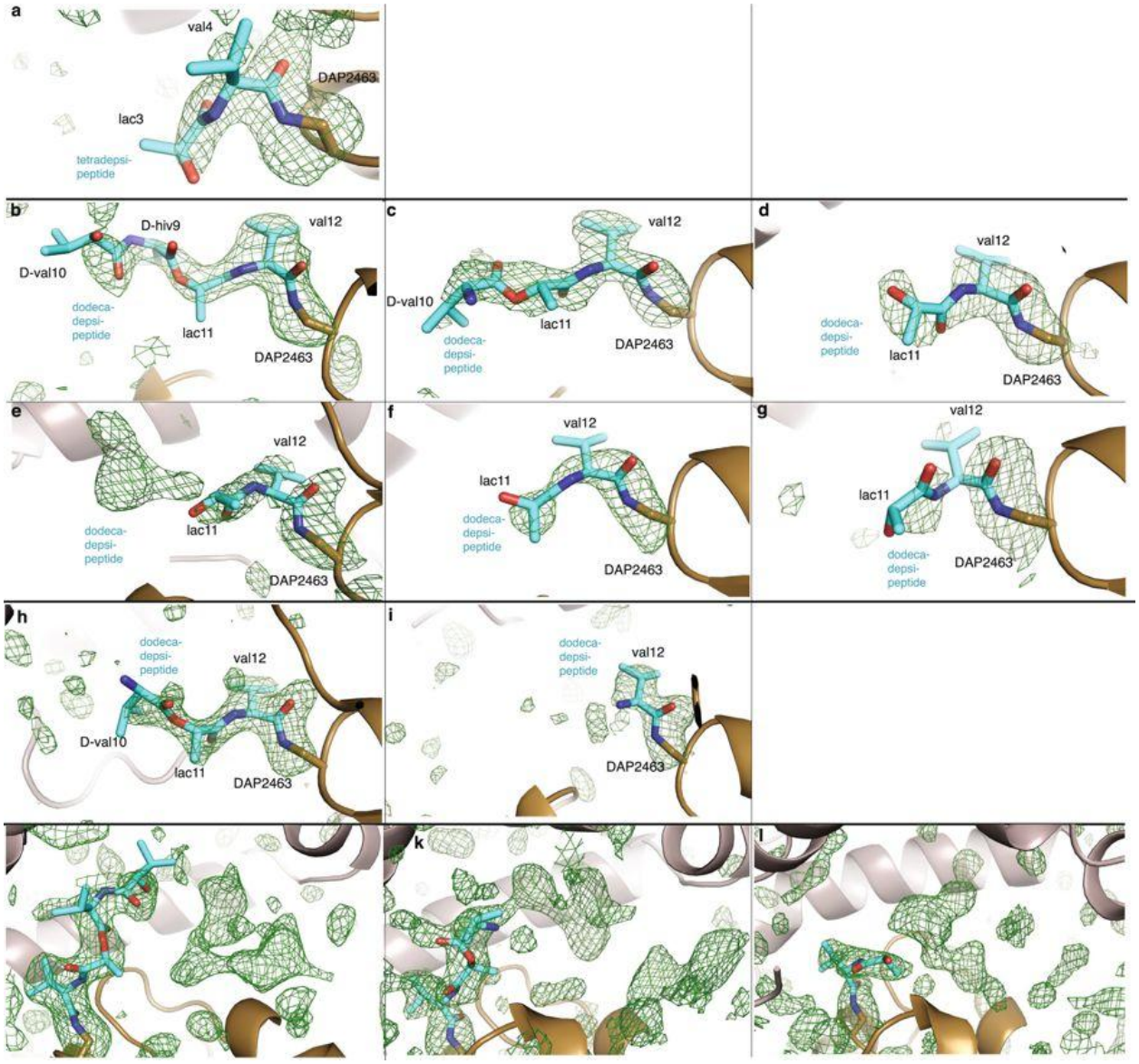

Figure 8. Electron density of the active site of covalent depsipeptidyl–TE_{DAP} complexes.

Unbiased mF_o – DF_c maps (green mesh, contoured at 2.5σ), calculated before depsipeptide residues were placed in the model. DAP (brown) and depsipeptide residues (cyan) are depicted as sticks. **a**, Tetradepsipeptidyl–TE_{DAP} (PDB accession number 6ECD). **b**–**g**, Dodecadepsipeptidyl–TE_{DAP} P_1 space-group structure (6ECF), with crystallographically independent molecules A to F shown in sequential order. **h**, **i**, Dodecadepsipeptidyl–TE_{DAP} H_3 space group (6ECE), for crystallographically independent molecules A and B. **j**–**l**, Electron density of the active site of covalent depsipeptidyl–TE_{DAP} complexes extends beyond modelled depsipeptides. Unbiased mF_o – DF_c maps (green mesh, contoured at 2.5σ), calculated before depsipeptide residues were placed in the model, for dodecadepsipeptidyl–TE_{DAP} P_1 space-group structure, with crystallographically independent molecules A, B and D in sequential order. The observed electron density that extends beyond the modelled

depsipeptides (cyan sticks) could accommodate extra depsipeptide residues in different orientations. However, unambiguous modelling into this density could not be achieved.

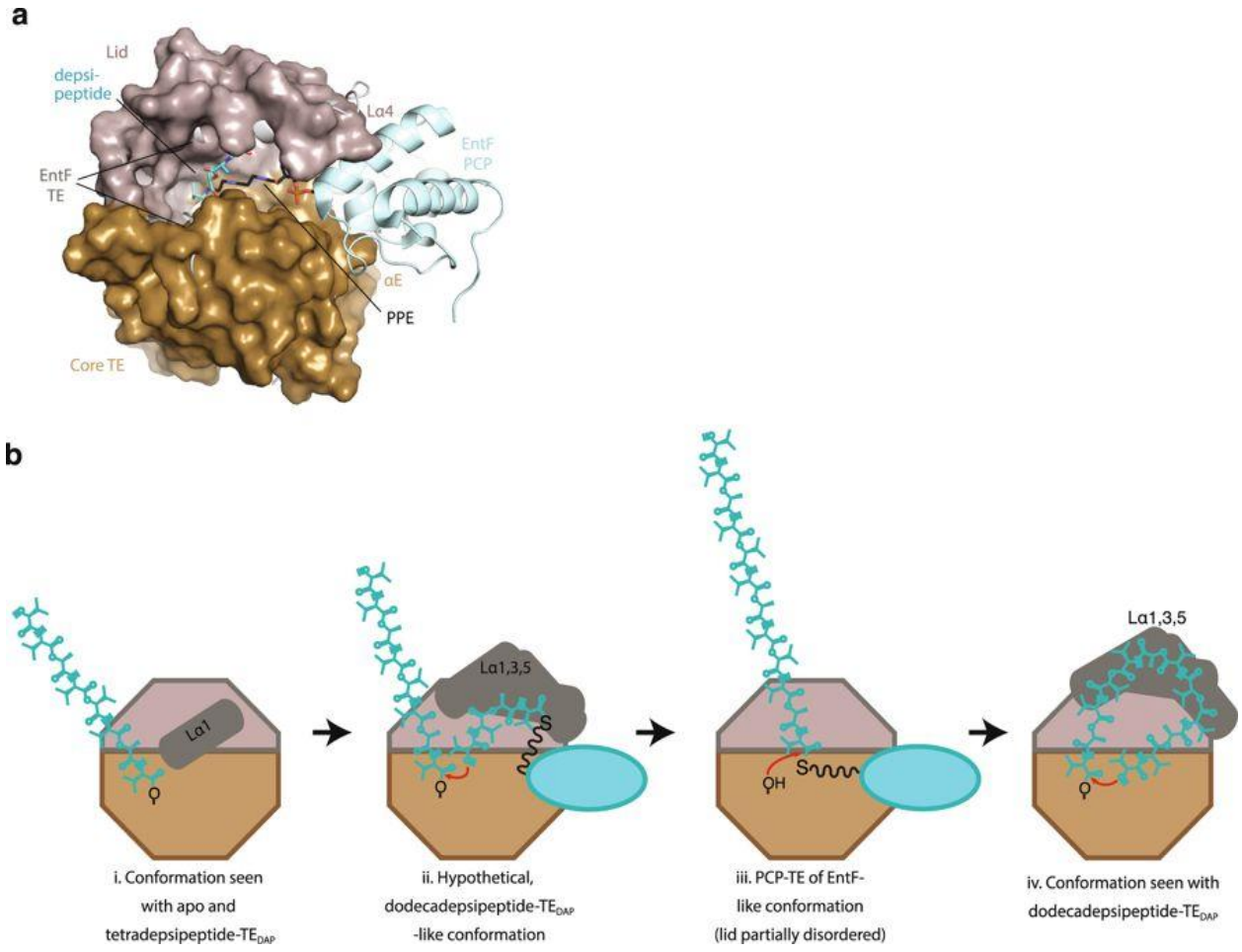

Figure 9. Modelling of interaction between the PCP domain and TE domain and putative pathway.

a, Superimposition of dodecadepsipeptidyl–TE$_{DAP}$ with the structure of the EntF PCP–TE didomain[2] (PDB accession number 3TEJ) shows the path of the PPE moiety to the active site. **b**, Hypothetical pathway for oligomerization and cyclization, starting from octadepsipeptidyl–TE. i, The position of Lα1 in the observed apo/tetradepsipeptide conformation promotes an extended peptide conformation. ii, The tetradepsipeptidyl–PCP accepts the octadepsipeptide onto its terminal hydroxyl, perhaps using a dodecadepsipeptide-like lid conformation which could accommodate the roughly 30-Å tetradepsipeptidyl–PPE bound to the PCP domain and guide it towards the active site. iii, The PCP domain presents the thioester for transfer back to serine 2463. iv, Finally, the lid conformation observed in the dodecadepsipeptide–TE$_{DAP}$ structures could help to curl the dodecadepsipeptide back towards serine 2463 for cyclization.

	TE_{wt} structure 1 (6ECB)	TE_{wt} structure 2 (6ECC)	TE_{DAP} bound with a tetradepsipeptide (6ECD)	TE_{DAP} bound with dodecadepsipeptide, space group H3 (6ECE)	TE_{DAP} bound with dodecadepsipeptide, space group P1 (6ECF)
Data collection					
Space group	P 4 3 2	P 4 3 2	P 4 3 2	R 3 : H	P1
Cell dimensions					
a, *b*, *c* (Å)	151.4, 151.4, 151.4	152.2, 152.2, 152.2	152.3, 152.3, 152.3	77.6, 77.6, 235.2	77.0, 77.1,90.3
α, β, γ (°)	90, 90, 90	90, 90, 90	90, 90, 90	90, 90, 120	91.8, 114.9, 118.0
Resolution (Å)	151.4-1.7 (1.73-1.7)	152.2-1.8 (1.84-1.8)	107.7-1.9 (1.94-1.9)	64.59-2.0 (2.05-2.0)	78.55-2.5 (2.589-2.5)
R_{sym} or R_{merge}	0.063 (1.059)	0.08 (1.525)	0.123 (3.917)	0.079 (0.845)	0.071 (0.320)
I / s*I*	21.83 (1.3)	19.0 (1.1)	23.3 (1.0)	9.8 (1.5)	4.06 (1.85)
Completeness (%)	98.3 (88.3)	99.4 (94.2)	100 (100)	100 (100)	97.58 (97.10)
Redundancy	12.3 (4.5)	12.7 (6.2)	37.2 (37.4)	5.0 (4.9)	1.7 (1.7)
Refinement					
Resolution (Å)	75.7-1.7	87.87-1.8	107.7-1.9	44.24-2.0	78.55-2.5
No. reflections	64286	55853	48056	35677	53933
R_{work} / R_{free}	0.1725/0.1874	0.1757/0.1898	0.1879/0.2143	0.2091/0.2426	0.1969/0.2489
No. atoms	2188	1917	1918	3739	11761
Protein	1984	1746	1807	3645	11518
Ligand/ion	0	0	5	5	37
Water	204	171	106	89	206
B-factors	33.45	39.71	54.47	48.06	44.16
Protein	32.52	38.92	54.39	48.09	44.13
Ligand/ion	n/a	n/a	117.62	52.13	65.2
Water	42.47	47.77	52.94	46.47	41.81
R.m.s. deviations					
Bond lengths (Å)	0.009	0.019	0.018	0.005	0.005
Bond angles (°)	1.31	1.69	1.65	0.96	0.99

Table 1. Data collection and refinement statistics for the crystal structures presented here

[1] J. M. Kavran, S. Gundllapalli, P. O'Donoghue, M. Englert, D. Söll, T. A. Steitz, *Proc. Nat. Acad. Sci. U.S.A.* **2007**, *104*, 11268–11273.

[2] Y. Liu, T. Zheng, S. D. Bruner, *Chem. Biol.* **2011**, *18*, 1482–1488.

Appendix 2. Copyright Permission Information

Title: Resorcylic Acid Lactone Biosynthesis Relies on a Stereotolerant Macrocyclizing Thioesterase

Author: Graham W. Heberlig, Monica Wirz, Meng Wang, et al

Publication: Organic Letters

Publisher: American Chemical Society

Date: Nov 1, 2014

Quick Price Estimate

Permission for this particular request is granted for print and electronic formats, and translations, at no charge. Figures and tables may be modified. Appropriate credit should be given. Please print this page for your records and provide a copy to your publisher. Requests for up to 4 figures require only this record. Five or more figures will generate a printout of additional terms and conditions. Appropriate credit should read: "Reprinted with permission from {COMPLETE REFERENCE CITATION}. Copyright {YEAR} American Chemical Society." Insert appropriate information in place of the capitalized words.

I would like to...	reuse in a Thesis/Dissertation
Requestor Type	Author (original work)
Portion	Full article
Format	Print and Electronic
Will you be translating?	make a selection
Select your currency	USD - $
Quick Price	Click Quick Price

QUICK PRICE CONTINUE

This service provides permission for reuse only. If you do not have a copy of the article you are using, you may copy and paste the content and reuse according to the terms of your agreement. Please be advised that obtaining the content you license is a separate transaction not involving Rightslink.

To request permission for a type of use not listed, please contact the publisher directly.

Chemoenzymatic macrocycle synthesis using resorcylic acid lactone thioesterase domains

G. W. Heberlig, J. T. C. Brown, R. D. Simard, M. Wirz, W. Zhang, M. Wang, L. I. Susser, M. E. Horsman and C. N. Boddy, *Org. Biomol. Chem.*, 2018, **16**, 5771
DOI: 10.1039/C8OB01512K

- For reproduction of material from all other RSC journals:
  [Original citation] - Reproduced by permission of The Royal Society of Chemistry

If you are the author of this article you still need to obtain permission to reproduce the whole article in a third party publication with the exception of reproduction of the whole article in a thesis or dissertation.

Information about reproducing material from RSC articles with different licences is available on our Permission Requests page.

SPRINGER NATURE

Title:	Trapping biosynthetic acyl-enzyme intermediates with encoded 2,3-diaminopropionic acid
Author:	Nicolas Huguenin-Dezot et al
Publication:	Nature
Publisher:	Springer Nature
Date:	Dec 12, 2018

Author Request

If you are the author of this content (or his/her designated agent) please read the following. If you are not the author of this content, please click the Back button and select no to the question "Are you the Author of this Springer Nature content?".
Ownership of copyright in original research articles remains with the Author, and provided that, when reproducing the contribution or extracts from it or from the Supplementary Information, the Author acknowledges first and reference publication in the Journal, the Author retains the following non-exclusive rights:
To reproduce the contribution in whole or in part in any printed volume (book or thesis) of which they are the author(s).
The author and any academic institution, where they work, at the time may reproduce the contribution for the purpose of course teaching.
To reuse figures or tables created by the Author and contained in the Contribution in oral presentations and other works created by them.
To post a copy of the contribution as accepted for publication after peer review (in locked Word processing file, of a PDF version thereof) on the Author's own web site, or the Author's institutional repository, or the Author's funding body's archive, six months after publication of the printed or online edition of the Journal, provided that they also link to the contribution on the publisher's website.
Authors wishing to use the published version of their article for promotional use or on a web site must request in the normal way.

If you require further assistance please read Springer Nature's online author reuse guidelines.

For full paper portion: Authors of original research papers published by Springer Nature are encouraged to submit the author's version of the accepted, peer-reviewed manuscript to their relevant funding body's archive, for release six months after publication. In addition, authors are encouraged to archive their version of the manuscript in their institution's repositories (as well as their personal Web sites), also six months after original publication.

v1.0

BACK | CLOSE WINDOW